



ENCYCLOPEDIA OF

Physical Science
AND Technology

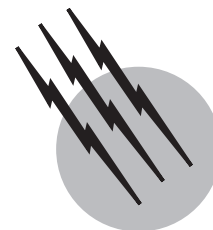
THIRD EDITION

Polymers



Table of Contents
(Subject Area: Polymers)

Article	<i>Authors</i>	Pages in the Encyclopedia
Biopolymers	<i>E. Ann MacGregor</i>	Pages 207-245
Macromolecules, Structure	<i>Peter A. Mirau, Lynn W. Jelinski and Frank A. Bovey</i>	Pages 857-901
Plastics Engineering	<i>R. J. Crawford</i>	Pages 457-474
Polymer Processing	<i>Donald G. Baird</i>	Pages 611-643
Polymers, Electronic Properties	<i>J. Mort</i>	Pages 645-657
Polymers, Ferroelectric	<i>T. C. Mike Chung and A. Petchsuk</i>	Pages 659-674
Polymers, Inorganic and Organometallic	<i>Martel Zeldin</i>	Pages 675-695
Polymers, Mechanical Behavior	<i>Garth L. Wilkes</i>	Pages 697-722
Polymers, Photoresponsive (in	<i>Elsa Reichmanis, Omkaram Nalamasu and Francis</i>	Pages 723-744
Polymers, Recycling	<i>Richard S. Stein</i>	Pages 745-750
Polymers, Synthesis	<i>Timothy E. Long, James E. McGrath and S. Richard</i>	Pages 751-774
Polymers, Thermally Stable	<i>J. P. Critchley</i>	Pages 775-807
Rheology of Polymeric Liquids	<i>Chang Dae Han</i>	Pages 237-252
Rubber, Natural	<i>Stephen T. Semegen</i>	Pages 381-394
Rubber, Synthetic	<i>Stephen T. Semegen</i>	Pages 395-405



Biopolymers

E. Ann MacGregor

University of Manitoba

I. General Characteristics of Polymers

II. Biopolymers

GLOSSARY

α -Amino acid Chemical compound containing a carboxylic acid group (COOH) and an amino group (NH₂) attached to one carbon atom.

Anomers Carbohydrates differing only in configuration of substituent groups at carbon 1 of an aldose sugar.

Configuration Arrangement of atoms in a molecule in space. One configuration cannot be changed to another without breaking interatomic bonds in the molecule.

Conformation Arrangement of the atoms of a molecule in space, which can be changed by rotation of chemical groupings around single bonds in the molecule.

Covalent bond Bond between two atoms in which each atom contributes one electron to the bonding.

Dalton Unit of atomic mass, equal to 1.66053×10^{-27} kg.

Gel Semisolid jelly of solid dispersed in liquid.

Hydrogen bond Weak bond formed when a hydrogen atom is shared between two electron-attracting atoms such as oxygen or nitrogen.

Primary structure Sequence of monomer residues in a polymer chain.

Quaternary structure Arrangement of subunits of a polymer molecule in space (especially for proteins). Each subunit must itself be a polymer chain.

Secondary structure Regular folding of a polymer chain, stabilized by hydrogen bonding.

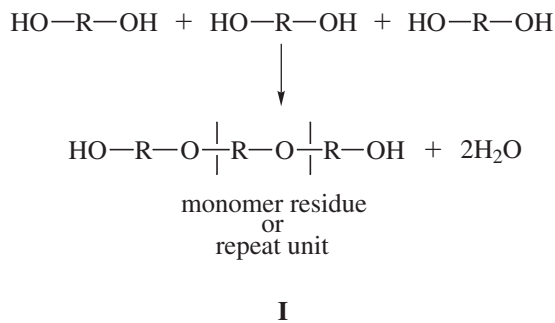
Tertiary structure Overall folding of a polymer chain, including relative orientations of secondary structures.

A POLYMER is a chemical substance whose molecules are large and consist of many small repeating units covalently bonded together. In nature, a wide variety of polymers, the biopolymers, are synthesized by living organisms. Among such biopolymers are the proteins which perform many different functions, such as acting as catalysts or regulators, the polysaccharides—important in structures and as energy reserves—and the nucleic acids which carry genetic information from one generation to the next. In addition, rubber, a plant polymer, is an industrially important elastomer, while little direct commercial use has yet been found for lignin, another abundant plant polymer. The microbial polyesters, polyhydroxyalkanoates, are, in contrast, growing in importance as biodegradable plastics made from renewable resources.

I. GENERAL CHARACTERISTICS OF POLYMERS

Polymer molecules, or macromolecules, are composed of large numbers of linked, small repeat units. The units from which polymers are synthesized are called monomers. Polymers may be made from one kind of monomer, giving

homopolymers, or from several kinds of monomers, giving copolymers. For many biopolymers the repeat units of the macromolecule are not identical in structure to the monomers, because a small molecule such as water is eliminated from the monomers during incorporation into the polymer. This leaves monomer residues or repeat units smaller than the original monomers (e.g., consider three hypothetical monomers becoming linked at the start of synthesis of a polymer, as in I).



The monomer is HOROH, while the repeat unit is $-\text{R}-\text{O}-$. Molecules consisting of a small number (<20) of repeat units are called oligomers, but there is no generally accepted value for the number of repeat units which distinguishes a large oligomer from a small polymer. In this article the molecules of the polymers discussed generally have a degree of polymerization (the number of repeat units in the polymer molecule) of more than 30.

Where polymers are synthesized from monomers containing two chemically reactive, or functional, groups, the resultant polymer molecules are linear. If monomers have more than two functional groups, however, branched or even network polymers may be formed (Fig. 1).

Carbon atoms are an important constituent of a biopolymer chain. Such atoms are usually bonded to four atoms or chemical groupings arranged tetrahedrally in space. When the four groups attached to one carbon atom are different, two possible arrangements in space, or configurations, are possible (Fig. 2). Biosynthesis of polymers is under strict stereochemical control, however, and usually only one possible configuration is incorporated into a biopolymer. Thus, proteins, which are polymers of α -amino acids, are synthesized from L- α -amino acids only, and not from D- α -amino acids (see Fig. 2).

In copolymers, where more than one monomer residue (say A and B) is present, these residues can be arranged along the polymer chain in different ways, giving for example an apparently random sequence A-B-A-A-B-A-B-B-B-A-A-, or an alternating sequence A-B-A-B-A-B-A-B-, or a sequence consisting of a block of one residue followed by a block of the other A-A-A-A-A-A-B-B-

B-B-B-. Examples of all these kinds of biopolymer arrangements are known.

A polymer sample may consist of a collection of identical molecules (i.e., with the same sequence of monomer residues, the same position and length of branches [where present] and the same degree of polymerization). On the other hand, polymers are known where the molecules are heterogeneous with respect to number and sequence of monomer residues and distribution of branches. Proteins and nucleic acids, for example, fall in the first category, while polysaccharides and lignin come in the second category.

One of the characteristics of polymers, apart from molecular size, which distinguishes them from substances made of small molecules is the importance of noncovalent bonding between two parts of the same polymer molecule or between two separate molecules. This noncovalent bonding can be of various kinds. Hydrogen bonding arises when hydrogen atoms are shared between two atoms such as oxygen or nitrogen which carry partial negative charges. Hydrogen bonds are particularly common in biopolymers, but they can be disrupted easily by heat or changes in acidity (or pH) of the environment of the polymer. Many groups attached to polymer main chains can ionize, and electrostatic attractions, or ionic bonding, can occur between positively and negatively charged groupings. Conversely, groups carrying like charges repel each other. Ionic bonding is important in many proteins and inorganic polymers but again can be lessened by changes in pH of the environment. In proteins, it is often found that hydrocarbon groups associate with each other. This hydrophobic interaction excludes water from the vicinity of the hydrocarbon groupings. In fact, it is this exclusion of water which provides the driving force for the association. In addition to these kinds of bonding, all atoms in close contact attract each other weakly. Such forces are called van der Waals forces and can be important in the interiors of highly folded and compact polymer molecules.

II. BIOPOLYMERS

A large number of polymers, differing widely in structure and function, are synthesized in living organisms. It is convenient, therefore, to discuss biopolymers in groups, rather than as a whole. The polymers described below have been assigned to groups on the basis of structure, but at best this division is approximate.

Although individual polymers are important, in living organisms it is often the interactions between biopolymers which confer on a tissue its form and function. Much work is now being carried out to elucidate these interactions.

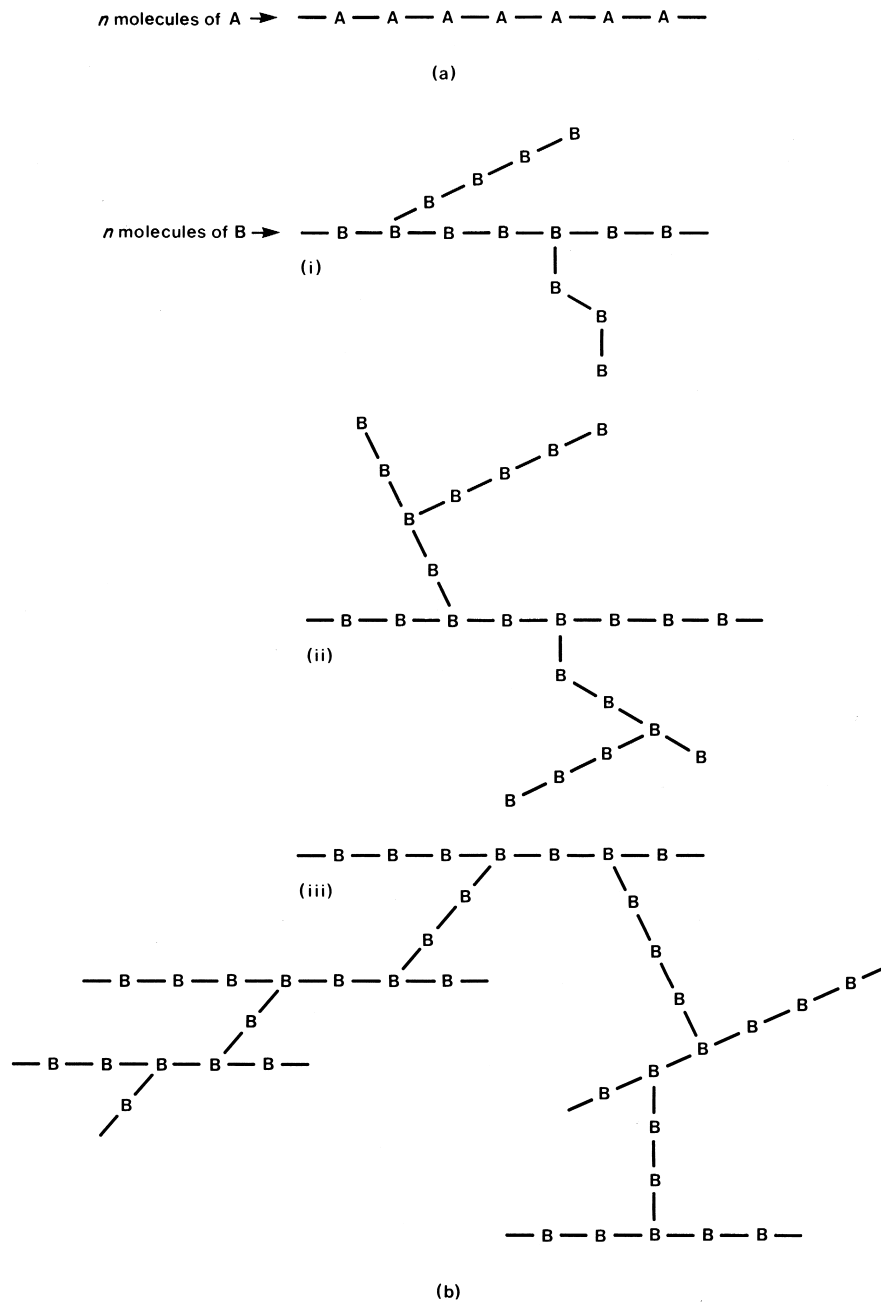


FIGURE 1 (a) Formation of a linear polymer from monomer A with two functional groups and (b) formation of nonlinear polymers from monomer B with three functional groups: (i) branched polymer, (ii) branch-on-branch polymer, and (iii) network polymer.

A. Proteins

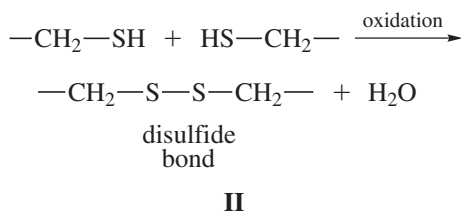
All proteins are polymers of α -amino acids, but they differ in three-dimensional molecular structure and in the functions they perform in living organisms. Protein molecules can, for example, have structural, transporting, or regulatory roles; in addition, as antibodies they protect mammals from disease and as enzymes act as the most efficient catalysts known. As our knowledge of protein structure has

increased, so also has our understanding of the relationship between structure and function.

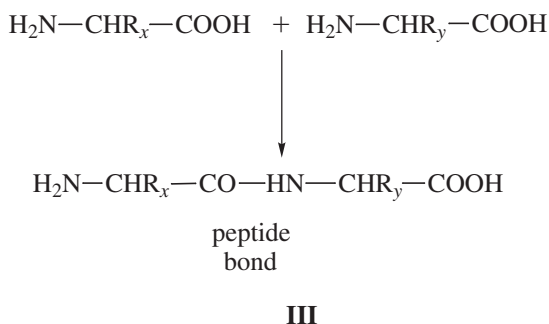
1. Structure

As mentioned earlier, the monomers of proteins are α -amino acids. Such acids can exist in two configurations (see Fig. 2), but the strict stereochemical requirements of the processes involved in protein biosynthesis result

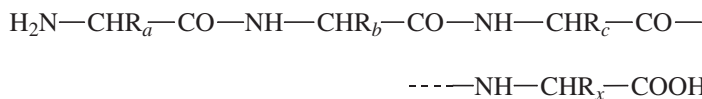
in only L- α -amino acids becoming incorporated into the polymers. Nineteen different amino acids of general formula $\text{H}_2\text{N}-\text{CHR}-\text{COOH}$ can be used as monomers in protein synthesis, and these vary only in the nature of the side group R. A list of possible side groups is shown in Table I. In addition an imino acid, proline, with a cyclic side chain and having an $-\text{NH}$ group instead of the $-\text{NH}_2$ of the amino acids, can act as a protein monomer. Some side chains (R groups) can be chemically modified after incorporation of the amino acid into a protein, and three of these modifications are also shown in Table I. Thus, hydroxyl groups can be introduced onto lysine and proline residues to give hydroxylysine and hydroxyproline, respectively. Oxidation, as in II, of two cysteine side chains close to each other in the protein molecule gives cystine, containing a new disulfide bond which helps to stabilize protein structure:



During protein biosynthesis, amino acids become linked together effectively by the elimination of water:



The new bond formed is called a peptide bond; two amino acids linked by such a bond constitute a dipeptide; three amino acids joined by two peptide bonds form a tripeptide. A chain of several (e.g., ten) amino acids so linked gives an oligopeptide, while a long chain of up to several thousand amino acids as in IV is called a polypeptide. A protein is simply a substance whose molecules consist of one or more polypeptide chains:



IV

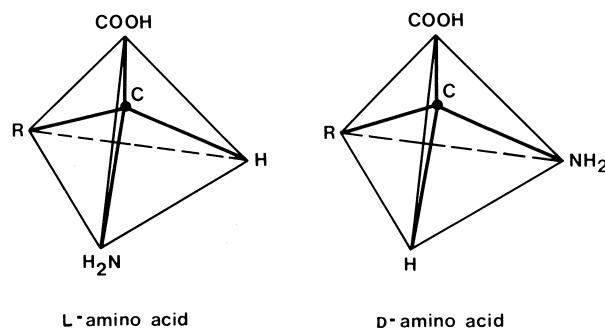


FIGURE 2 Two possible configurations of α -amino acids of structure $\text{H}_2\text{N}-\text{CHR}-\text{COOH}$.

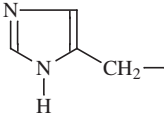
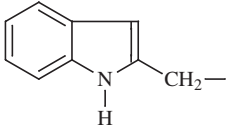
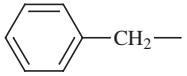
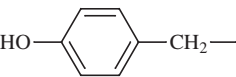
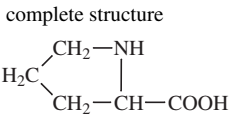
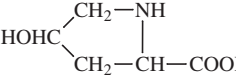
Protein biosynthesis is a complex process directed by other biopolymers, the nucleic acids, and this is described later in Section II.C.2. X-ray studies of peptides have shown that the atoms involved in the peptide bond are almost coplanar, and that adjacent side groups (R groups) project on opposite sides of the polypeptide chain (see Fig. 3). This imposes restrictions on the way a polypeptide chain can fold up in three dimensions.

All proteins have certain structural features in common. Each protein molecule consists of at least one polypeptide chain. Most polypeptide chains have a free amino group (NH_2) at one end—this is the N-terminal end of the chain—and a carboxylic acid group (COOH) at the other or the C-terminal end of the chain. By convention, polypeptide chain formulas are written with the N-terminal end at the left and the C-terminal end at the right.

The amino and carboxyl groups at chain ends and on the side groups of the amino acids, lysine, arginine, aspartic, and glutamic acids can ionize to give $-\text{NH}_3^+$ and $-\text{COO}^-$ groups, respectively. Thus, polypeptide chains are charged in solution, but the magnitude of the charge depends on the pH. For each protein there is a pH at which the net charge on the molecules is zero. This pH is known as the isoelectric point of the protein.

Proteins differ from one another in the number, modification, and sequence of amino acid residues in the polypeptide chains and in the number of chains making up the protein molecule. Hence, proteins differ widely in molecular weight. In addition, some proteins, the conjugated proteins, contain nonamino acid material such as complex organic molecules or simple metal ions. These are called prosthetic groups, and they alter the physical and chemical properties of proteins.

TABLE I The Common Amino Acids Found in Proteins

Name	Common abbreviation	Side group, R
Glycine	Gly	H—
Alanine	Ala	CH ₃ —
Valine	Val	$\begin{array}{c} \text{CH}_3 \\ \\ \text{CH}_3\text{—CH—} \end{array}$
Leucine	Leu	$\begin{array}{c} \text{CH}_3 \\ \\ \text{CH}_3\text{—CH—CH}_2\text{—} \\ \\ \text{CH}_3 \end{array}$
Isoleucine	Ile	$\begin{array}{c} \text{CH}_3 \\ \\ \text{CH}_3\text{—CH}_2\text{—CH—} \\ \\ \text{CH}_3 \end{array}$
Serine	Ser	HO—CH ₂ —
Threonine	Thr	$\begin{array}{c} \text{OH} \\ \\ \text{CH}_3\text{—CH—} \end{array}$
Aspartic acid	Asp	HOOC—CH ₂ —
Asparagine	Asn	H ₂ NOC—CH ₂ —
Glutamic acid	Glu	HOOC—CH ₂ —CH ₂ —
Glutamine	Gln	H ₂ NOC—CH ₂ —CH ₂ —
Arginine	Arg	$\begin{array}{c} \text{NH} \\ \\ \text{H}_2\text{N—C—NH—CH}_2\text{—CH}_2\text{—CH}_2\text{—} \end{array}$
Lysine	Lys	H ₂ N—CH ₂ —CH ₂ —CH ₂ —CH ₂ —
Hydroxylysine ^a	Hyl	$\begin{array}{c} \text{OH} \\ \\ \text{H}_2\text{N—CH}_2\text{—CH—CH}_2\text{—CH}_2\text{—} \end{array}$
Methionine	Met	CH ₃ —S—CH ₂ —CH ₂ —
Cysteine	Cys	HS—CH ₂ —
Cystine ^a	(Cys) ₂	—CH ₂ —S—S—CH ₂ —
Histidine	His	
Tryptophan	Trp	
Phenylalanine	Phe	
Tyrosine	Tyr	
Proline	Pro	<p>complete structure</p> 
4-Hydroxyproline ^a	Hyp	

^a Produced from preceding acid by chemical reaction after incorporation into protein.

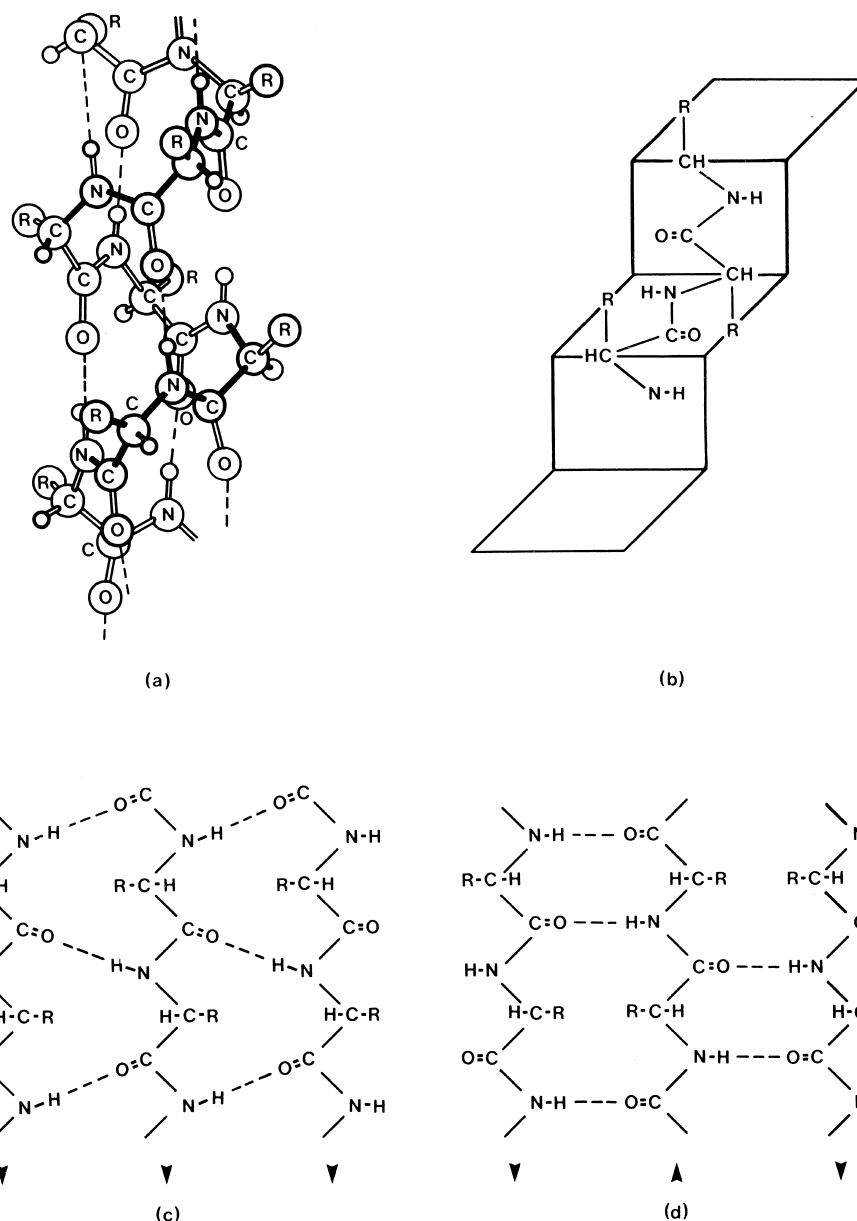


FIGURE 5 Secondary structures of proteins: (a) α -helix, (b) "pleated" extended polypeptide chain, (c) parallel pleated sheet, and (d) antiparallel pleated sheet. The arrow indicates chain direction from N-terminal to C-terminal.

the R groups project above or below the plane of the sheets, and frequently the sheets are not flat, but are bent or twisted. In some proteins, however, the polypeptide chain containing the β -strands may coil like a helix, giving a so-called β -helix.

Proteins do not have structures which are entirely helical or β -sheet. In general, a protein molecule made of one polypeptide chain consists of short stretches of helix and β -structure connected by apparently randomly folded segments of chain. Some proteins contain no helices, while others contain no β -structure. The proportion and relative

orientations of regular structures in a protein molecule are determined by the amino acid sequences of the polypeptide chains.

The overall fold of a polypeptide chain (i.e., the relative orientations of helices, β -strands, and the folding of segments between them) constitutes the tertiary structure of a protein (Fig. 6). This folding can be stabilized by additional hydrogen bonds between, for example, amino acid side groups brought close together by the folding, by ionic bonds if side chains carrying opposite electrical charges are brought into close proximity, by van der Waals forces

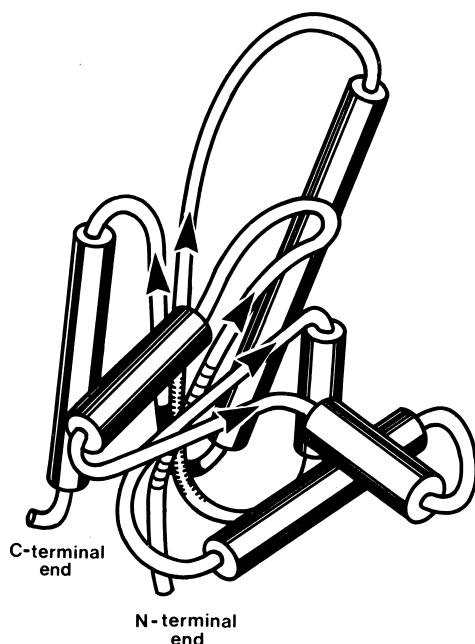


FIGURE 6 Tertiary structure of a hypothetical protein. The cylinders represent helices, while the arrows represent pleated sheet strands. The five strands of β -structure form a twisted parallel pleated sheet.

if side chains are packed closely together, by hydrophobic interactions where hydrocarbon side chains come together, and by the disulfide bonds of cystine (as in **II**).

Polypeptide chains of one protein usually adopt a preferred tertiary structure that is essential for biological activity. The noncovalent bonding, which stabilizes tertiary structure, can easily be weakened by heat or changes in pH and salt concentration. When this happens, the polypeptide chains unwind and become randomly coiled. Biological activity is lost and the protein is said to be denatured. For some proteins, removal of the denaturing agent permits a return of the preferred tertiary structure and of biological activity. The protein is then said to be renatured, and it is this ability to recover from unfolding which has led us to believe that the information required to specify the correct folding for biological activity is encoded in the amino acid sequences of polypeptide chains.

The tertiary structure of many proteins can be described in terms of “domains” rather than polypeptide chains. A domain is a polypeptide chain, or section thereof, often of molecular weight around 20,000 and which constitutes a geometrically separate entity (i.e., a region of regular and irregular folding separated from other such regions by a longer stretch of irregular folding). Comparisons of many proteins have shown that the same structural domain, characterized by its own folding pattern, may occur in different proteins or several times in one protein. As

the folding of more and more proteins is studied, we realize that most proteins can be described in terms of a small number of regular packing arrangements of helices and/or β -structures. Thus, proteins can be considered to be constructed of modules, each module being a structural domain of mainly α -helices and/or β -structure. One protein differs from another, then, in the number, type, and relative arrangement of domains within the molecule, and in the detailed arrangement of amino acid side groups, R groups, on the molecular surface.

The tertiary structure of a protein molecule encompasses the overall folding of polypeptide chains, where, if more than one chain is present, the chains are linked by covalent bonds—most often disulfide bonds (as in **II**). However, some proteins exist where the molecules consist of several separate polypeptide chains; such chains would be held together in the molecule by weaker bonds such as hydrogen and ionic bonds, hydrophobic interactions, and van der Waals forces and each chain can act as a separate subunit of the protein molecule. These proteins are said to possess quaternary structure (i.e., specific arrangements of subunits within the macromolecule). Changes in subunit arrangement and even, to a small degree, in tertiary structure of each subunit can take place while the protein carries out its biological function. Proteins in which such changes take place are said to be allosteric.

In summary, any one protein has a unique primary structure which in turn specifies the secondary and tertiary structure (i.e., folding of the polypeptide chains). Relatively minor changes in tertiary structure are possible as the protein functions in a living organism. Some proteins also possess quaternary structure which may undergo changes associated with biological activity.

2. Function

The functions of proteins are many and varied. Here representatives of some of the major functions are given, with a description where possible, of the relationship between structure and activity.

Enzymes are an extremely important group of proteins—the proteins that act as catalysts. These increase the rates of reactions by factors of from 10^8 up to 10^{20} , and so are the most efficient catalysts known. Unlike most man-made catalysts, enzymes are extremely specific; each enzyme catalyzes one reaction or a group of closely related reactions. The specificity extends not only to the chemical nature of the reactants and products of a reaction but also to the stereochemistry (i.e., arrangement of atoms in space) of the substances involved. Thus the enzymes of protein biosynthesis can distinguish between D- and L- α -amino acids and ensure that only L-amino acids are incorporated into a growing polypeptide chain. In a living organism,

there are many hundreds of reactions occurring, each catalyzed by a specific enzyme.

The way in which enzymes bring about such large increases in reaction rate is not understood completely, but a number of factors probably contribute to the rate enhancement. An enzyme forms a temporary complex with one or more of the reactants in a reaction. (The substances with which the enzyme interacts are called substrates for the enzyme.) There is often strain on a substrate in such a complex, allowing the substrate to react more readily than if the enzyme were absent. Immobilization of a substrate on the surface of an enzyme can also allow a reaction to occur more easily, particularly where a second reactant is involved. The enzyme brings the two substrates into close proximity. Some amino acid side groups are capable of donating and receiving protons (i.e., hydrogen ions), and if such groups on an enzyme are brought close to a bond to be broken in a substrate, then bond breaking can often occur more quickly. Some enzyme-catalyzed reactions proceed via formation of an intermediate covalently bonded to the enzyme; formation of such an intermediate seems to speed up the overall reaction.

Enzymes may act singly or may function as a group in a multienzyme complex. Usually each enzyme of a multienzyme complex is responsible for catalyzing one step of a complicated multistep biochemical pathway. Here greater acceleration of reaction rate is possible if one enzyme “passes on” the product of its reaction to the next enzyme in the pathway.

Although enzyme molecules are large, the catalytic activity is usually associated with a relatively small area of the molecular surface, where the substrate is bound and reaction takes place. This area is called the active site of the enzyme. When an enzyme possesses quaternary structure (i.e., consists of several separate polypeptide chains) there may be more than one active site per molecule. The active site is usually situated in a depression or a cleft on the enzyme surface and is lined with amino acid side groups that can bind the substrate—usually by weak bonds such as hydrogen bonds—and help to bring about the reaction being catalyzed. The active site is often formed from parts of the polypeptide chain, which are well separated in primary structure, but brought together by the folding of the chain. One enzyme differs from another in the shape of its active site and the nature of the side groups at the site. In many enzymes, the remainder of the macromolecule simply functions to maintain the shape and functionality of the active site.

The shapes of enzyme molecules, and proteins in general, have been investigated by X-ray diffraction of protein crystals (i.e., the folding of polypeptide chains in solid proteins has been studied). From studies of smaller proteins of molecular weight 25,000 or less in solution by nuclear

magnetic resonance spectroscopy, it has been concluded that a protein has the same overall shape in solution as in the solid state, but that some minor changes can occur. For enzymes it is known that a few amino acid side chains can change position by several angstroms (10^{-10} m) when the substrate becomes bound to the enzyme molecule. Thus, the active shape, or conformation, of an enzyme molecule is not rigidly defined, but alterations can take place as the enzyme carries out catalysis.

Many enzymes require the presence of ions or other small molecules in order to show catalytic activity. These nonprotein components are called cofactors, and a small organic cofactor is usually known as a coenzyme. A coenzyme may be covalently bound to an enzyme, in which case it would be classified as a prosthetic group of the enzyme, or it may be loosely associated with the enzyme. Here the coenzyme often acts as a substrate for the enzyme. Coenzymes are frequently derived from vitamins. Lack of such a vitamin in the human diet can result in an inactive enzyme or group of enzymes and can lead to development of a deficiency disease.

In living tissues, the activities of many enzymes are regulated by substances known as activators and inhibitors. These bind to enzymes and enhance or reduce the catalytic efficiency of the enzymes involved. Inhibitors can act simply by binding at the active site and preventing substrate binding. Certain lethal nerve gases, for example, modify the active site of an enzyme essential for the transmission of nerve impulses; the result is paralysis and death. Where the functioning of an enzyme is critical for the metabolism of a disease-causing bacterium or virus, administration of an enzyme inhibitor may be beneficial to an infected human being. Thus inhibitors of an HIV enzyme necessary for virus maturation are important anti-AIDS drugs.

Many natural regulators of enzyme activity, however, bind noncovalently at sites in the enzyme molecule other than the active site. For these enzymes, then, parts of the polypeptide chain(s) not involved in the active site have more than a structural role; they also have a regulatory role. It is believed that the activators and inhibitors bring about a change in the shape of the enzyme molecule and that this shape change controls the efficiency of the active site. Such enzymes are called allosteric enzymes, and many consist of several noncovalently bonded peptide chains. An inhibitor or activator may bind to one chain, while the active site is located on another. In a case like this, the active site is affected by a change in quaternary structure when the regulatory molecule is bound. Allosteric enzymes are believed to be capable of existing in inactive and active states; binding of inhibitor favors the inactive state, while binding of activators favors the active state. The active and inactive states differ slightly in tertiary and/or quaternary structure.

The details of the mechanism of action differ for each enzyme, but in each case a substrate is held by noncovalent forces at the enzyme surface. Amino acid side chains, and sometimes a coenzyme or metal ion, participate in transferring electrons, protons, or small functional groups to or from the substrate to facilitate the reaction being catalyzed.

Transport and storage of ions and small molecules is another function often performed by proteins. For example, metal ions such as iron or potassium are transported with the help of proteins. The transport and storage systems involved in the utilization of oxygen have been studied intensively. In human blood, oxygen is carried round the body bound to a protein called hemoglobin; the oxygen is stored temporarily before use in tissues such as muscles by a related but less complex protein, myoglobin.

Both proteins are conjugated proteins (i.e., contain a nonprotein prosthetic group). This group is heme, a flat organic ring system with an iron(II) ion at the center. This iron ion is normally surrounded by six atoms, each of which donates a pair of electrons to the iron. These atoms are four central nitrogens of the heme ring system, a ring nitrogen of a histidine residue (see Table I) of the polypeptide chain and the oxygen of the oxygen molecule being transported. The heme group is colored, but uptake and release of oxygen cause a color change. The oxy form of hemoglobin is the bright red characteristic of arterial blood, while the deoxy form is the more purplish color seen in blood in veins.

Myoglobin molecules consist of one polypeptide chain of about 150 amino acid residues and one heme group, while hemoglobin has four polypeptide chains and four heme groups. In myoglobin, the chain is folded up to give the overall shape of a flattened sphere, and about 80% of the amino acid residues are arranged in 8 α -helices. The heme group is bound to the polypeptide chain by noncovalent bonds. The polypeptide chain is folded in such a way as to provide a hydrophobic pocket for the heme group, and in fact the main purpose for the polypeptide chain of myoglobin seems to be to provide a hydrophobic environment for the iron(II) of the heme. This prevents the iron(II) from becoming readily oxidized to iron(III). Whereas the iron(II) of myoglobin and hemoglobin can bind oxygen easily, iron(III) attached to the same proteins cannot.

The common form of hemoglobin consists of two pairs of identical chains, α -chains containing 141 amino acid residues and β -chains of 146 amino acids. Each of the four chains of hemoglobin is folded to provide a hydrophobic pocket for the heme. Even though the primary structures of hemoglobin and myoglobin differ, their chains are folded in a similar way. The four chains of hemoglobin are not covalently linked to each other but

are held together by hydrophobic, ionic, and hydrogen bonding. Thus, hemoglobin molecules possess quaternary structure, and changes in this quaternary structure are important in the uptake and release of oxygen.

Myoglobin, the storage protein, is required to have a high affinity for oxygen at the oxygen pressure of muscles. Hemoglobin, on the other hand, must have more complex properties. The affinity for oxygen must be high at the oxygen pressure of the lungs and much lower in muscles so that the oxygen can be passed on to the myoglobin. This change is brought about by relatively small changes in tertiary and quaternary structure of the hemoglobin molecules. The pH in muscles is usually slightly less than that in lungs, and this favors the deoxy form of hemoglobin over the oxy form. At this lower pH the side chains of certain amino acids are positively charged and are involved in interchain ionic bonding with negatively charged groups close by in the quaternary structure. In addition, the iron ion lies out of the plane of the heme ring system. On one side of the iron ion in both α -chains is a space capable of accommodating the oxygen molecule; in the β -chains this space is blocked by the side chain of an amino acid residue. In lungs, when an oxygen molecule binds to the heme of one α -chain, the iron ion moves back into the plane of the heme ring, pulling part of the polypeptide chain with it. This in turn alters the position of one of the helices of the chain, and the movement causes the breaking of some ionic and hydrogen bonds between an α - and a β -chain. A second oxygen can bind to a second α -chain and bring about similar changes. With the breaking of noncovalent bonds between the hemoglobin subunits, however, changes in quaternary structure can take place. The α - and β -chains rotate with respect to each other and the two β -heme groups move about 6 Å closer to each other. The amino acid side groups of the β -chains which blocked the oxygen-holding space now move away and oxygen can also bind to the hemes of the β -chains. Further ionic bonds are broken and protons can be released, a situation favored at the higher pH of the lungs. In muscles the opposite changes take place. Although the first oxygen molecule is given up with some difficulty, the release of the other three oxygen molecules becomes easier as changes in quaternary structure take place, chain end ionic bonds are remade and the oxygen "pockets" of the β -chains become reblocked.

Small molecules other than oxygen can also bind at the heme groups. Unfortunately the affinity for carbon monoxide is much higher than for oxygen, and so in an atmosphere containing carbon monoxide this molecule is bound preferentially. If the carbon monoxide level is high enough, insufficient amounts of oxygen are transported from the lungs and death can ensue.

Other proteins in mammalian systems, the antibodies, serve to protect against invasion by bacteria or viruses. Foreign material such as bacterial protein or polysaccharide, on entering the bloodstream, provokes the synthesis of specific antibodies. The antibodies then combine with the “foreign” molecules, known as antigens, and render them harmless. Stimulation of antibody synthesis in man can be brought about by immunization, whereby a harmless form of disease-producing bacteria or virus is introduced into the body and specific antibodies are formed. These are active against virulent forms of the same bacterium and may remain in the bloodstream for years, affording protection against the disease. Unfortunately, “foreign” tissue in the body elicits the same response, and so, for organ transplants to be successful and not be rejected, the immune response must be minimized by the administration of powerful immunosuppressant drugs.

Antibodies constitute a group of proteins known as the immunoglobulins. In an adult human there are five classes of immunoglobulin, and the most prevalent, the IgG antibodies of blood, have been studied in some detail. Each IgG molecule contains two identical heavy chains of approximately 440 amino acids and two identical light chains of around 220 amino acids, all linked by disulfide bonds. It is believed that the chains are constructed of domains of approximately 110 amino acids. Each domain has similar folding of the polypeptide chains and consists essentially of two antiparallel pleated sheets. The light chains, therefore, contain two such domains, while the heavy chains have four each.

Antibodies are specific for the antigens with which they combine. Therefore, many different IgG molecules exist, but the primary structures of the three C-terminal domains of a heavy chain and the C-terminal domain of a light chain are very similar from one IgG molecule to another. These are referred to as the constant regions of the heavy and light chains, respectively. The N-terminal domains of both the heavy and light chains, however, show great diversity in amino acid sequence and are known as the variable regions of the chains.

Different classes of antibody vary in the nature of the constant regions of the heavy chains, but within one class (e.g., the IgG) the variable regions of the light and heavy chains confer specificity on an antibody. The binding site is believed to be situated in a cleft (for a small antigen) or on an irregular surface (complementary to part of the surface of a large antigen) formed by parts of two variable domains in close proximity, one domain belonging to a light chain and one to a heavy chain. Since each IgG molecule has two light and two heavy chains, then each has two antigen-binding sites. Binding of antigen is believed to involve noncovalent bonding between the antigen and amino

acid side chains on the antibody surface at the binding site.

Some proteins can serve yet another purpose in living organisms, where they can act as regulators of biochemical pathways. Hormones are substances that act on target cells and markedly alter the metabolism of those cells. Some hormones are small proteins or polypeptides, and it is believed that they interact with specific receptors on the outer surface of the target cell membrane. The receptors themselves are proteins, and binding of the hormone to the receptor protein causes changes to occur within the cell. In some cases it is known that a messenger molecule increases in concentration in the affected cell, and that this messenger modifies enzyme activities within the cell. Thus glucagon, a polypeptide of 29 amino acid residues secreted by the pancreas, acts on liver cells in this way and stimulates breakdown of glycogen (see Section II.B.6), giving an increase in blood glucose levels.

In many cases the direct effect (at the molecular level) of the hormone on its target cell is brought about by a complex “cascade” of reactions. This is true for insulin, the most widely studied polypeptide hormone. Insulin is secreted by the pancreas and consists of two short chains of 21 and 30 amino acids, linked by disulfide bonds (see Fig. 4). The hormone acts mainly on cells of liver, muscle, and fatty tissues, decreases glucose concentration in the blood, and promotes glycogen and fat synthesis. Amino acid side chains on the surface of the insulin molecule are important for interaction with the insulin receptor at its target cells. It is known that binding of insulin to the receptor stimulates the activity of an enzyme within the cell which is intrinsic to the receptor. This enzyme, in turn, activates other proteins and enzymes by adding phosphate groups to specific amino acid side chains. The newly activated proteins then affect other proteins to increase or reduce their activity and ultimately bring about the effects associated with insulin action. Thus, for example, the insulin receptor enzyme activates a second enzyme that stimulates glycogen synthase, which is capable of converting a modified glucose to the storage polysaccharide glycogen (see Section II.B.6). Hence insulin helps to control blood glucose levels.

Other protein regulators, such as the repressors, act not at cell surfaces but interact with the nucleic acids which control protein synthesis. These are described later (Sections II.C.2, and II.E).

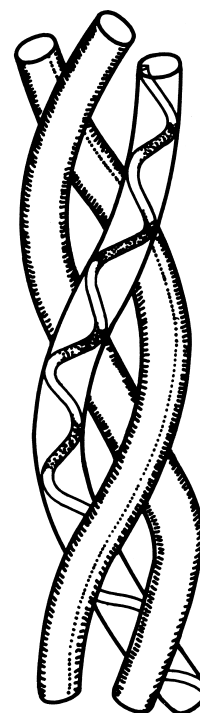
In addition to the functions discussed above, proteins can have a structural role in living organisms. Unlike many of the water-soluble proteins already described, which are often spherical in shape, structural proteins can be insoluble and fibrous. They are synthesized in a soluble form, processed to give the insoluble material, and then

may be cross-linked to other polymers to give the structural unit in living organisms.

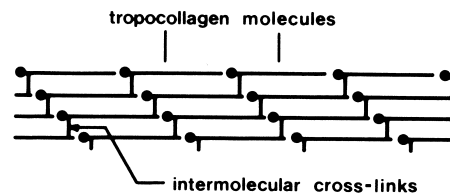
Collagen, a fibrous structural protein, is the most abundant protein in the animal kingdom. It is a major component of skin, cartilage, bone, tendon, and teeth. The basic "unit" is the tropocollagen molecule, consisting of three polypeptide chains, each approximately 1000 amino acid residues long. Many tropocollagens exist, differing in the amino acid sequences of the chains. In at least one collagen, the collagen II of cartilage, all three polypeptide chains in a molecule are identical; in other collagens this is not the case. All collagens have, however, certain features in common. The molecules are about 2800 Å long and 15 Å in diameter. The amino acid composition of tropocollagen is unusual, for one third of the residues may be glycine, while proline and hydroxyproline may constitute another quarter of the total protein. The sequence, -glycine-proline-hydroxyproline-, is common, which means that neither α -helices nor β -structures can be formed readily by the polypeptide chains, for neither proline nor hydroxyproline residues possess the NH groups necessary for hydrogen bond formation. The presence of glycine as every third residue in long stretches of the tropocollagen polypeptide chains allows another kind of regular structure to be formed. This is a triple helix of the three chains wound round each other; each single chain is coiled as a left-handed helix (Fig. 7a). The bulky side chains of proline and hydroxyproline project outward on the surface of the triple helix, while the side chains of glycine (H atoms) pack inside. The three chains are held together by hydrogen bonding between the NH of a glycine on one chain and C=O of another residue on a second chain. In addition there may be covalent cross-links between the three chains of the tropocollagen molecule near their N-terminal ends. In some tropocollagens, the amino acid sequence is less regular, and the molecules can consist of interrupted triple helices.

Heating collagen in water results in rupture of the hydrogen bonds and gives a denatured water-soluble protein with a random three-dimensional structure. This product is known as gelatin, and on cooling some molecules renature to give the original triple helical structure, while others partially renature to produce a cross-linked network, a gel. Because of its gel-forming abilities collagen is widely used in the food industry.

In structures such as bone and tendon, tropocollagen molecules are packed head to tail parallel to one another to form collagen fibrils. In the fibrils the molecules are covalently bonded side by side and are probably staggered by one-quarter of their length (Fig. 7b). The bonding is similar but not identical to that holding the three chains of one tropocollagen molecule together and involves the side chains of lysine and hydroxylysine, a less common amino



(a)



(b)

FIGURE 7 Structure of collagen. (a) The triple helix of a tropocollagen molecule; the left-handed helix of a single polypeptide chain is shown. (b) Packing of tropocollagen molecules in a collagen fibril.

acid found in collagen. The importance of such covalent bonding is indicated by the disease lathyrism, where severe skeletal deformities are found and which results from inhibition of the first enzyme involved in catalysis of cross-link formation.

Collagen fibrils are, in turn, packed side by side in tissues to form fibers. Fiber formation is probably influenced by the other polymers such as proteins and glycosaminoglycans (see Sections II.B.6 and 7) of a tissue. The long cylindrical shape of the tropocollagen molecules and their packing into fibrils and fibers gives collagen the high tensile strength necessary for a structural material. The

arrangement of fibers in a tissue depends on the nature of the tissue. In tendon, which requires great strength, fibers are arranged parallel to one another to give a structure with the tensile strength of a light steel wire, while in skin where strength and flexibility are required, the fibers are randomly oriented and woven together as in felt. Where rigidity is needed, as in bone, calcium salts are deposited to harden the tissue. The importance of the structural integrity of collagen is demonstrated by the human deficiency disease scurvy, affecting gums, joints, and wound healing. This results from a lack of vitamin C, ascorbic acid, now known to be required for the action of enzymes that modify proline and lysine to give the hydroxy forms during collagen synthesis.

Other structural proteins of some economic importance are the fibroins, the main constituents of silk, which appear to contain extensive antiparallel pleated sheets, and the keratins which are the main structural proteins of fur and wool, as well as of hair, skin, horn, hooves, nails, feathers, claws, and beaks. The keratin-containing structures are extremely complex, but in wool and hair, for example, there are α -helix-containing fibrils embedded in an amorphous matrix.

3. Utilization

The enzyme systems of microbes such as yeast have been used for centuries in brewing and breadmaking. In the first case the yeast enzymes catalyze the conversion of glucose to alcohol and in the second, carbon dioxide is produced and trapped in the dough to give a lighter texture to the bread. Microbial systems are also employed in the manufacture of cheeses and in the production of antibiotics.

Nowadays purified enzymes are used on an industrial scale, often in solution. Thus, purified starch-degrading enzymes can be added in the early stages of brewing to speed up production of glucose, and glucose syrups can be made from starch by the action of enzymes. Enzymes can also be immobilized on an inert solid support over which substrate is passed. Such immobilized enzymes are frequently employed to convert glucose to another sugar, fructose.

Many proteins are used in modern medicine. Antibody synthesis can be deliberately stimulated in the human body to provide protection against future exposure to disease-producing viruses or bacteria. In some cases of severe infection, antibodies can be administered directly to a patient. Purified antibodies of very high specificity, called monoclonal antibodies, can now be prepared and are used in diagnostic kits to confirm pregnancy or detect certain diseases. In addition, radioactive or modified antibodies to specific cell surface antigens can be synthesized. These antibodies can transport a radioactive isotope or a small

toxic molecule to target cells, which are then destroyed by the radioactivity or toxicity. In this way, for example, cancerous tumors can be reduced. Hormones can be given to alleviate diseases caused by a deficiency of that hormone. Thus, insulin is taken by those suffering from diabetes mellitus; growth hormones can prevent dwarfism. Yet other proteins that are involved in blood clotting can be used to prevent excessive bleeding in hemophiliacs.

Antibodies, because of their ability to bind specific molecules, can be utilized in the preparation of purified antigens, where the antigen itself has useful properties. The antibody can be immobilized on an inert solid support; antigen solution is allowed to flow over the support, and the antigens become bound selectively to the antibody-support complex. Disruption of antigen-antibody binding allows pure antigen to be released and collected. This technique can be used with many other proteins substituting for the antibodies, providing that these proteins show selective binding of useful substances.

Fibrous proteins such as found in wool and silk have been used for many centuries for clothing. The strength, flexibility, and water-holding abilities of the fibers have provided cloth which is both practical and comfortable.

Protein is also an essential foodstuff for man. We need amino acids from which to synthesize the proteins of our own bodies; certain amino acids can be made by conversion of other molecules in the body, but some—the essential amino acids (Trp, Phe, Lys, Met, Leu, Ile, and Val)—must be obtained in our diet from external protein.

Gelatin, the denatured water-soluble form of collagen, is used widely in the food industry as a gelling agent. It is commonly used in fruit-flavored jellies and canned meats. The gel melts, however, at around 25°C, so these foodstuffs should be kept at lower temperatures.

B. Polysaccharides

Polysaccharides are composed of small sugars, the monosaccharides, and a great variety of structure is found. Although they occur in almost all living organisms, their functions seem to be more limited than those of proteins. Quantitatively, the most important polysaccharides are energy reserves or perform a structural role, but other polysaccharides can act as lubricants or have a protective function.

Several polysaccharides have industrial importance; these are usually polymers that can be obtained easily, in good yield, from any one source. Commercially useful polysaccharides are often prepared from higher plants, but marine algae and bacteria are also important sources. In some cases, however, polysaccharide mixtures may be obtained as a by-product of an industrial process, e.g., hemicelluloses resulting from cellulose purification in

paper-making, but have not yet been fully developed as a resource.

1. Structure

As stated above, the monomers of polysaccharides are monosaccharides or sugars. Most of these have the general formula $(\text{CH}_2\text{O})_x$, and were considered initially as hydrates of carbon, hence the name carbohydrates. The most common monomers have five carbon atoms (the pentoses) or six carbon atoms (the hexoses). Each monosaccharide has many hydroxyl (OH) groups on the molecule, and one monosaccharide differs from another in the arrangement in space of the hydroxyl groups. In solution a monosaccharide can exist in a number of forms. The monosaccharides can be thought of as carrying an aldehyde or ketone group, and hence have reducing character. However, intra-molecular cyclization of a monosaccharide can occur to give a ring form, known as a hemiacetal or hemiketal, where the original aldehyde or ketone group is masked by reaction with a hydroxyl group of the same molecule. This cyclization gives a six-membered ring form (pyranose) or a five-membered ring form (furanose) (Fig. 8). Usually only one ring form of a monosaccharide is found in any one polysaccharide. Each monosaccharide can exist in two mirror-image forms, the D- and L-forms just as amino acids are found in D- and L-forms. Most monomer residues found in polysaccharides are D-sugars, but L-sugars do occur. This is unlike the case of proteins where only L-amino acids are incorporated into polymers.

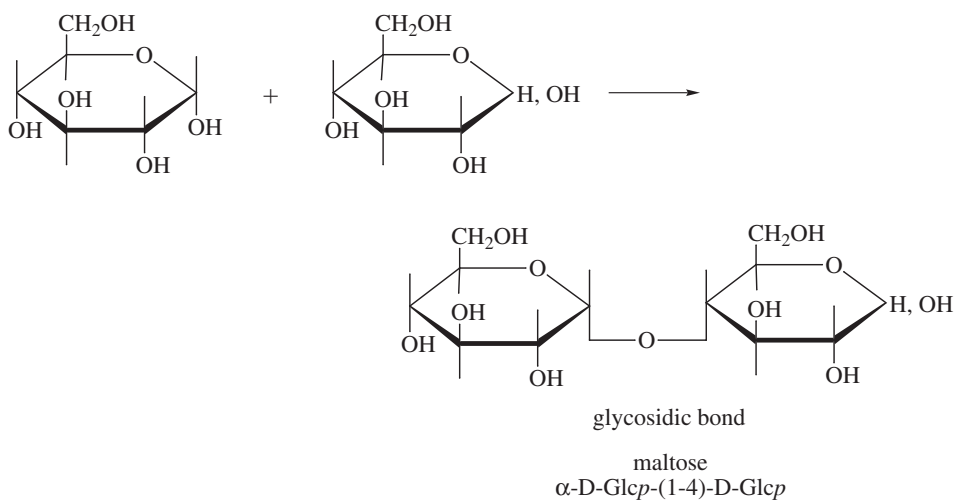
The hydroxyl group on carbon 1 of a sugar such as glucose or mannose can be found either below or above the sugar ring, as shown in Fig. 8a for glucose or mannose.

These two forms (anomeric forms) are distinguished as an α - or β -sugar. In the D-series of sugars, the α -form has the anomeric hydroxyl lying below the plane of the ring, while in the L-sugars, this hydroxyl lies above the ring plane in the α -form. The full name of a monosaccharide indicates whether the sugar is α or β , D or L, which kind of sugar is being dealt with, and the size of the sugar ring, hence the names α -D-glucopyranose and β -D-mannopyranose in Fig. 8a.

Neither the furanose nor pyranose rings are flat, but are puckered. The most stable conformations of pyranose sugars are "chair" forms, and these are designated ${}^4\text{C}_1$ or ${}^1\text{C}_4$, depending on whether the anomeric carbon (carbon 1) is at a top or bottom apex (Fig. 8). (Monosaccharides with six-membered rings may be represented either by the "flat" projection of the pyranose ring shown in Fig. 8a, or by the chair forms more closely related to three-dimensional shape shown in Fig 8b.)

A wide variety of monosaccharides can be incorporated into polysaccharides and some of the most common are shown in Fig. 8. Not all monosaccharides have the general formula $(\text{CH}_2\text{O})_x$. Some have one oxygen less; these are the deoxy sugars (Fig. 8d). Others have a substituted amino (NH_2) group usually on carbon 2; these are the amino sugars (Fig. 8e). Others may carry sulfate groups; yet others have acid groups (COOH) instead of $-\text{CH}_2\text{OH}$ at carbon 6; these are the uronic acids (Fig. 8f).

The anomeric hydroxyl group of a sugar is the most reactive and can act as a reducing group. Although polysaccharide synthesis is complex, the net effect is that monosaccharides become linked together by reactions involving the anomeric hydroxyl of one monomer and the hydroxyl at another carbon of a second monomer, with elimination of water as in VI.



VI

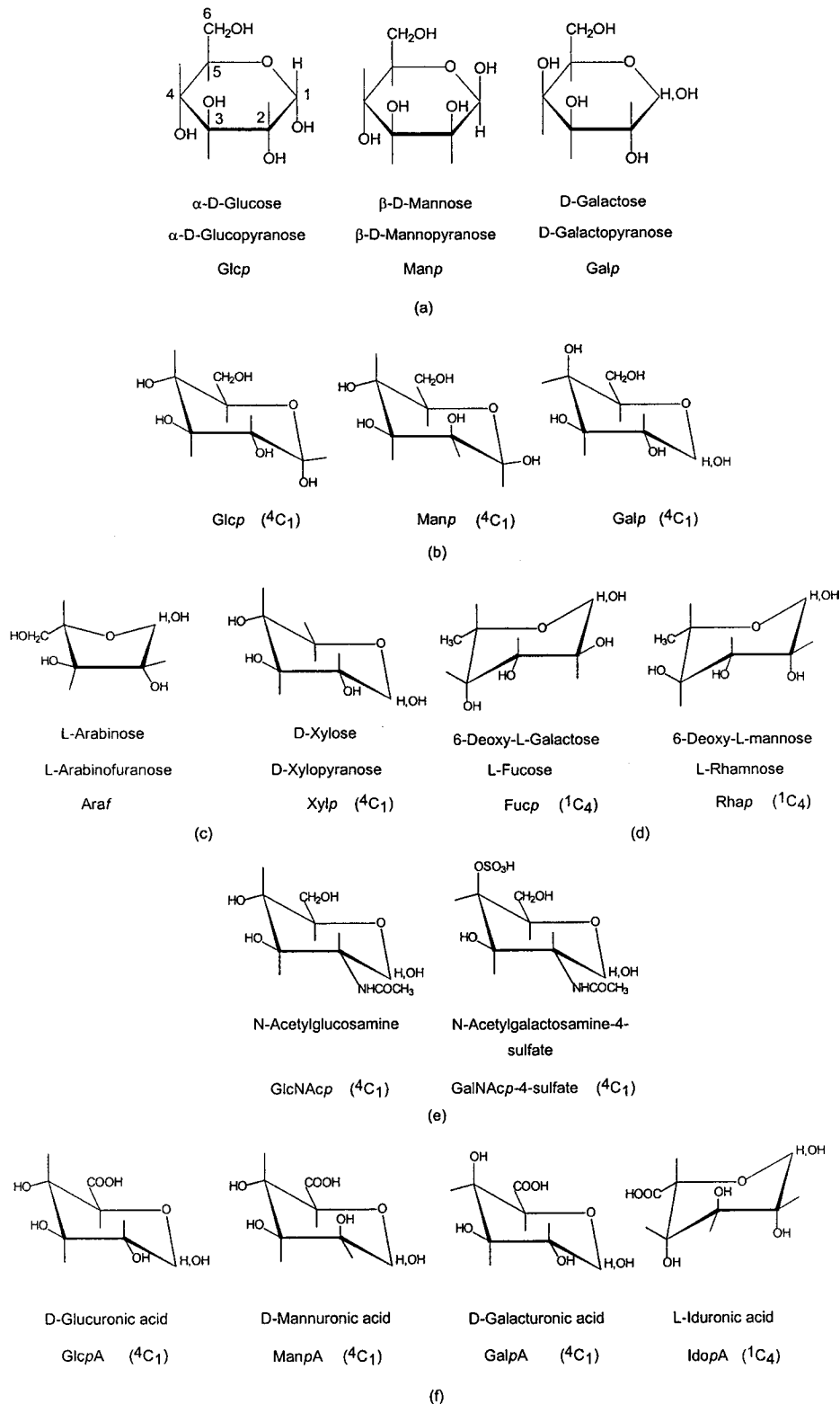


FIGURE 8 Monosaccharides commonly found in polysaccharides: (a) and (b) hexoses, (c) pentoses, (d) deoxy sugars, (e) amino sugar derivatives, and (f) uronic acids. (b)–(f) give a representation of molecular conformation. Note that H, OH at carbon 1 of a ring means either an α - or β -sugar. Common abbreviations of sugar names are given and *p* or *f* after an abbreviated name indicates a pyranose or furanose ring-form, respectively. The numbering of carbon atoms is shown for α -D-glucopyranose.

The product is a disaccharide, in which two monosaccharide residues are linked by a glycosidic bond. In **VI** the reaction has taken place between an α -hydroxyl on carbon 1 of one glucose and a hydroxyl on carbon 4 of the second monosaccharide. The new bond is therefore an α -(1 \rightarrow 4)-glycosidic bond. Reaction can, in fact, take place to link carbon 1 of one sugar through any of the free hydroxyl groups attached to carbons 2, 3, 4, or 6 on a second sugar, for example, glucose in the pyranose ring form, yielding 1 \rightarrow 2, 1 \rightarrow 3, 1 \rightarrow 4, or 1 \rightarrow 6 glycosidic bonds, respectively. In addition, the bond is designated as an α - or β -bond, depending on whether the anomeric hydroxyl of the first sugar lay originally below or above the plane of the monosaccharide ring. Many disaccharides have “trivial” (here maltose) and systematic names. An abbreviated form of the systematic name of maltose is shown. The sugar with the free hydroxyl on carbon 1 (the reducing end) is always written at the right of a disaccharide or polysaccharide, and the other monosaccharide residues are written to the left of it. In the systematic name for a disaccharide or polysaccharide, the name of the left-hand sugar is given first (here we have α -D-Glcp).

Besides the hydroxyl on carbon 1 of the right hand sugar, there are seven other hydroxyl groups which could, in theory, react with the carbon 1 hydroxyl of a third monosaccharide to give a trisaccharide. Thus a variety of different products can be formed. Two possibilities are shown in **Fig. 9**. In **Fig. 9a**, the third glucose residue is attached to the left-hand monosaccharide of **VI** to give a linear trisaccharide. Both glycosidic bonds in this product are α -bonds. The third glucose in **Fig. 9b**, however, is attached to the right-hand glucose of **VI** to yield a branched trisaccharide. The OH on carbon 1 of ring C was originally in the β -position (above the ring) and has given rise to a β -glycosidic link. Abbreviated names of the trisaccharides are given and forms like these are used to indicate polysaccharide structure.

Further monosaccharides could be linked by glycosidic bonds to the trisaccharides shown in **Fig. 9** to give larger molecules. Substances consisting of several monosaccharide residues (e.g., ten) joined by glycosidic bonds are oligosaccharides; polysaccharides consist of chains of very many linked monosaccharide residues, but again there is no formal definition of the distinction in size between a large oligosaccharide molecule and a small polysaccharide.

Polysaccharides differ from one another in the nature of the monosaccharide residues, the distribution of such residues along the chains, the types of glycosidic bonds

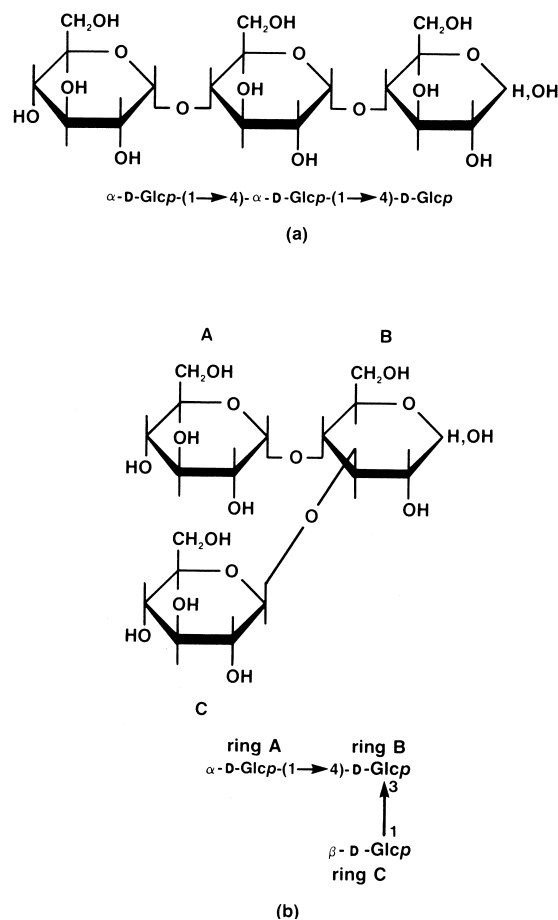


FIGURE 9 Two possible trisaccharides formed from D-glucopyranose. (a) An α -linked linear trisaccharide (b) A branched trisaccharide containing an α - and a β -glycosidic link.

(whether α or β), the linkage positions (e.g., whether 1 \rightarrow 4 or 1 \rightarrow 3 as in **Fig. 9b**), and in whether they are linear or branched. Branches may be one or several monosaccharide residues long or may themselves be branched.

At one end of almost all polysaccharide molecules, there is a monosaccharide residue with a free hydroxyl group at carbon 1. This is known as the reducing end of the molecule. For a linear chain molecule, the other end is the nonreducing end. Branched molecules can have several nonreducing ends, one for each branch. In **Fig. 9b**, for example, ring B forms the reducing end, while rings A and C are nonreducing ends of the molecule.

Unlike proteins, the molecules in a sample of one polysaccharide are not necessarily identical in size or even composition. Simple polysaccharides have linear chains made from one type of monomer; the polymer molecules, however, may be of different lengths. More complex polysaccharides can have branched molecules containing five or more different kinds of monomer residue.

Within a sample of a complex polysaccharide there can be molecules differing in length and distribution of branches, and in distribution and number of each kind of monomer residue. Because of this heterogeneity it has been more difficult to study the three-dimensional structure of polysaccharides, for conventional investigations require crystals made of large numbers of identical molecules.

The kinds of glycosidic bonds and linkage positions as well as the nature of the monosaccharide residues can have a profound effect on the shape of the polysaccharide molecules of which they are part. Polysaccharide chains fold, for the most part, by rotation about the C—O and O—C bonds of the interunit linkage. Free rotation is restricted, however, by the need for any large groups attached to the monosaccharide rings to keep as far apart as possible. In polysaccharides where monosaccharide residues give a regular repeating structure, only a small number of chain conformations are likely, and some polysaccharide chains are most stable with a secondary structure of extended ribbons, while others can coil up to give helices. A chain of β -(1 \rightarrow 4)-linked D-glucopyranose residues, for example, readily takes up an extended ribbon-like shape while a chain of α -(1 \rightarrow 4)-linked D-glucopyranoses can form a helix. The extended chains and helices can be stabilized by intrachain hydrogen bonding involving OH groups of the sugar residues. Bundles of extended chains can be held together by interchain hydrogen bonding, and helices can consist of one or more chains and also pack together in a regular way (Fig. 10). These organized

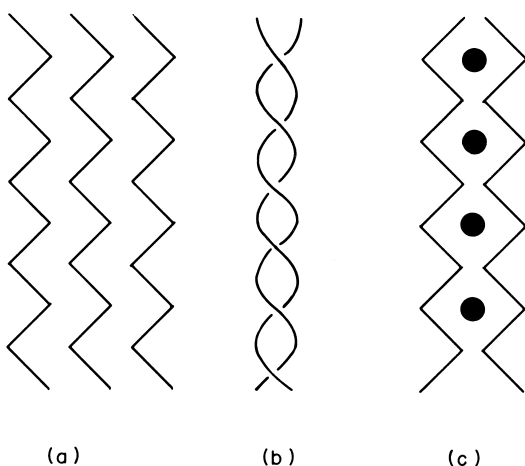


FIGURE 10 Stabilization of individual chain conformational preferences through interchain associations. (a) Extended ribbons in parallel or antiparallel alignment; (b) multiple helices as in amylose double helices or triple helices elsewhere; and (c) “egg box” model with anionic carboxyl groups cross-linked by divalent cations (●) with further coordination from hydroxyl groups (see Fig. 14). [From Aspinall, G. O. “Polysaccharides” in the Encyclopedia of Physical Science and Technology, Vol. 11, p. 176. Copyright 1987 by Academic Press, Inc., New York.]

structures can exclude water from the neighborhood of the sugar hydroxyl groups and render the polysaccharides insoluble.

When structures are not so regular, however, polysaccharides may be able to form gels, characterized by an open network that is stabilized by so-called junction zones, and where the open spaces are filled by solvent molecules. Such structures can be fairly rigid while containing as little as 1% polysaccharide. The junction zones are formed by close association of polysaccharide chain segments having a regular repeating structure, but are interrupted by segments of irregular structure. If a single polysaccharide molecule possesses more than one stretch of chain with structural regularity, each regular section can participate in a junction zone involving different molecules, thus generating a network where the junction zones are separated by segments of nonassociating chains of irregular structure.

Chain associations may be of the types indicated in Figure 10, i.e., extended chains held together by hydrogen bonding (Fig. 10a), chains wound round each other in multiple helices (Fig. 10b), or chains containing ionized acid groups may associate by electrostatic attraction of divalent cations such as Ca^{2+} to the negatively charged polysaccharide (Fig. 10c). The latter is called the “egg box” model for formation of pectate and alginate gels.

Junction zones may be interrupted by insertion of a different monosaccharide unit in the main chain, causing a kink in the structure, or alteration to an existing sugar residue so that the ring conformation changes, or changes to substituents on an existing monosaccharide, also causing a ring conformational change.

2. Classification

Whereas it is relatively easy to describe different proteins in terms of their functions, this becomes more complicated for polysaccharides. Some polysaccharides seem to fulfill both structural and reserve roles, for example. It is more convenient, therefore, to consider polysaccharides in groups based on structure; based, in fact, on the nature of the monosaccharide residues making up the main polymer chain.

Polysaccharides can then be classified according to structure and systematic names are given, depending on monosaccharide composition. In some cases, however, a trivial name is used, particularly for very complex polysaccharides, where the name preceded knowledge of structure. Homoglycans are composed of one kind of monosaccharide only; thus glucans consist of chains of glucose residues, while xylans contain xylose only. They may be linear, with one or more linkage type.

TABLE II Examples of Linear and Branched Homo- and Heteroglycans

Type	Common name	Monosaccharide sequence
Homoglycans		
Linear, one linkage type	Amylose	$\rightarrow 4)\text{-}\alpha\text{-D-Glc } p\text{-}(1 \rightarrow 4)\text{-}\alpha\text{-D-Glc } p\text{-}(1 \rightarrow$
	Cellulose	$\rightarrow 4)\text{-}\beta\text{-D-Glc } p\text{-}(1 \rightarrow 4)\text{-}\beta\text{-D-Glc } p\text{-}(1 \rightarrow$
Linear, more than one linkage type	Cereal β -glucan	$\rightarrow 3)\text{-}\beta\text{-D-Glc } p\text{-}(1 \rightarrow 4)\text{-}\beta\text{-D-Glc } p\text{-}(1 \rightarrow$
Branched	Amylopectin	$\rightarrow 4)\text{-}\alpha\text{-D-Glc } p\text{-}(1 \rightarrow 4)\text{-}\alpha\text{-D-Glc } p\text{-}(1 \rightarrow$ \uparrow 6 $\rightarrow 4)\text{-}\alpha\text{-D-Glc } p\text{-}1$
Heteroglycans		
Linear, one linkage type	Glucmannans	$\rightarrow 4)\text{-}\beta\text{-D-Man } p\text{-}(1 \rightarrow 4)\text{-}\beta\text{-D-Man } p\text{-}(1 \rightarrow 4)\text{-}\beta\text{-D-Glc } p\text{-}(1 \rightarrow$
Linear, more than one linkage type	Hyaluronic acid	$\rightarrow 4)\text{-}\beta\text{-D-Glc } pA\text{-}(1 \rightarrow 3)\text{-}\beta\text{-D-Glc } pNAC\text{-}(1 \rightarrow$
Branched	Galactomannan	$\rightarrow 4)\text{-}\beta\text{-D-Man } p\text{-}(1 \rightarrow 4)\text{-}\beta\text{-D-Man } p\text{-}(1 \rightarrow$ \uparrow 6 $\alpha\text{-D-Gal } p\text{-}1$

Typical examples (Table II) of the first group would be amylose or cellulose, containing only (1 \rightarrow 4)-glycosidic bonds, and of the second group, cereal β -glucans with both β -(1 \rightarrow 3) and β -(1 \rightarrow 4)-bonds. The most complex homoglycans are branched, as is the case for amylopectin, also a glucan. Heteroglycans contain at least two kinds of sugar unit, and the systematic name reflects the monomer composition. Again, the polysaccharide molecules may be linear, with one or more linkage type, or branched. Examples of linear heteroglycans (Table II) are glucmannans where glucose and mannose residues are linked by β -(1 \rightarrow 4)-bonds and hyaluronic acid (here a trivial name is commonly used) containing glucuronic acid and *N*-acetyl glucosamine joined by β -(1 \rightarrow 3)- and β -(1 \rightarrow 4)-linkages. Branched heteroglycans can be much more complex, with one or more type of monosaccharide in the main chain and yet other sugars in the branches, as is the case for plant pectins. With this degree of complexity, systematic nomenclature becomes difficult.

The functions and uses of the most widely studied and commercially important polysaccharides are described below, grouped according to source.

3. Plant Polysaccharides

Cellulose and starch are undoubtedly the plant polysaccharides of greatest importance, both in abundance and economic impact. Both are homopolymers of D-glucose, i.e., glucans.

Cellulose is the most abundant biopolymer and is the main structural material of the cell walls of higher plants. It has been estimated that there are approximately 10^{12} t

of cellulose present on the earth at any one time. Some plant fibers, such as ramie, hemp, jute, and notably cotton seed hairs, contain from 60% to over 90% cellulose and can be used with minimum processing as textile fiber. In wood, however, cellulose exists in close association with hemicelluloses and lignin (Section II.D) and harsh chemical treatments must be used to obtain cellulose, mainly for paper making.

Cellulose molecules are unbranched chains of β -(1 \rightarrow 4)-linked glucopyranose units up to 5000 residues long and are essentially rigid and extended. Individual β -D-glucopyranose units adopt the 4C_1 chair conformation. Within one molecule, the ribbon-like shape is stabilized by hydrogen bonding between the ring oxygen of one glucose unit and the OH on carbon three of the adjacent monomer residue, and also between the oxygen on carbon six of the first glucose and the OH on carbon two of the adjacent residue. Cellulose molecules can align themselves side by side, with adjacent chains running in the same direction; these sheets are stabilized by hydrogen bonds between the OH on carbon six of glucose on one molecule and the oxygen on carbon three of the closest glucose residue on an adjacent molecule. This structure is found in native, untreated cellulose and is called cellulose I. The forces between sheets are van der Waals forces, but the sheets associate to form microfibrils. These in turn aggregate to give fibers, which, in association with other polysaccharides and proteins, are the main structural components of plant cell walls. Cellulose II is a form of cellulose obtained by chemical treatment with, for example, alkali. Here chains run antiparallel to one another and intermolecular hydrogen bonding differs from that in cellulose I. Where structure is well-ordered,

as in cellulose I and II, crystallites can form, but samples of cellulose also contain amorphous regions where chain packing is less regular. Chemical modification of cellulose takes place more easily in these amorphous regions.

The cellulose derivatives of greatest commercial importance are regenerated cellulose, and cellulose ethers and esters. Regenerated cellulose can be prepared by acidifying cellulose solutions in cuprammonium hydroxide or alkaline solutions of cellulose xanthate, and by removal of ester groupings from cellulose esters in organic solvents. The regenerated cellulose can be spun as fibers for textiles, e.g., rayon, or cast as films such as cellophane which is used for packaging.

Paper consists of a network of tangled cellulose fibers and is made mainly from wood chips treated with alkali or sulfur dioxide in bisulfite solution to remove most of the noncellulosic constituents. Cellulose and cellulose derivatives are used to make textiles and plastics, and as thickeners and stabilizers. A variety of useful cellulose ethers are known, varying in degree of substitution and nature of substituents, and one of the most important is carboxymethyl cellulose. Since it is considered safe for human consumption and is not degraded in or absorbed by the human digestive tract, it is used in foodstuffs and pharmaceuticals. In laboratories it has become important in modern techniques for purifying proteins. Cellulose acetates and nitrates are probably the most useful esters. The acetates can be spun into fibers and used in textiles, but in bulk form the acetates are good thermoplastics. Cellulose trinitrate was first used as an explosive; nitrates are now used as membranes and protective coatings and can be cast as films (celluloid). Much interest is being shown in the possible utilization of glucose, resulting from cellulose hydrolysis, as a feedstock for chemical manufacture, to reduce reliance on petroleum as the major source of raw material for chemical industry.

Starch is probably the second most abundant carbohydrate polymer, and is an energy-reserve material of higher plants and some algae. It is granular in form and insoluble in cold water, and is a major constituent of cereal grains, potatoes, peas, and beans. Starch is generally considered to consist of two glucan components, amylose and amylopectin, with 15–30% of “normal” starches being made up of amylose. Genetic variants of plants such as maize can produce starches with no amylose or greater than 30% of this polysaccharide. Amylose molecules are mainly linear chains of α -(1 \rightarrow 4)-linked D-glucopyranose residues while amylopectin has a highly branched structure made up of chains of α -(1 \rightarrow 4)-linked glucose units joined by α -(1 \rightarrow 6) bonds. About 4% of the residues of amylopectin occur as branch points, while a small number

of branch points (<0.5%) can be found in some amylose molecules. Amylose can adopt a helical conformation, the ring conformations being stabilized by intramolecular hydrogen bonding between the OH on carbon 2 of a glucose residue and oxygen on carbon 3 of the adjacent glucose unit. Amylopectin probably has a structure where chains are arranged in clusters (Fig. 11), with the longer α -(1 \rightarrow 4)-linked glucose chains taking up double helical conformations. The (1 \rightarrow 6) bonds are more flexible than (1 \rightarrow 4) links, and this allows the amylopectin molecules to open up and give access to starch-degrading enzymes. The action of such enzymes is necessary when energy (in the form of glucose) is required by the plant. Amylose molecules in solution have a tendency to aggregate side by side and become insoluble. This phenomenon is known as retrogradation and is important in the staling of baked products. At high temperatures (>80°C) starch gives viscous solutions in water and, on cooling, forms a gel.

Starch is a natural energy source in the human diet. Because of this and its ability to form gels and highly viscous solutions, it is widely used in the food industry, as a

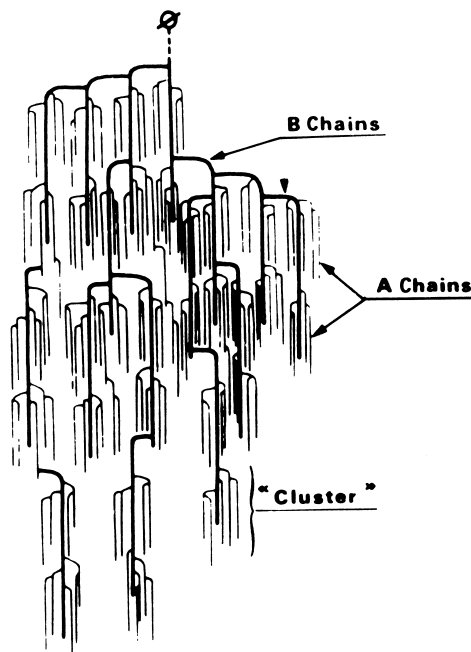


FIGURE 11 Cluster model for amylopectin wherein unbranched A-chains are attached through branch points to B-chains. Longer chain segments in clusters permit the formation of helical domains analogous to those in amylose. \emptyset = single reducing unit per molecule. [Modified with permission from Robin, J. P., Mercier, C., Duprat, F., Charbonniere, R., and Guilbot, A. (1975). *Die Starke* 27, 36–45. Copyright 1975 by Verlag Chemie, Weinheim. From Aspinall, G. O. “Polysaccharides” in the *Encyclopedia of Physical Science and Technology*, Vol. 11, p. 178. Copyright 1987 by Academic Press, Inc., New York.]

thickener or gelling agent in soups and desserts. Starch is broken down, mostly in the small intestine, to oligosaccharides and ultimately glucose. The most important enzymes involved in this hydrolysis are α -amylases (also found in plants and microorganisms) that bring about mainly random scission of α -(1 \rightarrow 4)-glucosidic bonds to yield oligosaccharides. Other enzymes then catalyze further hydrolysis to glucose. Some starch, particularly after heating and cooling of foodstuffs, is more resistant to attack and reaches the large intestine where it is fermented by the resident bacteria. This "resistant starch" is now believed to play a part in prevention of some bowel diseases and may contribute to lowering of blood cholesterol levels. Starch and starch derivatives are used in the textile and laundry industries—in the first as a warp size to strengthen the yarn or as a finish to give a polish to thread, in the second to stiffen clothing and some household linens. Starch products are important in the paper industry for strengthening the paper and improving the surface quality. Starch dextrins, prepared by heating dry starch, are widely used as adhesives on labels, envelopes, postage stamps, etc., while minor outlets for starch are the oil industry (in drilling muds), ore refining (as a flocculating agent), smelting (as a binder in refineries), and biodegradable plastics.

The production of alcohol for human consumption is based on the enzymic degradation of starch to glucose, followed by conversion of the glucose into ethyl alcohol. Alcohol for use as a fuel can also be made in this way.

Glucose and partially hydrolyzed starches (glucose syrups) are made by enzymic and/or acid hydrolysis and find wide use in the food and confectionery industries. Glucose is also used in pharmacy and medicine as an instant energy source. High fructose syrups, on a weight basis sweeter than glucose syrups, are produced commercially from glucose solutions by passage over an immobilized enzyme, glucose isomerase. The possibility of using glucose, from starch hydrolysis, as a feedstock for biodegradable polyester production is currently under investigation (Section D). Further, the incorporation of starch polysaccharides into nonbiodegradable plastics, to improve their rate of break-down in the environment, is also being studied.

In addition to cellulose, other polymers of β -linked glucose units exist; these are the β -glucans. Some, from microorganisms and seaweeds, contain mostly (1 \rightarrow 3) interunit links and seem to be food-reserve polysaccharides. Others are linear molecules containing (1 \rightarrow 3) and (1 \rightarrow 4) bonds in the ratio 1 : 3 and have a structural role in, for example, endosperm cell walls of barley kernels. Soluble β -glucans of this type can give solutions of high viscosity in water, presumably because of the formation,

by molecular association, of a loose polymer network, although in some cases aggregation of helices may be involved. Some barley β -glucans can thus cause filtration problems in the brewing industry. There is evidence that increased cereal β -glucan in the human diet can play a role in lowering blood cholesterol levels that are considered undesirably high.

Many structural tissues in living organisms appear to be constructed from fibers embedded in an amorphous matrix. In plant cell walls, the fibers are cellulose while the matrix consists of a complex arrangement of proteins and many polysaccharides. Historically, the matrix polysaccharides have been considered either as pectic substances, soluble in hot water or dilute acid solution, or hemicelluloses, soluble in alkali. The nature of the polysaccharides in each group varies with the type of plant under study, and also with the age and kind of tissue and even with the part of the cell wall being investigated.

Pectins are found in the primary cell walls and intercellular spaces in land plants. These polymers confer elasticity on, and hold water in, the cell walls and may be covalently bonded in the plants to arabinogalactans, which have galactose backbones and branches containing arabinose or arabinose and galactose. Pectins occur abundantly in fruits and vegetables, and are extracted commercially from citrus fruit peel, apples, sugar beet, and sunflower heads. They are polysaccharides where the main chains contain galacturonic acid and rhamnose, and side chains contain fucose, xylose, arabinose, and galactose. The structure is very complex. There may be stretches of uninterrupted (1 \rightarrow 4)-linked α -D-galacturonic acid residues and so-called "hairy" regions containing a high proportion of rhamnose in the main chain. The neutral sugars fucose, galactose, arabinose, and xylose are attached as side-chains, mostly on the rhamnose, and may occur as single monosaccharides or be part of long chains, often formed mainly of arabinose. The galacturonic acid units may be acetylated, but the most important feature of pectins is the degree to which these uronic acid residues are present as methyl esters. High-methoxyl pectins, with a high degree of esterification, and low-methoxyl pectins, prepared by longer extraction with acid, have different properties and are both commercially useful. The two types of pectin are capable of forming gels; the high-methoxyl pectin requires a large quantity of added sucrose for gel formation, and so fruit pectins are important in the jam and jelly and confectionery industries. Low-methoxyl pectin, on the other hand, carries a large number of acid groups and the polysaccharide chains cannot associate well unless the negative charges associated with these acid groups are neutralized. These pectins form gels in the presence of calcium ions and are believed to give an "egg box"

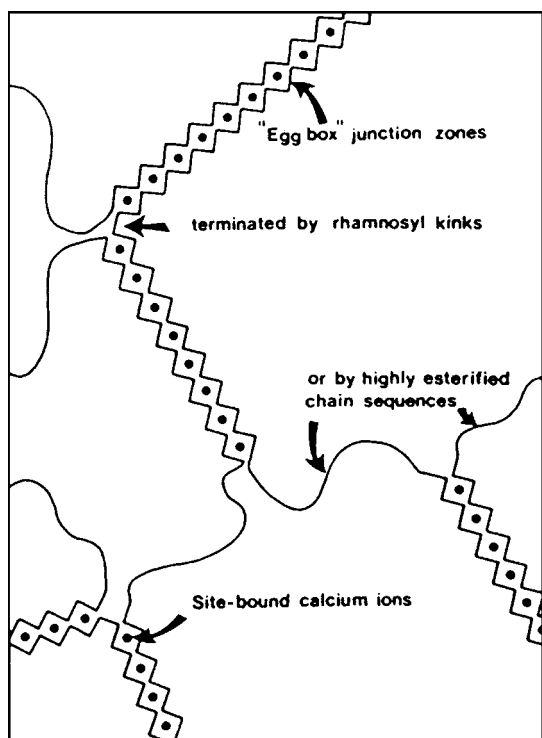


FIGURE 12 Representation of calcium pectate gels with "egg box" model for chain associations of nonesterified α -D-galacturonan regions through calcium ions, interrupted by esterified α -D-galacturonan regions, or terminated by insertion of L-rhamnose residues in the chain. [Adapted with permission from Rees, D. A., Morris, E. R., Thom, D., and Madden, J. K. (1982). In "The Polysaccharides", (G. O. Aspinall, ed.), Vol. 1, p. 265. Copyright 1982 by Academic Press, Inc., New York. From Aspinall, G. O. "Polysaccharides" in the Encyclopedia of Physical Science and Technology, Vol. 11, p. 184. Copyright 1987 by Academic Press, Inc., New York.]

structure where chains associate to form junction zones (see Figs. 10c and 12). Because high sucrose concentrations are not needed for gel formation, low-methoxyl pectins can be used for low-sugar jams and jellies. Enzymic degradation of pectins in cell walls is necessary for the softening of fruit during the ripening process. Apple juices must be clarified by enzymic degradation of pectins in freshly squeezed juice; in contrast the pectin-modifying enzymes of orange juice must be deactivated by storing the juice frozen, in order to maintain the cloudy appearance of the juice.

The polysaccharides generally considered as hemicelluloses have backbones composed of xylose residues, as in the xylans, or glucose units, as in the xyloglucans, or mannose sometimes in combination with glucose, as in the mannans and glucomannans. Few of these are isolated for commercial exploitation.

In many plant cell walls, the major hemicellulose is either arabinoxylan—main chains of xylose with branches of single arabinose residues on some of the xylose rings—or glucuronoarabinoxylans with additional branches of single unsubstituted or modified glucuronic acid residues on some xylose rings.

Xyloglucans may act as food reserves in seeds and have a structural role in mature plants. They probably have extended ribbon-like structures. Xyloglucans have backbone chains of β -(1 \rightarrow 4)-linked glucose residues with xylose units linked α -(1 \rightarrow 6) as branches on some of the glucose rings. Some branches can also contain galactose and fucose residues but there seems to be no regular repeat in the structure. This is a feature of many plant polysaccharides, and the apparent lack of regularity may be necessary for interaction with other proteins and polysaccharides in cell walls which can, as a plant grows, elongate to many times their original size. In addition, arabinoxyloglucans exist in some plants, with arabinose units linked α -(1 \rightarrow 2) to xylose.

Glucomannans and the related galactoglucomannans are important in softwood, and do not have a regular structure but have linear main chains containing, in an apparently random order, both mannose and glucose joined by β -(1 \rightarrow 4)-links. The galactoglucomannans have, in addition, single-residue branches of galactose joined by α -(1 \rightarrow 6)-bonds to some mannose units. Related polysaccharides are the galactomannans which have food reserve and structural functions in plants. These have backbone chains of β -(1 \rightarrow 4)-linked mannose residues, with single-residue branches of galactose joined by α -(1 \rightarrow 6)-bonds to some mannose units. Two of these galactomannans are commercially important. They are guar gum and locust bean (also known as carob) gum, isolated from the endosperm of seeds of the leguminous plants *Cyamopsis tetragonolobus* and *Ceratonia siliqua*, respectively. The guar gum has a higher content of galactose than the locust bean gum and is more water soluble. These galactomannans give high-viscosity solutions in water and so are used as thickening agents in the food industry and in the pharmaceutical industry. In particular, they give good gels with carrageenans, agarose, or xanthan (see next sections) and can be used in ice creams and cheese spreads. The galactose side groups are believed to interrupt junction zones in the gels. Derivatives of locust bean gum are of use in the textile industry as sizes, while guar gum can act as a dye thickener. Guar gum also increases the strength of cellulosic fiber in paper-making.

Matrix polysaccharides, mainly the pectins and hemicelluloses, of plant material, e.g., cereals, fruit, and vegetables, in the human diet are termed dietary fiber, although they may be more gel-like than fibrous. These polymers

are incompletely digested (or not at all) in the small intestine but may be fermented by resident bacteria in the large intestine. It is now believed that such polysaccharides are beneficial to human health in that they seem to contribute to the lowering of blood cholesterol levels and thus help to reduce heart disease. They modulate the absorption of glucose into the bloodstream, and possibly even lower the incidence of bowel cancer.

Some of the most complex polysaccharides known are found in gums that are exuded as a viscous fluid from some plants, often at the site of an injury. The fluid then hardens to a clear nodule consisting mainly of polysaccharide, which may have a protective function to prevent further damage to the plant. The major polysaccharide of gum arabic, for example, has a backbone of galactose residues, to which are attached branches containing arabinose, rhamnose, galactose, and glucuronic acid residues. Gums give highly viscous solutions or gels with water and so are used as thickening agents and binding agents in the food and pharmaceutical industries.

4. Marine Polysaccharides

Whereas in land plants polysaccharide structures often appear irregular, with an apparently random distribution of branches or monomers along a main chain, the structures of some seaweed polysaccharides are based on disaccharide repeats (Fig. 13). Two widely-used types of polysaccharides are obtained from red algae, the Rhodophyceae. These are the carrageenan and agar families of polysaccharide, the structures of both being based on an $-AB-$ repeat where A represents a 3-linked β -D-galactopyranose unit and B a 4-linked α -galactopyranose (Fig. 13). The commercially important κ -carrageenan contains anhydrogalactose residues (the right-hand sugar unit of Fig. 13a) derived from D-galactose. Sulfate groups are attached to galactose residues, and sometimes the regular repeat of β -D-galp-4-sulfate-(1 \rightarrow 4)- α -D-3,6-anhydrogalp-(1 \rightarrow 3) (see Fig. 13a) is interrupted by substitution of D-galactose-6-sulfate (Fig. 13b) for the anhydrogalactose. Chain segments of κ -carrageenan containing the regular repeat readily form double helices; the presence of the less common disaccharide in κ -carrageenan interrupts the helix. Interrupted helices are believed to favor gel formation where a large number of polymer molecules are cross-linked by stretches of helix to form a network. In red seaweed there is an enzyme that can convert the galactose-6-sulfate of κ -carrageenan to anhydrogalactose. This should encourage more helix formation and give greater strength to a gel, and indeed it is found that seaweeds growing where wave action is strong contain more anhydrogalactose, suggesting that the polysaccharide structure is controlled in response to environmental stress.

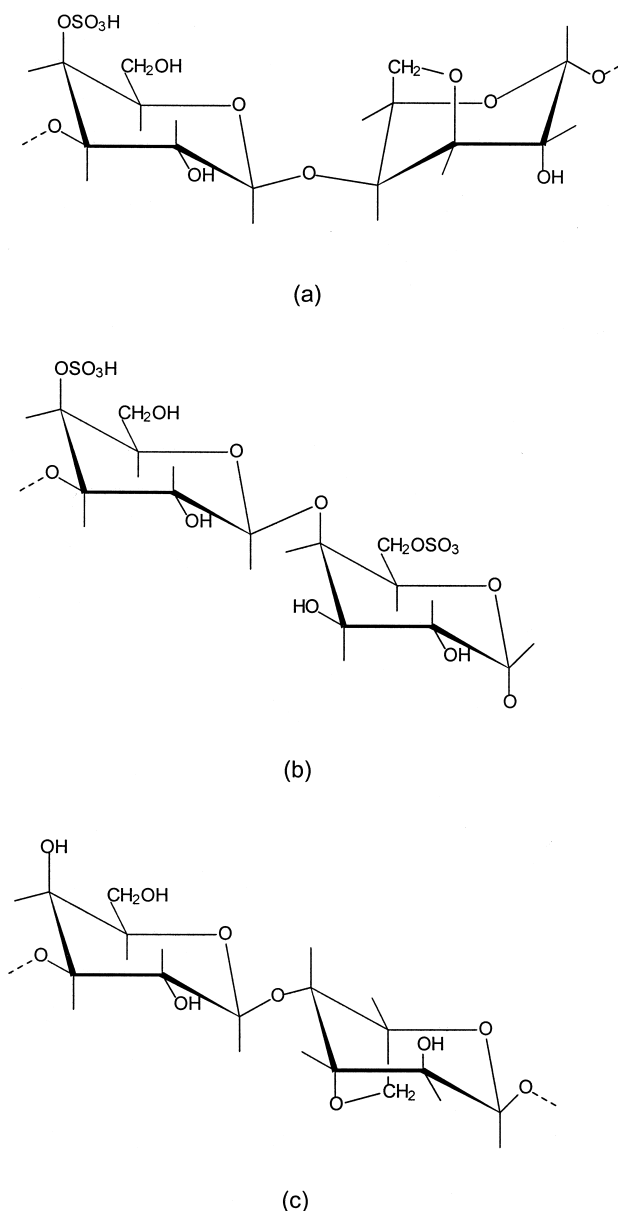


FIGURE 13 Partial structure of seaweed polysaccharides: (a) κ -carrageenan regular repeat, (b) κ -carrageenan, less common disaccharide, and (c) agarose regular repeat.

Agarose, the major component of agar, also contains anhydrogalactose residues, in this case formed from L-galactose (Fig. 13c). Again double helices can form, but the occasional presence of a galactose residue in place of the anhydrogalactose can interrupt the helix, and so agarose gels well.

Because carrageenans and agarose form strong gels, they are widely used in the food industry (e.g., in canned meats, gelled desserts and confectionery). Agarose is used also in laboratories as a molecular sieve like dextrans (Section II.B.5), and agar in gel form provides a good

culture medium for bacteria. Even stronger gels can be obtained in the presence of locust bean galactomannan (Section II.B.3).

Not all seaweed polysaccharides contain disaccharide repeats. Alginic acid, the major skeletal material of brown algae, may well be the marine equivalent of the pectins. It is a (1 → 4)-linked polymer of β -D-mannuronic acid and α -L-guluronic acid (which differs from β -D-mannuronic acid in having a mirror-image arrangement of substituents at carbon 5). The monomer residues are believed to occur in blocks (i.e., a stretch of chain containing one monomer only, followed by a stretch containing the other) as well as in alternating sequences. The guluronic acid blocks are thought to give a regular egg-box structure in the presence of common metal ions such as calcium, while the mannuronic acid blocks are unable to do this (Fig. 14). The regular structures form the cross-links, or so-called junction zones, of stable gels; again this gel-forming ability makes the alginates important in the food industry.

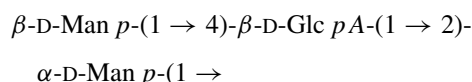
Chitin, while being common in insects and fungi, is extracted primarily from the shells of crustaceans such as crabs and lobsters. It is a linear polymer of (1 → 4)-linked 2-acetamido-2-deoxy- β -D-glucopyranose (*N*-acetyl glucosamine, Fig. 8e) residues and is insoluble in most solvents. It is extracted with dilute acid followed by hot, dilute alkali, and the process brings about deacetylation to give a polysaccharide of low acetyl content known as chitosan. Chitosan, because of the free amino groups on

carbon 2, is positively charged and can associate with negatively charged ions. It is therefore used as a flocculent for waste-water treatment. Chitosan and derivatives such as *N*-carboxymethyl chitosan are good chelating agents and can be used to remove transition metals in water reclamation projects.

5. Microbial Polysaccharides

Dextrans are extracellular polysaccharides synthesized from sucrose by bacteria of species *Leuconostoc*, *Lactobacillus*, and *Streptococcus*. The molecules are branched, usually with main chains of α -(1 → 6)-linked glucopyranose units and branches attached through α -(1 → 2), α -(1 → 3), or α -(1 → 4) bonds. Many different dextrans are found, the structure depending on the strain of bacteria from which they are obtained. Some dextrans are water soluble and again give highly viscous solutions. *Streptococcus* oral bacteria produce dextran which becomes a major component of dental plaque. The polysaccharide holds the bacteria near the tooth surface and traps nutrients required for bacterial metabolism. Sugar cane and sugar beet can become infected by dextran-synthesizing bacteria, and the resultant polysaccharides can interfere with sugar refining by blocking pipelines. On a commercial scale, *Leuconostoc* dextrans have been used as blood plasma extenders, and cross-linked derivatives are useful in modern laboratories as molecular sieves—materials which separate molecules on the basis of size. As such, they play an important part in the laboratory purification of other biopolymers, particularly proteins.

Xanthan is a widely used polysaccharide, produced extracellularly by *Xanthomonas campestris*. The molecules have a cellulose-like backbone of β -(1 → 4)-linked glucose residues, but side chains are attached at carbon 3 of every second glucose residue. The side chains themselves have the structure



The second mannose is usually acetylated at carbon 6 while a proportion of the first mannose units carry a pyruvic acid residue linked to carbons 4 and 6. The polysaccharide is therefore negatively charged, except at low pH, and gives solutions of high viscosity, stable over a wide range of temperature. In addition, the viscosity decreases markedly with high shear, and the polysaccharide is of special importance in drilling muds. Xanthan gum has wide use in the food, pharmaceutical, and cosmetic industries as a thickener and stabilizer of suspensions and emulsions. It forms strong gels with the galactomannans, guar and locust bean gum, and is used in this way in the food industry.

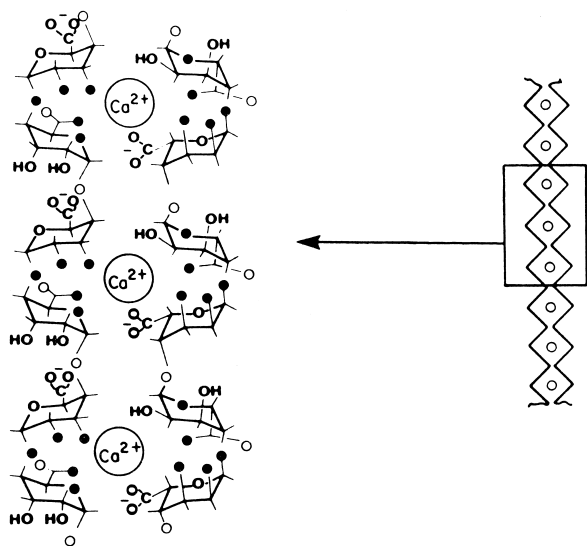


FIGURE 14 “Egg box” model for calcium ion-induced dimerization of α -L-guluronan regions of alginic acid chains. Oxygen atoms involved in cation chelation are represented by filled circles. [Modified with permission from Thom, D., Grant, G. T., Morris, E. R., and Rees, D. A. (1982). *Carbohydr. Res.* **100**, 29–42. Copyright 1980 by Elsevier, Amsterdam. From Aspirall, G. O. “Polysaccharides” in the *Encyclopedia of Physical Science and Technology*, Vol. 11, p. 180. Copyright 1987 by Academic Press, Inc., New York.]

Cell walls of bacteria often contain and may be coated by extremely complex polysaccharides. These polysaccharides seem to be constructed of regular repeats—frequently of four or more sugar units. A great variety of different polysaccharides have been found, some linear, some branched, some containing amino sugars, and others containing uronic acids; the structure depends on the bacterial source. The outer membrane of Gram negative bacteria contains lipopolysaccharide (i.e., polysaccharide chains covalently linked to lipid). Again the polysaccharide is made from regular repeats.

Many of these polysaccharides act as antigens and stimulate the formation of antibodies (see Section II.A.2), if the bacteria invade mammals. It is sometimes possible to confer immunity against one bacterial strain by immunizing a mammal at risk with the bacterial polysaccharide only, without the need for using intact bacteria. This procedure is obviously less hazardous than if whole bacteria were employed.

6. Animal Polysaccharides

Glycogen is a glucan that acts as a short-term energy reserve in animals although it is also found in some bacteria, algae, and fungi. It is much like amylopectin in structure but is more highly branched, with approximately 7% of the glucose residues carrying branches. The compact structure of glycogen allows for efficient storage and fast breakdown by enzymes to glucose when living organisms require energy.

Glycogen metabolism is of medical interest, for individuals are known that lack one or another enzyme important for glycogen synthesis or breakdown. Where an enzyme of glycogen breakdown is missing, the individual is said to have a glycogen storage disease. These genetic diseases are usually serious, and may be fatal, as in Pompe's disease, characterized by lack of one particular glucosidase in subcellular organelles called lysosomes.

Another group of polysaccharides, the glycosaminoglycans, are mostly of animal origin. They all contain modified amino sugars and disaccharide repeats along their linear chains (Fig. 15). Hyaluronic acid is found in skin, connective tissues, and joint fluid, while chondroitin and keratan sulfates occur in cartilage and bone. Chondroitin and dermatan sulfates form part of the structure of skin. All of these, except hyaluronic acid, exist in tissues covalently bonded to protein, that is, as proteoglycans (see Section II.B.7). The polysaccharide molecules may form a network that impedes the flow of water and so may be important for the correct hydration of tissues and in some cases for lubrication and shock absorption in joints. Hyaluronic acid can be used in eye surgery because of

its lubricating and cushioning effects, and direct injection of this polysaccharide can help patients suffering from osteoarthritis.

Heparan sulfate and heparin have backbones based on alternating glucuronic acid and *N*-acetyl glucosamine residues (Fig. 15). In both cases extensive modification of the monosaccharide units takes place after polymer synthesis. The *N*-acetyl group on the glucosamine can be removed and replaced with sulfate; D-glucuronic acid can be converted to L-iduronic acid and sulfate groups can be attached at carbons 3 and/or 6 of the *N*-sulfated glucosamine and at carbon 2 of the iduronic acid. Heparin differs from heparan sulfate in having a higher content of *N*-sulfated glucosamine (>85%) and iduronic acid (>70%). Both heparin and heparan sulfate occur mainly attached to proteins as proteoglycans (see next section). Heparin is used as a blood anticoagulant. A specific pentasaccharide sequence in the polysaccharide binds to a protein, antithrombin, and prevents a series of reactions taking place that would lead to blood clotting.

7. Peptidoglycan, Proteoglycan, and Glycoprotein

Several biopolymers contain both oligopeptide or protein and oligosaccharide or polysaccharide covalently bonded together in their molecules.

Peptidoglycans consist essentially of polysaccharide chains cross-linked by oligopeptides, producing a cage-like arrangement which can be the major structural component of a bacterial cell wall. The polysaccharide chains consist of disaccharide repeats based on glucosamine; one example is shown in Fig. 16a. The structure of the cross-linking peptides depends on the bacterial source, and one example is given in Fig. 16b. In these peptides, D-amino acids can be found, unlike the case of proteins, where only L-amino acids occur. Penicillins are antibacterial agents, because they act as inhibitors of peptidoglycan synthesis, by preventing cross-link formation. Other polymers, the teichoic acids, are found in bacterial cell walls covalently bonded to peptidoglycan through a phosphorylated derivative of the disaccharide shown in Fig. 16a. These acids are linear polymers of glycerol phosphate, $-\text{CH}_2-\text{CHOH}-\text{CH}_2-\text{OPO}_2-\text{O}-$ or ribitol phosphate $-\text{CH}_2-(\text{CHOH})_3-\text{CH}_2-\text{O}-\text{PO}_2-\text{O}-$ and may contain sugar rings as side chains or in the main backbone chain.

Proteoglycans contain protein and polysaccharide in the same molecule. In structural tissues of the fiber and matrix type, proteoglycans frequently occur in the matrix. Thus, in plant cell walls, cellulose fibers are embedded in a matrix which contains, among other polymers, arabinogalactans attached to protein. In animals collagen fibers

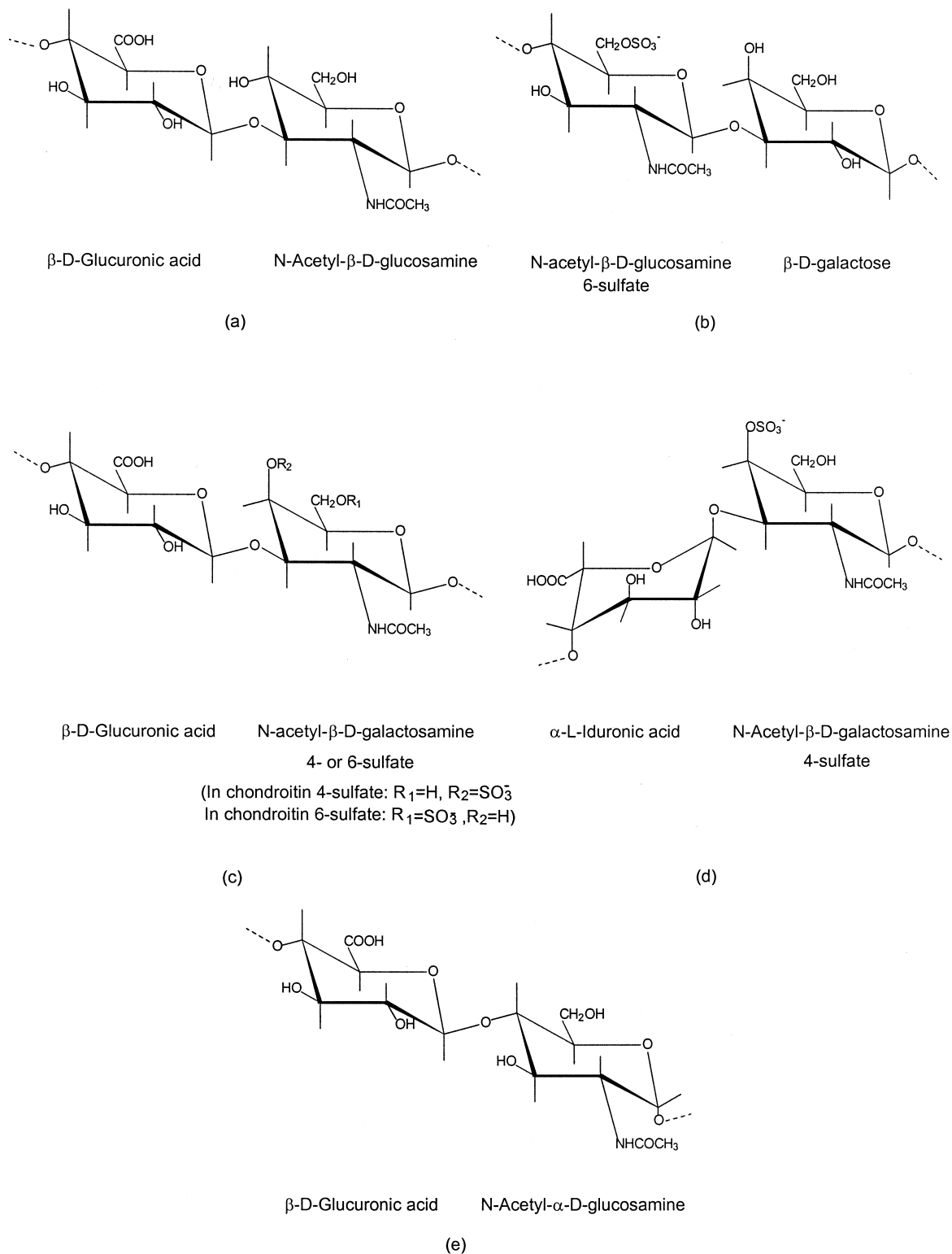


FIGURE 15 Repeating disaccharides of some animal glycosaminoglycans. Repeat of (a) hyaluronic acid, (b) keratan sulfate, (c) chondroitin sulfate, (d) dermatan sulfate, and (e) basic unit of heparan sulfate and heparin.

are found in cartilage, for example, in a matrix containing chondroitin and keratan sulfates attached to a protein core. The protein polysaccharide linkage usually involves the OH group on carbon 1 of the reducing end of the polysaccharide and hydroxyproline, serine, threonine or asparagine residues of proteins. A variety of proteoglycans are known, differing in the nature of the core protein and the number and nature of polysaccharide chains attached to it. In cartilage, several hundred chains of chondroitin sulfate and fewer of keratan sulfate are linked to a core protein called aggrecan. Several of these proteoglycan molecules are, in turn, noncovalently bonded to a single long hyaluronic acid chain. The whole complex is stabilized by the presence of another protein, a link protein. On cell surfaces, heparan sulfate is the main polysaccharide constituent of proteoglycans, and these molecules appear to be involved in cell adhesion and in modulating signals at the cell surface, and are implicated in inflammation and wound repair.

Glycoproteins consist of molecules that are mainly protein with some side branches of mono- or oligosaccharide. They can contain as little as one sugar residue per molecule or several complex chains each of about ten monosaccharide rings. The functions of glycoproteins are as diverse as those of the proteins themselves. Some are enzymes; antibodies are glycoproteins, as are many structural proteins. Indeed collagen contains some galactose and glucose units bonded to hydroxylysine residues of the protein. It is believed that glucose can be involved in cross-links binding collagen molecules together, and that an increase in such cross-links can bring about some of the deleterious effects of aging seen in collagenous tissues. Plant and animal structural tissues often contain glycoproteins in addition to proteoglycans and fibrous polymers. Glycoproteins are common on the outer surface of cell membranes; the oligosaccharides may function as probes with which the cell interacts with its environment. In fact, cancer cells are known to carry altered oligosaccharides on the glycoproteins of their surfaces.

C. Nucleic Acids

Nucleic acids are the basis of heredity—they transmit genetic information from one generation of living organisms to the next. The genetic information specifies, in a code form, the structure of all the proteins in a cell; the proteins, particularly the enzymes, then determine the characteristics of each cell and hence of the complete organism.

For all life forms, except a few viruses, protein structure is encoded in the deoxyribonucleic acids (DNA). These, in complex organisms, are found in cell nuclei, associated with protein in structures known as chromosomes. Other

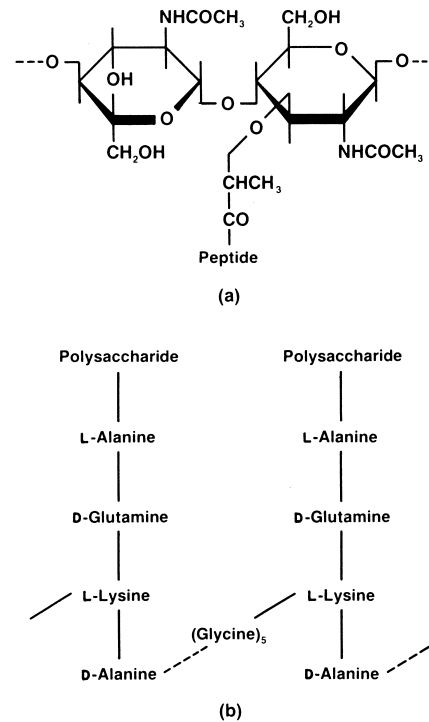


FIGURE 16 Structure of peptidoglycan: (a) repeat disaccharide of polysaccharide, and (b) oligopeptide cross-link.

nucleic acids, the ribonucleic acids (RNA), are involved in protein biosynthesis (i.e., the translation of the code on DNA into protein structure in a cell). Ribonucleic acids can be divided into three major types: messenger (m-) RNA which carries the coded message specifying protein structure from the DNA to the protein-synthesizing "machinery," the ribosomes; ribosomal (r-) RNA, which forms an integral part of those ribosomes, and transfer (t-) RNA, which brings to the ribosomes the amino acids to be incorporated into proteins. Some RNA is now known to have important catalytic properties.

1. Structure

The monomers from which nucleic acids are made are more complex than those of either proteins or polysaccharides. These are nucleoside triphosphates and they can be considered to consist of three parts (Fig. 17)—a triphosphate group, a five-carbon sugar in the furanose ring form, and a cyclic base—that is a ring system with basic properties (which can associate with H^+ in water). Five different bases are commonly found in nucleic acids.

In DNA the sugar is 2-deoxy-D-ribose. In RNA the sugar is D-ribose. From this difference came the names of the two polymers. The common bases are adenine, guanine, cytosine, thymine, and uracil; adenine and guanine are

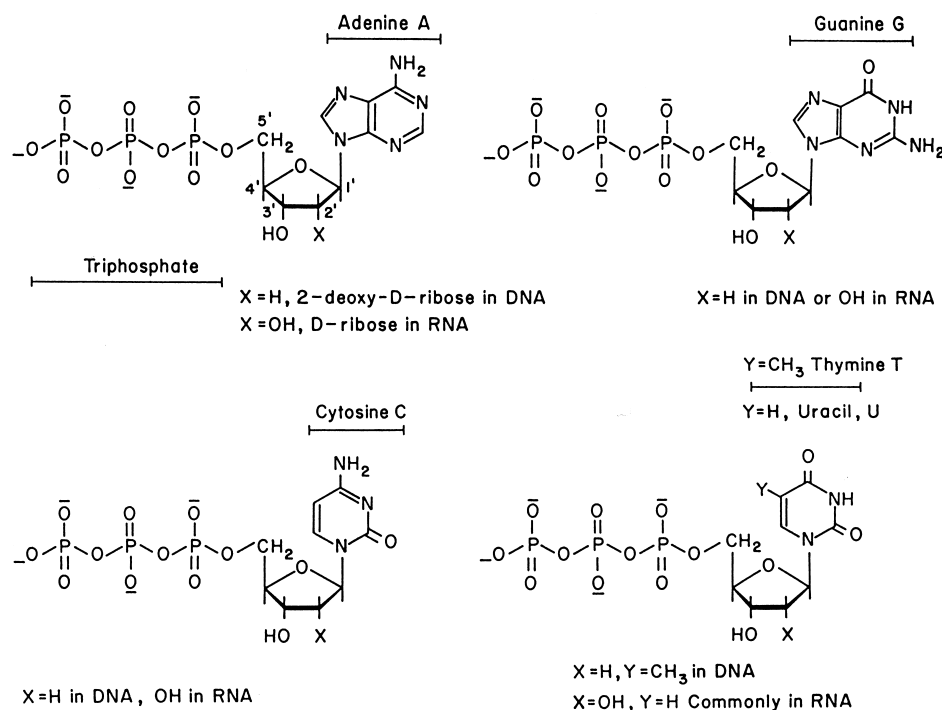


FIGURE 17 Common nucleoside triphosphates from which nucleic acids are made. The numbering system for the carbon atoms of the sugar rings and the initial letters commonly used as abbreviations for the base names are shown.

purines, while the others are pyrimidines. In each type of nucleic acid, DNA or RNA, only four bases occur commonly—in DNA these are guanine, adenine, cytosine, and thymine and in RNA they are guanine, adenine, cytosine, and uracil. Each base becomes attached to a sugar through a β -glycosidic link. Such a combination of sugar plus base is a nucleoside. The triphosphate is linked to carbon 5' of the sugar; nucleoside phosphates such as shown in Fig. 17 are also known as nucleotides.

During nucleic acid synthesis monomers are joined together with elimination of a pyrophosphate (diphosphate) grouping as shown in Fig. 18a. From two nucleotides, a dinucleotide is formed and the new link, a phosphodiester link, connects carbon 3' of one nucleotide sugar to carbon 5' of the next. A third nucleotide can become joined at carbon 3' of the right-hand sugar ring, and the process can continue to give a chain of several linked nucleotides—an oligonucleotide—or a chain of hundreds or even thousands of covalently bonded nucleotides, a polynucleotide (Fig. 18b). Most DNA molecules consist of two polynucleotide chains, while RNA molecules usually contain only one polynucleotide chain.

At one end of a chain the group attached to carbon 5' of the sugar ring is not involved in a phosphodiester link. This is referred to as the 5' end of the chain and by convention is written at the left end of the chain. At the other end,

the grouping on carbon 3' of the sugar is not involved in a phosphodiester linkage; this is the 3' end of the chain and is written on the right (Fig. 18b).

Nucleic acids differ from one another in the lengths of the polynucleotide chains of their molecules and in the sequence of bases along these chains. For any one nucleic acid, however, all the molecules are identical in size and base sequence. Any sequence of bases is possible in a nucleic acid. Abbreviations are often used to represent nucleic acid structure, and the simplest of these involves giving the base sequence of a chain in terms of the initial letters of the base names, starting from the 5' end of the chain; in this convention sugar and phosphate groups are not mentioned. Thus if, in Fig. 18b, Base 1 = guanine, Base 2 = thymine, Base 3 = adenine, and Base n = cytosine, the structure would be represented as GTA...C.

The two polynucleotide chains in DNA molecules are believed to be wound around each other to give a regular secondary structure, a right-handed double helix (Fig. 19). The two chains run in opposite directions with the phosphate and sugar groups on the outside of the helix and the bases in the interior. The proposal for this structure was first made by Watson and Crick and led to their being awarded the Nobel Prize in 1962. Since the bases are flat, they can stack on top of one another in any sequence almost at right angles to the helix axis. The two chains of

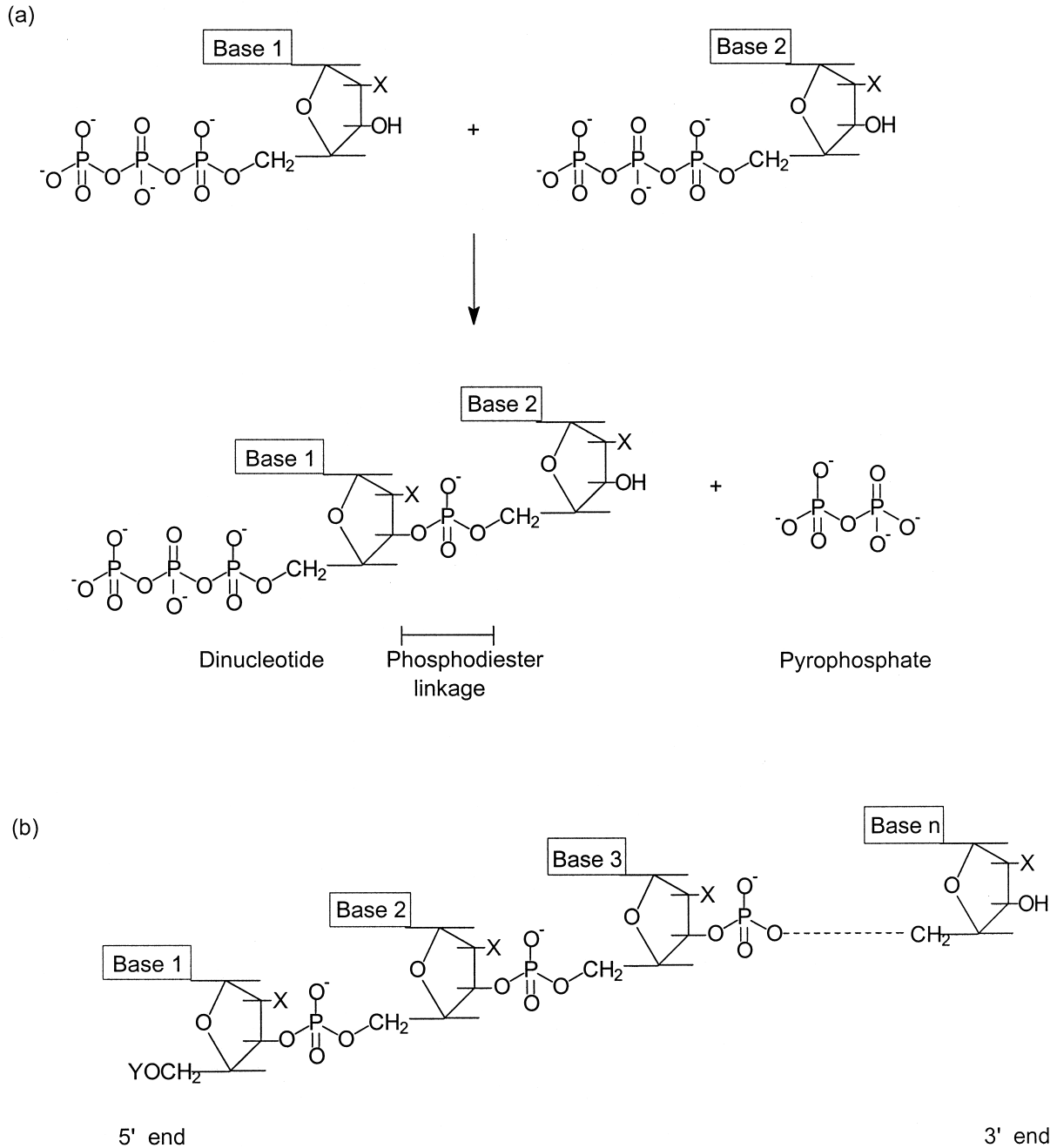


FIGURE 18 (a) Formation of a dinucleotide. (b) The chain structure of a polynucleotide or nucleic acid. X = H in DNA and OH in RNA; Y is often a triphosphate group.

the helix are held together by hydrophobic associations between the stacked bases and also by specific hydrogen bonding between pairs of bases, where one base of a pair is contributed by each chain. In an unstrained structure there are 10 base pairs per complete turn of the helix. The two chains of the helix are always approximately the same distance apart (the helix has a diameter of 20 Å) and

so the base pair must always consist of one double-ring base, a purine (A or G), hydrogen bonded to a single-ring base, a pyrimidine (T or C). This base-pairing is specific; adenine on one chain always bonds to thymine on another, while guanine on one chain bonds to cytosine on the other. The result is that the sequence of bases on one chain determines the sequence on the second chain, if base-pairing is

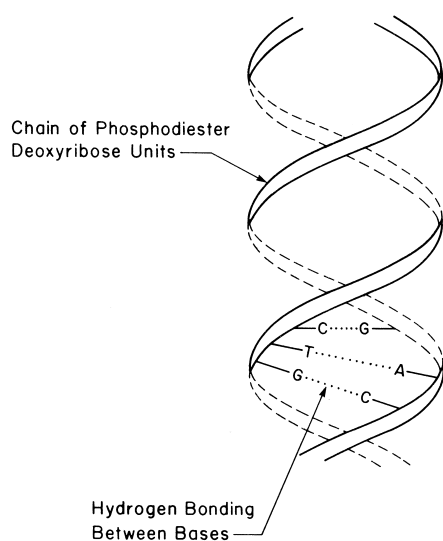


FIGURE 19 The double helix of DNA.

to take place. For example, if the base sequence of a chain segment is . . . ACTAGTC . . . then in the second chain T must bond to A, G to C, etc., and the double helix would have the sequence



VII

The sequences of the two chains are said to be complementary to each other. The helices are not completely regular along their length, but small variations in helix architecture occur with variations in base sequence. These relatively minor changes are important for DNA-protein recognition.

The DNA molecules may be several thousand to over a million nucleotides long, and some segments of the base sequence code for protein structure, while others form control elements. Yet other sequences code for the structures of the r-RNA and t-RNA essential for protein synthesis. The long DNA molecules behave as flexible rods that can coil up if long enough, and in some bacteria the two ends of a molecule can join together to give a closed loop. There is some evidence that, for GC sequences, a stretch of left-handed double helix can form. The importance of this secondary structure of DNA, called Z-DNA, in biological systems is not yet clear.

Except for a few viral ribonucleic acids, all RNA molecules are single-stranded. The polynucleotide chains can fold up on themselves, and if base sequences of two stretches of a chain are complementary, a stretch of right-handed double helix, similar to a DNA double helix, can

form. In an RNA double helix, there are approximately eleven base pairs per turn of the helix, and uracil, instead of the thymine of DNA, base-pairs with adenine. The single polynucleotide chains are folded to give short stretches of double helix separated by single-stranded nonhelical segments.

The secondary structures (helices) and tertiary structures (overall chain folding) of RNA are not uniform and differ with the type of RNA. The chain folding is often complex, involving short helices, loops, and even 3- or 4-way junctions of single-stranded chain. Messenger RNA molecules carry in their base sequences the information specifying protein amino acid sequence. There is one messenger for each protein, and so m-RNA molecules vary greatly in length and sequence; hence they differ in secondary and tertiary structure. Ribosomal ribonucleic acids form part of the structures known as ribosomes, where protein synthesis takes place in a living cell. In simple bacteria, each ribosome contains three sizes of r-RNA, designated 5s, 16s, and 23s RNA. (The numbers 5s, 16s, and 23s relate to the speed of movement of the RNA molecules through a solution spinning in a high speed centrifuge, and depend on the size of the RNA molecules). These molecules are typically 120, 1500, and 2900 nucleotides long, respectively. The base sequences of many r-RNAs are known, and segments of complementary base sequence have been observed, so that double helix formation is believed to occur within the ribosome. Transfer RNAs, which bring the amino acids to the sites of protein synthesis, are the smallest ribonucleic acids, being on average about 80 nucleotides long. The base sequences of many t-RNAs have been studied and it has been found that they contain many "unusual" bases, (i.e., bases other than A, G, U, and C). For example, thymine, a "normal" constituent of DNA, is found in t-RNA. All the t-RNAs examined so far have segments of complementary base sequence which can make up four short segments of double helix. Each t-RNA is specific for one amino acid, and so many t-RNAs exist, differing in the number and sequence of nucleotides. Despite this, it is believed all t-RNA molecules have approximately the same overall chain folding (i.e., tertiary structure) shown in Fig. 20. Unusual base pairs (e.g., G-U pairs) are found in this structure as well as base triplets (i.e., three bases held together by hydrogen bonding).

2. Function

The nucleic acids are all involved, directly or indirectly, in protein synthesis. DNA is essentially the "blueprint" for protein structure, but it does not participate in the biosynthesis of protein. In addition, however, it carries control elements which determine how much, if any, of

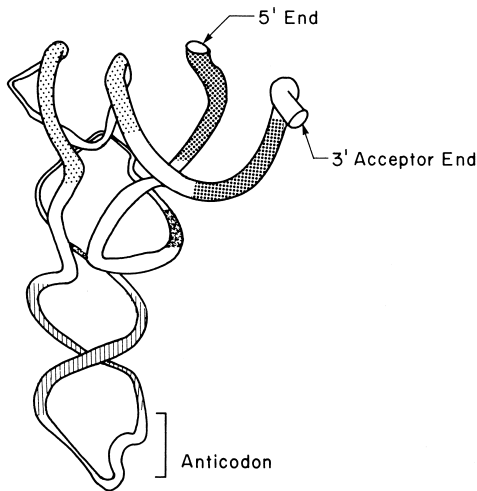


FIGURE 20 Tertiary structure of a t-RNA. The four short double helical segments are shown shaded. [Adapted with permission from Rich, A., and RajBhandary, U. L. (1976) *Annu. Rev. Biochem.* **45**, 805–860. Copyright 1976 Annual Reviews Inc.]

one protein is made in a cell at a particular time. The m-, r-, and t-RNA, in contrast, are all directly involved in the process whereby amino acids become joined together in the correct sequences.

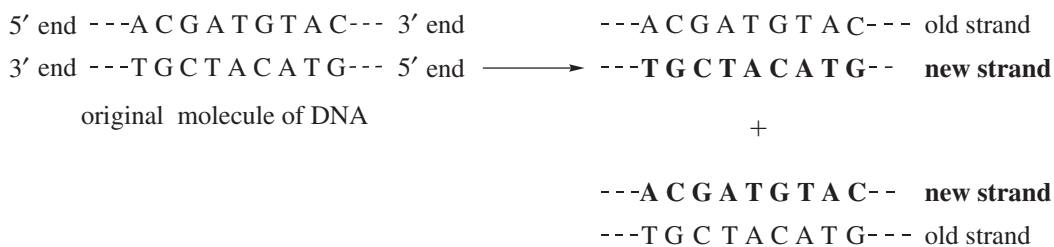
In higher organisms, most DNA is found in structures called chromosomes in the cell nuclei. The DNA functions as genetic material and is passed on from parent to offspring. As the offspring develop from single cells to multicelled organisms, by division of the original cells, each new cell usually contains DNA identical to that of the first cell. This is accomplished by a process called replication, where the two strands of an original DNA double helix separate and two new strands are synthesized, each with sequence complementary to one of the original strands, as in **VIII**.

The process is a complex one, for the original helix must be unwound and its two strands separated. Each “old” strand is used as a pattern or template for synthesis of a new strand. Enzymes, called DNA polymerases,

link together nucleoside triphosphates as shown in **Fig. 18**, ensuring that deoxyribonucleotides are incorporated with bases in the correct sequence for pairing with bases in the template strand. DNA polymerases cannot begin new strands, but rather lengthen strands that begin with a short stretch of RNA “primer” of base sequence complementary to a stretch of the DNA template strand. Each new DNA chain grows in the 5' to 3' direction, and, particularly for the new strand complementary to the upper left strand in **VIII**, is synthesized in segments. Later the RNA primers are removed and replaced with DNA segments, and the pieces of DNA making up one new strand are joined together by another enzyme, a ligase. The net result is that two new DNA molecules are formed, each identical in sequence to the one original molecule, as in **VIII**.

Although almost all DNA of a complex organism is located in cell nuclei, most protein synthesis takes place outside the nuclei. A messenger molecule, m-RNA, is necessary to carry the coded instructions from the DNA to the sites for protein biosynthesis. Since it is the base sequence of the DNA which carries these instructions, the base sequence of the m-RNA must be closely related to that of the DNA. This is ensured by a process known as transcription, whereby the m-RNA is synthesized in much the same way as a new DNA strand by using a DNA chain as template.

A section of DNA specifying one trait of an organism is a gene, and each gene codes for one protein or a group of related proteins. When an m-RNA molecule is formed, a segment of DNA must be unwound and one of the DNA chains is used as a template to specify the base sequence of the new RNA. An enzyme, RNA polymerase, links together ribonucleoside triphosphates with the elimination of pyrophosphate as in **Fig. 18a**, and the new chain grows in the 5' to 3' direction. Nucleotides are incorporated into the chain so that the bases pair with those in the template. This ensures that the base sequence of the m-RNA is complementary to that of the template DNA strand, as in **IX**. Uracil is incorporated into RNA to pair with adenine, instead of the thymine in a DNA strand:



VIII

3' end ---GCAC TAG--- 5' end DNA template
 5' end ---CGUGAUC--- 3' end new RNA strand

IX

A short stretch of RNA-DNA double helix forms between the new RNA and the DNA template, but this quickly dissociates. The “used” template strand then reforms a double helix with its original partner strand of the DNA molecule. (In a similar way, an RNA polymerase makes the short primers for DNA synthesis.)

The enzyme RNA polymerase, often with the aid of other proteins, recognizes sequences on the DNA which are the “start” and “stop” signals for synthesis of a particular m-RNA, so that messenger of the correct length is made. In higher organisms, the m-RNA usually carries the information specifying the structure of a single protein.

The other types of RNA, both ribosomal and transfer, are synthesized in the same way by using different stretches of the DNA as template. After transcription (i.e., RNA biosynthesis) the primary products are processed before being used to determine protein structure. Nucleotides are often trimmed off the 5' and 3' ends of the RNA, a special nucleotide “cap” is added to the 5'-end, and a stretch of adjacent adenine nucleotides is added to the 3' end of most m-RNA of higher organisms. Segments can be cut out of the interior of m-, r-, and t-RNA molecules. These stretches, called introns, are excised at specific base sequences, and the remaining sections, called exons in m-RNA, are joined together. For some RNA molecules, the introns are self-splicing, i.e., catalyze their own removal and joining together of the ends of the remaining stretches of RNA. These catalytic RNA segments are known as ribozymes. After intron removal bases can be modified, particularly in r- and t-RNA.

In the case of some m-RNA, different introns may be removed from the primary RNA produced by transcription (the transcript) to give different m-RNA molecules and hence different proteins from one transcript. This is one way in which a wide diversity of antibodies can be formed in the human body from a relatively small number of genes.

For protein synthesis to take place, the completed messenger RNA must now move to the ribosomes. Ribosomes are roughly spherical particles consisting of r-RNA and several proteins, but their size and composition depend on the source. Most bacteria contain ribosomes having a particle weight of 2.5×10^6 Da, but the ribosomes of the cell cytoplasm of higher organisms are larger. Bacterial ribosomes are made of two subunits, the 30s and 50s subunits. (Again these numbers refer to the speed of movement of the subunits through a solution spinning in a high-speed centrifuge and are related to subunit size.) The 30s subunit

contains one molecule of 16s RNA and 21 different proteins, while the larger subunit consists of one molecule of each of the 5s and 23s RNA and 32 different proteins. The ribosomes of higher organism cell cytoplasm have larger subunits, larger RNA molecules, one extra RNA molecule, and more proteins, but carry out the same function as bacterial ribosomes.

The initial step in protein biosynthesis is the binding of the smaller ribosomal subunit (30s in bacteria) to an m-RNA molecule at a specific base sequence on the m-RNA. This sequence is close to the start of the “message” coding for protein structure and is recognized by a complementary base sequence on the 16s RNA of the ribosome. In higher organisms, the “cap” at the 5' end of the m-RNA is recognized by the smaller subunit of the ribosome.

The base sequence of the m-RNA determines the amino acid sequence of the protein to be synthesized; in fact, a sequence of three bases, a unit called a codon, specifies one amino acid. From four different bases, A, G, C, and U, 64 different triplet codons can be made, but only 20 amino acids become incorporated into proteins. Hence many amino acids have more than one codon. The so-called genetic code (i.e., the base sequences coding for each amino acid) was first investigated in bacteria but is believed to be almost universal and is shown in [Table III](#). Some codons do not commonly specify an amino acid; these are UAA, UAG, and UGA, and are believed to be “stop” signals used to terminate protein synthesis. The codon AUG is the most common “start” signal, although GUG and UUG occasionally have this function.

The sequence of bases on m-RNA is read in the 5' to 3' direction, and is translated into an amino acid sequence starting at the N-terminal end of the protein. Amino acids, however, cannot interact directly with m-RNA. Instead, each amino acid becomes attached to the 3' end (the acceptor end) of a specific t-RNA (see [Fig. 20](#)); glycine, for example, becomes attached to glycine-specific t-RNA. The enzymes, amino acyl-t-RNA-synthetases, which catalyze this attachment, ensure that an amino acid is linked only to its correct t-RNA. The t-RNA carrying its amino acid can interact directly at the ribosome with m-RNA. In fact, each t-RNA has a three-base sequence complementary to the codon on m-RNA specifying its amino acid. This sequence on the t-RNA, called the anticodon, is located at the lower end of the molecule and the bases are held in such a way that a short stretch of double helix can be formed, with the bases of the anticodon pairing with the codon bases of the m-RNA.

After the m-RNA has become bound to the small subunit of the ribosome, a specific initiating t-RNA carrying methionine (or in bacteria, a modified methionine) forms a complex with the ribosome subunit and the AUG codon which signals the beginning of the amino acid sequence

TABLE III The Genetic Code

First base of codon ↓	Second base of codon				Third base of codon ↓
	U	C	A	G	
U	UUU } Phe	UCU } Ser	UAU } Tyr	UGU } Cys	U
	UUC } Phe	UCC } Ser	UAC } Tyr	UGC } Cys	C
	UUA } Leu	UCA } Ser	UAA } Stop	UGA } Stop	A
	UUG } Leu	UCG } Ser	UAG } Stop	UGG } Trp	G
C	CUU } Leu	CCU } Pro	CAU } His	CGU } Arg	U
	CUC } Leu	CCC } Pro	CAC } His	CGC } Arg	C
	CUA } Leu	CCA } Pro	CAA } Gln	CGA } Arg	A
	CUG } Leu	CCG } Pro	CAG } Gln	CGG } Arg	G
A	AUU } Ile	ACU } Thr	AAU } Asn	AGU } Ser	U
	AUC } Ile	ACC } Thr	AAC } Asn	AGC } Ser	C
	AUA } Ile	ACA } Thr	AAA } Lys	AGA } Arg	A
	AUG } Met, Start	ACG } Thr	AAG } Lys	AGG } Arg	G
G	GUU } Val	GCU } Ala	GAU } Asp	GGU } Gly	U
	GUC } Val	GCC } Ala	GAC } Asp	GGC } Gly	C
	GUA } Val	GCA } Ala	GAA } Glu	GGA } Gly	A
	GUG } Val	GCG } Ala	GAG } Glu	GGG } Gly	G

message on the m-RNA (Fig. 21). (GUG or UUG is used more rarely as an initiating codon.) The larger ribosome subunit then binds to the whole complex.

In a simplified picture of protein synthesis, we can consider that an intact ribosome has three binding sites, called the P-, A-, and E-sites, for t-RNAs. At this stage, the initiating t-RNA is bound at the P-site. A second t-RNA, with its amino acid, becomes bound at the A-site. The codon on the m-RNA next to AUG determines which amino-acyl-t-

RNA can bind (Fig. 22). In this example, the second codon codes for serine. A peptide bond is formed between the carboxyl group of the methionine and the amino group of the second acid serine, and the new dipeptide remains bound to the second t-RNA, at the A-site. The 23s RNA of the larger ribosomal subunit plays an important role in the catalysis of peptide bond formation. The ribosome now moves with respect to the t-RNA and m-RNA, so that the dipeptidyl-t-RNA is located at the P-site (Fig. 22), and the

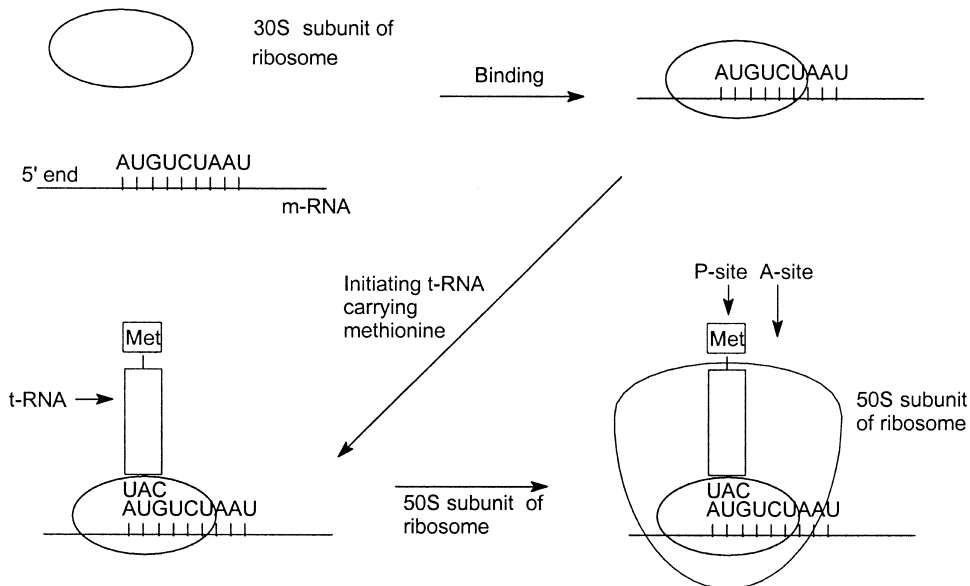


FIGURE 21 Initial stages of protein biosynthesis.

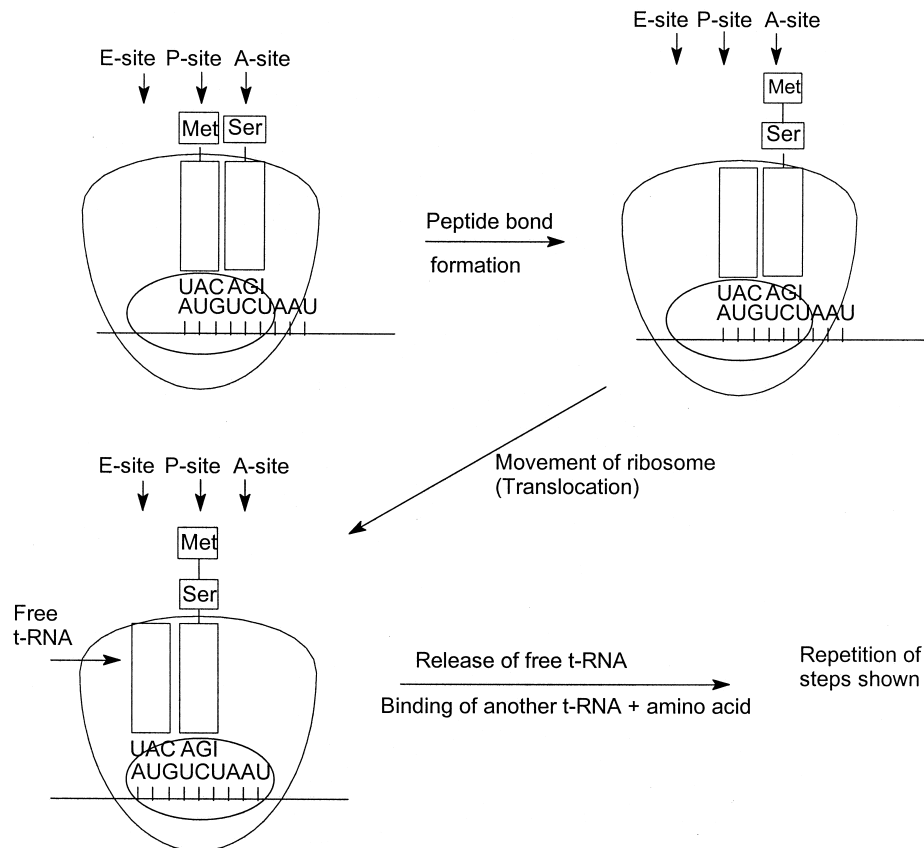


FIGURE 22 Elongation of a peptide chain. (I, on the serine t-RNA, signifies inosine, a base similar in structure to guanine, but lacking the NH_2 group. Inosine is common at t-RNA anticodons, and can pair with U, C, or A on a codon.)

free t-RNA moves to the E-site. A shape change at the ribosome surface and binding of a new amino-acyl-t-RNA at the A site cause the free t-RNA to drop out of the E-site. The processes shown in Fig. 22 can now be repeated over and over, to give a growing polypeptide chain. In this case, the third amino acid to be joined to the protein would be asparagine.

A ribosome moves along the m-RNA until a terminator codon appears at the A-site. The completed polypeptide chain is released from the last t-RNA, the t-RNA dissociates from the ribosome, and the ribosome itself splits into two subunits ready to recommence protein synthesis.

The whole process, whereby a sequence of bases on m-RNA becomes an amino acid sequence of a polypeptide chain, is called translation, and is much more complex than presented here. The ribosome plays an active part in the process and minor changes in its structure may occur at more than one stage of protein synthesis. Ribosome structure is more complicated than depicted in Figs. 21 and 22; a cavity exists between the two subunits in the intact ribosome, and it is in this cavity that the t-RNAs can bind. In addition, many protein factors are involved in protein

synthesis to help ensure correct initiation, elongation, and termination of the chain. After synthesis, many proteins undergo further modifications—amino acid side chains may be altered, segments of polypeptide chain may be removed, or prosthetic groups may be added.

Protein biosynthesis must at all times be under strict control. Much of this control, particularly in bacteria, is exerted at the level of transcription (i.e., production of m-RNA). In some cases, a protein known as a repressor recognizes and binds to a segment of DNA close to a site for initiation of m-RNA synthesis. The repressor binds in the grooves of the DNA helix and effectively prevents biosynthesis of the m-RNA. When that m-RNA is required, a shape-change can be brought about in the repressor protein by another molecule called an inducer; the repressor no longer binds to the DNA and transcription of m-RNA can take place. In other instances, specific proteins can bind to DNA and enhance the synthesis of particular m-RNA molecules. Translational control is also possible. Alterations in protein initiation factors or binding of proteins to m-RNA to alter its secondary structure or mask the initial ribosome recognition site can change the amount

of protein synthesis taking place from the m-RNA. Some proteins involved in enhancing transcription or initiating translation can themselves be activated as the result of a reaction cascade stimulated by a messenger molecule such as a hormone (see Section II.A.2), thus allowing another form of control.

Correct replication of DNA, transcription to RNA, and translation to amino acid sequences must be carried out if fully functional proteins are to be synthesized. A change of one base on a DNA or m-RNA can change a codon, so that an incorrect amino acid is inserted into a protein. Such a change in DNA is known as a mutation. For example, a change of GAA to GUA would substitute valine for glutamic acid in a protein. This kind of change is known in human hemoglobin where substitution of a valine for a particular glutamic acid causes a change in the surface properties of the hemoglobin molecules and produces a disease known as sickle cell anemia. At the level of DNA replication, DNA polymerases can “proofread” the new DNA, remove mismatched bases, and incorporate correct bases into the growing polynucleotide strand. Other enzymes can repair some damage to existing DNA. Thus mutations caused by errors in replication are rare, approximately 1 in 10^{11} bases. Lack of certain repair enzymes in human beings is known to be associated with particular kinds of cancer. RNA polymerases, on the other hand, do not have proofreading ability and so the rate of incorporation of mismatched bases is higher during RNA synthesis.

Other mutations can cause base additions or deletions in DNA, which can drastically alter protein structure, r-RNA or t-RNA structure or control systems, depending on the location of the alteration on the DNA. Mutations can occur spontaneously or by the action of chemicals. Some of these mutagenic chemicals are also carcinogens (i.e., cancer-causing agents).

In animals, certain viruses have been implicated in the development of cancer. These tumor-producing viruses can have DNA or RNA as their genetic material. Most RNA viruses contain an enzyme, reverse transcriptase, which is capable of synthesizing DNA on an RNA template. Both types of virus can bring about incorporation of viral DNA into the animal cell DNA, thus altering the genetic makeup of the cell. Some of the viral DNA may constitute an oncogene—a gene coding for a protein related, but not identical to, a normal cellular protein. The normal protein is often involved in control of cell growth, and the production of the altered protein from the oncogene may bring about transformation of the animal cells to malignant cells. Reverse transcriptases, like RNA polymerases, do not proofread the new nucleic acid strand being synthesized, and so a high mutation rate in viral DNA is possible. This can be important for human health. Some viral DNA codes for proteins, the so-called coat proteins, that form

the viral outer covering, and stimulation of antibodies in human beings against coat proteins can provide protection against viral diseases. Where a high mutation rate in viral DNA causes fast changes in coat protein amino acid sequences, it becomes difficult to produce a successful vaccine, since antibodies against the original coat protein may be ineffective against a new altered protein. In the case of the virus, HIV, that causes AIDS, the mutation rate is unusually high, making for great difficulty in producing a useful vaccine.

Antibiotics are compounds synthesized by some microorganisms, with the property of inhibiting the growth of others. Many of these act by interfering with nucleic acid function. Thus actinomycin D and mytomycin C bind to DNA and inhibit replication; streptomycin and the tetracyclines bind to ribosomes and inhibit translation, while puromycin, by its structure, mimics that end of a t-RNA which accepts an amino acid and brings about release of an incomplete polypeptide from a ribosome. AZT (azidothymidine), a modified form of a thymine nucleoside, inhibits the reverse transcriptase of HIV and hence is useful in slowing down the development of AIDS.

3. Utilization—Recombinant DNA and Genetic Engineering

Many medically important proteins, for example, human insulin and human somatotropin (a growth hormone) are in short supply. Now that the mechanisms of protein synthesis are understood, it is possible to introduce a segment of DNA, coding for say a human protein, into bacteria, culture the bacteria, allow them to synthesize the protein, and then harvest that protein. Such a process involves recombinant DNA technology.

First, the DNA segment which codes for the required protein must be prepared. This may be purified from cells in which it occurs, by partial degradation of the total cellular DNA, and isolation of the appropriate fragment. Alternatively, if purified m-RNA for the protein is available, the corresponding DNA can be made using reverse transcriptase. If the DNA segment required is short, a small amount can be synthesized chemically in a laboratory, and then greater quantities can be made by enzymic replication in the so-called polymerase chain reaction (PCR).

Second, this DNA must be incorporated into a “vector” which will carry the DNA into the bacterial cells. The vector may be the DNA of a virus which can invade the strain of bacterium to be used. More commonly, the foreign DNA is introduced into a plasmid, a small circular piece of DNA which can be replicated in the bacterial cells. The circular plasmid DNA is usually “nicked” by an enzyme, and another enzyme is used to join in the foreign DNA. If the cut ends of the plasmid DNA and the

foreign DNA have complementary sequences, then correct combination of the two is easier. These so-called “sticky” ends can be produced by enzymes or chemical synthesis. The product—an artificial combination of bacterial plasmid DNA and, for example, human DNA—is called recombinant DNA.

The plasmid is then introduced into a bacterial cell and the bacterium is cloned (i.e., the cell is allowed to divide several times) producing progeny bacteria with the same genetic constitution as the original cell. Each cell carries the DNA coding for the required protein, and if the DNA has been inserted with the correct control elements, each cell synthesizes the protein. The protein can later be purified from the bacterial culture.

In this way it has been possible to produce human insulin, growth hormone, and interferon (an antiviral protein) from *E. coli*—a common bacterium in the human digestive tract.

Fears that new and dangerous strains of *E. coli* might result from recombinant DNA experiments have mostly been allayed by stringent controls on the kinds of experiments that can be carried out and by greater understanding of the control mechanisms involved in bacterial nucleic acid metabolism.

It is hoped by these methods to produce medically useful proteins cheaply and on a large scale. In addition, new bacteria with useful properties may be “created” (e.g., bacteria able to convert cellulose to methane for energy production). (At present two different microorganisms must be used—one converts cellulose to acids, the second these acids to methane.)

By incorporating DNA with specific base changes into bacteria it is possible to obtain proteins with as little as one altered amino acid. This process, known as site-directed mutagenesis, has enabled detailed investigations to be made of the role of individual amino acids in, for example, enzyme activity and stability. It is hoped that, in the future, industrially important enzymes with improved thermal stability may be made in this way.

Genetic engineering can also be carried out on plants and animals, although there is usually some difficulty in introducing the new DNA into the plant or animal cell and ensuring that it is used to code for a new protein. Single plant cells can be transformed by infection with a bacterium, *Agrobacterium tumefaciens*, carrying a plasmid that contains the desired new DNA. When the bacterium contacts a plant cell, some of the plasmid DNA is transferred to the plant cell nucleus and is integrated into the plant cell’s DNA. Then whole plants can be produced from the single plant cells in culture by the administration of hormones. Thus, it is possible to grow complete plants with an altered genetic makeup. Disease resistance can be improved, for example, by incorporating a gene

for a virus coat protein into a plant. This appears to stop the virus replicating in the plant. The first commercially grown genetically modified plants contain DNA coding for an enzyme that confers herbicide resistance or for proteins that are insecticidal. In the first case, less herbicide need be used on crops to kill weeds, as spraying can be carried out when both the weeds and crop plants are well-grown. In the second case, application of external pesticide may not be required, since the crop plants themselves, containing the new insecticidal protein, may kill invading insects. Currently, cotton, soya, maize, and canola containing these modifications are grown commercially, but because of concerns about possible environmental problems such as potential harm to beneficial insects, introduction of new genetically-engineered crop plants has slowed down.

An extension of this work could lead to “genetic engineering” in human beings, where genetic diseases (i.e., diseases caused by a defective or missing enzyme) might be cured by incorporation of DNA coding for that protein. It will be difficult, however, to ensure that subsequent biosynthesis of the protein is under correct control, so that the protein is made in the right amounts in the appropriate tissues.

Small amounts of human DNA found at the scene of a crime can now be amplified by PCR technology, and the DNA can be hydrolyzed by enzymes specific for particular base sequences. Because the pattern of fragments produced is believed to be characteristic of one human individual, the process is now used to help identify perpetrators of serious crimes.

D. Rubber, Lignin, and Polyesters

Rubber is a hydrocarbon polymer produced by many tropical and a few temperate plants, such as the dandelion. Commercially, rubber is obtained from a tree originally found in Brazil, *Hevea brasiliensis*, which is now grown extensively in southeast Asia and Africa, as well as Central and South America. Rubber is obtained from the tree in the form of latex, a suspension of polymer particles in a slightly viscous aqueous solution; this latex oozes from the tree when a cut is made in the bark. Trees may be tapped again and again for more than 30 years, and commercial yields can be more than 3300 pounds per acre per year (3600 kg/ha/yr).

The monomer of rubber is isopentenyl pyrophosphate, and when the polymer is synthesized, the monomers become linked together, with the elimination of pyrophosphate, as in Fig. 23. During the joining of the monomer residues, the carbon-carbon double bond changes position (from left of the CH₃ group, to right of it) and the repeat unit in the polymer is an isoprene unit; rubber is, thus, a polyisoprene. In latex, the polyisoprene molecules are

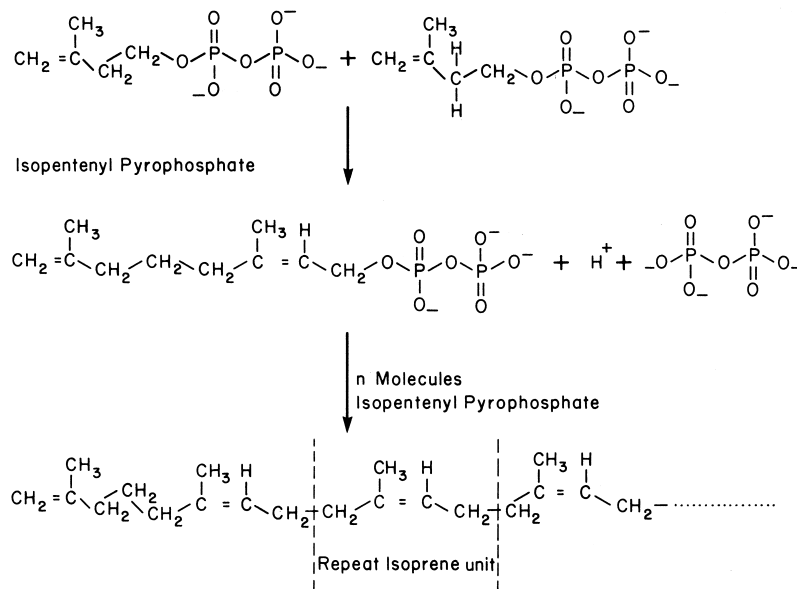


FIGURE 23 Synthesis and structure of rubber.

not all the same length, and the chains can vary from a hundred to tens of thousands of isoprene units long.

In rubber molecules, the carbon-carbon bonds of the polymer backbone always lie on the same side of the double bond (cis to the double bond) and this configuration conveys flexibility on the molecular chains. It is believed that rubber molecules coil up randomly and that this is their preferred conformation at temperatures around room temperature. On stretching, however, the molecules in a rubber sample become partially aligned with each other. When the stretching force is released, the rubber molecules return to their coiled shapes, and the sample regains its original length.

Synthetic rubber, with structure identical to natural rubber, can now be synthesized chemically from isoprene, but this is of much less economic importance than synthetic rubbers such as styrene-butadiene rubber, which are chemically distinct from natural rubber.

The small rubber particles in suspension in latex can be coagulated by the addition of acid. The resultant product can be passed through rollers and dried in air to give a sheet of raw rubber. If treated with sodium bisulfite before rolling, the product becomes crepe rubber and can be used to manufacture shoe soles. Other useful materials can be made by milling chemical compounds into the raw rubber and heating. Thus, addition of sulfuric acid can give adhesives and shellacs, while titanium and iron chlorides can be added to produce a rubber for molding into chemically resistant dishes and electrical apparatus.

Wrapping films can be made from rubber treated with hydrogen chloride and products used in paints and var-

nishes can be obtained from the reaction of chlorine with rubber.

Raw rubber, however, is limited in use because of its relatively low tensile strength (300 lbs/in.²), its solubility in some hydrocarbon solvents and its viscoelasticity; stretched raw rubber will not return to its original, unstretched length on release of tension if the tension is maintained for some time. This happens because some molecules slip past one another under tension, and do not return to their original positions when the tension is released.

The properties of raw rubber can be improved by a process called vulcanization, where rubber is heated with sulfur. The result of the treatment is the formation of monosulfide, $-S-$, and disulfide, $-S-S-$, cross-links between rubber molecules. Vulcanization is usually speeded up by incorporation of an accelerator, such as a thiazole, in the presence of an activator like zinc oxide. To increase the solubility of accelerator and activator in the rubber, the zinc salt of a fatty acid may be added.

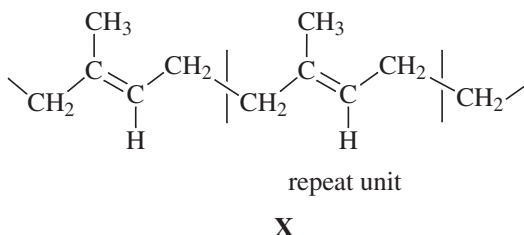
Vulcanization decreases the solubility of the rubber and its viscoelasticity. Now rubber molecules can uncoil on stretching but are less likely to slip past one another because of the cross-links, and so the rubber sample regains its original length when stretching ceases. The tensile strength of the rubber increases with the amount of sulfur incorporated, but simultaneously the elasticity decreases, because too many cross-links prevent molecular uncoiling when tension is applied to a rubber sample. If the sulfur content is less than 5%, the rubber is soft, pliable, and elastic and can be used for rubber tubing, elastic bands,

and rubber gloves. With high (30–50%) sulfur content, rubber is not elastic, but forms a hard, rigid substance called ebonite which can be used as a thermal and electric insulator.

The double bonds in rubber molecules are fairly readily oxidized; when this happens the rubber becomes less elastic. Thus antioxidants such as phenyl- α -naphthylamine are usually incorporated into a vulcanizing mixture.

Vulcanized rubber does not have high abrasion resistance, but this property can be improved by incorporating a filler before vulcanization. The most common filler is carbon black (soot) and this forms loose bonds to the rubber molecules. The result is a reinforced rubber with greater tensile strength (4500 lb/in.²), durability, and abrasion resistance. This reinforced rubber is used to make tires, particularly for aircraft and large trucks, and engineering components where heavy demand is made on physical performance.

Gutta percha or balata is another hydrocarbon found in some tropical trees. It, like rubber, is synthesized from isopentenyl pyrophosphate and is a polyisoprene. Unlike rubber, however, the carbon-carbon bonds of the polymer backbone always lie on opposite sides of (trans to) the double bond of the repeat unit:

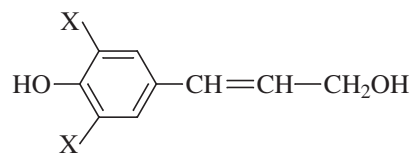


This configuration gives the molecules less flexibility, and there is a tendency for the molecules to pack together in a more regular fashion than the random coils of rubber. Thus, gutta is much less elastic than rubber and is of lesser industrial importance. It becomes softer and more elastic on heating, however, and can be molded into articles which retain their shape on cooling. It has been widely used as a submarine cable cover, and because of its acid resistance, can be used for containers for very strong acids.

Chicle, a mixture of low-molecular-weight rubber and gutta percha with some other plant products, is obtained from certain tropical trees and is used to make chewing gum.

Lignin, another plant polymer, has an obvious function—that of a structural material—but has little industrial application. Lignin is a biochemically inert polymer which acts as a support and cement in the cell walls of plants, where it is probably covalently linked to some of the cell wall polysaccharides. Lignin in a plant is extremely insoluble and so it has been difficult to study its

structure without degrading the molecules. It is believed that the monomers are alcohols like **XI**, where X may be H or OCH₃. The content of OCH₃ groups in the lignin depends on the plant source.



XI

Lignin is believed to be formed in a polymerization process involving oxidation of the monomers, to give a highly cross-linked polymer, with a molecular weight, in some cases, of over 50×10^6 Da. Many different cross-links can form so that it is probably not possible to write a simple structural formula for a lignin molecule. A possibility for part of a lignin molecule is given in Fig. 24.

Modified lignin is obtained as a by-product of papermaking (see Section II.B.3). Cellulose for paper manufacture is left as an insoluble residue, while the lignin is degraded and dissolved by treatment with sulfur dioxide and calcium bisulfite or alkali and sodium sulfide. In the first case lignin sulfonates are produced and are used as dispersants and wetting agents in the preparation of oil drilling muds. They may also be used in adhesives, cement products, and industrial cleaners, and on heating with alkali yield vanillin, a flavoring in the food industry.

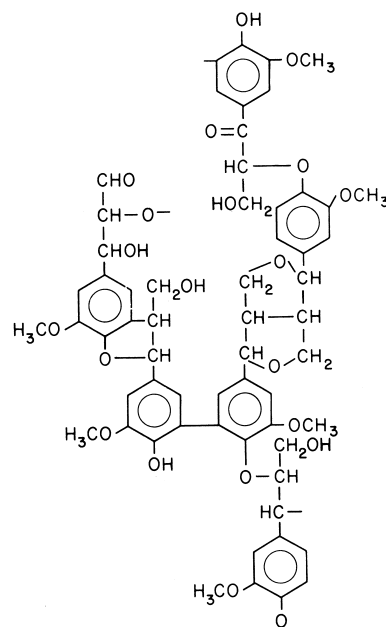


FIGURE 24 Possible partial structure of lignin.

Lignin from alkali extraction of wood is a stabilizer and emulsifying agent, an additive for concrete, and a filler for natural rubber. Much less lignin is used, however, than is produced by the paper industry and some is simply burnt as a fuel.

Cutin and suberin are polymers that provide physical barriers in plants to prevent or control diffusion of water and other small molecules. Leaves of plants are protected by a cuticle of cutin embedded in waxes, while underground organs such as roots have a barrier layer containing suberin and waxes. The monomers of both are thought to be a variety of hydroxy acids such as **XII**:



XII

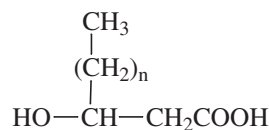
Trihydroxy acids, such as the above, are found more frequently in cutin than in suberin. In suberin, acids containing only one hydroxyl group at the end of the molecule or di-acids with a COOH group at each end are much more common. Both polymers contain some monomer residues related to those of lignin (with structures like **XI**, but having a COOH group instead of CH₂OH at the end of the side-chain); suberin can contain up to 60% of these residues, while cutin contains much less. The acid monomers probably become linked together by reaction between the COOH of one monomer and OH of another to give ester linkages as in **XIII**:



XIII

The molecules are highly cross-linked and, like lignin, cannot be described by a single simple repeat unit. Some of the phenolic residues of suberin may be covalently linked to cell wall polysaccharides. While both polymers have a protective function, break-down products from cutin may also be important for activating defense mechanisms when plants are invaded by pathogens.

Most commercial plastics are made from petrochemicals and are nonbiodegradable. Problems of supply may develop in the future as oil stocks run low, and the lack of degradability can currently result in environmental pollution when plastic objects are discarded. Thus investigations are ongoing to find materials that can be produced from renewable resources and are biodegradable, but have the properties of synthetic polymer thermoplastics or elastomers. Some bacteria synthesize polyesters, the poly(hydroxyalkanoates), with these properties. The monomers are usually of the type shown in **XIV**, where *n* is often 0 or 1.



XIV

The monomers become linked together essentially as in **XIII**, and the bacteria use the polymers as energy reserves. The most common polymer, poly(3-hydroxy butyrate) made from **XIV** where *n* = 0, resembles polypropylene in properties, but is stiffer and more brittle. A more useful polyester is a random copolymer of 3-hydroxy butyrate (**XIV** where *n* = 0) and 3-hydroxy valerate (**XIV** where *n* = 1), and is tougher and more flexible. This can be molded and is made into bottles and containers. Films, coatings for paper and board, and compost bags can also be produced from the copolymer. Polymers of longer chain acids (**XIV** with *n* = 4 for example) are rubbery and elastic, and may in future find uses as biodegradable elastomers. The poly(hydroxyalkanoates) are readily degraded to water and carbon dioxide, or in some cases methane, by enzyme systems occurring in bacteria of soil, sewage sludge, or compost. At present, however, the high cost of production of these polyesters limits their use. Research is under way to produce bacteria "engineered" (by transferring genes from one bacterium to another) to synthesize the polymers more efficiently from cheap carbon sources such as sugar cane and beet molasses, cheese whey and hydrolysates of starch, and hemicellulose (see Section II.B.3). New poly(hydroxyalkanoates), produced by supplying bacteria with a variety of acid starting materials, are also being investigated. In addition, attempts are being made to transfer the bacterial genes for polyester synthesis to plants, where the sun's energy, trapped via photosynthesis, could be utilized for poly(hydroxyalkanoate) production, thus lowering costs compared to expenditure on the bacterial fermentations currently necessary for polymer formation.

E. Polymer-Polymer Interactions

For very many biopolymers, their importance in the living organism lies in the way in which they interact with other polymers. In a few cases there is covalent bonding between polymers, for example, in the proteoglycans of animal connective tissue (see Section II.B.7), or between lignin and polysaccharides in plant cell walls. In many more instances, however, interactions are noncovalent and involve weaker bonds, such as hydrogen or ionic bonding or hydrophobic associations. Although the bonding is relatively weak, the interactions can be strong, because an area of the surface of one polymer molecule fits exactly

(sometimes after minor conformational changes) onto the surface of another.

Proteins, in particular, must be able to interact with other polymers, for enzymes are involved in the synthesis and degradation of all biopolymers. In addition, however, many examples are known of associations between nonenzymic proteins and other proteins, polysaccharides, or nucleic acids. Muscle movement, for example, is brought about and controlled by complex interactions between several proteins (myosin, actin, troponin, and tropomyosin) while collagen fibers are associated with both glycoproteins and proteoglycans in connective tissues. Protein antibodies can bind to protein or polysaccharide antigens, while polypeptide hormones must be recognized by their receptors, themselves proteins or glycoproteins. The proteins that interact with nucleic acids (e.g., repressors) bind to specific base sequences or secondary structures on the polymeric acids. In some cases these base sequences are almost palindromic (read the same backward or forward) as in **XV**, and the protein molecules which bind to them often have two subunits so that one may bind to each strand of the DNA.

5' end ---- GT TCACTC TGAAC---- 3' end
3' end ---- CAAGTGAGACT TG----5' end

XV

A "motif" found in several DNA-binding proteins consists of two helices linked by a short stretch of polypeptide chain in the form of a sharp bend. Such an arrangement fits easily into a groove of double helical DNA.

Within ribosomes, strong interactions between protein and r-RNA are essential for maintenance of the structure and functioning of the ribosome. Details of these interactions are not yet well understood.

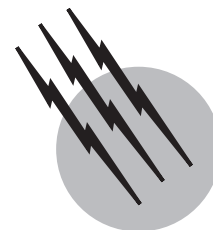
Polysaccharide-polysaccharide interactions can also take place, probably involving extensive hydrogen bonding and "shape fitting" over lengths of twenty or more monosaccharide residues. This is important in plant cell walls where cellulose fibers are embedded in a matrix of proteins and several different polysaccharides.

SEE ALSO THE FOLLOWING ARTICLES

BIOMATERIALS, SYNTHESIS, FABRICATION, AND APPLICATIONS • GLYCOPROTEINS AND CARBOHYDRATES • HYDROGEN BONDS • POLYMER PROCESSING • POLYMERS, RECYCLING • POLYMERS, STRUCTURE • POLYMERS, SYNTHESIS

BIBLIOGRAPHY

- Branden, C., and Tooze, J. (1999). "Introduction to Protein Structure," 2nd ed., Garland Publishing Inc., New York.
- Dey, P. M., and Harborne, J. B. (1997). "Plant Biochemistry," Academic Press, New York.
- Dumitriu, S., ed. (1998). "Polysaccharides," Marcel Dekker, New York.
- Fried, J. R. (1995). "Polymer Science and Technology," Prentice-Hall, New Jersey.
- Neidle, S., ed. (1998). "Oxford Handbook of Nucleic Acid Structure," Oxford University Press, New York.
- Voet, D., Voet, J. G., and Pratt, C. W. (1999). "Fundamentals of Biochemistry," John Wiley & Sons, New York.



Macromolecules, Structure

Peter A. Mirau

Bell Laboratories Lucent Technologies

Lynn W. Jelinski

Louisiana State University

Frank A. Bovey

Bell Laboratories Lucent Technologies (retired)

- I. The Nature of Macromolecules
- II. Molecular Weight and Size
- III. Microstructure of Macromolecules
- IV. Chain Conformations of Macromolecules
- V. Solid-State Morphology

GLOSSARY

Addition polymerization Polymerization reaction in which monomer units join by double bond or ring opening without splitting out small molecules. Also called chain polymerization.

Amorphous Polymers in which the chain packing is highly disordered or random.

Atactic Arrangement of successive units of a polymer chain so that the side-chain substituents are distributed randomly on both sides of the zigzag plane.

Block copolymers Polymers that contain relatively long sequences of one monomer covalently bonded to a similar sequence of another monomer. Block copolymers can be of the a-b, a-b-a, or random type.

Chain polymerization See addition polymerization.

Characteristic ratio C_{∞} , ratio between the unperturbed and the random walk dimensions of a polymer chain.

Condensation polymerization Polymerization reaction in which monomer units join with splitting out of

small molecules such as water. Also called step polymerization.

Configuration Stereochemical sequence, composed of isotactic (“meso,” symbolized by m) and syndiotactic (“racemic,” symbolized by r) monomer dyad sequences.

Conformation Spatial arrangement of a polymer molecule along its contour.

Copolymer Polymers that have chains of two or more comonomer units, generally classed into categories of random, block, and graft copolymers.

Crystalline State of solid polymers in which the individual chains are packed in a highly regular and repeating manner.

Defects Deviations from strictly ideal polymer structure caused by the reaction chemistry during or following synthesis. Defects can be branches (either short- or long-chain) or head-to-head;tail-to-tail structures.

End-to-end distance Root mean square end-to-end distance $\langle \bar{r}^2 \rangle^{1/2}$ of a polymer chain.

Excimer Association complex between an excited

chromophore and a chromophore in the ground state, the emission of which can be used to monitor spatial proximity and thereby establish polymer conformation.

Freely jointed chain Model for a polymer chain in which there are no restrictions on the bond angles between monomer units.

Geometrical isomers Isomers existing at carbon-carbon double bonds or other bonds that are not free to rotate.

Graft copolymer Homopolymer or copolymer onto which are covalently attached polymer chains of another type.

Heterotactic Triad configurational sequence containing one isotactic and one syndiotactic dyad, symbolized by m and r , respectively.

Isotactic Arrangement of successive units of a polymer chain so that all of the sidechain substituents are located on the same side of the zigzag plane.

Meso (m) Arrangement of two adjacent side-chains on the same side of a vinyl polymer chain in planar zigzag (all-*trans*) form (see isotactic).

Microstructure Precise way that monomer units are joined together to form a polymer.

Monomer Small chemical unit from which polymers are synthesized.

Morphology Describes the supramolecular organization of molecules.

Polydispersity Characterization of the molecular weight distribution of a polymer, given by \bar{M}_w/\bar{M}_n .

Polymer From the Greek words meaning “many parts,” used as an alternative term for macromolecule.

Polymerization Process of synthesizing a polymer.

Racemic (r) Arrangement of two adjacent sidechains on opposite sides of a vinyl polymer chain in planar zigzag (all *trans*) form (see syndiotactic).

Radius of gyration Root mean square distance $\langle s^2 \rangle^{1/2}$ of the units of a chain from its center of gravity.

Regioregularity Pertains to the occurrence of head-to-head: tail-to-tail defects in a linear polymer chain.

Rotational isomeric state Model for the theoretical treatment of polymer chains in which the main chain valence angles are fixed and the chain rotation is limited to a few states.

Spherulite Aggregate of crystals with a radiating fibrillar structure, a common habit in polymer crystallization.

Step polymerization See condensation polymerization.

Syndiotactic Arrangement of successive units of a polymer chain so that all of the side-chain substituents are located on regularly alternating sides of the zigzag plane.

⊖ **solvent** Solvent in which a particular polymer adopts its unperturbed dimensions.

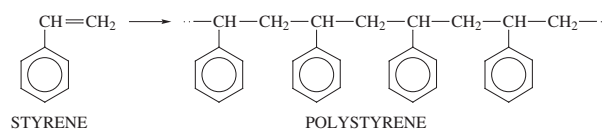
⊖ **temperature** Temperature at which a particular polymer adopts its unperturbed dimensions because the

polymer-polymer and polymer-solvent interactions are exactly balanced.

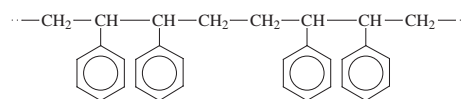
Tacticity Specification of the spatial arrangement of sidechains with respect to the zigzag plane of the polymer chain. Common types of tacticity are atactic, syndiotactic, and isotactic.

MACROMOLECULES are very large molecules. The word polymer is derived from the Greek words meaning “many parts” and is often used as an alternative term, one which emphasizes the nature of macromolecules as being built up by the joining of many small chemical units known as monomers (“single parts”). Polymers may be either of biological origin (e.g., proteins, cellulose, DNA, and RNA) or synthetic origin (e.g., polyethylene, polystyrene, nylon, and polyesters). We shall deal in this article mainly with the latter.

Macromolecules have structure on several levels. At the chemical level they are repeating sequences of a particular type of monomer unit covalently joined. Thus, units of the monomer styrene may be linked to form polystyrene:



The microstructural level refers to the precise way that these units are joined together. They are represented above as connected head-to-tail, but they may also be connected head-to-head: tail-to-tail and other options also exist. The conformation of a macromolecule describes the spatial arrangement of the polymer along its contour and may be altered by rotations about



bonds without alteration of the covalent structure. Many polymers are partially crystalline, and the chain conformation is markedly influenced and conditioned by the requirements of the crystal packing of the chains. Finally, the morphology of a macromolecular material refers to the supramolecular organization of the molecules, whether crystalline or amorphous, in the solid state.

I. THE NATURE OF MACROMOLECULES

A. The Macromolecular Concept

The utility of natural rubber was recognized two centuries ago, and cellulose esters were articles of commerce at the end of the nineteenth century. Leo Baekeland invented the

first entirely synthetic resin—the phenol-formaldehyde condensation product known as Bakelite—between 1905 and 1909. However, it is unlikely that any of the developers of these materials recognized their true chemical nature as macromolecules. Even at a time—the period of approximately 1900 to 1930—when organic chemistry was achieving an advanced state of development, the idea of covalently bonded molecules with molecular weights of 100,000 or even higher was not accepted. It was felt that such structures would be inherently unstable. Instead, it was commonly assumed that substances with polymeric properties—toughness, elasticity, no sharp melting point, and solutions of high viscosity—were aggregates of small molecules held together by vaguely defined “secondary” or “partial” valence forms. Referring particularly to natural rubber, these secondary valence associative forms were thought to require the presence of double bonds.

Hermann Staudinger was able to shake severely the foundations of the association theory by showing that on hydrogenation to a saturated hydrocarbon natural rubber still retained its polymeric character. By this and other evidence he was able, against strong opposition, to show that polymers were composed of molecular entities. Perhaps the most convincing evidence was provided by Wallace Carothers and his colleagues at the duPont company (1928–1931), who carried out straightforward polycondensation reactions that could lead only to long-chain molecules.

B. Types of Macromolecular Structure

Macromolecules of biological origin are familiar in nature. The protein of skin is predominantly the biopolymer collagen. Muscle is composed of the very large protein myosin, hair is mainly keratin, and DNA and RNA are well known as the macromolecules of the genetic code. Enzymes are proteins. We have already mentioned cellulose—to which starch is closely related—and rubber.

In contrast to natural macromolecules, synthetic polymers are by definition materials that can be prepared in the laboratory. They can be synthesized from monomers, as we have seen in the example of polystyrene. In a strict sense, the polymer, as in this instance, should have the same elementary composition as the monomer. However, the term monomer has now also come to be employed for molecules—adipic acid and hexamethylenediamine in the case of nylon 66—that undergo condensation reactions, with the splitting out of water of another small molecule, to yield a polymer, even though here the composition of monomer and polymer necessarily differ somewhat. Table I shows the chemical structures of selected polymers, and Table II lists trade names for some commercially important macromolecular materials.

The structure of a macromolecule—on chemical, microstructural, conformational, and morphological levels—has a vital relationship to the properties of the material. Because the properties of a material dictate its ultimate use, it is very important to obtain a fundamental understanding of the structure of macromolecules.

Although this article will deal mainly with macromolecules of the synthetic kind, essentially all methods of structural characterization described here pertain equally well to biological polymers. Before specifying the detailed chemical structure of the monomer units, we can describe a polymer chain more simply in terms of a series of beads linked together. With this physical picture in mind, we can illustrate several general types of structures (Fig. 1). Homopolymers are composed of one type of monomer unit and can occur in linear, branched, or cross-linked chains. Recent advances in polymer synthesis have also led to new polymer architectures, including star and hyperbranched polymers called *dendrimers*. New applications can be envisioned with such materials because they may have different rheological properties. Dendrimers consist of a core and successive generations of monomers. The number of end groups increases exponentially with each generation of monomers attached to the chain ends. Copolymers are

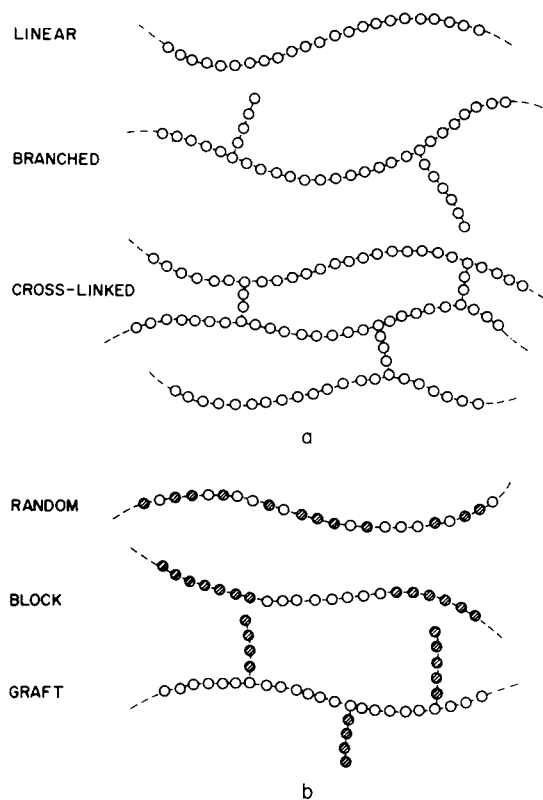
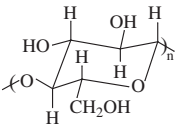
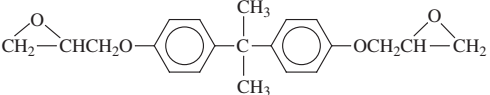
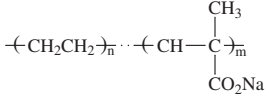
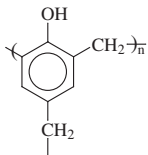
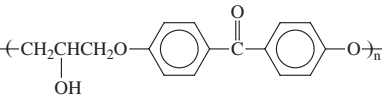
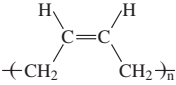
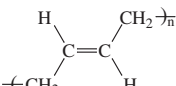
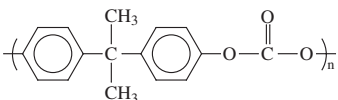


FIGURE 1 Schematic representation of various types of (a) homopolymer and (b) copolymer structures.

TABLE I Structures and Selected Thermal Data for Polymers

Polymer	Chain unit	T_m ($^{\circ}\text{C}$) ^a	T_g ($^{\circ}\text{C}$) ^b
Cellulose			
Epoxy resin (diglycidyl ether of bisphenol A)		43	
Ionomer resin			
Nylon 6	$\text{-(CH}_2\text{)}_5\text{CONH-}$		75 (dry)
Nylon 66	$\text{-NH(CH}_2\text{)}_6\text{NHCO(CH}_2\text{)}_4\text{CO-}$	265	49
Nylon 11	$\text{-(CH}_2\text{)}_{10}\text{CONH-}$		46
Nylon 12	$\text{-(CH}_2\text{)}_{11}\text{CONH-}$		37
Phenol-formaldehyde			
Phenoxy resin			
Polyacrylonitrile	$\text{-(CH}_2\text{CH-)}_n$ C≡N		~105 (two transitions)
Polybutene-1, isotactic	$\text{-(CH-CH}_2\text{)}_n$ CH ₂ CH ₃	142	-20 (several crystalline forms) -4
Polybutadiene	$\text{-(CH-CH}_2\text{)}_n$ CH=CH ₂	125	
1,2-isotactic		154	
1,2-syndiotactic		6	-108
Cis-1,4			
Trans-1,4		148	-18
Polycarbonate		267	149
Polychloroprene	$\text{-(CH}_2\text{C=CHCH}_2\text{)}_n$ Cl		-48

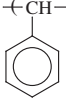
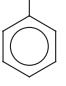
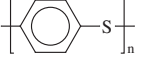
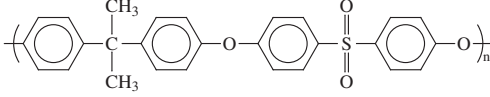
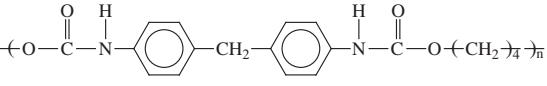
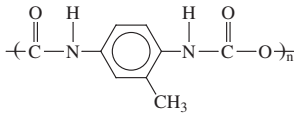
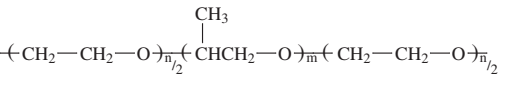
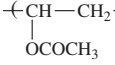
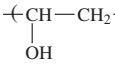
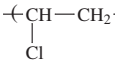
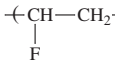
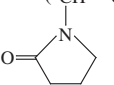
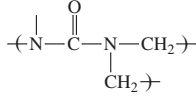
continues

TABLE I (Continued)

Polymer	Chain unit	T_m ($^{\circ}\text{C}$) ^a	T_g ($^{\circ}\text{C}$) ^b
Polychlorotrifluoroethylene	$\text{-(CF}_2\text{CF)}_n$ 	218	45
Poly(2,6-dimethylphenylene oxide)			
Poly(dimethylsiloxane)	$\text{-(Si(CH}_3)_2\text{-O)}_n$ 		-123
Polyisobutene	$\text{-(C(CH}_3)_2\text{CH}_2)_n$		-73
Polyisoprene <i>Cis</i> -1,4			-73 (natural rubber)
<i>Trans</i> -1,4			-58 (gutta percha)
Poly(ethyl acrylate)	$\text{-(CH}_2\text{CH)}_n$ 		-24
Polyethylene			
High pressure, branched		~115	
Linear	$\text{-(CH}_2\text{CH}_2)_n$	135	-125 (?)
Linear, low density (ethyl branches)			
Poly(ethylene oxide)	$\text{-(CH}_2\text{CH}_2\text{O)}_n$	66	-67
Poly(ethylene terephthalate)		265	69
Poly(methyl acrylate)	$\text{-(CHCH}_2)_n$ 		6
Poly(methyl methacrylate)			
Isotactic	$\text{-(C(CH}_3)_2\text{CH}_2)_n$ 	160	~45
Syndiotactic	$\text{-(C(CH}_3)_2\text{CH}_2)_n$ 	200	115
Atactic			105
Poly(oxymethylene)	$\text{-(OCH}_2)_n$	195	-85
Polypropylene			
Isotactic	$\text{-(CH(CH}_3)\text{-CH}_2)_n$ 	165	-10
Atactic			-20
Poly(propylene oxide)	$\text{-(CH(CH}_3)\text{-CH}_2\text{-O)}_n$ 	75	-75

continues

TABLE I (Continued)

Polymer	Chain unit	T_m ($^{\circ}\text{C}$) ^a	T_g ($^{\circ}\text{C}$) ^b
Polystyrene	$\left\langle \text{CH}-\text{CH}_2 \right\rangle_n$ 		
Atactic			100
Isotactic		240	100
Poly(styrene oxide)	$\left\langle \text{CH}-\text{CH}_2-\text{O} \right\rangle_n$ 	149	37
Polyphenylene sulfide	$\left[\text{C}_6\text{H}_4-\text{S} \right]_n$ 		
Polysulfone			219
Poly(tetrafluoroethylene)	$\left\langle \text{CF}_2\text{CF}_2 \right\rangle_n$	327	
Polyurethane	$\left\langle \text{O}-\text{C}(=\text{O})-\text{NH}-\text{C}_6\text{H}_4-\text{CH}_2-\text{C}_6\text{H}_4-\text{NH}-\text{C}(=\text{O})-\text{O}-(\text{CH}_2)_4 \right\rangle_n$ 		
4,4'-diphenylmethane Diisocyanate (MDI)			
Hard segment chain— extended with butanediol			
Toluene diisocyanate	$\left\langle \text{C}(=\text{O})-\text{NH}-\text{C}_6\text{H}_3(\text{CH}_3)-\text{NH}-\text{C}(=\text{O})-\text{O} \right\rangle_n$ 		
Hard segment			
Polyol soft segment	$\left\langle \text{CH}_2-\text{CH}_2-\text{O} \right\rangle_{n/2} \left\langle \text{CH}(\text{CH}_3)\text{CH}_2-\text{O} \right\rangle_m \left\langle \text{CH}_2-\text{CH}_2-\text{O} \right\rangle_{n/2}$ 		
Poly(vinyl acetate)	$\left\langle \text{CH}-\text{CH}_2 \right\rangle_n$ 		28
Poly(vinyl alcohol)	$\left\langle \text{CH}-\text{CH}_2 \right\rangle_n$ 	258	85
Poly(vinyl chloride)	$\left\langle \text{CH}-\text{CH}_2 \right\rangle_n$ 		81
Poly(vinylidene chloride)	$\left\langle \text{CCl}_2\text{CH}_2 \right\rangle_n$	190	
Poly(vinyl fluoride)	$\left\langle \text{CH}-\text{CH}_2 \right\rangle_n$ 	200	-20(?)
Poly(vinylidene fluoride)	$\left\langle \text{CF}_2\text{CH}_2 \right\rangle_n$	171	-45
Poly(vinylpyrrolidone)	$\left\langle \text{CH}-\text{CH}_2 \right\rangle_n$ 		
Urea-formaldehyde	$\left\langle \text{N}-\text{C}(=\text{O})-\text{N}-\text{CH}_2 \right\rangle_n$ 		

^a Melting temperature.^b Glass transition.

TABLE II Trade Names of Selected Polymers

ABS	Acrylonitrile–butadiene–styrene graft copolymers
Acrylic	Poly(acrylonitrile)
Amberlite	Ion-exchange resins
Bakelite	Phenol-formaldehyde
Buna N	Butadiene–acrylonitrile copolymer
Buna S (SBR)	Butadiene–styrene copolymer
Butyl rubber	Poly(isobutylene) + ~1% isoprene
Carbowax	Poly(ethylene glycol)
Cellophane	Cellulose hydrate
Celluloid	Cellulose nitrate
Cycolac	ABS
Dacron	Poly(ethylene terephthalate) fiber
Delrin	Poly(oxyethylene)
Dynel	Vinyl chloride–acrylonitrile copolymer
Epon	Epoxy resin
Estane	Polyurethane
HIPS	High-impact polystyrene—copolymer of styrene and butadiene
Hytrel	Poly(butylene terephthalate)–poly(butylene glycol) copolymer
Kapton	Polyimide
Kel-F	Poly(chlorotrifluoroethylene)
Kevlar	Polyaramide fiber
Lexan	Polycarbonate
Lucite	Poly(methyl methacrylate)
Marlex	Polyethylene
Mylar	Polyester film
Neoprene	Poly(chloroprene)
Orlon	Poly(acrylonitrile)
Plexiglas	Poly(methyl methacrylate)
PPO	Poly(2,6-dimethyl phenylene oxide)
PVC	Poly(vinyl chloride)
Rayon	Fibers from regenerated cellulose
Ryton	Polyphenylene sulfide
SBR	(See Buna S)
Silicone	Dialkyl siloxanes
Spandex	Fibers from elastic polyurethanes
Styrofoam	Polystyrene
Teflon	Poly(tetrafluoroethylene)
Viton	Vinylidene fluoride–hexafluoropropylene copolymer

composed of two or more monomer units and can occur in random, alternating, block or graft copolymers.

Figure 2 schematically illustrates the next level of detail—the chemical structure of the monomer unit. The polymer in this drawing is polyethylene, composed mainly of repeating $-(CH_2)-$ units. The main chain and a butyl branch are shown under the magnifying glass. (Butyl branches occur at the level of approximately 1 per 100 CH_2 groups.)

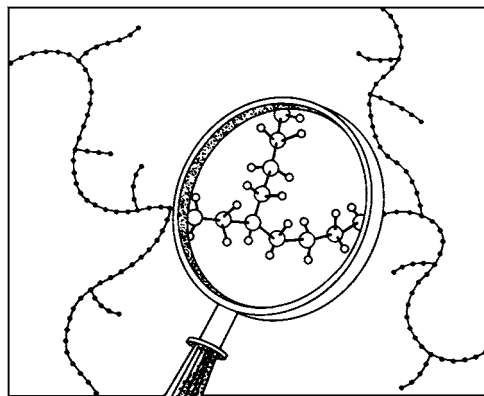


FIGURE 2 Examination of the chemical details in branched polyethylene. Within the magnifying glass, the large balls represent carbon atoms and the small ones are the hydrogen atoms. The four-carbon segment is a butyl branch.

C. Formation of Macromolecules

As an introduction to the understanding of structure, we must first consider the formation of macromolecules. Polymer formation involves either chain or step reactions, or living polymerization. Earlier, the terms *addition* and *condensation*, respectively, were used to describe chain and step growth polymerization. One important difference between the mechanisms is shown in Fig. 3, which shows a plot of the polymer molecular weight versus monomer consumption. In step polymerization, once the chain is initiated monomer molecules add in rapid succession to the reactive end group of the growing polymer chain until it terminates and becomes unreactive. In the growth or propagation step, several thousand monomer units add one at a time to each growing chain in a time interval of less than 1 sec. Thus, at any stage of a chain polymerization, the reacting system in effect consists of two species: monomers and very large molecular weight polymers. The formation of polystyrene from styrene is an example of chain polymerization.

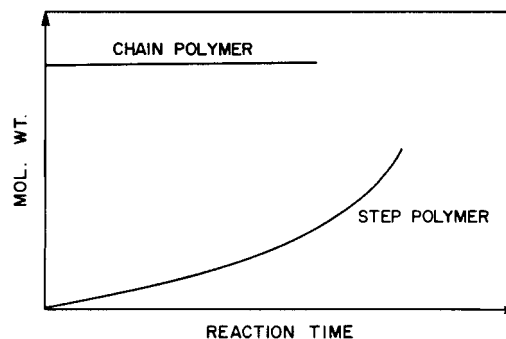
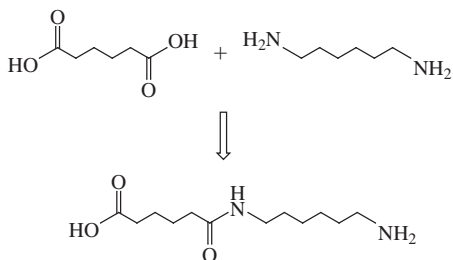


FIGURE 3 The dependence of molecular weight on monomer conversion for (A) chain polymerization, (B) step polymerization, and (C) living polymerization.

In step reactions, for example, in the reaction of adipic acid and hexamethylenediamine,



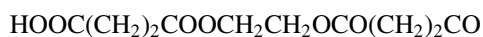
the growing molecules remain reactive and continue to grow by condensation through out the reaction period, which may be several hours. Although the “monomers” remain, their proportion on a weight basis rapidly becomes negligible (although on a molar basis they remain the most probable species).

In living polymerization, the chains continue to grow without chain transfer or termination. During the transferless polymerization, the number of polymer molecules remains constant. There is no termination, so the chain ends remain active when all of the monomer has been polymerized, and when fresh monomer is added, polymerization resumes. Because the chains are all growing at the same rate, they are more uniform than those prepared by other methods. This makes living polymerizations an invaluable method for preparing block, graft, and star copolymers.

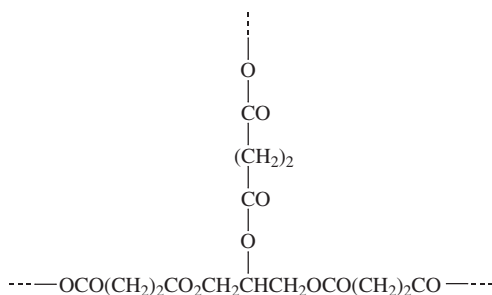
The polymer properties are often dependent both on the chain length (molecular weight) and the distribution in chain lengths. In chain reactions there is a large distribution in molecular weights because of the random nature of the initiation and termination processes. In step reactions, it results from random interactions of all species, the rates of which are independent of molecular weight. By comparison, the chains from the living polymerization are more uniform in molecular weight. The methods for measuring molecular weight distributions and averages are discussed in Section II.

D. Isomerism in Macromolecular Chains

In polymers produced by step reactions there is generally no formation of isomeric species in the usual sense except for those that may be readily predicted from the known composition of the starting mixture. Thus, for example, in the reaction of ethylene glycol and succinic acid to produce the polyester poly(ethylene succinate),



the introduction of a measured quantity of glycerol will produce a predictable proportion and distribution of trifunctional branch units:

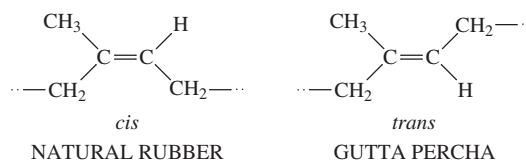


This predictability stems from the fact that the reactions involved are straightforward and well understood.

On the other hand, in the chain propagation reaction in vinyl monomer polymerization, many options are possible and their occurrence and structure are not so readily predictable. Hence, such isomeric species must be determined by spectroscopic or other means. One such option is the formation of inverted or head-to-head:tail-to-tail units, as we have seen. Actually, in polystyrene formed by the usual chain reactions of styrene, the occurrence of such units is negligible, but in the polymerization of such monomers as vinylidene fluoride and vinyl fluoride they occur with a substantial probability (see Section III).

Vinyl polymers may also exhibit marked differences in stereochemical configuration (i.e., the relative handedness of successive monomer units may vary). The simplest regular arrangements of successive units are the isotactic structure (Fig. 4a), in which all R substituents are located on the same side of the zigzag plane, representing the chain stretched out in an all-*trans* (see Section IV) conformation, and the syndiotactic arrangement, in which R groups alternate regularly from side to side (Fig. 4b). In the atactic arrangement, the R groups appear at random on either side of the zigzag plane (Fig. 4c). These isomeric forms are determined by the covalent bonding of each monomer unit and cannot be interconverted by rotations about the main chain bonds.

Another type of isomerism occurs in polymers having unsaturation in the main chain. Since carbon atoms linked together by double bonds are not free to rotate about the chain axis, repeating units in polymers such as polyisoprene can exist as two different geometrical isomers:



The *trans* polymer is a semicrystalline plastic whereas the *cis* form is normally a rubber at room temperature.

Yet another option is the production of branching, both short and long. An example of branching in polyethylene

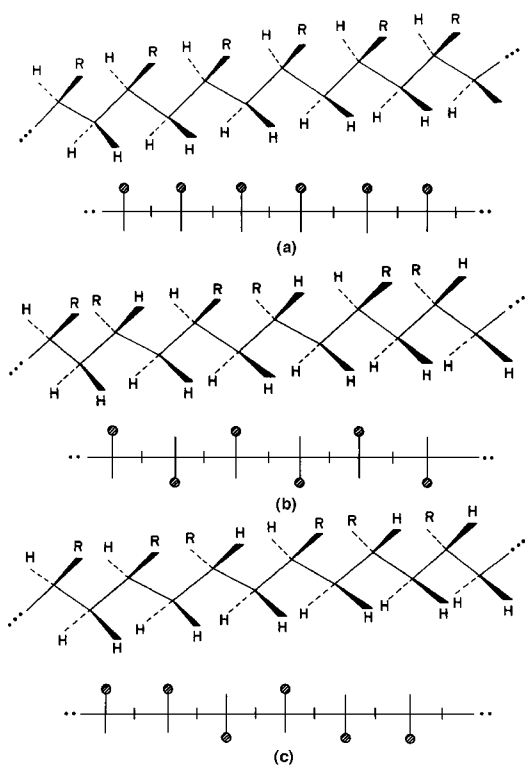


FIGURE 4 Schematic representation of structures of (a) isotactic, (b) syndiotactic, and (c) atactic chains.

is shown in Fig. 2. The observation and measurement of all these structures are discussed in Section III.

E. Physical and Mechanical Properties

We have seen that many macromolecular materials—usually those of fairly regular chain structure—may partially crystallize. Ordinary atactic polystyrene is amorphous, whereas the isotactic polymer readily crystallizes. Branched polyethylene (Fig. 2), made by free-radical polymerization of ethylene at very high pressure, is about 50% crystalline at room temperature, whereas linear polyethylene, formed at low pressure by heterogeneous catalysis, may be over 90% crystalline. As the temperature is raised, semicrystalline polymers exhibit crystalline melting points T_m , a first-order transition, accompanied by endotherms in the curves of heat capacity versus temperature.

As well as first-order transitions, exhibited by semicrystalline polymers, all polymers—whether crystalline or amorphous—show also second-order transitions, the most important of which is the glass transition T_g . This transition may be observed as a change in slope of a plot of the specific volume versus temperature and is usually measured by differential scanning calorimetry (Fig. 5).

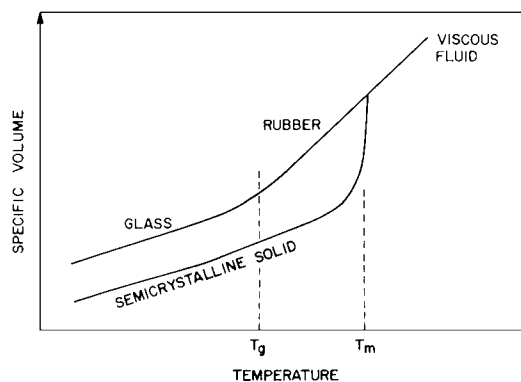
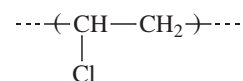


FIGURE 5 Specific volume as a function of temperature for glassy and semicrystalline polymers.

Marked changes in mechanical and other properties occur at this temperature, where hard, glassy materials become rubbery and extensible. This behavior results from the abrupt onset of extensive long-range molecular motion as the temperature is increased (or the suppression of such motion as it is lowered). These motions are inhibited in the glassy state, in which the viscosity is so high that the specific volume cannot attain its true or equilibrium value in a practical time span. Values of T_m and T_g for a selected group of polymers are presented in Table I.

Many important polymer properties, such as melting point, solubility, and viscosity, depend on secondary forces between adjacent molecules. These are variable but are one or two orders of magnitude less than the strength of the covalent bonds holding each molecule together. The strongest secondary forces involve hydrogen bonds. These account for the high melting temperature of nylon and for the insolubility and intractability of cellulose. The less polar carbon–chlorine bonds of poly(vinyl chloride) provide



interactions that are somewhat weaker yet sufficient to make this polymer hard and stiff even though it is essentially noncrystalline.

The chain segments in nonpolar polymers such as polyethylene are held together by weak dispersion forces common to all polymers. As the melting curves in Fig. 6 indicate, cumulative secondary forces are large even in nonpolar polymers. The melting point at first rises with increasing molecular weight but then levels off, showing that melting of high polymer fractions depends more on attractive forces between chain segments than on interactions between discrete molecules. The melting range reflects the molecular weight distribution in a typical polyethylene.

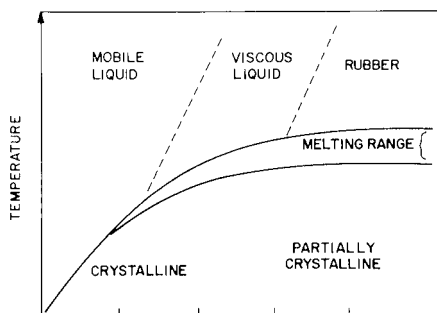


FIGURE 6 Melting curves for partially crystalline polymers as a function of molecular weight.

II. MOLECULAR WEIGHT AND SIZE

A. Molecular Weight Distributions and Averages

We have already seen that macromolecular materials, whether prepared by chain or step methods, usually contain a broad distribution of molecular weights. Two important averages specify the molecular weight distribution of a polymer. These are the number average molecular weight \bar{M}_n and the weight average molecular weight \bar{M}_w . We shall first illustrate the derivation of related quantities, the number average and weight average degrees of polymerization \bar{X}_n and \bar{X}_w . Statistical derivations of these averages depend upon the propagation mechanism, so we shall treat step polymerization and chain polymerization separately in the following sections. Monodispersity is difficult to achieve in step or chain growth polymerization, but a very low polydispersity (1.04) is possible with living polymerization.

1. Step Polymerization

Let us consider a difunctional monomer, A—B. We shall let p be the probability that one end (let us say A) has reacted at time t . Therefore the probability of finding an unreacted A group is $(1 - p)$. Since we want to calculate the number of molecules that are a particular number of units (let us say x) in length, we need to determine the probability of finding a chain which is x units long. Such a chain would have $(x - 1)$ A groups that had reacted, and this probability would be $p^{(x-1)}$. One A group would be unreacted, and its probability would be $(1 - p)$. So, the total probability of finding a chain x units in length is given by

$$p^{(x-1)}(1 - p). \quad (1)$$

If there are N molecules, the fraction of them that are x units in length, N_x , is given by

$$N_x = Np^{(x-1)}(1 - p). \quad (2)$$

The number average and weight average degrees of polymerization are calculated from

$$\bar{X}_n = \frac{\sum N_x x}{\sum N_x}, \quad (3)$$

$$\bar{X}_w = \frac{\sum W_x x}{\sum W_x} = \frac{\sum (N_x x) x}{\sum N_x x}, \quad (4)$$

where W_x is the weight fraction of molecules of degree of polymerization x . It is evident that

$$\bar{X}_n = 1/(1 - p), \quad (5)$$

and it can be shown that

$$\bar{X}_w = (1 + p)/(1 - p). \quad (6)$$

The polydispersity is characterized by \bar{X}_w/\bar{X}_n or $(1 + p)$. Thus, as the reaction approaches complete conversion, ($p \rightarrow 1$), $\bar{X}_w/\bar{X}_n \rightarrow 2$. A monodisperse polymer on the other hand, is one where all chains have identical molecular weights, and $\bar{X}_w/\bar{X}_n = 1$. Monodispersity is difficult to achieve in synthetic polymers, but occurs often for biomolecules.

On a number basis, there are more smaller chains than larger ones. However, these short chains comprise a small fraction of the total weight. Figure 7 illustrates this point. It shows the most probable distribution of polymer weights for an addition polymer of number average degree of polymerization \bar{X}_n of 100. Note that \bar{X}_n and \bar{X}_w are different by a factor of 2.

2. Chain Polymerization

Statistical derivations of number average and weight average molecular weights for chain polymerization follow arguments similar to those outlined in Eqs. (1)–(6). In the

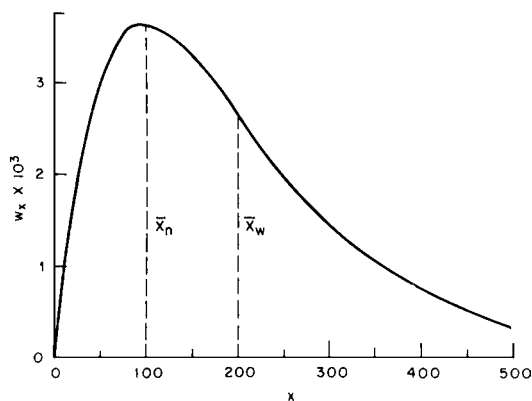


FIGURE 7 Weight fraction of degree of polymerization of x for an addition polymer having a number average degree of polymerization \bar{X}_n of 100; W_x is calculated by $W_x = (x/\bar{X}_n^2) \exp(-x/\bar{X}_n)$.

present case we are dealing with free radical reactions and need to make several assumptions. First, the concentration of the monomer is considered to remain constant throughout the polymerization. Second, we assume that the rate of initiation is constant throughout the polymerization. Finally, we assume that termination occurs either by disproportionation or by chain transfer (shortly we shall examine the effects of relaxing this third assumption).

A given radical can either propagate or terminate. We shall assign p to the probability that the radical will propagate. We can then obtain the probability of finding an x -mer, which requires $x - 1$ propagation steps [probability = $p^{(x-1)}$] and one termination [probability = $(1 - p)$]. As before, the probability of finding a chain x units long is then given by

$$p^{(x-1)}(1 - p), \quad (7)$$

and the number of molecules N_x is

$$N_x = Np^{(x-1)}(1 - p), \quad (8)$$

where N is the total number of molecules. The number average and weight average degrees of polymerization are obtained as before, and are given by

$$\bar{X}_n = 1/(1 - p), \quad (9)$$

$$\bar{X}_w = (1 + p)/(1 - p). \quad (10)$$

When propagation is highly favored over termination, $p \rightarrow 1$ and $\bar{X}_w/\bar{X}_n \rightarrow 2$.

So far we have considered the probability of finding an x -mer when termination occurs by disproportionation or chain transfer. These termination mechanisms are unimolecular in polymer—that is, only one polymer chain is involved in these reactions. Termination could also occur by chain combination, in which case the termination step requires two chains and is thus bimolecular in polymer. A chain combination to produce an x -mer requires $x - 2$ propagation steps [probability = $p^{(x-2)}$] and two termination steps [probability = $(1 - p)^2$]. In this case, \bar{X}_n and \bar{X}_w are given by

$$\bar{X}_n = 2/(1 - p), \quad (11)$$

$$\bar{X}_w = (2 + p)/(1 - p), \quad (12)$$

and thus $\bar{X}_w/\bar{X}_n \rightarrow 1.5$ as $p \rightarrow 1$.

3. Relationship between Degree of Polymerization and Molecular Weight

Now that we have derived expressions for the number average and weight average degrees of polymerization, we can convert these averages into \bar{M}_n and \bar{M}_w by multiplying the former quantities by the monomer molecular weight. In the following sections we shall describe experimental

methods for measuring \bar{M}_n and \bar{M}_w . However, before we can discuss experimental techniques for measuring molecular weights of polymers, we must digress briefly into the solution properties of macromolecules.

B. Solution Properties of Macromolecules

Solutions of macromolecules differ greatly from solutions of small molecules. In dilute solutions of small molecules, the molecules are effectively separated from each other by solvent. In contrast, dilute solutions of macromolecules have high local concentrations of monomer units because the chain segments are covalently bonded together. Furthermore, solutions of small molecules contain materials that are generally monodisperse in molecular weight. Solutions of polymers, on the other hand, contain macromolecules that have a dispersion in molecular weight.

In a general sense, liquids made up of small molecules are Newtonian in behavior. That is, they obey Newton's equation defining the viscosity of a fluid as the coefficient of proportionality between the shear stress and the velocity gradient. Liquids containing polymers, on the other hand, display non-Newtonian behavior. Some examples of non-Newtonian behavior are shown schematically in Fig. 8. These examples are described more fully in the figure legend.

1. Polymer Chain End-to-End Distance and Radius of Gyration

In a "good" solvent, where polymer-solvent interactions are favorable, a polymer chain adopts a somewhat extended shape. In a "poor" solvent, the polymer tends to coil back on itself because polymer-polymer interactions are more favorable than polymer-solvent interactions. We shall see later that these interactions are temperature-dependent and are exactly balanced at the θ temperature.

In an elementary approach, we can treat a polymer chain as being freely jointed. In such a model there are no restrictions on the bond angles between monomer units. Statistical random walk calculations show that a polymer with x monomer units each of length l at θ conditions has a root mean square (rms) end-to-end distance $\langle \bar{r}^2 \rangle^{1/2}$ given by

$$\langle \bar{r}^2 \rangle^{1/2} = lx^{1/2}. \quad (13)$$

This freely jointed chain model is clearly unreasonable for a real polymer, as bond hybridizations place restrictions on bond angles. We shall see later (Section IV) that this model can be improved by taking these restrictions into account. The actual end-to-end distance can be determined according to Eq. (68). The radius of gyration $\langle \bar{s}^2 \rangle^{1/2}$ is the rms distance of the units of a chain from its center of gravity. The radius of gyration and the actual end-to-end distance are related by

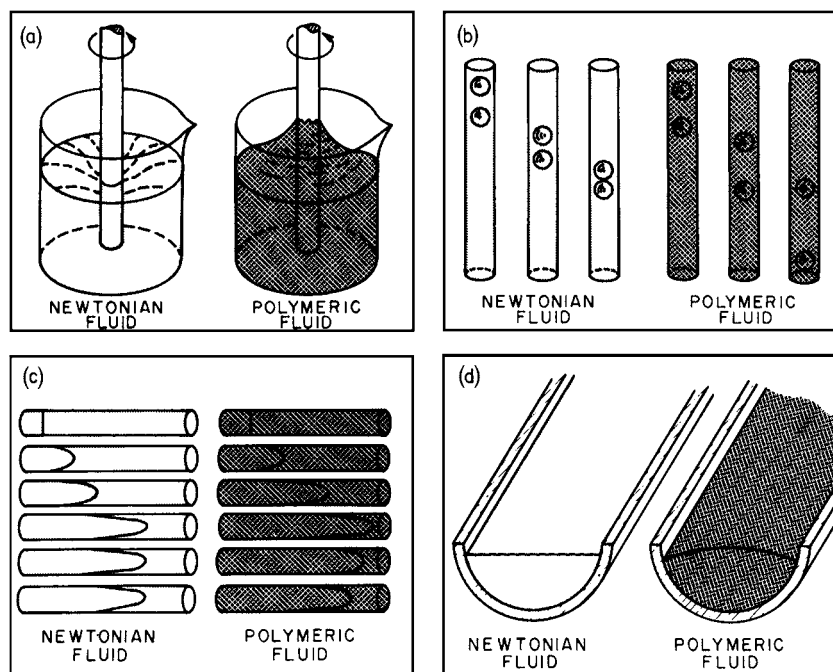


FIGURE 8 Several experiments illustrating the differences between a Newtonian fluid and a polymer fluid. (a) The surface of a Newtonian fluid is depressed near a rotating rod, whereas a polymeric fluid tries to climb the rod. (b) When two spheres are dropped one after the other into a Newtonian liquid, the second sphere always catches up and collides with the first one. In the polymeric liquid, if we wait a critical length of time between dropping the spheres, the spheres tend to move apart. (c) The two fluids are being pumped into circular tubes. The figure shows successive snapshots. The pump is turned off after the fourth frame. The Newtonian fluid comes to rest, whereas the polymeric liquid recoils, illustrating a “memory effect.” (d) When flowing in a trough, the surface of the Newtonian fluid is flat, except for a meniscus effect, whereas the polymeric liquid has a slightly convex surface. [From Bird, R. D., and Curtiss, C. F. (1984). *Phys. Today* **37**, 36–43.]

$$\bar{r}^2 = 6\bar{s}^2. \quad (14)$$

The radius of gyration is particularly important since it can be measured experimentally by light scattering and other techniques.

2. Polymer Solution Thermodynamics

As a consequence of their macromolecular size, polymers in solution exhibit large deviations from ideal behavior. (Ideal behavior is described by Raoult’s law, which states that the partial vapor pressure of a component in solution is proportional to the concentration of that species.) Polymers have very small entropies of mixing, which accounts for their large deviations from ideal behavior. The small entropy of mixing arises because of the size and interconnected nature of macromolecular chains. Whereas a small molecule can be distributed among solvent molecules in a great number of ways, there are fewer ways in which a polymer can be arranged.

The Flory–Huggins theory, developed in 1942 by P. J. Flory and M. L. Huggins, accounts for the restrictions that chain connectivity imposes on the arrangement of

solvent and solute. In this approach, the solution of solvent and macromolecule is treated as a lattice (Fig. 9). The number of distinguishable ways of arranging the N_1 solvent molecules of volume fraction v_1 and N_2 polymer molecules of volume fraction v_2 are then counted.

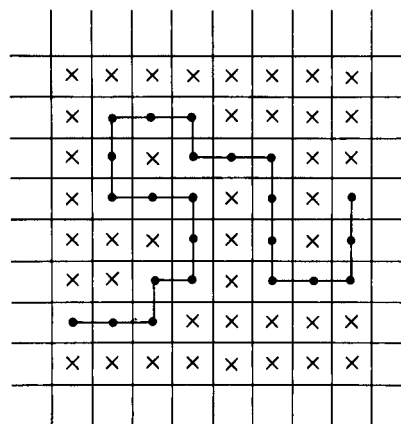


FIGURE 9 Lattice representation of a macromolecule (interconnected dots) in a solvent matrix. The x’s represent the solvent.

According to this method, the entropy and enthalpy of mixing are given by

$$\Delta S = -k(N_1 \ln v_1 + N_2 \ln v_2), \quad (15)$$

$$\Delta H = \chi kTN_1 v_2, \quad (16)$$

where χ is the Flory–Huggins interaction parameter. Because $\Delta G = \Delta H - T\Delta S$, the free energy of mixing is given by

$$\Delta G = kT(N_1 \ln v_1 + N_2 \ln v_2 + \chi N_1 v_2). \quad (17)$$

This master free-energy relationship can be used to obtain experimentally measurable quantities. These quantities can be used to determine molecular weight, as we shall see in the rest of this section.

For example, the chemical potential of a nonelectrolyte solution can be expressed as

$$\Delta\mu_1 = -RTV_1(A_1C_1 + A_2C_2^2 + A_3C_2^3 + \dots), \quad (18)$$

and the osmotic pressure π is

$$\pi = -\Delta\mu_1/V_1, \quad (19)$$

where V_1 is the molecular volume of the solvent and x is the number of chain segments. Here, A_2 is the second virial coefficient. When combined, Eqs. (18) and (19) give

$$\pi/C_2 = RTM_2^{-1} + RTA_2C_2 + RTA_3C_2^2 + \dots \quad (20)$$

We shall see later that light scattering measurements provide experimental determination of the second virial coefficient.

The Flory–Huggins theory holds for semidilute solutions, but does not address the consequence that very dilute polymer solutions must be discontinuous. Other theoretical treatments have been developed. The Flory–Krigbaum theory treats the system in terms of excluded volume effects. In this treatment, the θ temperature is the temperature at which the partial molar free energy from polymer–solvent interactions is zero, and the polymer adopts its unperturbed dimensions. The second virial coefficient goes to zero at the θ point.

A corresponding state theory has been set forth to correct the shortcomings of the above treatments. This theory can predict the volume changes that occur on mixing to 10–15% of the experimental value. More recently, deGennes has developed scaling concepts to describe the concentration region c^* (where polymer chains in solution begin to overlap), between the dilute ($c < c^*$) and semidilute ($c > c^*$) regimes (see Fig. 10). Scaling concepts make correct predictions about the dependence of the second virial coefficient on the number of links in a given polymer chain.

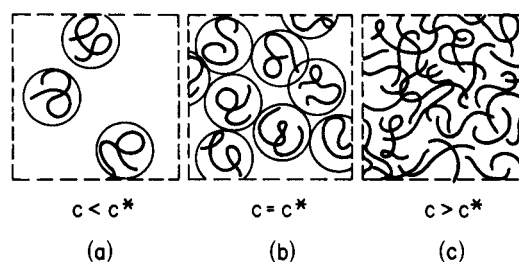


FIGURE 10 (a) Dilute coils swollen in a good solvent, below the overlap concentration. (b) Transition region c^* where the coils begin to overlap. (c) Semidilute region where coils overlap and display ideal size proportional to $\chi^{0.5}$.

C. Light Scattering

Light scattering from polymer solutions can be used to measure molecular weights between 10^4 and 10^7 g mol $^{-1}$. This method is very useful, as it provides the weight average molecular weight, the second virial coefficient, and the radius of gyration.

Polymer characterization by light scattering takes advantage of the fact that light is scattered whenever a beam of light impinges on matter. The electromagnetic wave interacts with the induced oscillating dipole in the molecule, thereby emitting light. We shall first develop the expressions for light scattering from small particles. We then amend these expressions to account for the situation when the wavelength of light and the size of the particle are comparable. This latter condition is generally true for polymers.

For dilute solutions of small molecules, we can treat each molecule as an independent point scatterer, and the scattering intensity will be proportional to the number of molecules. The Rayleigh's ratio R_θ , is the ratio between the scattered intensity (observed at angle θ from incident) and the incident beam. It is given by

$$R_\theta = 8\pi^4 \nu \alpha^2 (1 + \cos^2 \theta) / \lambda^4, \quad (21)$$

where ν is the number of molecules, α is the molecular polarizability, and λ is the wavelength of light. The molecular polarizability α is related to the dielectric constant D or to the refractive index n of the medium. In systems other than gases, destructive interference occurs and reduces the intensity of the scattered light.

The amount of this reduction in scattering intensity can be accounted for through fluctuation theory. In this treatment the local fluctuation of the dielectric constant is evaluated. Physically, the fluctuation in the dielectric constant arises from density or concentration fluctuations. According to Debye, the mean square concentration fluctuation is given by

$$\langle (\Delta c_2)^2 \rangle = \frac{kT}{(d^2G/dc_2^2)}, \quad (22)$$

where G is the free energy. A fluctuation in concentration is related to the osmotic pressure [recall from Eq. (19) that the osmotic pressure has the form dG/dc_2]. Equation (22) shows that a higher-than-equilibrium concentration fluctuation will be opposed by the osmotic pressure.

If we let ΔR_θ be the change in light scattering caused by concentration fluctuations, we can show that ΔR_θ is related to osmotic pressure π by

$$\Delta R_\theta = \frac{KTRc_2}{(d\pi/dc_2)}, \quad (23)$$

where

$$K = \frac{2\pi^2 n^2 (dn/dc_2)^2}{v\lambda^4}. \quad (24)$$

Proper evaluation of $(d\pi/dc_2)$ yields

$$Kc_2/\Delta R_\theta = 1/M + 2A_2c_2 + 3A_3c_2^2 + \dots, \quad (25)$$

where M is the solute molecular weight and A_2 is the second virial coefficient, as before. Equation (25) shows that a plot of $Kc_2/\Delta R_\theta$ versus c_2 will give an intercept of $1/M$ at $c_2 = 0$. Except in rare cases, polymers have a distribution in molecular weight. We can see the relationship between light scattering and weight average molecular weight \bar{M}_w by adding in the contributions from all species c_i with molecular weights M_i . In the limit of

$$c_2 \rightarrow 0, \quad \Delta R_\theta = \sum_i (\Delta R_\theta)_i = K \sum_i c_i M_i,$$

$$\lim_{c_2 \rightarrow 0} \frac{Kc_2}{\Delta R_\theta} = \frac{\sum_i c_i}{\sum_i c_i M_i} = \frac{1}{\bar{M}_w}. \quad (26)$$

We must now modify this expression to account for the generally encountered situation where the polymer dimensions are comparable to $\sim 1/20$ the wavelength of light. The particle can no longer be treated as a point scatterer because destructive interference occurs from light scattered by different parts of the particle itself. The destructive interference is largest at large angles θ between the incident and measured light, and it disappears as θ approaches zero. A correction factor, $P(\theta)$, is obtained by averaging over all possible angular relationships between the scattering points and the incident beam. The modified expression for $Kc_2/\Delta R_\theta$ becomes

$$\left(\frac{Kc_2}{\Delta R_\theta} \right)_{c_2 \rightarrow 0} = \frac{1}{\bar{M}_w P(\theta)}$$

$$= \frac{1}{\bar{M}_w} \left(1 + \frac{16\pi^2}{3\lambda^2} \langle s^2 \rangle \sin^2 \frac{\theta}{2} + \dots \right). \quad (27)$$

The weight average molecular weight, \bar{M}_w , is obtained by measuring $Kc_2/\Delta R_\theta$ at a number of concentrations

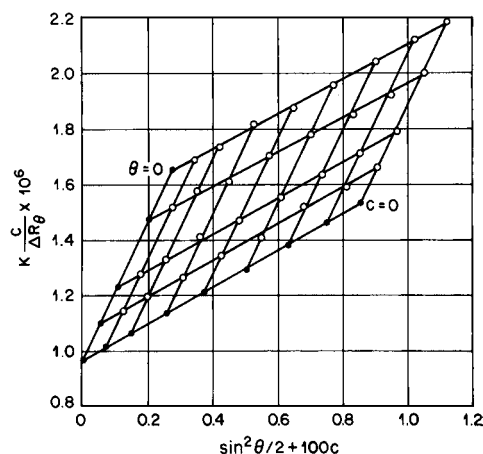


FIGURE 11 Zimm plot of light scattering data for polystyrene in butanone. [From Zimm, B. H. (1948). *J. Chem. Phys.* **16**, 1099.]

and as a function of scattering angle θ . A Zimm plot (see Fig. 11) is then constructed from the data. $Kc_2/\Delta R_\theta$ is plotted against $\sin^2(\theta/2)$. The points corresponding to the $c_2 = 0$ data and the $\theta = 0$ data are shown in Fig. 11 as filled circles. Lines through these points should intersect the ordinate at the same place, equal to $1/\bar{M}_w$. The second virial coefficient is obtained from the slope of the $\theta = 0$ line and the radius of gyration comes from the slope of the $c_2 = 0$ line.

D. Size Exclusion Chromatography

Size exclusion chromatography, also called gel permeation chromatography (GPC) is a widely employed method to determine molecular size. In this method, a chromatographic column is packed with porous beads. The beads are made either of glass or of polymeric material such as highly cross-linked polystyrene. They are prepared to have pore sizes that correspond approximately to the size of polymer molecules. The beads are equilibrated with the appropriate elution solvent before measurement is begun.

A solution of the polymer is introduced on the top of the column. Solvent is added to the top of the column to match the flux of solvent from the bottom of the column (Fig. 12). A detector, positioned immediately after the solvent has passed through the column, keeps track of the amount of solvent that has eluted (this amount is called the retention volume) as well as the amount of polymer in that volume. (The amount of polymer is detected by a number of methods, including ultraviolet spectroscopy or refractive index measurements.)

We can visualize how the column technique works by considering two extreme cases—a very small polymer

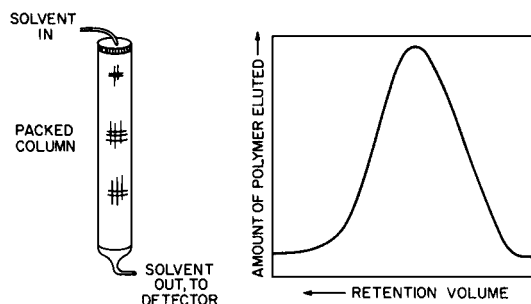


FIGURE 12 Schematic representation of a chromatographic column and typical data output (the chromatogram) from the detector. Large molecules elute first, at early retention volumes.

molecule and a very large one. When loaded onto the column, the small molecule begins its descent through the beads. Owing to its small size, it diffuses into the pores of the beads and is entrained in the internal structures of the beads during its journey to the bottom of the column. The very small molecule will spend much time on the column and will therefore have a large retention volume. The very large molecule, on the other hand, will be excluded, or mostly excluded, from the pores of the beads. Its journey to the bottom of the column will be relatively rapid, and it will appear in the early elution volumes.

So far we have shown that the molecules are eluted in order of decreasing molecular size. Calibrations are required to relate the retention volume to molecular weight. These calibrations are usually performed with commercially available polystyrenes of narrow molecular weight distributions. The position of the chromatogram peak thus gives \bar{M}_w indirectly through calibration curves. The width of the peak on the chromatogram is related to the molecular weight distribution \bar{M}_w/\bar{M}_n .

E. Ultracentrifugation

Ultracentrifugation methods are used primarily for the determination of biopolymer molecular weights. A solution of the polymer is placed in a centrifuge cell. (The solvent has been carefully selected for its density and refractive index differences from the polymer.) The centrifuge cell is placed in a rotor. The cell and rotor are constructed to allow refractive index measurements along the length of the cell. Centrifugation is then performed under vacuum at high speed and at controlled temperatures. There are several variations of the centrifugation experiment.

The sedimentation equilibrium experiment consists of centrifuging the sample at low speeds for long periods of time. At equilibrium the polymer is distributed according to its molecular weight. At this point the centripetal force is exactly balanced by the back diffusion of the polymer

along the concentration gradient in the cell. In mathematical terms, this means that force on a particle of mass m , which is a distance r from the center of the rotor rotating at angular velocity ω , is given by

$$F = \omega^2 r (1 - \bar{v}\rho)m, \quad (28)$$

where ρ is the density of the solution and \bar{v} is the partial specific volume of the polymer. For ideal solutions it can be shown from this expression that

$$\bar{M}_w = \frac{2RT \ln(c_2/c_1)}{(1 - \bar{v}\rho)\omega^2(r_2^2 - r_1^2)}, \quad (29)$$

where c_1 and c_2 are the concentrations at points r_1 and r_2 in the cell.

A variation of this experiment is sedimentation equilibrium in a density gradient. A centrifuge cell containing a known density gradient is prepared. (Sucrose density gradients are often used for biological polymers.) Upon centrifugation, the polymer distributes itself in the band with the density that exactly matches its own.

High speed centrifugation is used in the sedimentation transport experiment. The sedimentation constant, s_c , describes the rate at which the polymer moves to the bottom of the cell:

$$s_c = \frac{1}{\omega^2 r} \frac{dr}{dt} = \frac{m(1 - \bar{v}\rho)}{f}, \quad (30)$$

where f is the frictional coefficient. The frictional coefficient for a random coil polymer is not the simple one calculated for a hard sphere by Stokes' law but rather can be related to the diffusion coefficient D . At infinite dilution f is given by

$$f = kT/D, \quad (31)$$

and s_c becomes

$$s_c = Dm(1 - \bar{v}\rho)/kT. \quad (32)$$

The distribution in s_c can be converted to a distribution in molecular weight.

F. Viscosity Measurements

Solutions of polymers are viscous and viscosity measurements can be used to determine polymer molecular weights. Viscosity provides an indirect measure of molecular weight, since a calibration curve must be established for viscosity measurements, as is also the case for GPC measurements. Experimental viscosity measurements are performed in a capillary viscometer such as the one shown in Fig. 13(a). The viscosity experiment consists of first measuring the time t_0 that it takes for the solvent to pass between the two etched lines on the viscometer. Then the

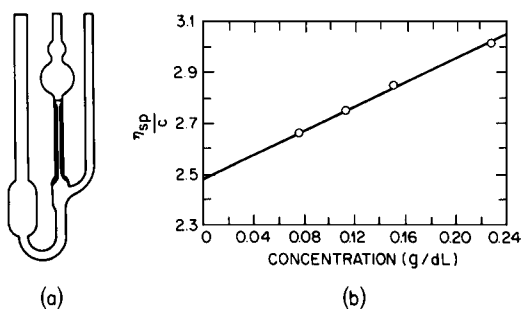


FIGURE 13 (a) A capillary viscometer of Ubbelohde design and (b) typical viscosity data.

times t are measured for polymer solutions of various concentrations c , expressed in g/dL, to pass between the two lines. The specific viscosity η_{sp} is given by

$$\eta_{sp} = (t - t_0)/t_0. \quad (33)$$

The viscosity data obtained as a function of concentration are plotted according to the Huggins equation

$$\eta_{sp}/c = [\eta] + k'[\eta]_c^2, \quad (34)$$

where k' is a constant for a particular polymer in a given solvent regardless of chain length. The graphical data are extrapolated to zero concentration to give the intrinsic viscosity, $[\eta] = (\eta_{sp}/c)_{c=0}$. Figure 13(b) shows such a plot; $[\eta]$ is customarily expressed in dL/g.

The viscosity average molecular weight \bar{M}_v can be determined after constructing a calibration curve. Such a curve is shown in Fig. 14. It is a double-log plot of intrinsic viscosity $[\eta]$ versus molecular weight of carefully fractionated samples. Such a plot provides the values of the constants K' and α for a given polymer-solvent pair, where

$$[\eta] = K' M^\alpha. \quad (35)$$

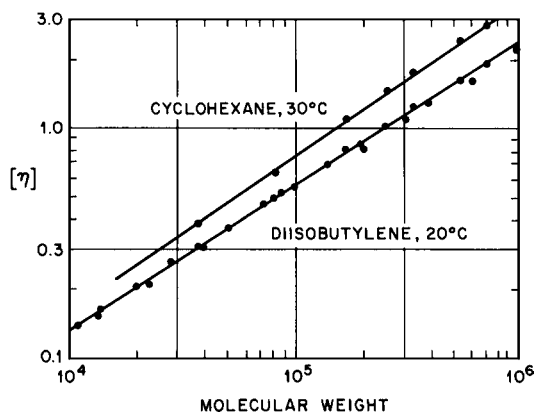


FIGURE 14 Intrinsic viscosity data for polyisobutylene as a function of molecular weight. Data are shown for two solvents.

The viscosity average molecular weight \bar{M}_v is given by

$$\begin{aligned} \bar{M}_v &= \left(\sum_i v_i M_i^\alpha \right)^{1/\alpha} \\ &= \left(\sum_i N_i M_i^{1+\alpha} / \sum_i N_i M_i \right)^{1/\alpha}. \end{aligned} \quad (36)$$

Note that \bar{M}_v reduces to \bar{M}_w when $\alpha = 1$. We shall later see that viscosity measurements made in θ solvents can be used to provide information about the unperturbed dimensions of a polymer chain.

G. Osmotic Pressure

Osmotic pressure, like the other colligative properties such as freezing point depression, boiling point elevation, and vapor pressure lowering, derives from Raoult's law. We have already seen in Eq. (19) that the osmotic pressure π is given by

$$\pi = \Delta \bar{G}_1 / V_1 = -(\mu_1 - \mu_1^0) / V_1, \quad (37)$$

where V_1 is the molecular volume of the solvent and μ_1 and μ_1^0 are the solvent activities with and without polymer. In analogy to the expansions in Eqs. (20) and (25),

$$\pi/c_2 = RT[(1/M) + A_2 c_2 + A_3 c_2^2 + \dots]. \quad (38)$$

At infinite dilution

$$(\pi/c_2)_{c_2=0} = RT/M, \quad (39)$$

and for polydisperse systems,

$$\pi = RT \sum_i \frac{c_i}{M_i} = \frac{RT c_2}{\bar{M}_n}. \quad (40)$$

There are two main types of osmometers. The vapor-phase osmometer is used for samples with low molecular weights ($<40,000$) and the membrane osmometer is best for higher molecular weights.

The vapor-phase osmometer works by measuring very small differences in temperature that arise from condensation of solvent. The pure solvent and the polymer solution are alternately dropped via a syringe onto a thermistor in a solvent-saturated chamber. The solvent in the polymer solution droplet has a lower activity than the pure solvent and therefore prefers to condense rather than evaporate. Condensation liberates heat of vaporization, thereby leading to a temperature differential. This difference temperature is proportional to the vapor pressure lowering, and thus to \bar{M}_n .

In a membrane osmometer, the solvent and the polymer solution are placed on opposite sides of a semipermeable membrane. The membrane allows the solvent to

pass through but not the polymer. The solvent diffuses through the membrane into the polymer solution in an attempt to equalize the solvent pressure on both sides of the membrane. This sets up a pressure difference that can be measured by a transducer or other appropriate methods.

III. MICROSTRUCTURE OF MACROMOLECULES

We have seen (Section I.B) the types of structural isomerism of which polymer chains are capable—in particular the occurrence of various types of stereochemical isomerism, branching and cross-linking, head-to-tail versus head-to-head:tail-to-tail isomerism, and monomer sequence isomerism in copolymers. We now describe briefly the two principal forms of spectroscopy that are used to observe and measure these structural features.

A. Vibrational Spectroscopy

The spectroscopic method that has the longest history for the study of macromolecules is infrared. More recently applied and very closely related is Raman spectroscopy. Both deal with relatively high-frequency processes that involve variation of internuclear distances (i.e., molecular vibration). (Rotational and translational processes will not concern us in polymer spectra.) As a first approximation we may imagine that these molecular vibrators can be considered as classical harmonic oscillators. For a diatomic molecule of unequal masses m_1 and m_2 connected by a bond regarded as a spring with a force constant k , the frequency of vibration expressed in wave numbers (i.e., cm^{-1} or reciprocal wavelength) is given by

$$\nu = (1/2\pi c)(k/m_r)^{1/2}, \quad (41)$$

where c is the velocity of light and m_r the reduced mass, given by

$$m_r = m_1 m_2 / (m_1 + m_2) \cong m_1 \quad \text{if } m_2 \gg m_1. \quad (42)$$

Thus, a small mass, such as hydrogen or deuterium, vibrating against a larger one, such as a carbon or chlorine atom, will have essentially the frequency characteristic of the smaller one. Most molecular vibration frequencies of interest for polymer characterization will be in the range of 3500 to about 650 cm^{-1} or in wavelength 2.5 to 15 μm .

Actual molecular vibrators differ from the classical oscillator in two respects. First, the total energy E cannot have any arbitrary value but is expressed in terms of integral quantum numbers n :

$$E = (n + 0.5)h/2\pi(k/m_r)^{1/2} = (n + 0.5)h\nu, \quad (43)$$

where h is Planck's constant. The transition energies are given by $h\nu$. Only transition between adjacent levels are allowed in a quantum mechanical harmonic oscillator. Second, the molecular vibrator is not strictly harmonic but rather anharmonic, with vibrational levels becoming more closely spaced and transitions somewhat smaller in energy as n is increased. Another consequence of anharmonicity is that selection rules are relaxed, permitting transitions to levels higher than the next immediately higher one. Transitions from $n = 0$ to $n = 2$ correspond to the appearance of weak but observable first overtone bands having slightly less than twice the frequency of the fundamental band.

The appearance of a vibrational absorption band in the infrared region requires that the impinging radiation supply a quantum of energy ΔE just equal to that of the vibrational transition $h\nu$. It is also necessary that the atomic vibration be accompanied by a change in the electric dipole moment of the system, thus producing an alternating electric field of the same frequency as the radiation field. This condition is often not met, as for example in the vibrations of homopolar bonds such as the carbon-carbon bonds in paraffinic polymers.

The Raman spectrum can give much the same information as the infrared spectrum, but they are in general not identical and can be usefully complementary. In Fig. 15 we see at the left the Rayleigh scattering process, in which the molecule momentarily absorbs a photon, usually of visible light, and then reradiates to the ground state without loss of energy. However, the excited molecule may also return to a higher vibrational state—the next highest in Fig. 15 (center)—and then the reradiated photon will be of lower frequency by $\Delta\bar{\nu}$. In a complex molecule there will be many such states, and so the Raman spectrum, like the

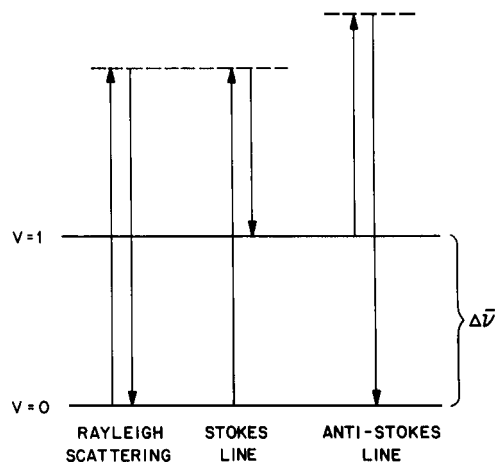


FIGURE 15 Energy level diagram for Raman scattering.

infrared spectrum, will appear as a number of lines, called the Stokes lines, much weaker than the exciting radiation and shifted to longer wavelength by a few hundred to two or three thousand wave numbers. (Antistokes lines corresponding to excitation from a higher vibrational state are also observed but are much weaker and not normally employed.)

For Raman emission to occur, the polarizability of the bond must change during the vibration. In polymers, most lines appear in both infrared and Raman spectra, an important exception being paraffinic carbon-carbon vibrations, which are inactive in the infrared (*vide supra*) but active in the Raman spectrum.

In polymers, as in small molecules, we may recognize vibrational bands specific to particular types of bonds and functional groups. These appear in the high-frequency region of the spectrum regardless of the actual compound or structure in which they occur. At the low-frequency end of the spectrum, the vibrational bands are more characteristic of the molecule as a whole. This region is commonly called the "fingerprint" region, since detailed comparison here usually enables specific identification to be made.

In the region near 3000 cm^{-1} appear the C-H bond stretching vibrations (Fig. 16), which may be asymmetric or symmetric, as illustrated in Fig. 17. These occur in nearly all polymer spectra and so are not structurally diagnostic, although useful in a more fundamental sense. At lower frequencies, corresponding to smaller force constants, are the deformation vibrations involving valence angle bending or scissoring, giving a large band near 1500 cm^{-1} ; wagging and twisting near 1300 cm^{-1} ; and

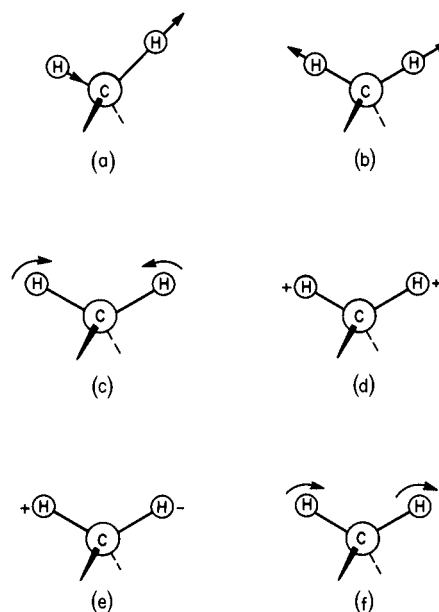


FIGURE 17 Stretching and deformation vibrational modes of the methylene group; (a) asymmetric stretching, 2926 cm^{-1} ($3.42\text{ }\mu\text{m}$); (b) symmetric stretching, 2853 cm^{-1} ($3.51\text{ }\mu\text{m}$); (c) scissoring deformation, 1468 cm^{-1} ($6.81\text{ }\mu\text{m}$); (d) wagging deformation, 1350 cm^{-1} ($7.41\text{ }\mu\text{m}$); (e) twisting deformation, 1305 cm^{-1} ($7.66\text{ }\mu\text{m}$); and (f) rocking deformation, 720 cm^{-1} ($13.89\text{ }\mu\text{m}$).

finally rocking deformations, appearing at the low-energy end of the usual spectrum. (At still lower frequencies are torsion and skeletal as well as intermolecular and lattice vibrations, which we shall not discuss here.)

In Fig. 16 a number of other characteristic vibrational bands and their frequency ranges are also shown. We may take particular note of the carbonyl stretch band near 1700 cm^{-1} , the C-C stretch band near 1600 cm^{-1} , and the olefinic C-H bending bands between 900 and 1000 cm^{-1} .

The design and operation of instruments for the observation of vibrational spectra—conventional and Fourier transform infrared spectrometers and Raman spectrometers—are described in other articles in this encyclopedia. We note here that polymer samples may be observed as mulls in Nujol or fluorolube and also (most commonly) as films. They may also be ground up with KBr, which is transparent to visible and infrared, and observed as pellets. Solutions in CS_2 or CCl_4 are occasionally also used. The initial radiation intensity falling on the sample I_0 will be attenuated in proportion to the path length b and, for solutions, to the concentration c ; thus

$$I = I_0 e^{-a'bc}, \quad (44)$$

where a' is the extinction coefficient or absorptivity characteristic of the band observed. For polymer films c , if

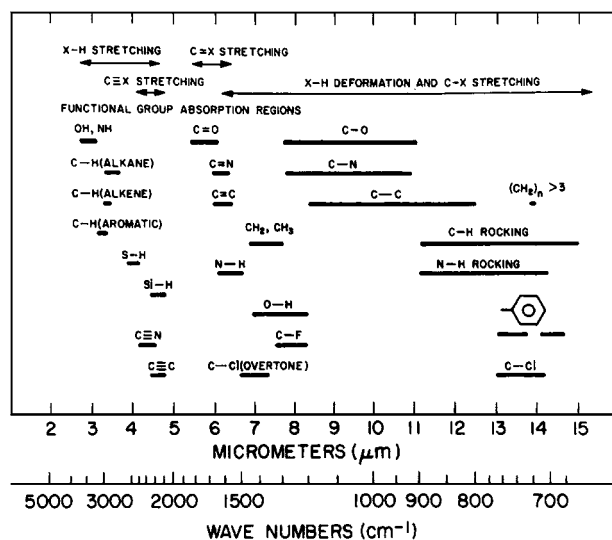


FIGURE 16 Infrared bands of interest in polymers.

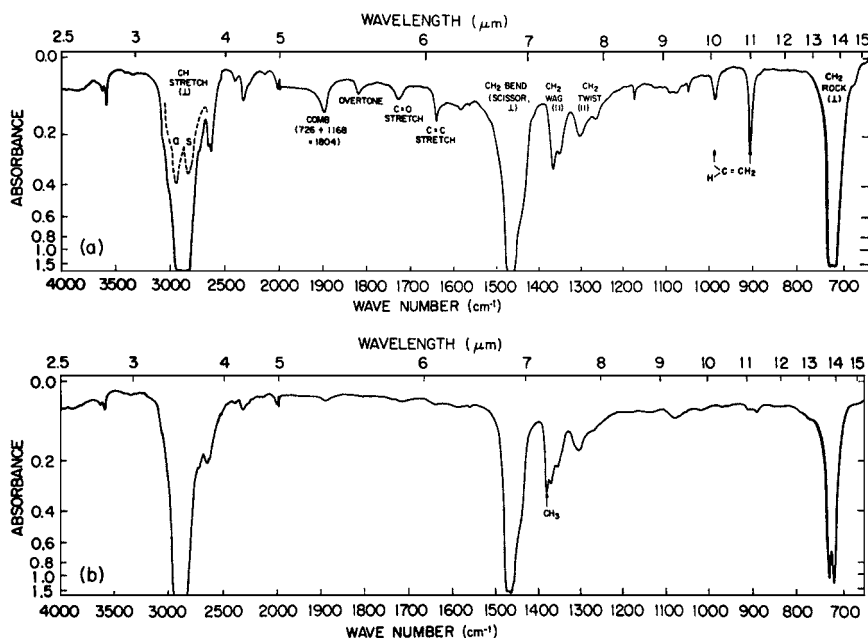


FIGURE 18 Infrared spectra of (a) linear and (b) branched polyethylenes.

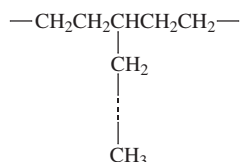
expressed in gm/cm^3 , will be approximately unity. We then have

$$2.303 \log_{10}(I_0/I) = a'bc. \quad (45)$$

The quantity $\log_{10}(I_0/I)$ is the absorbance or optical density and is the quantity on the vertical axis of typical infrared spectra.

In Fig. 18 the infrared spectra of (a) linear and (b) branched polyethylenes are shown. The principal bands are labeled in accordance with the vibrational assignments already discussed. The intense C—H stretch region is twofold owing to the splitting into asymmetric and symmetric bands, as shown in the inset dashed spectrum in Fig. 18a. Bands for carbonyl groups (1725 cm^{-1}), resulting from slight oxidation, and terminal vinyl groups are observable in the spectrum of the linear polyethylene. If accurate values of a' (from model compounds) and b are established, the content of these groups can be measured quantitatively.

Short branches in high-pressure polyethylene may be determined by counting their terminal methyl groups:



In Fig. 18b the CH_3 distortion band at 1375 cm^{-1} (arrow) provides a measure of the methyl content if linear material is employed as a blank. However, the determination of branch length, type, and distribution requires

carbon-13 NMR spectroscopy (see Section III.B). Such short branches are of particular importance in polyethylene since, as we have seen (Section I.E), their presence reduces the melting point and extent of crystallinity.

Vibrational spectroscopy is useful in many other determinations, including geometrical isomerism in polydienes (see Section III.D) and in the observation of conformational isomers, which may be too short-lived or otherwise unobservable by NMR. It is often quicker and simpler, especially in the solid state.

B. Nuclear Magnetic Resonance Spectroscopy (NMR)

This is a powerful and versatile technique, useful in both the solution and solid states for the qualitative and quantitative observation of polymer structure. The phenomenon of NMR depends on the fact that some nuclei possess spin or angular momentum. Such nuclei are described by spin quantum numbers I (the "spin") having integral or half-integral values. When placed in a magnetic field of strength B_0 , such nuclei occupy $2I + 1$ energy levels with relative populations normally given by a Boltzmann distribution. We shall deal here with the proton (^1H), ^{19}F , and the ^{13}C nucleus only, although ^{29}Si , ^{15}N , ^{31}P , and ^2H are also useful for polymers and biopolymers.

The spacing of magnetic energy levels is given by

$$\Delta E = h\nu_0 = 2\mu B_0, \quad (46)$$

where μ is the magnetic moment of the nucleus. Transitions between these energy levels can be made to occur

by means of a resonant radio frequency field having a frequency ν_0 . In modern instruments, this resonant field is supplied as a pulse of radiofrequency energy and the resonance signal appears as an oscillating current in the time domain (“free induction decay” or fid), which must be Fourier transformed by computer to the normal spectrum in the frequency domain.

The value of NMR to the chemist lies in the fact that at any particular value of ν_0 all nuclei of a given species—say, all protons—do not resonate at exactly the same value of B_0 (or vice versa). Resonance actually occurs at slightly different values of B_0 for each type of proton, depending upon its chemical binding and position in the molecule. The cause of this variation is the cloud of electrons about each nucleus. Protons attached to or near electronegative groups such as OR, OH, OCOR, CO₂R, or halogens experience a lower electron density and appear at the left in the NMR spectrum, while those removed from such groups, as in hydrocarbon chains, appear at the right. Similar structural relationships are observed for ¹³C nuclei, which also show a marked dependence on conformation. These variations are termed chemical shifts and are commonly expressed in relation to tetramethylsilane (TMS) as the zero of reference. For protons the total range of chemical shifts in organic compounds is ~ 10 ppm. For ¹³C it is much greater—over 200 ppm. The ¹³C nucleus constitutes only 1.1% of naturally occurring carbon (¹²C has no spin and is not observable by NMR) and consequently requires substantial spectrum accumulation.

For any nucleus, the separation of chemical shifts, expressed in hertz (Hz), is proportional to B_0 . An important advantage of high-field magnets is the improved resolution of resonances and finer discrimination of structural features. Spectrometers employing superconducting magnets, operating at 200 to 500 MHz for protons, are best suited for studies of polymers in solution.

Another important parameter in NMR spectra is nuclear coupling. If a nucleus has n sufficiently close equivalently coupled neighbors, its resonance will be split into $n + 1$ peaks, with intensities given by the coefficients of the binomial expansion. Thus, one neighboring spin splits the observed resonance to a doublet, two produce a 1:2:1 triplet, three a 1:3:3:1 quartet, and so on. The strength of the coupling is denoted by J and expressed in hertz. Proton–proton couplings through three intervening bonds—termed “vicinal”—are strongly dependent on the dihedral angle between the protons. This is dealt with in Section IV.

C. Stereochemical Configuration

In Fig. 19 the 500-MHz proton spectra of poly(methyl methacrylate) prepared (a) with a free radical initiator and

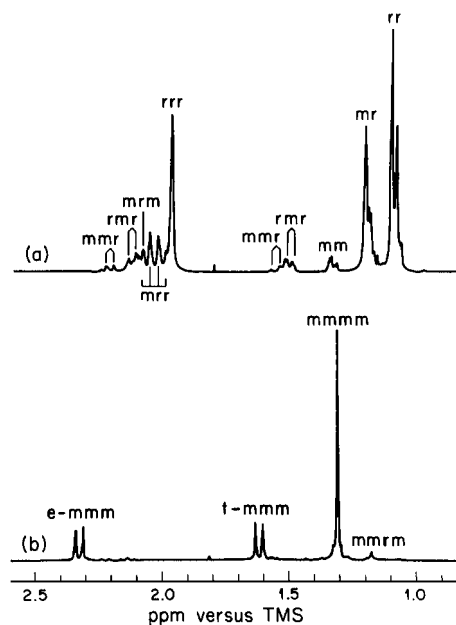
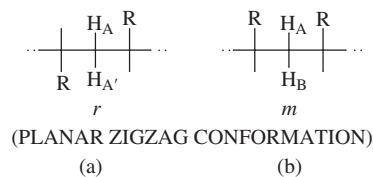


FIGURE 19 500-MHz proton NMR spectra of predominantly (a) syndiotactic and (b) isotactic samples of poly(methyl methacrylate), observed in 10% chlorobenzene-*d*₅ solution at 100°C. The methoxyl resonance is not shown, but appears as ≈ 3.4 ppm.

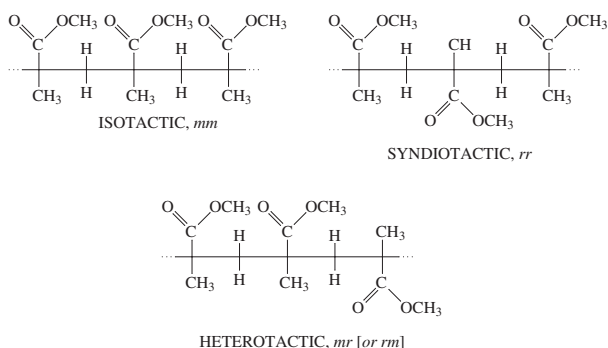
(b) with fluorenyllithium in toluene, an anionic initiator are shown. The profound effect of the nature of the initiator is evident in the marked differences between these spectra. To interpret these spectra, let us consider the chain in terms of sequences of two monomer units or dyads. There are two possible types of dyads and they have different symmetry properties. The syndiotactic or racemic (*r*) dyad has a twofold axis of symmetry and consequently the two methylene protons are in equivalent environments. They therefore have the same chemical shift and appear as a singlet resonance despite strong two-bond or geminal coupling between them. The isotactic or meso (*m*) dyad has no symmetry axis, and so the two protons are nonequivalent and should in general give different chemical shifts.



When there is no vicinal coupling to neighboring protons, as is the case in poly(methyl methacrylate), the syndiotactic sequences should exhibit a methylene singlet while the isotactic form should give two doublets, each with a spacing equal to the geminal coupling, ~ 15 Hz. We see in Fig. 19 that the methylene spectrum of the anionically

initiated polymer (b) is almost exclusively a pair of doublets; quantitative assessment shows that this polymer is 95% isotactic. The methylene spectrum of the free radical polymer (a) is more complex, but the principal resonance—at 1.9 ppm—is a singlet, showing that this polymer is predominantly syndiotactic but more irregular than (b). This is generally the case for free radically initiated vinyl polymers. (The other resonances are discussed later in this section.)

We see that proton NMR can provide absolute stereochemical information concerning polymer chains without recourse to X-ray or other methods. Somewhat more detailed, but not absolute, information can be gained from the methyl proton resonances near 1.2 ppm. [The ester methyl resonance at ~ 3.6 ppm (not shown) is less sensitive to stereochemistry.] In both spectra we note three peaks—or, more correctly, groups of peaks—appearing in similar positions but with greatly different intensities. These correspond to the α -methyl groups in the center monomer unit of the three possible triad sequences: isotactic, syndiotactic, and heterotactic. These may be more simply and appropriately designated by the m and r terminology, as indicated. Measurement of the relative intensities of the mm , mr , and rr α -methyl peaks, which appear from left to right in both spectra in this order, gives a valid statistical representation of the structure of each polymer.



From the triad data we may gain considerable insight into the mechanism of propagation. This is one of the principal uses of such information. Let us designate by P_m the probability that the polymer chain will add a monomer unit to give the same configuration as that of the last unit at its growing end (i.e., that an m dyad will be generated). We assume that P_m is independent of the stereochemical configuration of the growing chain. The generation of the chain is a Bernoulli trial process; it is like reaching into a large jar of balls marked m and r and withdrawing a ball at random. The proportion of m balls in the jar is P_m . Since two monomer additions are required to form a triad sequence, it is readily evident that the probabilities of their formation are

$$[mm] = P_m^2,$$

$$[mr] = 2P_m(1 - P_m),$$

$$[rr] = (1 - P_m)^2.$$

The heterotactic sequence must be given double weighting because both directions, mr and rm —observationally indistinguishable—must be counted. A plot of these relationships is shown in Fig. 20. Note that the proportion of mr (heterotactic) units rises to a maximum when P_m is 0.5, corresponding to a strictly random or atactic configuration for which $[mm]:[mr]:[rr]$ will be 1:2:1. For any polymer, if Bernoullian, the $[mm]$, $[mr]$, and $[rr]$ sequence intensities will lie on a single vertical line in Fig. 20, corresponding to a single value of P_m . Spectrum (a) in Fig. 19 corresponds to these simple statistics, P_m being 0.25 ± 0.01 ; the polymer corresponding to spectrum (b) does not. The propagation statistics in this case can be interpreted to indicate that the probability of isotactic placement is dependent on the stereochemical configuration of the growing chain and cannot properly be expressed by a single parameter such as P_m . Free-radical and cationic propagations always give predominantly syndiotactic chains. Anionic initiators may also do

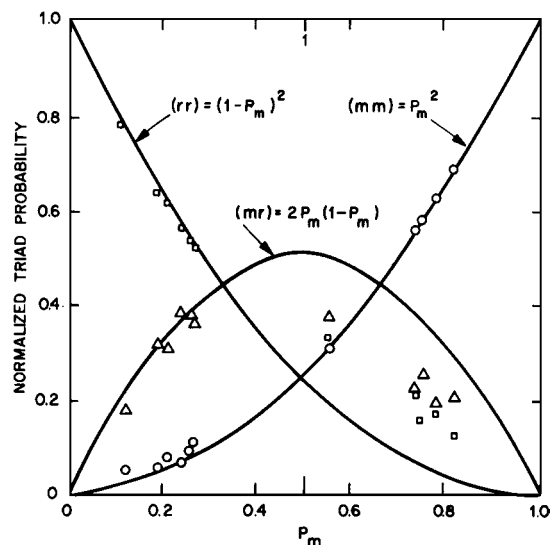


FIGURE 20 The probabilities of isotactic $[mm]$, heterotactic $[mr]$, and syndiotactic $[rr]$ triads as a function of P_m , the probability of m placement. The points on the left-hand side are for methyl methacrylate polymers prepared with free-radical initiators and those on the right-hand side are for polymers prepared with anionic initiators. For polymer (a) the points for $[rr]$ have been arbitrarily placed on the $[rr]$ curve and the others fall where they may and for polymer (b) the $[mm]$ points have been placed on the $[mm]$ curve.

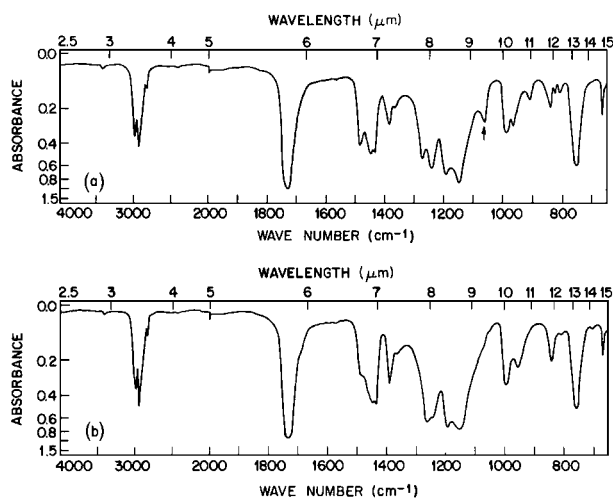


FIGURE 21 Infrared spectra of predominantly (a) syndiotactic and (b) isotactic films of polymethyl methacrylate.

so if strongly complexing ether solvents such as dioxane or glycol dimethyl ether are employed rather than hydrocarbon solvents as in polymer (b) of Fig. 19.

Vibrational spectra also reveal stereochemical differences. In Fig. 21 infrared spectra of films of predominantly syndiotactic (a) and isotactic (b) methyl methacrylate polymers are shown. In addition to other smaller differences, there is a conspicuous band at 1060 cm^{-1} in the syndiotactic polymer spectrum (arrow), which is absent in that of the isotactic polymer. Such observations can serve as quick measures of chain stereochemistry, but in general infrared is not as discriminating nor as quantitative as NMR.

It is evident that in the spectra of Fig. 19 there is fine structure in both the methylene and methyl regions that we have not discussed. In spectrum (a) this corresponds principally to residual resonances of the stereoirregular portions of the chains; in (b) such residual resonances are less conspicuous. These arise from sensitivity to longer stereochemical sequences than dyad and triad. In Table III planar zigzag projections of such sequences, together with their frequency of occurrence as a function of P_m , assuming Bernoullian propagation are shown. The tetrads—and all “even-ads”—refer to observations of β -methylene protons (or β carbons), while the “odd-ads” refer to substituents on the α -carbons (or α -carbons themselves). Resonances for tetrad sequences or higher even-ads should appear as fine structure in the dyad spectra, while pentad sequences or higher odd-ads should appear as fine structures on the triad resonances. The assignments to longer sequences as indicated on the spectra are based on Bernoullian probabilities in spectrum (a); those in spectrum (b) are primarily based on (a). It may be noted that r -centered tetrads (e.g., *mrr*)

do not necessarily appear as singlets if the sequence as a whole lacks a twofold axis.

The numbers of observationally distinguishable configurational sequences, or n -ads, designated $N(n)$, obey the relationship

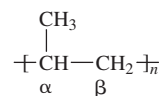
n	2	3	4	5	6	7	8	9
$N(n)$	2	3	6	10	20	36	72	136

or in general

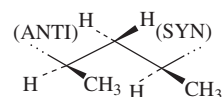
$$N(n) = 2^{n-2} + 2^{m-1}, \quad (47)$$

where $m = n/2$ if n is even and $m = (n - 1)/2$ if n is odd. Discrimination of these longer sequences is unlikely to be possible beyond $n = 6$ (hexads) or $n = 7$ (heptads). The observation of such sequences permits rather searching tests of polymerization mechanisms.

Another example is provided by polypropylene, particularly instructive as it is one of the few vinyl polymers that can be prepared in both



isotactic and syndiotactic forms with coordination catalysts. The proton spectra are relatively complex because of vicinal coupling between α and β protons and α and methyl protons as well as geminal methylene proton coupling in isotactic sequences. In Fig. 22, 220-MHz proton spectra of isotactic (a) and syndiotactic (b) polypropylene are shown. The β protons of the syndiotactic polymer appear as a triplet at 1.03 ppm corresponding to a single chemical shift and J-coupling to two neighboring α protons. In the isotactic polymer they appear as widely spaced multiplets at 1.27 and 0.87 ppm, corresponding to syn and anti positions in the *trans-trans* conformation:



Analysis of these spectra yields the following values for the vicinal main-chain couplings (in both polymers the vicinal $\text{CH}_3\text{---H}_\alpha$ coupling is 5 Hz and geminal methylene proton coupling is -13.5 Hz):

Isotactic

$$J_{\text{H}_\alpha\text{---H}_{\text{syn}}}: \quad 6.0 \text{ Hz}$$

$$J_{\text{H}_\alpha\text{---H}_{\text{anti}}}: \quad 7.0 \text{ Hz}$$

Syndiotactic

$$J_{\text{---CH}_2\text{---CH}_2}: \quad 4.8, 8.3 \text{ Hz}$$

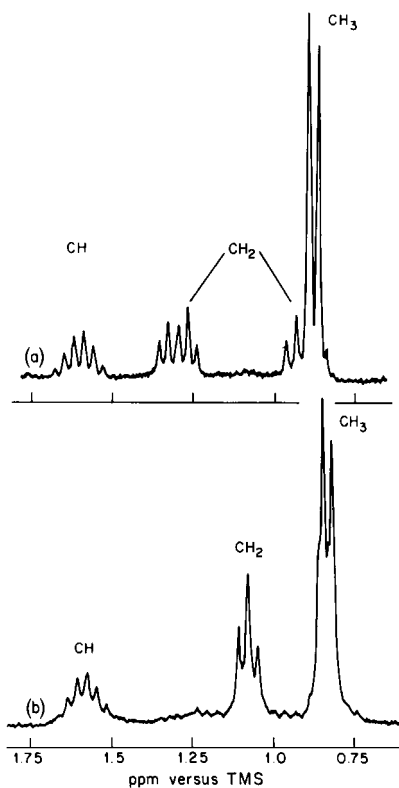


FIGURE 22 The 220-MHz proton NMR spectra of (a) isotactic and (b) syndiotactic polypropylenes observed in *o*-dichlorobenzene at 165°C.

The interpretation of these couplings in terms of chain conformation is discussed in Section IV.B.1.

The proton spectrum of atactic polypropylene (not shown) is virtually uninterpretable, being a complex of overlapping multiplets. In Fig. 23 the 25-MHz ^{13}C spectra of isotactic (a), atactic (b), and syndiotactic (c) polypropylene, observed in 20% 1,2,4-trichlorobenzene solution are shown. (In ^{13}C NMR it is customary to irradiate the protons at their resonant frequency to remove the multiplicity arising from ^1H - ^{13}C J-coupling; this increases observing sensitivity and simplifies the spectrum with no loss of essential information.) The isotactic and syndiotactic polymers give very similar spectra but with readily observable chemical shift differences, especially for the methyl carbons. This sensitivity to stereochemical configuration is particularly clear in the spectrum of the atactic polymer in which the methyl resonance is split into peaks corresponding to nine of the ten possible pentad sequences (Table III). It is also noteworthy that the syndiotactic polymer is less stereoregular than the isotactic and that the configurational statistics of both the atactic and syndiotactic polymers depart markedly from Bernoullian. This is generally the case for chains generated by coordination catalysts.

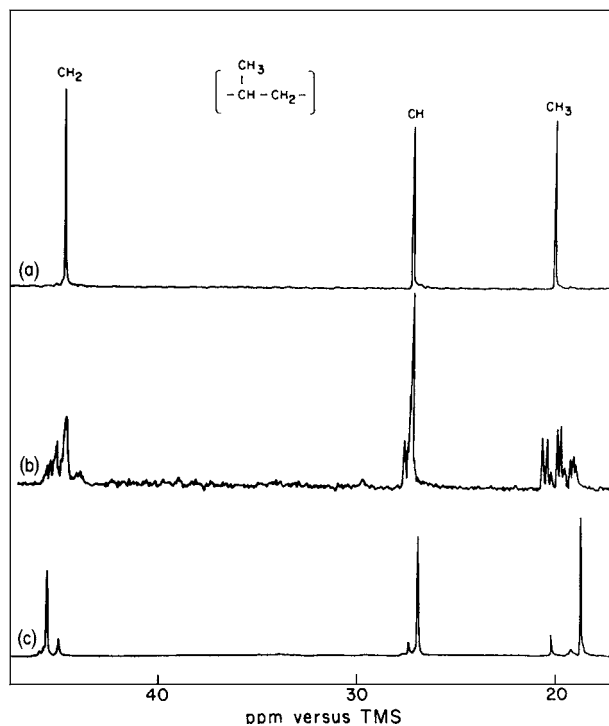
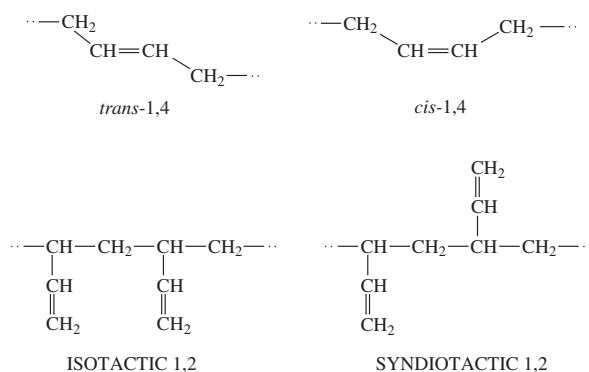


FIGURE 23 The 25-MHz ^{13}C spectra of three preparations of polypropylene: (a) isotactic, (b) atactic, and (c) syndiotactic observed as 20% (w/v) solutions in 1,2,4-trichlorobenzene at 140°C.


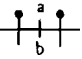

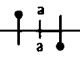
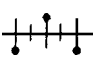
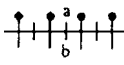
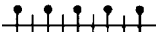
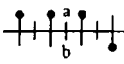

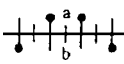

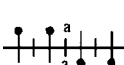
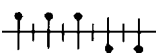
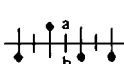
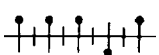
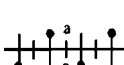
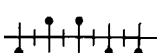
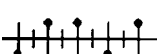
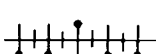
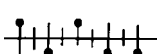
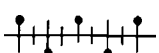
D. Geometrical Isomerism

Isomerism in diene polymer chains (Section I) can be detected and measured by both vibrational and NMR spectroscopy. In addition to the *cis* and *trans* structures found in natural isoprene polymers, the formation of such polymers by chain propagation of dienes proceeds also by incorporation of the monomer through one double bond rather than by 1,4 addition. Thus for butadiene, using coordination catalysts, these isomeric chains may be formed:



Polybutadiene formed by free-radical propagation contains all of these units, as we shall see. In Fig. 24 the

TABLE III Stereochemical Sequences and Their Probabilities

α Substituent			β -CH ₂		
Designation	Projection	Bernoullian probability	Designation	Projection	Bernoullian probability
Triad			Dyad		
Isotactic, <i>mm</i> (i)		P_m^2	meso, <i>m</i>		P_m
Heterotactic, <i>mr</i> (h)		$2P_m(1 - P_m)$	racemic, <i>r</i>		$(1 - P_m)$
Syndiotactic, <i>rr</i> (s)		$(1 - P_m)^2$	Tetrad		
Pentad			<i>mmm</i>		P_m^3
<i>mmmm</i> (isotactic)		P_m^4	<i>mnr</i>		$2P_m^2(1 - P_m)$
<i>mmmr</i>		$2P_m^3(1 - P_m)$	<i>rmr</i>		$P_m(1 - P_m)^2$
<i>rmmr</i>		$P_m^2(1 - P_m)^2$	<i>rrm</i>		$P_m^2(1 - P_m)$
<i>mmrm</i>		$2P_m^3(1 - P_m)$	<i>rrm</i>		$2P_m(1 - P_m)^2$
<i>mmrr</i>		$2P_m^2(1 - P_m)^2$	<i>rrr</i>		$(1 - P_m)^3$
<i>rrmm</i> (heterotactic)		$2P_m^2(1 - P_m)^2$			
<i>rmrr</i>		$2P_m(1 - P_m)^3$			
<i>mrrm</i>		$P_m^2(1 - P_m)^2$			
<i>rrrm</i>		$2P_m(1 - P_m)^3$			
<i>rrrr</i> (syndiotactic)		$(1 - P_m)^4$			

infrared spectra of (a) *cis*-1,4-polybutadiene, (b) *trans*-1,4-polybutadiene, and (c) atactic 1,2-polybutadiene are shown. These spectra cover only the 700–1200 cm⁻¹ CH out-of-plane bending vibration region, best suited for the observation of these polymers. The *cis* polymer shows a broad, strong band at 740 cm⁻¹; in the *trans* polymer the corresponding band appears at 965 cm⁻¹ and is narrower. Here, 1,2-polybutadiene shows the vinyl CH (995 cm⁻¹) and vinyl CH₂ (910 cm⁻¹) bending vibrations that we have already seen to arise from the terminal vinyl group of linear polyethylene (Fig. 18). The spectra show that none of the three polymers is entirely regular: the *trans* polymer contains some 1,2 structures and the *cis* polymer contains

both 1,2 and *trans*, while the 1,2 polymer exhibits a *cis* band at ~675 cm⁻¹. The spectra can yield quantitative analysis of the polymers by careful intercomparison even if extinction coefficients are not established.

Proton NMR may be employed for the analysis of diene polymers but ¹³C NMR is more discriminating. In Fig. 25, the 50.3-MHz ¹³C spectra of *cis*-1,4-polyisoprene and *trans*-1,4-polyisoprene observed in solution are shown. The olefinic carbons are relatively insensitive to isomerism at the double bond but the CH₃ and CH₂-1 carbons markedly shield each other in a *cis* arrangement compared to the *trans*. The CH₂-4 carbon, *cis* to a carbon atom in both isomers, is less affected.

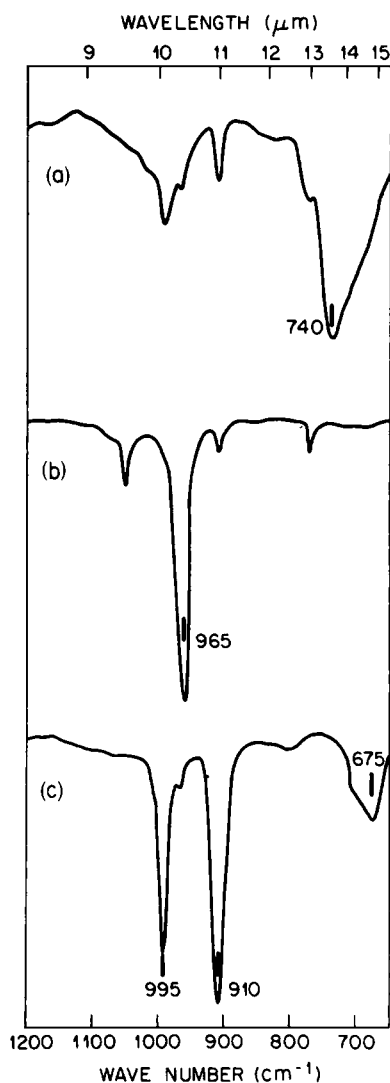


FIGURE 24 Out-of-plane bending bands in the infrared spectra of (a) *cis*-1,4-polybutadiene, (b) *trans*-1,4-polybutadiene, and (c) 1,2-polybutadiene.

Spectrum (a) is that of natural rubber or *hevea brasiliensis*. The biochemical pathway to natural rubber is an enzymatic process in which isoprene as such plays no part. The polymer is highly stereoregular, no trace of the *trans* structure being observable. Synthetic *cis*-1,4-polyisoprene is produced commercially using lithium alkyls or Ziegler-Natta catalysts. It contains 2–6% of *trans* units.

Chains of mixed structure exhibit more complex spectra because of sequence effects. In Fig. 26 the 50.3-MHz ^{13}C spectrum of a polybutadiene produced by free-radical initiation is shown. At the left (a) is the region of olefinic carbon resonance, not fully analyzed. The olefinic carbon singlets of the pendant vinyl groups flank those of the 1,4 units. At the right (b) are the aliphatic carbon resonances—

mainly 1,4 (and 1,2) methylene groups. This part of the spectrum is shown at two values of gain—1X and 5X—to show the small resonances of the sequences containing 1,2 units. The major peak (b) corresponds to central methylenes in *cis*–*cis* units; the principal peak (d) is that of the central 1,4-unit methylene group in *trans*–*trans* and *trans*–*cis* units, not discriminated. Peaks (a), (c), (e), and (m) correspond to sequences involving 1,4 units and one 1,2 unit, while the very small resonances (f) through (l) represent sequences containing two 1,2 units. The overall composition of the polymer is 23% *cis*-1,4, 58% *trans*-1,4, and 19% 1,2. Spectrum (c) is a computer simulation of (b) based on the assumption of a random distribution of units in these proportions. The satisfactory fit shows that free-radical propagation in butadiene polymerization is a Bernoullian process with regard to the generation of these isomeric structures.

It has been observed by infrared spectroscopy that the *trans*-1,4 content of free-radical polybutadiene or butadiene–styrene copolymers increases as the polymerization temperature is lowered—from ~51% at 97°C to 84% at –18°C. Butadiene–styrene copolymers in 75:25 mole ratio are produced commercially in emulsion as SBR synthetic rubber (see Table II). Most of it is produced at low temperature, because the higher *trans*-1,4 content improves its tensile strength and mechanical properties. By using rhodium salts in aqueous solution very highly stereospecific *trans*-1,4-polybutadiene can be prepared.

E. Copolymer Structure

A very important structural variable is provided by our ability to synthesize not only homopolymers with a single type of monomer unit but also copolymers having chains composed of two or more comonomer units. (We have seen, however, that even homopolymers may have different isomeric units and may be regarded as copolymers, although their composition is not so readily controlled as in true copolymerization.) Copolymers are broadly divided into three types, as shown in Fig. 1b: random, block, and graft. Block and graft copolymers contain relatively long sequences of one monomer bonded to similar sequences of another. Although they are of major scientific and technological interest, their overall composition is usually known from their method of synthesis, and they do not present microstructural problems essentially different from those of homopolymers. Our attention will be confined to the random type, in which two or more types of comonomer units are present in each chain. We shall discuss only copolymers of vinyl (or diene) monomers. Copolyesters and copolyamides are also significant but their composition is also usually readily predictable from the ratio of comonomers employed.

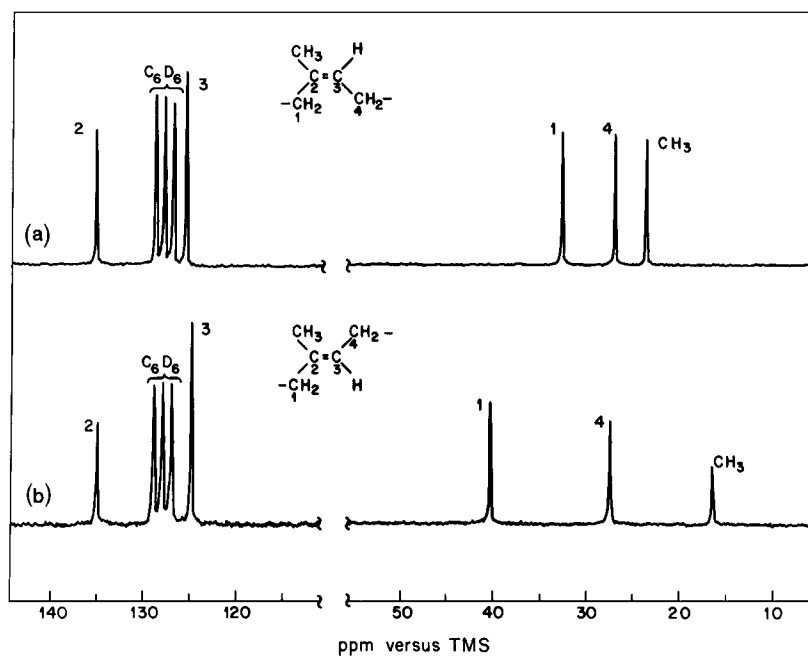


FIGURE 25 The 50.3-MHz ^{13}C spectra of (a) *cis*-1,4-polyisoprene and (b) *trans*-1,4-polyisoprene observed in 10% (w/v) solution in deuterobenzene at 60°C.

The composition of copolymers of vinyl and diene monomers is not in general the same as that of the monomer mixtures from which they are formed and cannot be deduced from the homopolymerization rates of the

monomers involved. The relationship between instantaneous copolymer composition and monomer feed composition (i.e., the starting ratio of monomers) is given by the differential equation

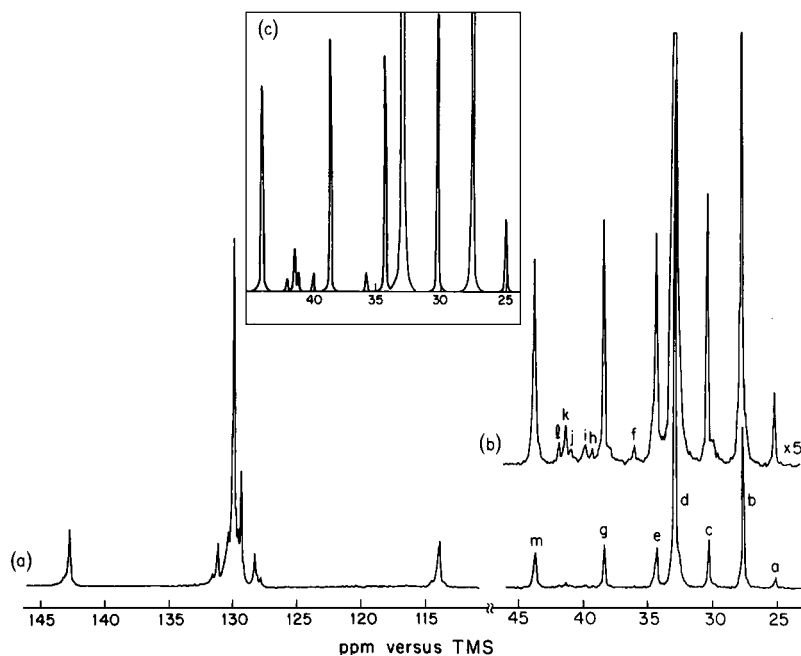


FIGURE 26 The 50.3-MHz ^{13}C spectrum of free-radical polybutadiene, observed at 50°C in 20% (w/v) CDCl_3 solution: (a) olefinic carbons, (b) aliphatic carbons, and (c) computer simulation of (b) (see text).

$$\frac{d[M_1]}{d[M_2]} = \frac{[M_1]}{[M_2]} \left\{ \frac{r_1[M_1] + [M_2]}{r_2[M_2] + [M_1]} \right\}, \quad (48)$$

where M_1 and M_2 represent the two comonomers. The left side of this equation gives the ratio of the rates at which the two monomers enter the copolymer, which in turn must represent the composition of the copolymer being formed at any instant. The ratio $[M_1]/[M_2]$ is the mole ratio of monomers in the feed. The quantities r_1 and r_2 are the reactivity ratios, defined as the ratios of propagation rate constants:

$$r_1 = k_{11}/k_{12}, \quad r_2 = k_{22}/k_{21}.$$

Here, k_{11} is the rate constant for the addition of monomer 1 to a growing chain ending in a monomer 1 unit; k_{12} is the rate constant for the addition of monomer 2 to the growing chain ending in monomer 1; k_{21} and k_{22} are the corresponding terms for growing chains ending in a monomer 2 unit.

Equation (48) is the copolymer equation in terms of the molar concentrations of the monomers. It is usually more convenient to express this relationship in terms of the mole fraction in both feed and copolymer. The feed mole ratio for monomer 1 is given by

$$f_1 = 1 - f_2 = \frac{[M_1]}{[M_1] + [M_2]}. \quad (49)$$

The instantaneous copolymer composition is given by

$$F_1 = 1 - F_2 = \frac{d[M_1]}{d[M_1] + d[M_2]}, \quad (50)$$

from which

$$F_1 = \frac{r_1 f_1^2 + f_1 f_2}{r_1 f_1^2 + 2 f_1 f_2 + r_2 f_2^2}. \quad (51)$$

(A parallel, but redundant, equation expresses F_2 .) We have stated that these relationships deal with the instantaneous composition of the copolymer. Since the comonomers generally do not enter the polymer in the same ratio as in the feed, the latter will drift in composition as copolymerization proceeds, becoming depleted in

the more reactive comonomer. As a result, the higher the monomer conversion the more heterogeneous the product. This in no way affects the determination of the overall composition or microstructure of the product but makes it more difficult to interpret in terms of relative reactivities. It is therefore customary in fundamental studies to limit the conversion to about 5% or less, although drifts in composition can be dealt with mathematically. In copolymer production on a practical scale, it is common practice to achieve greater structural regularity by adjusting the monomer input as the reaction proceeds. This usually means withholding the more reactive monomer.

The detailed discussion of various copolymerization cases will not concern us here. Traditionally, the determination of reactivity ratios, which provide important information concerning the behavior of monomers and growing chains, has required the determination of the overall comonomer composition of copolymers prepared from a series of feed ratios. Elemental analysis is most commonly used. A number of computational and graphic methods are employed to do this. It was realized very early that the theoretical treatment that predicts overall composition also predicts the frequency of occurrence of comonomer sequences, but at that time there was no way to observe and measure these. This can now be readily done by NMR, and the older and cruder methods are giving way to this more powerful approach. By NMR it is also possible to observe copolymer stereochemistry (never considered in earlier work) and the presence of anomalous units. One can also more readily detect deviations from the simple model employed here, in which only the terminal residue of a growing chain determines its reactivity; the effect of the penultimate unit, if any, may be clearly observed. Finally, it should be noted that by sequence measurements one can determine reactivity ratios from only a single copolymer provided the feed ratio is known. It may still be desirable to observe a range of compositions to assist in resonance assignments but it is not in principle essential.

For a random copolymerization, dyad, triad, and tetrad sequences may be represented (ignoring stereochemistry) as

Dyads		
$m_1 m_1$	$m_1 m_2$ (or $m_2 m_1$)	$m_2 m_2$
Triads		
$m_1 m_1 m_1$		$m_2 m_2 m_2$
$m_1 m_1 m_2$ (or $m_2 m_1 m_1$)		$m_1 m_2 m_2$ (or $m_2 m_2 m_1$)
$m_2 m_1 m_2$		$m_1 m_2 m_1$
Tetrads		
$m_1 m_1 m_1 m_1$	$m_1 m_1 m_2 m_1$ ($m_1 m_2 m_1 m_1$)	$m_2 m_2 m_2 m_2$
$m_1 m_1 m_1 m_2$ ($m_2 m_2 m_1 m_1$)	$m_1 m_1 m_2 m_2$ ($m_2 m_2 m_1 m_1$)	$m_2 m_2 m_2 m_1$ ($m_1 m_2 m_2 m_2$)
	$m_2 m_1 m_2 m_1$ ($m_1 m_2 m_1 m_2$)	
$m_2 m_1 m_1 m_2$	$m_2 m_1 m_2 m_2$ ($m_2 m_2 m_1 m_2$)	$m_1 m_2 m_2 m_1$

The dyad probabilities (i.e., frequencies of occurrence) are given by

$$[m_1m_1] = F_1P_{11}, \quad (52)$$

$$[m_1m_2](\text{or } [m_2m_1]) = 2F_1P_{12} = 2F_1(1 - P_{11}) \\ = 2F_2P_{21} = 2F_2(1 - P_{22}), \quad (53)$$

$$[m_2m_2] = F_2P_{22}. \quad (54)$$

Here, as we have seen, F_1 and F_2 are the overall mole fractions of m_1 and m_2 , respectively.

$$[m_1m_1m_1] = F_1P_{11}^2, \quad (55)$$

$$[m_1m_1m_2](\text{or } [m_2m_1m_1]) = 2F_1P_{11}(1 - P_{11}), \quad (56)$$

$$[m_2m_1m_2] = F_2(1 - P_{22})(1 - P_{11}). \quad (57)$$

The quantity P_{11} expresses the conditional probability that a chain ending in m_1 will add another m_1 , and P_{22} expresses the corresponding probability for m_2 . Here, P_{12} is the probability that a chain ending in m_1 will add m_2 , equal to the probability that it will not add m_1 (i.e., $1 - P_{11}$). Corresponding to the four rate constants k_{11} , k_{12} , k_{21} , and k_{22} are the four probabilities P_{11} , P_{12} , P_{21} , and P_{22} , related by

$$P_{11} + P_{12} = 1, \quad (58)$$

$$P_{21} + P_{22} = 1, \quad (59)$$

since a growing chain has only two choices. We choose to employ P_{11} and P_{22} ; it can be shown that they are given in terms of monomer feed mole fractions and reactivity ratios by

$$P_{11} = \frac{r_1f_1}{1 - f_1(1 - r_1)}, \quad (60)$$

$$P_{22} = \frac{r_2f_2}{1 - f_2(1 - r_2)}, \quad (61)$$

from which

$$r_1 = \frac{(1 - f_1)[m_1m_1]}{f_1(F_1 - [m_1m_1])}, \quad (62)$$

$$r_2 = \frac{(1 - f_2)[m_2m_2]}{f_2(F_2 - [m_2m_2])}. \quad (63)$$

Entirely analogous relationships apply to triad and tetrad sequences.

The system vinylidene chloride (m_1): isobutylene (m_2) is appropriate to consider since the copolymer has no asymmetric carbons and no vicinal J coupling. The proton NMR spectrum thus conveys only compositional sequence information. In Fig. 27, 60-MHz proton NMR spectra of the homopolymers (a) and (b) are shown. The homopolymer of vinylidene chloride gives a single resonance for the

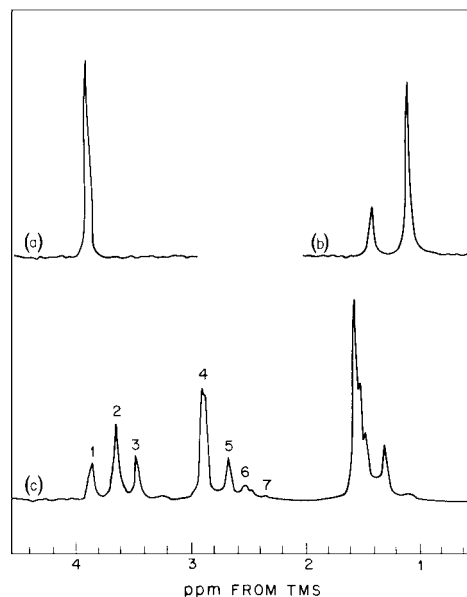
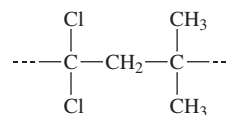


FIGURE 27 The 60-MHz proton spectra of (a) polyvinylidene chloride, (b) polyisobutylene, and (c) vinylidene chloride (m_1): isobutylene (m_2) copolymer containing 70 mol % m_1 . Peaks are identified with monomer tetrad sequences (a) $m_1m_1m_1m_1$; (2) $m_1m_1m_1m_2$; (3) $m_2m_1m_1m_2$; (4) $m_1m_1m_2m_1$; (5) $m_2m_1m_2m_1$; (6) $m_1m_1m_2m_2$; (7) $m_2m_1m_2m_2$. [From Hellwege, K. H., Johnsen, U., and Kolbe, K. (1966). *Kolloid-Z.* **214**, 45.]

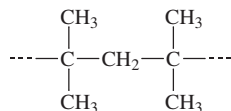
methylene protons (a); the homopolymer of isobutylene (which can be prepared with cationic but not with free radical initiators) gives singlet resonances of 3:1 intensity for the methyl and methylene protons. The spectrum of a copolymer, prepared with a free-radical initiator and containing 70 mol% vinylidene chloride is shown in (c). The methylene resonances are grouped in three chemical shift ranges: m_1m_1 -centered peaks at low field; peaks of methylene protons in



m_1m_2 -centered units near 3 ppm; and CH_2 and CH_3 resonances of m_2 -centered sequences at high field. It is evident that tetrad sequences are involved (assignments given in the figure caption). If only dyad sequences were distinguished, there would be only three methylene resonances corresponding to m_1m_1 , m_1m_2 (or m_2m_1), and m_2m_2 sequences. The upfield isobutylene peaks show considerable overlap and assignments here are less certain, but these resonances are not required for the analysis.

From dyad resonances r_1 and r_2 may be calculated. The relative intensity of the m_1m_1 resonances centered near 3.6 ppm gives $[m_1m_1]$ as 0.426, normalized over all dyad

methylenes, which from Eq. (62) gives a value of 3.31 for r_1 . Evaluation of the methylene resonance of



cannot be readily carried out because of overlaps, even though it would most directly provide a value of r_2 . Instead we note that

$$[m_1m_2](+[m_2m_1]) = 2F_2(1 - P_{22}) \quad (64)$$

or

$$[m_1m_2](+[m_2m_1]) = 2F_2 - \frac{2F_2r_2f_2}{1 - f_2(1 - r_2)}. \quad (65)$$

From the group of resonances near 2.8 ppm, a value of $[m_1m_2]$ of 0.56 is obtained, from which a value of r_2 of 0.04 is calculated. Conventional analysis of this system gives

$$k_{11}/k_{12} = r_1 = 3.3, \quad (66)$$

$$k_{22}/k_{21} = r_2 = 0.05, \quad (67)$$

in agreement within experimental error. These values show that vinylidene chloride radicals prefer to add vinylidene chloride and that chains terminating in isobutylene units have only a very small tendency to add another isobutylene.

More searching tests of the propagation mechanism can be obtained from consideration of tetrad intensities. By such analysis it is found that the relative reactivity of a growing free radical ending in vinylidene chloride depends on whether the penultimate unit is another vinylidene chloride unit or an isobutylene unit; if the latter, the chain is twice as likely to add vinylidene chloride.

A system of much interest is the copolymerization of ethylene and propylene. This reaction requires coordination catalysts rather than free-radical initiators. With insoluble coordination catalysts such as vanadium trichloride, together with aluminum alkyls or chloroaluminum alkyls, the heterogeneous propagation process is too complex for the simple treatment we have discussed. However, with soluble vanadium compounds— VOCl_3 , VCl_4 , or vanadium triacetylacetonate—the reaction takes place in a homogeneous phase and can be treated within our framework, although we shall not enter into details. In Fig. 28 the 25-MHz ^{13}C spectrum of a 50:50 (mole ratio) ethylene-propylene copolymer, observed in 1,2,4-trichlorobenzene at 120°C is shown. The principal chemical shift influence is that of the methyl-branched carbons, but stereochemical configuration is a substantial perturbation, as might be expected from the discussion of polypropylene (Section III.C). The methylene carbons prove to be the most useful. In a sequence of methylene carbons between branch carbons, each carbon gives a distinctive resonance up to a run length of 7. Established peak assignments (based on rules derived

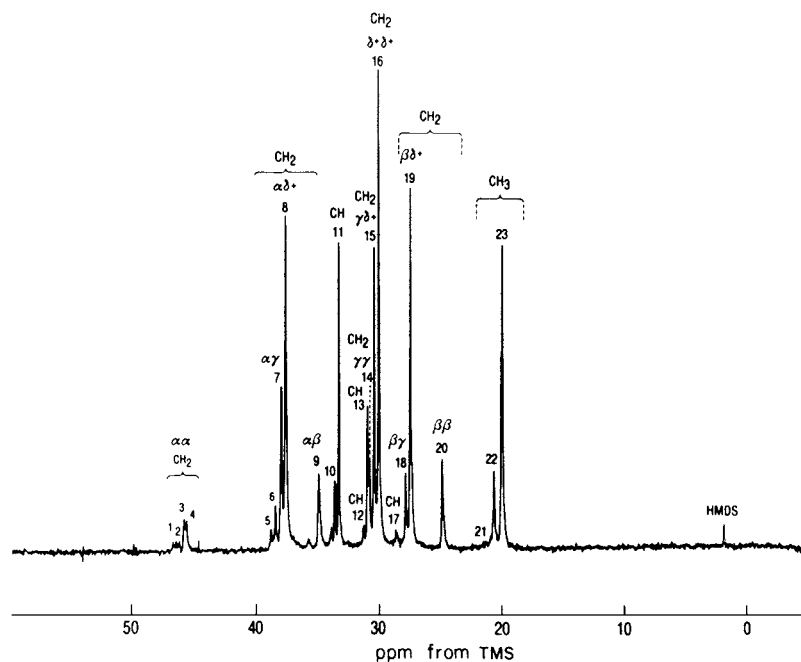
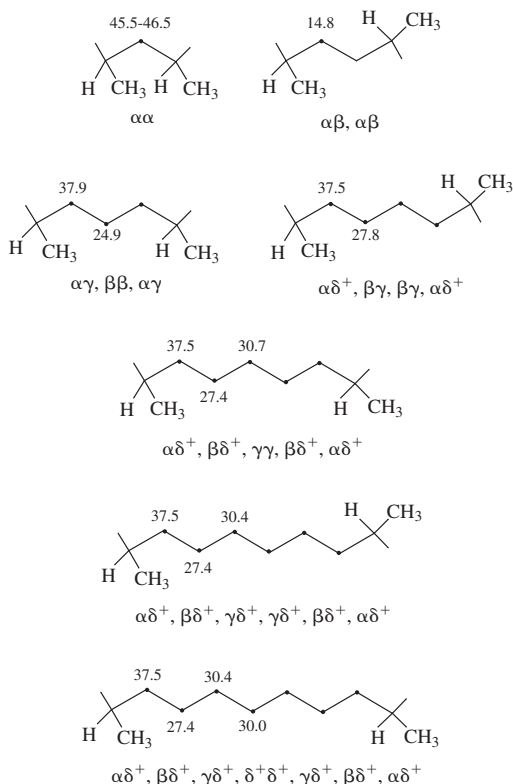


FIGURE 28 The 25-MHz ^{13}C spectrum of an ethylene-propylene copolymer of 50:50 mole ratio, observed at 120°C in 1,2,4-trichlorobenzene.

from extensive study of model hydrocarbons) are shown here:

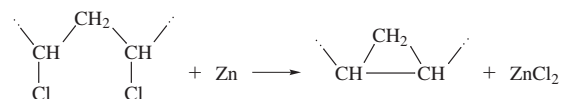


The Greek letter designations indicate the position of the nearest branch carbon. A plus sign indicates that the branch is at the δ or more distant position. Those methylene carbons that are four or more carbons removed from a branch carbon give the same chemical shift (30.0 ppm). Propylene inversions can be clearly identified through the presence of methylene sequences two and four carbons in length. From these assignments and using a mathematical model of chain growth that treats inverted propylene units as a third monomer, a complete analysis of the statistical distribution of sequences can be carried out. The extent of inversion is about 5%. A value of the product of reactivity ratios $r_1 r_2$ 0.35 ± 0.04 was found. This corresponds to a propagation process not far from random but with a moderate tendency toward alternation of monomer units.

F. Regioregularity

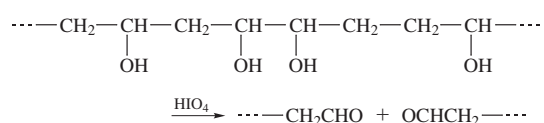
In the earlier days of polymer science it was not known whether vinyl polymers had head-to-tail or head-to-head: tail-to-tail structures (Section I). Because spectroscopy—

either vibrational or NMR—was not available, chemical methods had to be employed. Thus, to determine the structure of poly(vinyl chloride) the Freund reaction was employed. This employed metallic zinc and was believed to be specific for the removal of chlorine atoms in 1,3 positions:



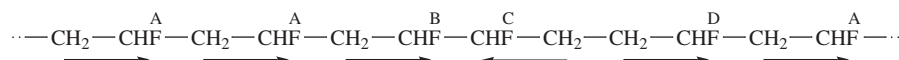
It thus would not proceed if the structure were head-to-head: tail-to-tail. Since it did in fact remove most of the chlorine from poly(vinyl chloride), it was concluded that the polymer had a head-to-tail structure. NMR confirms this conclusion.

A more subtle chemical approach has been applied to poly(vinyl alcohol). Here, it is assumed that the predominant structure is head-to-tail and the question posed was the frequency of occurrence of the occasional inverted unit. It is assumed that periodic acid reacts only with 1,2-glycol units and not with 1,3 units:



Inverted units in poly(vinyl alcohol) thus lead to chain scission, the extent of which can be measured by the reduction of solution viscosity (Section II.F). It is concluded that 1–2% of head-to-head units are present, this mode of propagation increasing with temperature.

Fluorine-substituted ethylenes are particularly subject to the generation of inverted units, presumably because fluorine atoms are relatively undemanding sterically. At the same time, the physical properties of their polymers may depend strongly on the presence of such units. The presence of ^{19}F offers an additional means for detailed study, as ^{19}F chemical shifts are highly sensitive to structural variables. Poly(vinyl fluoride), a commercial plastic having high resistance to weathering, has a substantial proportion of head-to-head units. The 188-MHz ^{19}F spectrum of a commercial polymer is shown in Fig. 29. The ^{19}F –H J-coupling multiplicity has been removed by proton irradiation as in ^{13}C spectroscopy (Section III.C). The resonance assignments, designated by capital letters, are:



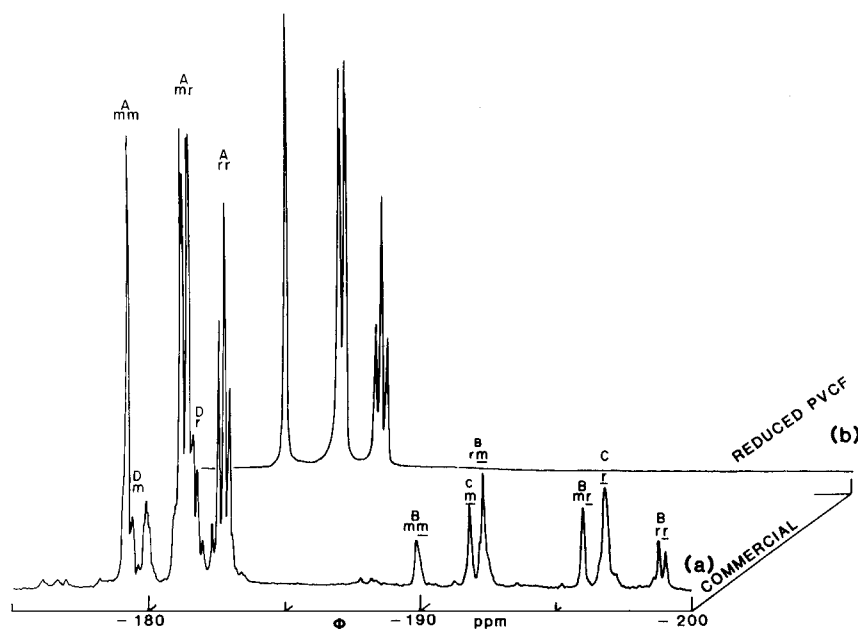
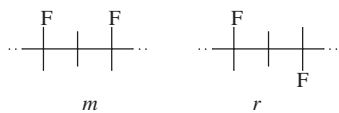
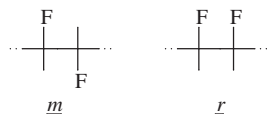


FIGURE 29 The 188-MHz ^{19}F spectrum of (a) commercial poly(vinyl fluoride) and (b) poly(vinyl fluoride) prepared by reductive dechlorination of poly(1-fluoro-1-chloroethylene): both spectra observed as 8% solution in N,N -dimethylformamide- d_7 at 130°C .

The stereochemical assignments are also indicated in Fig. 29. The m and r designations that are not underlined represent the usual relationships between substituents in 1,3 positions (in planar zigzag projection):



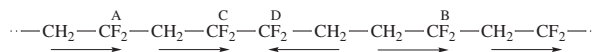
The underlined designations represent the substituents in 1,2 positions (also in planar zigzag projection):



It may be further noted in connection with the B resonances that \underline{rm} and \underline{mr} are quite different structures and do not differ merely in direction as with rm and mr . The fraction of inverted units is $\sim 11\%$.

Spectrum (b) is that of poly(vinyl fluoride) prepared without inversions by a special chemical route. The upfield portion of spectrum (a), as well as the D resonances, are absent, thus clearly identifying them as defect peaks. This material has a melting point of 210°C , compared to 190°C for the normal polymer. Both polymers are nearly atactic.

A similar study of poly(vinylidene fluoride)—a material of great interest because of its piezoelectric and pyroelectric properties—shows that 3–6% of its contents are inverted units:



The 188-MHz ^{19}F spectrum, shown in Fig. 30, is made somewhat simpler by the absence of asymmetric carbons.

G. Branching

Branching in vinyl polymers is an important structural variable. As with step polymers (Section I.C), it may be produced by the deliberate introduction of dienes and divinyl or polyvinyl monomers as comonomers. These comonomers yield double bonds in the copolymer chains, which can then polymerize to yield branches and

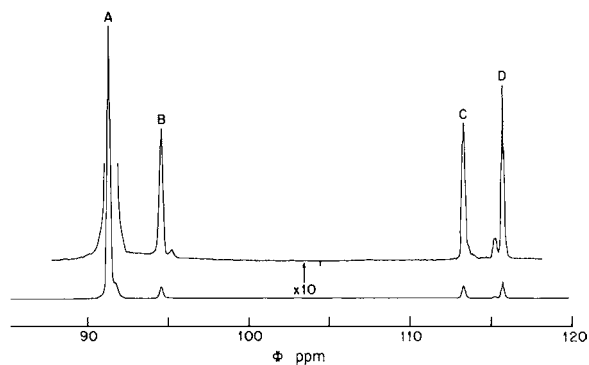
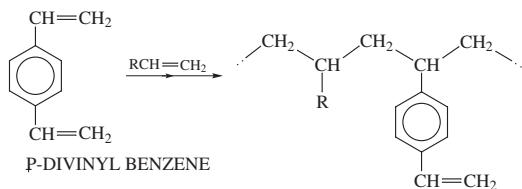


FIGURE 30 The 188-MHz ^{19}F spectrum of commercial poly(vinylidene fluoride) observed in 11% solution in dimethylformamide- d_7 at 21°C .

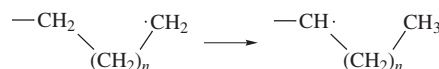
crosslinks. This is also true of course of homopolymers of such monomers:



Here, we discuss branching introduced by processes that are under less specific control and involve chain transfer reaction of various types.

Branches are of particular importance in polyethylene (see Fig. 2), as their presence reduces the melting point and extent of crystallinity (Section III.A). High-pressure polyethylene is found by infrared spectroscopy to have unusually large numbers of methyl groups, normally expected only at chain ends (Section III.A). When combined with molecular weight measurements, these results indicate that there are many more ends than molecules—or in other words that the chains contain branches. Carbon-13 NMR can supply details of the types and distribution of these branches because of the sensitivity of ^{13}C chemical shifts to such structural variables, already seen in the discussion of polypropylene (Section III.C) and ethylene-propylene copolymers (Section III.E). In Fig. 31 the 50.3-MHz ^{13}C spectrum of a high-pressure polyethylene observed in 5% solution in 1,2,4-trichlorobenzene at 110°C is shown. The resonances are labeled according to the scheme inset in the figure, using a large body of information obtained from model hydrocarbons and from ethylene copolymers with small proportions of olefins. The principal peak, at 30.0 ppm, not shown at its full height, corresponds to those methylene groups that are

four carbons or more removed from a branch or chain end: It constitutes about 80% of the spectral intensity. The C_1 carbons (i.e., methyl groups) and C_2 carbons are the most shielded, branch point carbons the least. Main-chain carbons β to the branch are more shielded while those α to the branch are less shielded than unperturbed methylenes. The composition of this polyethylene is shown in Table IV. The predominant branch type is *n*-butyl. Both amyl and butyl branches are believed to be formed by intramolecular chain transfer or “backbiting”:



This reaction is evidently most probable when $n = 3$ or 4, has a low but finite probability when $n = 1$, and has zero probability when $n = 0$ or 2.

The complex appearance of the ethyl branch methyl resonance at ~ 11.0 ppm suggests that these branches may occur in groups or with some similar complication. The branches described in Table IV as “hexyl or longer” are believed to be truly long, as illustrated in Fig. 2 (and at the right side of Fig. 31). Their frequency of occurrence is estimated from the unique peak labeled L-3-C in Fig. 31, corresponding to the third carbon from the chain end. Such branches are too few in number to influence crystallinity but are believed to have a significant effect on melt rheology. They are formed by transfer from the growing chain to a finished polyethylene molecule, resulting in a free-radical site on the latter, which then adds more monomer.

Branches of several types have also been observed by ^{13}C NMR in poly(vinyl chloride). They are nearly an order of magnitude fewer in number than in polyethylene but are

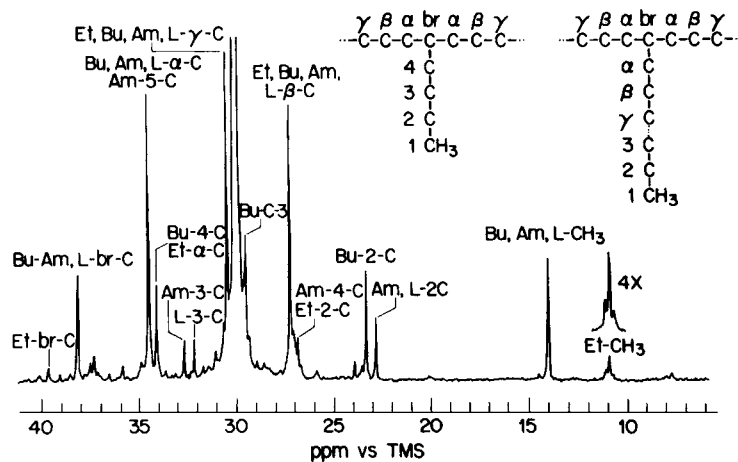
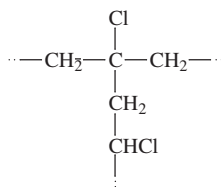


FIGURE 31 The 50.3-MHz ^{13}C NMR spectrum of high-pressure polyethylene observed in 5% (w/v) solution in 1,2,4-trichlorobenzene at 110°C .

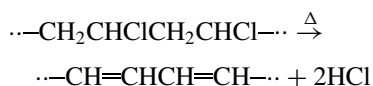
TABLE IV Branching in High-Pressure Polyethylene
 $\bar{M}_n = 18,400$, $\bar{M}_w = 129,000$

Types of branch	Number of branches per 1000 backbone carbons
—CH ₃	0.0
—CH ₂ CH ₃	1.0
—CH ₂ CH ₂ CH ₃	0.0
—CH ₂ CH ₂ CH ₂ CH ₃	9.6
—CH ₂ CH ₂ CH ₂ CH ₂ CH ₃	3.6
Hexyl and longer	5.6
Total	19.8

significant because some of them—those with a tertiary chlorine—are believed to be sites for the initiation of the



chemical decomposition of the polymer. Poly(vinyl chloride) is a valuable material, used in very large volume for molding and electrical insulation. It is fire resistant and relatively cheap, but when heated is subject to loss of hydrogen chloride, leading to the formation of deeply colored polyene structures:



The reaction is more complicated than this simple representation suggests and is believed to be sensitized by the presence of labile centers such as a tertiary chlorine.

Branches are an integral part of other polymers such as star polymers and dendrimers. Star polymers can have a variable number of arms with a controlled molecular weight. Dendrimer can have a high molecular weight and many functional end groups.

IV. CHAIN CONFORMATIONS OF MACROMOLECULES

A. Theoretical Introduction

We have already seen in Eq. (13) that the rms end-to-end distance of a polymer chain is given by

$$\langle \bar{r}^2 \rangle^{1/2} = lx^{1/2} \quad \text{or} \quad \langle \bar{r}^2 \rangle = l^2x,$$

where l is the length of a monomer unit and x is the number of monomer units. This relationship is derived from random walk statistics and assumes that bond rotation is free and that the bonds between two adjacent monomer units can assume any angle. This model is called the freely jointed chain and is clearly unreasonable for a polymer, where bond hybridization imposes restrictions on available bond angles. However, it is qualitatively correct in that any correlation between two monomer units must decrease as the distance between the units is increased.

We can improve this model by imposing a restriction on our hypothetical chain. If we allow the chain segments to rotate freely, but now fix the valence angles, we have what is known as a freely rotating chain. In this model, $\langle \bar{r}^2 \rangle$ is given by

$$\langle \bar{r}^2 \rangle = \left(\frac{1 - \cos \theta}{1 + \cos \theta} \right) xl^2, \quad (68)$$

where θ is the angle between successive bonds in a chain. For a tetrahedral chain, $\theta = 109^\circ$ and $\langle \bar{r}^2 \rangle = 2xl^2$.

A further refinement is required to obtain a reasonable model for a polymer chain. In the restricted rotation model, we take into account the fact that there are intrachain hindrances in a real polymer chain. The bond angles are fixed by virtue of hybridization, and the chain rotation is limited to a few rotational isomeric states. We shall first illustrate chain conformations with a simple model compound, and then extend our treatment to a segment of a polyethylene chain.

Referring to Fig. 32, we see several conformations of butane, generated by rotation about the C₂—C₃ bond. These are called *gauche*⁺, *trans*, and *gauche*[−] conformations and are usually abbreviated as *g*⁺, *t*, and *g*[−]. The available conformations are most easily visualized in Newman diagrams, shown in Fig. 32(a). Looking down the C₂—C₃ bond, the substituents are projected onto planes parallel to the paper. The C₂ carbon is in front, and the C₃ carbon, in this presentation, is obscured by the C₂ carbon. The Newman diagrams clearly show that in the *trans* arrangement, the bulky groups are opposite each other, separated by a dihedral angle of 180°. The *gauche*⁺ and *gauche*[−] conformations are formally generated by rotations about the C₂—C₃ bond. The bulky groups in the *gauche* conformations are separated by a dihedral angle of 60°.

Figure 32(b) shows how the torsional potential of *n*-butane varies as a function of conformation. The lowest energy conformation occurs when *n*-butane is in the *trans* conformation. The population of *n*-butane in the eclipsed conformations, corresponding to the tops of the energy barriers, is negligible. The *trans* and *gauche* conformers interchange very rapidly with each other, having lifetimes of approximately 10^{−10} sec at room temperature.

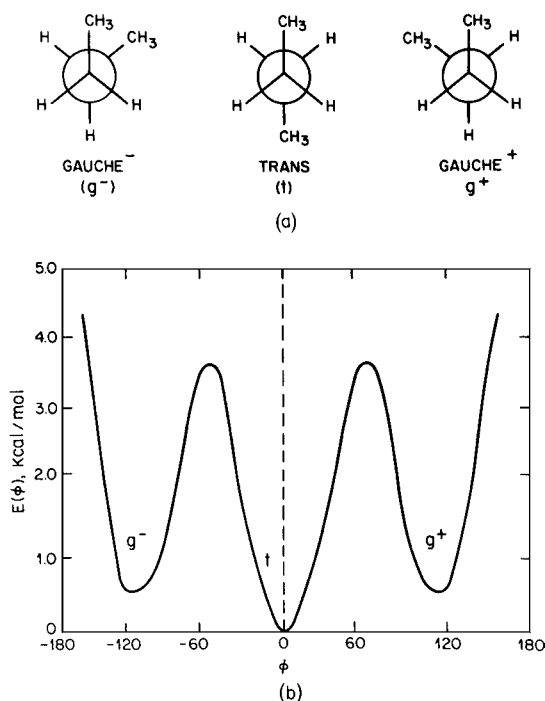
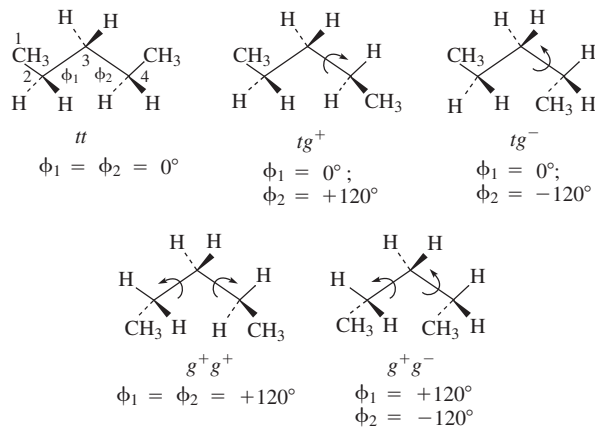


FIGURE 32 (a) Newman projections of the g^- , t , and g^+ conformations of *n*-butane and (b) torsional potentials for rotation about the central (C_2-C_3) bond in *n*-butane.

By virtue of its simple structure, *n*-butane has few available conformations. Once we lengthen the chain by one carbon we immediately see that the description of available conformations becomes more complicated. In *n*-pentane we must now specify two rotational angles, ϕ_1 and ϕ_2 :



Note that the tg^+ and g^+t conformations are identical, and that the tg^+ and tg^- states are mirror images of each other. Also, the g^+g^+ and g^-g^- conformations are equivalent, as are the g^-g^+ and g^+g^- states.

The energy of a given rotational state of the C_2-C_2 bond depends on the rotational state of the C_3-C_4 bond and vice versa. We now need an energy map, rather than the simple diagram of Fig. 32, in order to visualize the energies of the various conformations of *n*-pentane. Such a map is shown in Fig. 33. This diagram indicates that the *tt* conformation ($\phi_1 = \phi_2 = 0^\circ$) has the lowest energy. Other low-energy conformations are the tg^+ and tg^- states ($\phi_1 = 0^\circ$, $\phi_2 = \pm 120^\circ$). The g^+g^+ state ($\phi_1 = \phi_2 = +120^\circ$) is of lower energy than the g^+g^- ($\phi_1 = +120^\circ$, $\phi_2 = -120^\circ$). This is because the methyl groups in the g^+g^+ state experience neither attractive nor repulsive forces, whereas in the g^+g^- state the methyl groups are nearly eclipsed and experience severe repulsion.

It is important to note that although the g^+g^- (and g^-g^+) state is very unfavorable, there are local minima near this conformation at $\phi_1, \phi_2 = 77^\circ, -115^\circ$ and $120^\circ, -70^\circ$ (see Fig. 33).

The main difference between the *n*-butane and *n*-pentane cases is that there are only three-bond, or first-order interactions in *n*-butane, whereas in *n*-pentane there are second-order interactions. These second-order interactions must be taken into account in polymer chains. The rotational isomeric state (RIS) model, introduced above, is successful in treating both the first-order and higher order interactions.

The RIS model is a statistical treatment of all possible chain conformations in which the bond lengths and valence angles are fixed. The conformation of a polymer chain of *n* bonds can be specified by assigning a rotational state to each of the $n - 2$ nonterminal bonds. If there are *v* rotational states about each of *n* bonds, there will be v^{n-2} possible conformational states. Even for the common case of $v = 3$, a chain of 20 bonds will have 3.8×10^8 conformational states. The RIS model readily lends itself to computer calculation by matrix methods. Statistical weight matrices are used with the RIS model to

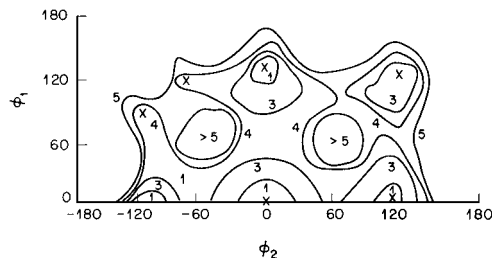


FIGURE 33 Energy map for *n*-pentane for rotation angles ϕ_1 and ϕ_2 . The numbers on the contours refer to energies in kcal/mol. The minima are indicated by x 's [From Abe, A., Jernigan, R. L., and Flory, P. J. (1966). *J. Am. Chem. Soc.* **88**, 631.]

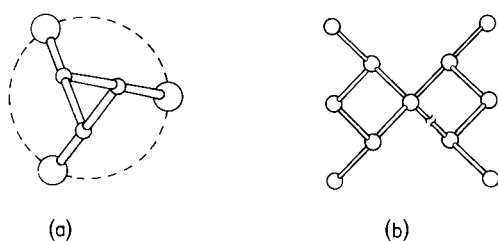


FIGURE 34 Representative conformations of polymers: (a) 3_1 helix $(gt)(gt)(gt)$ viewed down the helix axis; and (b) syndiotactic $(gg)(tt)$ sequences found in polypropylene.

define the energies of various conformers. The matrices include the effects of both first- and second-order steric interactions. Using the RIS model and matrix operations, any conformation-dependent property of a polymer chain can be calculated, although such a calculation requires some estimate of the bond rotational states and their associated energies.

A detailed account of RIS model and associated calculations is beyond the scope of this article. However, we summarize several of the conclusions concerning the relationship between structure and conformation of vinyl polymers that can be drawn from a combination of RIS calculations and experimental results. Isotactic chains tend to assume alternating gauche and trans rotational states. These $\cdots(gt)(gt)(gt)\cdots$ sequences favor the formation of a 3_1 helix. [A 3_1 helix makes one turn for every three monomer units. When viewed along the helix axis the 3_1 helix exhibits threefold symmetry, as shown in Fig. 34(a).] As we have seen, such helical sequences will have equal probability of being either left- or right-handed. In solution these conformations will reverse chirality rapidly and at random, as the conformation states have very short lifetimes.

Syndiotactic chains, in contrast to the isotactic sequences discussed above, generally favor tt conformations. There is a substantial occurrence of helical conformations of the type $\cdots(gg)(tt)(gg)(tt)\cdots$. Figure 34(b) shows a view of this helix along the helix axis. This is a special case found for syndiotactic polypropylene. We shall return to this structure later (Section IV.C.3). In solution the conformations responsible for such a helical sequence also undergo rapid interconversions.

B. Experimental Observation of Chain Conformation in Solution

Examples of the conformation-dependent properties that can be calculated from the RIS model include the dipole moment, the molar Kerr constant, the characteristic ratio,

and the NMR chemical shift and other spectroscopic parameters. In this section we shall describe briefly some of the methods for experimentally observing polymer chain conformations in solution. Combined with such experimental measurements, the results from RIS calculations provide valuable insight into the structure and conformation of macromolecules.

1. The Characteristic Ratio, C_∞

Recall from our previous discussion (Section II.F) that the intrinsic viscosity $[\eta]$ is obtained by extrapolating the specific viscosity, η_{sp} to zero concentration:

$$[\eta] = \lim_{c \rightarrow 0} \left[\frac{\eta - \eta_0}{\eta_0} \right] / c. \quad (69)$$

In this expression, η and η_0 are the polymer solution and solvent viscosities, respectively, and c is the polymer concentration in g/dL, or grams per deciliter.

Flory has shown that the intrinsic viscosity may also be expressed as

$$[\eta] = \phi \langle r^2 \rangle^{3/2} / M, \quad (70)$$

where ϕ is a universal constant equal to approximately 2.5×10^{21} and M is the polymer molecular weight. The mean squared end-to-end distance is $\langle r^2 \rangle$ (see Section II.B.1), which in a non- θ solvent may be somewhat greater than the unperturbed dimensions $\langle \bar{r}^2 \rangle$. In real solvents the degree of expansion of the molecular coil is designated as α , such that

$$\langle r^2 \rangle = \alpha^2 \langle \bar{r}^2 \rangle. \quad (71)$$

For a θ solvent, where the expanding effect of excluded volume is exactly balanced by polymer-polymer interactions, $\alpha = 1$.

The characteristic ratio C_∞ is the ratio between the unperturbed and the random walk dimensions and is given by

$$C_\infty = \langle r^2 \rangle / xl^2 \quad (72)$$

where x is the number of chain segments and l is the length of a single monomer unit, as before.

For all real polymers, C_∞ is greater than unity and is a measure of departure from a freely jointed or freely rotating model.

Substituting into Eq. (72) for $\langle r^2 \rangle$, we can obtain a relationship between C_∞ and $[\eta]$:

$$C_\infty = \frac{1}{xl^2} \left[\frac{[\eta]_\theta M}{\phi} \right]^{2/3} \quad (73)$$

If we let m be the monomer molecular weight,

$$C_\infty = \frac{m}{Ml^2} \left[\frac{[\eta]_\theta M}{\phi} \right]^{2/3} \quad (74)$$

TABLE V Characteristic Ratios C_∞ for Selected Polymer Chains

Polymer	Conditions	$C_\infty = \langle r^2 \rangle_0 / nl^2$
Polymethylene	Decanol-1, 138°C	6.7
Polyoxymethylene		~10.0
Polyoxyethylene	Aqueous K ₂ SO ₄ , 35°C	4.0
Polytetramethylene oxide		~2.0
Polypropylene	Diphenyl ether	
Isotactic	145°C	4.7
Atactic	153°C	(5.3)
Polystyrene	Diphenyl ether	
Atactic	Cyclohexane, 35°C	10.2
Poly(methyl methacrylate)		
Atactic	Various solvents	6.9
Isotactic	Acetonitrile, 28°C	9.3
Polydimethylsiloxane	Butanone	6.2

The length, l , is usually 0.15 nm and M can be obtained from any of the usual molecular weight measurements (see Section II.B). Thus, the characteristic ratio can be determined directly from intrinsic viscosity measurements under θ conditions. Table V lists characteristic ratios for selected polymers.

The RIS model can be used to calculate characteristic ratios, and these calculations can be compared with experimentally derived values. Such comparisons are useful for testing various assumptions used in RIS calculations. Table VI shows such a comparison for a polymethylene chain. The experimental value for C_∞ is 6.7. Table VI lists C_∞ calculated for (a) a freely rotating chain; (b) a chain with a reasonable gauche energy of 500 cal but with independent rotational states for the neighboring bonds; and (c), (d), and (e) neighbor-dependent three-state model with different values for the energy of the gauche and of the gauche⁺–gauche[−] conformations. Table VI shows that entry (c) comes closest to matching the experimental values. [The energies used in (c) were deduced from studies on small paraffins.]

2. Spectroscopic Determination of Chain Conformation in Solution

Many spectroscopic techniques are useful for observing polymer chain conformations. Ultraviolet spectroscopy (UV) is used almost exclusively for biopolymers to establish the degree of helicity and to study other aspects of protein and nucleic acid tertiary structure. For example, the UV spectra of nucleic acids and nucleotides show hypochromic effects when helical conformations are

TABLE VI Calculated and Experimental Values of the Characteristic Ratio $C_\infty = \langle r^2 \rangle_0 / nl^2$ (300 K) and Its Temperature Coefficient for the Polymethylene Chain

Model	Characteristic ratio C_∞	Temperature coefficient $dC_\infty/dT \times 10^3$
Experimental	6.7	-1.1 ± 0.1 (390–420 K)
(a) Freely rotating	2.1	0
(b) 3-State RIS, $E_g = 500$ cal $E_{g^+g^-} = 0$ (independent rotations)	3.4	
(c) 3-State RIS, $E_g = 500$ cal $E_{g^+g^-} = 2200$ cal	6.7	−1.0
(d) 3-State RIS, $E_g = 800$ cal $E_{g^+g^-} = 2200$ cal	8.3	−1.5
(e) 3-State RIS, $E_g = 500$ cal $E_{g^+g^-} = 3500$ cal	7.1	−0.7

formed. With respect to synthetic polymers, there is some UV evidence that isotactic polystyrene partially retains a helical conformation in solution. This is confirmed by infrared measurements.

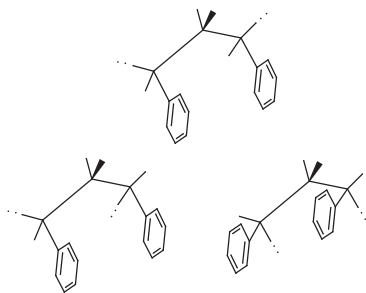
Infrared spectroscopy (IR) (Section III.A) is used primarily for characterizing polymer conformations in bulk samples and will be discussed in this regard in the following section. However, it can also be used to study solution state conformations, since the skeletal vibration frequencies are conformationally sensitive. Bands can be identified that are signatures for the tt , tg , and longer sequences. Using these conformationally sensitive IR bands, researchers have observed helical sequences in isotactic polystyrene and have also shown the absence of cooperative helix-coil transitions in this material. IR spectroscopy is also very useful for studying hydrogen bonding interactions bond in biopolymers and in synthetic polymers.

Raman spectroscopy (Section III.A) provides information that is complementary to that obtained from IR measurements. We have already seen that to be IR active, a vibrational mode must undergo a change in dipole moment. Thus, –OH, –NH, and –CH bonds are examples of IR-active groups. In fact, the –OH infrared bands are so strong that they often make difficult the use of water as a solvent for some IR studies. In contrast, a symmetrical bond, for example a carbon–carbon bond C–C, has an IR-inactive stretching vibration. However, the C–C stretching vibration gives a strong Raman band. Furthermore, aqueous solvents can be used in Raman studies, making Raman spectroscopy an ideal method for studying the conformations of biological macromolecules. Raman spectroscopy provides much new information concerning

the conformational changes that occur in heme-proteins upon binding small molecules.

Fluorescence measurements have long been used to study the conformations of biopolymers. Phenylalanine, tyrosine, and tryptophan fluoresce. Because solvents affect the fluorescence intensity of proteins, solvent studies can, in favorable cases, be used to establish the hydrophobicity of the environment surrounding these residues. Fluorescent dyes, or fluorescence probes, can be attached to or entrained in biological molecules to provide additional conformationally sensitive information.

Excimer formation studies are very useful in probing the conformations of synthetic polymers in solution. An excimer is an association complex between an excited chromophore and a chromophore in the ground state. The excimer emission band is shifted toward longer wavelengths than normally would be observed. Efficient formation of excimer complexes depends on spatial proximity of the chromophores, which can thus be used to establish conformation. Excimer fluorescence can also be used to probe conformational mobility in polymer chains, since excimer formation, in some cases, requires that a conformational transition take place within the fluorescence lifetime. For example, these conformations of a polystyrene chain can undergo excimer formation:



We have already seen that NMR spectroscopy (Section III.A) is a powerful tool for establishing both the chemical structure and microstructure of polymer chains. NMR spectroscopy can also be used to measure the chain conformation in solution using the through-bond J -coupling constants, the distances between atoms measured by the nuclear Overhauser effect and the chemical shifts.

It has long been recognized that the magnitude of the vicinal proton–proton coupling constant has a strong dependence of the dihedral angle between the two protons. This angular dependence (known as the Karplus relationship) and is given by

$${}^3J_{HH} = \begin{cases} 8.5 \cos^2 \varphi - 0.28 & 0^\circ \leq \varphi \leq 90^\circ \\ 9.5 \cos^2 \varphi - 0.28 & 90^\circ \leq \varphi \leq 180^\circ \end{cases} \quad (75)$$

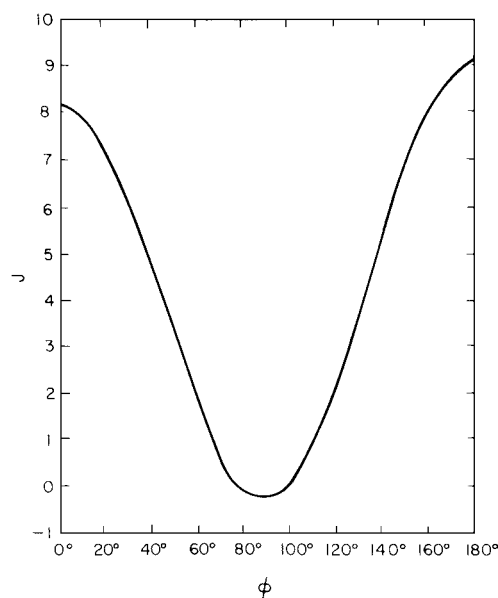


FIGURE 35 Karplus equation showing the variation of J as a function of dihedral angle.

Figure 35 shows a plot of this equation. In polymers, a gauche arrangement generally has a coupling constant of ~ 2 – 4 Hz whereas a *trans* conformation has a value between 8 and 13 Hz. A time-averaged value of J is observed due to rapid conformational equilibration. This averaged value of J can be used to estimate the populations of gauche and *trans* conformers.

The nuclear Overhauser effect arises from through-space dipolar interactions between nearby protons. The magnitude of this effect depends on the inverse sixth power of the distance, and it is very sensitive to distances in the range of 2–5 Å. Like the J -couplings, an average value is observed that depends on the equilibrium concentration of gauche and *trans* states. The J -couplings and distances can be very effectively measured using multidimensional NMR methods.

A combination of RIS calculations and experimental chemical shift (primarily ^{13}C and ^{19}F) measurements has established the validity of the γ -gauche effect with respect to vinyl polymer chains. In this treatment, it is observed that when two carbons are gauche to each other, they shield each other by ~ 5 ppm, compared to the chemical shift of the corresponding *trans* arrangement. For example, we would expect the CH_3 chemical shift of polypropylene to be sensitive to the gauche content of the chain. In Fig. 36, top, we see that the methyl group experiences different numbers of γ -gauche interactions, depending on the local chain conformation. The ^{13}C chemical shifts of the methyl groups in all 36 heptad sequences can be satisfactorily predicted with the RIS model by assuming

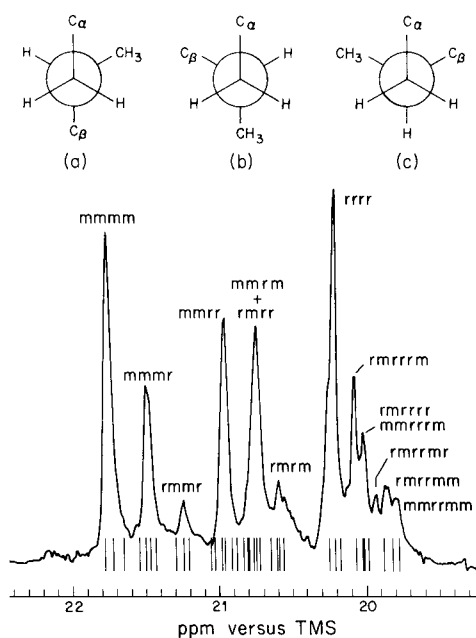


FIGURE 36 Top: conformations of a fragment of a polypropylene chain: (a) *trans*, $C_\alpha-C_\beta$: *t*, $C_\alpha-CH_3$: *g*; (b) *gauche +*, $C_\alpha-C_\beta$: *g*, $C_\alpha-CH_3$: *t*; (c) *gauche -*, $C_\alpha-C_\beta$: *g*, $C_\alpha-CH_3$: *g*. Bottom: 90-MHz ^{13}C NMR spectrum of the methyl region of atactic polypropylene. The “stick” spectrum shows the RIS-predicted chemical shifts for the 36 heptad sequences, based on the γ -*gauche* effect.

appropriate populations of the *trans* and *gauche* conformations about the central bonds of each heptad. The γ -*gauche* model can be successfully extended to other vinyl polymers including poly(vinyl chloride) and polystyrene.

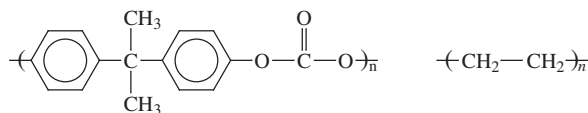
3. Kerr Effect and Dipole Moment Measurements of Chain Conformation in Solution

Kerr effect (electric birefringence) measurements are exceptionally sensitive to solution state conformations. Results from Kerr effect measurements can be used to provide a critical test of a particular RIS model. Likewise, dipole moments are conformationally sensitive and can also be predicted by RIS methods.

Taken together, characteristic ratios; UV, IR, and NMR spectra; fluorescence measurements; molar Kerr constants; and dipole moments provide a fairly clear and consistent view of polymer chain conformation in solution. The fact that the experimental results can be predicted from the RIS model and other semiempirical treatments suggests that our understanding of solution state chain conformations is at a fairly advanced state.

C. Experimental Observation of Chain Conformation in the Solid State

Polymers in the solid state can generally assume both crystalline and amorphous states, oftentimes together in the same sample. The fraction of crystallinity in a sample is generally dependent on both the chemical structure and microstructure of the polymer chain and on the thermal history of the sample. For example, the tetrahedral bonding of the quaternary carbon in polycarbonate introduces a “bend” in the backbone and prevents efficient crystal packing. On the other hand, the regular structure of polyethylene in the planar zigzag form enhances its tendency to crystallize:



Polymer chains in the solid state adopt primarily *gauche* and *trans* conformations, in close analogy to the situation we have already encountered in the solution state. The chief physical methods for determining solid-state polymer chain conformations include vibrational spectroscopy, X-ray diffraction, neutron scattering, and NMR spectroscopy. We shall discuss representative results from each of these methods.

1. Vibrational Spectroscopy

IR and Raman spectroscopy (Section III.A) can be used to determine chain conformations. The CH_2 rocking band is sensitive to the interaction of chains with their neighbors. Using the method of normal coordinate analysis, it is possible to establish interchain and intrachain force fields. Furthermore, once conformationally sensitive bands are identified, they can be used to identify the fraction of *gauche* bonds. Using Fourier transform IR techniques and digital subtraction, difference spectra can be generated. Thus, a spectrum of an unfavorable conformer can be obtained, even if it is present as only a small fraction of the total sample.

2. X-Ray Diffraction

X-ray diffraction is one of the primary methods for determining macromolecular conformations in the crystalline solid state. The intramolecular conformational considerations we have already discussed for polymer chains in solution appear to be the dominant forces for determining solid-state conformations. However, in the solid state we must also consider the intermolecular requirements of

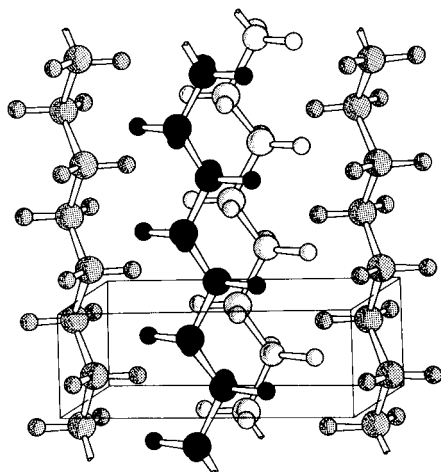


FIGURE 37 The crystal structure of polyethylene. The unit cell is indicated by the parallelepiped. The chains are reproduced in different tones for the purpose of clarity. [From Bovey, F. A. (1982). "Chain Structure and Conformation of Macromolecules," Academic Press, New York, 1982.]

chain packing. For example, we have already seen from a theoretical viewpoint that for polyethylene the planar zigzag, or all-*trans* conformation, has the lowest energy. The crystal structure of polyethylene is shown in Fig. 37, where it can be seen that the chains adopt the planar zigzag form.

Figure 37 actually represents an oversimplification of the morphology of polyethylene. Complexities that are related to the occurrence of amorphous regions, chain folds, lattice defects, and branching are omitted. However, crystallographic data provide important information about chain packing, as well as about molecular conformation.

Crystal structures of polymers, such as the structure shown in Fig. 37, can also be used to establish the conformations of the crystalline regions of fluoropolymers, the conformations of polymers that prefer gauche conformations (such as polyoxymethylene), and the conformations of stereoregular materials. Crystallography is also useful for determining the crystallization that occurs upon stretching rubbery polymers such as polyisobutylene or natural rubber. These structures are generally more complex than that of polyethylene. For example, Fig. 38 shows a side view of the 3_1 helix of isotactic polystyrene. The aromatic side chains are stacked on top of each other, radiating outward from the helix. Figure 38 also illustrates two additional variations in structure—a sense of direction and handedness, or chirality. This 3_1 helix is right-handed, and the α substituents are all pointing up with respect to the chain axis. The packing energy of such helices will vary, depending on the chirality and directions of

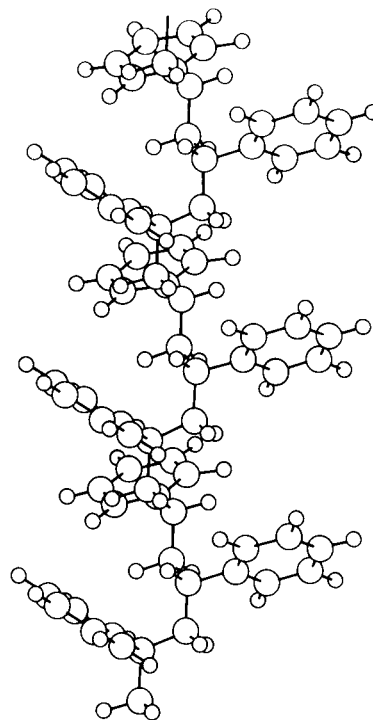


FIGURE 38 Side view of the 3_1 helix of isotactic polystyrene. [From Bovey, F. A. (1982). "Chain Structure and Conformation of Macromolecules," Academic Press, New York.]

their surrounding chains. For chains such as polystyrene or polypropylene, it is clear that alternating chirality is favored. However, it is not certain whether the directions of the helices are entirely random or whether they are uniform over whole domains.

The nylon polyamides are an example of a class of polymer where intermolecular forces, in this case hydrogen bonding, exert a large influence on the chain structure in the solid state. The chain conformations of nylon 66 and nylon 6 are shown in Fig. 39. In nylon 66 the chains do not have a sense of direction and are packed in the crystalline α form as shown in Fig. 39(a). However, the nylon 6 chains have a sense of direction. The most stable arrangement is the one shown in Fig. 39(b), where successive chains are antiparallel and the maximum number of hydrogen bonding interactions is realized.

3. Neutron Scattering

X-ray diffraction, by its nature, provides detailed information about the ordered regions of polymers that are crystalline, but does not bear directly on noncrystalline or glassy materials. For years there was substantial controversy concerning the conformation of macromolecules

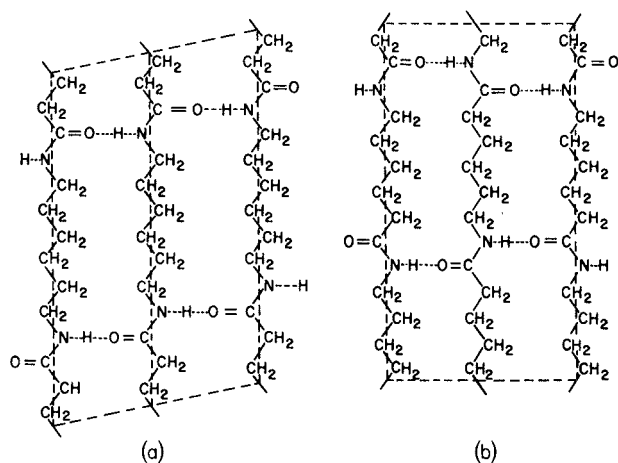


FIGURE 39 Chain conformations of (a) nylon 66 and (b) nylon 6. [From Holmes, D. R., Bunn, C. W., and Smith, D. J. (1955). *J. Polym. Sci.* **17**, 159.]

in the amorphous state. One school maintained that the chains did not mingle with their neighbors but rather coiled back on themselves. Another school insisted instead that the chains interacted with their neighbors forming microbundles or lamellae too small to be seen by X-ray diffraction. Flory, in 1953, postulated that neither of these ideas is correct, and that in the solid state macromolecules exhibit their unperturbed, θ -condition dimensions, since a polymer chain surrounded by itself and like chains has nothing to gain by expanding.

The advent of small-angle neutron scattering has suppressed essentially all further controversy in this regard. In this method, deuterated polymer is diluted in a protonated polymer matrix. The deuterated polymer has a greater scattering cross section than the corresponding protonated materials, thereby providing contrast. The information from neutron scattering provides $\langle \bar{r}^2 \rangle$ and $\langle s^2 \rangle$, as is the case for light scattering. Results from neutron scattering experiments show that polymer chains in the amorphous solid state exhibit their unperturbed dimensions.

Neutron scattering experiments are also particularly useful for determining copolymer morphology (see Section V). The scattering profile can be analyzed to provide information about the degree of phase mixing and also about the interfacial gradient.

4. Solid-State NMR Spectroscopy

NMR spectroscopy of solid polymers is a powerful method for establishing the degree of orientation in stretched polymers, the degree of crystallinity in bulk samples, and the conformation in the solid state. Generally, ^{13}C , ^{29}Si , ^{19}F ,

^2H , and ^1H NMR are most useful for synthetic polymers, whereas ^2H , ^{15}N , ^{31}P , and ^{13}C are often used for materials of biological origin.

Studies of the degree of polymer or biopolymer orientation with respect to a strain direction take advantage of the orientation-dependent NMR chemical shift or dipole-dipole interaction in the solid state. NMR spectra of oriented materials can provide information about the arrangement of individual chain segments with respect to the draw direction. Often, the amount of orientation in amorphous regions can also be determined.

NMR quantification of the fraction of crystalline and amorphous components in a solid relies upon differences in molecular motion between these regions. The crystalline regions have very little molecular motion and thus have very long relaxation times. The amorphous regions, on the other hand, are generally quite mobile and have much shorter relaxation times. These differences in relaxation times are generally sufficient for spectral discrimination, thereby affording quantification of the fraction of crystalline and amorphous components.

Solid-state NMR spectra of polyethylene provide a particularly clear example of the differences between crystalline and amorphous components. We have already seen that polyethylene in the crystalline solid state exists in a planar zigzag conformation. The amorphous regions are expected to have some gauche character and according to the γ -gauche model (see Section IV.C) would be expected to have a different chemical shift. We see from Fig. 40 that this is the case. The peaks arising from the crystalline and the amorphous regions are separated by approximately 2.4 ppm, which is what we expect for an equilibrium amount of gauche bonds in the amorphous region.

Solid-state NMR chemical shifts are also sensitive to packing effects. The ^{13}C spectra of isotactic and syndiotactic polypropylene (Fig. 41) illustrate this point. As we recall, isotactic polypropylene adopts a 3_1 helix composed of alternating gauche and *trans* conformations. The methyl groups occupy positions on the surface of the coil, and the methine and methylene groups are stacked one over the other in alternating fashion. These three types of carbons give rise to the three resonances observed in Fig. 41(a).

Syndiotactic polypropylene, on the other hand, adopts a repeating $(gg)(tt)(gg)(tt)$ conformation, with four monomer units per repeat. In this conformation the methylene groups can reside in one of two distinct environments [Fig. 41(b)]. These groups are magnetically nonequivalent and produce two peaks. The separation between these two resonances can be explained in terms of the γ -gauche shielding effect. The external CH_2 experiences two *trans*

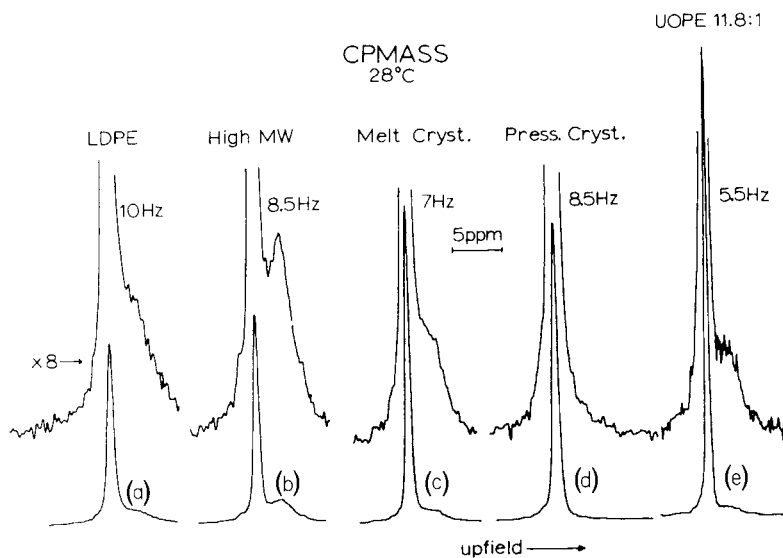


FIGURE 40 Solid-state ^{13}C spectra of five polyethylene samples: (a) low-density polyethylene, (b)–(d) high-density linear polyethylene, and (e) ultraoriented polyethylene. [From Earl, W. L., and VanderHart, D. L. (1979). *Macromolecules* **12**, 762.]

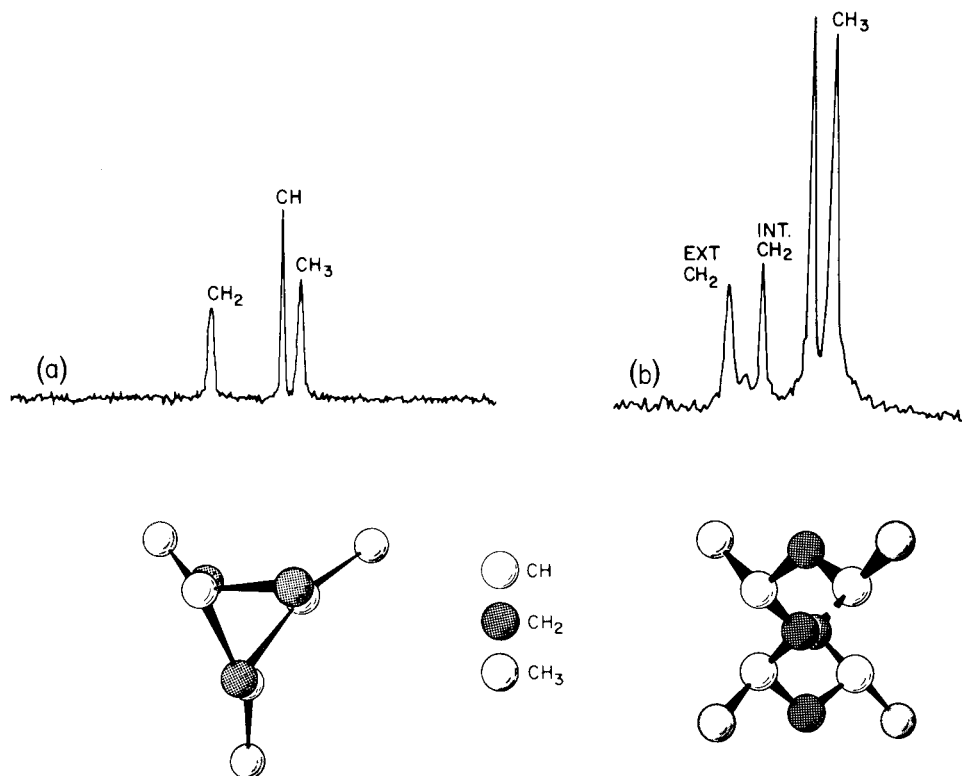


FIGURE 41 Solid-state ^{13}C NMR spectra of (a) isotactic and (b) syndiotactic polypropylene shown with the corresponding representations of their conformations. [From Bovey, F. A. (1982) "Chain Structure and Conformation of Macromolecules," Academic Press, New York.]

carbons in the γ positions, whereas the internal CH_2 experiences two *trans* carbons in the γ . Therefore, the internal carbon chemical shift is expected to occur upfield by two γ -gauche interactions, or 8 ppm (2×4 ppm). The peaks are actually separated by 8.7 ppm, in good agreement with the γ -gauche model.

NMR methods have been evolving rapidly in recent years and much progress has been made in developing methods to measure the distances and relative orientations between nearby atoms in polymer chains. These studies typically involve introducing isotopic labels into the polymer chain. In polycarbonate, for example, the distances between the carbonate groups depend strongly on chain conformation. The chemical shifts in solids are anisotropic and depend on how an atom is oriented relative to the external magnetic field. From such effects it is possible to measure the relative orientation of neighboring atoms, such as those in polyethylene. The fraction of *trans* and gauche conformations can be directly measured from these spectra.

V. SOLID-STATE MORPHOLOGY

A. Crystalline Polymers and Chain Packing

In order for crystallinity to occur, synthetic polymer chains must be capable of packing closely together in a regular, parallel array. Some natural polymers, notably globular proteins, may crystallize even though their chains are folded into complex spheroidal shapes. But such polymer molecules are usually—for a given type—all identical in chain length and manner of folding and can be stacked like tennis balls. For synthetic polymers, this is not the case, and crystallinity requires packing side by side in extended form either as planar zigzags or helices (see Section IV.C.2). To do this, the chain must be at least fairly regular in structure. Unless the chain is predominantly isotactic or (much more rarely) syndiotactic, it usually cannot be fitted sufficiently well to its neighbors to crystallize. Exceptions are polychlorotrifluoroethylene ($-\text{CFCICF}_2-$)_n, poly(vinyl fluoride), and poly(vinyl alcohol). On the other hand, natural rubber, although perfectly regular in covalent structure (Section III.D), crystallizes only on very long standing or on stretching.

The conformations of representative polymer chains in the crystalline state have been discussed in Section IV.C. Our concern here is with the morphology of polymer crystals at the level of the optical and electron microscope. Polymers never crystallize completely even though the chains may be entirely regular in structure. The degree of disorder far surpasses that corresponding to the oc-

casional vacancies and dislocations found in crystals of small molecules. The nature and significance of the amorphous phase is not entirely straightforward, but the notion of a degree of crystallinity is useful and well established. It is commonly estimated by comparing the density and heat of fusion to those of an appropriate standard. Defining the degree of crystallinity as χ , it is found that most polymers vary in χ from less than 0.5 to 0.95. Even for single crystals of linear polyethylene, χ is usually no more than 0.9. For high pressure branched polyethylene, χ is about 0.5.

For the crystallization of linear polyethylene, typical conditions involve preparation of an approximately 0.01% solution at 130–140°C, which is then held at a fixed temperature of 70–80°C until a crop of crystals is obtained. (Since the crystal habit of polymers varies markedly with crystallization temperature, it is not desirable to simply let the solution cool to room temperature.) The crystals so obtained take the form of thin, flat platelets or lamellae a few micrometers in long dimensions and approximately 10 nm in thickness. The latter dimension increases with the temperature of crystallization and in fact crystals once formed at lower temperatures will increase in thickness upon annealing at a higher temperature. The chain or *c* axis of the molecules is oriented across the thickness of the platelet rather than in its plane. Since the molecules may be 1000 nm or more in length, it follows that the chains must be folded many times. These features are shown schematically in Fig. 42. The nature of the surface at which the chains emerge, fold, and reenter is a matter of some controversy and no doubt varies from case to case, particularly as the degree of crystallinity varies. On the one hand, the appearance of the seemingly regular and planar surfaces of lamellae, with well-defined edges and corners, suggests that the chains fold back with minimum loops and probably with reentry into the crystal at adjacent positions, particularly when the extent of crystallinity is high. It has been proposed, on the other hand, that at least in some cases the fold surface has

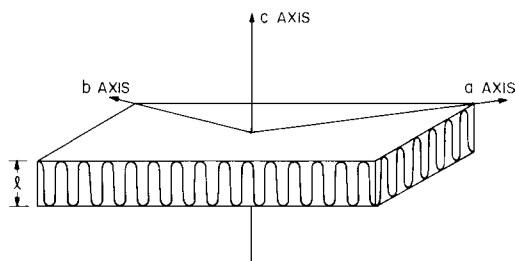


FIGURE 42 Schematic representation of crystalline lamellae showing folded chains, crystal faces, and axes.

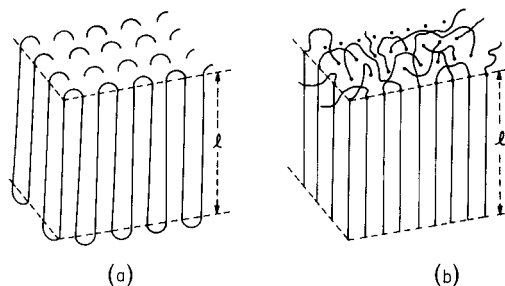


FIGURE 43 Models of chain morphology in a single crystal with (a) regular folding with adjacent reentry and (b) irregular, random "switchboard" fold surface.

the form of a "switchboard" with reentry occurring more or less at random and with loops much larger than the minimal size. Such a model will clearly tend to be favored at low extents of crystallinity. These two pictures of the morphology of a single crystal are presented in Fig. 43.

Although represented in Figs. 42 and 43 as planar for simplicity, lamellar crystals often take complex forms of hollow pyramids. Viewed along the c axis such crystals would appear lozenge-shaped. What is seen under a microscope as a planar lamella may actually represent a collapsed pyramid, as shown in Fig. 44. In such hollow pyramids the stems of the molecules remain parallel to

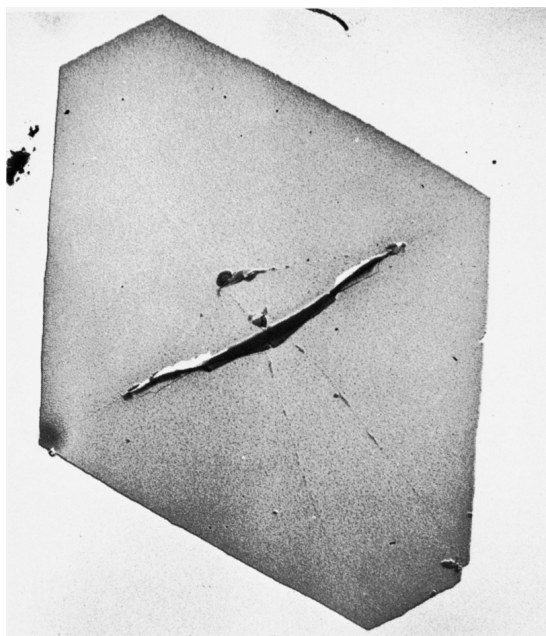


FIGURE 44 A single crystal of polyethylene that is actually a collapsed hollow pyramid as indicated by the pleats in the center.

the pyramid axis and are therefore inclined to the faces of the pyramid. Another deviation from the idealized form is often observed in crystals prepared at high degrees of undercooling. Under such circumstances the growth of polymer crystals is not limited to the laying down of chains in a lateral growth pattern. The formation of multilayered crystals consisting of several superimposed chain-folded layers all of equal thickness, and originating from a screw dislocation, is often observed. Their spiral terraces have a ziggurat-like form.

Single polymer crystals from solution are mainly of scientific rather than technical interest. In practical use, semicrystalline polymers crystallize from the melt, and the dominant form is the spherulite, which is uncommon for small molecules. Spherulites are aggregates of crystals with a radiating fibrillar structure. In polymers they are microscopic in size, usually of the order of $100\ \mu\text{m}$ or less in diameter. In Fig. 45 spherulitic growth in a melt of isotactic polystyrene, observed under the polarizing microscope between crossed polarizers, is shown. Being birefringent the spherulites show up against a dark background of molten polymer. They are seen in cross section, having grown in two dimensions in a film of molten polymer between cover slips, which have a small separation compared to the spherulite diameter. In bulk polymer, of course, their growth would take place in three dimensions. The maltese cross pattern is typical, reflecting their birefringent and symmetric nature. In this stage, growth is not yet complete. When it is complete, the spherulites impinge on one another with more or less straight boundaries, as shown in Fig. 46. These spherulites also exhibit a banded pattern that is quite common.

It is found from the sign of the birefringence and from X-ray study that the molecular chains are normal to the

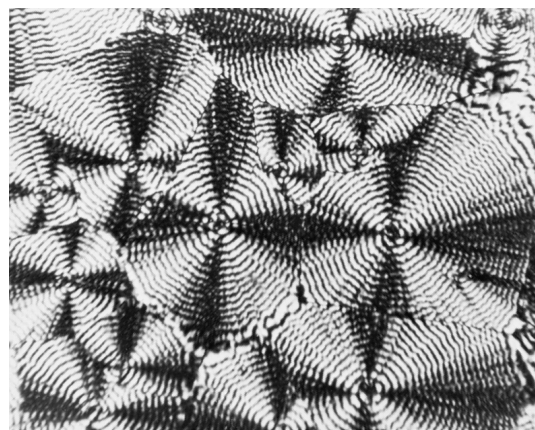


FIGURE 45 Spherulitic growth in a melt of isotactic polystyrene (magnification: $115\times$).

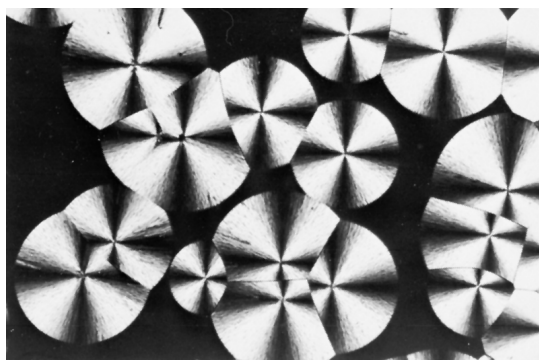


FIGURE 46 Banded spherulitic structure in polyethylene (magnification: 700 \times).

chain direction. The radiating fibrils of the spherulite are actually elongated, chain-folded lamellae. The concentric bands, when present, arise from the fact that the lamellae twist about the radius like ribbons and do so in a regular and cooperative manner. The period of twist corresponds to the separation of bands seen in the optical microscope. When the bands are absent the structure is essentially the same but without the twisting.

B. Block Copolymer Morphology

We have seen (Section III.E) that an important class of copolymers, both scientifically and technologically, are those of the block type. Usually, the synthesis of block copolymers is designed to produce macromolecules of either the AB or the ABA type, where the letters designate different kinds of chains. A much studied class of block copolymers is that containing polystyrene and polybutadiene sections. It is a general rule that polymers of different structure, even though closely related, will not mix. The fundamental reason is that such large molecules are necessarily few in number, and the entropy gain on mixing them is negligibly small (Section II). As a consequence, the A and B segments cannot exist in a molecularly dispersed state but must form small separate domains, the covalent bonding preventing separation into macroscopic phases. The domains may take the form of spheres, rods, or lamellae, the dimensions of which depend on the end-to-end length of the segments (usually close to the unperturbed dimensions) (Section II) and the interfacial tension between the domains. The segments present in greater volume fraction will generally form a continuous phase in which the lesser phase exists as separate microphases. In Fig. 47 electron micrographs of a 70/30 polystyrene–polybutadiene (mole ratio) AB block copolymer are shown. Although the appearance of the domains is of almost crystalline regularity, the dimensions are at least an order of magnitude

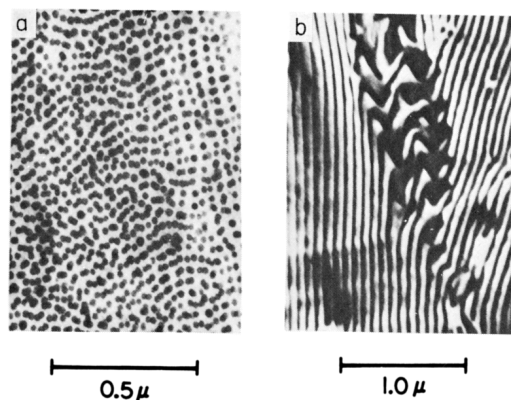


FIGURE 47 Electron micrographs of a 70/30 mol ratio polystyrene–polybutadiene AB block copolymer: (a) microtomed normal to the long dimensions and (b) microtomed along the long dimension.

greater than true crystalline dimensions. In (a) the polybutadiene segments are actually rods, but appear as circles because the sample has been microtomed normal to their long dimensions. In (b) the direction of microtoming is that of their long dimension and their elongated form is evident.

SEE ALSO THE FOLLOWING ARTICLES

BIOPOLYMERS • INFRARED SPECTROSCOPY • MICROANALYTICAL ASSAYS • NUCLEAR MAGNETIC RESONANCE • POLYMER PROCESSING • POLYMERS, SYNTHESIS • RAMAN SPECTROSCOPY • RUBBER, NATURAL • RUBBER, SYNTHETIC

BIBLIOGRAPHY

- Allcock, H. R. (1990). "Contemporary Polymer Chemistry," Prentice-Hall, Upper Saddle River, NJ.
- Bovey, F. A. (1982). "Chain Structure and Conformation of Macromolecules," Academic Press, New York.
- Bovey, F. A., and Mirau, P. A. (1996). "NMR of Polymers," Academic Press, New York.
- deGennes, P. G. (1979). "Scaling Concepts in Polymer Physics," Cornell University Press, Ithaca, NY.
- Elias, H. G. (1997). "Introduction to Polymer Science," John Wiley and Sons, New York.
- "Encyclopedia of Polymer Science and Engineering" (1988). Wiley Interscience, New York.
- Flory, P. J. (1953). "Principles of Polymer Chemistry," Cornell University Press, Ithaca, NY.
- Flory, P. J. (1969). "Statistical Mechanics of Chain Molecules," Wiley Interscience, New York.

Hunt, B. J., and James, M. I. (1993). "Polymer Characterization," Blackie Academic and Professional, Glasgow.

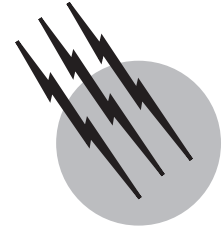
Koenig, J. L. (1990). "Chemical Microstructure of Polymer Chains," Kreiger, Melbourne, FL.

Odian, G. (1970). "Principles of Polymerization," McGraw-Hill,

New York.

Painter, P. C., and Coleman, M. M. (1997). "Fundamentals of Polymer Science: An Introductory Text," Technomic Publishing, Lancaster, PA.

Salamone, J. C. (1998). "Concise Polymeric Materials Encyclopedia," CRC Press, Boca Raton, FL.



Plastics Engineering

R. J. Crawford

University of Auckland

- I. General Types of Plastics
- II. Design Considerations
- III. Material and Process Selection
- IV. Successful Engineering Applications for Plastics

GLOSSARY

Composite A material that is a combination of two or more constituents, each of which retains its own identity. In the context of this article, the constituents are fibers within a thermoplastic or thermosetting matrix.

Creep The time-dependent change in the dimensions of a plastic under the action of a static load.

Cross-linking The formation of an infusible structure by the joining together of individual molecular chains into a three-dimensional network.

Ductility The ability of a material to deform plastically before fracture.

Elastomers Plastics that exhibit the large deformation/elastic recovery characteristics of rubbery materials.

Engineering plastics A general name for plastics suitable for use in load-bearing applications.

Fatigue The failure of a material as a result of the repeated application of a fluctuating stress or strain.

Fiber A general term for a filament of material that has a length at least 100 times its diameter.

Heat-deflection temperature The temperature at which a standard test piece deflects by a specified amount when subjected to a specified force.

Modulus The ratio of stress to strain in a material, at a specified level of strain.

Speciality plastics Materials with special characteristics usually in regard to high-temperature properties.

Stiffness A measure of the ratio of load to deformation; there is usually a direct correlation with modulus, but modulus is an inherent material property whereas stiffness depends on the shape of the material being stressed.

Thermoplastic A material capable of being repeatedly softened by heat and hardened by cooling.

Thermoset A plastic that when subjected to heat (or a chemical process) changes into an infusible, insoluble material.

Viscoelasticity A property of a material whereby it exhibits the combined effects of viscous and elastic behavior.

PLASTICS are now well established in all branches of engineering as cost-effective, high-performance materials. A major attraction of plastics is that when one takes into account the overall costs of conversion from raw material to final product, plastics almost always come out best.

In addition, although the absolute mechanical property values of plastics are less than those for metals, the low density of plastics means that their specific properties compare very favorably with other materials. When one adds on the other attractive properties of plastics such as chemical and environmental resistance, toughness, and resilience, and in particular, ease of processing into complex shapes, it is clear that the engineering applications for plastics will continue to increase.

I. GENERAL TYPES OF PLASTICS

The most characteristic feature of the structure of plastics is that they consist of relatively long molecules. These molecules are usually referred to as “chain-like” because during the manufacture of the plastic a large number of small units have been linked together. In most cases the molecular chain has a carbon backbone, and it is the varying nature of the side groups off the backbone that gives the different types of plastics their individual characteristics.

The forces between molecular chains are relatively weak, so that when a plastic is heated the thermal energy is capable of moving the chains apart. In this state the structure has a random configuration, and the plastic can easily flow into a mold or through a die to take any desired shape. When heat is extracted from the plastic it is transformed from a melt to a solid and retains its new shape.

If the side groups on the molecular chain are simple, it is possible for the structure of the plastic to attain a very ordered structure. If this occurs the plastic is said to be *crystalline* or, perhaps more accurately, *semicrystalline* since no plastic is capable of becoming totally crystalline. The degree of crystallinity can be controlled, to some extent, during molding operations, and it is important that the molder is aware of the effects on properties that can be produced. Crystallinity in a plastic improves some of its mechanical properties (such as modulus) but shrinkage is greater, and in a particular plastic the toughness is reduced as the degree of crystallinity increases. Chemists can also take steps to control crystallinity; this can be used as one method to obtain, for example, high-temperature plastics.

Some plastics have a molecular structure that does not permit any type of crystalline structure. These plastics are referred to as *amorphous* in that they have a random molecular structure in both the molten and the solid states. Amorphous plastics are always capable of being transparent, although the addition of fillers and pigments results in their being available in a wide range of opaque colors. Semicrystalline plastics contain both amorphous and crystalline regions in their structure. The way that these regions co-exist has a major effect on the properties of the plastic. Semicrystalline plastics are naturally opaque, but

if crystallization is prevented (by, for example, rapid cooling from the melt) transparent moldings can be produced. The classic example of this is the manufacture of bottles from polyethylene terephthalate (PET).

The semicrystalline and amorphous types of plastic referred to above are more generally known as *thermoplastics*. This is because they are capable of going through an almost indefinite cycle of being softened by heat and becoming solid again when the heat is removed. The most distinguishing feature of this type of plastic is that the polymer chains remain linear and separate after molding. In contrast to this it is possible to have *thermosetting* plastics, which can be softened only once to take up the shape of the mold. Once these materials have solidified they cannot be softened by the application of heat or by any other method. When heat and pressure are applied to a thermosetting plastic during the initial molding process, the structure undergoes a chemical reaction that locks it into a three-dimensional network. This is called *cross-linking*; it is initiated by heat, chemical agents, irradiation, or a combination of these. As a result of this cross-linking, thermosets have an obvious advantage in that they will not soften in high-temperature environments. Thermosets also have improved resistance to chemical attack, stress cracking, and creep. However, they are not so easy to mold as the thermoplastics, and generally they cannot offer the same level of toughness.

Examples of thermoplastics are polypropylene, polycarbonate, polyvinyl chloride, ABS, polystyrene, acetal, and nylon (polyamide). Examples of thermosets are epoxies, phenolics, ureas, and melamines. Polyesters and polyurethanes can be available as both thermoplastic and thermosetting materials. It should be noted that some thermoplastics, such as polyethylene, are now commercially available in cross-linkable grades, so the distinction between a thermoplastic material and a thermosetting material is becoming less clear-cut.

The types of plastics used successfully in engineering applications cover the full range of thermoplastics and thermosets that are available. This means that the designer has access to materials ranging from polyethylene to polyetheretherketone (PEEK). In the former case the elastic modulus is low (300 to 400 MN/m²), but with proper design it may be used in critical, demanding applications—for example, nationwide pressurized gas-distribution pipes. The modulus of polyethylene can also be increased by a factor of 100 if its structure is highly oriented by stretching the material under controlled conditions in the solid state. In the case of PEEK, it is an expensive material that possesses unique properties. When combined with carbon fibers, it provides a material that is stronger and has a higher modulus than many metals (see [Table I](#)).

TABLE I Short-Term Properties for Engineering Plastics

Material	Density (kg/m³)	Modulus (GN/m²)	Strength (MN/m²)	Specific modulus (MN m/kg)	Specific strength (kN m/kg)	Deflect. temp. (°C)
Aluminum	2700	71	80	26.3	29.6	—
Brass (70Cu/30Zn)	8500	100	550	11.8	64.7	—
Mild steel	7860	210	460	26.7	58.5	—
Polyacetal	1410	2.9	65	2.1	46.1	110
Polyacetal/30%g	1610	8	100	5	62.1	163
Polyamide (66)	1140	3	85	2.6	74.6	77
Polyamide 66/30%g	1300	9.5	190	7.3	146.2	249
Polyamide-imide	1380	4.6	63	3.3	45.7	260
PAI/30%g	1570	11.3	196	7.2	124.8	274
PAI/30%C	1420	18	210	12.7	147.9	274
Polycarbonate	1240	2.3	60	1.9	48.4	129
Polycarbonate/30%g	1420	8	125	5.6	88	149
Polyetherimide	1270	3.3	100	2.6	78.7	200
PEI/30%g	1510	8.7	196	5.8	129.8	210
PEI/30%C	1390	17	238	12.2	171.2	210
Polyethersulfone	1370	2.5	84	1.8	61.3	204
PES/30%g	1600	8.3	132	5.2	82.5	213
PES/30%C	1470	14	180	9.5	122.4	216
Polysulfone	1240	2.9	78	2.3	62.9	171
Polysulfone/30%g	1450	8.3	120	5.7	82.8	185
Polyimide	1400	4.5	100	3.2	71.4	315
Polyimide/30%g	1850	19	180	10.3	97.3	315
Mod. PPO	1100	2.7	65	2.5	59.1	129
Mod. PPO/30%g	1270	9	147	7.1	115.7	154
Polyester (PET)	1360	3.1	55	2.3	40.4	38
PET/30%glass	1680	9	150	5.4	89.3	225
Polyph. sulf (PPS)	1350	3.8	66	2.8	48.9	138
PPS/30%glass	1650	14	131	8.5	79.4	260
PPS/30%C	1450	21	175	14.5	120.7	263
PEEK	1320	3.6	100	2.7	75.8	182
PEEK/30%g	1490	10.5	225	7	151	310
PEEK/30%C	1420	13.7	240	9.6	169	315
Liquid crystal	1600	14	140	8.8	87.5	346
Polyarylates	1210	2.2	70	1.8	57.9	170
Fluoropol. (ECTFE)	1580	1.7	40	1.1	25.3	77
Allyls	1820	3.8	37	2.1	20.3	145
Allyls/glass	2000	12	65	6	32.5	220
Aminos (urea)	1500	10	45	6.7	30	130
Aminos (melamine)	1500	10	52	6.7	34.7	130
Cyanates	1250	3	80	2.4	64	250
Epoxies	1300	3	60	2.3	46.2	120
Phenolics	1400	8.2	80	5.9	57.1	190
Unsat. polyesters	1300	3.4	40	2.6	30.8	130
Polyester/40%glass	1500	9	124	6	82.7	220

Traditionally, plastics have been divided into a number of specific categories. Although these tend to be somewhat imprecise in that many plastics can belong to several categories, the terminology does help to give a broad indication of the potential uses of individual plastics.

1. *Engineering plastics*: Although most plastics can be used in engineering applications, one group has been distinguished by the description engineering plastics. These are polyamides, polycarbonates, polyacetals, modified polyphenylene ethers, and thermoplastic polyesters. The use of the term *engineering plastic* probably arose when it was established that these materials could be used as successful substitutes for metals in light engineering applications (for example, gear wheels, pulleys, etc.).

2. *Speciality plastics*: Other high-performance plastics, such as polysulphone and polyphenylene sulphide, are sometimes included in the list of engineering plastics, but the consumption of these materials is relatively small because economic factors restrict them for the more demanding types of application. Hence, these materials, along with exciting recent arrivals such as polyimides, fluoropolymers, polyetherketones, and polyarylates, tend to be more accurately described as speciality plastics. A particular feature of this type of plastic is the ability to be used continuously at service temperatures up to 300°C in circumstances where some metals cannot even be considered candidate materials. Typical properties of these materials are shown in [Table I](#).

3. *Elastomers (thermoplastic rubbers)*: Conventional vulcanized rubbers possess a range of very desirable properties, such as resilience and flexibility, over a wide temperature range and resistance to oils, greases, ozone, etc. However, they require careful, relatively slow processing, and it is not possible to reuse any waste material. To overcome the latter disadvantages, in recent years a range of thermoplastic rubbery materials has been developed. These exhibit the familiar feel and performance of rubbers but have the ease of manufacture associated with thermoplastics. There are several basic types of thermoplastic rubber (TPR). These differ in the way they impart rubber-like properties to the thermoplastic. In the polyurethane, styrenic, and polyester TPRs the chemists have grafted thermoplastic molecules on the rubber molecules. In the olefinic TPR there is a polypropylene matrix with fine rubber particles embedded in it to provide the elastomeric properties. Other types of TPR are based on polyamide and are essentially alloys. New advancements in polymer chemistry have created other families of elastomers—plastomers, metallocene-based EPDM alloys, styrene-ethylene block copolymers, and other blends and alloys.

4. *Polymer alloys*: Blends and alloys have become an important part of the plastics materials scene in recent

years. The concept of combining different materials to bring together their desirable attributes into one material has been utilized with metals for centuries, but its exploitation has been slow with plastics. ABS (acrylonitrile-butadiene-styrene) was one of the first commercially available plastic alloys but its success could not be generally extended to other materials due to the inherent incompatibility of most plastics. A recent revival of interest in polymer alloys has been caused by two factors. The first is the result of breakthroughs in the blending technology, so that some very interesting and exciting combinations have become possible. The second factor is that some lucrative market sectors (for example, the automotive industry) are demanding property specifications not available in a single plastic. As a result, there is an ever increasing range of commercially available alloys, and the material suppliers are prepared to listen to requests for combinations not yet available. Some of the most interesting and successful alloys are polyphenylene oxide/polystyrene (modified PPO), polycarbonate/ABS, polyamide/polypropylene, polyamide/polyphenylene ether, ASA/polycarbonate, and PBT/polycarbonate.

5. *Structural foam*: Many plastics can be foamed by the introduction of a blowing agent so that after molding the product consists of a cellular foam core and a solid skin. This type of structure is very efficient in terms of stiffness per unit weight. The foam effect is normally achieved by preblending the plastic granules with a heat-activated blowing agent. Polycarbonate, polypropylene, and modified PPO are popular materials for foam molding.

6. *Liquid-crystal polymer (LCP)*: These polymers arrived on the materials scene in the mid-1980s. They have an exciting new type of structure that is highly ordered, even in the molten state. The structure has been likened to a stack of uncooked spaghetti: if subjected to stress the stiff rods can slide past one another, but the same ordered orientation is retained. It is this retention of structural order in LCPs that gives them exceptional properties. They have outstanding dimensional stability, high strength, stiffness, toughness, and excellent chemical resistance. They also have very good high-temperature performance (up to 300°C), and they are easy to process.

7. *Oriented polymers*: When the chain-like structure of polymers is drawn out so that the chains become highly oriented, it is possible to achieve very high strength and stiffness values. For example, the modulus of polyethylene can readily be increased from under 1 GN/m² to about 70 GN/m². Hot stretching of the plastic can bring about some improvement in properties, but the maximum benefit is gained by cold drawing. In addition to mechanical properties, it has been shown that conductivity, diffusion/solubility, and piezoelectric properties are also enhanced, and this opens the door to new application areas.

Materials that have shown themselves to be amenable to high degrees of structural orientation include polyethylene, PVC, and PMMA.

8. *Composites*: Although unreinforced plastics can be used in engineering applications, it is only when fiber reinforcement is added that they become serious challengers for metals in the more demanding applications. Both thermoplastics and thermosets can benefit from fiber reinforcement. In the past these two types of composites tended to develop in separate ways and targeted different market sectors. However, in recent years the reinforcement technologies have moved closer together and now they often compete directly for the same applications. When fiber reinforcement was first identified as a means of obtaining very significant improvements in the mechanical properties of plastics, it was continuous-fiber reinforcement that attracted most attention. As the very large surface area of the continuous fibers needed to be completely wetted, it was necessary to use the low-molecular-weight resins that could be subsequently polymerized when the structure had been shaped. Hence, thermosetting resins dominated the continuous-fiber, high-performance sector, but the manufacturing processes were slow. In contrast, the thermoplastic industry concentrated on their fast production methods, such as injection molding, but were obliged to accept lower property enhancement through the use of short fibers. In recent years this situation has changed in that the thermosetting industry is prepared to sacrifice properties, that is, use shorter fibers to speed up production rates. Similarly the thermoplastic industry has devised ways of wetting continuous fibers with thermoplastic resins to get into the more lucrative high-performance application areas (for example, aerospace). The main advantages that thermoplastics have over thermosets are that they offer better toughness (damage tolerance) and they have better water resistance. It is evident that for thermosets it is possible to improve either one of these characteristics to acceptable standards but not both at the same time.

The continuous-fiber reinforced thermoplastics are normally available as a flat sheet containing the reinforcement. This is heated and shaped between matched halves of a mold to produce the desired shape. Also available in the thermoplastic sector are long (as opposed to continuous) fibers for reinforcement. The raw material is available as injection-moldable pellets containing wetted fibers that are the full length of the pellet, typically 10 mm. Normally, short fibers have lengths in the range of 0.75 to 0.5 mm so that the long fiber-reinforced thermoplastics have very significantly improved properties while retaining the easy, fast processing associated with injection molding.

The type of fiber used in plastics has a major effect on the properties and economics of a product. Glass fibers are

generally the least expensive, and they improve the creep resistance, thermal conductivity, and high-temperature capability of the plastic at short and long times. The extent of the improvement depends on the efficiency of the bond between the fiber and the base resin. This is where aramid fibers have had difficulty in the past. Although they offer a better property enhancement than glass, the high surface energy of the lightweight fibers makes wetting the fibers and dispersion of the base resin difficult. These problems have to a large extent been overcome by the development of special proprietary sizing/coupling systems. Characteristic features of aramid-reinforced plastics are low warpage and thermal expansion and uniform properties in all directions.

Carbon fibers offer the best improvements in strength, stiffness, and thermal conductivity, albeit at a price. There are also very significant increases in the heat-deflection temperature, creep resistance, and fatigue endurance. Carbon fibers also offer the ability to dissipate static electric charges very effectively; this is becoming a crucial feature in many new application areas for plastics. The resistivity of most plastics is in the region of 10^{12} – 10^{16} Ω cm, which means that they are excellent electrical insulators. However, there is a developing market in areas such as electronic component housings, EMI shielding, and battery construction where some degree of electrical conductivity in plastics would be desirable. The simplest way to achieve this is to load the plastic with a conductive filler such as metal or carbon. The developing technology is to devise structures in plastics that are intrinsically conductive, and some exciting advances have already been made in this field.

Natural fibers, such as jute, sisal, flax and hemp, are also used in plastics. There are attractive because they are low-cost, low-density materials offering good specific properties and they are friendly to the environment. However, there are also problems to be overcome. The poor moisture resistance of natural fibers and their incompatibility with the matrix resin are problems that attract a lot of research activity in some parts of the world.

An exciting development area in plastics is nanocomposites. This involves the addition of 2–5% of nanometer-size particles into a plastic to enhance fire resistance, improve mechanical properties, reduce thermal conductivity, and reduce permeability. The low addition levels of these very fine particles does not alter density or transparency. The automotive industry has been one of the first to utilize these materials for under-the-hood components. The original nanocomposites were produced by adding the small particles at the reactor stage but recent success has been achieved by compounding them into the plastic using an extruder.

II. DESIGN CONSIDERATIONS

Plastics offer the designer a very wide range, and interesting combinations, of attractive properties. Their ease of manufacture into complex shapes also presents exciting opportunities for the creative mind. As a result, plastics are serious contenders for most types of engineering components, and they are only excluded from those in which the demands are extreme—for example, continuous-service temperatures above 400°C or situations in which high electrical or thermal conductivity are required.

However, it is important that the designer recognize that plastics are only part of the portfolio of materials—metals, ceramics, etc.—that are available. In the early days of plastics it was very common to find them misused, so that the public image of these materials was low. The problem was not with the plastic but with the designer, who would quite often replace a metal article with a plastic one without any redesign to cater to the special characteristics of plastics. It

is very important that these early mistakes not be repeated, so it is essential that designers are aware of the advantages and limitations of plastics. This applies to their physical properties, their performance characteristics, and their molding/fabrication methods. Most material suppliers now recognize that it is better not to choose plastics if the performance specification dictates use of another material.

Of course, this puts a lot of responsibility on the designer because it means that he or she must be aware of the broad spectrum of properties of a very wide range of plastics and also be knowledgeable about their processing characteristics. Not all plastics can be injection-molded. (See Table II.) Many shapes cannot be produced by blow-molding. Processes such as rotational molding may put restrictions on the production rate. In many cases the molding operation will alter the properties of the plastic. For example, the molder may be obliged to use process conditions that improve the flowability of the melt, but this will in turn reduce the ductility and toughness of the product.

TABLE II Compatibility of Plastics with Processing Methods

Material	Process							
	Blow-molding	Compression molding	Extrusion	Foaming	Injection molding	Rotational molding	Thermo-forming	Transfer molding
ABS	✓	—	✓	✓	✓	—	✓	—
Acetal	✓	—	✓	—	✓	—	—	—
Acrylic	✓	—	✓	✓	—	—	✓	—
Aminos	—	✓	✓ ^a	✓ ^a	—	—	—	✓
Epoxides	—	✓	—	—	—	—	—	—
Fluoroplastics	—	✓	✓ ^a	—	✓	—	—	—
Ionomers	✓	—	✓	—	✓	—	✓	—
PEEK	—	✓	✓	—	✓	✓	—	—
Phenolics	—	✓	✓	✓	✓	—	—	✓
Polyamides	✓ ^a	—	✓	—	✓	✓ ^a	—	—
Polycarbonate	✓	—	✓	—	✓	—	✓	—
Polyester (unsaturated)	—	✓	—	✓	—	—	—	—
Polyester (thermoplastic)	✓	—	✓	—	✓	—	—	—
Polyimides	—	✓	—	—	—	—	—	—
Polyphenylene oxide	✓	—	✓	—	✓	—	—	—
Polyphenylene sulfide	✓	✓	—	—	✓	—	—	—
Polypropylene	✓	—	✓	✓	✓	✓	✓	—
Polysulfone	✓	—	✓	—	✓	—	✓	—
Polyurethane	—	✓	✓	✓	✓	—	—	—
Thermoplastic polyetheresters	✓	—	✓	—	✓	✓	—	—
Thermosets	—	✓	—	—	✓	—	—	✓

^aSpecial grades.

A good designer must be aware of such factors. This is particularly true in our modern society, which has come to expect high performance and regular design upgrades.

The task of choosing the correct plastic may appear daunting, but to most designers plastics offer an exciting challenge. The design process is not difficult but it requires a clear, logical, and open-minded approach. The first step must always be a precise statement of the design specification. This must define (1) the structural demands on the material, (2) the environmental factors relevant to the product, (3) the special codes of approval that may apply (e.g., food contact or aircraft authorities), (4) the appearance required (transparent, colored, decorated, etc.), and (5) the number of articles required.

On the basis of this type of information, it is possible to draw up a short list of materials. Many materials suppliers and a number of commercial organizations provide computerized databases that assist greatly at the material selection stage. The internet is also an excellent source of data and information on plastics.

Using these data, it is necessary to finalize the shape and then identify the most appropriate molding method. These must be considered together because each molding method places limitations on shape (e.g., wall-thickness distribution, undercuts, etc.). At the detailed mold design stage, when one is considering corner radii, draft angles, positioning of vents, shrinkage, etc., it is usual to seek advice from both the molder and the moldmaker because each will have a unique contribution to make. By the time that metal for the mold is being cut it is extremely important to have the selection of a plastic made because the shrinkage, dimensional tolerances, etc., that must be allowed for will be different for each plastic. Some of the general characteristics of thermoplastics and thermosets are indicated below.

A. Thermoplastics

1. *ABS (acrylonitrile-butadiene-styrene)*: Easily molded, tough, hard, plastic with a relatively high modulus. Good dimensional stability with low water absorption. Good wear resistance and some grades can be electroplated.

2. *Acetal*: Available as a homopolymer or copolymer. Strong engineering plastic with a good modulus, low water absorption, and excellent dimensional stability. High resistance to wear and chemicals and excellent property retention in hot water. Low tendency to stress-crack.

3. *Acrylic*: Hard, glossy plastic with high optical clarity and excellent resistance to outdoor weathering.

4. *Cellulosics*: Family of tough, hard plastics comprising cellulose acetate, butyrate, propionate, and ethyl cellulose. Dimensional stability is generally fair. Moisture

and chemical resistance is variable depending on the grades.

5. *Fluoroplastics*: Large family of low-strength, high-cost plastics that have a number of distinguishing features. In particular, they offer excellent dielectric properties, high-temperature stability, and chemical resistance. PTFE has a coefficient of friction that is one of the lowest for any material. Other plastics in this group are FEP, PFA, CTFE, ECTFE, ETFE, and PVDF.

6. *Ionomers*: Tough, tear-resistant plastics with excellent outdoor weathering resistance. Can be transparent and have good chemical resistance.

7. *Polyamide*: Engineering plastic with high toughness and wear resistance. Coefficient of friction is low and chemical resistance is excellent. Water absorption is high, so dimensional stability tends to be low.

8. *Polyamide-imide*: A high-cost amorphous plastic that offers high strength, high-temperature performance.

9. *Polyarylates*: Family of tough, heat-resistant plastics with excellent outdoor weathering resistance. Very low inherent flammability and high resistance to creep and warpage.

10. *Polyaryletherketones*: Strong, heat-resistant crystalline plastics capable of continuous service at 250°C. Excellent chemical and wear resistance. Family comprises polyetheretherketone (PEEK), polyetherketone (PEK), and polyetherketoneketone (PEKK).

11. *Polycarbonate*: An amorphous plastic with outstanding toughness. Excellent outdoor weathering resistance and good creep resistance. Susceptible to chemical attack and stress cracking.

12. *Polyester*: Polybutylene terephthalate (PBT) and polyethylene terephthalate (PET). Characterized by toughness with excellent dimensional stability. Good chemical resistance (except to strong acids and bases) and low water absorption. Generally notch-sensitive and not suitable for outdoor use. PET is capable of high optical clarity if prevented from crystallizing.

13. *Polyetherimide*: A strong, tough amorphous plastic suitable for use at high temperatures. Easily processed, with good dimensional stability and broad chemical resistance.

14. *Polyethylene*: Basically a commodity plastic but capable of performing in load-bearing applications if properly designed. Easily processed, tough, inexpensive plastic with excellent chemical resistance. Medium and high density grades are stronger and harder.

15. *Polyimide*: A tough plastic with good wear resistance and low coefficient of thermal expansion. Outstanding high-temperature properties but expensive and not easy to process.

16. *Polyphenylene ether*: The homopolymer is frequently referred to as polyphenylene oxide (PPO). Rigid,

amorphous plastics offering a broad working-temperature range. Very low water absorption and so excellent dimensional stability. Very amenable to blending with other plastics to produce alloys.

17. *Polyphenylene sulfide*: Good strength characteristics from low to high temperatures. Inert to most chemicals and inherently flame retardant.

18. *Polypropylene*: Part of the same generic group as polyethylene. Low-density, tough plastic (above room temperature) and very easy to mold. Outstanding fatigue resistance and stress-crack resistance.

19. *Polysulfone*: A clear, rigid, tough plastic capable of continuous use at 160°C. Excellent chemical resistance but notch-sensitive and expensive. Polyether sulfone is one of the most commercially successful members of the polysulfone family.

20. *Polyurethane*: Versatile material available in a wide range of forms. Very tough, with high abrasion and chemical resistance. Popular foaming material (rigid or flexible foams). Susceptible to ultraviolet attack. Also available as a thermoset.

21. *Polyvinyl chloride*: Wide range of formulations from hard-rigid to soft-flexible material. Hard and tough with excellent electrical insulation properties. Good outdoor weatherability and resistance to moisture and chemicals.

B. Thermosets

1. *Alkyd*: Easy, fast-molding material with no volatile by-products. Excellent electrical insulation with good heat resistance and low moisture absorption. Developed in the 1930s; one of the earliest applications was for automotive distributor caps.

2. *Allyl*: Excellent all-round electrical properties even under long-term heat and moisture. Also good resistance to chemicals even at high temperatures.

3. *Aminos*: Urea and melamine formaldehyde are the most common forms. Very easily colored. Urea is less expensive and molds more easily but melamine has higher hardness and better chip resistance and is more resistant to temperature and chemicals.

4. *Bismaleimide (BMI)*: Excellent high-temperature performance but, like most thermosetting materials, it lacks toughness.

5. *Cyanates*: Tough materials with excellent adhesive peel strength. Low dielectric loss and moisture absorption. Good dimensional stability.

6. *Epoxies*: Excellent combination of mechanical strength, electrical resistance, and adhesion to most materials. Low mold shrinkage, and some formulations cure without heat or pressure. Most grades are relatively brittle.

7. *Melamine formaldehyde*: The hardest of all plastics, this material is excellent for food contact applications and is fire resistant. Requires higher pressure than phenolics to mold but its color properties are superior to those of the polyesters.

8. *Phenolics*: General purpose, cost-effective resins. One of the first synthetic plastics; developed by Leo H. Baekeland in the early 1900s. Color limited to black or brown. Easily molded into complex shapes with good dimensional stability. Good creep resistance and very hard surface.

9. *Polyesters*: Unlimited colors and also available transparent. Easy to mold but shrinkage is high. Very popular resin for use with glass fibers; product is often referred to as fiberglass. Also form basis for the popular (easily molded) bulk molding compound (BMC) and sheet molding compound (SMC).

10. *Polyimides*: These materials have a low dielectric constant and a high dielectric strength. Their chemical resistance and creep resistance are both excellent. Also available as a thermoplastic.

11. *Polyurethane*: Wide range of formulations. The greater the degree of cross-linking, the greater the hardness. Excellent toughness, good traction properties, and resistance to wear make it ideal for skate wheels and shoe heels. Also available as a thermoplastic.

12. *Silicones*: Can be available as elastomeric or rigid materials. They are very inert and can be used over a broad temperature range. Popular as gaskets, sealing rings, and O-rings. They have good weatherability and excellent electrical properties.

13. *Urea formaldehyde*: Can be available in a range of colors. Good surface hardness and electrical properties but relatively poor heat resistance.

C. General Behavior Characteristics of Engineering Plastics

The successful design of plastic articles requires a broader range of knowledge of materials behavior than would be the case for designing a metal product. This is because factors such as time, temperature, environment, etc. are variables that must be considered in almost all cases for plastics, whereas these are only relevant in extreme cases for metals. The simplest illustration of this is the design of a product to be subjected to a static load at room temperature. If the product is made from metal and it is able to withstand the applied load in the short term, one can have reasonable confidence that there will be no problems in the long term. However, with plastics the modulus (related to the stiffness) of the material will decrease with time, so the ability to withstand the applied load in the short term should not lead one to assume that it will

be a successful design in the long term. After a period of a month, or six months, or several years, the product could fail as a result of the sustained action of the static load. To avoid this, it is essential to design plastic articles with a full awareness of the long-term material characteristics.

D. Mechanical Properties of Plastics

1. *Short-term tests:* The majority of tabular data (e.g., Table I) generated for plastics is based on short-term tests. This is clearly because it is quick and easy to obtain such information and to a large extent it can be correlated directly with data for other materials (e.g., metals). However, from the foregoing comments it should be apparent that this type of data is not suitable for most types of design calculations for plastic products. The short-term data are supplied simply to facilitate initial sorting of plastics for a particular application and to provide a basis for quality control checks. It should also be noted that the short-term data for plastics are very sensitive to test conditions. Figure 1 illustrates how temperature and testing speed can alter the stress-strain characteristic for a thermoplastic. For this reason it is important to adhere to standard, recommended test procedures. The main international standard test methods for plastics are summarized in Table III. The principal short-term properties quoted for plastics are strength and modulus, using a tensile and/or flexural test mode. Occasionally, data are quoted for compression or shear behavior, but this is not common.

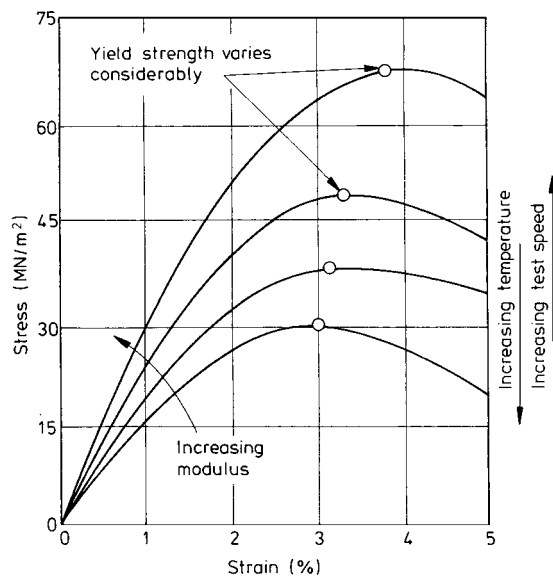


FIGURE 1 Effects of temperature and testing speed on mechanical properties of plastics.

2. *Impact tests:* The ability of a plastic to resist impact forces is one of its most practically relevant properties. However, this is also one of its least understood properties. Impact strength is not an inherent material property that can be used in a design calculation. It is simply a quantitative measure of the ability of a material to absorb impact energy. It is known that this ability is very sensitive to factors such as geometry, structural variations produced by molding, the speed of the impact, and environmental conditions. In some cases the impact strength of a plastic may be assessed using an arbitrary test that matches quite closely the service conditions of the product. However, due to the difficulty of comparing impact test data obtained in a wide range of test methods, there has been a move in recent years toward standardization of all impact tests. To a large extent this has been prompted by the desire to have a uniform data presentation format in all computerized databases. The Izod impact test (essentially flexure of a notched sample) and the tensile impact test are becoming the most widely used tests. Although it is recognized that the results do not always correlate well with the behavior of real moldings, the tests are clearly defined and are unambiguous. Thus, they provide a useful ranking of materials to indicate which are most likely to be successful in a particular application. For research purposes, instrumented impact tests are preferred in which the load and deformation of the material are recorded simultaneously throughout the brief impact event.

3. *Long-term tests:* The two main long-term properties that are relevant for plastics are *creep* and *fatigue*. The former reflects behavior under long-term static loads, and the latter reflects performance under long-term fluctuating loads. The creep behavior of plastics arises essentially from their viscoelastic nature. Thus, when a static load is applied, there is an almost instantaneous (elastic) increase in strain followed by a time-dependent (viscous) increase in strain. The latter is called *creep*. Similarly, if the static load is removed or decreased there will be an instantaneous decrease in strain followed by a time-dependent decrease in strain (called *recovery*). This type of strain response to an applied stress is illustrated in Fig. 2. In the creep situation where the strain is increasing at constant stress (ignoring small changes in cross-sectional area), the most practical implication is that the modulus of the material (ratio stress/strain) is decreasing. As most design calculations involve the use of a modulus for the material, it is very important that the correct value be used. For metals, of course, the modulus is usually regarded as a constant, and the values of the modulus for most common metals are familiar to designers. However, for plastics one must choose a modulus that is relevant to the time scale of the loading. For example, if the design involves the application of a static load for a design life of, say, five years, then

TABLE III Standard Test Method for Plastics

Physical property	Standard organization ^a			
	ASTM	ISO	DIN	British
Density	D792 D1505	1183	55749	BS2782, 602A
Vol. resistivity	D257	IEC 93, 167	53482	BS6233
Surf. resistivity	D257	IEC 93, 167	53482	BS6233
Dielectric constant	D150	IEC 250	53483	BS2782
Dielectric strength	D149	IEC 243	53981	BS2782
Arc resistance	D495			BS2782
Thermal conduct.	C177, C518		52612	BS874
Melt. temperature	D2117	3146, 1218	53736	BS2782, 103A
Heat dist. temp.	D648	75	53461	BS2782, 115A
Transition temp.	D3418			
Vicat softening	D1525	306	53460	BS2782, 120A
Melt flow index	D1238	1133	53735	BS2782, 720A
Melt rheology	D3835		54811	
Oxygen index	D2863	4589		BS2782, 141A
Flammability	D635	1210		BS2782, 508A
	D568, 3713			BS6336
	D3801		53438	BS4422
Smoke emission	D2843, E662			BS5111, 6401
Water absorption	D570	62	53495	BS2782, 430A
		117	53457	
Weathering	D4459	877	53388	BS2782, 540A
	D1435	4507	53386	
	D2565	4892	53387	
Chemical resistance	D543	175	53476	BS4618, 3505
Stress crack	D2552	4600	53449	BS4618
Wear resistance	D1044	3537	52347	BS2782, 310A
			53754	
Gas transmission	D1434	2556	53380	BS2782
Water vapor trans.	E96	1195	53122	BS3177
Static tensile	D638	527	53455	BS2782, 320
Static flexure	D790	178	53452	BS2782, 335A
Creep	D2990	899	53444	BS4618
Relaxation	D2991			
Compression	D695	604	53454	BS2782, 345A
Creep rupture	D2239			BS3505
	D1598			BS3506
Fatigue	D671		53442	
			53398	
Impact	D256	178, 180	53448	BS2782, 350
	D1822		53448	
	D3029	6603	53443	BS2782, 306B
	D1709			
	D4272			
Ball hardness		2039	53456	BS2782, 365D
Rockwell hardness	D785	2039		BS2782, 365C
Shore hardness	D2240	868	53505	BS2782, 365B
Barcol hardness	D2583	EN59	EN59	BS1001
Material specs.	D4000			
Sample preparation	D647, 1897	293	53451	BS2782, 901A
				BS7008

^aSome tests are also standardized by Underwriters Laboratories, Northbrook, Illinois.

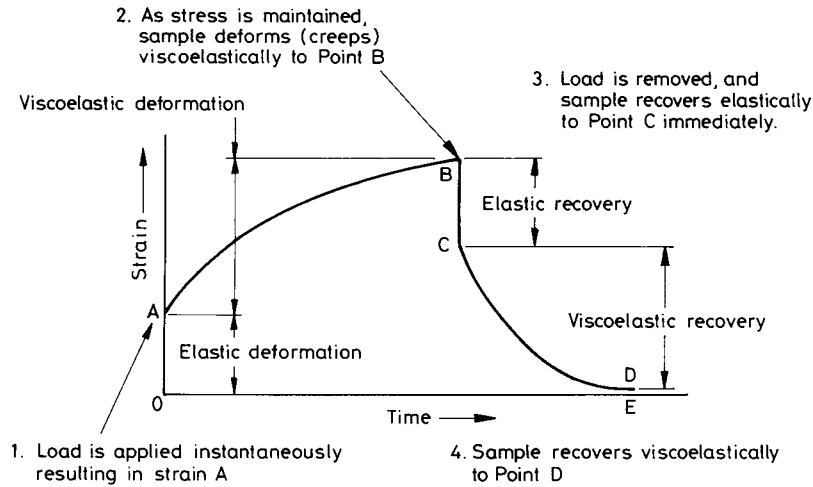


FIGURE 2 Typical creep and recovery behavior of a plastic.

the five-year modulus should be used in the calculations, not the short-term modulus quoted in [Table I](#). This design approach usually results in a considerable over-design at short time scales, but this can be accommodated in any safety factors used. [Figure 3](#) shows the type of creep modulus vs. time design graph that can be obtained for plastics.

From the foregoing it is clear that creep can result in unacceptably high deformations of a product if it is not designed correctly. In some cases, *creep fracture* may occur. Thus, although a plastic product is able to withstand an applied stress at short times, it may fracture under the same stress at long times. A situation where this can occur is in gas- or water-pressurized plastic pipes. The problem is also made worse by the fact that, whereas short-term creep-fracture failures are normally ductile, the long-term failures are often brittle. Thus, the short-term fractures provide a visual warning that failure is imminent and they

have an inherent energy-absorbing mechanism, but the long-term fractures occur without warning and sometimes with catastrophic results. [Figure 4](#) shows the type of design chart that should be used for this type of situation. Note in particular the “knee” in the curve, which should alert one to the danger of extrapolating short-term data if that is all that is available.

Another aspect of viscoelasticity that the designer must be aware of is *relaxation*. If a plastic product is in a situation where the strain is not permitted to increase (or decrease), the stress necessary to maintain this strain will decrease with time. Although it might appear that this relaxation of stress is not a concern, it can lead to problems in some situations—for example, in cases where the stress level must be maintained to prevent leakage of a fluid.

As plastics are used in more and more demanding engineering applications, it is inevitable that they will be subjected to fluctuating stresses as well as to static stresses.

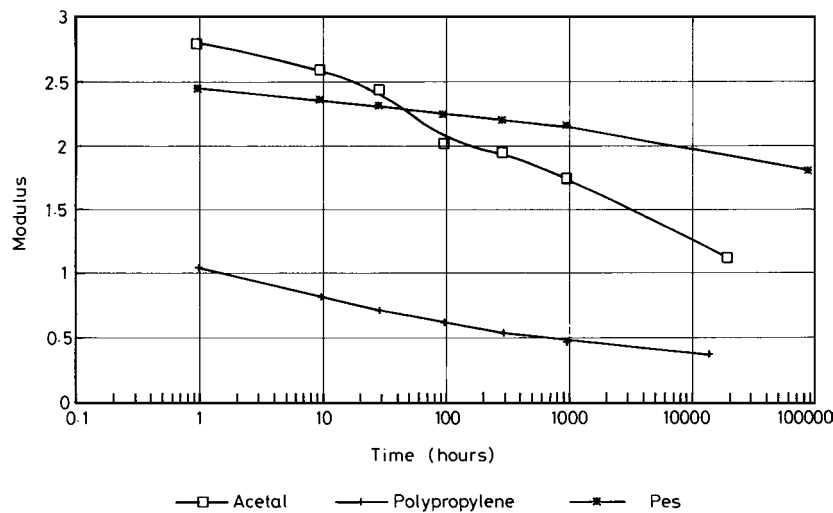


FIGURE 3 Creep modulus for plastics. Modulus values in MN/m².

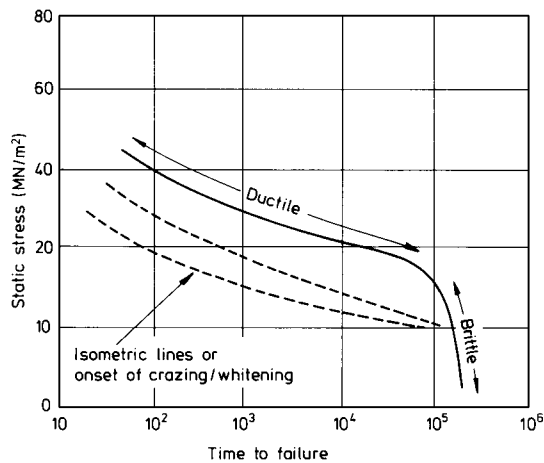


FIGURE 4 Typical creep fracture behavior of plastics.

Experience has shown that when the stress level is fluctuating, plastics are susceptible to *fatigue-crack* growth in the same way metals are. However, with plastics two separate failure mechanisms can occur. On the one hand, if the applied stress amplitude or the cyclic frequency is high then hysteritic heating of the plastic can result in catastrophic softening of the material. Under other conditions where hysteritic heating does not occur, the product may still fail as a result of the more conventional slow crack growth through the material. In the case of thermosetting plastics, only the latter failure mechanism can occur.

E. Electrical Properties of Engineering Plastics

Plastics are probably most familiar as electrical insulators, and this is used to great advantage in many applications, but they do have a wide range of other electrical properties that designers of engineering components need to consider:

1. *Dielectric strength*: The voltage gradient (V/m) across a plastic that will cause conduction through the plastic.
2. *Volume resistivity*: A measure of the resistance to the flow of electricity through a plastic.
3. *Surface resistivity*: A measure of the resistance to the flow of electricity over the surface of a plastic.
4. *Arc resistance*: A measure of the time taken for a conductive track to develop along the surface of a plastic.
5. *Dissipation factor*: A measure of the heat dissipated in a plastic when it is subjected to an alternating current.
6. *Dielectric constant*: A measure of the electrical energy stored in a plastic. It reflects the way plastics change the nature of nearby electric fields.

The standard test procedures for these properties are listed in Table III. It should be noted that, as with mechanical properties, the electrical properties of plastics are not constants. For example, the dielectric strength of a plastic decreases as time and temperature increase.

F. Thermal Properties of Engineering Plastics

The high-temperature performance of plastics is usually quantified by the heat-deflection test. A test sample of the plastic is loaded in flexure and the temperature rise necessary to cause a predefined deflection is measured (see Tables I and III). The Vicat softening temperature is a similar type of test in that the temperature at which a needle penetrates the plastic by a prescribed amount is recorded. Other thermal properties such as coefficient of linear thermal expansion, thermal conductivity, and specific heat are defined and measured as for other materials. However, it should always be remembered that for plastics these properties will be dependent on factors such as temperature and the structural variations brought about by processing conditions. Flammability is, of course, one of the most crucial and topical behavior characteristics for plastics. As fire performance is very much linked to ignition source, geometry of plastic, environmental conditions, etc., it is clear that it is not possible to define flammability as a single inherent property of the material. Properties such as smoke-emission rate, flame spread, the ability to self-extinguish, etc. are all important, and in many cases it is best to conduct tests on the final product rather than laboratory samples. The Underwriters Laboratory has defined a series of standardized test procedures for measuring the flammability of plastics (UL 94), and its classifications are a valuable indicator of the suitability of a material for a particular application.

G. Degradation of Engineering Plastics

Under this heading one has to consider all the environmental factors that can contribute to a deterioration in the performance of a plastic. Generally, crystalline plastics offer better environmental resistance than amorphous plastics, but it can be dangerous to take the generalization too far. It is always wise for the designer to explore thoroughly the likely environmental factors and then check the vulnerability of specific plastics. The chemical resistance of plastics varies widely. Some plastics are resistant to concentrated acids but are attacked by everyday substances such as butter or soap. The circumstances in which the latter substances can cause problems are usually referred to as *environmental stress cracking*. This is a phenomenon whereby a stressed plastic product develops crazes or cracks when it comes in contact with a certain

substance. *Weathering* is another factor that must be taken into account. Basically, it relates to the attack on the plastic by ultraviolet (UV) radiation, often coupled with water absorption. Absorption of water into plastics has a plasticizing effect that increases flexibility, but it leads to brittleness when the water is eliminated. The UV radiation effectively causes a breakdown of the bonds in the molecular structure, and this also leads to brittleness. A loss of color is the usual warning of weathering attack on plastics.

III. MATERIAL AND PROCESS SELECTION

It was indicated earlier that a wide range of processing methods can be used to convert engineering plastics from a raw material into an end product. The choice depends on many factors. In particular, the number of parts required and their shape will have a major influence. At the next stage in the decision process, the plastic chosen for the product may put a limitation on the possible molding methods. Finally it may be necessary to do a detailed cost comparison to select from a short list of possible molding methods.

In general terms, engineering thermoplastics may be processed by injection molding, extrusion, blow molding, thermoforming, rotational molding, or foam molding. Thermosets may be shaped using compression molding, transfer molding, injection molding, or reaction injection molding (see Table II). Fiber composites can be manufactured using injection molding, filament winding, pultrusion, stamping, manual or automatic lay-up, and various types of resin injection molding. A number of new hybrid moulding methods are also becoming available for both thermoplastics and thermosets. These often arise out of the need to create a special geometry for a specific application, and the versatility of plastics gives scope for ingenious minds to create novel manufacturing methods. Examples of such methods include twin-sheet thermoforming, gas injection molding, and three-dimensional blow molding.

Each molding method has its own advantages and peculiarities. For example, injection molding has high mold costs, but fast production rates can make this less significant if the number of articles required is very large. Rotational molding, on the other hand, has low mold costs but is best suited to short production runs due to its relatively long cycle time (see Fig. 5). Other processes such as hand lay-up are very labor intensive, and product quality relies to a large extent on the skills of the operator. In recent years, major advances have been made in achieving volume production with high-performance fiber-reinforced plastics.

The key point to remember is that engineering plastic parts must be designed for production. On a simplistic

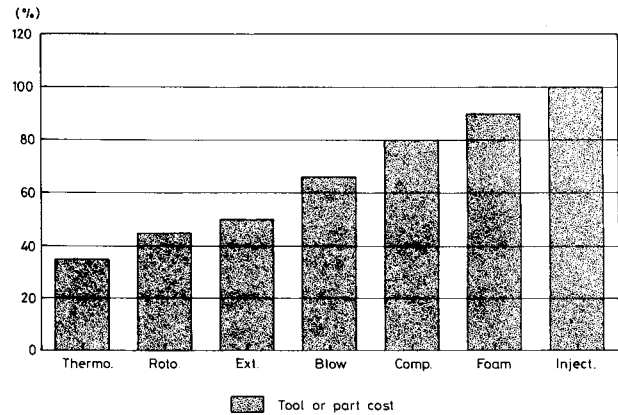


FIGURE 5 Relative costs of various molding methods.

cost-per-unit-weight basis, high performance plastics would be selected for very few applications, because the material cost is so high. Indeed, contrary to popular belief, it is often not as a weight-saving measure that plastics are used. For example, in the car industry the improvement in fuel consumption is very small relative to weight saving, so that very large mileages would need to be covered to achieve any sensible payback. Instead, the advantages to the car industry of using high-performance plastics are related to the major savings in production costs and the combination of functionality and aesthetics that comes with the design freedom offered by plastics. However, it should also be noted that there are other special market sectors where a high price premium is acceptable for any genuine weight savings. To take an extreme case, a space satellite project may not succeed unless weight savings can be made. Hence, this industry accepts that a high cost may have to be paid for such weight savings. Even in the civil aviation industry, price premiums of \$400/kg are generally acceptable due to the reduced fuel consumption or increased payload that this represents. Also, in the sports industry, it has been clearly demonstrated that the market will bear high-cost products if there is a perceived improvement of performance.

It may be seen from Table IV that the costs of engineering plastics can vary widely, as can their relative properties. To rationalize the choice of plastic for a particular application, the following procedure may be adopted. Consider the design of a flexural element in which the width and length are fixed but the depth is variable in order to achieve a defined stiffness at minimum cost. Standard strength-of-materials texts show that the flexural stiffness of this system is given by:

$$\text{Stiffness} = \alpha_1 EI \quad (1)$$

where α_1 is a constant, E is the modulus of the plastic, and I is the second moment of area. Hence,

TABLE IV Typical Prices of Engineering Plastics (Relative to Polypropylene)

Material	Density (kg/m ³)	Price (vol. basis)	Price (wt. basis)
Polypropylene	905	1	1
ABC	1040	2.6	2.3
Polyacetal	1410	5.7	3.7
Polyamide(66)	1140	5.7	4.5
Polyamide(66)/30%g	1300	6.3	4.4
Polyamide-imide	1380	82.8	54.3
Polycarbonate	1240	5.5	4
Polyetherimide	1270	13.8	9.8
Polyethersulfone	1370	19.3	12.7
Polysulfone	1240	13.8	10.1
Polysulfone 30%g	1450	13.4	8.4
Polyimide	1400	160	103.4
Mod. PPO	1100	3.4	2.8
Mod. PPO/30%g	1270	6.8	4.8
Polyester(PET)	1360	5.4	3.6
PET/30%glass	1680	6.2	3.3
Polyph. sulf(PPS)	1350	15.2	10.2
PPS/30%glass	1650	12.4	6.8
PEEK	1320	75.9	52
PEEK/30%C	1420	82.8	52.8
Liquid crystal	1600	69	39
Fluoropol. (ECTFE)	1580	42.9	24.6
Allyls	1820	9.7	4.8
Allyls/glass	2000	11.7	5.3
Aminos (urea)	1500	2.6	1.6
Aminos (melamine)	1500	2.9	1.7
Cyanates	1250	63.4	45.9
Epoxies	1300	4.8	3.3
Phenolics	1400	2.1	1.4
Unsat. polyesters	1300	2.3	1.6

$$\text{Stiffness} = \alpha_2 E d^3 \quad (2)$$

where α_2 is a constant.

Now the cost of the beam will be given by:

$$\text{Cost} = \alpha_3 \rho d C \quad (3)$$

where ρ is density, C is cost per unit weight, and α_3 is a constant.

So substituting from Eq. (2) into Eq. (3) for the depth d ,

$$\text{Cost} = \alpha_4 (\rho C / E^{1/3}) \quad (4)$$

Hence, the desirability factor in the material, in order to minimize cost for the given stiffness, is the ratio ($E^{1/3} / \rho C$), which should be maximized. Using this relationship it is possible to compare a range of materials

(plastics, metals, ceramics, etc.) to obtain a ranking of the cost effectiveness of each. If it is desired to make the comparison on the basis of maximum stiffness for minimum weight, the bottom line of the equation should be simply ρ instead of ρC .

A similar analysis can be carried out for a range of other structural shapes. The relevant equations are summarized in Table V.

IV. SUCCESSFUL ENGINEERING APPLICATIONS FOR PLASTICS

There are many success stories where the use of plastics and composites has resulted in improved performance and new markets for products that had previously been manufactured from more traditional materials. Some examples of these applications are as follows.

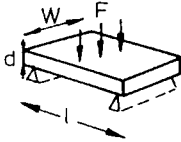
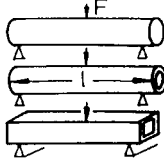
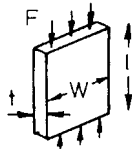
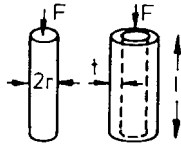
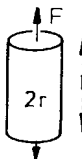
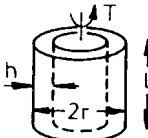
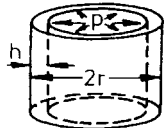
A. Automotive Applications

It has been evident for many years that the plastics industry views the automotive sector as one of its most demanding challenges, both in terms of materials performance, quality, and the production rates required. Initially the vast majority of uses of plastics were in vehicle trim (that is, secondary, non-loadbearing applications). In 1960 a typical family car contained about 1% by weight of plastic. Today the average weight of plastic in a car is about 175 kg, representing between 9 and 18% of the weight of the vehicle.

Interior trim still accounts for the biggest proportion of plastics in cars (about 40% of the total) but the use of plastics in demanding under-the-hood applications is increasing rapidly and is expected to reach 20% soon. At present more than 25% of the air inlet units made for cars world wide are plastic. Cost savings of over 50% are quoted in regard to this conversion from metal to plastic, accompanied by similar benefits in weight reduction. Exterior body panels also represent an exciting challenge for plastics in terms of design for manufacture and performance. Sheet molding compound (SMC) is a composite that is popular in this sector, and at the current time approximately 13 million units are manufactured annually for automotive use. Body panels from other materials such as PET or polypropylene blends reinforced with glass fibers and alloys of polycarbonate/polybutylene terephthalate are also proving to be very successful. A primary target in this application is to achieve a Class A, durable finish straight from the mold so as to remove the need for the relatively expensive painting stage.

Polypropylene continues to be the popular choice for automotive applications. U.S. consumption of this material for cars is currently about a billion pounds. Many

TABLE V Desirability Factors to be Maximized for Minimum Cost Design (for Minimum Weight Replace should be ρC by ρ)

Mode of loading	Minimize cost for given:	
	Stiffness	Ductile strength
Bending of plate		$\frac{E^{1/2}}{\rho C}$ $\frac{\sigma_y^{1/2}}{\rho C}$
Bending of rods and tubes		$\frac{E^{1/2}}{\rho C}$ $\frac{\sigma_y^{2/3}}{\rho C}$
Buckling of plate		$\frac{E^{1/3}}{\rho C}$ —
Buckling of slender column or tube		$\frac{E^{1/2}}{\rho C}$ —
Tie		$\frac{E}{\rho C}$ $\frac{\sigma_y}{\rho C}$
Torsion tube		$\frac{G}{\rho C}$ $\frac{\sigma_y}{\rho C}$
Cylinder with internal pressure		$\frac{E}{\rho C}$ $\frac{\sigma_y}{\rho C}$

factors are pushing the increasing use of plastics in cars. Not least are the “green” or environmental issues that require lighter vehicles (to minimize energy consumption and/or facilitate alternative energy sources for the vehicle) as well as the need for recycleability. Many car manufacturers continue to strive for the all-plastic car and a number of prototypes have been made and tested by

the major manufacturers. In one of the most recent innovations, Chrysler produced a Composite Concept Vehicle (CCV), which features an almost totally plastic (reinforced PET) body. Table VI shows some of the other plastics used by the automotive industry. And of course, when one looks at high performance vehicles, such as Formula One racing cars or fighter aircraft, then there is a very high reliance on fiber reinforced plastics.

B. Sporting Applications

Although sporting applications do not, in most cases, present critical (life or death) problems for the designer, they do make very stringent demands on the properties of materials. For this reason, the plastics industry takes the sporting, and indeed the toy, industries very seriously. There is no doubt that any development that is good enough for a sporting goods application is going to make its mark in other fields also.

Composites, in particular, can be used to very good effect in sports and leisure goods. The racing yachts used in the Americas Cup depend almost totally for their high performance on fiber-reinforced plastics. Using these materials provides combinations of lightness, strength and high modulus not available in any other materials. Modern tennis rackets used by professionals are usually hollow molded structures utilizing fiber-reinforced plastic. The height records that pole vaulters can achieve increased dramatically with the introduction of the fiber-reinforced plastic poles. The key property required in this application is a high elastic limit. A fiberglass composite has an elastic limit of 2–3%, whereas a high strength aluminium alloy is less than 1%. The high elastic limit of the composite means that it can bend into a radius of about 1 m without breaking, and in doing so stores enough energy to propel the vaulter over the bar, which is typically 6 m above the ground.

C. Medical Applications

Plastics have been a major boon to the medical profession. In North America the value of the industry has been estimated to be over \$4 billion. The packaging of medical products, tubes, and pharmaceutical closures are routine applications for plastic materials. Their high impact and chemical resistance and ability to be easily sterilized make them the first choice in many cases. Almost 80% of polymers used in the medical industry is represented by PVC, polypropylene, and polystyrene. The excellent resistance to steam exposure of some plastics (such as polyphenylsulfone) is used very effectively in special applications such as microfiltration devices for immunoassays, reusable syringe injectors, respirators, nebulizers, prosthesis packaging, sterilizer

TABLE VI Application of Plastics in the Automotive Industry

Application	Properties sought	Typical materials used
Bumpers, fenders, side protection bars	Impact resistance, paintability (or Class A finish)	Polypropylene, alloys of PC, PPE/PA alloys
Fascias	Rigidity, good surface detail	Polypropylene
Body panels	Rigidity, energy absorption, Class A finish	Reinforced PP or PET, SMC or alloys of PC/PBT
Wheel arches	UV resistance, impact strength, abrasion resistance	PP, HDPE
Electrical components, gears, etc.	High modulus, dimensionally stable	PPS, PBT, polyacetal, reinforced nylons
Fuel tanks	Impact resistance, low permeability	HDPE, multi layers
Seat foams, soft touch trim	Lightweight, flexible, durable	Polyurethane
Grills	Stiff, dimensionally stable, easily molded	ABS, polypropylene
Cable sheathing	Electrical and thermal resistance, impermeable to water	PVC and cross-linked PE
Fuel lines	Low permeability, flexible, tough	Nylons, multi layer materials
Transparent fittings	Clarity, surface hardness, toughness	Polycarbonate acrylic (PMMA)
Washer bottles	Tough, inert to chemicals, impermeable	HDPE, PP
Headlights	Tough, good optical properties	Polycarbonate
Intake manifolds	Stiff, high temperature and oil/fuel resistance	Nylons
Safety belts	High strength, flexible, tear resistant	Nylons

trays, and dental tools. Polyetheretherketone (PEEK) is sterilizable by autoclave, gas, or high-energy radiation and offers good chemical resistance. Common uses include catheters, disposable surgical instruments, and sterilization trays. Polyurethane can be sterilized using dry heat, gas, or radiation, and its applications include tubing, catheters, connectors/fittings, pacemaker leads, tensioning ligatures, wound dressings, and transdermal drug-delivery patches. Polycarbonate and its blends are capable of being sterilized by all the common methods, and its uses include equipment housings and reservoirs. Liquid-crystal polymers (LCPs) can also be sterilized by all the common methods and are used in products such as dental tools, surgical instruments, and sterilizable trays.

Examples of life-saving devices based on the unique properties of plastics are evident in every hospital ward and operating theater. Some typical examples are the use of carbon-fiber-reinforced plastics in operating tables, NMR imagers, and radiotherapy simulators. In these applications the combination of lightness, strength, stiffness, and good fatigue resistance are supplemented by relatively low absorption of X-rays. This means that much clearer, sharper images are obtained with lower dosages of radiation.

In general, the drive to reduce healthcare costs and the need to use disposable medical supplies are important factors generating a higher demand of medical plastics. New materials, with improved properties, are being developed in order to satisfy the requirements of infection control standards. Current research is being conducted to determine the biological reactivity of polymeric materials. Some new types of polymeric material can match very closely the performance of bone. This enables broken

limbs to be repaired or replaced by a synthetic material that is accepted by the human body and encourages new tissue growth.

Plastic/fiber composites are also being used very effectively to meet the tough weight and strength demands made by artificial limbs. In this application lightness is crucial because if, for example, a patient needs to have a whole leg replaced, the prosthesis acts like a pendulum and is difficult to control if it is too heavy. The successful development of fiber composites in artificial limbs has meant that patients are able to adapt and use the new limb quickly and easily and without pain or discomfort.

D. Electrical Applications

The effects caused by static (electrostatic discharge, ESD) and electromagnetic/radiofrequency interference (EMI/RFI) are familiar as sparks jumping from fingertips to a doorknob or clothing and electronic noise in communications networks. In some cases these are just an inconvenience (or can be used to advantage such as in packaging cling film), but when they are present in, on, or near electronic circuitry or flammable environments, they create hazards that must be or eliminated. ESD can damage or destroy electronic components, erase or alter magnetic data storage, and initiate explosions or fires. Electromagnetic and radiofrequency waves radiate from computer circuits, radio transmitters (including cellular phones), fluorescent lamps, electric motors, lightning, and many other sources. In most cases they are harmless but they become undesirable when they interfere with other electrical equipment. An example of this is interference with medical devices such as pacemakers.

Plastics are inherently electrical insulators and they are often used to exploit this characteristic. However, conductive thermoplastics offer parts designers extra freedom in the control of static (ESD) and EMI/RFI. The mechanism of conductivity in plastics is similar to that of most other materials. Electrons travel from point to point when under a driving force, following the path of least resistance. Conductive modifiers with low resistance can be melt blended with plastics to alter the polymers inherent electrical resistance. At a threshold concentration unique to each conductive modifier and resin combination, the resistance through the plastic mass is lowered enough to allow electron movement. The speed of electron movement depends on the modifier concentration—in other words, on the separation between the modifier particles. Varying the percentage or type of conductive additive used in the compound permits one to control the degree of electrical resistivity. Nearly every type of polymer can be compounded with conductive fillers and most conductive thermoplastics can be made in a variety of colors.

The types of conductive additives that can be used include carbon-based powder and fibers, metal powder and fibers, and metal-coated fibers of carbon or glass. Recently, unique conductive additives such as metal-coated substrates, intrinsically conductive polymers (ICPs), and inherently dissipative polymers (IDPs) have found commercial use in conductive thermoplastic compounds. Conductive thermoplastic compounds prevent static accumulation from reaching dangerous levels by reducing the parts electrical resistance. This allows static to dissipate slowly and continuously rather than accumulate and discharge rapidly as a spark. Conductive thermoplastic compounds provide protection against EMI/RFI by absorbing electromagnetic energy and converting it to electrical or thermal energy. They also function by reflecting energy.

There are numerous application areas for conductive plastics in the computer industry in the form of housings to protect sensitive electronics, and in industries using powders there is often a strong dependence on the unique characteristics of these materials. In the pharmaceutical industry, for example, antistatic surfaces, containers, and packaging must be used to eliminate dust attraction into the product. An example of an application in the medical field is the body for asthma inhalers where the correct dosage of the medication is critical and any static “capture” of the fine-particulate drugs can affect recovery from a spasm.

E. Aircraft/Aerospace Applications

The very stringent demands that the aircraft/aerospace area makes on materials has made it very much the final frontier for plastics and composites. The fact that

some plastics are already well established in this field is further confirmation that they have come of age as engineering materials. Plastics and composites are now widely used for primary and secondary components in civil and military aircraft. The Lear Jet and the Beech Starship are two examples of what can be achieved in that the complete outer structure of the planes utilize carbon-fiber-reinforced plastic (CFRP). Another very significant example is the vertical and horizontal tail-plane of the Airbus 320. These structures are predominantly made from CFRP in both monolithic and honeycomb-cored sandwich panels. Glass-fiber-reinforced plastics are used for the bridging layers between the honeycomb cores and the CFRP skins. The weight saving achieved is about 20%, which represents a very considerable reduction in fuel consumption or increase in payload. Another major advantage of using composites in this type of application is that the fabrication methods used reduce the number of individual parts that must be assembled. In the case of the Airbus 320 the reduction was from about 2000 parts in older designs to less than 100 parts in the latest design. Future generations of commercial aircraft will make even more extensive use of plastic composites.

In military and space applications, the advantages of composites are utilized to their utmost effect. The cost of launching rockets is so high that a high price can be tolerated for any weight saving that can be achieved. As a result, thousands of composite parts have been used successfully in spacecraft. The bank of information that has been built up in this application area has shown that CFRP can outperform other materials because of their very high specific strengths and stiffnesses, excellent fatigue resistance, and low coefficients of thermal expansion. As the trend continues toward longer design lifetimes of spacecraft, it seems certain that the use of composites will also continue to grow rapidly in this application area.

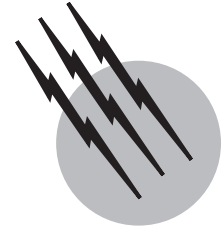
SEE ALSO THE FOLLOWING ARTICLES

CHEMICAL PROCESS DESIGN, SIMULATION, OPTIMIZATION, AND OPERATION • COMPOSITE MATERIALS • CONSTITUTIVE MODELS FOR ENGINEERING MATERIALS • FRACTURE AND FATIGUE • PLASTICITY • PLASTICIZERS

BIBLIOGRAPHY

- Astrom, B. T. (1997). “Manufacturing of Polymer Composites,” Chapman & Hall, London, p. 469.
 Berins, M. L., ed. (1991). “Plastics Engineering Handbook,” 5th ed., Hanser, Munich, p. 869.
 Crawford, R. J. (1998). “Plastics Engineering,” Butterworth-Heinemann, Oxford.

- Dominghaus, H. (1993). "Plastics for Engineers," Hanser, Munich, p. 785.
- Dyson, R. W. (1990). "Engineering Polymers," Chapman & Hall, New York, p. 195.
- Epel, J. N., *et al.*, eds. (1998). "Engineered Materials Handbook—Engineering Plastics," Vol. 2, ASM International, Metals Park, OH, p. 882.
- Gibson, L. J., and Ashby, M. F., "Cellular Solids," 2nd ed., Cambridge University Cambridge, U.K., p. 510.
- Grosberg, A. Y., and Khokhlov, A. R. (1997). "Giant Molecules," Academic Press, San Francisco, CA, p. 244.
- Gruenwald, G. (1992). "Plastics—How Structure Determines Properties," Hanser, Munich, p. 357.
- Huang, J. C. (1995). "EMI shielding plastics: a review," *Advances in Polymer Technology* **14**(2), 137–150.
- Kelly, T., and Clyne, B. (1999). "Composite materials—reflections on the first half century," *Physics Today* **Nov.**, 37–41.
- Maier, C., and Calafut, T. (1998). "Polypropylene," *Plastics Design Library*, Norwich, NY, p. 432.
- Mascia, L. (1989). "Thermoplastics: Materials Engineering," 2nd ed., Elsevier Applied Science, London, p. 537.
- Mathews, G. (1996). "PVC: Production, Properties, and Uses," *Institute of Materials*, London, p. 379.
- Miller, E. (1996). "Introduction to Plastics and Composites," Marcel Dekker, New York, p. 434.
- Pardos, F. (1999). "Forecast for the World Plastic Industry to 2020," *Plastics Engineering* **55**(11), 53–57.
- Portnoy, R. C. (1998). "Plastomer modified PP films for medical product packaging," *Plastics Engineering* **54**(4), 33–35.
- Reinhart, T. J., ed. (1987). "Engineered Materials Handbook—Composites," Vol. 1, ASM International, Metals Park, OH, p. 983.
- Saheb, D. N., and Jog, J. P. (1999). "Natural fiber polymer composites: a review," *Advances in Polymer Technology* **18**(4), 351–363.
- Sawyer, L. C., Linstid, H. C., and Romer, M. (1998). "Emerging applications for neat LCPs," *Plastics Engineering* **54**(12), 37–41.
- Selke, S. E. M. (1997). *In* "Understanding Plastics Packaging Technology" (E. H. Immergut, ed.), p. 206, Hanser, Munich.
- Throne, J. L. (1996). "Thermoplastic Foams," Sherwood Publishers, Hinckley, OH, p. 692.
- Walder, A. J. (1998). "Characteristics of medical polyurethanes," *Plastics Engineering* **54**(4), 29–31.
- Weber, M. E. (1995). "The processing and properties of electrically conductive fiber composites," *In* "Chemical Engineering," McGill University, Montreal, Canada.
- Wigotsky, V. (1998). "Medical plastics," *Plastics Engineering* **54**(4), 22–27.
- Woods, G. (1987). "The ICI Polyurethanes Book," Wiley, Chichester, p. 330.



Polymer Processing

Donald G. Baird

Virginia Polytechnic Institute and State University

- I. Introduction
- II. Rheology of Polymer Melts
- III. Thermal Physical Properties
- IV. Extruders
- V. Compounding
- VI. Extrusion Dies
- VII. Post-Die Processing
- VIII. Molding and Forming

GLOSSARY

Blow molding A polymer tube, referred to as a *parison* if extruded and a *preform* if injection molded, is expanded into a cavity by means of air pressure where it is rapidly solidified on contact with the mold walls. It is used for producing hollow objects such as bottles, containers, and fuel tanks.

Compounding The process by which other polymers and organic and inorganic additives are combined with a polymer to improve processing performance and properties of the given polymer.

Compression molding A process by which a polymer mass is subjected to high mechanical pressure within a cavity to cause it to take the shape of the cavity, solidified, and the part removed. Used primarily for highly filled polymers with a high viscosity and for highly filled thermosetting resins.

Extruder A device used to melt and pump polymeric fluids consisting of a screw rotating within a metallic barrel.

Extrusion die A metal channel attached to the end of an extruder to provide shape to an emerging polymer stream.

Film blowing An extrusion process for producing thin films of polymers with biaxial orientation based on extruding from an annular die and subjecting the bubble to both axial (drawing) and radial (air pressure) stretching.

Injection molding A cyclic automated process by which polymer pellets are melted in an extruder, the melt is injected into a cavity, solidified, and the part removed. The process is used to make small intricate parts as well as large parts for automobiles.

Melt index The mass flow of a fluid (in grams) in the period of 10 min from a capillary of known dimensions under a specified pressure and temperature.

Newtonian fluid A fluid in which the shear stress is linearly proportional to the velocity gradient; i.e., a fluid of constant viscosity.

Non-Newtonian fluid A fluid whose viscosity is not constant and may exhibit a wide range of time-dependent responses.

Rheology Science of the deformation and flow of materials.

Rheometry The equipment and process by which the rheological properties of polymeric fluids are determined.

Thermoforming A process by which a sheet of polymer is heated, usually by radiation heating, to the point at which it is pliable and then pushed or pulled into a cavity by applied mechanical force or pressure or applied vacuum. Used frequently for producing materials for packaging applications, but large parts for recreational use can also be produced.

Viscoelasticity The response of a fluid or solid which is a combination of viscous and elastic behavior as determined by the rate of deformation relative to the relaxation time of the material.

IN THE CONTEXT of this article, polymer processing refers to the operations by which polymer resin is converted to finished plastic parts and objects. Of particular interest are those resins referred to as *thermoplastics* which can be softened by the application of heat, processed, solidified, and reheated and processed again. This is opposed to *thermosetting* resins which, once solidified via the process of cross-linking, cannot be softened for reprocessing. Virgin resin is rarely processed; instead, a wide variety of additives are compounded into the resin to improve processing performance and properties. These resins plus appropriate additives are then heated and shaped by flow and deformation using a number of processing operations (extrusion, injection molding, film blowing, fiber spinning, blow molding, thermoforming, compression molding, etc.).

I. INTRODUCTION

The conversion of polymers to finished parts and articles differs significantly from that used to process low molar mass (sometimes molecular weight is used) fluids because of their unique molecular features that lead to high viscosity and viscoelastic behavior. Polymeric mate-

rials typically have molar masses in the range of 20,000 to 150,000 g/g-mol. When the molar masses are greater than some critical value, M_c , the large molecules physically entangle with each other as shown schematically in Fig. 1. This entanglement network leads to not only highly viscous fluids but fluids with elastic properties. Under finite deformations, macromolecules stretch, disentangle, and orient (Fig. 1). On cessation of flow, thermal motion causes the molecules to recover their initial conformation and re-entangle. As a result of this recovery process, polymeric fluids partially resemble purely elastic materials such as cross-linked rubber and are therefore referred to as being viscoelastic.

The processing behavior of polymeric melts is highly dependent on several molecular features. The size of the molecule or its molar mass is one of the key factors. Polymers rarely consist of a single molar mass; they are instead a distribution of molar masses. Because of the distribution of chain sizes it is common to use moments of the distribution to specify the molar mass of a resin. For example, the number average molar mass, M_n , is the total mass of polymer divided by the number of polymeric chains (i.e., the average molecular weight). The weight average molar mass, M_w , is the number of chains of given weight times the weight of material with that given molar mass divided by the total weight of polymer. It is a higher moment of the distribution. The ratio of M_w/M_n is referred to as the *polydispersity* of the polymer. For polymers synthesized by means of a step polymerization process (e.g., PET and nylon), this ratio is around 2.0 (the most probable distribution), whereas for polymers produced by means of addition polymerization (polyethylenes), the ratio can vary from 4.0 to 30.0. With the advent of metallocene catalysts, polyethylenes with polydispersity indices in the range of 2.0 are possible.

Although techniques such as gel permeation chromatography or size exclusion chromatography are typically used to provide details about the molar mass distribution, several other techniques are used by manufacturers to specify the molar mass of their polymers. For polymers such as those produced via means of step polymerization the inherent viscosity (IV) is commonly used.

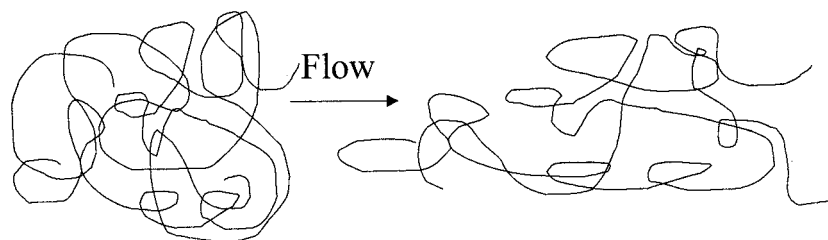


FIGURE 1 Entangled macromolecules in the undeformed and deformed states.

The IV is obtained from measurements of the viscosity of a dilute polymer solution relative to the viscosity of the solvent. Typically, it is measured at a specific polymer concentration. The IV is directly related to the intrinsic viscosity, which is obtained by the extrapolation of solution viscosities to zero polymer concentration. Well-known relations between the intrinsic viscosity and the molar mass of a polymer exist (this relation is referred to as the Mark–Houwink relation). For polymers such as those produced by means of addition reactions, the melt index (MI) is used to categorize the molar mass. The measurement of MI is discussed in the rheology section.

Another factor affecting processing is whether the chain is linear or branched. Branching refers to arms that extend from the main backbone of a chain. These branches may be long or short depending on whether the molar mass of the branch, M , is greater than the critical molar mass for entanglements, M_c , or less than M_c . Branching may be quite dense, in which every chain contains many branches, or sparse, in which not every chain contains a branch. The branching architecture can be described as *random*, *comb*, *star*, or *H*. Random branching involves irregular spacing of the branches along the backbone as well as the branches. Combs are systems in which the branches protrude from one side of the chain. Star-branched polymers consist of three or four arms emanating from a central point. H-branched polymers consist of multiple branches at the end of the chains. The processing behavior as well as the mechanical properties of a polymer are dependent on the branching architecture.

The thermal conditions for processing are determined by two important thermal transition temperatures. These temperatures are the glass transition temperature, T_g , and the melting point, T_m . For amorphous polymers that exhibit no crystallinity, the T_g determines where it becomes deformable and, hence, processible. For semicrystalline polymers, T_m determines the primary temperature at which the polymer will flow and become processible. Some semicrystalline polymers can be processed to limit the formation of crystallinity and thereby behave somewhat like an amorphous polymer. Temperature T_g is associated with an increase in free volume, which allows mobility of the polymer chains. Hence, one must be above T_g to process amorphous polymers.

II. RHEOLOGY OF POLYMER MELTS

A. Purely Viscous Behavior

When a simple fluid, such as water, is placed between the two plates, as shown in Fig. 2, in which the top plate is moved to the right with constant velocity, V , the relation

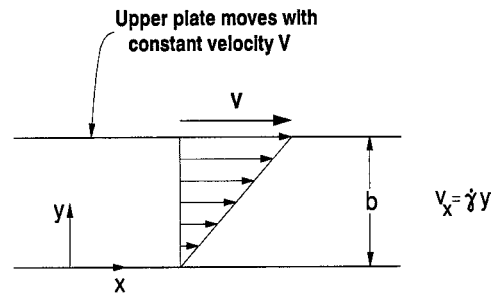


FIGURE 2 Steady simple shear flow with shear rate equal to V/b .

between force, F , divided by the area of the plates, A , and the velocity divided by the separation distance, b , is given as follows:

$$\frac{F}{A} = \mu \frac{V}{b}. \quad (1)$$

The constant of proportionality, μ , is called the viscosity of the fluid. F is the force required to keep the top plate moving with a constant velocity. The force per unit area acting in the x direction on a fluid surface at constant y by the fluid in the region of lesser y is the shear stress, τ_{yx} . Because the velocity of the fluid particles varies in a linear manner with respect to the y coordinate, it is clear that $V/b = dv_x/dy$, which is the derivative of the velocity with respect to the distance y . Equation (1) can be rewritten as:

$$\tau_{yx} = -\mu(dv_x/dy). \quad (2)$$

This states that the shear force per unit area is proportional to the negative of the local velocity gradient and is known as Newton’s law of viscosity. Fluids that obey this simple linear relationship are termed *Newtonian fluids*. From Eq. (2) we can determine the dimensions of viscosity, which are mass/unit length/unit time. For the *Système International* (SI), the units of viscosity are Pa sec (or kg/m/s), whereas for the CGS system they are the Poise (dyn/cm²/sec or g/cm/sec).

The flow behavior of most thermoplastics does not follow Newton’s law of viscosity. To quantitatively describe the viscous behavior of polymeric fluids, Newton’s law of viscosity is generalized as follows:

$$\tau_{yx} = -\eta dv_x/dy, \quad (3)$$

where η can be expressed as a function of either dv_x/dy or τ_{yx} . Some typical responses of polymeric fluids are shown in Fig. 3, where τ_{yx} is plotted versus the velocity gradient. For a *pseudoplastic* fluid, the slope of the line decreases with increasing magnitude of dv_x/dy , or in essence the viscosity decreases. Some polymeric fluids (in some cases polymer blends and filled polymers) exhibit a *yield stress*, which is the stress that must be overcome before flow

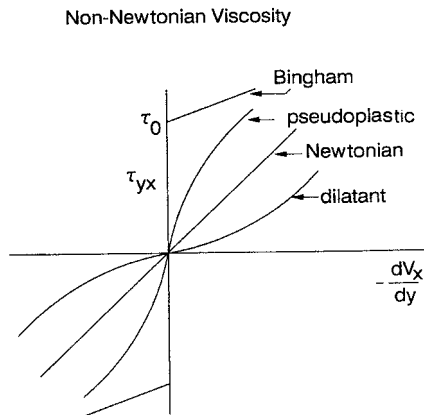


FIGURE 3 Shear stress versus velocity gradient or shear rate for several different types of fluids. [From Baird, D. G., and Collias, D. I. (1998). "Polymer Processing: Principles and Design," Wiley, New York.]

can occur. When flow occurs, if the slope of the line is constant, then the fluid is referred to as a *Bingham fluid*. In many cases the fluid is still pseudoplastic once flow begins. Finally, in some cases the viscosity of the material increases with increasing velocity gradient. The fluid is then referred to as being *dilatant*.

Many empiricisms have been proposed to describe the steady state relation between τ_{yx} and dv_x/dy , but we mention only a few of the most useful for polymeric fluids. The first is the power law of Ostwald and de Waele:

$$\eta = m \left| \frac{dv_x}{dy} \right|^{n-1}. \quad (4)$$

This is a two-parameter model in which n describes the degree of deviation from Newtonian behavior; m , which has the units of Pa sec^n , is called the *consistency*. For $n = 1$ and $m = \mu$, this model predicts Newtonian fluid behavior. For $n < 1$, the fluid is pseudoplastic while for $n > 1$ the fluid is dilatant. In particular, the model describes the viscosity behavior as shown in Fig. 4 in the region where the viscosity decreases linearly with increasing velocity gradient (which is also called shear rate). The curves shown in Fig. 4 are also referred to as *flow curves*. Actually most polymeric fluids exhibit a constant viscosity at low shear rates and then shear thin at higher shear rates (Fig. 4). A model that is used often in numerical calculations, because it fits the full flow curve, is the Carreau–Yasuda model:

$$\frac{\eta - \eta_\infty}{\eta_0 - \eta_\infty} = \left[1 + \left(\lambda \frac{dv_x}{dy} \right)^a \right]^{\frac{n-1}{a}}. \quad (5)$$

This model contains five parameters: η_0 , η_∞ , λ , a , and n . η_0 is the zero shear viscosity just as above; η_∞ is the viscosity as the shear rate or dv_x/dy goes to very high

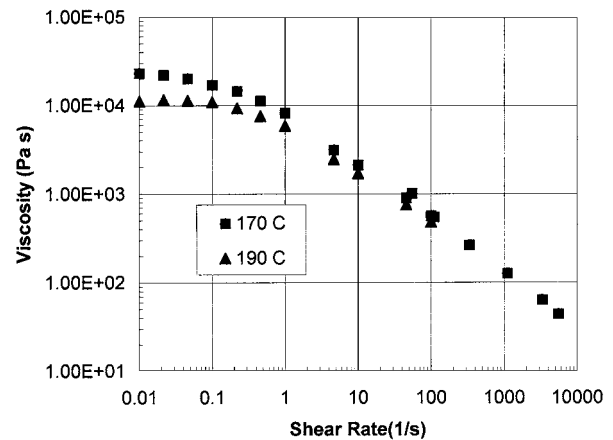


FIGURE 4 Viscosity versus shear rate (i.e., flow curves) for a metallocene catalyzed polyethylene at temperatures of 170 and 190°C.

values (e.g., $>10,000 \text{ sec}^{-1}$) and for polymer melts this can be taken as zero; λ has units of seconds and approximately represents the reciprocal of the shear rate for the onset of shear thinning behavior; and n represents the degree of shear thinning and is nearly the same as the value in the power-law model. Finally, a is a parameter that controls how sharp the transition is into shear-thinning behavior.

B. Viscoelastic Behavior

The term *viscoelastic behavior* refers to the fact that a polymeric fluid can exhibit a response which resembles that of an elastic solid under some circumstances, while under others it can act as a viscous liquid. Viscosity alone is not sufficient to describe the flow behavior of polymer melts. Additional material functions are needed which reflect their viscoelastic nature. Before defining several of the most important material functions in addition to viscosity, it is necessary to discuss the kinematics or deformation associated with these material functions.

Two basic flows are used to characterize polymers: shear and shear-free flows. (It so happens that processes are usually a combination of these flows or sometimes are dominated by one type or the other.) The velocity field for rectilinear shear flow (Fig. 2) is given below:

$$v_x = \dot{\gamma}(t)y \quad v_y = v_z = 0, \quad (6)$$

where $\dot{\gamma}(t)$ may be constant or a function of time. The velocity field for shear-free flows can be given in a general form as

$$\begin{aligned} v_x &= -1/2 \dot{\epsilon} (1 + b)x, \\ v_y &= -1/2 \dot{\epsilon} (1 - b)y, \\ v_z &= +\dot{\epsilon}z, \end{aligned} \quad (7)$$

where $\dot{\epsilon}$ is the extension rate and b is a constant that is either 0 or 1. When $b = 0$ and $\dot{\epsilon} > 0$, the flow is *uniaxial extensional flow*. When $b = 0$, but $\dot{\epsilon} < 0$, the flow is *equibiaxial extensional flow*. When $b = 1$ and $\dot{\epsilon} > 0$, the flow is called *planar extensional flow*.

The deformational types are shown for a unit cube of incompressible material in Fig. 5. In shear flow, the unit cube is merely skewed with the degree of strain given by the angle, $\dot{\gamma}(t_2 - t_1)$, the edge makes with the y axis. The term $\dot{\gamma}(t_2 - t_1)$ represents the shear strain. Three types of shear-free flow are described in Fig. 5. In uniaxial extensional flow the unit cube is stretched along the z axis while it contracts uniformly along the x and y axes in such a manner that mass is conserved. The elongational strain is given by $\dot{\epsilon}(t_2 - t_1)$. In biaxial elongational flow, the unit cube is stretched equally along the x and y directions but must contract in the z direction in such a way that mass is conserved. In planar extensional flow, the unit cube is stretched along the z axis but is constrained so that it contracts only in the x direction.

Significant differences are seen the behavior of polymeric fluids in these two types of deformation, and each type of deformation has a different effect on the orientation of macromolecules. For example, uniaxial and planar extensional flows impart significant molecular orientation to polymers during flow compared to shear flows. On the other hand, biaxial extensional flow is a weak flow and

does not lead to a strong degree of molecular orientation. Furthermore, the rheological response can be significantly different for a polymer in extensional flow versus shear flow.

Various types of shear flow experiments are used in the characterization of polymeric fluids, depending on whether the flow is steady or unsteady. When $\dot{\gamma}(t)$ is constant, $\dot{\gamma}_0(t)$, then three material functions are defined in steady shear flow:

$$\begin{aligned} \tau_{xy} &= -\eta(\dot{\gamma})\dot{\gamma}_0, \\ \tau_{xx} - \tau_{yy} &= -\Psi_1(\dot{\gamma})\dot{\gamma}_0^2, \\ \tau_{yy} - \tau_{zz} &= -\Psi_2(\dot{\gamma})\dot{\gamma}_0^2, \end{aligned} \tag{8}$$

where η is the viscosity, Ψ_1 is the primary normal stress difference coefficient, and Ψ_2 is the secondary normal stress difference coefficient. The values $\tau_{xx} - \tau_{yy} = N_1$ and $\tau_{yy} - \tau_{zz} = N_2$ are the primary and secondary normal stress differences, respectively, and are related to the elastic nature of polymer melts.

There are numerous transient shear flows in which $\dot{\gamma}(t)$ varies in a specific way with time. One of the most frequently used experiments is when $\dot{\gamma}(t)$ varies sinusoidally with time:

$$\dot{\gamma}_{yx} = \dot{\gamma}_0 \cos \omega t, \tag{9}$$

where $\dot{\gamma}_0$ is the amplitude and ω is the angular frequency. Because polymeric fluids are viscoelastic, the stress lags

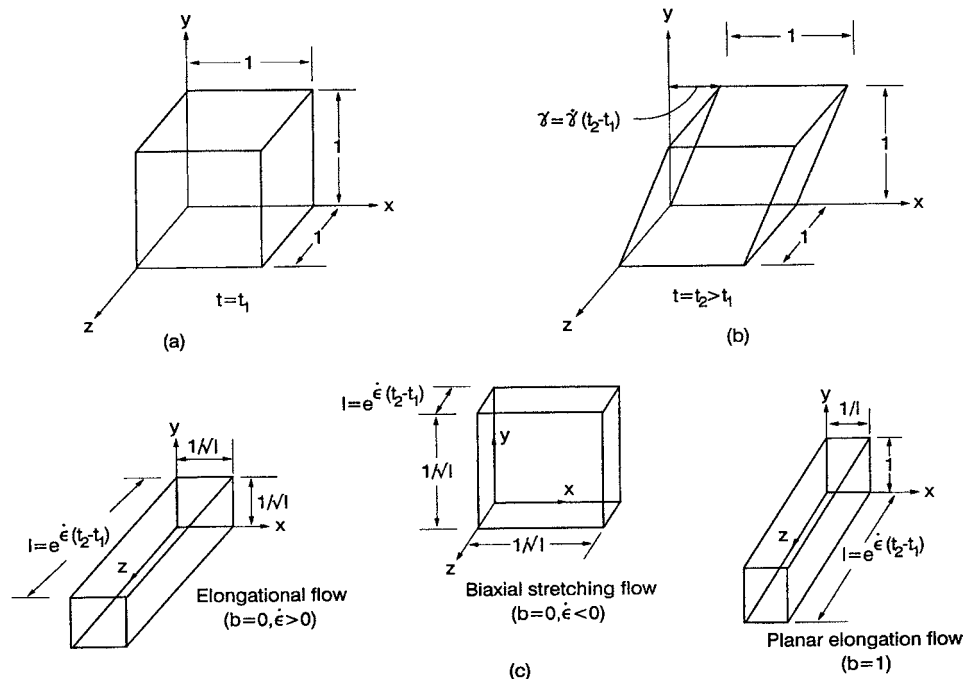


FIGURE 5 The deformation of (a) a unit cube of material from time t_1 to t_2 in (b) steady simple shear flow and (c) three kinds of shear-free flow. [From Bird, R. B., Armstrong, R. C., and Hassager, O. (1987). "Dynamics of Polymeric Liquids: Volume I, Fluid Dynamics," Wiley, New York.]

behind the input frequency. One component of the stress is in phase with the rate of deformation given by Eq. (9) and one is out of phase. When the strains are small, and the stress is linearly proportional to strain, one is said to be in the linear viscoelastic region. The complex viscosity is defined as

$$\eta^* = \eta' - i\eta'' \quad (10)$$

where η' is the dynamic viscosity (viscous contribution) and η'' is the elastic contribution associated with energy storage per cycle of deformation. For a number of polymeric resins, $|\eta^*(\omega)| = \eta(\dot{\gamma})$ when $\omega = \dot{\gamma}$, which is known as the Cox–Merz relation.

Some prefer to treat polymeric fluids as viscoelastic solids and thereby represent τ_{yx} as a function of shear strain, in which case the complex shear modulus is defined as:

$$G^* = i\omega\eta^* = G' + iG'' \quad (11)$$

where G' is the storage modulus and G'' is the loss modulus. Part of the value of the G' measurements rests on the fact there is a good correlation between $2G''$ and N_1 . It should also be pointed out that η' and G'' and η'' and G' are interrelated; i.e., $\eta'\omega = G''$ and $\eta''\omega = G'$.

Other transient shear flows are used including the start-up of flow, cessation of flow, creep, and constrained recoil. The coverage of these flows and the corresponding material functions is beyond the scope of this chapter (see Bird *et al.*, 1987).

Similar flow histories can be described for shear-free flows as described for shear flows. Here we discuss only steady and stress growth shear-free flows. For steady simple (i.e., homogeneous deformation) shear-free flows, two viscosity functions, η_1 and η_2 , are defined based on the two normal stress differences given in Eq. (12):

$$\tau_{zz} - \tau_{xx} = -\bar{\eta}_1(\dot{\epsilon}, b)\dot{\epsilon} \quad \tau_{yy} - \tau_{xx} = -\bar{\eta}_2(\dot{\epsilon}, b)\dot{\epsilon}. \quad (12)$$

For uniaxial extensional flow where $b=0$ and $\dot{\epsilon} > 0$, $\eta_2=0$, and η_1 is called the extensional or elongational viscosity, $\bar{\eta}$. Most often it is not possible to reach steady-state conditions and, hence, only the stress growth data at the start-up of flow is measured. Representative data are shown in Fig. 6 where $\bar{\eta}$ versus tensile stress and η versus shear stress values are compared for a polystyrene melt. At low stress values, $\bar{\eta} = 3\eta_0$, which is called the Trouton ratio. However, when η shear thins, $\bar{\eta}$ tends to increase slightly with stress and then decrease. At higher values of stress, η is several decades lower than $\bar{\eta}$.

C. Rheometry: Shear Flow Measurements

Measurements of rheological properties at low shear rates are usually carried out in rotary rheometers such as the cone-and-plate (C-P) shown in Fig. 7 or the plate-plate (P-P) systems. In rotary rheometers one of the members of the system is driven, which transmits force through the fluid to the bottom plate. The torque, T , and the normal force, F , are recorded at the bottom member by means of

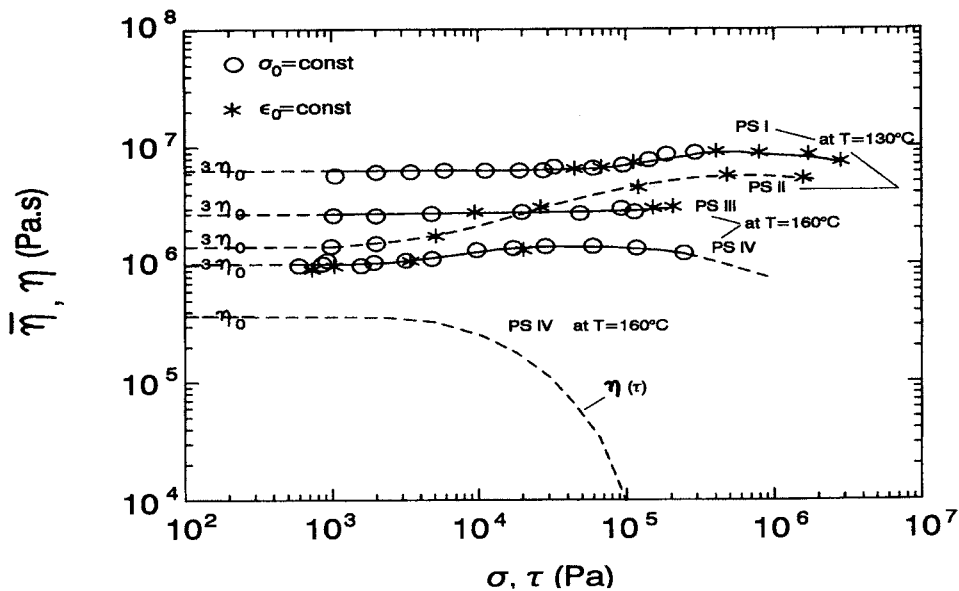


FIGURE 6 Steady shear and uniaxial extensional viscosity versus shear stress and extensional stress, respectively, for a polystyrene melt. [From Münstedt, H. (1980). *J. Rheo.* 24, 847–864.]

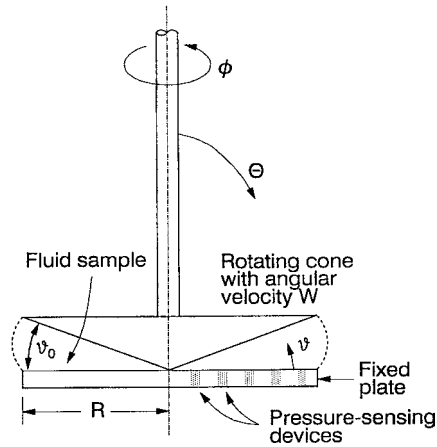


FIGURE 7 Cone-and-plate rheometer. The geometric variables are the cone angle, ϑ_0 , and the radius, R . The torque, T , required to turn the cone at an angular velocity W is converted to viscosity while the normal force exerted on the bottom plate is converted to the primary normal stress difference.

transducers. The C-P configuration has the advantage that the shear rate is nearly uniform through the gap. Because the shear rate is uniform throughout the gap, it is possible to use the C-P to measure the transient response of polymeric fluids. For the case of the P-P device the shear rate varies with the distance r from the center of the plates. Hence, one must make a series of measurements at various shear rates before obtaining values of η and $\Psi_1 - \Psi_2$ at specific values of shear rate. For the C-P device the maximum shear rate for which measurements are possible (the melt usually fractures and comes out of the gap) is about 1 sec^{-1} while slightly higher values of shear rate are possible with the P-P device.

The capillary rheometer (Fig. 8) is commonly used to obtain η at high shear rates. Basically the device consists of a barrel for melting the polymer and a plunger that pushes the melt through the capillary. The data obtained from this device consist of the pressure required to push the melt through the capillary and the volumetric flow rate (plunger speed and cross-sectional area). Two corrections are applied to these data. First, the pressure drop must be corrected for the additional pressure required for the melt to pass through the contraction between the barrel and the capillary. For any fluid, the wall shear stress is given by:

$$\tau_R = \left(\frac{-dp}{dz} \right) \frac{R}{2}, \quad (13)$$

where dp/dz is the pressure gradient in the capillary. Usually $-dp/dz$ is approximated by $\Delta P/L$, where ΔP is the pressure drop across the whole capillary including the entrance and L is the capillary length. For a Newtonian fluid the pressure gradient is nearly constant over the length of the capillary. The pressure gradient is nonlinear for poly-

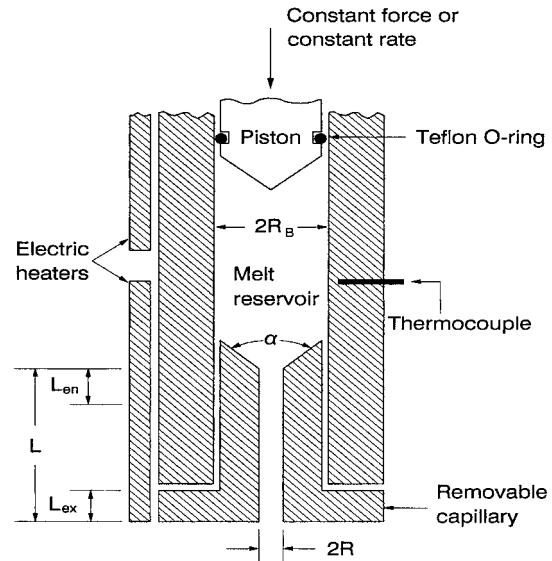


FIGURE 8 A capillary rheometer in which polymer pellets are melted by heat conducted through the barrel and then pushed by the plunger through the capillary. Viscosity data are obtained from the force and plunger speed measurements. [From Baird, D. G., and Collias, D. I. (1998). "Polymer Processing: Principles and Design," Wiley, New York.]

meric materials and approximating it as $\Delta P/L$ would lead to large errors in the determination of τ_R . The difference between the pressure extrapolated from the linear region and the true pressure is called the entrance pressure, ΔP_{ent} . There may be residual pressure at the die exit, called the exit pressure, ΔP_{ex} , but it is quite small relative to ΔP_{ent} and hence is neglected. If there is additional pressure at the die exit, then the method used to obtain ΔP_{ent} actually includes ΔP_{ex} . The total pressure correction for exit and entrance regions is called the end pressure, ΔP_{end} , i.e.,

$$\Delta P_{\text{end}} = \Delta P_{\text{ex}} + \Delta P_{\text{ent}}. \quad (14)$$

The true wall shear stress, τ_R , is then obtained by plotting the total pressure, ΔP_{tot} , versus L/D at each value of shear rate for several L/D values (these are called Bagley plots). The extrapolation of ΔP_{tot} to $L/D = 0$ is ΔP_{end} . One now obtains τ_R as follows:

$$\tau_R = \left(\frac{\Delta P_{\text{tot}} - \Delta P_{\text{end}}}{L} \right) \frac{R}{2}. \quad (15)$$

Because the velocity profile is nonparabolic, one must correct the apparent wall shear rate, $\dot{\gamma}_a$, defined as $4Q/\pi R^3$. The true wall shear rate for a shear-thinning fluid is:

$$\dot{\gamma}_w = \frac{\dot{\gamma}_a}{4} \left(3 + \frac{d \ln \dot{\gamma}_a}{d \ln \tau_R} \right). \quad (16)$$

Hence, by plotting τ_R versus $\dot{\gamma}_a$ on a ln–ln plot one obtains the reciprocal of the required correction factor. It turns out that this value is just $1/n$, where n is the power-law index.

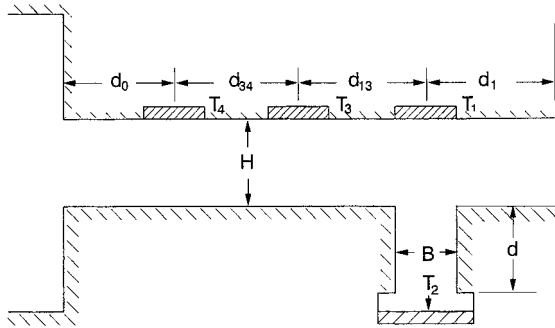


FIGURE 9 A slit-die rheometer consisting of two parallel plates through which polymer melt is pumped. The wall shear stress is determined from the pressure measurements along the upper wall and the shear rate from the volumetric flow rate. [From Baird, D. G., and Collias, D. I. (1998). "Polymer Processing: Principles and Design," Wiley, New York.]

Slit-die rheometers (Fig. 9) are useful devices for measuring the viscosity of polymer melts because it is possible to measure the pressure gradient directly. The geometry is that of two flat plates with a rectangular cross section. If the aspect ratio, W/H , is greater than or equal to 10, then there is no sidewall effect. The wall shear stress, τ_w , is then

$$\tau_w = \left(\frac{-dp}{dz} \right) \frac{H}{2} = \frac{P_3 - P_1}{d_{31}} \frac{H}{2}, \quad (17)$$

where P_3 and P_1 are the pressures recorded by transducers T_3 and T_1 , respectively, and d_{31} is the distance between the center of the transducers. The wall shear rate, $\dot{\gamma}_w$, is obtained from the following relation:

$$\dot{\gamma}_w = \frac{\dot{\gamma}_a}{3} \left[2 + \frac{d \ln \dot{\gamma}_a}{d \ln \tau_w} \right], \quad (18)$$

where $\dot{\gamma}_a = 6Q/WH^2$ (this is just the wall shear rate for a Newtonian fluid) for flow through flat plates.

The slit-die rheometer also offers the possibility of obtaining values of N_1 at high shear rates. The method is based on the measurement of a quantity called the hole pressure, P_H , which is the difference of pressures P_1 and P_2 where P_2 is the pressure measured by transducer T_2 mounted at the bottom of a rectangular slot placed perpendicular to the flow direction, i.e.:

$$P_H = P_1 - P_2. \quad (19)$$

The value of N_1 is obtained from the following equation:

$$N_1 = 2\tau_w \frac{dP_H}{d\tau_w}. \quad (20)$$

Hence, from data of P_H versus τ_w one can obtain N_1 as a function of τ_w .

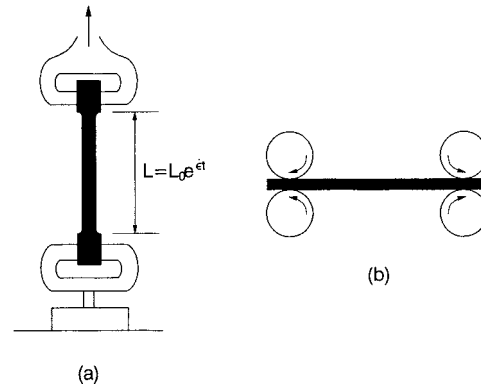


FIGURE 10 Two methods for generating uniaxial extensional flow: (a) Ballman method and (b) Meissner method. [From Baird, D. G., and Collias, D. I. (1998). "Polymer Processing: Principles and Design," Wiley, New York.]

D. Rheometry: Shear-Free Flow Measurements

Two techniques for measuring the extensional viscosity of polymer melts are shown in Fig. 10. In the first technique (Ballman method) polymer melt is either glued or clamped at both ends, and then one end is moved in such a manner as to either generate a uniform extension rate or a constant tensile stress. In the Meissner method, both ends of the melt are pulled at either a constant velocity to achieve a uniform extension rate or to provide a constant stress.

For the Ballman method in order to generate a uniform extension rate throughout the sample, one end of the sample must be deformed such that the length of the sample is increased exponentially with time; i.e., $L = L_0 e^{kt}$. The Meissner method has several advantages and disadvantages relative to the Ballman method. First, it is possible to reach very high strains (of the order of 7.0). Second, the sample is usually deformed horizontally so that the matching of the oil density with that of the polymer melt is not as critical. Finally, finding a suitable glue is not necessary. On the other hand, the construction of the apparatus is more complicated and expensive. Larger samples are required, and they must be nearly free of inhomogeneities.

There are two methods for obtaining approximate values of $\bar{\eta}$. The first method is based on the fiber spinning technique shown in Fig. 11 (the device is called the Rheotens). The second method for estimating $\bar{\eta}$ is based on entrance pressure data. It must be emphasized that these two methods will give only approximate values for $\bar{\eta}$, but the correlation between values obtained using exact methods and the approximate values is sometimes quite good.

E. Squeeze Flow Rheometer

A device that can be used to handle complex materials, such as highly filled polymers, and that can generate both

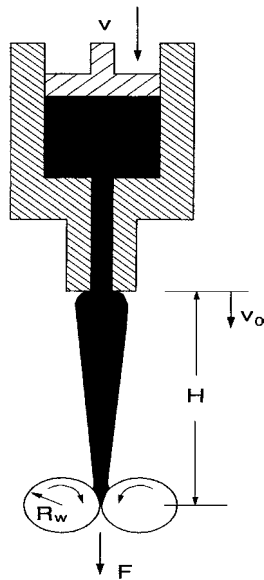


FIGURE 11 Rheotens apparatus for estimating uniaxial extensional viscosity. [From Baird, D. G., and Collias, D. I. (1998). "Polymer Processing: Principles and Design," Wiley, New York.]

shear and shear-free flows is the squeezing-flow rheometer shown in Fig. 12. For small gaps and no slip at the walls, the kinematics are primarily that of shear flow. For large gaps and in the presence of lubrication at the interface between the plates and polymer, biaxial extensional

flow is generated. The device can be operated by either applying a constant squeeze rate or a constant force. The device is very useful for making viscosity measurements on fluids with high viscosity (e.g., $\eta > 10^5$ Pa sec) such as composite materials containing long-fiber reinforcement or propellants.

F. Effect of Molar Mass on Viscosity

Molar mass (M) has a significant effect on the rheological properties of polymer melts and hence on their processing performance. At low molar mass, i.e., below some critical molar mass (M_c), for flexible chain polymers η_0 depends on M_w , while above M_c , η_0 depends on M_w to the 3.4 to 3.6 power for most flexible linear polymer chains:

$$\eta_0 \propto \begin{cases} M_w & \text{for } M_w < M_c \\ M_w^{3.4} & \text{for } M_w > M_c \end{cases} \quad (21)$$

The 3.4 power dependence has been observed experimentally and predicted theoretically. Furthermore, the primary normal stress difference coefficient in the limit as the shear rate goes to zero, $\Psi_{1,0}$, is observed to be proportional to M_w raised to the 7.0 power, i.e.:

$$\Psi_{1,0} \propto \eta_0^2 \propto M_w^{7.0} \quad (22)$$

For branched polymers the dependence of η_0 on M_w can be to higher or lower powers than 3.4 to 3.6 depending on the molecular weight between branch points. For rodlike

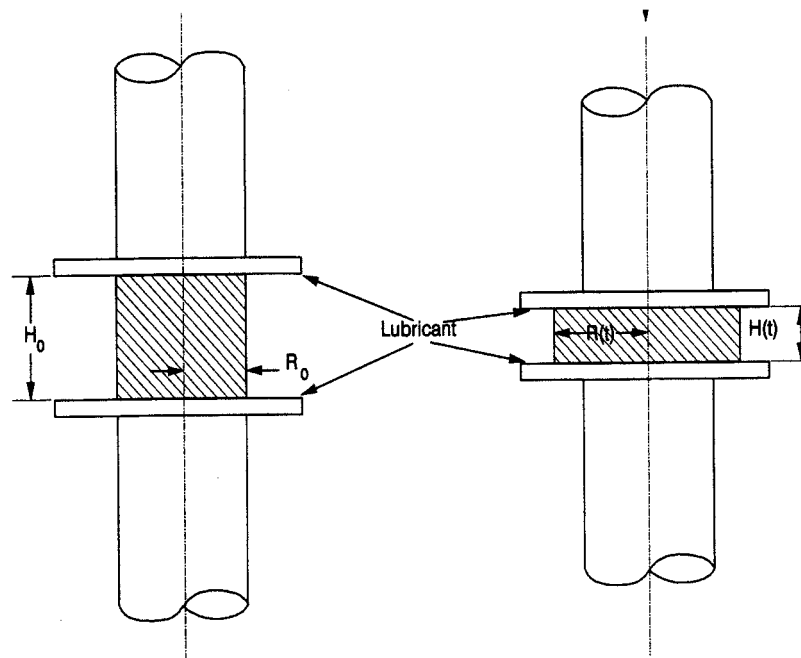


FIGURE 12 Squeezing-flow rheometer showing displacement of parallel disks. [From Baird, D. G., and Collias, D. I. (1998). "Polymer Processing: Principles and Design," Wiley, New York.]

molecules there is some evidence that the following relations hold:

$$\eta_0 \propto \bar{M}_w^{6.8} \quad (M > M_c) \quad \Psi_{1,0} \propto \bar{M}_w^{13.0}. \quad (23)$$

In addition to the dependence of the magnitude of η_0 and $\Psi_{1,0}$ on M_w , the onset of shear-thinning behavior is affected by M . As M increases, the onset of shear thinning moves to lower shear rates. An increase in the breadth of the molar mass distribution will also cause shear thinning to occur at lower shear rates.

The *melt flow index* (MI) is commonly used in the polyolefin industry to distinguish between polymers of different molar mass. A schematic of an MI device is shown in Fig. 13. A known weight is applied to a plunger, which pushes polymer melt through a capillary of specified dimensions (American Society for Testing of Materials, ASTM, specifications). The mass of polymer leaving the capillary over a 10-min period is collected and weighed. Hence, 1.0 MI polymer means that 1 g of polymer was collected in 10 min. The higher the MI, the lower the molar mass.

G. Effect of Temperature

The viscosity of homogeneous polymer melts is known to depend on temperature in a well-defined manner given by the following expression:

$$\eta(T) = \eta(T_0) \exp \left[\frac{\Delta E}{R} \left(\frac{1}{T} - \frac{1}{T_0} \right) \right], \quad (24)$$

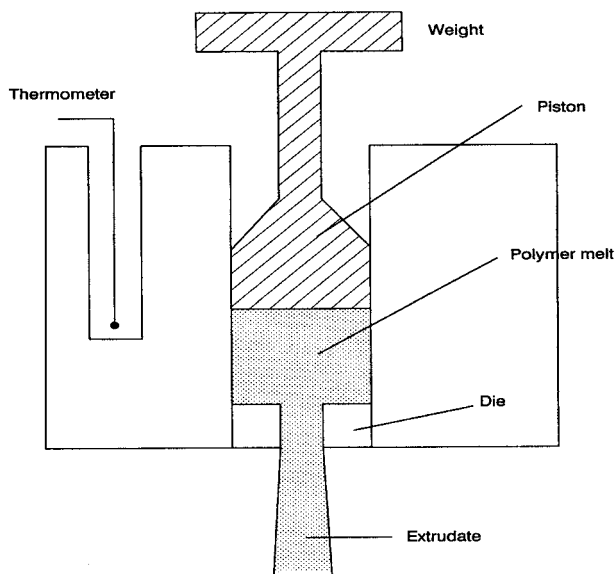


FIGURE 13 Melt flow index device. [From Baird, D. G., and Collias, D. I. (1998). "Polymer Processing: Principles and Design," Wiley, New York.]

where R is the gas law constant, T_0 is the reference temperature, and ΔE is the *flow activation energy*. Typical values of $\Delta E/R$ for low-density polyethylene (LDPE), high-density polyethylene (HDPE), and polypropylene (PP) are 4.5×10^3 K, 2.83×10^3 K, and 5.14×10^3 K, respectively. The flow curves shown in Fig. 4 for LDPE measured at various temperatures have the same shape. Because of this they can be reduced to a single *master curve* plotting the viscosity in reduced form (i.e., η_r versus $\dot{\gamma}_r$) where $\dot{\gamma}_r = a_T \dot{\gamma}$ and $\eta_r = \eta/a_T$ and where a_T is called the shift factor and is basically $\eta_0(T)/\eta_0(T_0)$. This shifting of viscosity to a master curve is reflective of the principle of *time-temperature superposition*. This principle is based on the concept that at elevated temperatures the relaxation processes associated with changes in chain conformation are much faster and hence the molecule can respond to higher deformation rates. At low temperatures the relaxation processes are retarded and the molecule can respond to only low deformation rates.

III. THERMAL PHYSICAL PROPERTIES

The thermal material properties that are pertinent to the processing of polymers are the density ρ , the constant pressure heat capacity C_p , (*note*: when ρ is constant $C_p \approx C_v$, the constant volume heat capacity), and the thermal conductivity k . Representative thermal properties for an amorphous polymer, in this case polycarbonate, are shown in Fig. 14 as a function of temperature. Here it is observed that all the quantities except C_p change continuously with increasing temperature. At about 153°C , a discontinuity in C_p is associated with the glass transition

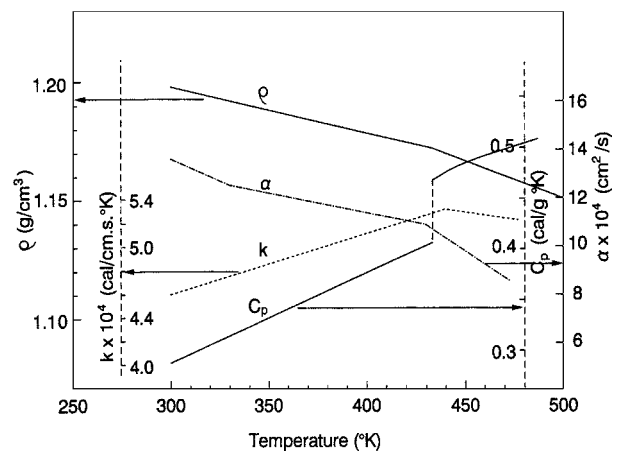


FIGURE 14 Thermal physical properties of an amorphous polymer, polycarbonate. [From Baird, D. G., and Collias, D. I. (1998). "Polymer Processing: Principles and Design," Wiley, New York.]

temperature, T_g . At T_g there is an increase in the free volume allowing molecules more freedom of movement. Above T_g , the polymer chains become more mobile and more easily deformed. It is observed that above T_g there is very little change in the thermal properties. For example, C_p changes from 0.46 kcal/g K at 435 K to 0.5 kcal/g K at 480 K (K is degrees Kelvin). The thermal conductivity changes even less. The density changes less than 5% over the whole temperature range shown. On the other hand, the changes in thermal properties for a semicrystalline polymer are more distinct as shown in Fig. 15. Here it is observed that C_p increases rapidly with temperature passing through a maximum and then decreasing with temperature. The temperature at the peak value is taken as the melting point, T_m . The area under the curve is associated with the melting of the crystalline phase and is referred to as the heat of fusion, ΔH_f . Above T_m the thermal properties are observed not to change significantly with temperature. The density changes markedly for polypropylene varying from about 0.5 g/cm³ at 300°C to 0.9 g/cm³ at 50°C. This large change in density leads to large changes in the dimensions of parts on cooling down from the melt and can lead to warpage of large injection molded panels.

For semicrystalline polymers it is observed that melting occurs leading to the absorption of energy. The energy

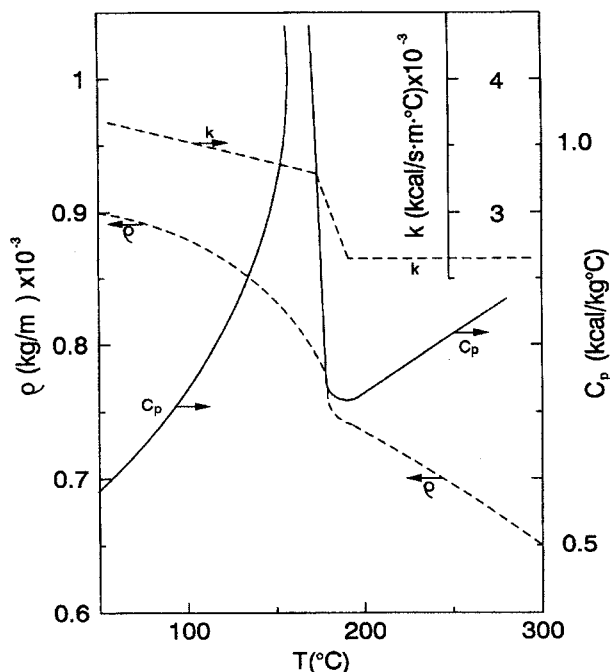


FIGURE 15 Thermal physical properties of a semicrystalline polymer, polypropylene. [From Baird, D. G., and Collias, D. I. (1998). "Polymer Processing: Principles and Design," Wiley, New York.]

associated with the change from the crystalline phase to the completely amorphous state is obtained by integrating the area under the curve of C_p versus temperature. The energy associated with this phase transition is called the heat of fusion, ΔH_f . Note also that the melting point is not really distinct, but covers a broad temperature range. The cooling of a semicrystalline polymer from a temperature above T_m to some lower temperature leads to crystallization. The energy associated with crystallization, called the heat of crystallization (ΔH_c), is affected by the temperature at which crystallization takes place and depends on M_w . Furthermore, the values of ΔH_c are somewhat lower than those of ΔH_f .

The ratio, $k/\rho C_p$, is called the thermal diffusivity, α , and has units of m²/sec. It represents the rate at which heat can penetrate a polymeric material and change its temperature. For most polymers in the melt state, α is about the same with a value of about 1.0×10^{-7} m²/sec. The low value is primarily due to the low value of k , as most polymers are insulators. In other words, it takes a long time to raise and lower the temperature of a polymer, which represents the limiting step in their processing.

IV. EXTRUDERS

A. Single-Screw Extruders

The most frequently used extruder is a plasticating extruder, which is shown in Fig. 16. Polymer pellets are fed to the extruder by means of a hopper (sometimes the pellets are metered in). The gravitational flow of solids in the hopper is rather complex and will not be covered here. The pellets are compressed in the channel of the screw and then dragged forward by friction between the pellets and the barrel. Heat generated by sliding friction at the barrel surface and transferred from the heated barrel causes the pellets to melt. The melt film is scraped away and collects at one end of the channel. The solid-bed width decreases as the solid plug advances along the screw channel until the solid is completely melted. The melt is pressurized by means of a drag flow mechanism. The pressure generated in the extruder and the performance of the extruder are significantly affected by the resistance at the end of the extruder due to filter packs and shaping channels called dies.

The single-screw extruder consists of a metallic barrel and a rotating screw as shown in Fig. 16. The screw is a metallic shaft in which a helical channel has been machined. Sometimes parallel channels are machined in the shaft at the same time leading to what are called multiflighted screws. Typical barrel diameters used in the United States are 0.75, 1.0, 1.5, 2.0, 2.5, 3.5, 4.5, 6.0,

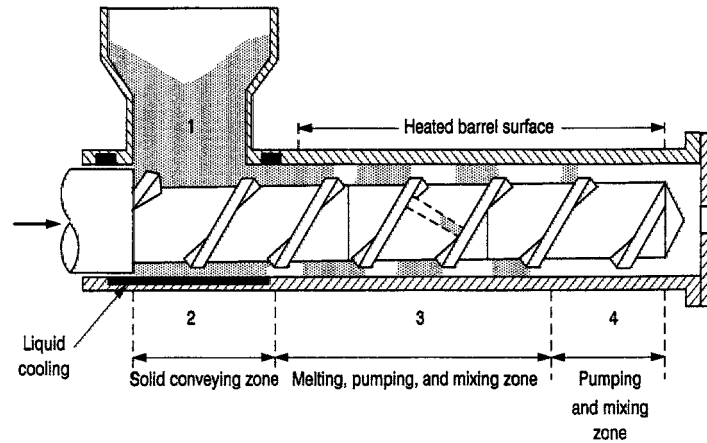


FIGURE 16 Single-screw plasticating extruder showing the four primary zones: hopper, solids feed, melting, and pumping. [From Baird, D. G., and Collias, D. I. (1998). "Polymer Processing: Principles and Design," Wiley, New York.]

8.0, 10.0, 12.0, 14.0, 16.0, 18.0, 20.0, and 24.0 inches. The length to diameter ratios (L/D) range from 20 to 30, but the most common ratio is 24.

The main geometrical features of a screw are shown in Fig. 17. The diameter of the screw at the tip of the flight (the flight is the metal that remains after machining the channel), D_s , is less than the diameter of the barrel, D_b , by an amount $2\delta_f$ (i.e., $D_s = D_b - 2\delta_f$), where δ_f is of the order of 0.2–0.5 mm. Of course, as the screw and barrel wear, δ_f increases and the leakage flow over the flights increases to the point where the screw loses its pumping efficiency. The lead of the screw, L_s , is the axial distance covered in completing one full turn along the flight of the screw. The helix angle, ϕ , is the angle formed between the flight and the plane normal to the screw axis. The helix angle at the flight tip is related to the lead and diameter as follows:

$$\tan \phi_s = L_s / \pi D_s. \quad (25)$$

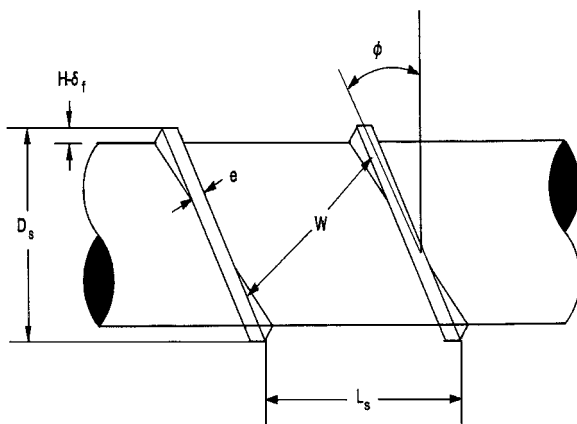


FIGURE 17 Geometrical aspects of a screw. [From Baird, D. G., and Collias, D. I. (1998). "Polymer Processing: Principles and Design," Wiley, New York.]

The helix angle is a function of the diameter and hence is different at the base of the flight than at the flight tip. The radial distance between the barrel surface and the root of the screw is the channel depth. The main design variable of screws is the channel depth profile along the helical direction. The width of the channel, W , is the perpendicular distance between the flights and is given by

$$W = L_s \cos \phi - e, \quad (26)$$

where e is the flight width. We note here that W varies with radial position, and it is also a function of the distance from the root of the screw.

Although the main function of the single-screw extruder is to melt and pump polymer, it has a number of other applications. Extruders can be used to remove volatiles such as water or trace amounts of monomers. They can be used to generate foamed polymers because the temperature and pressure history can be controlled. They also serve as continuous mixing and compounding devices. Hence, extruders have a wider range of applications than other pumping devices.

B. Twin-Screw Extruders

Twin-screw extruders consist of two screws mounted in a barrel having a "figure-eight" cross section. The "figure-eight" cross section comes from the machining of two cylindrical bores whose centers are less than two radii apart. Twin-screw extruders are classified by the degree to which the screws intermesh and the direction of rotation of the screws. Figure 18 shows three types of screw arrangements. Figure 18a shows an intermeshing counterrotating type, whereas Fig. 18b shows a corotating intermeshing type. Figure 18c shows a nonintermeshing counterrotating type. Figure 19a shows an intermeshing self-wiping corotating twin-screw extruder. Not all the elements of

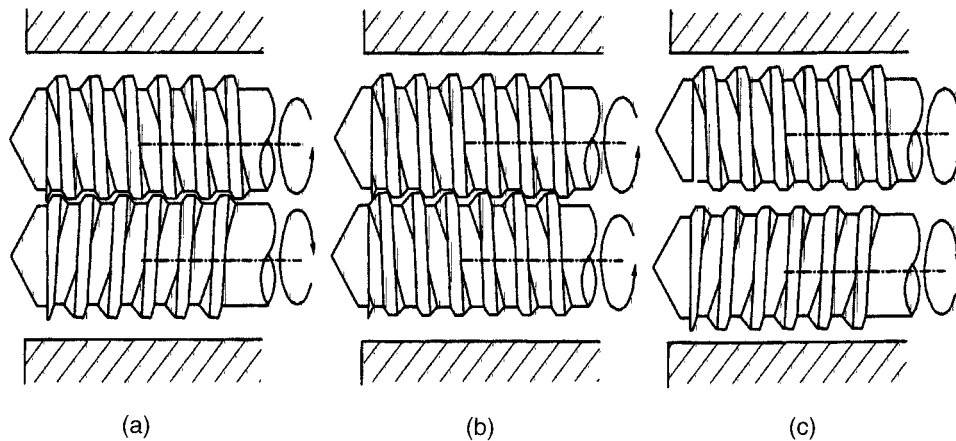


FIGURE 18 Various types of twin-screw extruders: (a) counterrotating intermeshing elements, (b) corotating intermeshing elements, and (c) counterrotating nonintermeshing elements. [From Baird, D. G., and Collias, D. I. (1998). "Polymer Processing: Principles and Design," Wiley, New York.]

a twin-screw extruder are screw elements as shown in Fig. 19b; kneading elements may also be used. Probably the most frequently used twin-screw extruders are the corotating intermeshing and the counterrotating types.

Twin-screw extruders are used in two main areas. One is in the processing of polymers that are difficult to process because they do not flow easily and they degrade readily. For example, twin-screw extruders are used in the profile extrusion of PVC compounds, which are thermally sensitive and do not flow well. The other is for specialty processing operations such as compounding, devolatilization, and chemical reactions. In the case of profile extrusion counterrotating closely intermeshing extruders are used, because their positive conveying characteristics allow the machine to process hard-to-feed materials (powders, rub-

ber particles, etc.) and yield short residence times and a narrow residence time distribution. In the case of specialty operations, high-speed intermeshing corotating extruders are often used, but a wide variety of other designs are also used.

One of the major differences between twin- and single-screw extruders is the type of transport that takes place in the extruder. Material transport in a single-screw extruder is by drag-induced transport of the solid particles and the molten material. In particular, friction between the barrel walls and the solid pellets advances the polymer in the solids-conveying zone, while viscous drag advances the molten polymer. On the other hand, the transport in an intermeshing twin-screw extruder is to some degree positive displacement. The degree of positive displacement

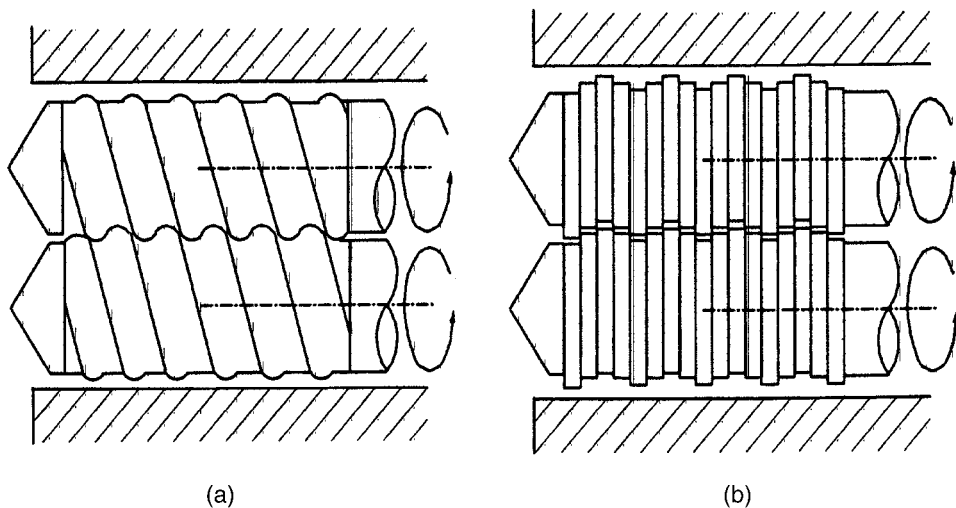


FIGURE 19 Corotating screw extruder: (a) self-wiping intermeshing screw elements and (b) self-wiping intermeshing kneading block elements. [From Baird, D. G., and Collias, D. I. (1998). "Polymer Processing: Principles and Design," Wiley, New York.]

depends on how well the flight of one screw closes the opposing channel of the other screw. Closely intermeshing counterrotating twin screw extruders provide the most positive displacement. However, some leakage will occur, which will reduce the degree of positive conveying that can be achieved. Counterrotating self-wiping twin-screw extruders actually operate in a mode similar to that of a single-screw extruder. However, because elements can be easily interchanged in a twin-screw extruder, it is possible to change the channel depth profile and add more mixing elements.

The flow of material in twin-screw extruders is very complex, and the flow patterns are difficult to predict mathematically. For this reason the simulation of processes in twin-screw extruders is not as well developed as it is for single-screw extruders. It is, therefore, difficult to predict the performance of a twin-screw extruder based on geometrical features, polymer properties, and processing conditions. Hence, it is difficult to carry out accurate design calculations. For this reason twin-screw extruders are constructed in modules in which the screw and barrel elements can be changed. The screw design can be changed by changing the sequence of the screw elements. Hence, much of the design of twin-screw extruders is done on an empirical basis. One can use a combination of screw elements and kneading blocks to accomplish a given operation.

The sizes of twin-screw extruders range from 25 to 244 mm (this is the diameter of one of the barrels). The barrel length to diameter ratio, L/D , ranges from 39 to 48. The length can be altered as required for most twin-screw extruders because of their modular construction.

V. COMPOUNDING

Polymers are rarely used in neat form but usually in the presence of other additives. These additives may be in the form of other polymers, processing aids, stabilizers, colorants, fillers, etc. The process by which additives are combined with polymers is called *compounding*. Fundamental principles of mixing are described briefly followed by commercial techniques used for compounding, and then a description is given of some types of additives that influence processibility and to some degree properties.

A. Principles of Mixing

The term *mixing* refers to operations that have a tendency to reduce nonuniformities or gradients in concentration, temperature, size of a dispersed phase, or other properties of materials. Equivalently, a mixing operation increases the configurational entropy of the system, which reaches

a maximum as the configuration becomes random. Mixing is considered to be one of the most widespread industrial unit operations, and it is found in the core of many areas in the general industry. This unit operation might be a process in itself or it might be part of a more extended sequence of processes.

In this article we will restrict ourselves to the study of the mixing of two-component systems. The two components are defined as either *major* or *minor* components by the level of their total concentration. The goal of the mixing process is usually to achieve a homogeneous dispersion of the minor component into the major one obtaining the *ultimate particle* or *subdivision* (or *volume element*) level of the minor component. The above term is used in a restricted sense, because in its general form the ultimate particle is the molecule and ultimate mixing is molecular mixing. However, in typical mixing operations the two parameters that define the size and form of the ultimate particle are the form of the component and the level of satisfaction of the final dispersion. For example, in the mixing of carbon black agglomerates in polyethylene (PE) the ultimate particle is one particle of carbon black defined by the form of the initial agglomerates (many particles together) as well as by the satisfactory dispersion level of one carbon black particle. In general, typical ultimate particles are molecules and colloidal and microscopic particles.

Mixing is accomplished by movement of material from various parts by the flow field. This movement occurs by a combination of the following mechanisms, two of which are hydrodynamic and one is molecular. The first is *convective transport*. It is present in both laminar and turbulent regimes, and it can also be called "bulk diffusion." Generally speaking, a colored pigment being dispersed in a bucket of paint is an example of laminar mixing. In this case, layers of pigment are thinned, lumps are flattened, and threads are elongated by laminar convective flow. Stirring of cream in a cup of coffee is an example of turbulent mixing, in which the mechanism of turbulent bulk flow predominates at the first stages.

The second mechanism is *eddy diffusion* which is produced by local turbulent mixing. This mechanism prevails at the later stages in the example of the stirring of cream into a cup of coffee mentioned above. The turbulent eddies in the flow field create small-scale mixing, which is sometimes thought to be analogous to molecular diffusion. However, eddy diffusivity is much higher than molecular diffusivity, and it occurs over longer length scales. For gases and low-viscosity liquid systems eddy diffusion becomes the usual mode of mixing.

Finally, there is *molecular diffusion* or interpenetration of molecular species. It is responsible for the ultimate homogenization on a molecular scale (the ultimate particles are the molecules), and it is considered to be true

mixing. This diffusion is driven by the chemical potential difference due to concentration variation, and it is a very slow process, because its timescale is proportional to the value of the diffusion coefficient. Thus, this mechanism becomes important in gases and low molecular weight, miscible liquid systems, although there are timescale differences in those two cases.

The major difference between mixing in general and in polymer processing stems from the fact that the viscosity of polymer melts is usually higher than 10^2 Pa sec, and thus mixing takes place in the laminar regime only ($Re < 2000$; to achieve such a number the polymer would have to flow down a 1-m-wide channel at a velocity of 20 cm/sec). This has a severe consequence: the lack of eddy and molecular diffusion, which greatly enhance the rate of mixing and reduce the scale of homogenization. Thus, all mixing theories and practices should be adjusted to the laminar regime to find applicability in the polymer processing area. This remark applies also to solid–solid mixing in polymer processing, but it does not find application to the addition of low-molecular-weight substances into polymers, like dyes, where molecular diffusion plays a role.

Two basic types of mixing can be identified as *extensive* and *intensive* mixing. Distributive, convective, repetitive, simple mixing, and blending are the main names that extensive mixing is also associated with, whereas compounding, dispersive, and dispersing mixing are the corresponding names associated with intensive mixing. Extensive mixing refers to processes that reduce the nonuniformity of the distribution (viewed on a scale larger than the size of the distributed components) of the minor into the major component without disturbing the initial scale of the minor component. It can be achieved through two mechanisms: rearrangement and deformation in laminar flow. Also, deformation achieved in shear, elongation, and squeezing flows plays a major role in distributing the minor component.

The term *intensive mixing* refers to processes that break down the liquid dispersed phase or the initial particle agglomerates, and they decrease the ultimate particle of the dispersion. A typical example is the dispersion of agglomerates of colloidal carbon black particles in PE. In this case the initial ultimate particle is the agglomerate, and the final is the particle itself. Another example is the dispersion of a polymer into another polymer where the minor component should be dispersed into small droplets or elongated fibers (both of them have a length scale of about $10\ \mu\text{m}$). The analysis of dispersive mixing follows the lines of the analysis of the distributive mixing with the complication that the breakup forces should now be included.

The geometry of the mixing equipment; physical parameters such as viscosity, density, interfacial tension, elasticity, and attractive forces for solids; and operating

conditions such as temperature, speed of rotating parts, flowing velocity, and residence time are the important factors which determine the relative strengths of the mixing mechanisms. As a consequence, this relative strength affects the efficiency of mixing and the quality of the product. In almost all cases, both good distribution and good dispersion are required. In some cases, only distributive mixing can be tolerated if the next step offers dispersive characteristics and, respectively, dispersive mixing is used when a finely dispersed mixture is required and when the next step does not offer any dispersion characteristics.

Some of the nomenclature mentioned above gets a specific connotation when referred to polymer processing, and thus we will give here some specific definitions. *Compounding* refers to the process of softening, melting, and compaction of the polymer matrix and dispersion of the additive into that matrix. *Blending* refers to all processes in which two or more components are intermingled without significant change of their physical state. Finally, *kneading* refers to mixing achieved by compression and folding of layers over one another; *milling* refers to a combination of smearing, wiping, and possibly grinding, and *mulling* refers to wiping and rolling actions.

Dispersive mixing is the term used to describe mixing associated with some fundamental change of the physical characteristics of one or more of the components of the mixture. Generally, dispersive mixing is divided into two parts: The first part is the incorporation of the additives in terms of agglomerated particles or the second polymer component into the polymer matrix, and the second part is the dispersion (or deagglomeration) of the second phase to yield the final product. The microstructures of the blends are determined by rheological, hydrodynamic, and thermodynamic parameters. The rheological parameters are viscosity, elasticity, and yield stress of all components. The hydrodynamic parameters determine the flow fields. The thermodynamic parameters are related to solubility, adhesion, and diffusion of all components.

This type of dispersion has been applied in the polymer processing industry for at least 50 years. It is concerned with the incorporation and deagglomeration of additives in the polymer matrix with the ultimate goal being the reduction of the price or the improvement of the properties of the final product. Of course, if the additive exists in the form of isolated noninteracting particles then the task of mixing is only to distribute these particles uniformly throughout the final product. However, when the additive exists in the form of clusters of particles (interacting or noninteracting), then dispersive mixing ensures that the agglomerates break into isolated particles, which then should be distributed by extensive mixing mechanisms.

The size of the particles as well as their ability to interact with each other characterize the type of cluster as

cohesionless or *cohesive*. A cohesionless cluster is formed from noninteracting particles or from large particles ($> 1\text{mm}$), and its dispersion is determined only by the total deformation of the primary phase. On the other hand, a cohesive cluster includes interacting particles or very small particles, and its dispersion depends on the applied stresses (or equivalently on the deformation rates). In the case of cohesionless clusters, the dispersion is achieved by “peeling off” particles from the surface of the cluster by tangential velocity components close to the particles.

It is common practice in the polymer processing industry to make *masterbatches* or *superconcentrates* of the dispersed to the continuous phase and thus to increase the applied stresses by increasing the viscosity. In highly concentrated batches, the viscosity of the medium can be orders of magnitude higher than the viscosity of the polymer matrix. For example, the masterbatch of carbon black in PE contains about 50% carbon black while the final product contains about 2–5% only. The deagglomeration takes place in the masterbatch where the viscosity is high, and it is followed by dilution steps in extensive type of mixing.

Liquid–liquid dispersion is characterized by two phases: the dispersed and the continuous. The physical parameters of the two phases affecting a liquid–liquid dispersion are viscosity, elasticity, interfacial tension, solubility, and diffusion rate. On the basis of solubility, the system is considered to be miscible, immiscible, or partially miscible. Interfacial tension is lowest for miscible systems and highest for immiscible systems. All high molecular substances have a diffusion coefficient, D , of about 10^{-12} to 10^{-14} cm^2/sec . Consequently, the diffusion rates in molten polymer systems are extremely small, and the relative penetration depths in the timescale of the blending process are extremely small.

Both the dispersed and the continuous phases are fed into the blending or compounding equipment in the form of pellets. The deformation and the dispersion start after heating both components to temperatures above their melting point. Similar to the dispersion of agglomerates, the hydrodynamic force is the deforming and disruptive force and the interfacial tension force is the cohesive force of the dispersed phase. The ratio of these two forces or stresses is called the *capillary* (or *Weber*) number, Ca :

$$Ca = \frac{F_h}{F_c} = \frac{\mu_c \dot{\gamma} R}{\gamma}, \quad (27)$$

where R is the characteristic length (radius) of the dispersed phase and μ_c is the viscosity of the continuous phase. The initial characteristic length of the dispersed phase is the pellet radius, which is large enough for interfacial forces, γ/R , to play any role at that stage. For example, a dispersed system with characteristic length

2 mm, interfacial tension 30 mN/m, continuous phase viscosity 100 Pa sec and subjected to a shear rate of 100sec^{-1} experiences a viscous disruptive stress of 10,000 Pa while the resisting interfacial tension stress is only 15 Pa.

As blending proceeds, the characteristic length of the dispersed phase decreases to the point of equilibrium between the disruptive hydrodynamic and cohesive interfacial tension forces. Of course, during the blending process, dispersed droplets come in contact with each other and may coalesce, so that coalescence and breakup are two competitive mechanisms in polymer blends. In the final blending stages, miscible and immiscible systems behave differently. On the one hand, in miscible systems homogenization is achieved to a very small scale, possibly the molecular scale, if sufficient time is allowed. On the other hand, immiscible systems exhibit a two-phase structure whose characteristics depend on the physical parameters of both polymer phases.

In summary, miscible and immiscible systems show similar behavior in the initial steps of the dispersive mixing process, where hydrodynamic forces deform and disrupt the units of the dispersed phase. In the next stages, interfacial tension forces come into play and induce motion (interfacial tension driven Rayleigh or capillary disturbances). Then, at the final stages, miscible systems are expected to be homogenized at the molecular level (if sufficient time is allowed), while immiscible systems retain the coarser structure of a two-phase system.

As the deformation of the droplets increases, they assume elongated shapes and finally at some value of the capillary number, called the critical capillary number, Ca_c , the disruptive forces exceed the cohesive forces and the droplets burst. In Fig. 20, the critical capillary number times a function of the viscosity ratio $f(p)$, where $f(p) = (19p + 16)/(16p + 16)$, is plotted against the viscosity

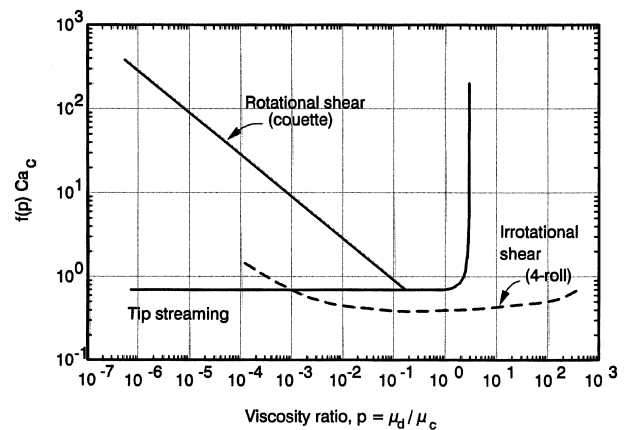


FIGURE 20 Critical capillary number versus viscosity ratio p . [Data from Grace, H. P. (1982). *Chem. Eng. Commun.* **14**, 225–277.]

ratio for the two modes of bursting, i.e., tip streaming (for $p < 0.1$) and regular bursting. Tip streaming refers to the situation where droplets assume a sigmoidal shape with tiny droplets shedding off the tops. The important feature shown in Fig. 20 is the inability of shear flows to cause droplet breakup at viscosity ratios exceeding 3.5, while for shear-free flows (i.e., extensional flow) breakup occurs over a wide range of viscosity ratios.

B. Commercial Compounding Lines

Compounding lines fall into two broad categories: batch and continuous systems. A commonly used batch mixer is the Banbury high-intensity internal mixer shown in Fig. 21. It consists of a figure-eight-shaped chamber with two rotors that rotate in a counterrotating direction. The materials to be mixed are fed through the hopper door and then pushed into the mixing chamber by means of a pneumatic plunger. Dispersive mixing takes place in the high shear region between the rotors and the walls. Distributive mixing takes place as the material is moved back and forth between the rotors. Once mixed, the material is discharged as a large molten drop through a door at the bottom of the machine into a two-roll mill to be converted to a ribbon-like form, which is easier to handle. Batch mixers allow control of residence time, shear rate, and temperature. Direct translation of performance to continuous systems is sometimes difficult.

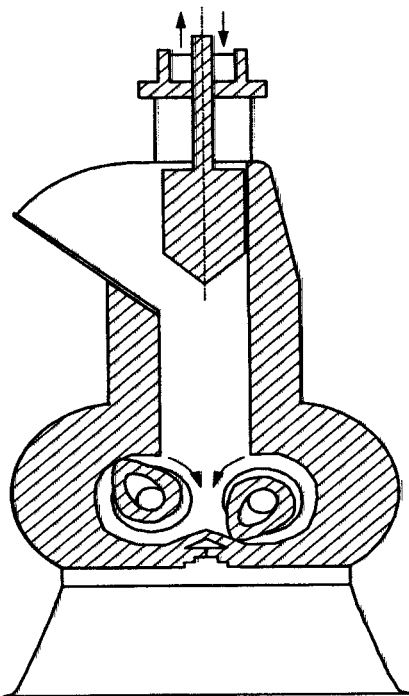


FIGURE 21 Banbury high-intensity internal mixer.

Continuous compounders are for the most part designed around one or more extruders, either of the single- or twin-screw type. The most versatile screw-extruder compounding lines are the so-called two-stage compounding lines, which combine high-performance continuous melt mixers, such as planetary gear extruders, twin-screw extruders, twin-rotor continuous mixers, and reciprocating screw kneaders, with a single-screw extruder. These melt mixers provide excellent control over shear, stock temperature, dwell time, and homogeneity. The second stage, usually a short single-screw extruder, receives the melt and meters it to a strand die. Vacuum venting is normally available in the transition area between the extruders, which ensures that any volatile matter is extracted from the plastics. Normally, both extruders have separate drive motors and the capacity to vary the compounding rpms independently of metering.

A variety of melt-mixer configurations are used in the first stage. *Planetary-gear* extruders consist of a single screw that changes after a certain length into a helical gear, as shown in Fig. 22. The toothed planetary screws are driven by the main screw, which intermeshes with them. They also intermesh with a fixed internally toothed barrel and are retained in the planetary roller system by a stop ring on the outlet side. They are used mainly for compounding PVC formulations. *Twin-rotor continuous mixers* (see Fig. 23) are a development based on the stationary Banbury mixers. They are also known as continuous high-intensity fluxing mixers or *Farrel* continuous mixers. Premix is continuously fed from the feed hopper into the first section of the rotors, which act as a feed conveyor, propelling the material to the mixing section. The mixing section consists of Banbury-type rotors housed in a close-fitting twin-bore mixing chamber. Here the material undergoes intensive shear between the corotating tangential rotor blades and the walls of the mixing chamber. There is also a rolling action of material as it moves back and forth between the bores of the mixing chamber. The continuous mixer and the cross-head extruder have been closed-coupled by means of a short heated transition piece.

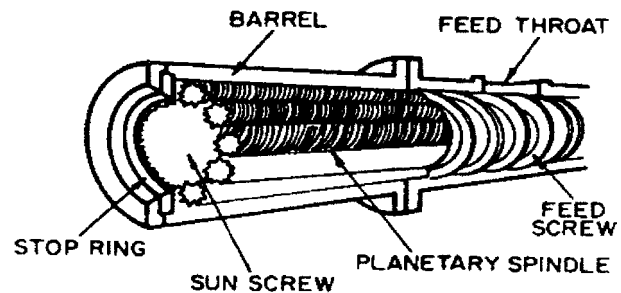


FIGURE 22 Planetary-gear extruder.

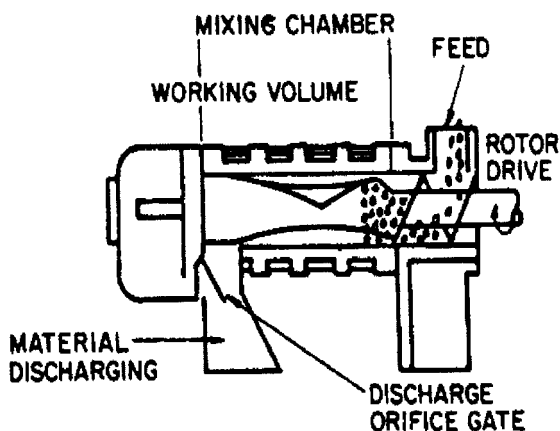


FIGURE 23 Twin-rotor continuous internal mixer.

This transition piece eliminates the need for the adjustable discharge orifice previously used to control backpressure and mixing. Due to their great versatility, they are used to compound all sorts of thermoplastic compounds. *Twin-screw extruders*, as discussed in the previous section, offer a number of advantages including high-power economy, greater versatility, closer control of shear history and temperature, and higher loading of additives. Corotating self-wiping screws with mixing elements (i.e., kneading elements) are used most frequently for compounding operations. Material is moved back and forth between screws in a figure-eight path as it moves down the barrel. In addition to shear, material is subjected to high extensional deformation in the region between the tip of the kneading element and the surface of the opposite element. A kneading action is applied to the material in which it is stretched and folded continuously. Although mixing can take place in counterrotating twin screw extruders, it primarily relies on shear to disperse and distribute the additives and, hence, is not as efficient as the corotating devices.

Reciprocating-screw kneader compounding extruders use a single screw that not only rotates but also reciprocates as shown in Fig. 24. A series of three rows of teeth run axially along the inside of the barrel, corresponding to a series of three wedge-shaped gaps per turn in the screw thread. As the screw rotates, it simultaneously reciprocates. When the plastic material passes through the narrowing gaps, it is deformed and sheared. Each turn of the screw corresponds to a complete forward-backward cycle of the reciprocating screw. The kneading teeth pass through the gaps in the screw flights in both directions, moving material two steps forward and one back for each revolution of the screw. As with all other two-stage compounding lines, the kneader stage is mated to an extruder provided with a metering screw as shown in Fig. 24 for a Buss kneader system used for compounding of fiber-reinforced thermoplastics.

C. Additives Affecting Polymer Processability

A wide variety of additives are used to enhance the properties and processing performance of polymers. We emphasize only those additives which are incorporated for the purpose of enhancing processability or are added for some other reason but lead to significant changes in polymer processability.

1. Antioxidants

Antioxidants are compounds that retard oxidation and hence degradation of the polymer. The susceptibility of polymers to oxidation starts with the formation of free radicals on exposure to heat, UV radiation, ozone, metallic impurities (from catalysts, raw materials, and equipment), etc. The radicals thus initiated have a high affinity for reacting with oxygen to form unstable peroxy radicals. These radicals, in turn, abstract neighboring labile hydrogens to produce unstable hydroperoxides plus additional free radicals that keep the process going. Only when a nonradical inert product is formed will the cycle be terminated. Degradation, which results in the loss of mechanical properties and viscosity, can occur during processing, utilization, and recycling. The antioxidant functions by intercepting the radicals or preventing radical initiation during the plastic's life cycle.

2. Heat Stabilizers

Heat stabilizers are used to protect polymers like PVC from chemically breaking down and discoloring under heat. This instability in PVC is due primarily to the presence of allylic chloride atoms. Prompted by the exposure to heat or UV light, the chemical breakdown results in the release of hydrogen chloride, which leads to discoloration, polymer degradation, and potential corrosion of processing equipment. Heat stabilizers are typically organic and inorganic compounds containing metals, and organic compounds containing active functions other than metals. These stabilizers are known to plate out on equipment and have an effect on melt rheology.

3. Lubricants and Processing Aids

Polymers such as PVC are processed in the presence of additives referred to as *internal* and *external lubricants*. Internal lubricants, such as stearic acid or glycerol monoricinoleate, are typically compatible with PVC and on melting stay absorbed within the PVC molecules. They tend to lower the temperature at which the melt must be processed. External lubricants, such as low-melting hydrocarbons and PE waxes, tend to separate from PVC during melt processing and work their way to the metal surfaces.

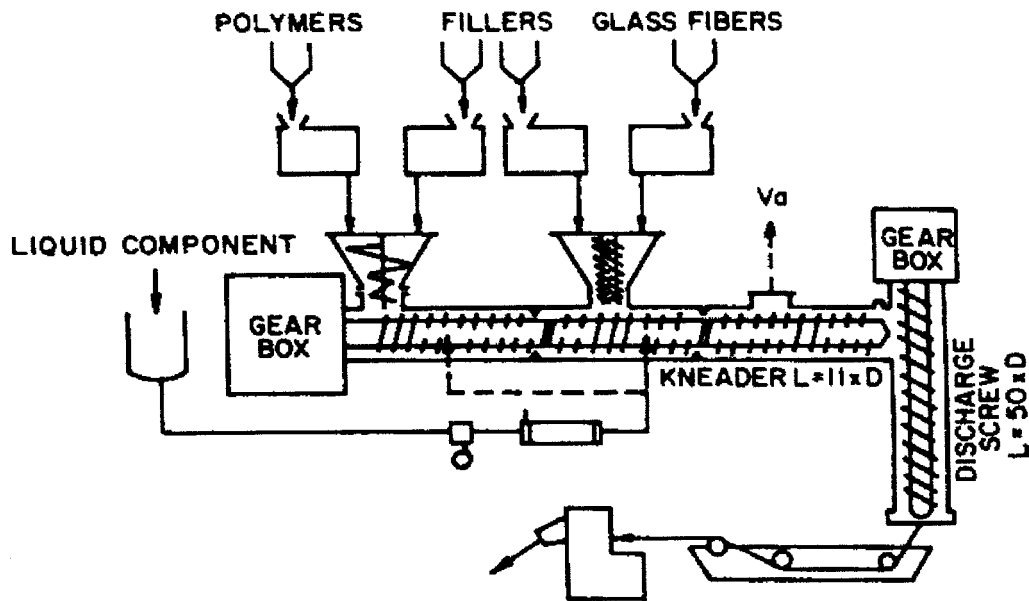


FIGURE 24 Setup of kneader system for compounding of reinforced thermoplastics.

Sometimes, it is difficult to determine exactly what their effect is on melt processing as a drop in melt viscosity is not always observed. In the case of a linear low-density polyethylene (LLDPE), flourinated copolymers are added to delay the onset of an instability referred to as *melt fracture*, which is discussed in the section on extrusion dies. They are used at levels in the range of about 0.02 wt % and hence have no significant effect on the rheology of LLDPE. However, they attach to the die walls and promote controlled slip (much in the same way Teflon reduces adhesion between metal surfaces and food).

4. Fillers and Reinforcements

Fillers are particulate material, such as minerals, diatomaceous earths, and talc, which are added to polymers to reduce cost. *Fibrous reinforcements*, such as glass and carbon fibers, are added to polymers to increase stiffness and to some degree strength. Both types of materials tend to increase the viscosity of the polymer, especially at low shear rates, resulting in the formation of a yield stress. At high shear rates, the effect is less pronounced as the viscosity approaches that of the neat resin. In addition to leading to increases in pressure drops associated with processing these composite materials, they tend to lead to wear of the screws, eventually reducing the performance of the extruder.

5. Compatibilizers

Most polymers are highly incompatible with each other, which makes dispersion of one component within another very difficult. Furthermore, the adhesion between the two

polymer phases is very poor, leading to poor mechanical properties. *Compatibilizers* are used to reduce interfacial surface tension and thereby promote better dispersion of the minor component within the major component. An example of a compatibilizer is maleated polypropylene, MAPP (maleic anhydride is grafted onto polypropylene), which is used in the blending of PP with nylon 6. These two polymers are highly incompatible, and it is difficult to disperse PP within nylon 6. MAPP reacts with the amide linkage of nylon 6 to form a graft copolymer, which is then miscible with each of the two phases. Because the drops of the minor component are much smaller in the presence of MAPP, the viscosity of the blend at low shear is lower than when MAPP is not present.

VI. EXTRUSION DIES

A. Extrudate Nonuniformities

Extrusion dies are metal channels that impart a specific cross-sectional shape to a polymer stream. The design difficulty centers on achieving the desired shape within set limits of dimensional uniformity at the highest production rate possible. Because of the viscoelastic nature of polymers and the associated flow behavior, it is no simple matter to design a die that will produce a smooth extrudate with the desired product dimensions.

There are basically two types of nonuniformities. Those that occur along the machine direction (MD), or along the extrusion direction, and those that occur in the transverse direction (TD). The nonuniformities that arise along the

MD are usually due to pressure and temperature variations that affect the flow rate, the rheological properties of the melt, and to some degree the die design. The irregularities that occur in the TD are due nearly totally to the die design, but in some cases the rheological properties are responsible for irregularities.

In the case of the MD, variations in the flow rate due to pressure or temperature variations in the pumping device are the main cause of the irregularities. However, flow instabilities associated with the phenomena of *melt fracture* (discussed later in this section) and *draw resonance* (discussed in Section VII) can lead to variations in the dimensions of the extrudate. These variations are closely connected to the rheological properties of the melt, but die design can at least alleviate the severity of the irregularities.

The TD variations are nearly totally due to die design. The major problem is to design a feed system (i.e., *manifold*) that will distribute the melt uniformly to the shaping portion of the die (see Fig. 25 for definition of parts of a die). In the event this is not possible, then it must be possible to adjust the die lips in such a way that the fluid will leave the die with a uniform thickness. Even when the manifold is designed to feed the die uniformly, the phenomenon of *die swell* can affect the degree of uniformity across the die. Because the degree of swell may vary nonuniformly over the cross section due to variations in the deformation history, then the die lips (main shaping section) may have to be designed to compensate for this.

Three phenomena are associated with the flow behavior of polymeric fluids that must be considered in the design of extrusion dies: pressure drops in contractions (or expansions), die swell, and melt fracture. The latter two bear a

direct relation to extrudate uniformity, while the flow behavior in contractions may only be indirectly related to extrudate uniformity. In this section, for illustrative purposes, we present results based primarily on studies in the capillary geometry. One must recognize that the extension of results from a capillary to other geometries may be difficult to make quantitatively.

B. Extrusion Instabilities

The limiting factor in the extrusion rate of polymeric fluids is the onset of a low Reynolds number instability called *melt fracture*. The onset of melt fracture leads to varying degrees of imperfections that may affect only the clarity of a material on one hand, or on the other, may be so severe as to significantly reduce the physical properties. There are basically five types of melt fracture: *sharkskin*, *ripple*, *bamboo*, *wavy*, and *severe*. These types of melt fracture are shown in Figs. 26 and 27. Sharkskin is shown in Fig. 26 for a LLDPE. At the lowest apparent shear rate the extrudate is smooth but at an apparent shear rate of $\dot{\gamma}_a = 112 \text{ sec}^{-1}$, the extrudate exhibits a mild roughness, called sharkskin, which affects the appearance of the surface. This type of fracture is extremely detrimental to the manufacture of packaging films, which must meet certain requirements for clarity. As $\dot{\gamma}_a$ is increased, another form of fracture arises. At $\dot{\gamma}_a = 750 \text{ sec}^{-1}$, the fracture present is called bamboo. Finally, at $\dot{\gamma}_a$ of 2250 sec^{-1} the fracture is severe. LLDPE does not seem to exhibit wavy fracture. HDPE does not seem to exhibit sharkskin, but does seem to exhibit bamboo (sometimes referred to as *spurt* or *slip-stick*) fracture at lower shear rates as shown in Fig. 27. As $\dot{\gamma}_a$ is increased, HDPE is observed to exhibit the wavy form

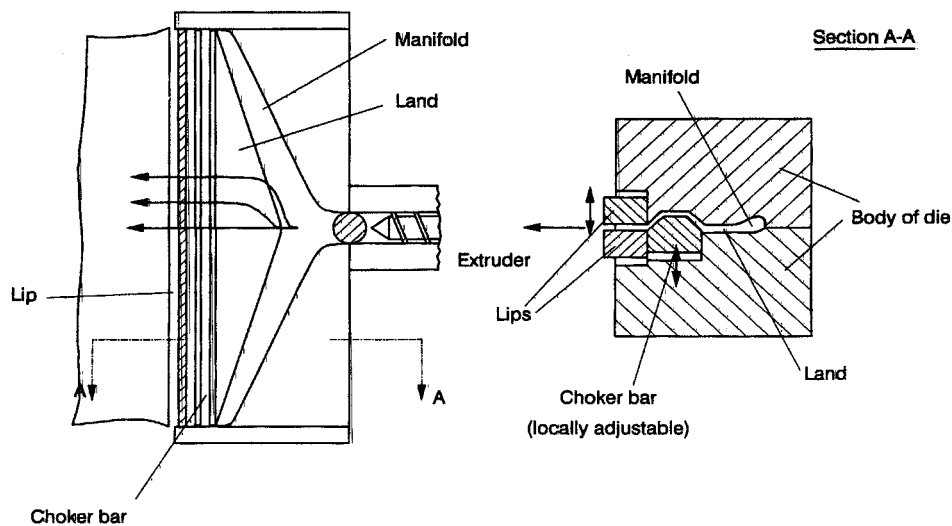


FIGURE 25 Film or sheet die with a coathanger manifold: top and side views. [From Baird, D. G., and Collias, D. I. (1998). "Polymer Processing: Principles and Design," Wiley, New York.]

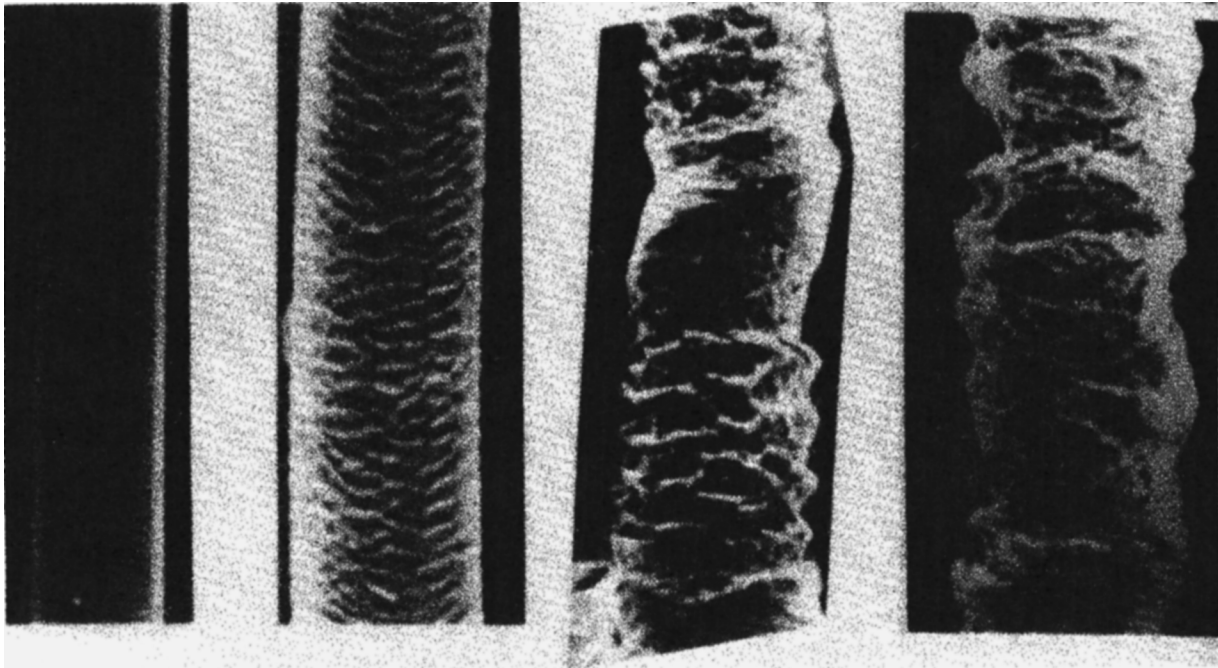


FIGURE 26 Different types of melt fracture exhibited by LLDPE with increasing apparent shear rate from left to right: smooth, sharkskin, bamboo or slip-stick, and gross. [From Baird, D. G., and Collias, D. I. (1998). "Polymer Processing: Principles and Design," Wiley, New York.]

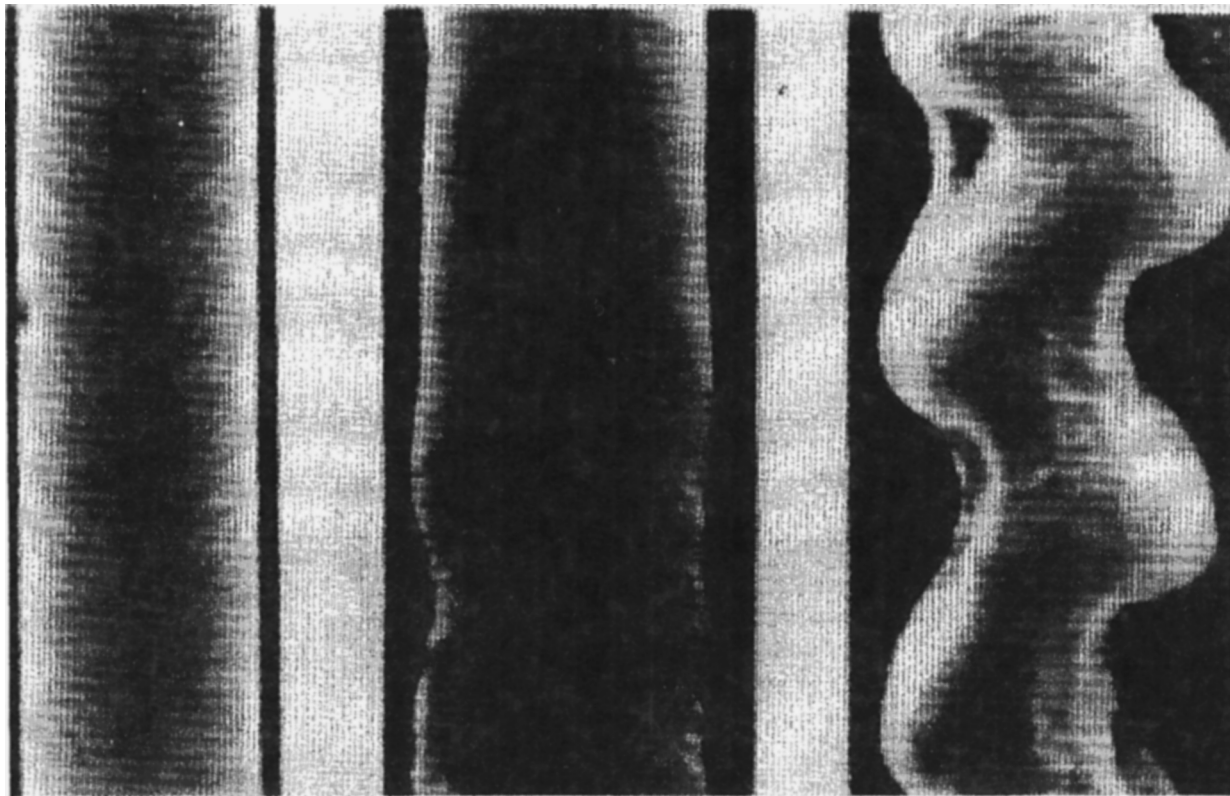


FIGURE 27 Different types of melt fracture exhibited by HDPE from left to right: smooth, slip-stick, wavy, and a form of gross fracture. [From Baird, D. G., and Collias, D. I. (1998). "Polymer Processing: Principles and Design," Wiley, New York.]

of fracture. When slip-stick fracture occurs, the pressure in a capillary begins to oscillate and the magnitude does not rise with increasing throughput. However, for gross fracture (and sharkskin for that matter) there are no signs of pressure oscillations.

To reduce the detrimental effect of melt fracture through die design or polymer modification, it is important to know the origin of melt fracture. The major sources for melt fracture are the die entry region, the die land, and the die exit. For a polymer such as LDPE, fracture originates at the die entry. Large vortices form in the contraction at the die entry. As the extrusion rate is increased, the vortices no longer grow in size or intensity. Instead the flow takes on a spiral motion in the die entry sending sections of the nearly stagnant fluid into the die at regular intervals. This leads to regions of various flow histories passing through the die and leaving the die exit. When this type of fracture occurs, there is no indication of the flow problems in the pressure measured along the die. By streamlining the die entry or increasing the length of the die land it is possible to reduce the amplitude of the distortion, but the critical wall shear stress for fracture is unchanged. The critical wall shear stress for the onset of fracture for LDPE is of the order of 10^5 Pa.

LLDPE typically exhibits no strain hardening and the onset of shear thinning is pushed to higher shear rates than for LDPE. This is because there is usually no long-chain branching and the polydispersity is fairly low (<5.0). When a critical wall shear stress is reached (e.g., $\sim 1.8 \times 10^5$ Pa), the polymer begins to stick and slip at the die exit leading to sharkskin. As the throughput is increased, the polymer begins to stick and slip in the die land leading to large pressure oscillations and an irregular extrudate (the critical stress for slip-stick is of the order of 3×10^5 Pa). There is a distinct flattening of the flow curve (i.e., shear stress versus shear rate) indicating a region where multiple flow rates are possible for the same wall shear stress. Eventually the flow curve appears to become normal again at high shear rates, but then the sample exhibits severe fracture. HDPE also exhibits very little strain hardening, but the onset of shear thinning occurs at low shear rates because of the high degree of polydispersity. Usually HDPE does not exhibit sharkskin but slip-stick and then gross fracture. When slip-stick fracture occurs (which results in the ripple and then bamboo types of fracture), increasing the die length just makes the degree of distortion worse. Using short lands can eliminate slip-stick, but enhance sharkskin.

C. Extrudate Swell

The phenomenon associated with the increase of the diameter of an extrudate as a polymer leaves a capillary is

known as *die swell* or *extrudate swell*. The common view is that die swell is related to unconstrained elastic recovery (S_∞) following shear flow. S_∞ is related to the ratio of the primary normal stress difference to the shear stress through the equation:

$$S_\infty = \frac{N_1}{2\tau_{yx}}. \quad (28)$$

Tanner's theory for die swell for flow through a capillary predicts

$$D_p/D_o = 0.1 + [1 + \frac{1}{2}(S_\infty^2)]^{1/6}. \quad (29)$$

Extrudate swell is more complicated than indicated by Eq. (29) because it depends on a number of factors such as die length, exit geometry, and length of recovery time. First it depends on the measurement method. The highest values are obtained for polymers that are extruded isothermally into an oil bath. The lowest values are for the extrudate, which is extruded into ambient air. Annealing allows the sample to almost reach the values obtained under isothermal conditions. It depends on the capillary L/D with the greatest swell being for the shortest capillary. This behavior has been attributed to the large amount of elastic energy stored during the extensional flow in the entry region. It is also observed that die swell depends on time after the extrudate leaves the die. It is observed that a large portion of the diameter increase can occur over a period of several minutes. Finally, D_p/D_o (equilibrium swell) is a function of the wall shear stress, τ_R . In summary, capillary die swell, $B = D_p/D_o$, is a function of the following variables:

$$B = f(L/D, \tau_R, EG, E, t, t_p/\lambda), \quad (30)$$

where EG is the entrance geometry, E is the exit geometry, t is the time after a fluid element leaves the die, t_p is the time required for the melt to pass through the die, and λ is the longest relaxation time for the fluid. The last quantity, t_p/λ , is referred to as the Deborah number. Certainly the ideas of elastic recovery are involved, but stresses other than those generated in shear flow (e.g., extensional flow at the die exit) must be considered.

D. Dies

1. Flat Film and Sheet Dies

The salient features of a film (or sheet) die are shown in Fig. 25. A film die consists of four major parts: the manifold, the choker bar, the land, and the lips. The purpose of the manifold is to distribute the melt uniformly over the width of the die. The land tends to act as a resistance to flow and also promotes better flow uniformity. In the event that the manifold does not quite provide the required

uniformity in flow rate across the die width, the choker bar can be used to adjust the flow rate locally. The die lips provide the final film thickness and can also be adjusted locally to account for a nonuniform flow rate or nonuniform die swell. The manifold design shown in Fig. 25 is referred to as a *coathanger*. Other designs include the *T-die* and the *fishtail die*.

2. Annular Dies

Dies with annular cross sections are used to extrude pipes, tubes, tubular films, and parisons for blow molding. Center-fed dies are commonly used for extruding pipes, while side-fed dies are used for tubular films and parisons. The four basic annular die designs in use at the present time are shown in Fig. 28. These include (1) center-fed spider-supported mandrel dies, (2) center-fed screen pack dies, (3) side-fed mandrel dies, and (4) spiral mandrel dies. At the die exit there is usually an outer die ring that forms the die land. Plastic pipes are primarily extruded using center-fed dies. The melt stream from the extruder passes from the circular opening to the annular

die by means of the mandrel support tip. The melt then passes over the *spider legs* which support the mandrel, and through a converging annular region, which for pipes is usually 10° to 15° . The converging region is followed by an annular region with parallel walls which imparts the final dimensions to the pipe. The outer diameter of the pipe can range from a few millimeters to approximately 1.6 m. The ratio of the mandrel radius to outer wall radius usually falls in the range of 0.8 to 0.925. The spider legs usually lead to problems in that not only are flow markings visible, but mechanically weak regions are generated. These flow lines are also referred to as weld lines and are due to a higher degree of molecular orientation caused by the high stresses imparted to the melt and the inability of the molecules to re-entangle during the time the melt spends in the die. The strength of the weld line is most likely related to the degree of re-entanglement of the molecules, which occurs as the melt passes through the die at the melt temperature. The re-entanglement time appears to be much longer than the longest relaxation time. It has been estimated from interrupted-shear experiments for polystyrene, for example, to be of the order

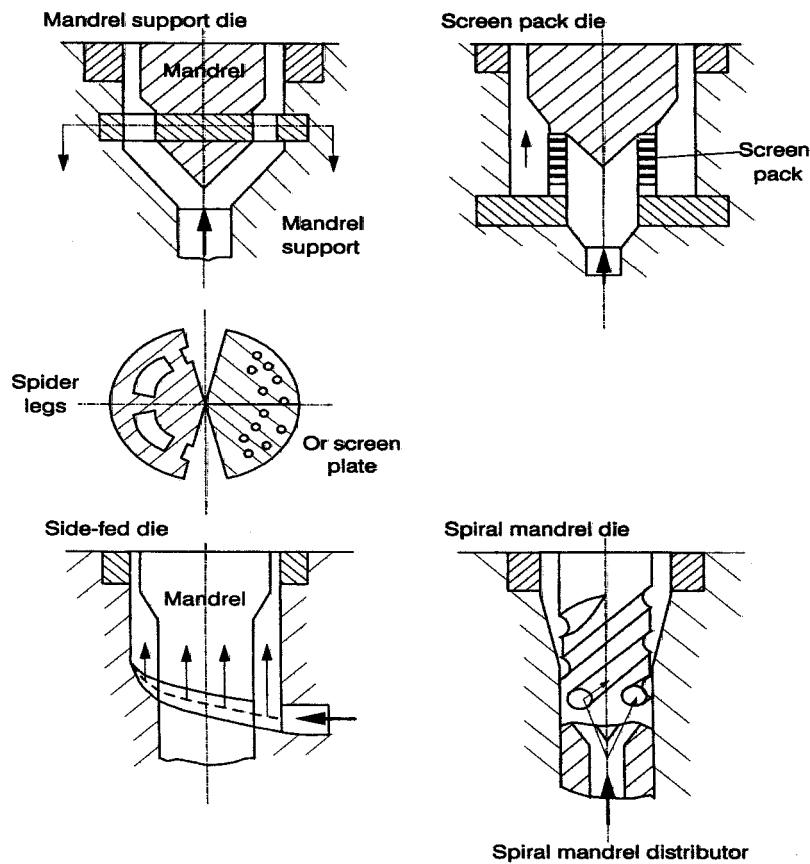


FIGURE 28 Four common annular die designs. [From Baird, D. G., and Collias, D. I. (1998). "Polymer Processing: Principles and Design," Wiley, New York.]

of 300 sec and is related to self-diffusion of polymer molecules.

One way of reducing the effect of the flow lines is through the design of the support system. Instead of arranging the spider legs radially, tangential arrangement as shown will displace the defect circumferentially over the extrudate. A better way for reducing the flow marks is the use of offset spider legs. Here the flow marks do not extend all the ways through the wall of the extrudate, which offers at least mechanical improvements. Finally, another way to reduce flow marks is through the use of a screen plate. In this design the melt passes into the annular region by first passing through a plate with many small holes bored in it. In effect, the annular die is fed by multiple capillaries.

The *side-fed mandrel die* is used in both blown film and pipe extrusion. The main consideration is to provide a uniform flow rate at the die land. This is done in much the same way as for flat film extrusion by the use of a manifold. The spiral mandrel die seems to offer the best possibility for providing a uniform flow rate circumferentially at the annular die exit. The die is usually fed from the extruder by means of either a star-shaped or ring-shaped distributing system. The melt then passes into spiral-shaped channels that are machined into the mandrel. The depth of the channels decreases with spiral distance, which ensures that there will be mixing of the melt from channel to channel as the result of leakage. Because of the design of this system there are no mandrel support elements, and hence flow lines are eliminated completely.

3. Wire-Coating Dies

Wire-coating dies also involve annular cross sections. The melt usually enters from the side and so resembles the side-fed annular dies. The goal in the design of wire coating dies is to provide a coating that is of the desired thickness, free of imperfections, and with the wire centered in the insulation. Again the even distribution of the melt from the die entry is the key design element. Two basic types of coating dies are used at present: pressure coating and tube coating dies (Fig. 29). In the pressure coating die the wire is coated under pressure in the die. This technique is usually used for the application of the primary coating where good adhesion is important. In the case of the tube coating die, the polymer coating is applied outside the die and is used for applying a secondary coating.

4. Profile Extrusion Dies

Profile extrusion refers to the extrusion of polymer melts through dies of cross sections that are neither round, annu-

lar, or rectangular with an aspect ratio, W/H , greater than 10.0. At present three types of profile dies are used: orifice dies, multistage dies, and tapered profile dies. Basically the orifice die consists of a die base and a die plate in which the profile is formed. These dies are used for the extrusion of inexpensive profiles where dimensional accuracy is not necessary. Because of the abrupt change in cross-sectional area, there is usually a buildup of stagnant material behind the die plate and high extrusion rates are not possible. These dies are not commonly used for most thermoplastics but are restricted primarily to PVC and rubber. Multistage dies exhibit step changes in the cross-sectional area of the flow channel. They consist of a series of die plates of similar geometry but of a decreasing cross-sectional area. Certainly these represent an improvement over the orifice dies, but they still suffer from some of the same deficiencies as the orifice die. Whenever profiles of high-dimensional accuracy are to be produced at high extrusion rates, profile dies with a gradual change of cross-sectional area are required.

5. Multiple-Layer Extrusion (Coextrusion)

It is becoming more common to combine multiple layers of different polymers to form products with properties that take advantage of the best properties of each component. For example, packaging film might be composed of several different types of polyethylene along with a layer of adhesive and a barrier polymer. There are basically three types of multiple-layer extrusion (or coextrusion) techniques:

1. Melt streams flow separately.
2. Melt streams flow separately and then together.
3. Melt streams flow together.

In type 1, polymer streams are extruded through separate flow channels and then joined outside the die. The advantage in this type of multilayer extrusion is that polymers with widely different processing temperatures and rheological properties can be used. The major problem is that of generating satisfactory adhesion between the components. Usually the technique is only used for two polymers. In the second technique the streams are brought together inside the die, and then they pass through a common land region. Because the streams are brought together under pressure, adhesion is improved. However, it is not possible to have the streams at widely different temperatures. Likewise the rheological properties cannot be too widely different or flow instabilities will arise. Furthermore, at the point where the streams converge, interfacial instability problems may arise. In the third method, which is not too dissimilar from the second method, the polymer streams are brought together

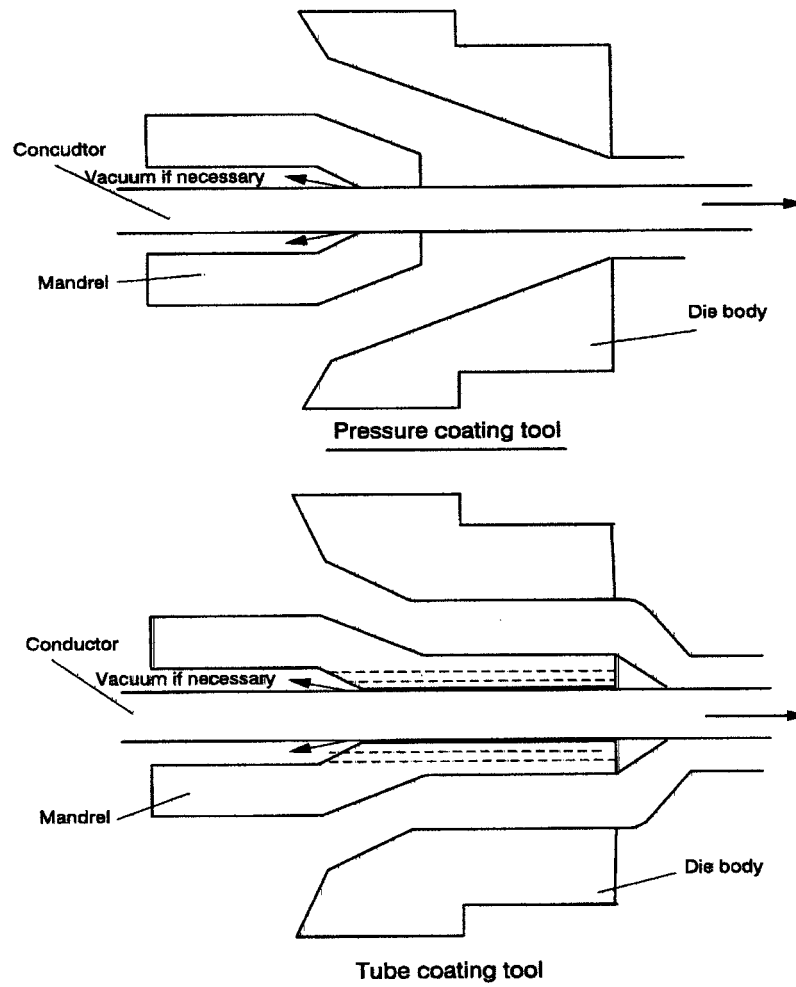


FIGURE 29 Two types of wire-coating processes: pressure and tube coating. [From Baird, D. G., and Collias, D. I. (1998). "Polymer Processing: Principles and Design," Wiley, New York.]

in an adapter, and then they pass through a common die. In this case the same die as that used for single-component extrusion can be used. Again the melt rheological properties cannot be too dissimilar or an instability will arise that will disrupt the laminar nature of each stream. However, this is one of the most inexpensive and simplest methods for generating multiple-layer films and sheets.

Basically, two problems arise when trying to extrude multiple layers of different fluids through the same die. First, if there are distinct viscosity differences between the fluids, then the lower viscosity component will try to encapsulate the higher viscosity component. Second, there are situations when the viscosities of two polymers are closely matched, but the interface still becomes wavy and distorted. This type of instability is thought to be due to slip at the interface between the two polymers. However, the most probable region for the onset of the instability

is at the die exit where large stresses arise as the velocity profile undergoes a rapid rearrangement.

VII. POST-DIE PROCESSING

A. Fiber Spinning

A *fiber* is the fundamental unit of textiles, and it is defined as a material unit of axial length scale about 100 times the length scale in the cross direction (width or radius). There are two types of fibers: *natural* and *synthetic* (or *manmade*). The term *spinning* has a different meaning for natural and synthetic fibers. Spinning of natural fibers refers to the *twisting of short fibers* into continuous lengths (also called *filaments*). On the other hand, spinning of synthetic fibers refers to production of continuous lengths *by any means*. Finally, the *yarn* is made by twisting many filaments together.

The production of manmade fibers usually includes the following processes:

1. Preparation of polymer (polymerization, chemical modification, etc.)
2. Preparation of the spinning fluid (polymer melt or solution)
3. Spinning (extrusion, solidification, and deformation of the spinning line or filament)
4. Drawing (due to a higher linear speed at the take-up roll relative to that at the die; drawing is used to increase the degree of molecular orientation and improve the tensile strength, modulus of elasticity and elongation of the fibers)
5. Heat treatment
6. Textile processing (twisting, oiling, dyeing, etc.).

The spinning process can be achieved mainly by three procedures: *melt spinning*, *solution dry-spinning*, and *solution wet-spinning*. Of these three procedures, melt spinning is the simplest and the most economical one. Its simplicity stems from the fact that it involves only heat transfer and extensional deformation, whereas the other methods in addition to the above processes involve also mass transfer and diffusion. The melt spinning procedure can be applied to polymers that are thermally stable at the extrusion temperature and that exhibit relatively high fluidity at that temperature. Typical examples of melt-spun polymers are polyamides, polyesters, polystyrene, polyolefins, and inorganic glasses.

In the solution dry-spinning procedure the polymer is dissolved in a volatile solvent and the solution is extruded. Then the spinning line meets a stream of hot air and the solvent is evaporated. The recovery of the solvent increases the cost of the whole process. Typical examples of dry-spun polymers are cellulose acetate, acrylonitrile, vinyl chloride, and acetate. Lately, extended-chain PE fibers (ECPE, Spectra fibers) are made by solution spinning in a typical melt-spinning apparatus. The solution wet-spinning procedure is applied to polymers that meet neither criteria of the previous two methods (i.e., thermal stability and solubility in a volatile solvent). It involves the extrusion of a polymer solution into a liquid bath of coagulating agents, which drive the solvent out of the filament. Four other spinning procedures (*phase separation spinning*, *emulsion spinning*, *gel spinning*, and *reaction spinning*) are not addressed here.

A schematic (not in scale) of the typical melt-spinning procedure is shown in Fig. 30. Polymer is pumped by means of an extruder through a screen pack, in which the polymer is filtered through layers of screens and sand. Then it is divided into many small streams by means of a plate containing many small holes, the *spinneret*.

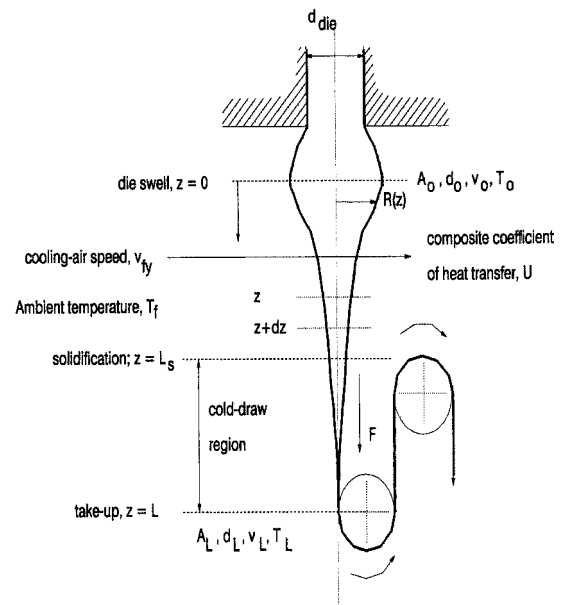


FIGURE 30 Schematic of the melt-spinning process for a single filament. [From Baird, D. G., and Collias, D. I. (1998). "Polymer Processing: Principles and Design," Wiley, New York.]

Some spinnerets can have as many as 10,000 holes (rayon spinning from a 15-cm platinum disk spinneret). Extrusion through the spinneret (or die), subsequent *die swell* (due to the relaxation of the elastic stresses of the polymer), cooling of the filament by cooling air (or water vapor) flowing perpendicularly to the filament axis, solidification of the polymer, and its cold drawing in the region from the solidification point to the take-up roll are shown in this figure. Part of the time the holes in the spinneret are circular in shape, but mostly they are irregular in shape. Typical shapes include *trilobal*, *square*, and *cross*. Note that dry- and wet-spinning from circular spinneret holes usually results in irregularly shaped fibers.

In terms of the number of the filaments per spinneret plate, as well as the spinning speed, melt spinning is divided into various groups. Monofilaments are produced by one-hole spinneret plates, while most of the time numerous filaments are extruded through the spinneret (multifilament yarns). Very low-speed spinning, with speeds ranging from 30 to 100 m/min, usually occurs for thick monofilaments spun through liquid baths. Low-speed spinning is usually carried out at speeds in the range of 100 to 750 m/min, where the filament tension is constant along the entire length. To enhance the degree of orientation and crystallinity and, hence, physical properties, the yarns are subsequently drawn and annealed and, therefore, the melt-spinning process is considered to be a two-step process (first step: spinning; second step: drawing;

TSP). At intermediate speeds of 750 to 3500 m/min, the filament tension is increased due to inertia and air drag. Finally, at high spinning speeds of 3500 m/min and above polymers such as PET undergo stress-induced crystallization. At high spinning speeds the structure, morphology, and resulting physical properties are somewhat different from those obtained in conventional low-speed spinning processes.

Typical physical and mechanical properties of melt-spun fibers include the following: density, boil-off shrinkage, birefringence, tensile strength, percent elongation, modulus of elasticity, shrinkage tension, and dyeability. In practice, some of the above properties might be found under different names. *Denier per filament* (dpf; unit: denier, d) is usually substituted for density, and *tenacity* (unit: g-force/d or gf/d) is used in place of tensile strength. Denier refers to the weight in grams of 9000 m of fiber and, hence, represents the linear density of the fiber.

B. Film Casting

A large activity of the polymer processing industry is the production of films and sheets of thermoplastic polymers. By definition, the term *film* is used for thicknesses less than $250\ \mu\text{m}$ (equal to about 0.010 in.), and the term *sheet* is used for thicker films. Note that in this section we will use the term *film* generically, and we will occasionally mention the term *sheet* when confusion might occur. These products are primarily used in the packaging industry for either foodstuffs (groceries, dairy produce, etc.) or other consumer products. Quite frequently, the properties of various polymers need to be combined by either coating, lamination, or coextrusion. The major properties of the films and sheets are transparency, toughness, flexibility, and a very large aspect ratio (width or length to thickness) of about 10^3 . Typical values of the thickness range from about 10 to $2500\ \mu\text{m}$, whereas the other two dimensions can vary from 40 to 320 cm.

Flat film production consists mainly of the following three processes: extrusion, casting, and stabilization. Depending on the film thickness there are three major groups: fine film, with thicknesses of $10\text{--}50\ \mu\text{m}$; thicker cast film and sheet, with thicknesses of $100\text{--}400\ \mu\text{m}$; and thermoformable sheet, with thicknesses of $200\text{--}2500\ \mu\text{m}$. The first two groups are produced on chrome-plated chill-roll or water-bath lines, whereas the third one is produced with a special roll. All film types, after the chill-roll or water bath, are trimmed at the edges (some curling might occur there) and either wound or undergo stretching (uniaxial or biaxial) or thermoforming. Polypropylene, polyethylene, polyester, and polyamide are the four most frequently used polymers on chill-roll lines.

C. Film Blowing

One method to produce film with a good balance of mechanical properties is by extruding a polymer through a film die and then subsequently stretching the film in two directions as described in the previous section. The other technique involves extrusion through an annular die. Then, the moving tubular film is stretched and inflated by an air stream flowing from inside the annular die (the pressure is slightly higher than atmospheric pressure; Fig. 31) creating a "bubble." This bubble is cooled by an air jet flowing from an air ring toward its outside surface. The cooling results in crystallization and solidification, which start at the freeze line. Beyond this line the bubble boundaries become parallel to the centerline, and the polymer melt is transformed into a two-phase mixture consisting of molten and solidified polymer. The frost line is the other boundary of the region that starts with the freeze line. Beyond the frost line the deformation of the bubble is not very significant, and the bubble consists of one-phase material only, the solidified polymer. Thus, the bubble beyond the freeze line is a constant radius cylinder. This cylinder is then flattened by a set of guide rolls and taken up by a set of rubber nip rolls, which form an airtight seal at the upper end of the bubble. The takeoff at the nip rolls may be either of constant speed or constant torque. Finally, the film is wound onto cylinders and sold as "lay-flat" tubing or trimmed at the edges and wound into two rolls of flat

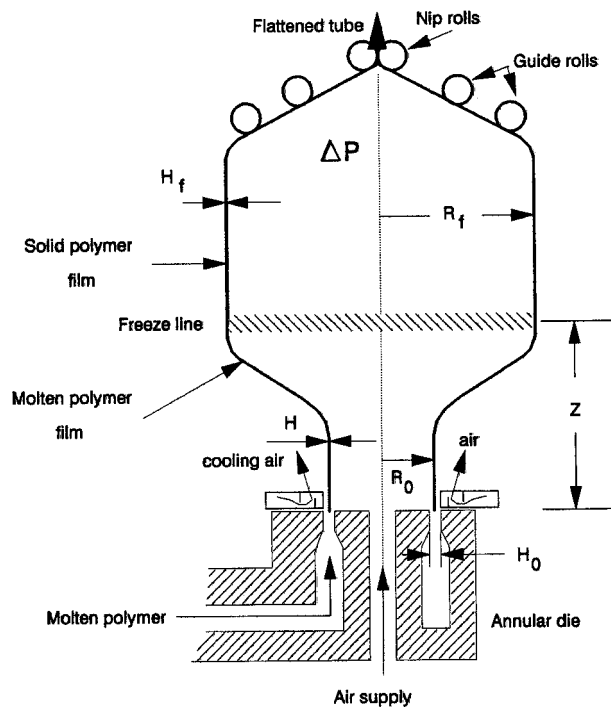


FIGURE 31 Schematic of the film blowing process.

film. In terms of direction, most frequently this process takes place vertically upward and less frequently vertically downward and horizontally. The major advantages of this method over the first method are the economics and the speed of production.

Film blowing and fiber spinning have general similarities. Both processes have free boundaries, and the flows are predominantly elongational. They differ with respect to the orientation generated. The fiber spinning process imparts orientation in the axial direction only, whereas the film blowing process imparts unequal (in general) biaxial orientation. The two axes of orientation are the axial (*machine*; MD) direction due to the drawing of the tube and the circumferential (*nonmachine*, or *transverse*; TD) direction due to the blowup of the tube. The mechanical properties of blown film are nearly uniform in both directions as a result of biaxial orientation, and this is the reason for producing flat film by the film blowing process.

The two main parameters of this process are the *blow ratio* (or *blow-up ratio*), B_R (or BUR), and the *machine-direction draw* (or *drawdown*) *ratio*, D_R . The blow ratio is defined as the ratio of the final tube radius, R_f , to the initial tube outside radius just downstream of the annular die, R_0 :

$$B_R = \frac{R_f}{R_0}. \quad (31)$$

Similarly, the draw ratio is defined as

$$D_R = \frac{V}{v_0}, \quad (32)$$

where V is the takeup speed, and v_0 is the die extrusion rate. The final film thickness, H_f , can be calculated from the blow and draw ratios and the mass conservation equation as follows:

$$H_f = \frac{H_0}{B_R D_R}; \quad (33)$$

where H_0 is the initial film thickness or, equivalently, the die gap thickness. Typical parameters in the film blowing process are $H_0 = 1\text{--}2$ mm, $R_0 = 2.5\text{--}25$ cm; $v_0 = 1\text{--}5$ cm/sec; $B_R = 1.5\text{--}5$; $D_R = 5\text{--}25$; $\Delta P = 50$ Pa (i.e., the internal pressure is about 0.05% of the atmospheric pressure); and freeze-line height $Z = 0.25\text{--}5$ m. An average value of the blow and draw ratios and of the initial film thickness yields a final film thickness on the order of $50 \mu\text{m}$ (i.e., about 2 mils in English units). In terms of nomenclature, the final film is considered to be thick-gauge blown film whenever its thickness exceeds $75 \mu\text{m}$ or equivalently 3 mils. In terms of applications, thick-gauge blown film is used in the production of dunnage bags, heavy-duty shrink film, greenhouse film, lawn and garden bags, and resin and chemical packaging.

As far as the mechanical properties are concerned, the tear (test name: Elmendorf tear), impact (test name: dart drop), and tensile strengths give an indication of the mechanical strength of the tubular film. The amorphous as well as the crystalline orientation development during the blowing process depend on the stretching imparted in the machine and transverse directions. Finally, besides orientation, the amount of crystallinity as well as the size of the crystallites may play a significant role in the mechanical and physical properties of the blown film.

This process is not as fast as fiber spinning, which results in a more uniform temperature distribution in the film relative to that in the fiber. Usually, cooling is achieved by blowing an air stream from an axisymmetric air ring toward the external film surface. In some cases, in addition to the external air ring, an internal air cooling system is provided. Finally, in some other cases, especially in thick tube and large bag production, cooling is achieved by a water spray or ring. Note that in the latter cases the film must be dried before winding up, which leads to an additional step.

Commercially, the film blowing process is extensively used for the production of polyolefin (LDPE, HDPE, and PP) wrapping film. Mechanical strength, optical clarity, which depends on the degree and type of crystallinity for crystallizable polymers, and the uniformity of thickness (variations of about 5% for films with a length scale of 10 mm to 10 m is acceptable) are the three most important and general properties of the film.

D. Stability

The rate of production in one of the three processing operations just discussed, i.e., fiber spinning, film casting, and film blowing, is limited by the onset of instabilities. Two major types of instabilities are encountered in these processes. A significant degree of drawdown is used to reduce the fiber diameter or film thickness. If the stresses become too high, the polymeric material can fail by means of *cohesive fracture*. The filament or film merely ruptures. In the second type of instability, called *draw resonance*, the fiber diameter begins to oscillate periodically when a critical drawdown ratio is reached. In the case of blown film, this is manifested in variations in the film thickness leading to fluctuations in the bubble diameter. For Newtonian fluids the critical draw ratio for the onset of draw resonance, D_{RC} , is about 20. For polymeric materials D_{RC} is significantly lower with values of less than 5.0 observed. The type of instability depends on the nature of the polymer. Polymers that exhibit strainhardening extensional viscosity (i.e., the extensional viscosity increases with increasing strain and strain rate) such as LDPE tend to exhibit cohesive fracture but not draw resonance, whereas polymers such as LLDPE

that are not strain hardening are prone to draw resonance. In the case of film blowing, the bubble can also start a spiral motion due to the turbulent flow of the cooling air being emitted from the cooling ring at the base of the bubble. The instabilities are detrimental because they can be so severe as to cause the process to break down or at least lead to variable mechanical properties.

VIII. MOLDING AND FORMING

A. Injection Molding

Injection molding is probably the most widely used cyclic process for manufacturing parts from thermoplastics. In essence polymer pellets are plasticated in a single-screw extruder, and the molten polymer accumulates at the tip of the screw in a reservoir. The melt, which has accumulated in the reservoir, is pushed forward by the screw whose displacement is controlled by hydraulic pressure. The melt flows through the nozzle, as shown in Fig. 32, which connects the extruder to the mold, passes through the sprue, along the runner, through the gate, and into the mold cavity. The sprue is designed to offer the least resistance to flow as possible while minimizing the amount of polymer that is wasted. The runner is designed to carry melt to the mold cavity, and when multiple cavities are involved, it must be designed to ensure that each cavity fills at the same time. The gate represents the entrance to the mold. Its location is of utmost importance to the appearance of the part. Furthermore, it is desirable to make the gate as small as possible for not only cosmetic reasons but to facilitate the separation of the part from the rest of the material solidified in the runner. The melt enters the mold cavity where it begins to solidify as it touches the mold wall. As semicrystalline polymers solidify, they shrink as a result of increases in density. Pressure is maintained during the cooling process to ensure that melt continues to flow into the mold. Once solidification is complete, the mold plates

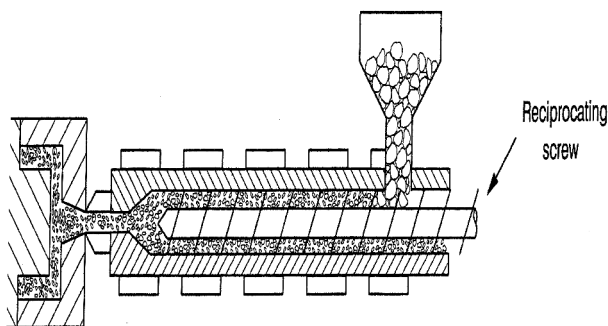


FIGURE 32 Schematic of the injection molding process.

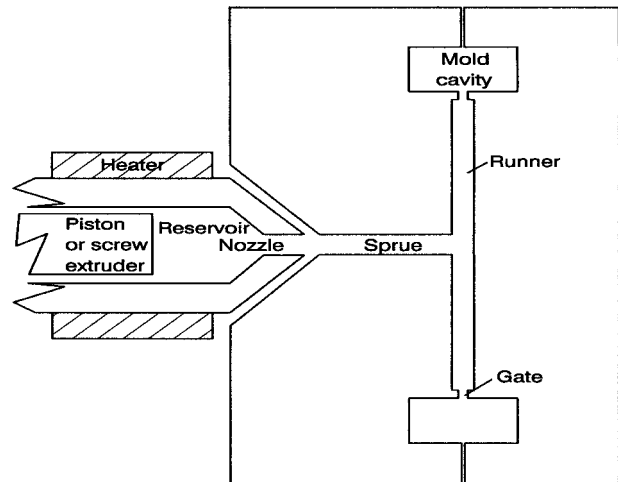


FIGURE 33 Injection molding tooling showing the tip of the injection system and its connection to the mold. [From Baird, D. G., and Collias, D. I. (1998). "Polymer Processing: Principles and Design," Wiley, New York.]

open, and the part is ejected. While the screw is being pulled back, it rotates plasticating more polymer.

The flow rate and pressure in the reservoir are shown schematically in Fig. 33. The injection pressure, which is the hydraulic pressure applied to the screw, is one of the variables that can be selected. Because of little resistance to flow in the beginning, the flow rate through the nozzle is constant. However, as the melt advances through the sprue and runner, the resistance to flow increases, and the pressure increases. As the cavity fills, the set pressure reaches a constant pressure (this is the injection pressure and is a machine setting), but the resistance to flow continues to increase. The flow rate through the nozzle as well as the flow rate into the cavity must decrease. If the resistance to flow is too great either as a result of the polymer solidifying or the melt viscosity being too high, the polymer will fail to fill the mold leading to what is known as a *short-shot*. Once the mold fills, the hydraulic pressure applied to the screw is reduced (this is called the holding pressure) to a value which maintains enough flow of material into the mold to compensate for the volume changes due to shrinkage. Some pressure is maintained during the complete cooling cycle.

In Fig. 34 the flow patterns in normal mold filling are shown schematically. As the melt leaves the gate, the front is found to occupy various positions in the mold at different times. The velocity profiles in the fully developed flow behind the front are shown in Fig. 34b. The flow well behind the front is primarily shear flow, while that at the front involves stagnation flow. In essence, fluid passes through the center of the cavity to the front where it turns and then is laid up on the wall of the mold where it solidifies.

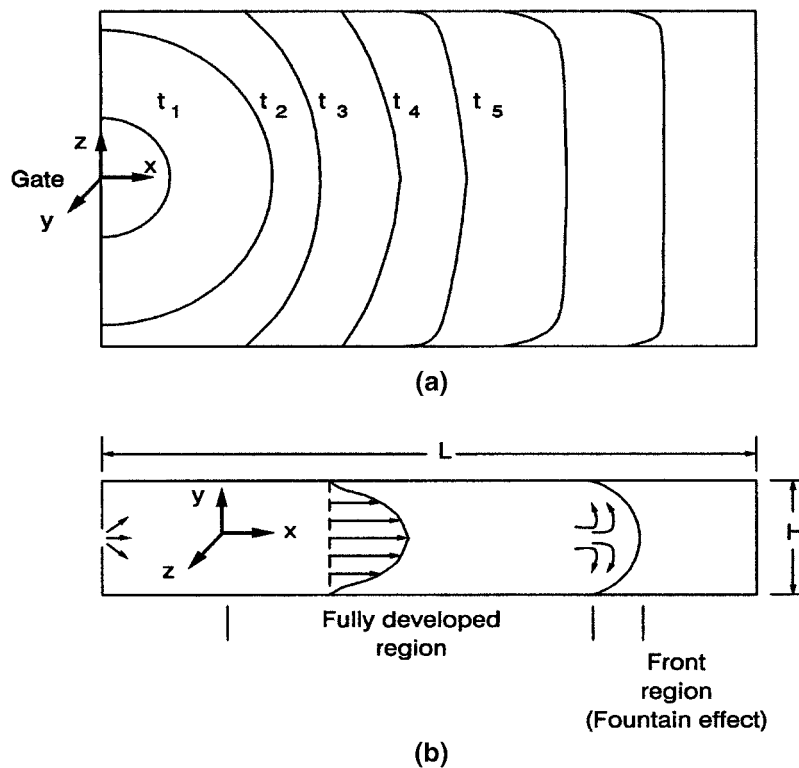


FIGURE 34 Flow patterns in an end-gated mold: (a) top view of fronts as a function of time and (b) side view showing velocity profiles and frontal region. [From Baird, D. G., and Collias, D. I. (1998). "Polymer Processing: Principles and Design," Wiley, New York.]

The velocity gradient, and hence stress, pass through a maximum at an interior point in the flow. A fluid element near the centerline will decelerate as it approaches the front and become compressed along the flow direction and stretched along the transverse direction. The element is then stretched further at the front and laid up on the wall where it is rapidly solidified in a highly oriented state. Hence, the extensional flow at the front stretches the fluid element and leads to a higher degree of orientation in the material at the mold wall than at the interior of the material.

On occasion the opening at the gate is smaller than the cavity thickness, and the melt no longer fills the mold by an advancing front mechanism. Rather, it "snakes" its way into the mold leading to a material with a poor surface appearance and reduced physical properties. Snaking does not seem to be a common method found in the filling of molds, but it can occur.

One of the major problems in injection molding of parts is the formation of weld lines, which lead to surface imperfections and weak spots in the part. Weld lines arise from the presence of obstructions in the flow and from the impingement of advancing fronts from different gates. The former type of weld line is referred to as a *hot weld*, while the latter is referred to as a *cold weld*. In the case of the hot weld the melt, the polymer stream is split by an ob-

struction such as a pin, for example, and then the streams are brought back together. Usually the temperature at the interface does not change much, and hence the streams are brought back together at the processing temperature. On the other hand, when two fronts impinge on each other, the temperature of the free surfaces has dropped somewhat, leading to the formation of what are called cold welds.

B. Thermoforming

Thermoforming is used primarily for the manufacture of packaging and disposable containers. However, it is also becoming a useful technique in the processing of engineering thermoplastics to produce parts used in the transportation industry. Polymers that are processed by this technique must have sufficient melt strength that on heating they do not sag significantly under their own weight, yet they can be deformed under pressure to take the shape of a mold. Hence, highly crystalline polymers with high melting temperatures and low molecular weight cannot be readily thermoformed. For example, nylon 6,6 ($T_M = 265^\circ\text{C}$ and $M_w = 30,000$) is not usually processed by means of thermoforming, while LDPE ($T_M = 110^\circ\text{C}$ and $M_w = 200,000$) is.

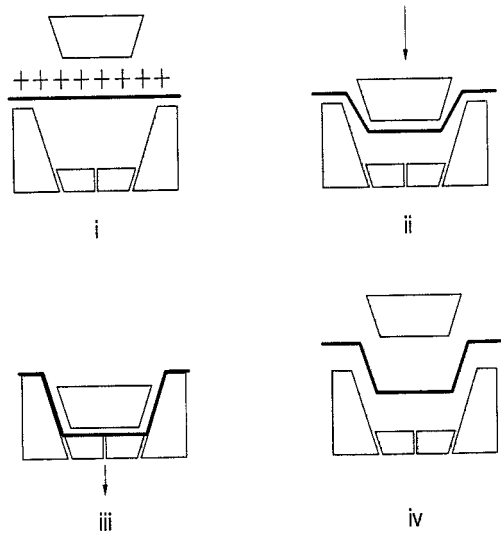


FIGURE 35 Plug-assisted vacuum thermoforming process. [From Baird, D. G., and Collias, D. I. (1998). "Polymer Processing: Principles and Design," Wiley, New York.]

The essential features of the thermoforming process are shown in Fig. 35. Thermoplastic sheet is heated usually by means of radiation but sometimes in conjunction with convection cooling to temperatures either just above T_g in the case of amorphous polymers or T_m in the case of semicrystalline polymers. The exact temperature depends on the degree of sag exhibited by the material under its own weight, which is determined by its rheological properties. The sample is then removed from the heating system and brought into position over the mold. The sample is forced to take the shape of the mold by applying pressure to the top of the sheet or by generating a vacuum on the underside of the sheet. The forming step occurs in the matter of a second. The sample is maintained in the mold until it is rigid enough to be removed from the mold without altering its shape.

There are a number of variations on the basic process. For example, in plug-assisted vacuum forming the heated sheet is forced by a plug into the mold with the remainder of the shape being produced by the application of vacuum to the underside of the sheet. This method is used to help maintain a more uniform wall thickness throughout the part. Another example is matched-die molding. The heated sheet is forced to take the shape of the female portion of the mold by the male part. This process is characterized by the formation of parts with more intricate shapes and uniform wall thickness. Finally, one last technique is that of twin sheet thermoforming. Here two sheets are heated and then forced to take the shape of the mold by applying air pressure on the inside of the sheets and possibly vacuum on the outside. This process resem-

bles somewhat that of blow molding, which is discussed next. However, the sheets can be forced to take on different shapes because each half of the mold can have a different shape. Furthermore, different polymers can be used for each half. The sheets must be held in the mold long enough for bonding to occur.

Thermoforming can be divided into four sections: (1) sheet heating without deformation; (2) sheet stretching without significant heat transfer; (3) part cooling in the mold; and (4) postmolding operations such as trimming. The time to make a part is primarily determined by steps 1 and 3 because these are of the order of minutes. However, the successful functioning of the part is determined by step 2 because the distribution of wall thickness is determined in this step.

C. Blow Molding

Blow molding is a process for generating hollow plastic articles such as bottles and containers. This process was initially used by the packaging industry but more recently has been used by the automotive industry to produce parts such as fuel tanks, bumpers, dashboards, and seatbacks. In other words, plastic parts are being manufactured for applications where some structural integrity is required.

Although a number of variations are possible in the way in which blow molding is carried out, there are a number of common steps. First, conventional melt processes are used to make a cylindrical tube (*note*: the preformed sample may be of other shapes). When extrusion is used, this tube is referred to as a parison, and when injection molding is used, it is referred to as a preform. The softened preformed tube is transferred to a mold consisting of two halves, where it is sealed and inflated to assume the internal contours of the mold. The part is cooled in the mold, until it reaches a temperature where it will maintain the shape of the mold when the mold is opened.

Extrusion blow molding is used frequently for polymers that exhibit high melt strength such as polyolefins. The process is shown schematically in Fig. 36. In this figure the tubular parison is continuously extruded from a die into position between the two mold halves and then separated from the main stream by means of a knife. The mold closes, sealing the end of the parison, and air pressure is applied inflating the parison against the walls of the mold. The time for inflation is very short, usually in the range of a second depending on the size of the part. The longest step in the process is the cooling of the part. The time for cooling depends on the temperature to which the part must be lowered in order for it to maintain the shape of the mold and the rate of heat transfer between the mold wall and the part. The mold opens finally and the part is ejected.

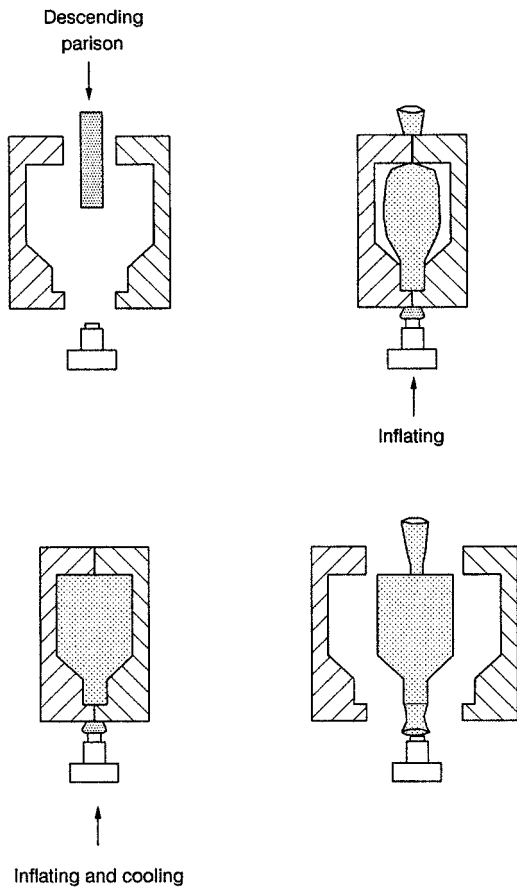


FIGURE 36 Blow-molding process. [From Baird, D. G., and Collias, D. I. (1998). "Polymer Processing: Principles and Design," Wiley, New York.]

In some cases injection molding is used to generate preforms rather than extrusion, but otherwise the process is nearly the same. Injection molding is used primarily when the screw-thread dimensions must be precise and to avoid flash, weld lines, and material waste at the base of the container. Just as in the case of extrusion blow molding, it is possible to generate preforms with multiple layers for situations where barrier properties are required.

In continuous processes the parison or preform must have sufficient melt strength so that it does not sag under its own weight. Sagging leads to unacceptable variations in the wall thickness of the part. For polymers such as PET it is usually not possible to use extrusion blow molding because of severe sagging problems. To overcome sagging problems, preforms are injection molded in a separate step where they can be rapidly quenched to inhibit crystallization and, hence, remain clear. The preforms are then heated by means of radiation to a temperature about 30°C above T_g , where crystallization kinetics are slow, but the material is deformable. The heated preforms are then transferred to the mold, where they are inflated by means of air pressure.

The process of inflating the parison is primarily one of planar extensional flow especially away from the ends of the parison. Because the ends of the parison are constrained as the parison expands, the thickness of the wall decreases as the diameter expands leading to primarily planar extensional deformation. For this reason the blow molded part contains primarily orientation along the circumferential or hoop direction and hence will exhibit mechanical anisotropy.

To generate a better balance of mechanical properties it is necessary to create biaxial orientation in the part. *Stretch blow molding* is used to accomplish this. In essence the parison is stretched along the axial direction before being inflated. Biaxial orientation is specifically required in large containers for fluids. For example, bottles for carbonated beverages are typically processed by means of stretch blow molding.

D. Compression Molding

Compression molding is primarily used to process thermosetting systems and difficult to process thermoplastics, such as fiber-filled systems or thermoplastic elastomers. The essential features of the compression molding process are illustrated in Fig. 37. In the case of thermoplastics, a preheated mass of polymer, which may be either a sheet or a pile of pellets or powder, is placed in the mold. The temperature of the mold is set low enough to cause the polymer to solidify but not so rapidly that it will not flow. Hydraulic pressure is applied to the top or bottom plate pushing the plattens together. The molds are designed to prevent the top part of the mold from touching the bottom part, which would squeeze the resin from the mold.

The design of a compression molding process consists of four aspects. The first is the selection of the proper amount of material to fill the cavity when the mold halves are closed. The second is determining the minimum time

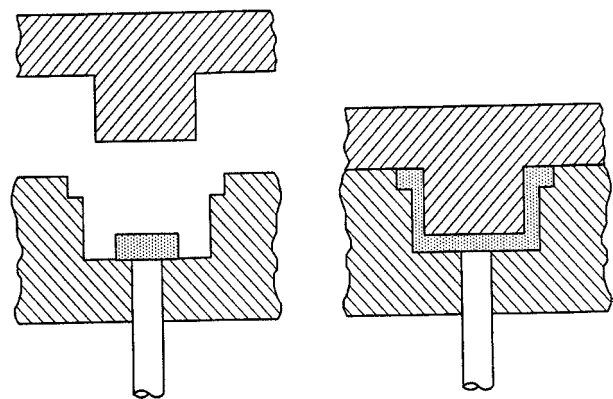


FIGURE 37 Compression molding process. [From Baird, D. G., and Collias, D. I. (1998). "Polymer Processing: Principles and Design," Wiley, New York.]

required to heat the blank to the desired processing temperature and the selection of the appropriate heating technique (radiation heating, forced convection, etc.). It is necessary to make sure that the center reaches the desired processing temperature without the surface being held at too high of a temperature for too much time. The third is the prediction of the force required to fill the mold. Finally, the temperature of the mold must be determined, keeping in mind that one wants to cool the part down as rapidly as possible, but too rapid of a cooling rate will prevent the polymer from filling the mold.

E. Rotomolding

Rotomolding or *rotational molding* is a process for making hollow plastic articles that cannot be easily produced by techniques such as blow molding. Examples of objects produced by this method include underground storage tanks for fluids, playground equipment, and recreational items such as coolers and kayaks. The objects are usually larger and have thicker walls than can be handled in blow molding. The process consists of placing polymer powder (typically 40 mesh or 500 μm in size) into a mold and then placing the mold into a forced convection oven where it is rotated around two axes to distribute the powder over the mold walls. The polymer particles are fused into a solid mass by the process of sintering, which is governed by surface tension and the polymer melt viscosity. High MI polymers (i.e., low molar mass) are typically used because it is the viscosity that leads to the resistance of fusion of the particles. The part must be cooled slowly to ensure dimensional stability and minimize warpage. The process

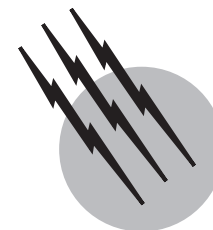
is relatively slow taking in the range of an hour or more to make a part. However, extremely large hollow objects can be made this way (e.g., a storage tank having a length of 20 ft and diameter of 8 ft). HDPE is most frequently used, but there are reports of nylons, ABS, and polycarbonate being used.

SEE ALSO THE FOLLOWING ARTICLES

ELASTICITY, RUBBERLIKE • PLASTICIZERS • POLYMERS, MECHANICAL BEHAVIOR • POLYMERS, RECYCLING • POLYMERS, THERMALLY STABLE • RHEOLOGY OF POLYMERIC LIQUIDS

BIBLIOGRAPHY

- Baird, D. G., and Collias, D. I. (1998). "Polymer Processing: Principles and Design," Wiley, New York.
- Bird, R. B., Armstrong, R. C., and Hassager, O. (1987). "Dynamics of Polymeric Liquids. Volume I: Fluid Mechanics," Wiley, New York.
- Dealy, J. M., and Wissbrun, K. F. (1990). "Melt Rheology and Its Role in Plastics Processing," Van Nostrand Reinhold, New York.
- Green, E., ed. (2000). "Modern Plastics Encyclopedia," McGraw-Hill, New York.
- Michaeli, W. (1984). "Extrusion Dies," Hanser, Munich.
- Morton-Jones, D. H. (1989). "Polymer Processing," Chapman and Hall, London.
- Rauwendall, C. (1986). "Polymer Extrusion," Hanser, Munich.
- Rodriguez, F. (1996). "Principles of Polymer Systems," Taylor and Francis, Washington, DC.
- Van Krevelen, D. W. (1990). "Properties of Polymers," Elsevier, Amsterdam.



Polymers, Electronic Properties

J. Mort

Xerox Corporation

- I. Conductivity
- II. Electronic States
- III. Triboelectricity and Electrets
- IV. Piezo- and Pyroelectricity
- V. Photoelectronic Properties of Pendant-Group Polymers
- VI. Conducting Polymers: Polyacetylene
- VII. σ -Bonded Polymers
- VIII. Applications

GLOSSARY

- Amorphous** Pertaining to a structurally disordered material in which the building blocks, atoms, or molecules are randomly arranged without the periodicity characteristic of a crystalline solid.
- Carrier range** Distance an excess electronic carrier can move in an applied field E before being immobilized by trapping.
- Chromophore** Strictly speaking, a term denoting the molecular unit responsible for the color of a molecular solid but also used as a generic description of a molecular unit such as a pendant group.
- Conjugated polymer** Polymer consisting of alternating single and double bonds.
- Electret** Material in which real or polarization charges can be stored for a long period of time.
- Extended states** Used synonymously with the term *band states* and describing a range of allowed energies, originating from the condensed nature of a solid, for electronic carriers.
- Fermi level** Parameter in quantum statistics defining the energy of the highest occupied energy states.
- Geminate recombination** Recombination of photogenerated electron-hole pairs before they ever become free of their mutual Coulomb attractive field.
- Mobility μ** Critical parameter of electronic charge transport defined as the carrier velocity per unit field.
- Molecular ion** Charged molecular unit with either an excess (anion) or deficit (cation) of electronic charge.
- Pendant group** Molecular unit attached to the polymer backbone at an angle to the chain direction.
- Piezoelectricity** Change in electric polarization due to either stress or strain.
- Plasmon** Collective excitation of free or bound carriers.
- Poling** Technique for forming electrets involving the application of a high electric field at an elevated temperature followed by cooling to room temperature with the field still applied.

Pyroelectricity Change in electric polarization due to temperature change.

Soliton As applied to conducting polymers, it refers to a bond alternation defect that results in a particlelike field pattern.

Triboelectricity Transfer of charge between two solids due to their contact and separation.

A POLYMER SOLID is composed of a collection of very long molecular chains that are characterized by strong chemical bonding within the chain and much weaker inter-chain bonding. In this sense, a polymer can be considered to be an assembly of individual chains. Each chain can contain a very large number ($\sim 10^5$ or more) of identical subunits bonded together. Each subunit can be viewed as a separate molecule with electronic states consisting of the molecular orbitals of the molecule. In describing the electronic states of polymers, the degenerate molecular orbitals that overlap in a periodic fashion lift their degeneracy by forming extended, that is, bands of, electronic states. Thus, bonding and antibonding molecular orbitals lead to polymer valence and conduction bands, respectively. To this degree, polymers can be viewed as organic semiconductors and, by analogy with the more familiar inorganic crystalline semiconductors such as silicon, the concepts of energy band theory can be used to characterize their electronic states and properties.

I. CONDUCTIVITY

Polymers are a familiar part of everyday life and, because of the ability of chemists to tailor-make their properties, have found widespread application. Until recently, these applications capitalized on advantageous properties such as chemical inertness and durability. By contrast, the most valued electrical property of polymers was their capacity to inhibit conductivity, that is, act as insulators, and little concerted work was done to examine and understand the fundamentals in order to enhance electrical conductivity in polymers. Beginning in the 1970s, a resurgence of effort occurred in the study of polymers as electronic materials. This has been characterized by an interdisciplinary approach involving physicists, chemists, materials scientists, and device engineers. This renewed interest was stimulated by the interplay of scientific and technological motivations. For the scientist, polymers posed new and often unconventional questions regarding the interpretation of experimental results. From the technological perspective, it was an explicit goal to explore the potential for combining useful electronic functions of polymers with their unique materials properties. Figure 1 shows the

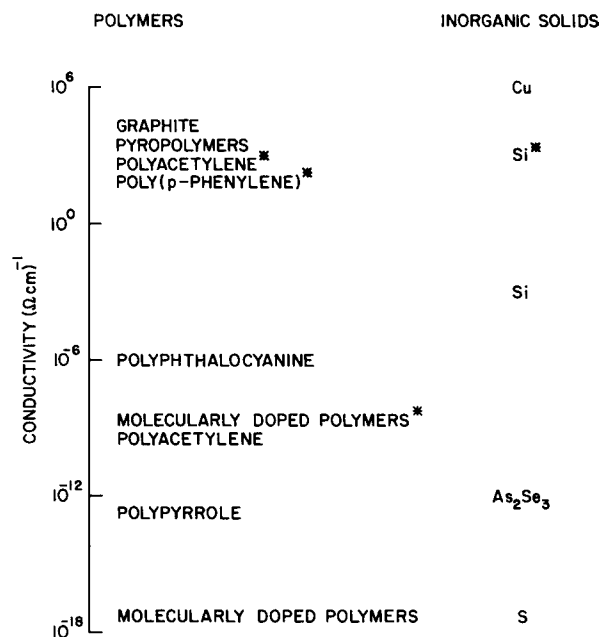


FIGURE 1 Representative conductivities of polymers and inorganic materials. The asterisk denotes that these values are achieved in doped materials. [From Mort, J., and Pfister, G., eds. (1982). "Electronic Properties of Polymers," Wiley, New York, by permission.]

range of conductivities that have been reported in polymer materials compared with the more familiar inorganic materials.

This article provides a review of the development of this new area of solid-state science. Emphasis is placed on key ideas, particularly as they contrast to more traditional concepts in the solid-state properties of crystalline or ordered solids. Topics covered include electronic states in polymers, an essential precursor to understanding the electronic properties of polymers; charge storage; piezo- and pyroelectricity; photoconductivity and electronic transport in polymers (e.g., pendant-group polymers) where localized molecular ion states play a determining role and in polymers (e.g., conjugated polymers) where delocalization of electronic charge is significant.

Finally, the actual and potential technological applications and commercial use of polymers as electronic materials are discussed. Particular stress is placed on how the contrasting properties of the various types of polymers determine their advantage in specific applications.

II. ELECTRONIC STATES

It is convenient for the discussion of this aspect of polymers to consider separately two classes that have quite different optical and electrical properties. The first consists

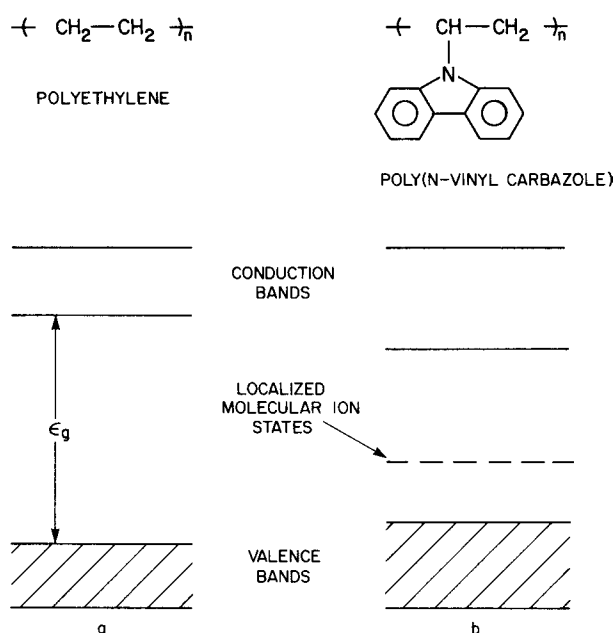


FIGURE 2 Examples of a saturated polymer (a) without pendant groups, polyethylene, and (b) with a pendant group, poly(*N*-vinyl carbazole), and associated energy level picture.

of polymers with the bonds saturated (i.e., complete bond satisfaction) or unsaturated but no pendant groups. Examples of these are polyethylene and polyacetylene, respectively. The second class comprises polymers with saturated backbones with appended aromatic chromophores that project out of the polymer chain. Polystyrene and poly(*N*-vinyl carbazole) (PVCA) are representative examples. Figure 2 schematically represents examples of these two polymer classes together with the appropriate electronic energy level picture. As alluded to above, the strong intrachain covalent bonding leads to wide bands of states with an energy gap, ϵ_g between the last-filled and first empty band. This is applicable even for amorphous polymers because of the maintenance of periodicity in the chain direction. An important requirement for the applicability of the band theory relates the strength of any electron-phonon interaction with the width of the energy band. In order for a carrier to remain within an energy band of width W after a phonon-scattering event, the Heisenberg uncertainty principle states that $W\tau > \hbar$, where τ is the electron-phonon scattering time. Since $\mu = e\tau/m^*$ (m^* is the effective mass of the carrier), then μ must be $> \hbar e/m^*W$. For reasonable choices of m^* , a minimum mobility of $\sim 0.2 \text{ cm}^2 \text{ V}^{-1} \text{ sec}^{-1}$ is required for the valid application of band theory. This value is typical of those experimentally measured for molecular crystals such as anthracene. By contrast, calculations for polyethylene and polyacetylene predict mobilities considerably higher than this minimum value and suggest that the con-

cepts of band theory may have validity for these polymers. These considerations are further amended if, as is the case in reality, the polymer materials are not ordered as in single crystals. Any variation in the energy of a molecular orbital due to disorder (compositional, translational, or rotational) can impede band formation by the disruption of the required periodicity. Experimental values for mobilities in pendant-group polymers reveal values much lower ($\sim 10^{-4} \text{ cm}^2 \text{ V}^{-1} \text{ sec}^{-1}$ or less), which reflects the consequences of strong electron-phonon interactions relative to bandwidths together with substantial effects of disorder.

The conventional method of experimentally studying electronic states in polymers is that of optical absorption, including increasingly sophisticated techniques such as low-energy electron-loss spectroscopy and synchrotron radiation source spectroscopy. These techniques allow such optical properties as absorption, reflectivity, and dielectric loss to be measured over an energy range from 0.2 to 1000 eV with a resolution of 0.1 eV. With these energies, it is also possible to do core-level spectroscopy in which the very narrow deep-lying atomic levels, by acting as a source of electrons of well-defined energies, can be used to probe the structure in the broader, higher lying empty extended states. Photoemission spectroscopy, in which electrons are excited out of the polymer, can give complementary information regarding filled-valence molecular states.

A. Pendant-Group Polymers

The extension of the pendant group perpendicular to the chain direction and its typically planar character can lead to very little overlap and therefore interaction even between adjacent pendant groups. Amorphous pendant-group polymers are therefore similar to a random assembly of isolated pendant molecules. This fact has several far-reaching consequences. The electronic states of pendant-group polymers bear a remarkable resemblance to those of the isolated pendant group. Similarly, the aromatic pendant groups give rise to electronic states in the gap between the valence and conduction band and play a dominant role in the static and dynamic electrical properties, as is discussed in Sections III and V.

The most obvious feature of their electronic absorption spectra is the close similarity to those of the effectively isolated chromophores, which can be observed in the gas phase. Figure 3 shows a typical energy-loss function and its derivative for polystyrene. The features indicated by the arrows, covering the range from 9 to 19 eV on the rising edge of the plasmon peak, correspond to strong peaks in the ultraviolet absorption spectrum of benzene, which is closely related to the styrene chromophore.

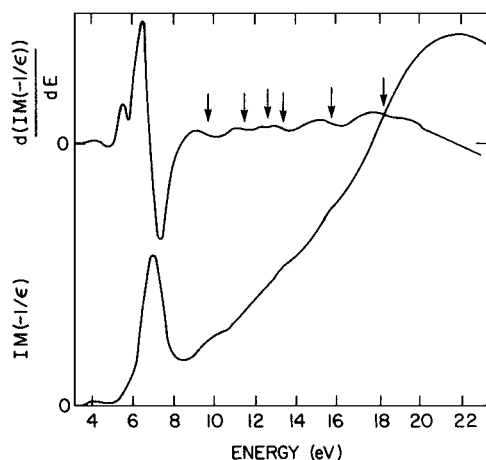


FIGURE 3 Energy-loss function and its derivative (from which the optical constants can be derived) for polystyrene. The arrows correspond to strong peaks in the ultraviolet absorption of benzene, which is closely related to the styrene chromophore. [From Ritsko, J. (1978). *J. Chem. Phys.* **69**, 4162, by permission.]

B. Alternating Conjugated Polymers

In the case of polymers without pendant groups, the electronic properties are determined by states associated with the strong covalent bonding between the atomic building blocks within the chain. The most extensively studied member of this class is polyacetylene, the structure of which is shown in Fig. 4. In this simple linear conjugated polymer, each carbon atom has three of its four valence electrons in saturated bonds pointing to neighboring carbon or hydrogen atoms within the plane (σ bonds). The remaining electron (the so-called π electron) has a wave function component perpendicular to the plane and overlapping with neighboring π -electron orbitals. The π electrons are therefore available to delocalize into a band. For an idealized case of a uniform chain, metallic conduction should ensue. However, such a system is unstable with respect to bond alternation and a characteristic gap opens up in the electronic energy spectrum. Figure 5 shows the

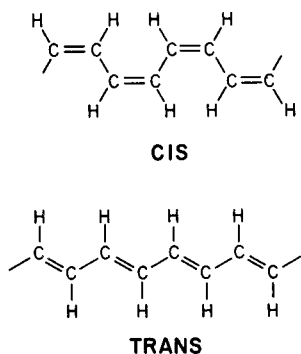


FIGURE 4 Structure of *cis*- and *trans*-polyacetylene.

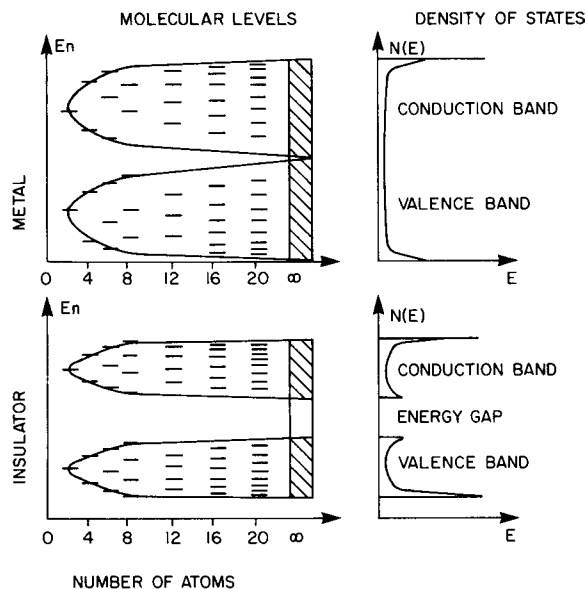


FIGURE 5 Molecular levels and density of states for regular (top) and alternant (bottom) polyenes. [From Andre, J. M., and Ladik, J., eds. (1975). "Electronic Structure of Polymers and Molecular Crystals," Plenum Press, New York, by permission.]

evolution of the molecular levels as a function of atoms in a finite chain and the band structure and density of states for both uniform and alternating polymers. The characteristic feature of the alternating configuration, the energy gap, is seen in the absorption spectrum of polyacetylene (Fig. 6).

III. TRIBOELECTRICITY AND ELECTRETS

Triboelectrification is the process by which two originally uncharged bodies become charged when brought

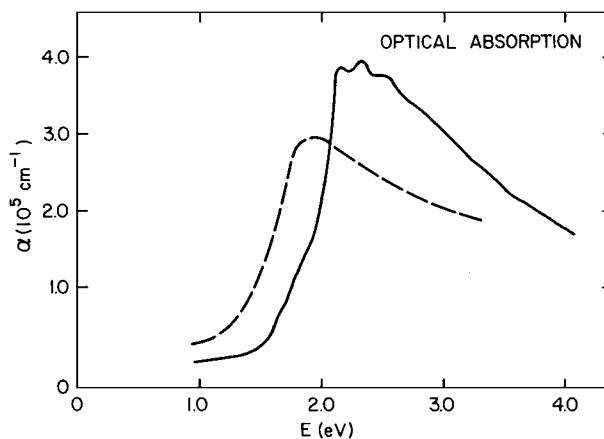


FIGURE 6 Absorption of *cis*-polyacetylene (solid line) and *trans*-polyacetylene (dashed line), $(CH)_x$. [From Fincher, R., Jr. *et al.* (1979). *Phys. Rev.* **B20**, 1589.]

into contact and then separated. This process occurs for all highly insulating materials, but its occurrence in polymers has enormous technical and commercial significance in electrophotography and as the cause of troublesome static electricity. Triboelectricity is a particular case of the general phenomenon of charge storage exhibited by electrets. Polymers are capable of storing electrical charges for a long period of time, if sufficiently insulating. The stored charges may be real (i.e., net charge is added) or polarization charges or a combination of both. The real charges consist of layers of positive or negative charges trapped at or near surfaces or distributed throughout the bulk (volume charges). The real charges may also be inhomogeneously located within molecular or domain structures resembling a dipole polarization. True polarization charges result from the frozen-in alignment of dipoles that may be a consequence of molecular structure. This aspect, which produces piezo- and pyroelectric properties, is discussed in Section IV. The permanence of charge storage in polymers depends on conductivity, charge transport properties, and polar relaxation frequencies. Since most of these properties are thermally activated, the storage times are strongly temperature dependent.

Triboelectrification or the formation of electrets (resulting from real charges) can be understood only by considering the band structure of polymers and, as an example, a contacting metal as a source of additional charges. Referring to Fig. 7, it can be seen that if insulating polymers are viewed as wide-band-gap solids with no states within the gap then no charge transfer from the contacting metal can occur. The fact that both triboelectrification and electrets are well known implies that, contrary to this simple view, states must exist essentially isoenergetic to the metal Fermi

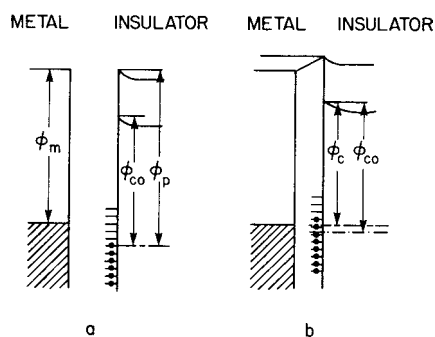


FIGURE 7 Energy level diagram of a contact between a metal and an insulator with surface states. (a) Before contact, (b) after contact. ϕ_m and ϕ_p are the metal and polymer work functions, respectively; ϕ_c and ϕ_{co} represent the energy difference between the polymer conduction band and the Fermi level after and before contact, respectively. [From Mort, J., and Pfister, G., eds. (1982). "Electronic Properties of Polymers," Wiley, New York, by permission.]

level, thus enabling charge transfer to occur. These states can be of two general types. The first are extrinsic surface states that occur only at the surface of the polymer. Unsaturated defects, chain-end groups, adsorbed molecules, or chemically modified surfaces due to ambients or even additives introduced in the synthesis process are candidates for these extrinsic states (Fig. 7).

The second type of state is more fundamental, since it consists of intrinsic bulk states. This is particularly true of pendant-group polymers in which, as was discussed previously, the electronic states of the pendant group play a dominant role. For such materials, any excess charge is localized on the individual pendant groups, forming molecular ions. The energy of these electronic states is subject to large relaxation effects because of the strong electron-phonon interaction between the excess charge and the large degrees of freedom existing within the large and easily deformable molecules. The extended or wide energy bands associated with the saturated chain are separated by a wide band gap, while the molecular ion states associated with the addition (anion) or withdrawal of an excess electron (cation) lie within this gap. Inhomogeneous broadening of these states occurs due to static polarization fluctuations arising from the disordered amorphous nature of the polymer. In this picture, charge is transferred to polymer states localized in energy to within ~ 0.4 eV of the Fermi level of the contacting metal. The sign of triboelectrification of the polymer depends on whether it is energetically more favorable to add or withdraw an electron. The occupied molecular ion state is presumed to be highly stable in that the transferred charge does not percolate, due to its extreme localization, to empty states of lower energy. This question of localization of charge on pendant groups is of central importance in understanding the motion of charge in molecular solids and is discussed further in Section V.

Many details remain unclear, not the least of which is the consistency of experimental results. This is hardly surprising since both of these phenomena are controlled by defect or impurity states and surface contamination can overwhelm the other, more fundamental effects due to intrinsic states. Nonetheless, the general features of the phenomena and their causes are now based on a picture that takes into account the electronic energy level description of polymers.

IV. PIEZO- AND PYROELECTRICITY

Piezo- and pyroelectricity are phenomena associated with the stress and temperature dependence, respectively, of remanent or frozen-in polarization. Although a number of polymers possess these properties, none match the

magnitude of the effects in polyvinylidene fluoride (PVF₂), which is the most widely studied and commercially used piezo- and pyroelectric polymer.

Substantial piezo- and pyroelectricity can be permanently induced by heating stretched films to $\sim 100^\circ\text{C}$, followed by cooling to ambient temperature with a strong dc electric field ($\sim 300\text{ kV cm}^{-1}$) applied. This treatment is called "poling." Such polarization, attributed to redistribution of electronic or ionic charges within the solid or injected from electrodes, characteristically vanishes on exceeding some polarization temperature, T_p . The effect in PVF₂ is totally different in that the induced polarization is thermally reversible and polarization currents are produced on either heating or cooling.

Polyvinylidene fluoride is a crystalline polymer that exists in at least three and possibly more crystalline phases. Since the polymorphism is a critical ingredient in determining the piezo- and pyroelectric properties, it is worthy of some discussion. Phase I (β form) has a planar zigzag conformation and ordered C–F bonds, giving a large unit dipole of 2.1 debye (D). This large moment and the facility with which it can orient, because of the small atomic volume of fluorine, accounts for the high permittivity. Phase II (α form) has a conformation with two chains of opposite dipole moment per unit cell. Melt-crystallized samples below 150°C are largely phase II, although phase I films can be made by casting from appropriate solvents and by high-pressure techniques. Induced strain by biaxial stretching at temperatures around 60°C can result in α - to β -phase transformations. Contrary to early expectations, phase II is not nonpolar under all circumstances but can have unit cell dipole moments of $\sim 1.5\text{ D}$ after orientation of poled films. More recent studies have revealed the existence of a third phase, called γ , in films cast from dimethylformamide and annealed at $\sim 170^\circ\text{C}$. The γ phase is uncertain, but it has been proposed that it is a modified phase II with a double repeat unit.

The necessity of poling to induce permanent piezo- and pyroelectric behavior and the intuition that these phenomena are intimately associated with the polymorphic form have induced several workers to attempt to detect structural changes due to poling. Reversible changes were detected in the polarized infrared absorption at 510 and 445 cm^{-1} when poling and depolarization were repeated. A minor change in the X-ray diffraction when β -phase PVF₂ was poled was reported, and variations in dielectric constant and loss have also been reported. On the basis of these observations, one might conclude that the origin of spontaneous polarization in PVF₂ is due to dipole orientation in β crystallites and that the orientation can be in part reversed by electric field; that is, PVF₂ has some aspects of ferroelectric behavior. However, direct evidence has yet to be found for the existence of domains or a Curie

point in PVF₂. The fact that quite efficient poling occurs at temperatures of $\sim 130^\circ\text{C}$, compared with transition temperatures of β to α phase of 180°C and the α -phase melting point of $\sim 200^\circ\text{C}$, suggests that dipole orientation does not occur in the crystalline phase. Instead, it is believed to occur in disordered regions that have conformational similarity to the β form but with lateral disorder between chains.

The structure–property relationship for PVF₂ is an extremely complex question that remains an area of some controversy and contention. There is some evidence that other effects, such as charges injected during the poling process, in addition to dipole reorientation, may also be important. Other evidence has been found for nonuniform pyroelectric constants and internal electric field after poling. There seems little question that internal space charges in the films can have a significant influence on the poling process.

In summary, it is perhaps wise to highlight the fact that piezoelectric and pyroelectric properties can be quite sample dependent in terms of purity, morphology, and detailed processing procedure. It thus becomes very difficult to identify a specific mechanism when in fact several inter-related ones may be operative.

V. PHOTOELECTRONIC PROPERTIES OF PENDANT-GROUP POLYMERS

The weak intermolecular interactions in molecular solids lead to very narrow energy bands, even for ordered molecular crystals such as anthracene. This results in low mobilities for electronic charge carriers. If, in addition to this weak interaction between the molecular building blocks, one introduces the feature of disorder, rather dramatic effects on carrier transport may be expected. Pendant-group polymers, as we have seen, are examples of polymers in which the optical properties are dominated by those of the pendant-group molecules themselves. Extensive studies of the photoelectronic properties of such polymers have verified these features to a dramatic degree. It is therefore found that dynamic charge transfer, including both photogeneration and transport, is determined by charge exchange between neighboring, essentially isolated molecules.

The full range of these effects has been examined, but not by studying pendant-group polymers themselves, although in the case of PVCA this has been done. Rather, the concept of molecular doping of polymers has been employed as a powerful way of exploring the intuitive concepts. A typical example of a molecularly doped polymer is the molecular dispersion of *N*-isopropyl carbazole (NIPCA) in a polycarbonate polymer. The doping

is achieved by dissolving the dopant molecule and polymer matrix of appropriate weight ratios in a common solvent. From this solution, films are cast and the solvent driven off thermally. In the absence of doping, the polycarbonate behaves as essentially an ideal insulator with immeasurably small currents that are unaffected by light even of ultraviolet energies. In contrast, with the introduction of NIPCA in concentrations of $\sim 10^{20}$ molecules per cubic centimeter, significant photocurrents are observed. It should be stressed that this system is a true molecular solid solution; that is, the NIPCA molecules are dispersed on a molecular level. The photoconductivity excitation spectrum confirms that the photocarriers are produced by optical excitation of the NIPCA molecules. By shining short light pulses, highly absorbed in the film, it is possible to create a thin sheet of photogenerated charge and, by monitoring the time evolution of the photocurrent, to measure the time the sheet of charge (moving under an applied electric field) takes to traverse the film thickness. This allows the measurement of a fundamental parameter of the motion of charge: its mobility, μ . By varying the weight ratios of the NIPCA and polycarbonate, it is possible to control the average distance between NIPCA molecules and measure how the mobility depends on this separation.

Intuitively, in such a system the charge transport is expected to occur via the hopping of charge from one molecule to another. This is a quantum mechanical effect wherein the probability of such an event is determined by the product of the electronic wave function associated with each molecule. Mathematically, this can be expressed by $\mu\alpha\rho(-2\gamma\rho) \exp(-\Delta/kT)$, where ρ is the average separation of the molecules, γ is a parameter describing the decay of the electronic wave function outside the molecule, and Δ is any activation energy required for the hop. Figure 8 shows the dependence of μ/ρ^2 on ρ (the average intermolecular separation). The linearity of the semilogarithmic plot is strong evidence for a transport mechanism involving hopping between the randomly distributed molecules. The slope of this line gives a measure of the localization parameter γ , which measures the extension of the molecular wave function outside the molecule. This extension controls the degree of overlap of the wave functions on neighboring molecules and this in turn determines the probability with which a hop will occur. Values of γ are typically $\sim 2 \text{ \AA}^{-1}$, indicating a very high degree of localization. This is consistent with the picture of the excess carrier interacting very strongly with the intramolecular vibrational modes of the individual molecules. Temperature dependence studies reveal the hopping process to be thermally activated, also reflecting the intramolecular relaxation of the molecular ion and the self-trapping of the excess carrier. The study of molecularly doped matri-

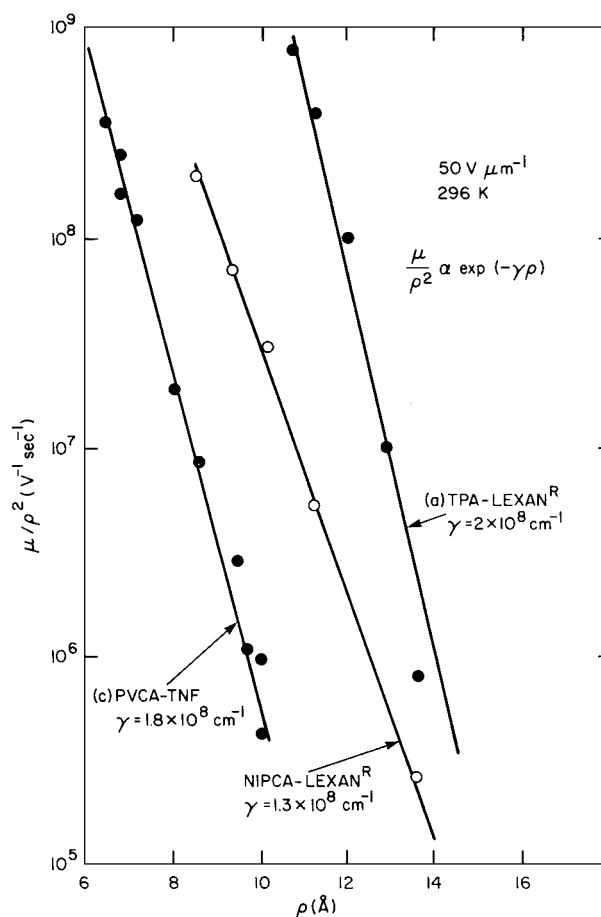


FIGURE 8 Concentration dependence of hole mobility in the molecularly doped polymers NIPCA-Lexan[®] and TPA-Lexan[®] and the charge-transfer complex PVCA-TNF-Lexan[®]. [From Mort, J., and Pfister, G. (1979). *Polym. Plast. Technol. Eng.* **12**, 89. Reprinted courtesy of Marcel Dekker, Inc.]

ces has proved to be a particularly powerful tool because of the ability, simply by gravimetric means, to control the number and type of hopping sites. This is difficult to do in actual pendant-group polymers. However, mobility measurements made in the way previously described have been carried out on pendant-group polymers such as PVCA. The magnitudes of the mobilities observed, the activation energies, and the details of the time evolution of the transport suggest that the same basic transport mechanism prevails. That is, the charge transport occurs via hopping between the pendant groups attached to the polymer backbone, which merely provides the mechanical integrity of the polymer.

Carrier propagation in pendant-group polymers can also be described from a more chemical viewpoint as being a reversible oxidation-reduction reaction. In the case of hole transport, for example, as a result of a photoexcitation process some dopant molecules (or pendant groups)

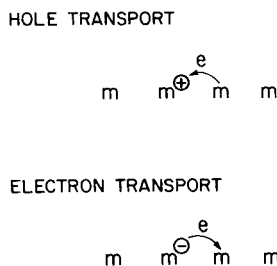


FIGURE 9 Charge transport in doped polymer systems visualized as a donor–acceptor or an oxidation–reduction process.

become radical-cations (positively charged). As illustrated in Fig. 9, under the influence of an applied electric field, neutral molecules will repetitively transfer electrons to neighboring cations. The macroscopic manifestation of this microscopic process is hole transport. It must be stressed that this is purely electronic and not ionic motion since no mass transport is involved. For hole transport to occur, therefore, one expects that the neutral molecule should be donorlike in its neutral state, whereas for electron transport the neutral molecule should be acceptorlike. This has been confirmed experimentally since donorlike molecules such as NIPCA, triphenylamine (TPA), and tri-*p*-tolylamine (TTA) exhibit only hole transport. For molecules that are acceptorlike, that is, have a high electron affinity, such as trinitrofluorenone (TNF), only electron transport is observed.

Many of these concepts play a role in the process of photogeneration in which free carriers are created by photoexcitation. There are many potential consequences of photoexciting a molecule. The excitation can either relax internally within the molecule via nonradiative or radiative (fluorescence or phosphorescence) processes or it can thermalize (i.e., lose excess energy) into a bound electron–hole pair. This electron–hole pair can self-annihilate due to the mutual attractive Coulomb force, or there is always a probability, which can be enhanced by temperature or applied electric field, for the pair to dissociate into a free electron and hole. Many studies have demonstrated that this process, or one very much like it, does occur in pendant-group polymers. A theory commonly invoked to explain this phenomenon is due to Onsager and describes the probability of dissociation of a thermalized electron–hole pair. Figure 10 shows the general predictions of theory; ϕ_0 is the number of initially thermalized pairs, ϕ the number which dissociate, and r_0 the separation of the bound electron–hole pair after thermalization. A final critical parameter is the Coulomb radius of the carrier pair, which is the distance at which they just begin to feel their mutual attraction. This is determined primarily by the dielectric constant κ of the material and for most polymers is ~ 250 Å. From Fig. 10, it can be seen that the number of dissociated

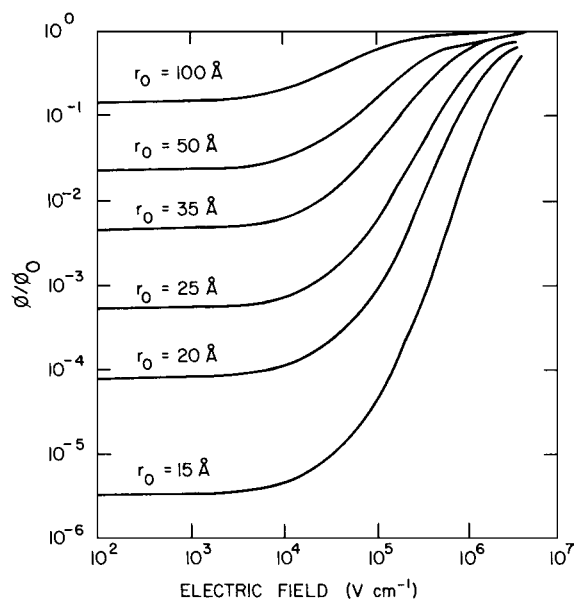


FIGURE 10 Escape probability predicted by Onsager theory for isotropic initial distribution of electron–hole pairs, $T = 296$ K, $\kappa = 3$.

electron–hole pairs (i.e., the number of free carriers) is essentially independent of the applied electric field but is a strong function of r_0 . This simply reflects the fact that, the closer the electron–hole separation after thermalization relative to the Coulomb radius, the more difficult it becomes for them to escape. For a given value of r_0 the number of dissociated pairs is a strong function of electric field and ultimately approaches unity; that is, all pairs dissociate. Similar considerations apply to phenomena in polymers such as photosensitization in which a visibly absorbing molecule (i.e., a dye or pigment) is incorporated into a pendant-group or molecularly doped polymer. In this case, the details become more complicated because of the interaction between dissimilar molecules. The photoexcited molecule is the sensitizer, and the photogeneration involves both this molecule and the pendant-group molecule of the host polymer, whereas the ultimate transport of the freed charge may involve only the pendant-group specie.

As just discussed, transient increases in conductivity can be achieved by exposure to light of appropriate wavelengths. This photoconductivity decays to the quiescent equilibrium dark level, often with very large time constants due to trap emptying, on termination of the illumination. Typically in these insulating systems, this steady-state dark conductivity is extremely small. The excess conductivity is produced by transient photooxidation of the pendant groups. This suggests that it should be possible to produce controlled increases in the equilibrium dark electrical conductivity (σ) by the use of variable equilibrium chemical oxidation or reduction of the pendant groups.

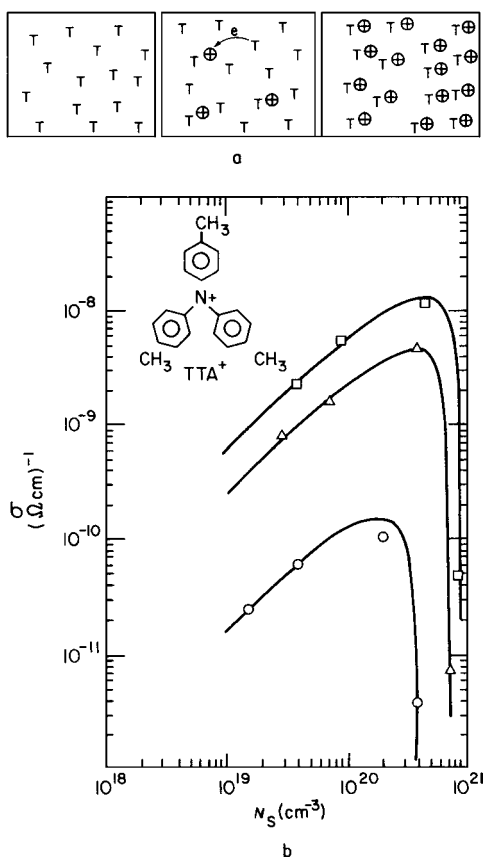


FIGURE 11 (a) Chemical control of conductivity in a molecularly doped polymer matrix. Fractional oxidation of neutral transport molecules T is achieved by the addition of an oxidizing agent, SbCl_5 . Oxidized transport molecules are radical-cations T^\oplus , which constitute free carriers. (b) Dependence of conductivity on concentration of oxidized transport molecules measured by electron spin resonance N_S . The molecule tri-*p*-tolylamine (TTA) is dispersed in polycarbonate. Total molecule concentrations are 8.6×10^{20} , 7.2×10^{20} , and $0.86 \times 10^{20} \text{ cm}^{-3}$. [From Troup, A. *et al.* (1980). *Solid State Commun.* **33**, 91, by permission.]

This has been reported, as shown in Fig. 11a. At low oxidation levels of the neutral transport molecule T, the conductivity rises as the number of “free” carriers (i.e., cations of the transport molecule) increases (Fig. 11b). These “free” carriers can move by the hopping of electrons from the neighboring, more numerous neutral molecules. However, since no extended states exist and the carriers are highly localized and associated with specific molecules, at high oxidation levels the “free” carriers created begin to result in a significant loss of the neutral molecules necessary for transport. In the extreme case, in which total oxidation has occurred, no neutral molecules necessary for the transport process remain, and after going through a maximum, the conductivity falls dramatically to that of an insulator. The levels of dark conductivity achievable in these systems are limited by

the intrinsically low mobilities associated with the hopping transport mechanism through the localized molecular states.

VI. CONDUCTING POLYMERS: POLYACETYLENE

In order for an organic polymer to exhibit high electrical conductivity in the dark, it must have a high density of free dark carriers that possess relatively high mobilities. This requires the polymer to have extended π electrons along the chain. This can occur either by having aromatic rings within the chain with large overlap across any atomic linkages between the rings or by having unsaturated bonding within the chain, which also leads to delocalization of π electrons. The canonical example of the latter type, and the most extensively studied, is polyacetylene. To put the previous discussion in perspective, fully saturated polymers such as polyethylene have no π -electron system to provide the necessary free carriers, although the mobilities in the extended state bands would have the necessary values. On the other hand, the pendant aromatic groups in pendant-group polymers have the necessary π -electron system but an exceedingly low intermolecular overlap of the π orbitals. This is exacerbated by the effect of disorder on the orientation of the planar groups and results in extremely low mobilities.

Polyacetylene possesses both a π -electron system because of the unsaturated bonding, and strong overlap of orbitals since the chain is an extended molecule and the coupling is intramolecular. As we have seen, in an ideal infinite chain of $(\text{CH})_x$, the π electrons should form a half-filled band, leading to metallic behavior. However, because of bond alternation (Peierl's distortion) a system of infinitely long $(\text{CH})_x$ chains is actually a semiconductor with a Peierl's band gap of $\sim 1.5 \text{ eV}$. Polyacetylene films consist of randomly oriented fibers with diameters of 200 \AA and indefinite length. As might be expected, such inhomogeneity on a macroscopic scale plays a significant role in both determining and interpreting the properties of polyacetylene, particularly for electrical transport. The absorption spectrum of nominally undoped $(\text{CH})_x$ of either cis or trans form reveals an absorption edge characteristic of a semiconductor, although the two edges do differ in detail. The absorption spectrum should show a singularity if the material were composed of perfect linear chains, and the smoothed-out edge (see Fig. 6) reflects the inhomogeneous nature of the material. Substantial changes occur in the absorption spectra when the polymer is doped with electron acceptor such as AsF_5 or iodine. For low doping levels, that is, $y < 0.005$, where y is the number of dopant molecules incorporated per (CH) unit, the interband



FIGURE 12 Bond alternation defect in an odd-numbered chain.

absorption is reduced and a band grows below the absorption edge and roughly at half the band-gap energy. It is believed that this absorption is due to transitions from the valence band to the unoccupied localized states. The latter may be associated either with excitations related to the dopant or with a bond alternation defect induced in the $(\text{CH})_x$ chain (so-called soliton) by the dopant (Fig. 12). This type of bond alternation defect is intuitively expected to be a feature of characteristically twofold-coordinated polymers.

The dopant molecules may be of two different types. In the first, the impurity is spatially localized (so-called quenched impurities), or it may relax depending on the detailed local environment (annealed impurities). Since the dopants are charged, they tend to screen the induced bond alternation defects, which otherwise, because of mutual Coulomb repulsion, would undergo further modification. Quenched impurities have a strong phase-disordering effect at high concentrations, which makes the Peierl's distortion unstable. This eventually leads to a disordered metallic phase wherein the Peierl's gap is closed. With annealed impurities, on the other hand, the Peierl's distortion could persist and an impurity band form at high concentrations within the gap. Effects of these kinds are found in $(\text{CH})_x$ doped to high concentrations (i.e., $y > 10^{-2}$) with AsF_5 or I_2 . In the case of iodine doping (Fig. 13), even at the highest doping levels the fundamental absorption edge is still discernible. On the other hand, in the case

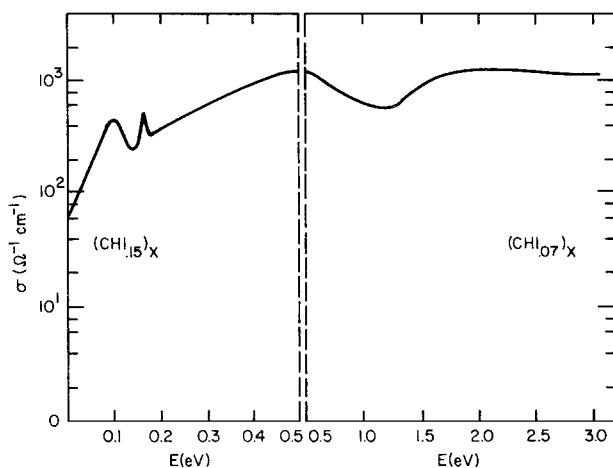


FIGURE 13 Optical conductivity of polyacetylene highly doped with iodine. [From Mort, J., and Pfister, G., eds. (1982). "Electronic Properties of Polymers," Wiley, New York, by permission.]

of AsF_5 the band gap is no longer detectable and the optical properties are those normally associated with a metal.

The property of polyacetylene that has produced the most excitement is the dramatic increase in the dc electrical conductivity on doping. It is found that there are two regimes of doping, that below $y = 0.01$ and that above $y = 0.01$ within which a semiconductor-to-metal transition is observed. Conductivity measurements have been made from 40 mK to room temperature. For doping levels $y < 0.01$ the log σ versus T^{-1} curves for both undoped and doped samples typically show a curvature that can be associated with a distribution of activation energies associated with disorder. Some studies have been made relating to the degree of anisotropy due to charge transport along or perpendicular to the fiber axes. In stretch-aligned films, elongation ratios of ~ 3 produce $\sigma_{\parallel}/\sigma_{\perp} \sim 10$ for undoped films and somewhat larger after doping. These conductivity studies can be interpreted in terms of a conventional extrinsic semiconductor picture. Alternative interpretations of the conductivity in this low-doping regime include hopping between localized states due to, or caused by, the dopant. An example of the latter is transport by charged solitons. In this case, the activation energy for conduction would be determined by the binding energy between the charged soliton and the neighboring impurity.

Above doping concentrations of $y \sim 0.01$, the electrical conductivity increases very rapidly to very high, almost metalliclike values (Fig. 14). In many respects these results are similar to the insulator-metal transitions observed in inorganic semiconductors. However, important and significant differences are observed. In highly conducting inorganic semiconductors (e.g., InSb) a Burstein shift is observed (i.e., a shift of the absorption edge to higher energies with increasing conductivity) since the first empty available states lie above the Fermi level and the optical transition associated with the band gap remains. For polyacetylene, in the highly conducting state no Burstein shift is seen and the band-gap transition disappears (except for the special case of I_2 doping). Some reports of the field and temperature dependence of the conductance have been seen as evidence of a "cermetlike" behavior. A cermet is a system of conductive (usually metallic) particles dispersed in an insulating matrix. At low loadings of the conductive particles, the system behaves as an insulator, but above a relatively sharp threshold (the percolation limit) the conductivity rises dramatically toward that of the bulk conductive material. No overwhelming evidence for any one process, in either doping regime, has been established from electrical measurements.

The Royal Swedish Academy of Sciences awarded the Nobel Prize in Chemistry for 2000 jointly to Alan J.

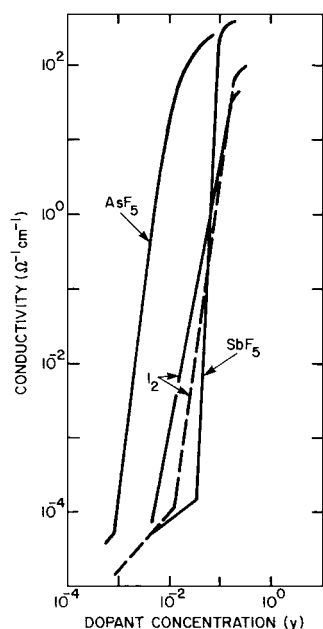


FIGURE 14 Direct current conductivity of *trans*-(CH)_x as a function of concentration for various dopants. The concentrations are expressed as the number of dopant molecules per CH group. [From Mort, J., and Pfister, G., eds. (1982). "Electronic Properties of Polymers," Wiley, New York, by permission.]

Heeger of the University of California at Santa Barbara, Alan G. MacDiarmid of the University of Pennsylvania, Philadelphia, and Hideki Shirakawa of the University of Tsukuba, Japan, for the discovery of conductive polymers based on doped polyacetylene.

Most research in highly conducting polymers has centered on polyacetylene. This is principally because of the wide range of interesting phenomena observed in a material that from a chemical viewpoint is relatively simple. Nonetheless, this has spawned efforts to uncover other polymers that exhibit similar properties. This offers the chance to explore intuitive concepts as to the connection between structure and electrical properties. To reiterate, it is expected that high conductivity in polymers requires an extended π -electron system along the chain direction together with large intra- or interchain overlap (or both) of molecular wave functions. A number of polymers have been found that exhibit high conductivity on doping. These polymers are characterized by six-membered phenylene rings or five-membered hetero rings linked together. In most of these systems, the optical absorption shift with increasing number of units within the chain is not as great as that for (CH)_x. This is indicative of a lack of wave function overlap across the bridging atoms connecting the rings or a lack of planarity of the rings. The effects of doping on the optical properties are similar to those of polyacetylene on the growth of a sub-band-gap absorption and a

maintenance of an absorption edge in the highly doped, conducting material.

VII. σ -BONDED POLYMERS

Recently, it has been shown that σ -bonded polymers, which have no conjugated π bonds in their backbone or side groups, exhibit photoconductive properties and observable charge transport. Certain polysilane polymers are known to be photosensitive in the ultraviolet and indeed are useful as self-developing photoresists. The σ -electron delocalization plays an important role in the electronic states of low-molecular-weight polysilanes because the energy of the σ - σ^* transition is highly dependent on the polymer conformation. Photogeneration, with an efficiency of about 1% at high fields, has been shown to be associated with excitation diffusion to the surface. Dissociation at the surface only leads to the creation of free holes, since only hole motion is detectable using the time-of-flight technique, in which well-defined transits are observed, yielding hole drift mobilities of about 10^{-4} cm² V⁻¹ sec⁻¹ at room temperature. The initial measurements made on poly (phenylmethylsilane) were thought to be due to the hopping of holes through the attached phenyl groups with their associated π electrons. However, subsequent studies have revealed that essentially the same mobility is found in all alkyl polysilanes containing no π electrons. It is now believed that the nondispersive transport intimately involves the σ -electron states of the polymer backbone (in contrast to the case of PCVA). The low mobility and its thermal activation, activation energies ranging from 0.1 to 0.25 eV, imply a motion of carriers in the σ -electron states which is trap controlled. Since the measured mobilities at room temperature appear remarkably insensitive to the purity of the polymer, it is thought that the traps are intrinsically associated either with chain ends or self-trapping by the formation of small polarons.

VIII. APPLICATIONS

The commercial use of polymers as electronic materials is growing rapidly, and several major applications are already firmly entrenched. As applications have proved their value and as awareness of their utility has grown, increasing attention has turned to applications of polymeric electronic materials in which their unique combination of properties may offer significant technical or economic benefit or both. As a consequence, many applications have not yet been commercialized but are rather in various stages of research and development. In this section, no attempt will be made to specify the particular

stage that potential applications have reached except to indicate those that have already entered the marketplace and proved their worth.

Conductive plastics are presently used in, or being developed industrially for antistatic substances for photographic film, shields for computer screen against electromagnetic radiation, and for "smart" windows (that can exclude sunlight on demand). In addition, semiconductive polymers have recently been developed for use in light-emitting diodes and solar cells and as displays in mobile telephones and miniformat television screens.

A major commercial application of polymer electrets is as electroacoustic transducers such as microphones. Their commercial acceptance is based on several advantages over condenser microphones. Among these are an insensitivity to mechanical shock and electromagnetic pickup. They are much simpler in design and less expensive. In a typical microphone, a thin polymer electret is attached to a back electrode and a front diaphragm. Incident sound induces vibration of the diaphragm, and the vibration of the electret thus generates an ac signal. This type of microphone and variations are used in cassette recorders, hearing aids, stereo equipment, and sound level detection and telecommunications. Current worldwide production is ~ 100 million units on an annual basis. The piezoelectric properties of PVF_2 have also led to its use in commercial electroacoustic applications. In all cases, the chief advantages of polymers are their flexibility, toughness, and capacity to be easily processed in large-area, thin films of practically any shape. They also possess low mechanical impedance and therefore have the virtue of good acoustic coupling to water and the human body. These two qualities, together with the others, have suggested potential important applications ranging from medical, biological, and geological to military. The good impedance match to the human body suggests use as real-time, *in vitro* heart rate monitoring (e.g., fetal phonocardiographs). In marine technology, the monitoring of underwater acoustic signals whether from marine life or human-made objects such as submarines becomes possible. The piezoelectric properties of PVF_2 allows its use as transducers in inkjet printers, printing pressure monitors, blood pressure monitors, strain gauges, accelerometers, and the like. The pyroelectric properties have led to the use of PVF_2 as an infrared detector with a fast response time because of the small heat capacity achievable with thin films. These detectors can also be produced in very large areas and therefore have potential security applications such as burglar and fire alarms.

The triboelectric properties of polymers have enormous applications in the area of electrophotography and dry-ink electrophotography. The basic feature of electrophotography is the production of a latent electrostatic pattern that

replicates the information to be produced either from an original or from electronic input. This electrostatic pattern can be produced by selective photodischarging of a uniformly charged photoreceptor surface or by selective charging of a surface with an ion beam. The latent electrostatic pattern must then be developed. In dry copying, as opposed to liquid ink development, the image is rendered visible by moving a developer material across the surface of the photoreceptor. This developer material is a fine powder that consists of black or colored toner particles, which are polymer spheres ($\sim 10 \mu\text{m}$ in diameter) in which a colorant such as carbon black is encapsulated. These toner particles are charged by a triboelectric process to a sign opposite to that with which the photoreceptor was originally charged. (By proper choice of materials either polarity of triboelectric charge can be obtained.) The oppositely charged toner particles are therefore attracted by the latent electrostatic pattern and render it visible. This toner pattern is then transferred to paper from the photoreceptor and fixed. This is usually done thermally, by which process the polymer spheres melt and adhere to the paper. Considering that billions of copies are made per year, the commercial significance of triboelectricity in polymers can be appreciated.

Another significant application of polymers as electronic materials in electrophotography is as photoreceptors. Polymers that are electrically insulating in the dark but can transport nonequilibrium carriers produced by light are well suited to function as photoreceptor elements. Polymers such as PVCA or molecularly doped polymers have strong intrinsic optical absorption only in the ultraviolet, and since visible light is employed in practice, the polymer photosensitivity must be extended into the visible. This can be done by (1) the formation of a charge-transfer complex with absorption in the visible, (b) dye sensitization with an appropriately absorbing dye, or (c) the use of a thin, contiguous sensitizing layer such as amorphous selenium or an organic pigment. The ability to make large-area flexible polymer films at relatively low cost by solution coating accounts for the application of these materials in electrophotography. Although in pendant-group polymers or polymers doped with aromatic molecules charge transport is a hopping process with inherently low mobilities, less than $10^{-3} \text{ cm}^2 \text{ V}^{-1} \text{ sec}^{-1}$, this is not a limitation for electrophotographic usage. In this process, the most important parameter, within limits, is how far the carriers move before they are immobilized rather than how fast they travel. For most process speeds, such mobilities are adequate provided that the photogenerated carriers can traverse the total device thickness, that is, $\mu E \tau > \text{sample thickness}$, where μ is the mobility, E the electric field, and τ the lifetime of carriers with respect to deep traps. Remarkably, such polymers do exhibit large

carrier ranges because of their very long deep-trapping lifetimes.

For systems in which the photogeneration occurs by photoexcitation within a polymer, such as the charge-transfer complexes or dye-sensitized systems, the photogeneration efficiency can be controlled by a geminate recombination mechanism. This type of carrier recombination in molecular systems can lead to quantum efficiencies for photogeneration that are substantially less than unity and are strongly field dependent. This may result in a photosensitivity limitation, depending on the particular system, and can be overcome to some degree by increasing the light exposure in a machine.

For other electronic applications, the magnitudes of the carrier mobilities are of paramount importance, since they determine the frequency response of devices or, through the related diffusion lengths, determine ultimate collection efficiencies in devices such as photovoltaic cells. Pendant-group polymers and disordered molecularly doped systems are not likely to find applications in these areas because of their low mobilities and the probable importance of geminate recombination processes.

A major commercial application of highly conductive polymers, such as doped polyacetylene, has yet to be realized. Potential uses that have been explored or are currently under study include experimental photovoltaic and photoelectrochemical cells and lightweight rechargeable batteries. Organic batteries, based on reversible electrochemical doping, in particular, appear to hold the most

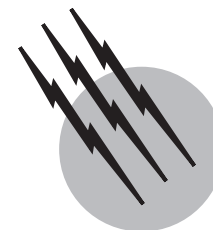
technological promise, although, because of the infancy of this class of electronic polymers, further advances leading to other innovations cannot be ruled out.

SEE ALSO THE FOLLOWING ARTICLES

ELECTRONS IN SOLIDS • FULLERENES AND CARBON NANOTUBES • ORGANIC CHEMICAL SYSTEMS, THEORY • PHOTOGRAPHIC PROCESSES AND MATERIALS • POLYMERS, FERROELECTRIC • POLYMERS, SYNTHESIS

BIBLIOGRAPHY

- Chiang, C. K., Druy, M. A., Gau, S. C., Heeger, A. J., Louis, E. J., MacDiarmid, A. J., Park, Y. W., and Shirakawa, H. (1978). "Synthesis of highly conducting films of derivatives of polyacetylene (CH)_x," *J. Am. Chem. Soc.* **100**, 1013.
- Farges, J.-P. (1994). "Organic Conductors: Fundamentals and Applications," Marcel Dekker, New York.
- Kahol, P. K., Harbeke, G., and Clark, G. C. (1992). "Conjugated Conducting Polymers," Springer-Verlag, Berlin/New York.
- Kroschwitz, J., ed. (1988). "Electrical and Electronic Properties of Polymers: A State-of-the-Art Compendium," Wiley, New York.
- Nalwa, H. S. (1997). "Handbook of Organic Conductive Molecules and Polymers: Vol. 1, Charge-Transfer Salts, Fullerenes and Photoconductors," Vol. 1, Wiley, New York.
- Okamura, S., and Ranby, B. (1994). "Photoconducting Polymers/Metal-Containing Polymers," Springer-Verlag, Berlin/New York.
- Skotheim, T. A., and Elsenbaumer, R. L. (1997). "Handbook of Conducting Polymers," 2nd ed., Marcel Dekker, New York.



Polymers, Ferroelectric

T. C. Mike Chung

A. Petchsuk

Pennsylvania State University

- I. Definition of Piezo-, Pyro-, and Ferroelectrics
- II. Conventional Piezoelectric Polymers: Poly (vinylidene fluoride) and Its Copolymers
- III. New Piezoelectric VDF/TrFE/CTFE Terpolymers
- IV. Other Ferroelectric Polymers
- V. Applications

GLOSSARY

Actuator Transducer capable of transducing an input energy into mechanical output energy (displacement/force).

Dielectric constant The relative permittivity (compared with vacuum) that represents the charge-storing capacity of a dielectric material in the presence of an external electric field.

Electroactive polymer Polymer whose shape can be changed under an electric field to perform energy conversion between the electric form and the mechanical form.

Electrostriction Phenomenon in all dielectric materials which gives rise to a strain that is proportional to the square of the applied electric field.

Ferroelectric polymer Polymer whose direction of spontaneous polarization can be reversed under an electric field.

Poly(vinylidene fluoride) Polymer consisting of vinylidene fluoride monomer units.

Sensor A detection device that produces a measurable response to a change in a physical condition, such as temperature or pressure.

VDF/TrFE/CTFE terpolymer A random copolymer consisting of three different monomers: vinylidene fluoride, trifluoroethylene, and chlorotrifluoroethylene.

STRONG INTEREST has been generated in recent decades regarding the development of ferroelectric, piezoelectric, and magnetostrictive materials with high performance for such applications as electromechanical transducers, actuators, and sensors. However, many traditional electroactive materials (piezoceramic and magnetostrictive materials) have been found to suffer from low strain response (<1%), despite their high dielectric constant, low hysteresis, and fast speed. Developing new ferroelectric, piezoelectric, and magnetostrictive materials with high strain, high elastic density, and high electromechanical coupling has been a scientific and technological challenge. Recently, polymeric materials have received much more

extensive attention as new ferroelectric or piezoelectric materials. Compared to current ceramic-based materials, polymeric materials could offer many unique features, such as light weight, low cost, great mechanical strength, easy processability into thin and flexible films of various shapes and sizes, high reliability, large strain, and, most importantly, flexible architecture design via molecular tailoring.

It was not until 1969 that Kawai demonstrated the significant increase of piezoelectricity in poly(vinylidene fluoride); pyroelectricity and ferroelectricity were reported in 1971. Since then, tremendous growth in the new field of ferroelectric polymers has occurred. The exploration of the chemistry, physics, and technology of poly(vinylidene fluoride) led to the search for other classes of novel ferroelectric polymers, such as its copolymers, odd-numbered polyamides, cyanopolymers, polyureas, polythioureas, biopolymers (including polypeptides), and ferroelectric liquid crystal polymers. Significant progress has been made both in finding new materials and in better understanding structure–property relationships.

In this review, the primary goals are to update current research in ferroelectric polymers and provide a fundamental understanding of ferroelectric physics. Since many extensive reviews of poly(vinylidene fluoride) and its copolymers already exist in great detail, only a brief summary is given of their chemical synthesis, structure–electrical property relationships, and applications. Some emphasis will be on the newly developed VDF/TrFE/CTFE terpolymers containing vinylidene difluoride (VDF), trifluoroethylene (TrFE), and chlorotrifluoroethylene (CTFE) units. These processable terpolymers show high dielectric constants, narrow polarization hysteresis loops, and large electrostrictive responses at ambient temperature. The last section will cover some other novel ferroelectric polymers, such as polyamides, polyurethanes, and polyureas. No attempt is made to discuss ferroelectric biopolymers and ferroelectric liquid crystal polymers, comprehensive reviews of which are available elsewhere.

I. DEFINITION OF PIEZO-, PYRO-, AND FERROELECTRICS

It is well established that electrical properties such as piezoelectricity and pyroelectricity can only exist in materials lacking a center of symmetry. In fact, among the 32 classes of the crystal point symmetry group, only 20 can exhibit piezoelectric and pyroelectric effects. A piezoelectric material is one that develops electric polarization only when mechanical stress is applied. Pyroelectric materials possess a permanent polarity (spontaneous polarization)

which responds not only to stress, but also to temperature change. Pyroelectric crystals whose spontaneous polarization can be reversed by an external electric field are called ferroelectrics.

A. Piezoelectric d Constant

The magnitude of the induced strain x by an external field E or the dielectric displacement D by a stress X is represented in terms of the piezoelectric d constant (an important parameter for acoustic applications)

$$x = dE \quad (1a)$$

$$D = dX. \quad (1b)$$

The effect in Eq. (1b) is the direct piezoelectric effect, where the induced charge is proportional to the mechanical stress, whereas the effect in Eq. (1a) is the converse piezoelectric effect. Extending Eqs. (1a) and (1b) with the use of the linear elastic (Hooke's law) and dielectric equations, and writing the results in matrix notation form yields

$$x_i = s_{ij}^E X_j + d_{mi} E_m, \quad (2a)$$

$$D_m = d_{mi} X_i + \varepsilon_{mk}^X E_k, \quad (2b)$$

where s_{ij}^E is the elastic compliance, ε_{ik}^X is the dielectric permittivity, $i, j = 1, 2, \dots, 6$, and $m, k = 1, 2, 3$. The superscripts refer to the conditions under which these quantities are measured, that is, compliance is measured under constant electric field, and permittivity is measured under constant stress. ε_0 is the vacuum dielectric permittivity ($=8.85 \times 10^{-12}$ F/m).

B. Piezoelectric g Constant

The induced electric field E is related to an external stress X through the piezoelectric voltage constant g , which is an important parameter for sensor applications:

$$E = gX. \quad (3)$$

Taking into account $D = dX$, we obtain

$$g = \frac{d}{\varepsilon \varepsilon_0}. \quad (4)$$

C. Field-Related and Charge-Related Electrostrictive Coefficients

Generally, there are two phenomenologies used to describe the electric field-induced strain: the electrostrictive and piezoelectric effects. The piezoelectric effect is a primary electromechanical coupling effect in which the

strain is proportional to the electric field, whereas the electrostrictive effect is a secondary effect in which the strain is proportional to the square of the electric field (this effect exists in any polymer). Electrostriction can be expressed as

$$x = ME^2, \quad (5)$$

$$x = QP^2. \quad (6)$$

where $P = \varepsilon\varepsilon_0E$ in the *paraelectric* phase and $P = P_s + \varepsilon\varepsilon_0E$ in the *ferroelectric* phase. The electric field-related electrostrictive coefficient M and charge-related electrostrictive coefficient Q are related to each other through $M = Q\varepsilon_0^2\varepsilon^2$.

For an isotropic polymer,

$$x_{33} = Q_{33}P^2, \quad x_{31} = Q_{31}P^2, \quad (7)$$

where the two numerals in the subscripts refer to the electric field direction and the measured polarization direction, respectively. Therefore, x_{33} and x_{31} are strains parallel to and perpendicular to the polarization direction, known as longitudinal and transverse strains, respectively. For isotropic polymers, both experimental and theoretical data show that $Q_{11} < 0$, $Q_{13} > 0$, $M_{33} < 0$, and $M_{13} > 0$, hence the polymer will contract along the polarization direction as the polarization increases. In other words, the polymer will contract along the thickness direction and will expand along the film direction when an electric field is applied across the thickness.

It should be noted that most polymers exhibit nonlinear dielectric behavior and deviate from Eq. (5) in a high field, where the field-induced strain will be saturated.

D. Electromechanical Coupling Factor K

The electromechanical coupling factor K is related to the conversion rate between electrical energy and mechanical energy; K^2 is the ratio of stored mechanical energy to input electrical energy, or the ratio of stored electrical energy to input mechanical energy.

When an electric field E is applied to a piezoelectric material, K^2 can be calculated as

$$K^2 = d^2/\varepsilon\varepsilon_0s. \quad (9)$$

There are many electromechanical coupling factors corresponding to the direction of the applied electric field and to the mechanical strain (or stress) direction. For instance, in cases where a polymer actuator is made with the electric field along the 3-direction, the mechanical coupling factor is longitudinal to the electromechanical coupling factor K_{33} , which can be related to the Eq. (9) as

$$K_{33}^2 = d_{33}^2/\varepsilon_{33}^X\varepsilon_0s_{33}^E. \quad (10)$$

E. Acoustic Impedance Z

The acoustic impedance Z is a parameter used for evaluating the acoustic energy transfer between two materials. It is defined as $Z^2 = \text{pressure}/\text{volume} \cdot \text{velocity}$. In solid material,

$$Z = \sqrt{\rho \cdot c} \quad (11)$$

where ρ is the density and c is the elastic stiffness of the material.

Piezoelectric ferroelectrics fall into four classes: optical active polymers, poled polar polymers, ferroelectric polymers, and ceramic/polymer composites. *The poling procedure involves the application of an external field to a ferroelectric to induce a cooperative alignment of constituent dipoles.* Most polymers in the first group are biological materials, such as derivatives of cellulose, proteins, and synthetic polypeptides. The origin of piezoelectricity in these polymers is attributed to the internal rotation of the dipoles of asymmetric carbon atoms, which gives rise to optical activity. The second class of piezoelectric polymers includes polyvinyl chloride (PVC), polyvinyl fluoride (PVF), polyacrylonitriles (PAN), odd-numbered nylons, and copolymers of vinylidene cyanide. The piezoelectricity in these polymers is caused by the trifluoroethylene (TrFE) or tetrafluoroethylene (TFE). Recently, other polymers were found to show ferroelectric behavior, such as copolymers of vinylidene cyanide, odd-numbered nylons, and polyureas, in which piezoelectricity arises from the functional polar groups in the polymer molecules. In the fourth class (polymer/ceramic composites), the piezoelectric activity comes from the intrinsic piezoelectricity of ceramics. Physical properties of these composites can be controlled by the choice of the ferroelectric ceramics and the polymer matrix. They have a combination of high piezoelectric activity from the ferroelectric ceramics and flexibility from the polymer matrix.

Table I compares the piezoelectric properties of the ferroelectric ceramics and polymers. The piezoelectric strain constant d_{31} of polymers is relatively low compared to that of ceramics. However, the piezoelectric voltage constant g_{31} is larger. In addition, polymers have a high electromechanical coupling factor and low acoustic impedance, which permit their use in ultrasonic transducer applications and medical instrumentation. The combination of these properties with their flexibility, light weight, toughness, and availability in large-area sheets has led to tremendous growth in research on novel ferroelectric polymers.

TABLE I Typical Physical, Piezoelectric, and Pyroelectric Properties of Various Materials

Material ^a	Density ρ (g/cm ³)	Modulus C_{11} (GN/m ²)	Piezoelectric constants			Pyroelectric constant ($\mu\text{C}/\text{K}\cdot\text{m}^2$)	Dielectric constant (ϵ_r)	Coupling factor k_{31}	Acoustic impedance (Gg/m ² -sec)
			d_{31} (pC/N)	e_{31} (pC/N)	g_{31} (mV-m/N)				
PVDF	1.78	1–3	20	6.0	174	30–40	10–15	0.1	2–3
P(VDF/TrFE)	~1.9	1.2	15–30	2–3	100–160	30–40	15–30	0.2	
PVF	1.4	1	1			10			
PVC	1.5	4	1			1–3	3		
Nylon-11	1.1	1.5	3	6.2		3	4	0.1–0.15	
Nylon-11/PVDF Laminate film		2.3	41	109			13.8		
P(VDCN/VAc)	1.2	4.5	6	2.7	169		4.5	0.06	
PTUFB						3.0	20–30		
PVDF/PZT	5.3	3.0	20	6.0	19		120	0.07	
Rubber/PZT	5.6	0.04	35	1.4	72		55	0.01	
POM/PZT	4.5	2.0	17	3.4	20		95	0.08	
Quartz	2.65	77.2	2	15.4	50		4.5	0.09	
PZT	7.5	83.3	110	920	10		1200	0.31	

^a PVDF, poly(vinylidene fluoride); P(VDF/TrFE), poly(vinylidene fluoride-co-trifluoroethylene); PVF, polyvinyl fluoride; PVC, polyvinyl chloride; P(VDCN/VAc), poly(vinylidene cyanide-co-vinyl acetate); PTUFB, polyurea-formaldehyde; PZT, lead zirconate titanate.

II. CONVENTIONAL PIEZOELECTRIC POLYMERS: POLY(VINYLDENE FLUORIDE) AND ITS COPOLYMERS

A. Poly(vinylidene fluoride)

1. Synthesis

Poly(vinylidene fluoride) (PVDF) is commercially produced by free radical polymerization of 1,1-difluoroethylene ($\text{CH}_2=\text{CF}_2$) at high temperature (50–150°C) and high pressure (10–300 atm). The most common polymerization process is emulsion or suspension using water as a reaction medium. The catalysts used in these processes are either inorganic (persulfate) or organic peroxides. Since the monomer units of PVDF have a directionality (CH_2 is denoted the “head” and CF_2 the “tail”), typically 5% of the monomer units enter the growing chain with a reverse orientation, leading to head-to-head and tail-to-tail defects. These defects cause a reduction of the average dipoles by 6–10%. Polymers with defect concentrations ranging from 0.2% to 23.5% have been synthesized and the effect of defects on crystal structure has been studied.

2. Molecular and Crystal Structure

PVDF ($-\text{CH}_2-\text{CF}_2-$) has a chemical structure in between those of PE ($-\text{CH}_2\text{CH}_2-$) and PTFE ($-\text{CF}_2\text{CF}_2-$). Unlike PTFE, which has a helical conformation due to the steric hindrance of the fluorine atom, or PE, which takes

the most stable conformation (all-*trans* conformation due to low rotational barrier), PVDF can take several conformations. The three known conformations are tg^+tg^- , all-*trans*, and $tttg^+tttg^-$. The first two conformations are the most common and important ones, and are schematically drawn in Fig. 1.

The C–F bond is a polar bond (dipole moment $\mu = 6.4 \times 10^{-30}$ C-m), and contributes to the polar conformation. The all-*trans* conformation has the highest dipole moment ($\mu = 7.0 \times 10^{-30}$ C-m/repeat) due to the alignment of all dipoles in the same direction. The tg^+tg^- conformation is also polar, but the net dipoles that are perpendicular and parallel to the chain are approximately the same, giving rise to lower net dipole.

The packing of these polar chains in a crystal adopts several distinct morphologies in PVDF. At least four are known, the α , β , γ , and δ phases, which can easily be transformed into one another. The most common one is the α phase, which may be obtained by crystallization from the melt. As depicted in Fig. 1, the unit cell of the α phase consists of two tg^+tg^- chain conformations whose dipole components normal to the chain are antiparallel and neutral to each other. Thus the α phase is a nonpolar phase. The polar analog δ phase can be obtained by poling under a high electric field. The lattice dimensions of these two phases are essentially the same: $a = 4.96$ Å, $b = 9.64$ Å, and $c = 4.96$ Å.

The β phase is the most highly polar and important phase, and is typically prepared by stretching polymer film at room temperature or by crystallization from the melt

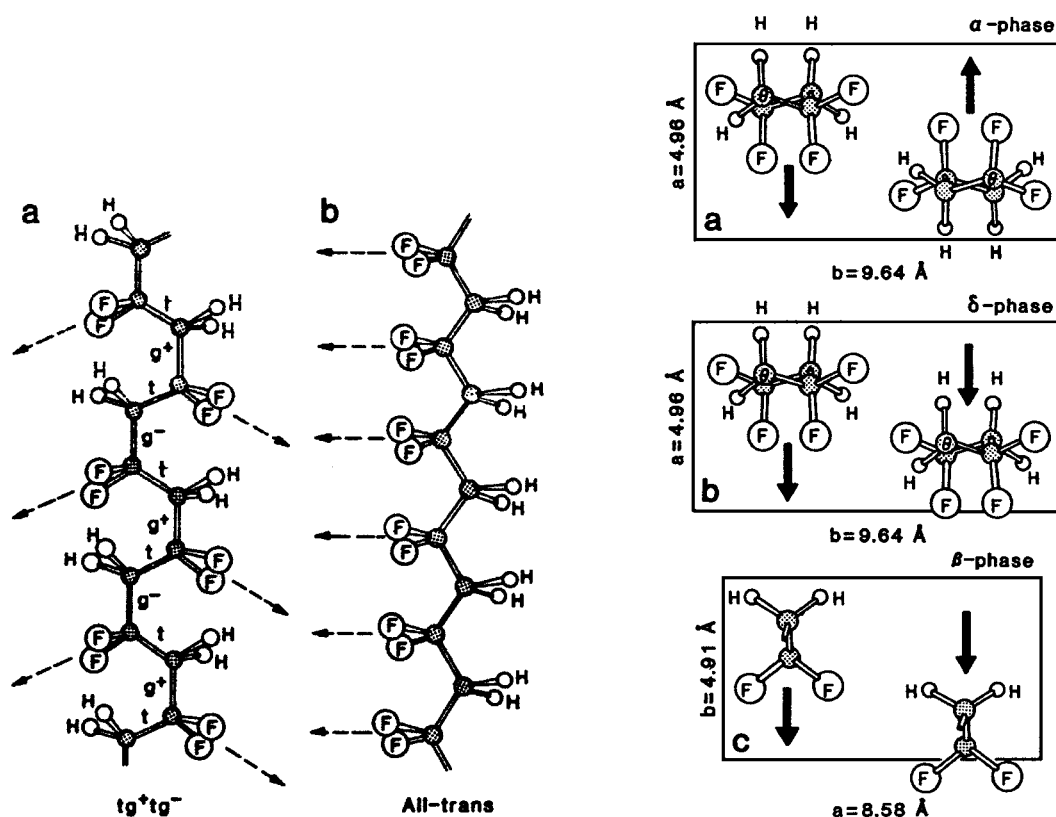


FIGURE 1 (Left) Schematic depiction of the two most common chain conformations in PVDF: (a) tg^+tg^- and (b) all-trans. (Right) Unit cells of (a) α phase, (b) δ phase, and (c) β phase of PVDF in projection parallel to the chain axis.

under high pressure or epitaxial technique. The unit cell of the β phase contains two all-trans chain conformations in orthorhombic symmetry with the lattice with $a = 8.45 \text{ \AA}$, $b = 4.88 \text{ \AA}$, and $c = 2.55 \text{ \AA}$. The dipole components normal to the chain (b axis) are parallel. Thus, the β phase is a polar phase that possesses spontaneous polarization and exhibits piezoelectricity as well as pyroelectricity.

The γ phase contains two $tttg^+tttg^-$ chain conformations that are packed in a polar fashion. It has unit cell dimensions of $a = 4.96 \text{ \AA}$, $b = 9.58 \text{ \AA}$, and $c = 9.23 \text{ \AA}$. This phase may be obtained by the crystallization of a molten sample at high temperature or solution cast from dimethylacetamide (DMA) or dimethylformamide (DMF).

3. Morphology of PVDF

The crystallization of PVDF from the melt results in spherulitic morphologies in which the lamella stacks have a periodicity of about 10 nm and have no net dipoles. A number of papers have reported on the morphology of melt-solidified PVDF. There are two types of spherulites grown from the melt at high temperature (up to 60°C). The most common is a spherulite from the nonpolar phase

(α form), which is larger and has high birefringence and tightly spaced concentric bonding. The second type is smaller and has less birefringence, and comes from the γ phase. The morphology of PVDF has recently been investigated as a function of head-to-head defects and crystallization temperature for a wide range of temperatures.

4. Ferroelectricity and Related Properties of PVDF

Although the β and δ phases are known to be polar since the components of their dipoles are arranged in the same direction, the β phase has stronger pyroelectric and piezoelectric coefficients than the other phase. Therefore, to obtain a useful PVDF as a transducer material, a polymer film must be oriented and polarized. The orientation or stretching can be performed between the glass temperature T_g and melting temperature T_m by stretching a polymer film to several times its original length. Poling can be accomplished either at room temperature with a high electric field or at high temperature with a low field. For conventional thermal poling, a polymer film is stretched, annealed, electroded on both surfaces, and subjected to

an electric field of about 0.5 MV/cm at high temperature (80–100°C), followed by cooling in the presence of the applied field. Other methods of poling include corona discharge, plasma, and poling during orientation.

For many years, there was debate over the origins of the piezoelectric and pyroelectric properties in PVDF. The arguments seem to have reached the conclusion that the properties primarily arise from the dipole orientation, rather than from trapped space charge. The discovery of the enhancement of piezoelectric activity in PVDF by Kawai led to the revelation of others properties, such as pyroelectricity and ferroelectricity. Although there is no obvious evidence of a Curie transition in PVDF, the existence of polarization loops together with polarization reversal and the switching phenomenon is generally accepted as proof of ferroelectricity in PVDF. Figure 2 shows the D–E hysteresis loops at various temperatures. Even at –100°C a square-shape hysteresis loop is clearly observed with a remanent polarization P_r about 60 mC/m², which does not change with temperature. However, the coercive field E_c , which is the electric field used for neutralizing polarization in the material, is temperature-dependent. The value is about 50 MV/m at room temperature and remains almost constant above the glass transition temperature (–50°C), but increases sharply at lower temperatures.

The remanent polarization P_r , which is the polarization after the field has been removed, is dependent on the crystallinity. For PVDF, the calculated macroscopic polarization for 100% alignment of all dipoles is 130 mC/m², and the measured polarization of 60 mC/m² is consistent

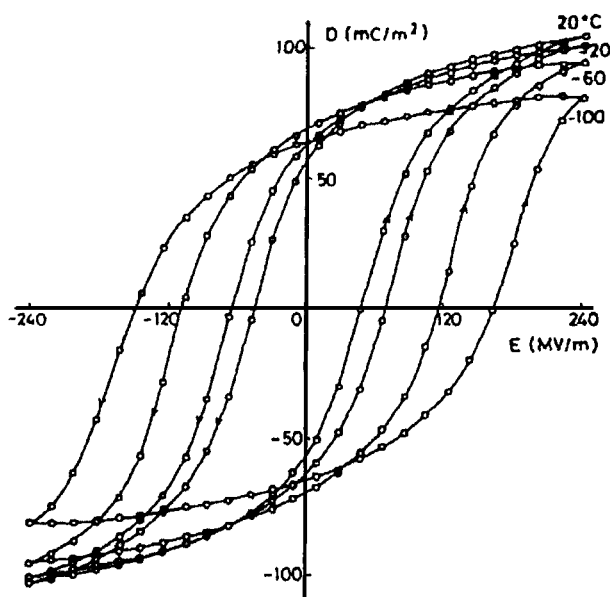


FIGURE 2 The D–E hysteresis loops of PVDF at various electric fields.

with about 50% crystallinity and perfect alignment. The direction of P_r can be reversed by subsequent application of the field in the opposite direction. This phenomenon, called ferroelectric switching, has been investigated extensively to elucidate the mechanism of polarization reversal.

Although PVDF exhibits strong piezoelectric and pyroelectric properties, it is necessary that the polymer film be subjected to mechanical stretching and electrical poling to get the β phase. Such procedures include, for example, subjecting the ferroelectric polymer to mechanical deformation, electron irradiation, uniaxial drawing, crystallization under high pressure, and crystallization under high electric field. It is tempting to speculate about how much improvement of the dielectric, piezoelectric, and pyroelectric properties may yet be achieved by modification of the chemical structure of the polymer. Some improvement has been achieved by synthesizing copolymers of vinylidene fluoride with trifluoroethylene (TrFE), tetrafluoroethylene (TFE), or vinyl fluoride (VF), and, indeed, some of these copolymers exhibit even higher piezoelectric and pyroelectric properties that will be discussed in the next section.

B. Poly(vinylidene fluoride–trifluoroethylene) (VDF/TrFE) Copolymer

P(VDF/TrFE) is the most studied copolymer. Lando *et al.* and Yagi *et al.* initially studied the properties and structure of this copolymer. The randomly distributed VDF and TrFE units form the cocrystalline phase in the whole composition range of the copolymers. The greater proportion of bulky trifluorine atoms in PVDF prevents the molecular chains from accommodating the tg^+tg^- conformation. Therefore, copolymers crystallize at room temperature into a ferroelectric phase with the extended planar zigzag (all-*trans*) conformation, whose crystalline phase is similar to the β phase of PVDF homopolymer.

1. Ferroelectric–Pараelectric Phase Transition

Probably the solid evidence for the ferroelectricity in this copolymer is the existence of the ferroelectric to paraelectric (F–P) phase transition or Curie temperature T_c . The Curie temperature of synthetic polymer was discovered in 1980 by Furukawa *et al.* At this temperature, the dielectric constant shows a maximum value, the polarization and piezoelectric constants go down to zero, and the Young's modulus and elastic constant decrease. The phase transition of copolymers has been found to be affected by several factors, especially the VDF content. As shown in Fig. 3, copolymers with VDF content below 82 mol% exhibit a phase transition below the melting point.

The lowest Curie temperature of the copolymer is about 60°C, and this phase temperature increases linearly with

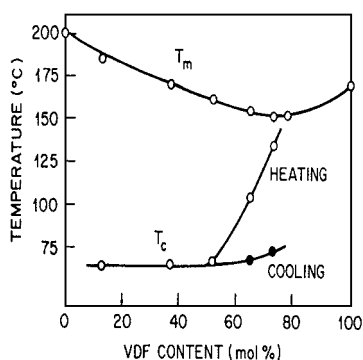


FIGURE 3 The thermal transition temperature in VDF/TrFE copolymers.

increasing VDF content, which allows an extrapolation of the Curie transition temperature of PVDF homopolymer to about 215°C. Other widely studied factors that affect the Curie transition are hydrostatic pressure, tensile stress, external electric field, annealing temperature and time, mechanical drawing, poling, irradiation, solution history, thermal history, and crystallization conditions.

2. Crystal Structures

A number of experimental techniques such as differential scanning calorimetry (DSC), dielectric constant determination, ferroelectric measurement, and X-ray diffraction have been employed to investigate structural change during the phase transition. It is not clear whether the double peak at the ferroelectric transition of 70/30 VDF/TrFE copolymer is associated with the formation of different sizes of ferroelectric domains or the two-step phase transformation. Tashiro suggested the existence of two types of ferroelectric phases: a low-temperature phase (LT) consisting of a parallel arrangement of dipoles in planar zigzag (*all-trans*) chain (as seen in the β phase of PVDF homopolymer) and the cooled phase (CL) consists of long *trans* segments connected by irregular *gauche* linkages along the chain axis (depending on the VDF content of the copolymer as well as the sample preparation conditions).

The transition behavior of the copolymer change with change in the VDF content in the copolymer. For instance, in a copolymer with a VDF content of 70–80 mol%, a first-order transition between the LT and HT phases at high temperature is observed, whereas a second-order transition between the CT and HT phases occurs in copolymer with a VDF content of <50 mol%. The 50–60% VDF samples show more complicated transitional behavior. The *trans* zigzag chains transform to the irregular *trans* form of the LT phase, which easily changes to the random *gauche* conformation. Recently, the phase transition from the LT to CL phases has been confirmed.

During the transition from the ferroelectric to the paraelectric phase, structural changes in the crystal lattice and the domain size are clearly demonstrated. The phase transition occurs through the *trans-gauche* conformational change, where all-*trans* molecular chains change their conformation to a disordered sequence of conformation isomers (tg^+ , tg^- , tt), resulting in the nonpolar unit cell structure of hexagonal packing, with unit cell dimensions of $a = 9.96 \text{ \AA}$, $b = 4.96 \text{ \AA}$, and $c = 4.64 \text{ \AA}$.

Interestingly, during the phase transition, there is large strain change associated with the phase transformation. For 65/35 mol% VDF/TrFE copolymers, respective lattice strains as high as 10% and 7% in the crystalline phase along (001 reflection) and perpendicular to (200, 110 reflections) the polymer chain have been detected during the phase transition. Therefore, for a high-crystalline (>50% crystallinity) copolymer, these strains can be transformed into macroscopic strains; indeed, a thermal strain of more than 6% in 65/35 copolymer has been observed. More importantly, for a ferroelectric polymer, the phase transformation can be controlled by an external electric field, hence the high-field induced strain can be achieved by exploring the lattice strain at the phase transition.

3. Ferroelectricity and Related Properties

Copolymers were demonstrated to possess ferroelectricity over a wide composition range. Piezoelectric and pyroelectric properties of these copolymers have also been reported. Since the electrical properties originate from the crystal units, chain orientation by drawing, crystallization by annealing, and CF_2 dipole orientation by poling are important for achieving high piezoelectric and pyroelectric constants. The dipole orientation can result in a change of chain conformation, chain packing, crystallinity, and crystal size. Recently, the structural and crystal changes of copolymers have been reported as functions of poling conditions and high-pressure crystallization. The polarization reversal of copolymers strongly depends on their thermal and mechanical treatment. The polarization reversal of quenched copolymers proceeds over several decades if annealed above the Curie temperature T_C , whereas it is completed within one decade if annealed below T_C .

The phase transition T_C of all VDF/TrFE copolymers occurs at high temperatures (>60°C) and the transition is relatively sharp. In addition, the early experimental results showed a large hysteresis at the phase transition, which is not desirable for practical applications. Therefore, many attempts have been devoted to broadening and reducing the phase transition to room temperature and minimizing or eliminating the hysteresis. Zhang *et al.* found that by systematic study of the irradiation conditions of the copolymer, high electromechanical response

can be achieved. The longitudinal strain S_3 measured at room temperature and 1 Hz frequency reaches -4% at 150 MV/m. The irradiation significantly reduces the hysteresis in the polarization loop. However, the polarization was also significantly reduced, and the sample becomes completely insoluble in common solvent because of a severe crosslinking side reaction during the high-energy irradiation.

The increase in hardness of the copolymer due to crosslinking was also revealed in the electromechanical response. A very high field was required to get high strain response. It appears that the irradiation process produces many undesirable side reactions that increase the amorphous phase content and diminish the processability of the sample.

C. Poly(vinylidene fluoride–tetrafluoroethylene) (VDF/TFE) Copolymer

The second mostly studied copolymer is the VDF/TFE random copolymer, which can be viewed as a PVDF polymer containing an increased amount of head-to-head and tail-to-tail defects. The steric hindrance created by the TFE unit effectively stabilizes the *trans* conformer of the VDF chain. As the content of TFE units increases, the *trans* conformation is stabilized overwhelmingly and the generation of the *gauche* bonds is suppressed. The copolymers of VDF/TFE with at least 7% are crystallized in the β form. The Curie transition was clearly observed in 18–23 mol% TFE. The crystal structure and phase transition behavior of copolymers have been studied by X-ray, IR, and Raman spectroscopies.

Piezoelectric and pyroelectric studies of VDF/TFE copolymers showed highly inhomogeneous polarization across the thickness of the copolymer films. Ferroelectric studies revealed a hysteresis loop, but no Curie transition in the temperature-dependent dielectric curve. However, there was some evidence showing that the Curie transition occurs in the vicinity of the melting temperature.

III. NEW PIEZOELECTRIC VDF/TRFE/CTFE TERPOLYMERS

In our laboratory, we have adopted a new chemical strategy of altering crystalline domains and creating relaxor ferroelectric behavior of VDF/TrFE copolymer, with the objective of achieving a processable polymer with controllable phase transition temperature, high dielectric constant, and fast and large electromechanical response at ambient temperature. The chemistry involves homogeneous incorporation of a small amount of bulky ter-monomer units, such as chlorotrifluoroethylene (CTFE), as the crystalline

defects into a VDF/TrFE copolymer chain. The resulting VDF/TrFE/CTFE terpolymers are completely solution and melt processable, and exhibit high dielectric constant and electrostrictive response at ambient temperature.

A. Synthesis

Prior to our research, there were some reports discussing the terpolymerization reactions involving VDF, TrFE, and a small amount of termonomer, such as hexafluoropropene (HFP), chlorotrifluoroethylene (CTFE), or tetrafluoroethylene (TFE), by conventional free radical polymerization processes. The ter-polymerization was usually carried out in the emulsion or suspension process using inorganic or organic peroxides as initiator at elevated temperatures.

Recently, we have developed a bulk (room temperature) polymerization process initiated by the oxidation adducts of the organoborane molecule, as illustrated in Fig. 4.

Upon exposure to a controlled quantity of oxygen, asymmetrical alkylborane (I) is selectively autoxidized at the linear alkyl group to produce ethylperoxyborane (II). The peroxyborane (II) behaves very differently from regular benzoyl peroxides and consequently decomposes to alkoxy radical ($C-O^*$) and a borinate radical ($B-O^*$) (III) that is relatively stable due to the back-donating of electron density to the empty p orbital of boron. In the presence of fluoro-monomers, the homolytic cleavage of peroxide occurs even at very low temperatures (-30°C). The alkoxy radical is very reactive and initiates the radical polymerization at ambient temperature. On the other hand, the borinate radical forms a weak and reversible bond with the growing chain end, which assures the “stable” radical polymerization. During the propagating reaction, a coordination intermediate (IV) may form due to the B–F acid–base complex between the active site and the incoming monomer. Such an interaction will regulate

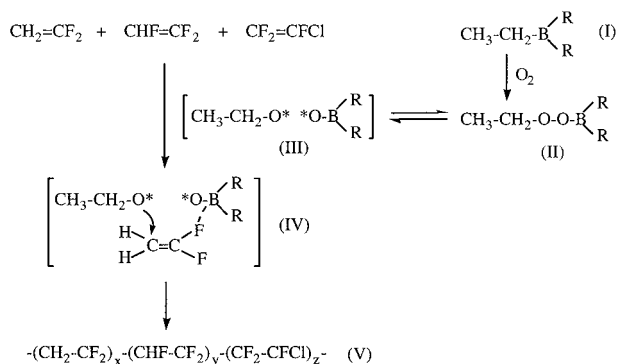


FIGURE 4 An equation showing selective auto-oxidation of organoborane and terpolymerization of VDF, TrFE, and CTFE monomers.

TABLE II A Summary of VDF/TrFE/CTFE Terpolymers Prepared by Borane/Oxygen Initiator^a

Sample no.	Terpolymer mole ratio			Melting temperature		Phase transition temperature		$[\eta]$ (MEK) ^b (35°C)	P_{\max} (mC/m ²)	E_c (MV/m)	Dielectric constant ^c	Dielectric loss
	VDF	TrFE	CTFE	T_m (°C)	ΔH_m (J/g)	T_C (°C)	ΔH_C (J/g)					
1	72.2	17.8	10.0	107.8	17.8	25.0	0.4	0.38	82	19.6	27.0	0.04
2	66.0	22.5	11.5	117.2	21.6	25.2	2.5	0.42	78	24.1	22.4	0.03
3	66.1	21.4	12.5	115.6	20.5	25.8	1.8	0.42	—	—	40.9	0.04
4	63.1	25.4	11.5	113.7	18.5	None ^d	None	0.49	76	19.8	53.5	0.06
5	61.4	25.3	13.3	111.3	17.8	15.6	1.5	0.69	75	33.7	53.1	0.06
6	58.0	33.1	8.9	130.0	21.3	31.6	2.5	0.63	63	16.4	33.0	0.05
7	60.0	36.0	4.0	140.9	25.7	43.8	6.5	0.58	87	21.8	26.4	0.04
8	55.6	36.1	8.3	124.6	21.2	None	None	0.54	36	7.6	42.4	0.07
9 ^e	60.0	35.1	6.9	126.6	20.9	33.5	1.6	0.78	110	55.9	52.7	0.07
10 ^e	59.3	32.9	7.8	125.1	20.3	24.8	1.4	0.80	70	11.5	51.0	0.07
11 ^e	57.3	31.2	11.5	111.1	14.8	None	None	0.75	45	39.4	50.5	0.06

^a P_{\max} and E_c at 100 MV/m, 10 Hz, 22°C. Dielectric constant and dielectric loss at 1 KHz, 22°C.

^b MEK, methylethylketone.

^c Value measured in the heating cycle.

^d None: no observable.

^e Sample prepared by constant monomer feed ratio during the polymerization.

the insertion of monomers in a preferred head-to-tail sequence. No chain transfer and termination reactions are expected during the propagating process, which will lead to a linear polymer structure with relatively narrow molecular weight and composition distributions. Figure 5 shows that the VDF/TrFE/CTFE terpolymer increases in molecular weight with the conversion of monomers.

In addition, this chemistry produces terpolymers that have relatively uniform molecular structure and few impurities (boric acid and butanol), which can be easily

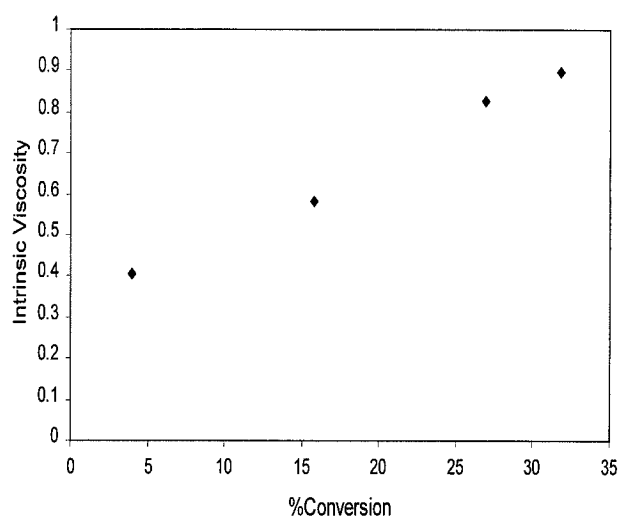


FIGURE 5 Intrinsic viscosity of VDF/TrFE/CTFE terpolymer versus monomer conversion.

removed by methanol. Table II summarizes several VDF/TrFE/CTFE terpolymers prepared by the same method. All terpolymers are high-molecular-weight (>20,000 g/mole) polymers with good solubility in common organic solvents and are melt processable at >150°C.

B. Thermal Properties

Despite having relatively high concentrations of CTFE units, all the terpolymers are still semicrystalline thermoplastics with melting temperatures >100°C and a crystallinity of $\Delta H > 17$ J/g. Figure 6 compares the DSC curves of three VDF/TrFE/CTFE terpolymers (samples 9, 10, and 11). The relatively well-defined melting and crystalline phase transition temperatures imply a relatively uniform molecular structure and polymer morphology. In addition to the reduction of melting temperature, the incorporated CTFE units also significantly reduced the F–P phase transition temperature. It is interesting to note that the effect of incorporated CTFE units resembles that seen from crosslinking in irradiated VDF/TrFE samples. The CTFE units may not affect the crystal unit cell of VDF/TrFE segments, and instead serve as a defect (by introducing a *gauche* bond) to prevent the extension of crystallization, which results in the reduction of the lamella thickness of the crystal. Detailed studies of the molecular structure and the crystal polar domain size are underway.

In general, the third CTFE monomer units in VDF/TrFE/CTFE terpolymers shift (and broaden) the phase transition to lower temperatures, to near ambient

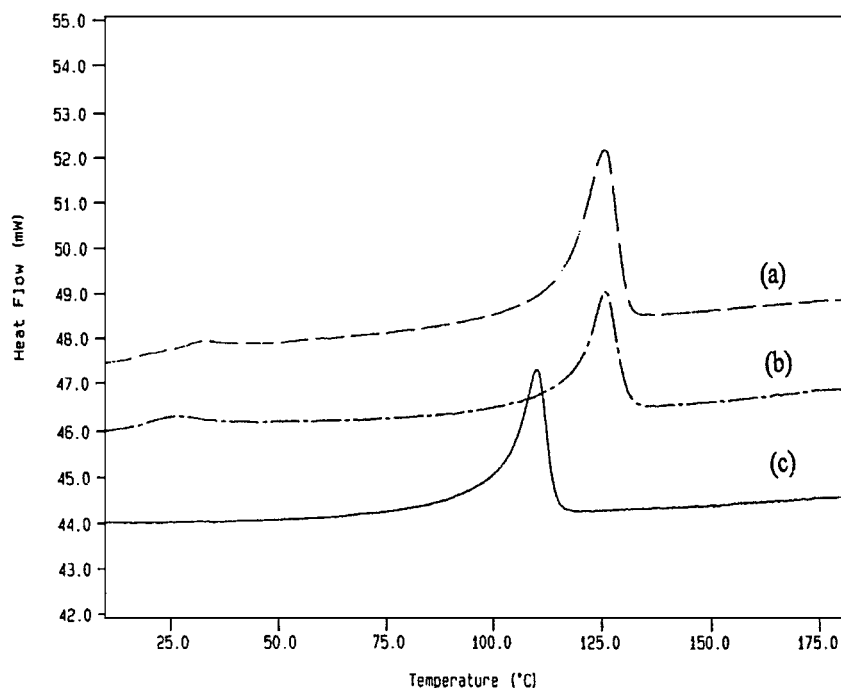


FIGURE 6 DSC comparison of three VDF/TrFE/CTFE terpolymers: (a) sample 9, (b) sample 10, and (c) sample 11 in Table II.

temperature for samples 1, 2, 3, and 10, and almost disappearing for samples 4, 8, and 11. That indicates a very small energy barrier in the phase transition and implies a smaller crystalline domain. The results are consistent with the electric responses of the terpolymer under an electric field.

C. Electric Properties

For electrical measurements, polymer films ($\sim 30 \mu\text{m}$ thickness) were prepared either by solution casting on a glass slide from *N,N*-dimethylformamide solution containing 8–10 wt% polymer or melt-pressing polymer powder at 200°C . The polymer films were annealed at 110°C under vacuum for 5 hr. Gold ($<1 \mu\text{m}$ thickness) was sputtered on both surfaces of the polymer film. The dielectric constant was measured by an HP multifrequency LCR meter equipped with a temperature chamber. Figure 7 shows the dielectric constant of 59.3/32.9/7.8 VDF/TrFE/CTFE terpolymer (sample 10) and 57.3/31.2/11.5 VDF/TrFE/CTFE terpolymer (sample 11) during the heating–cooling cycles.

In general, the dielectric constant hysteresis during the heating–cooling cycles is very small, and the dielectric peak appears near the ambient temperature, well below the dielectric peak observed in 55/45 VDF/TrFE copolymer ($>60^\circ\text{C}$) with a big hysteresis loop. Diffuse dielectric peaks and peaks shifting toward higher temperatures as

the frequency increases are common features of relaxor ferroelectrics.

As shown in Table II, most of the terpolymers show high dielectric constants at ambient temperature. Samples 4 and 5 exhibit dielectric constants as high as 53.5 and 53.1 (1 kHz), respectively, at 22°C . In sharp contrast, prior research reported that high dielectric constants (>25) only existed in the VDF/TrFE/CTFE terpolymers with a narrow range (18–22%) of TrFE content. In addition, the mechanical stretching of the polymer film, usually very important for increasing the dielectric constant in VDF/TrFE copolymers, is not necessary in these terpolymers. The effective orientation of dipoles under an electric field may be attributed to the low phase transition energy which occurs at near-ambient temperature.

The polarization hysteresis loop was measured by a Sawyer–Tower circuit with a frequency range between 1 and 10 Hz. Figure 8 compares the polarization hysteresis loops of two terpolymers (samples 2 and 8) and a 55/45 VDF/TrFE copolymer. Both terpolymers show significantly smaller hysteresis than the 55/45 copolymer, which has the narrowest polarization hysteresis loop observed in the copolymer samples. Sample 2 (VDF/TrFE/CTFE = 66/22.5/11.5 mole ratio) maintains a high polarization level ($P_{\text{max}} = 78 \text{ mC/m}^2$ at $E = 100 \text{ MV/m}$) and reduces both a coercive field (17.3 MV/m at $P = 0$) and remanent polarization (25.2 mC/m^2 at $E = 0$). Sample 8 (VDF/TrFE/CTFE = 55.6/36.1/8.3 mole ratio) exhibits a

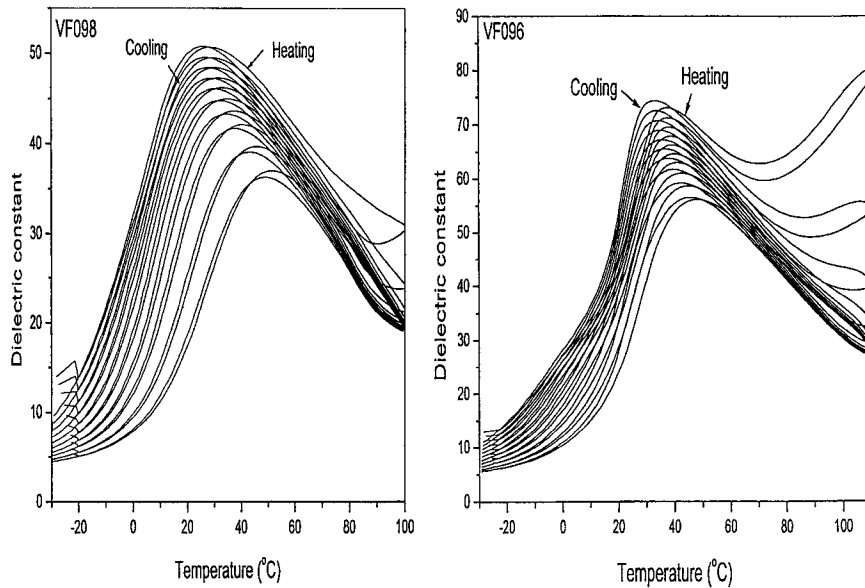


FIGURE 7 Temperature dependence of dielectric constant in two terpolymers: (right) sample 10 (VDF/TrFE/CTFE = 59.3/32.9/7.8) and (left) sample 11 (VDF/TrFE/CTFE = 57.3/31.2/11.5) during heating–cooling cycles. The frequencies from top to bottom of the dielectric curve range from 1 to 300 kHz.

very slim loop with very small coercive field and remanent polarization, as well as an overall reduced polarization level. These results indicate that the VDF/TrFE crystalline defects introduced by the incorporated CTFE termonomer units cannot be recovered by the application of a high electric field. It is interesting to note that the polarization hysteresis loop of sample 8 gradually appears with re-

duced temperature ($<0^{\circ}\text{C}$), another feature common to all relaxor ferroelectrics.

The electric field-induced strain was measured at ambient temperature in the field range of 0–150 MV/m using a bimorph-based strain sensor. Figure 9 shows three samples, 9–11, having VDF/TrFE/CTFE mole ratios of 60.0/35.1/6.9, 59.3/32.9/7.8, and 57.3/31.2/11.5,

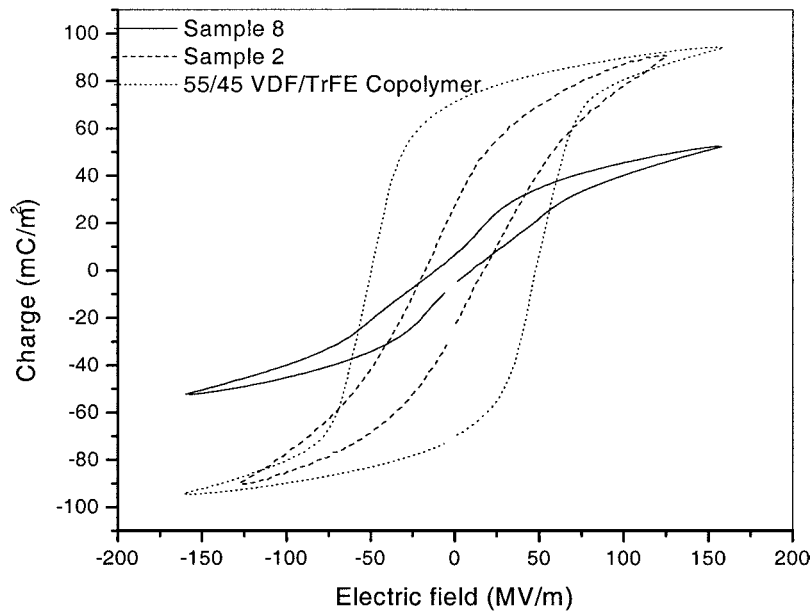


FIGURE 8 The comparison of polarization hysteresis loops between two VDF/TrFE/CTFE terpolymers (samples 2 and 8) with 66/22.5/11.5 and 55.6/36.1/8.3 mole ratios, respectively, and a VDF/TrFE (55/45) copolymer.

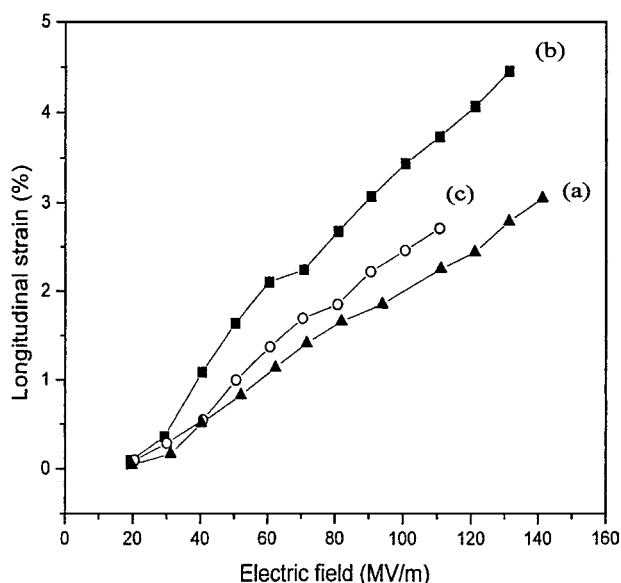


FIGURE 9 Electric field-induced strain of three VDF/TrFE/CTFE samples 9–11.

respectively. At ambient temperature, the longitudinal strain was about 4.5% for samples 10 under an electric field of 130 MV/m. A nearly straight line of S versus P^2 for sample 10 indicates the electrostrictive response in the VDF/TrFE/CTFE terpolymer. Based on the electrostrictive relationship $S = QP^2$, this yields an electrostrictive coefficient Q of about $-5.57 \text{ m}^4/\text{C}^2$.

IV. OTHER FERROELECTRIC POLYMERS

A. Ferroelectric Nylon

1. Polymeric and Crystal Structure

The discoveries of piezoelectric and pyroelectric properties in PVDF polymer led to the search for other classes of novel ferroelectric polymeric materials. Recently, odd-numbered nylons have emerged as a new class of ferroelectric polymer similar to PVDF. These materials have attracted much interest in the past two decades because of the stability of their electroactive properties at relatively high temperatures and relatively high electromechanical coupling coefficient.

Polyamides, commonly known as nylons, have molecular repeated units of $(-\text{HN}(\text{CH}_2)_x\text{CO}-)$. Generally, nylons are named after the number of carbon in the repeating unit of the polymer backbone. For example if $x = 5$, the corresponding nylon is identified as nylon-5. Nylons with an odd number of carbon atoms are called “odd nylons” and nylons with an even number of carbon atoms are called “even nylons.” Other categories of polyamides having molecular repeating units of

$[-\text{HN}(\text{CH}_2)_x\text{NHOC}(\text{CH}_2)_y\text{CO}-]$ are termed odd–odd nylons if the numbers of carbon atoms in the repeating units (x and y) are both odd numbers. Nylons are prepared by melt polymerization solution and interfacial polymerization, ring-opening polymerization, and anionic polymerization. The morphology and degree of crystallinity of the nylons depend on the basic structure of their chemical linkages. Strong interactions between the amide group of neighboring chains account for the unique physical properties of nylons, such as toughness, stiffness, high melting points, and low coefficients of friction.

Odd nylons and odd–odd nylons are important classes of ferroelectric polymers. Nylons crystallize in all-*trans* conformation and are packed so as to maximize the hydrogen bonds between the adjacent amine and carbonyl groups, as seen in Fig. 10. The dipoles of odd nylons are aligned in the same direction and give rise to a large dipole moment and spontaneous polarization in the unit cell of the crystalline phase, whereas the dipole components of even nylons cancel each other out. The density of $\text{NH}\cdots\text{C}=\text{O}$ dipoles per unit volume of nylon is larger for lower-numbered nylons; thus nylon-5 is expected to possess a larger dipole moment (i.e., remnant polarization) than nylon-7, nylon-9, and nylon-11. Indeed, the experimental results show that the remnant polarization

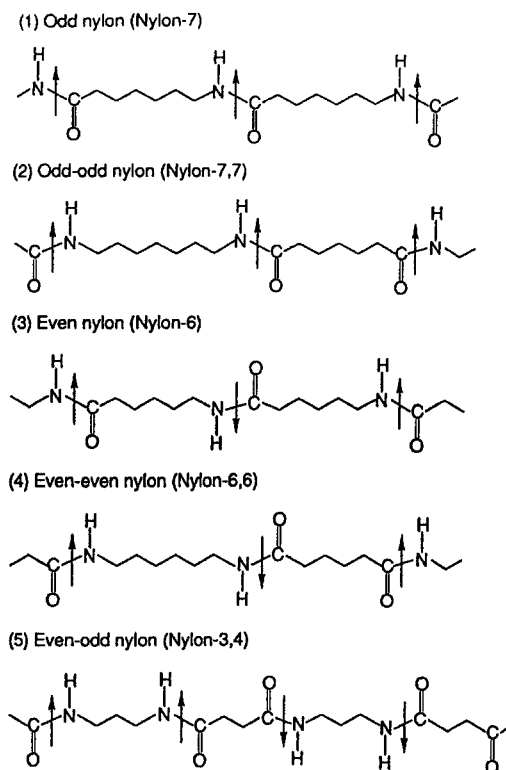


FIGURE 10 All-*trans* conformation of odd-numbered and even-numbered nylons. Arrows indicate the dipole direction.

of nylon-5 is ~ 135 mC/m². Odd-numbered nylons have polymorphs. Nylon-11 has at least five different crystal structures: triclinic α form I, monoclinic form II, pseudo-hexagonal γ form III, δ' phase, γ' and phase. The α form of nylon-11 is polar in nature, with dipoles that are hydrogen-bonded and aligned in the same direction, whereas the γ form is nonpolar and has amide groups that lie in the plane perpendicular to the chain axis. The crystal phase transformation of nylon-11 occurs between a triclinic α form and a pseudo-hexagonal γ form at high temperature ($>90^\circ\text{C}$) through the randomization of the hydrogen bonding. Polymorphs of nylon-9, nylon-5,7, and nylon-7,7 have also been prepared. The α form seems to be the most common polymorph in many odd-numbered nylons.

2. Ferroelectricity and Related Properties

Nylons exhibit very interesting dielectric behavior in that the dielectric constant changes significantly with changes in temperature and frequency. The dielectric constants of poled and annealed nylons are relatively low (about 2.5–3) at various frequencies below 0°C , and increase rapidly above the glass transition. The peak position, magnitude of dielectric constant, and relaxation process in nylons change with poling conditions and the presence of absorbed water. Several articles have been focused on the high-frequency properties that are of interest for ultrasonic transducers.

The pyroelectricity and piezoelectricity of the α and γ phases of nylon-11 films with variation of poling conditions have been reported. The γ phase nylon films show much higher piezoelectric response than α -phase films under the same poling conditions. This characteristic difference was interpreted as the breaking and re-forming of hydrogen bonds under a high electric field. The γ phase has a more regular arrangement of dipoles and has stronger hydrogen bonding, and thus is more strongly influenced by an applied electric field. However, it is found that a mixture of α phase and γ phase, rather than pure α phase or γ phase, has the highest piezoelectric constants. The piezoelectricity and pyroelectricity of odd nylons were also affected by anisotropy, absorbed water, orientation, and annealing temperature.

Ferroelectric properties of nylons have been investigated by several research groups. Polarization reversal was found to be complete in a few tens of milliseconds under 140 MV/m at 20°C . This fast polarization reversal and the rectangular D–E hysteresis loop are evidence of the dipoles' origin. The effect of annealing on the ferroelectric behavior of nylon-11 and nylon-7 has been investigated. The remanent polarization decreases with increasing annealing temperature and disappears at an annealing temperature of 185°C , whereas the coercive field increases as

annealing temperature increases, indicating the rearrangement of the hydrogen bonding structure. The mechanism of ferroelectric polarization in odd nylons has not been addressed, except for nylon-11. The ferroelectricity of poled nylon-11 is related to the hydrogen bond breaking, followed by the reorientation of the amide groups toward the electric field's direction and the re-forming of hydrogen bonds in a new direction. The orientation is retained in the glassy state below T_g even after the electric field is removed. Ferroelectricity has also been observed in polyamides containing *m*-xylylenediamine, aliphatic dicarboxylic acids, and fluorinated odd–odd nylons.

Ferroelectricity in aliphatic odd nylons has been reported recently. Unlike nylons with ring systems, in which the ferroelectric nature arises from the orientation of the amide dipoles in the amorphous region, the ferroelectric polarization of aliphatic odd nylons originates from the crystalline phases. A slightly higher density of amide dipoles contributes to a larger value for the remanent polarization, as seen in other nylon systems. Recently, a new class of ferroelectric and piezoelectric polymers, nylon-11/PVDF laminated films prepared by a co-melt-pressing method, has been reported. The laminated films exhibit a typical ferroelectric hysteresis loop with high remanent polarization, higher than that observed in PVDF homopolymers or nylon-11 under the same measurement conditions. The film's piezoelectric stress constant ($d_{31} = 41$ pC/N) and piezoelectric strain constant ($e_{31} = 109$ mC/m²) are significantly higher than those of PVDF and nylon-11. Another new class of ferroelectric polyamides recently reported is the ferroelectric polyamide blends. The D–E hysteresis curves were observed in all blends of nylon 6I/6T copolymers (6 = hexamethylenediamine, I = isophthalic acid, T = terephthalic acid) and *m*-xylylenediamine-6 (MXD6). It was concluded that the intermolecular exchange of hydrogen bonding in the amide groups is responsible for the ferroelectricity.

B. Cyanopolymers

Cyanopolymers discussed here include polyacrylonitriles (PAN), poly(vinyl cyanide), and cyanocopolymers. The cyano group (C–CN) has the unique feature of a large dipole moment (3.5 D) and the ability to form complexes with transition metals. The polymerization can occur through free radical and ionic polymerization, leading to nonstereoregular (atactic) cyano groups in the polymer structure. Thus, cyanopolymers have no clear melting temperature because of their high cohesive force and low thermal stability. It has been accepted that the strong interaction and repulsion of the cyano groups force polymer chains to adopt a helical conformation. However, the all-*trans* conformation is more stable.

The ferroelectricity of poled and annealed PAN has been studied by X-ray and IR spectroscopy. It is believed that the ferroelectricity of PAN is related to the dipole orientation and kinking of the chain above the glass transition temperature. The piezoelectric and pyroelectric properties of PAN were initially studied by Ueda and Carr, and were proved by Von Berlepsch using copolymer with methylacrylate. The D - E hysteresis loop of a stretched film of this copolymer has been measured at 68°C, which is below the glass transition temperature. The copolymer showed very low remanent polarization and high coercive field at low temperature. However, an alternating copolymer of PAN, poly(allylcyanoide[35%]/acrylonitrile[65%]), showed very high remanent polarization, 200–700 mC/m² at 105°C.

Another alternating copolymer that has received more attention as an amorphous copolymer is vinylidene cyanide/vinyl acetate copolymer. The dipole moment of the repeating unit is 4.5 D in *trans* conformation, thus contributing to a large piezoelectric constant after poling. The piezoelectricity (d_{31}) of drawn and poled films is comparable to that of PVDF in the temperature range 20–100°C. Interestingly, this copolymer shows a very large dielectric strength of more than 100, one of the largest values among polymers. It is concluded that the large dielectric relaxation strength originates from the cooperative motion of 10 or more CN dipoles. The exceptionally high dielectric peaks occur near the glass transition temperature, similar to a ferroelectric transition. A most unique feature of this copolymer is its low density, which results in low acoustic impedance, close to the levels seen in water and the human body. This makes this copolymer very useful in medical applications.

C. Polyureas and Polythioureas

Polyureas and polythioureas are amino resins, and are thermosetting polymers. They are usually synthesized by condensation polymerization, and their products are mostly in the form of powder. The preparation of thin films was not possible due to their insolubility until a technique of vapor deposition polymerization was developed. The synthesis and characterization of different kinds of thin-film polyureas have been reported. A typical polymerization consists in vapor deposition of monomers onto the surface of a substrate in a vacuum chamber. The monomers diffuse on the surface and react with each other to form urea bonds between an amino (NH₂) group and an isocyanate (CNO) group. The urea bond (NHCONH) has a dipole moment of 4.9 D and is responsible for high piezoelectric and pyroelectric properties.

The dielectric constants of aromatic polyureas [P(4,4'-diphenylmethane diisocyanate (MDI)/4,4'-diamino diph-

enylmethane (MDA))] have been reported. The dielectric constant of MDA-rich films of poled and annealed P(MDA/MDI) are relatively constant up to 200°C, whereas the MDI-rich films have a low dielectric constant but show good stability up to 200°C. The dielectric constants of the balanced stoichiometric films increase with increasing temperatures above 100°C. Pyroelectric and piezoelectric constants are also large for the balanced composition films. This is due to the fact that a crosslinked network structure does not form in balanced film the way it does in unbalanced films. The high-molecular-weight molecules are oriented or crystallized in a local region under a high poling field and form a semicrystalline structure; thus, stabilized residual polarization is produced and gives rise to high piezoelectric and pyroelectric constants.

The pyroelectric and piezoelectric properties of aliphatic polyureas display similar features to those seen in nylons, i.e., there is no observation of these activities if the number of carbon atoms between the urea bond is even. This is because alternating urea bond dipoles arrange in antiparallel direction, and the dipole moments cancel out. Strong hydrogen bonds are possible in cases where the parallel orientation of dipoles in a planar zigzag chain gives rise to high glass transition and melting temperatures. Dielectric peaks above 125°C have been observed in poly(heptamethylene/nanomethyleneurea). The relatively large dielectric constant is believed to be related to the crystal transition from the mobile dipole state to the rigid dipole state corresponding to the different hydrogen bonding states. The value of remanent polarization obtained from D - E hysteresis of the same sample is as high as 200–440 mC/m² at 90°C, which may be attributed to the effect of the ionic currents of impurities. The remanent polarization disappears above 110°C, which suggests the rearrangement of the hydrogen bonding at this temperature.

Polythioureas are known pyroelectric, piezoelectric, and ferroelectric polymers. Their chemical structure is H₂N—CS—NH₂. Ferroelectric thiourea polymers have been prepared by condensation reaction of thiourea and formaldehyde under different conditions. Thiourea [SC(NH₂)₂] has a large dipole moment of 5.4 D. Ferroelectricity in polythioureas was initially studied in 1978. The sharp dielectric constant of thiourea-formaldehyde (PTUBFB) observed at 145°C is as high as 320. Recently, an odd-numbered aliphatic polythiourea, polythiourea-9, has been synthesized. The odd number of carbons was chosen to ensure a polar chain and polar packing. Large dielectric relaxation as well as a large dielectric constant were observed in the glass transition region. According to the theoretical data of Meakins *et al.*, the dielectric relaxation and dielectric loss increase with any increase in hydrogen bonding. As a result, the hydrogen-bonded thiourea dipoles in the intermolecular chains are easily

rotated under an electric field above the glass transition. The ferroelectric transition in thiourea is essentially due to both crystalline domains and an “incommensurate phase,” which are due to both hydrogen bonding and dipole interactions. The D – E hysteresis was first observed in drawn polythiourea-9 above T_g . The remanent polarization is very small. This may be due to the fact that only a small amount of chains can form hydrogen bonding. Therefore, the remanent polarization stabilized by hydrogen bonding is small.

D. Polyurethane

Polyurethanes have emerged as nonlinear optic, ferroelectric, and piezoelectric materials in which molecular structures can be tailored for specific applications. Polyurethanes have the chemical structure $[-(\text{CH}_2)_x\text{OC}(\text{O})\text{NH}(\text{CH}_2)_y\text{NHCO}(\text{O})-]$. The dipole moment of the urethane group is 2.8 D. Polyurethanes are usually composed of a polyester or polyether soft segment and a diisocyanate-based hard segment. From the viewpoint of the chemical structure of the hard segments, polyurethanes can be classified into urethane polymers (PU), which are formed by extending a diisocyanate with low-molecular-weight diols, and urethane–urea polymers (PUU), which are formed by extending a diisocyanate with low-molecular-weight diamine. Polyurethanes undergo microphase separation due to the immiscibility of the hard-segment and soft-segment. The hard segment domain acts as the physical crosslink as well as the filler particles for the soft-segment matrix. The driving force of the domain formation is the strong intermolecular interaction of the hydrogen bondings between the hard–hard segments and the urea/urethane linkages.

Both the temperature dependence and pressure–temperature effects on the dielectric constant and relaxation processes of aliphatic polyurethanes have been studied. The relaxation times for both the I process, associated with the molecular motion in hard segments, and the α process, associated with the glass transition temperature, increase with pressure, and that these shifts are much more pronounced for the I process. Dielectric properties of polyurethanes were also studied as a function of drawing and poling effects.

The D – E hysteresis of polyurethanes can be obtained above the glass transition temperature (at 70°C). Ferroelectricity originated from the crystal region by controlling the hydrogen bonding. Recently, there was a report on the origin of ferroelectricity that suggested it derives from the amorphous region above the glass transition temperature. The electrostrictive responses, which are proportional to the square of the electric field, have been investigated in polyurethane. The field-induced strain was found to be

very sensitive to the processing conditions and the thickness of the specimen. The increase of the strain response as the sample thickness is reduced is suggested to be caused by a nonuniform electric field across the thickness direction. In nonpiezoelectric materials, the field-induced strain can be caused by the electrostrictive and also the Maxwell stress effects. Experimental results show that the Maxwell stress can significantly contribute to the strain response at temperatures higher than the glass transition temperature, and that the electrostrictive coefficient is much higher than those of other materials.

V. APPLICATIONS

In recent years, many kinds of piezoelectric devices have been developed from organic polymer materials and widely used in industrial settings as well as in medical instruments. These device applications can be grouped into sensors, medical instrumentation, robotics, low- or audiofrequency transducers, ultrasonic and underwater transducers, electroacoustic transducers, electromechanical transducers, actuators, pyroelectric devices, and optical devices. The pyroelectric, biomedical, and robotic applications and the optical devices will not be discussed here.

The first commercial application of piezoelectric polymer film was in audio transducers (tweeters) and loudspeakers. The merits of ferroelectric polymers for piezoelectric devices over ferroelectric ceramics is their softness, light weight, toughness, flexibility, and ability to be fabricated into large sheets. In addition to these traits, they have a good electromechanical coupling factor and much lower acoustic impedance (this property is proportional to the product of density and stiffness) than ferroelectric ceramics. Therefore, they are suitable for acoustic applications in media such as air, water, and human tissue. Such applications include audio transducers (headphones, microphones, loudspeakers), underwater acoustic hydrophones, and biomedical transducers (sensors and probes, imaging systems, and acoustic sources). Another merit of polymer piezoelectrics is their thin-film-forming ability. This could lead to very promising applications, such as ultrasonic transducers or paperlike speakers for the future’s thin TVs, decorations, and interiors. The main disadvantages of polymer piezoelectrics are their relatively low piezoelectric constant and relatively poor dimensional stability.

Devices based on the conversion of a mechanical input (stress or strain) into an electrical output signal are often used as sensors to detect displacement, stress, vibration, and sound. Typical sensors are hydrophones, blood pulse counters, blood pressure meters, pressure sensors,

acceleration sensors, shock sensors, vibration sensors, touch sensors, microphones, antinoise sensors, and keyboards. Reverse devices, in which the input is an electrical signal and the output is a mechanical signal, include position controls, acoustic systems, and actuators.

SEE ALSO THE FOLLOWING ARTICLES

NONLINEAR OPTICAL PROCESSES • ORGANOMETALLIC CHEMISTRY • POLYMERS, ELECTRONIC PROPERTIES • POLYMERS, SYNTHESIS • ULTRASONICS AND ACOUSTICS

BIBLIOGRAPHY

- Brown, L. F., Scheinbeim, J. I., and Newman, B. A. (1995). *Ferroelectrics* **171**, 321.
- Chung, T. C., and Janvikul, W. (1999). *J. Organomet. Chem.* **581**, 176.
- Cross, L. E. (1996). *Ceram. Trans.* **68**, 15.
- Furukawa, T., Date, M., Fukada, E., Tajitsu, Y., and Chiba, A. (1980). *Jpn. J. Appl. Phys.* **19**, L109.
- Kawai, H. (1969). *Jpn. J. Appl. Phys.* **8**, 1975.
- Lovinger, A. J. (1982). "Poly(vinylidene Fluoride)," In "Developments in Crystalline Polymers," Vol. 1, pp. 195–273 (Basett, D.C., ed.), Applied Science, London.
- Lovinger, A. J. (1983). *Science* **220**, 1115.
- Nalwa, H. S. (1991). *J. Macromol. Sci. Rev. Macromol. Chem. Phys.* **C-31**, (4), 341.
- Nalwa, H. S. (ed.). (1995). "Ferroelectric Polymers," Marcel Dekker, New York.
- Ueda, H., and Carr, S. H. (1984). *Polymer J.* **16**, 661.
- Von Berlepsch, H., Kunstler, W., and Danz, R. (1988). *Ferroelectrics* **81**, 353.
- Wang T. T., Herbert, J. M., and Glass A. M. (eds.). (1988). "The Applications of Ferroelectric Polymers," Blackie, Chapman and Hall, Glasgow.
- Zhang, Q. M., Bharti, V., and Zhao, X. (1998). *Science* **280**, 2102.



Polymers, Inorganic and Organometallic

Martel Zeldin

Hobart and William Smith Colleges

- I. Morphological Classification
- II. Compositional Classification
- III. Inorganic Polymers of the Main Group Elements
- IV. Inorganic Polymers with Transition Metals

GLOSSARY

Chain polymer A macromolecule composed of difunctional repeating units that are devoid of inter- or intrachain crosslinks.

Crosslink polymers Polymers containing two or more chains that are interconnected by chemical bonds.

Inorganic polymers Polymers containing a metal or semimetal (metalloid) in the backbone or pendant to the polymer chain.

Molecular weight Unless otherwise stated, the number-average value (M_n).

Network polymers Giant three-dimensional structures in which many chains are connected through crosslinks.

Oligomers Molecules with relatively few (usually less than 10) repeating units in the chain.

Organometallic polymers Polymers containing a metal or semimetal (metalloid) directly bonded to carbon in the macromolecule. The metal may be in or pendant to the polymer backbone.

Sheet polymers Two-dimensional, layered (lamella)

structures in which the primary valences of the atoms are satisfied by covalent bonds and secondary weaker interactions (e.g., van der Waal forces, hydrogen bonds) more loosely holding the layers intact.

Silicone An organometallic polymer that contains the siloxyl (Si—O—Si) unit.

INORGANIC and organometallic polymers are macromolecules that contain metals or semimetals (metalloids) either in or pendant to the polymer backbone. Many of these materials have been designed to withstand the extremes of temperature and erosion, but still maintain the highly desirable properties of oxidative stability, elasticity, electric conductivity or resistivity, tensile strength, fire retardancy, low density, and/or inertness to solvents and chemicals. Representative examples are illustrated in [Fig. 1](#).

Inorganic and organometallic polymers are often classified in terms of morphological structure (e.g., chains, sheets, and networks) and elemental composition (e.g., homoatom and heteroatom).

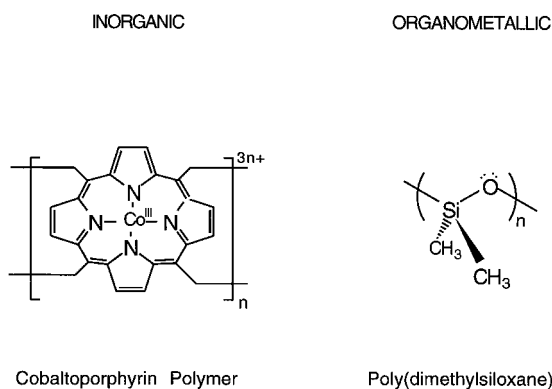


FIGURE 1 Examples of inorganic and organometallic polymers.

I. MORPHOLOGICAL CLASSIFICATION

A *chain* polymer is a one-dimensional macromolecule composed of linear difunctional repeating units that are devoid of inter- or intrachain crosslinks. Polythiazyl, $(\text{SN})_x$, and poly(dialkylstannanes), R_2Sn , are examples of linear chain polymers (Fig. 2). Under certain circumstances, the ends of a linear chain can join to form a large macrocyclic polymer. For example, cyclic poly(hydrogenmethylsiloxane) with as many as 50 skeletal repeating units is known (Fig. 3). However, cyclic chain molecules with a relatively small number of repeating units (oligomers) are very common. Some well-known cyclic oligomers are octamethylcyclotetrasiloxane, $(\text{Me}_2\text{SiO})_4$, and one of the allotropic forms of elemental sulfur, S_8 (Fig. 4). In addition, chains may also assume a random coil, helical (protein-like), or rigid-rod structure.

Sheet polymers are two-dimensional (2D) macromolecules in which the primary valences of the atoms are satisfied by covalent bonds. In some cases, weaker interactions such as van der Waals forces or hydrogen bonds connect one sheet to another in a layered (lamella) structure. Graphitic carbon and boron nitride, $(\text{BN})_x$, are examples of sheet polymers (Fig. 5). Both polymers consist of flat sheets of hexagonal rings in which each atom is bonded to three other atoms in the same layer. The sheets are stacked in a lamella fashion permitting the sheets to “flake.”

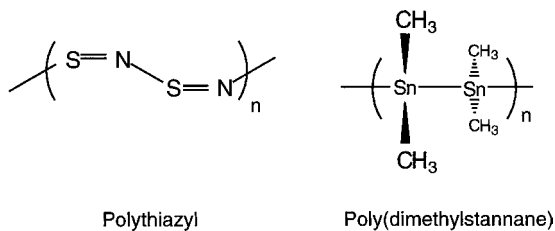


FIGURE 2 Chain polymer.

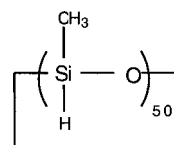


FIGURE 3 Cyclic poly(hydrogenmethylsiloxane).

Another variation of a 2D sheet occurs if two chains are crosslinked at regular intervals to give a ladder-type structure. An example of a siloxane ladder polymer is given in Fig. 6. Ladder polymers are unusually high-melting solids with extraordinary oxidative, hydrolytic, and thermal stability.

Network polymers are highly crosslinked materials in which some of the atom valencies are satisfied by bonds that result in a three-dimensional (3D) structure. Such polymers are usually difficult to characterize owing to their refractory nature. Network polymers are usually hard, infusible, insoluble substances such as diamond and silicon dioxide (silica) (Fig. 7).

II. COMPOSITIONAL CLASSIFICATION

Homoatom polymers are macromolecules with only one kind of element in the backbone. Poly(diphenylsilane), $(\text{Ph}_2\text{Si})_n$ (Fig. 8), is an example of a homoatom polymer because it contains only silicon atoms along the chain's backbone. Some metal salts have semimetal anions with polymeric structure. For instance, metal borides have the formula M_xB_y in which the boride anion may be in the form of chains, ladders, 2D sheets, or 3D networks (Table I). These anionic polymers possess high thermal stability, resistance to chemical attack, and interesting electrical properties.

Certain elements prefer to aggregate as low-molecular weight (MW) oligomers. Phosphorus, for example, exists in several allotropic forms. The allotrope, white phosphorus, is a tetramer (P_4) in which the phosphorus atoms lie at the corners of a tetrahedron (Fig. 9). Black phosphorus is obtained by heating P_4 under pressure (200°C, 12 000 atm) in the presence of a catalyst. It is a sheet polymer in which each P atom is bonded to three neighbors in double layers (Fig. 10A). In this giant molecule the double layers are

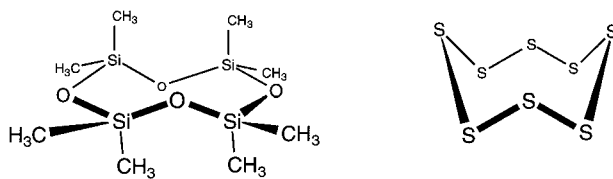


FIGURE 4 Common cyclic polymers.

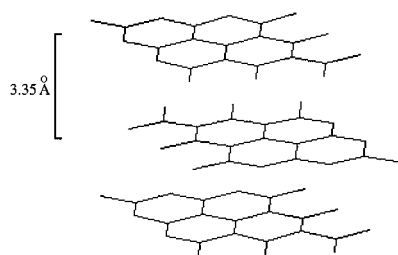


FIGURE 5 Graphite sheet polymer. In graphite (above), the C atoms are located at each vertex and the layers are staggered. In boron nitride, the B and N atoms are located at alternate vertices and the layers are eclipsed.

stacked in a manner similar to graphite. In addition to flaking, black phosphorus is a good electrical conductor. Red phosphorus results from heating P_4 at $\sim 400^\circ\text{C}$ in a sealed vessel. One crystalline form of red phosphorus (Hittorf's phosphorus) has a linear tubular arrangement of eight P atoms in a pentagonal wedge structure (Fig. 10B).

Like phosphorus, elemental sulfur is a polyatomic, polymorphic substance. Oligomeric sulfur rings that contain from 6 to 12 sulfur atoms have been identified (Fig. 11). The orthorhombic form, $\alpha\text{-S}_8$, has the most thermodynamically stable structure and exists as a yellow crystalline solid consisting of eight-member puckered rings in a crown conformation stacked together in "crankcase" fashion. The chain polymer form of sulfur called *catena* or *plastic* sulfur is obtained by quenching molten S_8 in water. If stretched, catena sulfur has a helical polymeric structure. Selenium forms polymers similar to those of sulfur.

Heteroatom polymers contain a metal or semimetal in addition to one or more other atoms (e.g., O, S, N, P, and C) in the polymer backbone. It is well-known that polymer stability and inertness increases when the heteroatom is electron rich. Presumably, such atoms serve as electron sources toward low-lying vacant orbitals on the metal or semimetal (Fig. 12). The resulting coordinate (dative) interaction generally decreases the nucleophilicity of the metal or semimetal thereby reducing the susceptibility of the polymer to attack by Lewis acids and bases. Further-

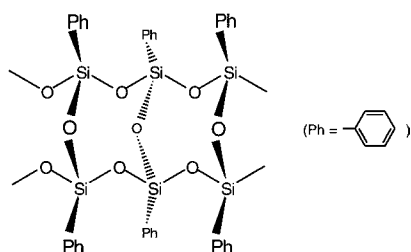


FIGURE 6 Poly(diphenylsiloxane) ladder polymer.

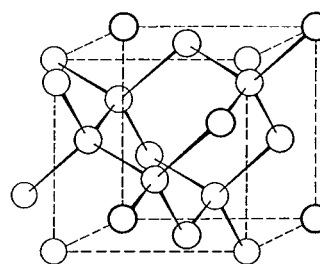


FIGURE 7 Network polymer (diamond and silica). In diamond, each atom is carbon; in silica, silicon is surrounded tetrahedrally by four oxygen atoms.

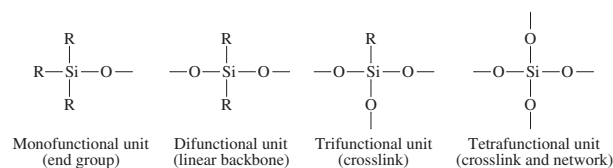
more, the dative interaction tends to stabilize the polymer toward thermal degradation and aids in the regulation of structure, chain mobility, and interchain forces that enhance useful dynamic-mechanical properties.

III. INORGANIC POLYMERS OF THE MAIN GROUP ELEMENTS

A. Silicon-Based Polymers

1. Polysiloxanes (Silicones)

Polysiloxanes are chains, rings, ladders, and 3D network polymers that contain siloxane (Si—O—Si) bonds in the backbone. The basic structural units of polysiloxanes are



Chain polysiloxanes are composed of difunctional units. The framing groups (R) are either H or organic moieties and the end groups are usually —OR or a monofunctional siloxyl unit. Chain polysiloxanes such as poly(dimethylsiloxane)s are synthesized by the hydrolysis of dichlorodimethylsilane [Eq. (1)].

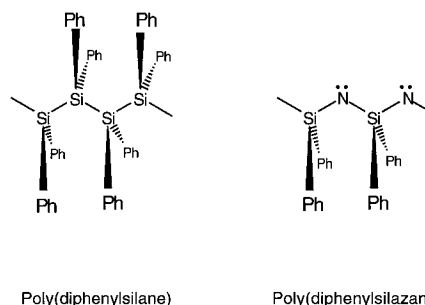


FIGURE 8 Homoatom and heteroatom polymers.

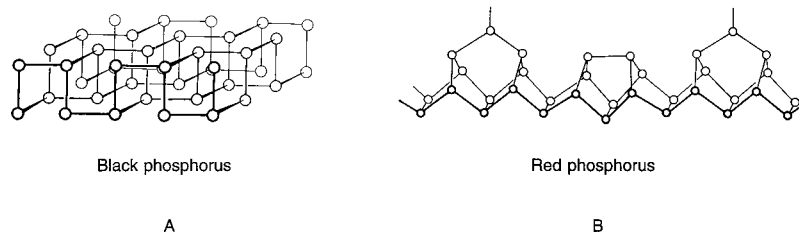
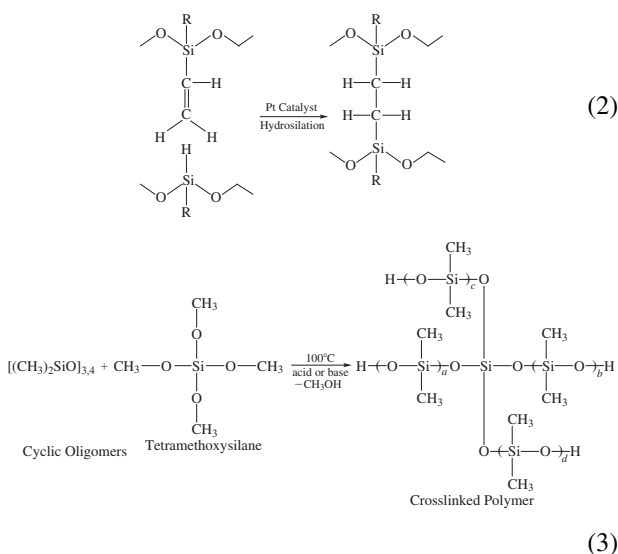


FIGURE 10 Black and red phosphorus.



Resins differ from elastomers in the proportion of crosslinks that are present. Highly crosslinked polysiloxanes are sometimes called T-resins. In general, T-resins are prepared by the hydrolysis of tri- and tetrafunctional silanes. The resulting resins have a complex network structure and are insoluble in common organic solvents. Under specially controlled synthetic conditions, lower MW materials containing ladder and polyhedral oligomeric siloxanes called silsesquioxanes (Fig. 13) are obtained that are soluble in organic solvents. The resins are used as coatings in microelectronic devices and binding agents in high-performance refractory materials.

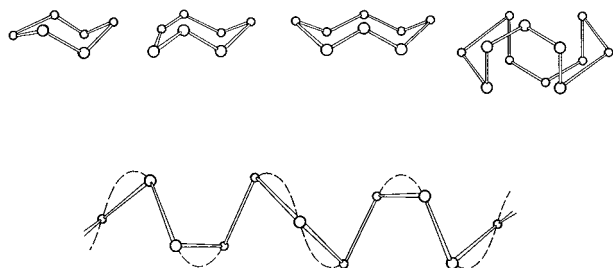


FIGURE 11 Allotropic forms of elemental sulfur.

Polysiloxanes have many commercial and consumer applications. Some of the uses of polysiloxane fluids, elastomers, and resins are summarized in Table II. Some of the important physical properties of polysiloxanes that lead to applications are their low glass transition temperature T_g , low bulk viscosity, low thermal coefficient of viscosity, high gas permeability, low surface energy, and low surface tension.

2. Polysilanes

Polysilanes are chains, rings, and 3D network polymers of silicon that contain the Si—Si bond in the polymer backbone. The tetravalency of silicon is usually completed with H or organic groups. The basic structural unit of a polysilane is shown in Fig. 14.

There are several methods of polysilane synthesis: reductive or Wurtz coupling [Eq. (4)], dehydrogenative coupling [Eq. (5)], ring-opening polymerization of cyclic silane oligomers [Eq. (6)], ring-opening of cyclic organodisilanes [Eq. (7)], and polymerization of silylenes [Eq. (8)]:

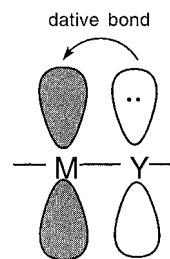
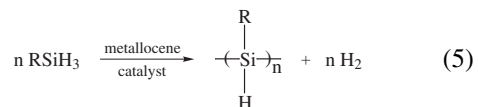
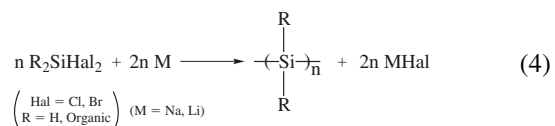


FIGURE 12 Coordinate (dative) bond.

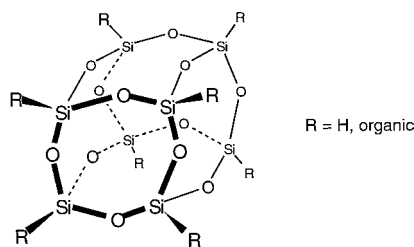
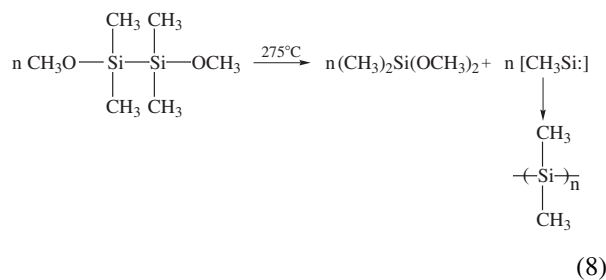
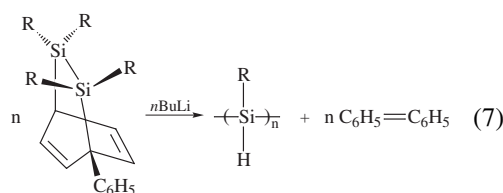
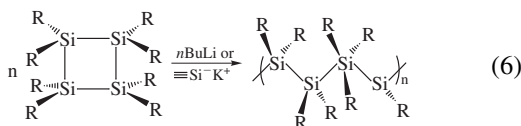


FIGURE 13 Polyhedral silsesquioxanes.



Reductive coupling is a heterogeneous reaction involving well-dispersed alkali metals with difunctional dihalosilanes. If the product conversion is kept low, high-MW polymers are obtained. As the reaction proceeds, the cyclic oligomers (mainly Si_6 and Si_8) are also formed to give an overall binodal distribution of chain and ring products. If a trifunctional silane (e.g., RSiCl_3) is used, a network polysilane is formed.

Dehydrogenative coupling of primary alkylsilanes (RSiH_3) using titanocene, zirconocene, or organolanthanum compounds (e.g., $[\text{C}_5(\text{CH}_3)_5]_2\text{LaH}$) gives good

TABLE II Some Applications of Polysiloxanes

Insulators	Surgery implants	Coupling agents
Dielectric materials	Mold-forming agents	Water repellants
Heat exchange fluids	Antifoaming agents	Lubricants
Seals and gaskets	Masonry additives	Hydraulic fluids
Caulking agents	Surfactants	Ceramic composites
Emulsifying agents	Paper release coatings	Pressure-sensitive adhesives

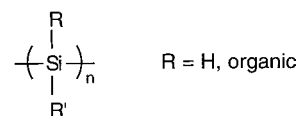


FIGURE 14 Polysilane repeating unit.

yields of soluble polysilanes with MW as high as 17 500. Arylsilanes couple more rapidly than alkylsilanes. Diorganosilanes (R_2SiH_2) under the same reaction conditions give only dimers, $(\text{R}_2\text{Si})_2$.

Ring-opening polymerization of strained cyclosilanes leads to polysilanes. The reaction is anionically catalyzed with $n\text{-BuLi}$ or $\text{R}_3\text{Si}^- \text{K}^+$. This method is most effective if the rings are small (e.g., Si_4) and the substituents are not excessively bulky (e.g., H, CH_3 , C_6H_5).

Polysilanes are formed by ring-opening polymerization of strained organodisilanes. To illustrate, when a disila-bicyclooctadiene [Eq. (7)] is treated with $n\text{-BuLi}$, polysilanes with MW as high as 50 000 are obtained. Biphenyl is eliminated as a by-product. This synthetic method is particularly useful since addition of vinyl monomers such as methyl methacrylate can lead to block copolymers [e.g., poly(methyl methacrylate-co-polysilane)].

Polysilanes can also be prepared from silylenes. Consequently, thermolysis of 1,2-dimethoxytetramethylsilane generates the transient intermediate dimethylsilylene that polymerizes at ambient temperature to poly(dimethylsilane) [Eq. (8)].

The physical properties of polysilanes depend on the groups attached to the silicon. Polymers with relatively small and identical organic groups (e.g., $\text{R} = \text{CH}_3$, C_2H_5 , C_6H_5) bonded to Si are highly crystalline and generally insoluble and infusible solids. The crystallinity decreases and the solubility increases with the length of the alkyl substituent and the presence of two different substituents on Si. For example, $[\text{CH}_3\text{SiR}]_n$ in which $\text{R} = n\text{-hexyl}$ is an elastomer at room temperature with $T_g = -75^\circ\text{C}$. However, if $\text{R} = \text{C}_6\text{H}_5$, resinous solids that are soluble in organic solvents and have reasonable melting points are formed.

An interesting and potentially useful property of polysilanes is their sigma electron delocalization that results from relatively loosely held σ -bonding electrons and relatively low-lying σ^* antibonding orbitals associated with the Si-Si backbone. These unusual molecular orbitals are responsible for strong electronic absorptions, electro- and photoconductivity, thermochromism, and photosensitivity. Polysilanes have found applications as photoresists in microlithography and free radical photoinitiators in polymerization of unsaturated hydrocarbons. Soluble polysilanes can be spun into fibers that, when pyrolyzed, give silicon carbide (SiC) ceramic materials (see Section III.A.3).

For example, if $R = R' = H$ in ring-opening polymerization, only chain oligomers of relatively low MW (~ 1000) are obtained. If $R = CH_3$ and $R' = H$, the products are a mixture of cyclic and chain oligomers. If R is larger than methyl, only cyclotri- and cyclotetrasilazanes are formed (Fig. 16B, C). Products with higher degrees of polymerization are obtained by dehydrocoupling of the oligomers.

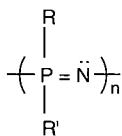
The primary use of polysilazanes is as prepolymers in the manufacture of silicon nitride ceramics. Thus, heating ($<1000^\circ\text{C}$) the oligomers results in progressive deamination–condensation to give a cyclomatrix polymer. Ceramic silicon nitride is formed upon further heating ($>1000^\circ\text{C}$) under vacuum. The high tensile strength coupled with thermal and oxidative stability of silicon nitrides makes them useful as tough ceramic coatings or high-impact composites in heat engine parts, power-generating turbines, and machine bearings. They are also used as refractory materials for heat- and corrosion-resistant jigs and in devices where high-temperature insulation is required.

B. Phosphorus-Based Polymers

1. Polyphosphazenes

Polyphosphazenes are polymers that contain alternating phosphorus and nitrogen atoms. Two organic, inorganic, or organometallic substituents are bonded to phosphorus (Fig. 17). An important feature of polyphosphazenes is their synthetic methodology that provides an enormous variety in the types of R groups attached to the P. As a result, a large number of polyphosphazenes have been synthesized and characterized (Fig. 18). The diverse chemical and physical properties of these polymers make them important candidates for many industrial and consumer applications. Some applications associated with different substituents on the PN chain are summarized in Table III.

There are several methods of polyphosphazene synthesis: ring-opening polymerization (ROP), condensation polymerization (CP), and more recently anionic polymerization (AP). In the case of ROP, the primary commercial starting material is highly purified hexachlorocyclotriphosphazene, $[\text{NPCl}_2]_3$. The cyclic trimer, which is



R, R', R'' { alkyl, aryl, alkoxy, aryloxy, halo, amino,
thio, organometallo (e.g. ferrocenyl, polysiloxy)}

FIGURE 17 Polyphosphazene repeating unit.

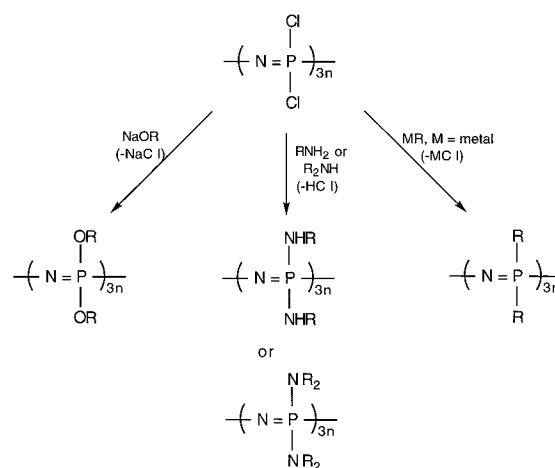
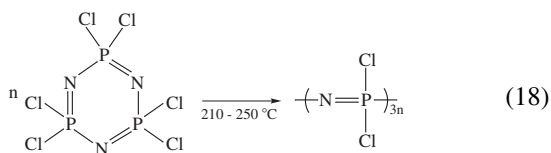
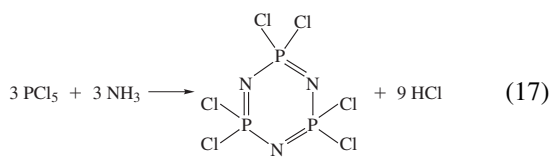


FIGURE 18 Synthesis of substituted polyphosphazenes.

prepared from PCl_5 and NH_3 (or NH_4Cl), is then carefully heated above 200°C to induce polymerization [Eqs. (17), (18)]:



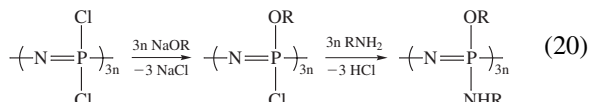
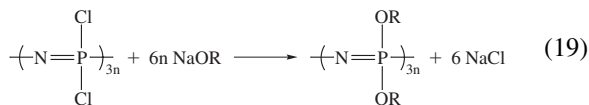
The product is a linear polymer that is soluble in organic solvents. The degree of polymerization using this method

TABLE III Applications of Polyphosphazenes with Various Substituents

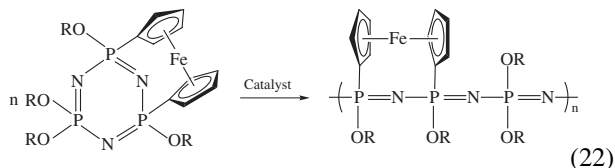
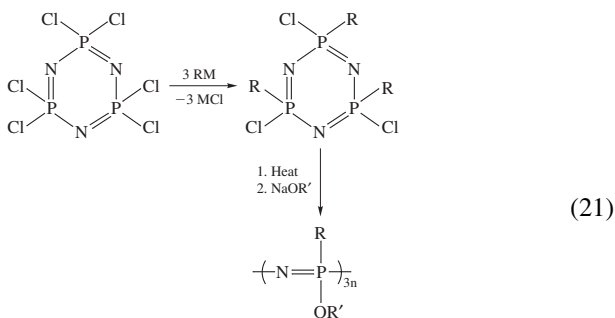
Substituents	Applications
$-\text{OCH}_2(\text{CF}_2)_x\text{CF}_3$	Hydrocarbon-resistant O-rings, gaskets, coatings, and fuel lines and nonflammable polymers
$-\text{OC}_6\text{H}_5$	Electrical, heat, and sound insulation materials, immobilized enzymes
$-\text{OC}_2\text{H}_4\text{OC}_2\text{H}_4\text{OCH}_3$	Polymer electrolytes in batteries, hydrogels for soft tissue medical applications
$-\text{O}[\text{Si}(\text{CH}_3)_2]_n\text{OSi}(\text{CH}_3)_3$	Hydrophobic polymers
$-\text{NHC}_2\text{H}_5$	Hydrophilic polymers
$-\text{NHCH}_2\text{COOC}_2\text{H}_5$	Bioerodible polymers
$-\text{O-Steroid}$	Drug delivery polymers
$-\text{O-Procaïne}$	Local anesthetic

can exceed 15 000. If the linear polymer is heated further or at higher temperatures, a crosslinked elastomeric polymer is formed.

The high reactivity of the P–Cl bond toward nucleophilic substitution provides a facile route to polymers with a variety of organic, organometallic and inorganic substituents. For example, homopolymers [Eq. (19)] and copolymers [Eq. (20)] are available through this route:



Halogen substitution reactions on linear polymers sometimes suffer from incomplete halogen replacement or unwanted chain scission. These problems are sometimes precluded by ROP of cyclic trimers that have one or more of the halogens replaced with R groups [Eq. (21)]. This modified approach controls the substituent distribution. Although polymers have been obtained with several different organic groups attached, polymerization becomes more difficult as the number of groups increase. It is noteworthy that polymerization is more facile if the substituents cause steric ring strain as in the ferrocenyl phosphazene trimer [Eq. (22)]:



The second, somewhat limiting method of preparing linear polyphosphazenes involves a condensation reaction. Usually reaction of a chlorophosphine with an amine gives a cyclic oligomer. However, a multistep reaction sequence (Fig. 19) that entails several noncyclic intermediates has been developed. The linear polymer is formed from a phosphorimine by elimination of a volatile silyl es-

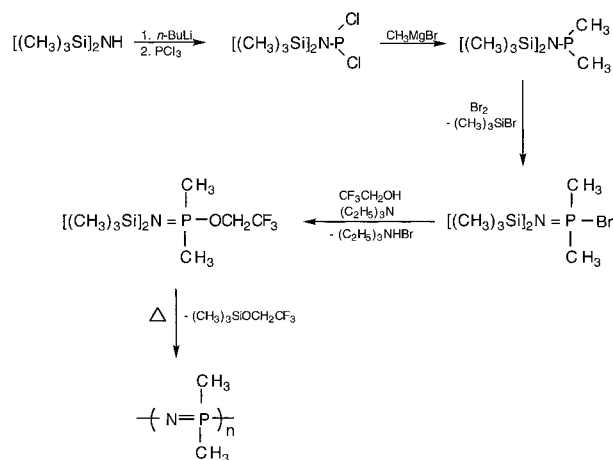
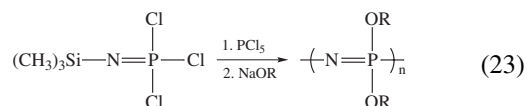


FIGURE 19 Synthesis of linear polyphosphazenes via noncyclic intermediates.

ter. Polymers generated by this process are often difficult to obtain by other means.

Polyphosphazenes are also prepared using “living” cationic catalysts at room temperature [Eq. (23)]. This direct synthesis from monomer to polymer allows control over polymer architecture, MW, polydispersity, and block copolymer composition. It has also been used to prepare star-branched polymers and organic–PN hybrid copolymers. The active initiator in this synthesis is believed to be the short-chain ionic intermediate $[\text{Cl}_3\text{P}=\text{NPCl}]^+[\text{PCl}_6]^-$.



Polyphosphazenes have been prepared with MW from several thousand to several million. Although the formula is usually written as alternating single and double bonds ($-\text{P}=\text{N}-\text{P}=\text{N}-$), all the P–N lengths are approximately equal. Therefore, unlike the corresponding unsaturated organic polymers, where $p\pi-p\pi$ delocalization is extensive, the participation of 3d orbitals on P with a 2p orbital on N generates an orbital symmetry with nodes at every P atom. This bonding arrangement limits delocalization to three adjacent atoms [namely $(d-p-d)\pi$; Fig. 20].

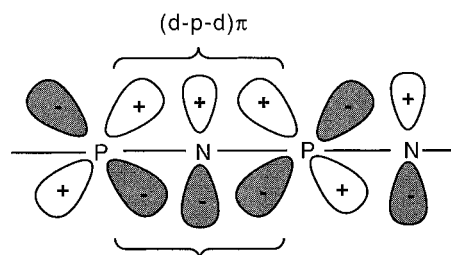


FIGURE 20 Orbitals involved in polyphosphazene bonding.

The ability to alter pendant substituents and control MW, polydispersity, solubility, polymer architecture, and copolymer composition gives versatility to polyphosphazenes. The polymers can vary from elastomers to ceramics, from hydrophobic to hydrophilic, from bioactive to bioinert, and from electrical conductor to insulator. In addition, many of these polymers have low T_g values (e.g., $T_g([\text{Cl}_2\text{PN}]_n) = -63^\circ\text{C}$) that result in rubbery behavior at fairly low temperatures.

2. Poly(carbophosphazene) and Poly(thiophosphazene)

The backbone of the polyphosphazene chain can be modified by insertion of heteroatoms such as carbon [poly(carbophosphazene)] or sulfur [poly(thiophosphazene)]. These polymers are obtained by heating the heterocyclic trimer analogs that are prepared by a 3 + 3 cocondensation reaction as illustrated in Fig. 21. Unless the poly(thiophosphazene) has bulky sidegroups, it is hydrolytically unstable. However, if the oxidation state of sulfur is increased to VI [poly(thionylphosphazene), Fig. 22], the polymer is stable to atmospheric moisture. Moreover, only the halogens on P undergo substitution with NaOR (R = phenyl).

An interesting feature of these polymers is the increase in T_g relative to $[\text{R}_2\text{PN}]_n$. This suggests that the presence of carbon or sulfur significantly reduces chain mobility and flexibility presumably because of the higher rotational barrier in C=N and S=N and the increase in intermolecu-

lar interactions in the more polar C=O or S=O bonds. The MW of the thionyl polymers, determined from light scattering, range from 5000 to 140 000 with polydispersities from 1.4 to 2.3 depending on the substituents. The combination of low T_g and high oxygen diffusion coefficient for some of these polymers has led to applications as matrices for pressure and phosphorescence sensor composites in the aerospace industry.

3. Other Phosphorus-Containing Polymers

Oligomers and polymers of elemental phosphorus were mentioned previously (Section II). Although they are rather sensitive toward atmospheric oxygen and moisture, in small quantities they have applications as fire retardants, surface treatment of metals for coatings, and in ion-exchange resins. Oligomers and polymers of phosphorus with oxygen $[\text{P}_4\text{O}_6, \text{P}_4\text{O}_{10}, \text{P}_8\text{O}_{16}, (\text{PO})_n, \text{P}_3\text{O}_8^{5-}, \text{P}_6\text{O}_{12}^{6-}$ and $(\text{PO}_3)_n^{n-}]$ are well known. Several examples are given in Fig. 23. The small neutral P–O and P–S compounds have polyhedral cage structures. $(\text{PO}_3)_n^{n-}$ polymers, however, are composed of orthophosphate (phosphoanhydride) residues in which n may be several multiples of 10 to several hundred. These macromolecules are constituent parts of all living cells and are responsible for cellular energy transfer and other biochemical processes. Phosphorus–sulfur oligomers (P_4S_x , $x = 3, 5, 7, 9, 10$) are also known.

Aromatic polyphosphates that are prepared from phosphodichloridates and aromatic diols [Eq. (24)] possess the

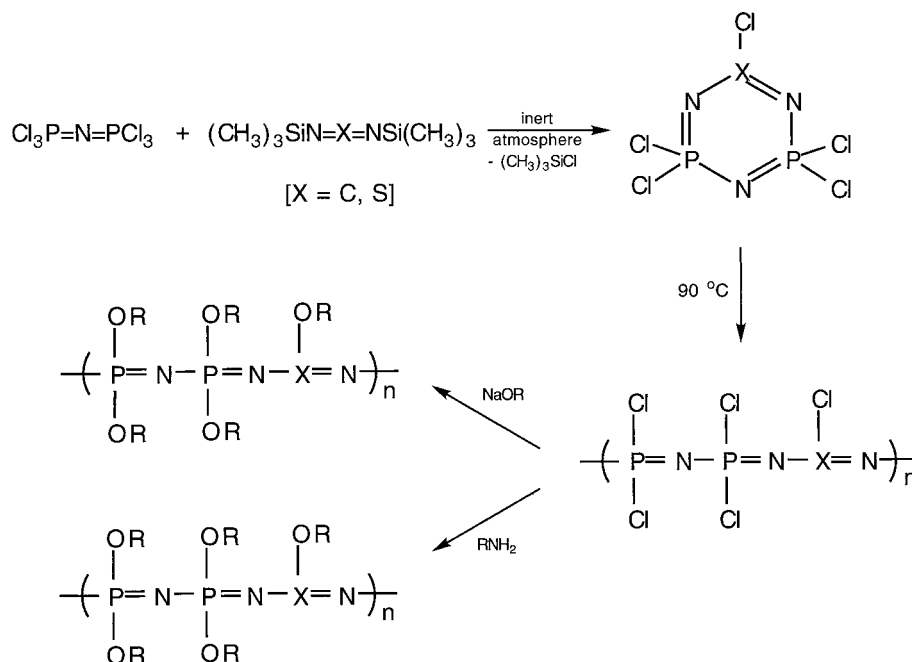


FIGURE 21 Synthesis of poly(carbophosphazene) and poly(thiophosphazene).

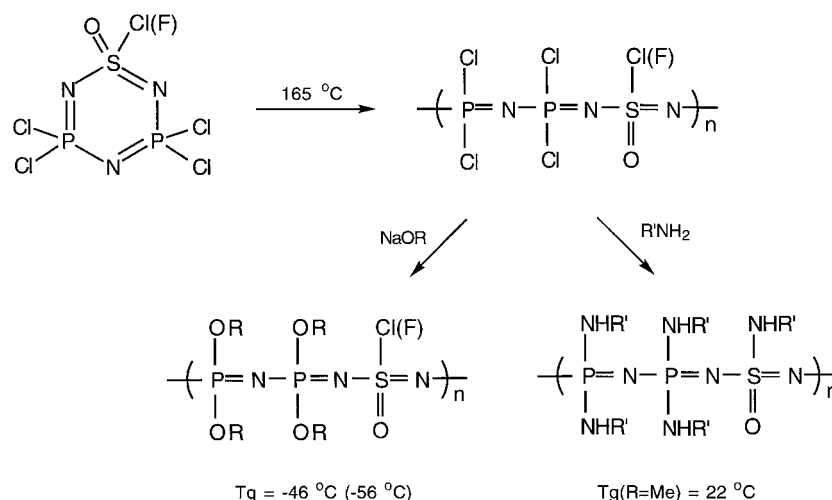
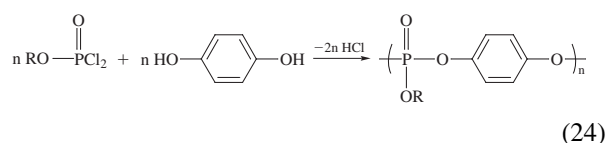
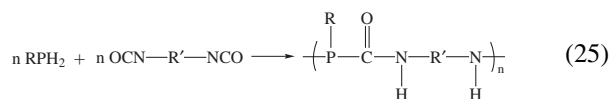


FIGURE 22 Synthesis of poly(thionylphosphazene).

useful properties of hardness, high transparency and flame retardancy:



However, these materials lack long-term hydrolytic stability. The hydrolysis problem has been partially overcome by elimination of the P–O linkage as in the poly(phosphinoisocyanate)s [Eq. (25)]:



If metal alkoxides (e.g. MOR, M = Al, Co, Cr, etc.) react with a diorganophosphinic acid [$\text{R}_2\text{PO}(\text{OH})$], poly(metal phosphinate)s with general formula $[\text{M}(\text{OPR}_2\text{O})_2]_n$ are formed.

Poly(phosphoryldimethylamide)s are obtained from a complex reaction of P_4O_{10} , $[(\text{CH}_3)_2\text{N}]_3\text{P}=\text{O}$, and $\text{Cl}_3\text{P}=\text{O}$ (Fig. 24). This class of polymer has elastomeric properties.

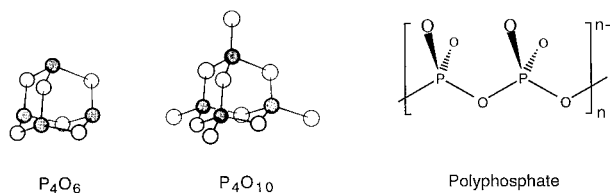


FIGURE 23 Phosphorus–oxygen oligomers and polymer (polyphosphate)

C. Boron-Based Polymers

1. Boron–Hydrogen Polymers: Polyboranes

Polymers that contain boron may be classified into two categories: homoatom polymers that are anionic (see Table I) or neutral and heteroatom polymers that contain boron with carbon, oxygen, nitrogen, phosphorous, or other elements. The latter may be neutral or ionic. Some of the homoatom anionic polymers (borides) were mentioned earlier (Section II). A simple homoatom polymer of boron is $[\text{BF}]_n$, which presumably contains BF repeating units with B–B bonds in the backbone. $[\text{BF}]_n$ is prepared from elemental boron and BF_3 at high temperature. The polymer is an elastomer. However, owing to its pyrophoricity and sensitivity to moisture, it has not been fully characterized. Boron oligomers that contain B–H (polyboranes) are interesting because of their “nonclassical,” multicenter covalent bonds (Fig. 25) and their unusual weblike (*arachno*), nestlike (*nido*), and cagelike (*closo*) structures (Fig. 26).

The structures of some neutral polyboranes with formulas B_nH_{n+4} ($n = 5, 6, 10, 16, 18$) and B_nH_{n+6} ($n = 4, 5, 10$) and several anionic polyboranes ($\text{B}_6\text{H}_6^{2-}$, $\text{B}_{12}\text{H}_{12}^{2-}$, and $\text{B}_{18}\text{H}_{20}^{2-}$) are given in Fig. 26. Although these unusual cluster oligomers have fascinating structures and remarkable bonding, the difficulties encountered in large-scale

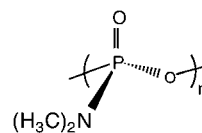
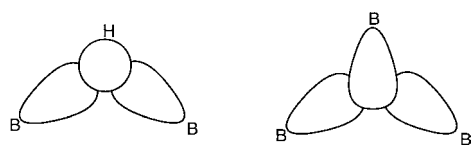


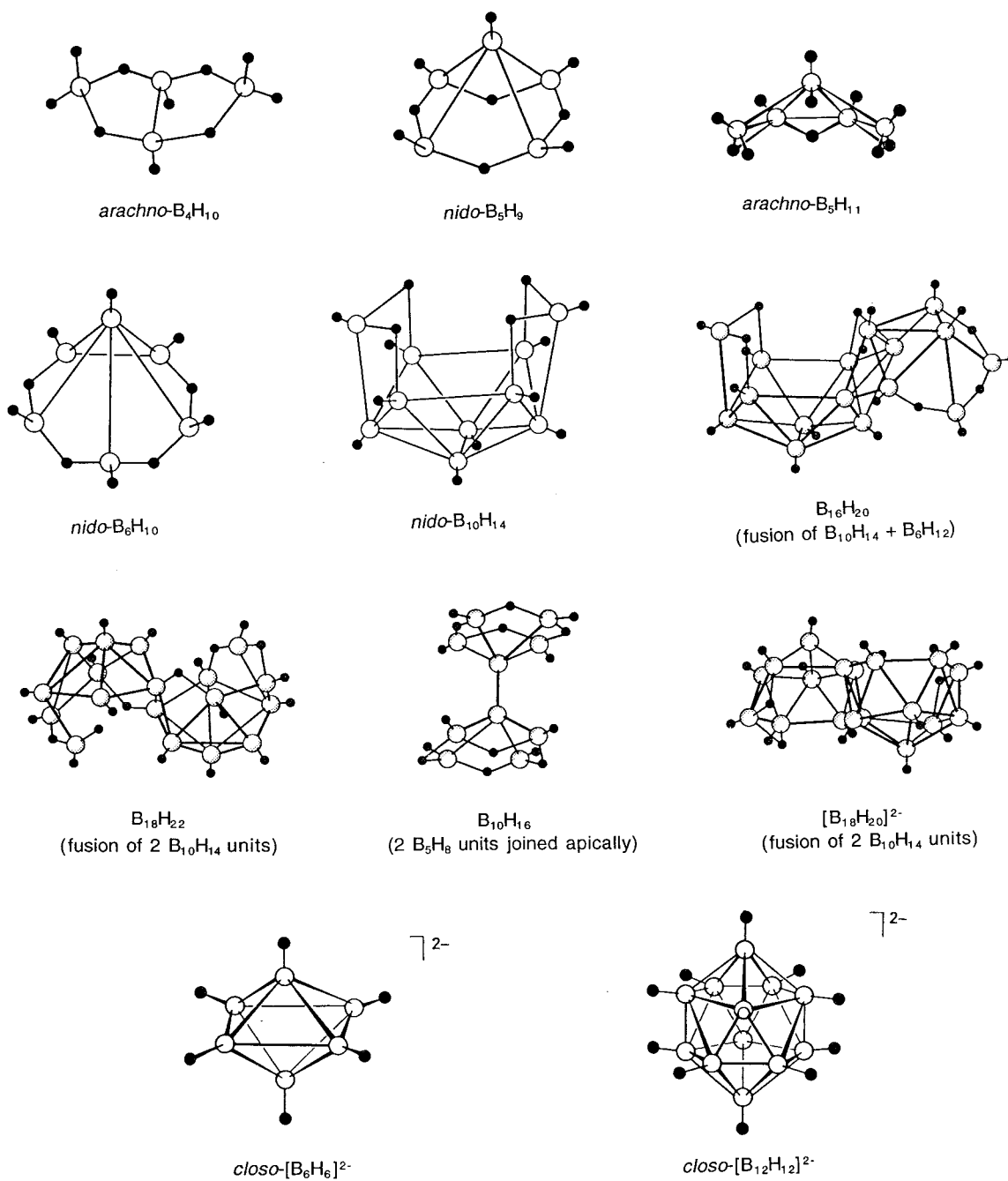
FIGURE 24 Poly(phosphoryldimethylamide) repeating unit.

Open B-H-B
three-center bondClosed B-B-B
three-center bond**FIGURE 25** Three center bonds in boranes.

synthesis and purification, coupled with their hydrolytic instability, have inhibited commercialization.

2. Boron–Carbon Polymers: Carboranes

An important group of heteroatom boranes are the *closo*-carboranes (or carbaboranes). *Closo*-carboranes are oligomers of boron that contain one or more carbon atoms

**FIGURE 26** Neutral and ionic polyhedral borane structures.

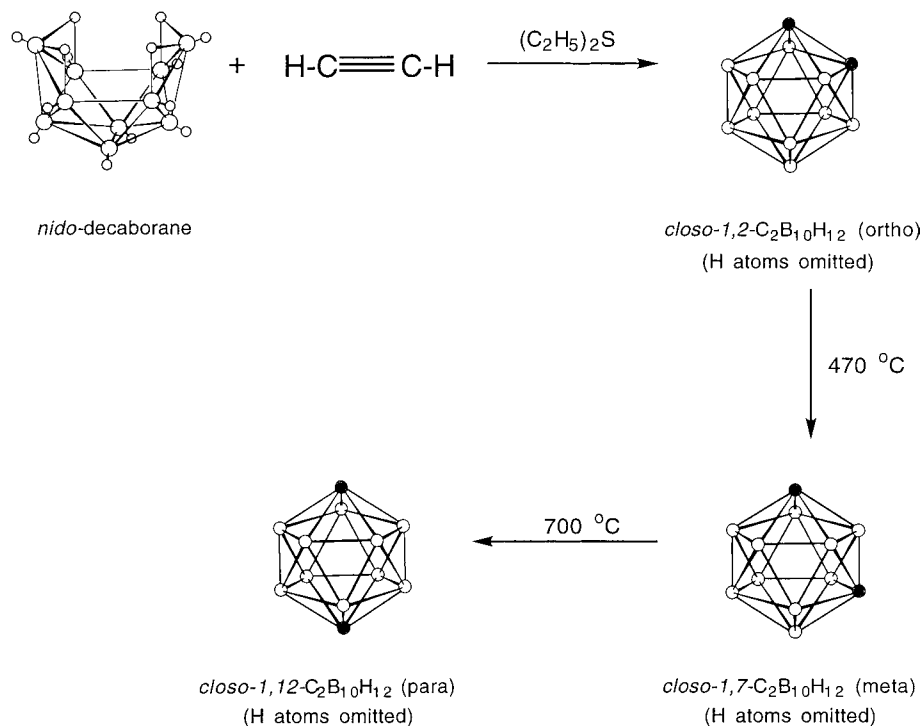


FIGURE 27 Synthesis of *closo*-dodecacarboranes.

in the polyhedral cage structure. These oligomers are generally unaffected by atmospheric oxygen and moisture. Some of the materials are thermally stable to 500°C. A particularly important group of carboranes are the derivatives of *closo*-decaborane. These compounds are prepared from *nido*-decaborane and acetylene in the presence of ethyl sulfide (Fig. 27). The primary product of the reaction is *closo*-1,2- $\text{C}_2\text{B}_{10}\text{H}_{12}$ (*ortho* isomer). The *ortho* isomer undergoes rearrangement at 450°C to *closo*-1,7- $\text{C}_2\text{B}_{10}\text{H}_{12}$ (*meta* isomer), and at 700°C to *closo*-1,12- $\text{C}_2\text{B}_{10}\text{H}_{12}$ (*para* isomer). The H atoms attached to the electropositive carbons, like acetylene, are acidic. Thus the C–H bonds may be metallated with reagents like *n*-BuLi. The lithiated derivative reacts with nucleophiles to produce a wide variety of organometallic products. For example, the reaction of the *meta* isomer with a dichloro end-functional oligomeric siloxane will give a carborane–siloxane copolymer (Fig. 28). Some of these materials are commercially available (Dexil[®]) as rubbers and resins. They preserve their elasticity and mechanical properties at low temperatures, and are thermally stable to 600°C.

3. Boron–Nitrogen and Boron–Oxygen Polymers

Nonoxide, solid-state ceramics of boron and nitrogen (boron nitrides) are of commercial interest owing to their chemical inertness and robust physical, mechanical,

and thermal properties. BN materials have applications as ceramic coatings, fiber-reinforced plastics, and bulk composites. Boron nitride may be obtained from simple reagents such as elemental B and N_2 or B_2O_3 and NH_3 , using high-energy reaction conditions (Fig. 29). Boron nitride prepared in this manner has a hexagonal crystalline form (α form) of planar sheets with six-member fused rings containing alternating B–N bonds. The structure is similar to graphite except (1) the layers are directly aligned (as opposed to offset) with the B on one sheet directly over the N on the neighboring sheet and (2) the sheets are closer together (1.45 Å vs. 3.35 Å in graphite). There are also salient differences in some of the physical properties of α -BN. For example, α -BN is colorless and an electrical insulator, whereas graphite is black and an electrical conductor. However, the lamella layers in both α -BN and graphite easily slip past one another, giving rise to their lubricity.

α -BN undergoes structural reorientation to the more dense β -BN (cubic) form when heated under pressure. The boron atoms in the cubic form occupy tetrahedral sites in the crystal lattice analogous to carbon in diamond. Thus β -BN is extremely hard, second only to diamond, and is used industrially as a high-temperature abrasive.

Alternate synthetic routes to boron nitrides through BN-containing oligomers and preceramic polymers have been developed. For example, pyrolysis of poly(borazylene),

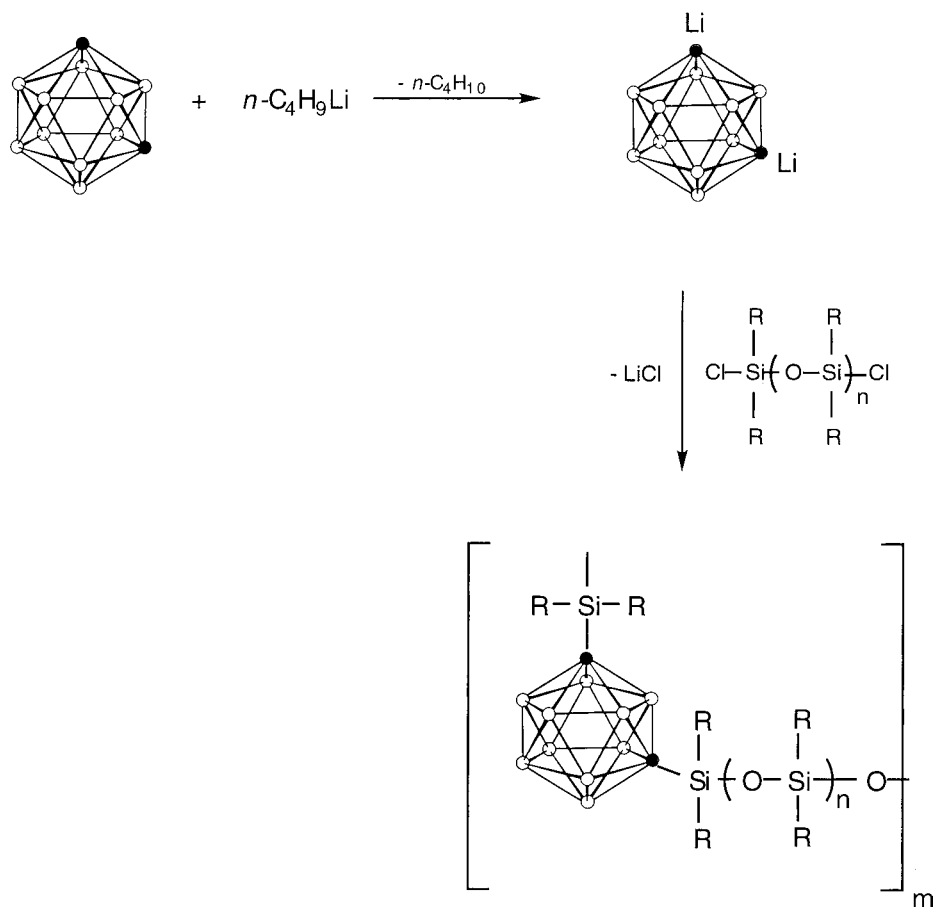


FIGURE 28 Synthesis of carborane-siloxane copolymer.

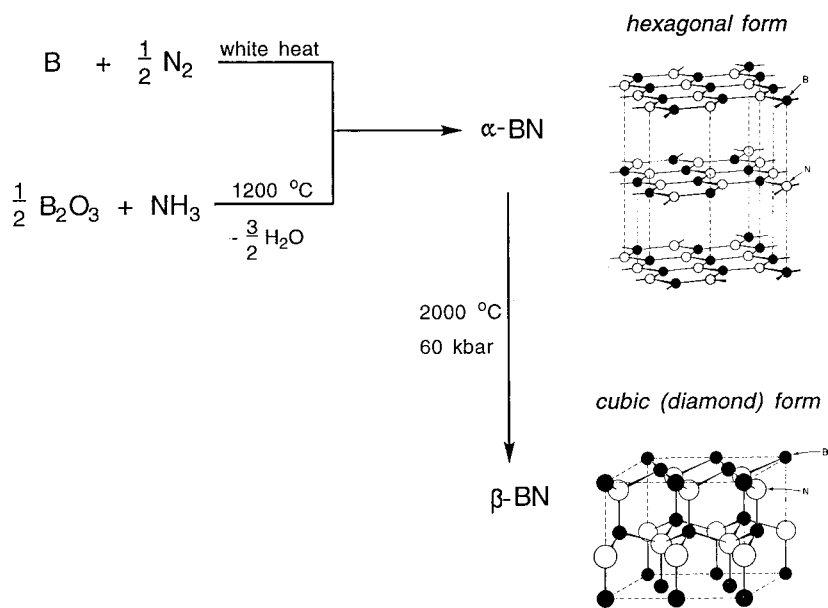


FIGURE 29 Synthesis of α - and β -BN.

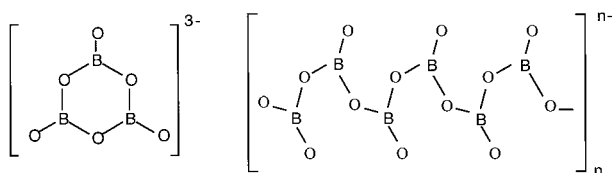
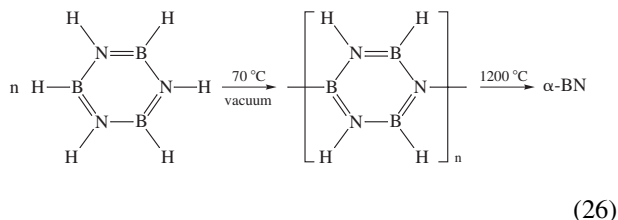


FIGURE 30 Boron–oxygen polymers.

which is prepared by warming liquid borazine under vacuum, gives α -BN [Eq. (26)]:



The advantage of preceramic polymers is that they are soluble in polar solvents, readily purified, and produce ceramic materials in high purity and high yield.

Like silicon, boron forms a large number of anionic oligomers and polymers with oxygen (borates). Some of these anions have been well characterized. For example, anhydrous metal metaborates have the general formula $M_x(\text{BO}_2)_y$. These polymeric salts are stable at atmospheric pressure and contain the cyclotrimeric $\text{B}_3\text{O}_6^{3-}$ anion or the infinite linear $(\text{BO}_2)_n^-$ anion where each B atom is trivalent (Fig. 30). At high pressures, however, they undergo reorganization to tetravalent boron with a zinc-blend superstructure.

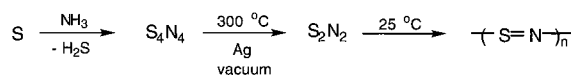


FIGURE 31 Synthesis of polythiazyl.

D. Other Main Group Element Polymers

1. Heteroatom–Sulfur Polymers

Catenated sulfur polymers were discussed earlier. The low cost and ready supply of sulfur has led to the development of a number of heteroatom polymers involving sulfur with other main group elements (e.g., N, C, O, P, B, etc.). Several examples with their applications are given in Table IV.

A particularly interesting polymer of sulfur and nitrogen known as polythiazyl or poly(sulfur nitride) is obtained by the sequence of reactions illustrated in Fig. 31. The polymer is crystalline and fibrous like asbestos. It has a gold-luster color when viewed perpendicular to the chain axis and behaves in many ways like a metal: high malleability, reflectivity, and electrical conductivity at room temperature. Moreover, it exhibits anisotropic superconductivity at 0.26 K. The conductivity has been explained in term of the polymer structure (Fig. 32) and bonding in which long S–N chains assume a *cis–trans–planar* conformation with π -bond delocalization along the chains and from S–S, S–N, and N–N orbital overlap between adjacent chains. Polythiazyl absorbs bromine to produce $(\text{SNBr}_x)_n$ ($x = 0.25\text{--}0.40$), a black, fibrous polymer with increased conductivity. Despite their unusual properties, polythiazyls have not been commercialized because of their oxidative and thermal instability in air and their tendency to detonate with heat and pressure.

TABLE IV Sulfur-Containing Polymers and Applications

Polymer	General formula	Applications
Poly(thioethers)	-(R-S)-_n	Engineering plastics, elastomers, photoresists, optical filters, heat-resistant adhesives
Poly(thiazoles)		Conducting polymers, heat-dissipating coatings
Poly(sulfamides)	-(N-S-C(=O)-R)-_n	Coatings for imaging paper
Poly(thiophenes)		Antistatic coatings and films, biosensors, storage batteries
Poly(sulfones)	-(R-SO2)-_n	Engineering plastics

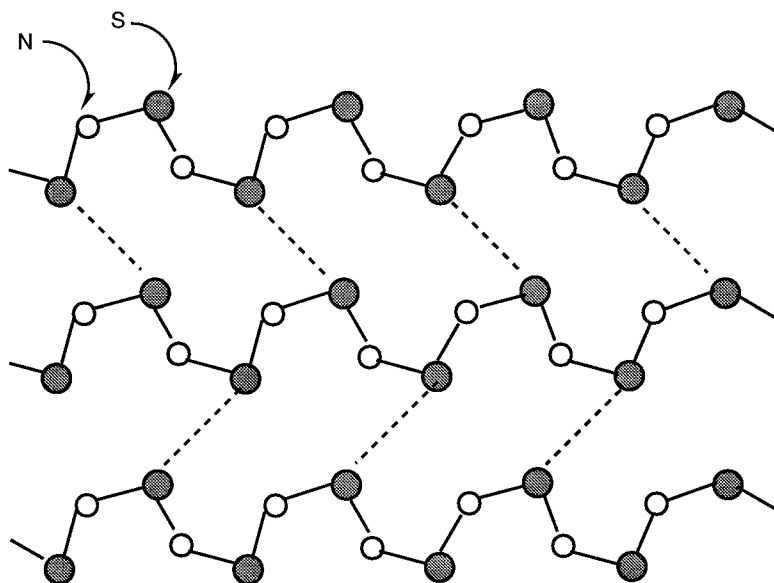
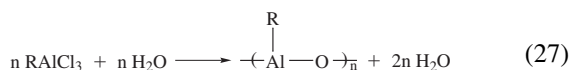


FIGURE 32 Structure of polythiazyl.

2. Aluminum-Containing Polymers

Aluminum forms heteroatom oligomers and polymers mainly with oxygen and nitrogen. The Al–O polymers are formed by (1) hydrolysis of multifunctional alanes (R_nAlX_{3-n} , $n = 0, 1$; R = organic; X = Cl, OR) to give poly(organoaloxane)s [Eq. (27)] or (2) the reaction of trialkyl- or trialkoxyalanes with organic acids to give poly(acyloxyaloxane)s (Fig. 33A, B):



In the latter reaction, an excess of carboxylic acid or chelating reagent such as acetylacetonate (Fig. 33C), diol, or aminoalcohol produces a more soluble, higher MW, and processible material. The bulk of the evidence suggests that the products are highly crosslinked network structures. These preceramic polymers are used to prepare high-performance alumina (Al_2O_3) fibers. Generally, Al–O polymers range from gums to brittle solids. In addition

to ceramic fibers, they have applications as lubricants, fuel additives, catalysts, gelling and drying agents, water repellants, and additives to paints and varnishes. If oxygen in the backbone is replaced with NH or NR, the polymers are thermally unstable and sensitive to acids, bases, and water.

A variety of Al–O–Si–O polymers, poly(alumino-siloxanes), with Si:Al ratios from 0.8 to 23, are known. These materials are prepared by the reaction of sodium oligo(organoaloxane)s with $AlCl_3$ [Eq. (28)]:

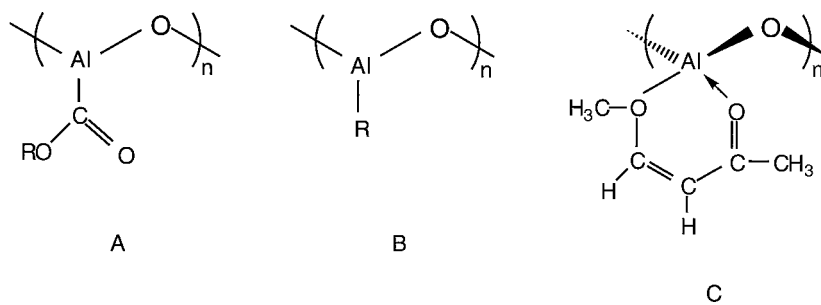
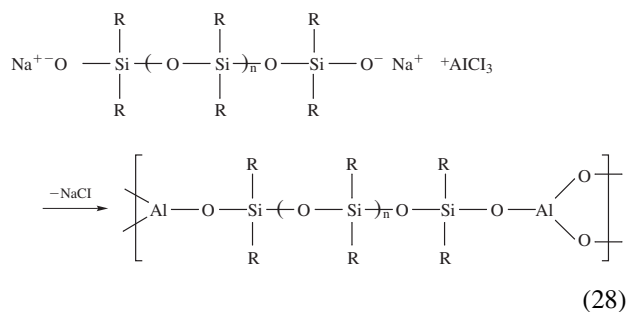


FIGURE 33 Al–O polymer repeating units.

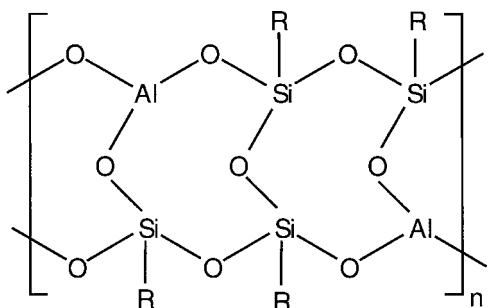


FIGURE 34 Poly(aluminosiloxane) ladder polymer.

If a trifunctional silane is used, the Si:Al ratio is larger than 7 and a soluble polymer, believed to have a ladder structure, is obtained (Fig. 34).

The aluminosilicates are anionic polymers that are present in natural and synthetic minerals where Al(III)

ions replace Si(IV) in the lattice. Examples of 2D sheet aluminosilicates are clays, micas, and talc. Feldspar and zeolites (molecular sieves) are 3D network structures in which AlO_4 and SiO_4 units share tetrahedral vertices. The cavities created in these network polymers are accommodated by cations such as Na^+ and K^+ . Depending on the size of the cavity, these cations can be displaced by other cations, hence their use as ion exchange materials. Moreover, by synthetically controlling the size and shape of the cavity, small molecules like water, methanol, or gases can be selectively trapped. Thus these materials are used in laboratory and industrial separations and purification processes (Table V).

3. Tin-Containing Polymers

Polystannanes as analogs to polysilanes were mentioned earlier. There are also a number of heteroatom polymers of

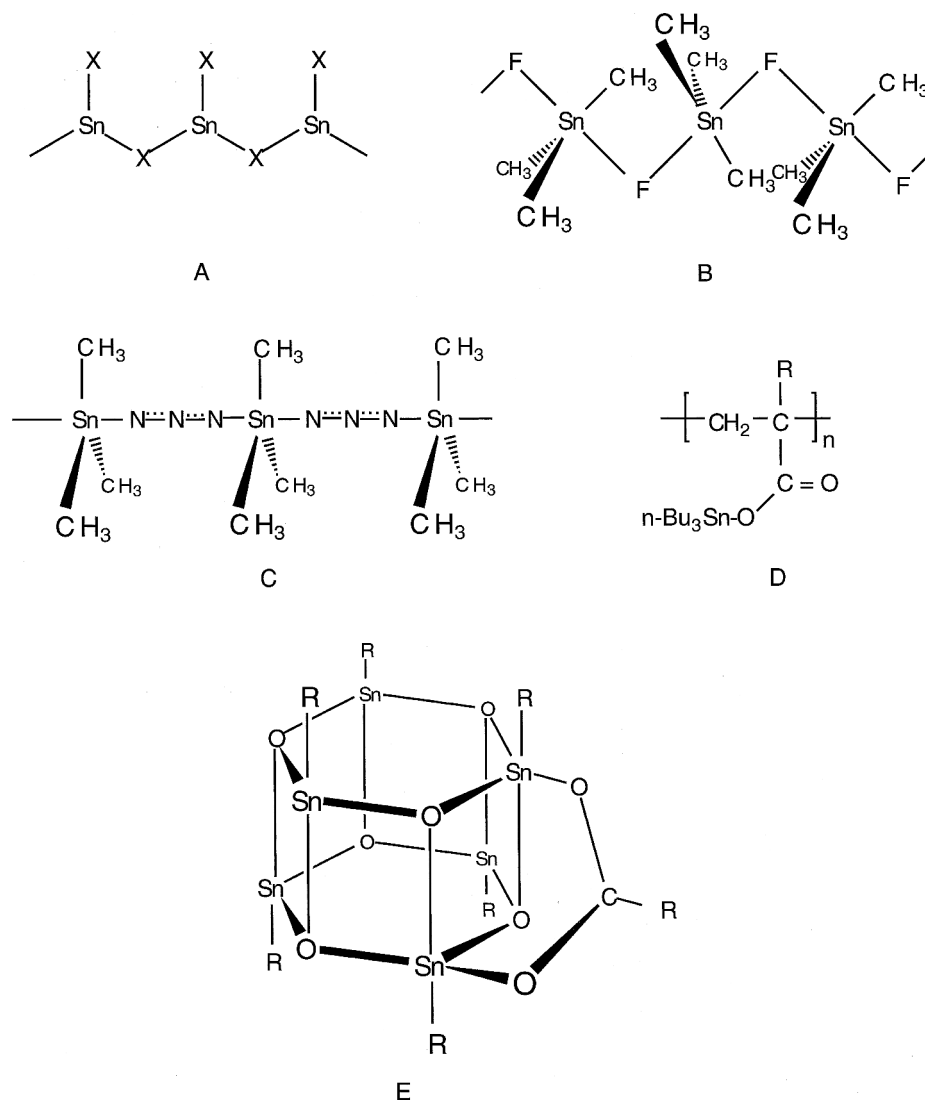


FIGURE 35 Heteroatom tin-containing polymers.

TABLE V Some Common Aluminosilicate Minerals, General Formulas, and Applications

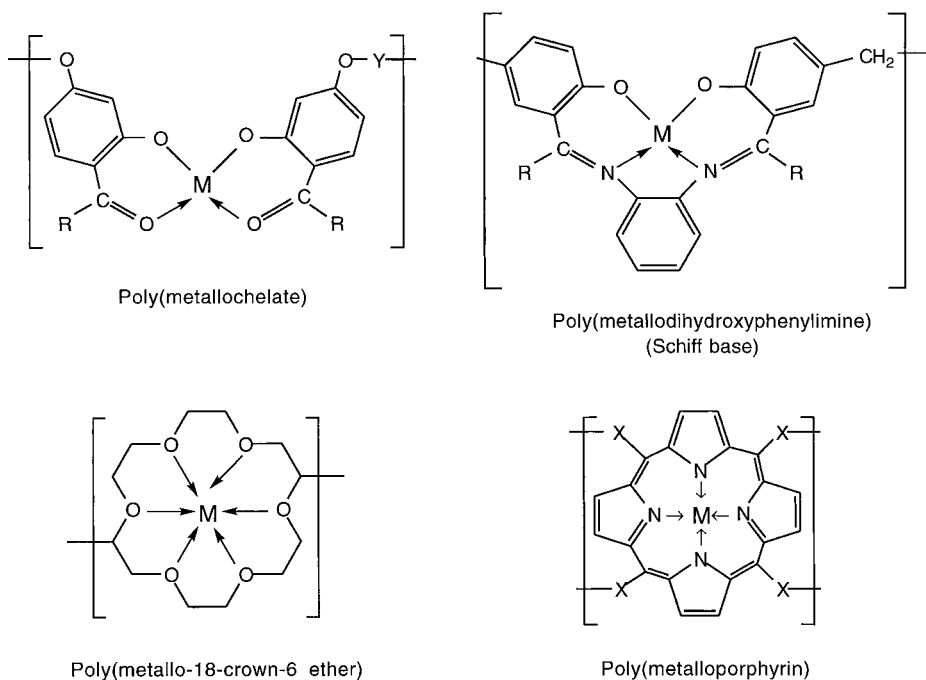
Structural type	Example	General formula	Applications
Sheet	Mica	$K(\text{Mg}, \text{Fe})_3(\text{HO})_2\text{AlSi}_3\text{O}_{10}$	Electronics (capacitors, diodes), cosmetics (powders)
3D	Feldspar	$K[(\text{AlO}_2)(\text{SiO}_2)_3]$	Glass, ceramics, semiprecious stones
	Zeolites	$\text{Na}_{13}\text{Ca}_{11}\text{Mg}_9\text{KAl}_{55}\text{Si}_{137}\text{O}_{384}$	Water softener, gas separation and purification
	Molecular sieves (A)	$\text{Na}_{12}[(\text{AlO}_2)_{12}(\text{SiO}_2)_{12} \cdot x\text{H}_2\text{O}]$	Small-molecule (4 Å) absorber (e.g., H_2O)
	Molecular sieves (X)	$\text{Na}_{86}[(\text{AlO}_2)_{86}(\text{SiO}_2)_{106} \cdot x\text{H}_2\text{O}]$	Medium-molecule (8 Å) absorber (e.g., CH_3OH)

tin in which tin is part of or pendant to the polymer backbone. Examples of the former are $\text{Sn}^{\text{II}}\text{X}_2$ ($\text{X} = \text{Cl}, \text{OCH}_3$), which has an extended chain structure of three-coordinate Sn with two $-\text{X}-$ units in the chain (Fig. 35A), and $(\text{CH}_3)_3\text{Sn}^{\text{IV}}\text{Y}$ ($\text{Y} = \text{F}, \text{azide}$), which is a strongly associated polymer of five-coordinate Sn with $-\text{Y}-$ units forming bridges between tin moieties (Fig. 35B, C). $(\text{CH}_3)_2\text{Sn}^{\text{IV}}\text{F}_2$ forms a 2D infinite-sheet structure in which each Sn is in an octahedral environment with the methyl groups lying above and below the plane of the sheet and the F atoms forming bridges to four Sn atoms. Other types of tin-containing polymers with $-\text{Sn}-\text{O}-\text{M}-$ ($\text{M} = \text{Si}, \text{Ti}, \text{and B}$) units in the chain have also been prepared. Some of these polymers have uses as plasticizers, fungicides for paints, fillers and reinforcing agents, and resin additives to enhance thermal and mechanical properties.

Vinyl esters such as tributyltin methacrylate can undergo polymerization to poly(tributyltin methacrylate)

(Fig. 35D) using free radical, ionic, or coordination catalysts. These polymers have the Sn moiety pendant to the polymer backbone. Some of these polymers readily release the tin moiety in water and have potent antifouling, antifungal, and antibacterial properties. However, their toxicity to the environment has precluded widespread commercial applications. In an effort to circumvent the rapid hydrolytic release problem, styrene polymers with $n\text{-Bu}_3\text{Sn}$ bonded directly to the phenyl group have been prepared.

Unusual “cage” oligomeric organotin carboxylates that are prepared by the condensation of organostannoic acids with carboxylic acids or their salts are mainly tetramers and hexamers with formula $[\text{RSn}(\text{O})\text{O}_2\text{CR}']_{4 \text{ or } 6}$. Evidence suggests that the reaction proceeds through the formation of ladder type intermediates (see Fig. 6) prior to closure to yield a stable drum-shaped product (Fig. 35E; only one of six carboxylate units is shown).

**FIGURE 36** Examples of transition metal coordination polymers.

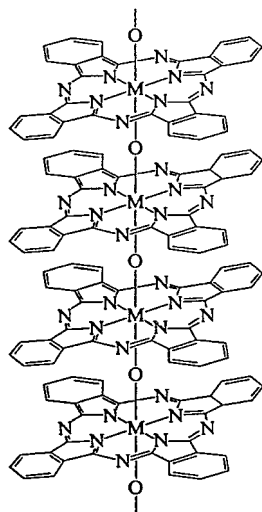


FIGURE 37 Metallophthalocyanine (*shish kebab*) polymers.

IV. INORGANIC POLYMERS WITH TRANSITION METALS

A. Transition Metal Coordination Polymers

There are numerous examples of inorganic polymers with transition elements. These polymers have the metal as an integral part of or pendant to the polymer backbone. Generally the metal is attached to a ligand (L) by one or more σ -coordinate covalent bonds ($M \leftarrow L$) through heteroatoms such as O, N, P, or S on L. The polymer arises by connecting metal units through the ligands. Examples of coordinating ligands are polydentate chelating compounds such as porphyrins, phthalocyanines, phosphinates, β -diketonates, dioximes, Schiff bases, and crown ethers. Several coordination polymers with different ligands are shown in Fig. 36.

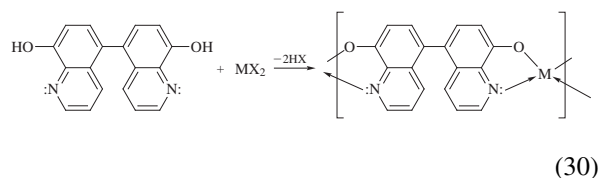
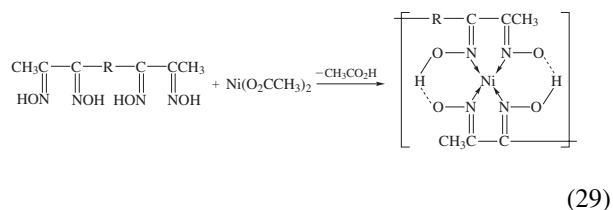
Two interesting cases are worth noting:

1. The poly(metallophthalocyanine) (*shish kebab*) polymers in which $M = \text{Si}$, Ge , Sn , or Ni . These polymers are made up of planar phthalocyanine units with the N atoms tetracoordinated to M. The macrocycles are stacked one dimensionally through metal-oxo bonds (Fig. 37). The materials are prepared by dehydration

of the metallophthalocyanine dihydroxide. Similar polymers with S, Se, and Te as bridging atoms are known and are soluble in strong acids. Moreover, they have favorable dynamic-mechanical properties comparable to polyamides (e.g., Kevlar®). If doped with iodine, *shish kebab* polymers exhibit potentially useful magnetic, electronic and optical behavior.

2. The molecular photonic wire composed of a zinc-porphyrin chain with a boron dipyrromethane group at one end and a free base porphyrin at the other end (Fig. 38). This oligomer is photochromic and absorbs blue-green light at boron and emits red light at the uncomplexed site. Such macromolecules have potential as *molecular wires* in molecular devices.

A general method of preparing coordination polymers involves the reaction of the free metal, metal salt, or metal complex with a polydentate ligand. For example, the reaction of nickel acetate with *bis*(1,2-dioxime) gives a polymer with tetracoordination of the ligand nitrogen atoms with nickel (Eq. 29). Metal-containing polymers with two or more different atoms of the ligand bonded to the metal are also possible (Eq. 30).



To date, owing to their low solubility, aggregation to give intractable solids, and difficulty in processing, there are relatively few commercial applications for coordination polymers. Some materials have found promise as nonlinear optical materials, electrical conductors, photosensitive coatings and films, and bioactive releasing agents. For

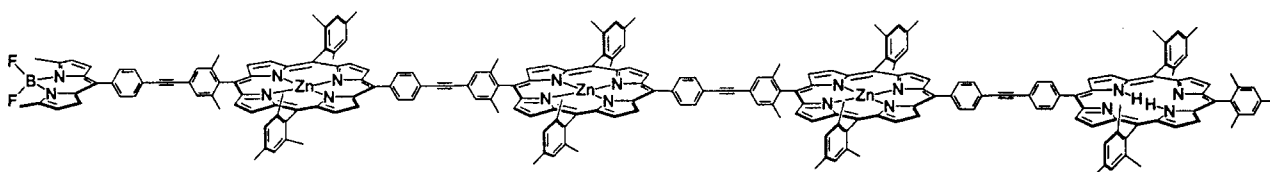


FIGURE 38 Zinc-porphyrin (*photonic wire*) polymer.

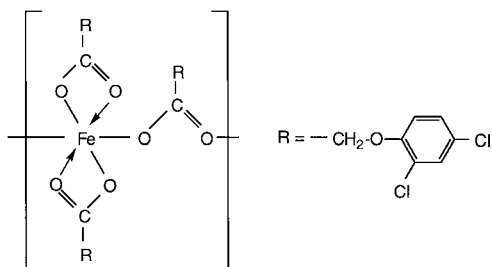


FIGURE 39 Iron-containing coordination polymer with herbicidal properties.

example, the herbicide 2,4-dichlorophenoxyacetic acid forms a coordination polymer with iron (Fig. 39) that slowly and effectively releases the bioactive agent in soil. The metallic by-product is nontoxic.

B. Metallocene Polymers

Metallocenes are organometallic compounds that contain a metal atom (e.g., Fe, Cr, Ti, Mn, etc.) “sandwiched” between two aromatic cyclopentadienyl (Cp) rings. Metallocene polymers are constructed by extending a chain either through one (homoannular) or both (heteroannular) Cp rings (Fig. 40A, B). In addition, polymers have

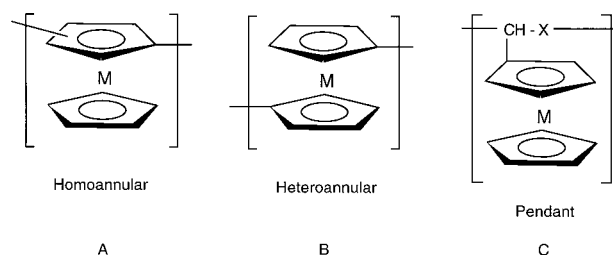
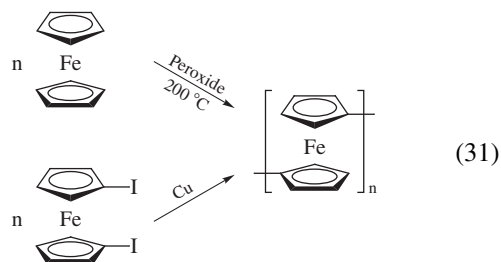


FIGURE 40 Polyferrocenes. (A) Homoannular. (B) Heteroannular. (C) Pendant.

been synthesized with the metallocene group pendant to a hydrocarbon chain (Fig. 40C).

Although metallocenes have been made with many different metals, current work and commercial applications have focused mainly on $M = \text{Fe}$ (ferrocene). Therefore, this section will explore the synthesis and properties of polyferrocenes. The great interest in polyferrocenes stems from the variety of their useful properties (e.g., high thermal stability, radiation resistance, diversified chemistry, high energy content, and, recently, catalytic activity). There are numerous examples of ferrocenyl polymers as constituent parts of elastomers, adhesives, electron transfer resins, semiconductors, UV absorbers, solid-propellant additives, combustion activators, heat transfer fluids, lubricants, and antioxidants.

Polyferrocenes were first obtained by heating ferrocene in the presence of a free radical catalyst [Eq. (31)]. Although the product was stable to 400°C , the yields were low ($\sim 10\%$) and the polymer had a relatively low MW (< 3000). Grignard and Wurtz-type coupling reactions on 1,1'-diiodoferrocene have improved yields considerably ($> 80\%$); however, the degree of polymerization remained low.



Since the Cp functionality has aromatic properties, it undergoes electrophilic substitution reactions in much the same manner as benzene. Therefore, many ring-containing derivatives can be synthesized for use in step-growth, chain-growth, and ring-opening polymerization

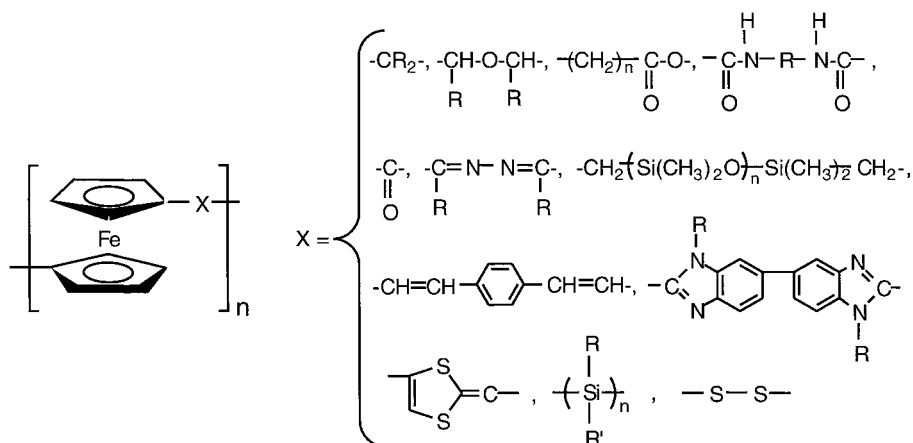
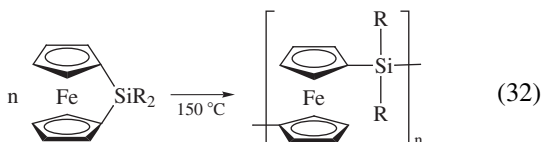


FIGURE 41 Polyferrocenes with various bridging groups.

(ROP) reactions. Thus polyferrocenes with alkyl, ester, amide, urea, urethane, ether, sulfur, siloxyl, and other functionalities between ferrocenyl units have been reported. Some examples are given in Fig. 41. For example, poly(ferrocenylmethylene) has been obtained with MW 20 000.

High-MW, soluble, film-forming polymers as well as random and block copolymers with $-\text{SiRR}'_2-$ units (R , $\text{R}' = \text{H}$, alkyl, aryl) bridging the ferrocenyl groups can be prepared by anionic or ROP at moderate temperatures [Eq. (32)]:



MW values ranging from 10^5 to 10^6 have been obtained. These polymers exhibit electrochromism, photoactivity, and semiconductor behavior.

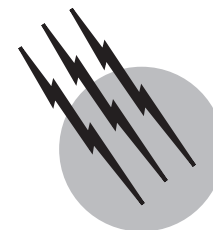
SEE ALSO THE FOLLOWING ARTICLES

BIOPOLYMERS • MACROMOLECULES, STRUCTURE • ORGANOMETALLIC CHEMISTRY • POLYMER PROCESS-

ING • SILICONE (SILOXANE) SURFACTANTS • SOL-GEL PROCESSING

BIBLIOGRAPHY

- Laine, R. M., Sanchez, C., Brinker, C. J., and Giannelis, E. (eds.). (1998). "Organic-Inorganic Hybrid Materials," Materials Research Society, Warrendale, PA.
- Mark, J. E., Allcock, H. R., and West, R. (1992). "Inorganic Polymers," Prentice Hall, Englewood Cliffs, NJ.
- Mark, J. E., Lee, C. Y.-C., and Bianconi, P. A. (eds.). (1995). "Hybrid Organic-Inorganic Composites," American Chemical Society, Washington, DC.
- Pittman, C. U., Jr., Carraher, C. E., Jr., Zeldin, M., Sheats, J. E., and Culbertson, B. M. (eds.). (1996). "Metal-Containing Polymeric Materials," Plenum Press, New York.
- Sheats, J. E., Carraher, C. E., Jr., Pittman, C. U., Jr., Zeldin, M., and Currell, B. (eds.). (1990). "Inorganic and Metal-Containing Polymeric Materials," Plenum Press, New York.
- Wisian-Neilson, P., Allcock, H. R., and Wynne, K. J. (eds.). (1994). "Inorganic and Organometallic Polymers II. Advanced Materials and Intermediates," American Chemical Society, Washington, DC.
- Zeldin, M., Wynne, K. J., and Allcock, H. R. (eds.). (1987). "Inorganic and Organometallic Polymers," American Chemical Society, Washington, DC.
- Ziegler, J. M., and Fearon, F. W. (eds.). (1990). "Silicon-Based Polymer Science," American Chemical Society, Washington, DC.



Polymers, Mechanical Behavior

Garth L. Wilkes

Virginia Polytechnic Institute and State University

- I. Introduction
- II. Types of Deformation
- III. Important Stress–Strain Deformation Parameters
- IV. Effect of Temperature on Stress–Deformation Behavior
- V. Time and Temperature with Respect to Molecular Considerations
- VI. Stress Relaxation and Creep Behavior
- VII. Effect of Crystallinity on Properties
- VIII. Effect of Covalent Cross-Linking
- IX. Effect of Fillers on Mechanical Behavior
- X. Molecular Orientation and Anisotropic Systems
- XI. Miscellaneous Considerations and Final Remarks

GLOSSARY

Bulk modulus In the limit of small pressures, it represents a change in hydrostatic pressure with change in volume when a material is placed under hydrostatic loading. This parameter is related to the compressibility of a material.

Deborah number D_e Dimensionless parameter related to the ratio of the molecular relaxation time of a material to that of the time frame over which the material is observed, that is, the experimental time window.

Engineering stress Force obtained in extension divided by the sample's original cross-sectional area.

Extension ratio Variable expressing how a given dimension is changing in a sample with deformation; defined as the deformed length divided by the undeformed length in the same direction.

Glass transition temperature T_g Important parameter that is related to the temperature at which the onset of cooperative segmental motion occurs for a polymer

within the time frame of the experiment. It applies only to amorphous regions of a material.

Loss modulus Parameter that is related to the viscous dissipation of a material undergoing small cyclic deformations; generally obtained by dynamic mechanical spectroscopy techniques.

Mechanical hysteresis Important parameter that is related to the amount of energy dissipated during cyclic deformation. No hysteresis would be obtained if the unloading stress–strain profile were identical to the loading profile.

Permanent set Parameter that is related to the degree of irrecoverable flow that exists after a material has been deformed in either shear or tension.

Poisson's ratio Variable indicating whether a material undergoes dilation during extensional deformation; usually denoted by μ .

Secant modulus Slope of the line that extends from the origin of an engineering stress–strain curve and intersects that curve at a given elongation. The secant

modulus must be specified with respect to the degree of deformation.

Shear modulus Initial slope of a shear stress–shear strain deformation curve; an indication of the resistance to deformation by shear.

Storage modulus Parameter that is related to the elastic behavior of a material when undergoing small cyclic deformations; generally obtained by dynamic mechanical spectroscopy.

Strain Variable expressing how the dimensions of a material change under deformation.

Tensile strength Engineering stress at the point of sample failure. In the case of sample tearing, generally the peak value of the engineering stress is quoted as the tensile strength.

Thermal mechanical spectrum Graphic representation of a specific mechanical property as a function of temperature in which the data have been obtained under the same loading rate. Generally, either the dynamic storage or loss modulus is reported. These values are obtained by either dynamic shear or extensional methods.

True stress Force of deformation obtained in extension divided by the cross-sectional area that exists at the elongation at which the stress is determined.

THE MECHANICAL BEHAVIOR of a material extends from its stress–deformation response, in which the mode of deformation (uniaxial, biaxial, etc.) is particularly important to define, as are the loading profile and environment under which a given test is carried out. Often in the application of polymeric materials, the mode of failure may be induced by a more complex loading scheme than is easily applied within a testing laboratory. However, it is important to develop, where possible, a basic understanding of the properties of any new polymeric material through a well-defined loading profile and to learn how these properties depend on molecular or “system” variables as well as the nonmolecular or “external” variables mentioned above.

I. INTRODUCTION

The mechanical behavior of polymeric materials is a vast subject and one that is particularly important for the practical application of these materials. Often it is the mechanical properties, in conjunction with economics, that dictate whether a given polymeric material can be utilized for a specific purpose. Other properties, such as optical transparency and dielectric behavior also play a significant role, but this article focuses only on the basics of mechanical properties and, in particular, the means by which

these properties are measured and expressed. In addition, some of the molecular origin of the observed behavior is considered following basic definitions. Because of space limitations, only the basics are provided; hence, only the terminology and general characteristics of different behavioral patterns of polymers in terms of their response to internal (macromolecular) variables, such as molecular weight, chain topology, cross-linking, and crystallinity, will be considered along with the influence of external parameters, such as temperature, time, and pressure, the former two being of extreme importance.

Before we address the mechanical parameters and their definition, a few comments are in order concerning the molecular systems that we will be discussing. In particular, polymeric or macromolecular systems are composed of long chains whose backbone is made up either of like units (homopolymers) or of varied units (copolymers, terpolymers, etc.), and if only two distinct ends are present the system is said to be linear. In many cases macromolecules are not linear but may possess branches, which are short or long, depending on the procedures used to synthesize these materials. These branches can have a considerable effect on mechanical properties since randomly placed branch points will not fit into a crystal lattice. Therefore, the percentage of crystallinity is decreased by branching in those systems that have otherwise suitable chain symmetry to pack into a lattice. In addition, these branch points also influence the general flow properties of the system in melt processing or solution processing particularly if the branches are long enough to undergo entanglement with neighboring chains. Network structures are also common due to cross-linking between chains if the reactants have sufficient functionality to promote network development at high conversion.

Many of the polymers utilized today in the marketplace such as polyethylene, polypropylene, polystyrene, styrene–butadiene rubber, and polymethyl methacrylate are viewed as flexible or coil-like chains. This is due to the ease of bond rotation in these covalently connected repeat units, which can occur under appropriate conditions and are in contrast to rigid rod polymers where ease of bond rotation is highly limited at any reasonable temperature at which the system would be used or processed. It is important to recognize the general “long-chain” nature of many of these materials. As an example, consider a polyethylene molecule of 100,000 molecular weight. What would be the necessary tube length and tube diameter to place this molecule into if one were to stretch it out in its fully extended form (see Fig. 1)? For that molecular weight a first-approximation calculation would show that this number (length/diameter), or aspect ratio of the molecule, is of the order of 1800. This number far exceeds the same aspect ratio that would be obtained for

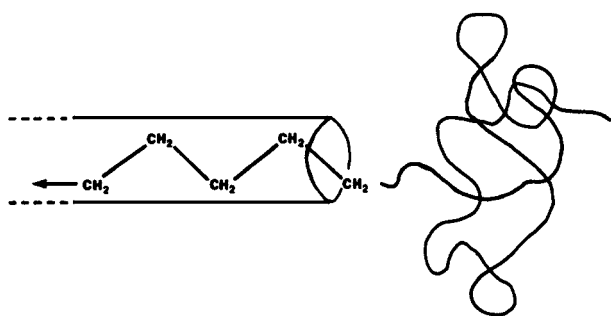


FIGURE 1 General schematic showing how a coiled polyethylene molecule might be extended into a rodlike shape.

a strand of spaghetti, which is often used as an analogy to linear polymer molecules. This long threadlike nature or high aspect ratio is an important feature, for it leads to the physical entanglement of a given molecule with many of its neighbors through the intertwining or interweaving of one molecule with several others including itself. The consequences of these entanglements and the time-dependent behavior of these molecules becoming unentangled or changing their *entanglement density* are discussed in Section V. It should be recognized, however, that in the above-calculated estimate of aspect ratio, a rather “skinny” chain was utilized. If one were to carry out the same calculation for a 100,000 molecular weight polystyrene molecule that contains bulky phenyl groups on alternate carbons, the same calculation would lead to a much smaller aspect ratio, this being about 240. However, even this number is still greater than the typical aspect ratio for a strand of spaghetti!

Another important feature of molecular systems is that their behavior under a given set of loading conditions is very dependent on a balance of three types of energy: (1) intramolecular, which is related to energy changes involved with bond rotations within the backbone and other types of intramolecular interactions such as changes in secondary bonding that occurs between atoms or groups within the same molecule; (2) intermolecular, which results from the energies concerned with secondary bonding but is now between groups or atoms or different molecules; and (3) thermal energy, which is dictated by the product kT , where k is the Boltzmann constant and T is absolute temperature. When T is ~ 300 K (ambient), the value of RT , where R is the molecular gas constant, is of the order of 0.6 kcal/mol. This may be contrasted with van der Waals energies involved with secondary bonding, which are of the order of 2 to 3 kcal/mol, while stronger hydrogen bonding may reach levels of the order of 7 to 11 kcal/mol. The intramolecular bond rotation energies or more specifically the difference between various rotational isomeric states may be as little as a fraction of a kilocalorie per mole to many kilocalories per mole. The lower this value

the more flexible the chain is and the easier it will be for it to undergo changes in its conformation. As expected, the bond rotational potential energies will be a function of the steric hindrance by side groups extending from the chain backbone. In the case of the presence of a double bond within the backbone, there is of course no rotation allowed about this type of bond. As we shall learn, temperature is a particularly important variable in the discussion of the mechanical properties of polymers; higher temperatures provide higher thermal energy (higher kT) and therefore permit higher degrees of thermal Brownian motion that may promote changes in the inter- and intramolecular energy states of the molecules.

The mechanical behavior of a material extends from its stress–deformation response, in which it is particularly important to define the mode of deformation (uniaxial, biaxial, etc.) and the loading profile and environment under which a given test is carried out. Often times in the application of polymeric materials, the mode of failure may be induced by a more complex loading scheme than is easily applied within a testing laboratory. However, it is important to develop, where possible, a basic understanding of the properties of any new polymeric material through a well-defined loading profile and to learn how these properties depend upon molecular variables and the external variables mentioned above. In this article, the general mechanical or stress–deformation responses of materials are often illustrated in this article in the form of a schematic diagram showing how this behavior may change with specific variables rather than by presenting actual experimental data.

Due to the macromolecular or chainlike nature of the components, the orientation of polymer chains may well occur during loading or may already exist within the system to be tested due to previous orientation inducement caused by such common fabrication schemes as fiber spinning, film drawing, and injection molding. Hence, it is important to recognize whether the material can be viewed as isotropic, that is, possessing equal properties in all directions, or whether it is anisotropic in that the properties are directionally dependent such as would occur if one were to test a previously oriented system, two common examples being a drawn monofilament or a deformed film. For the purposes of our discussion, emphasis will be placed on the mechanical behavior of isotropic systems; anisotropic systems will be discussed in Section IX.

II. TYPES OF DEFORMATION

There are three principal modes by which systems undergo deformation: (1) tensile or extensional deformation, (2) shear deformation, and (3) bulk or hydrostatic

deformation. In many tests, the loading profile can be analyzed in terms of a combination of the above, but for simplicity we shall discuss each of these separately; we shall place emphasis on the uniaxial mode of tensile deformation since this is a particularly common procedure for testing the mechanical response of a solid system. (Polymer fluids and their mechanical response are most often characterized by simple shear deformation.)

These three modes of deformation are sketched in Figs. 2a–c. Only a uniaxial deformation scheme is illustrated for tensile deformation, but biaxial or multiaxial tension behavior could occur. Furthermore, the shear deformation mode shown is that for simple shear in which a rotational component of the deformation exists, as is obvious if one “shears” a ball between one’s hands (i.e., rotation occurs). No such rotation occurs in the case of tensile deformation of the same ball; rather, the deformation leads only to the shape of an ellipsoid if uniaxial deformation is applied—a quite different phenomenon than for the simple shear. Thus, extensional deformation is an *irrotational* deformation. This is the first indication that there are likely to be differences in terms of the mechanical response of materials when placed under a tensile mode of deformation in contrast to simple shear. Clearly, bulk deformation carries no rotational component.

Referring to Fig. 2, let us define terminology that will help describe the mechanical response of the system. Considering uniaxial tensile deformation at this point, if one deforms a rubber band in this mode, there will be a positive

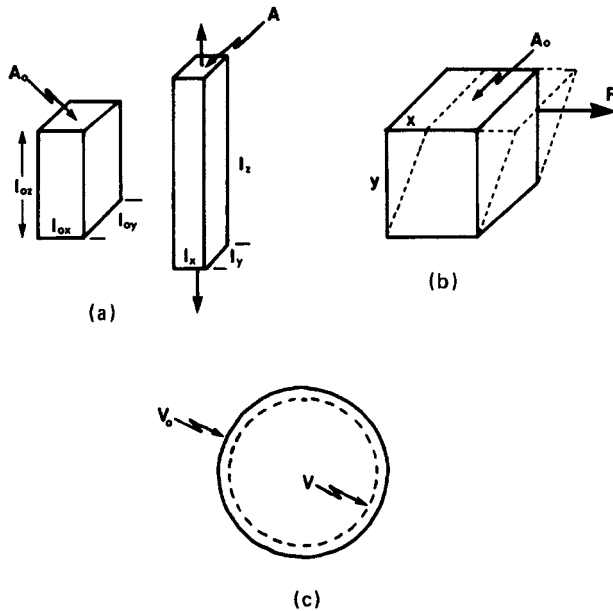


FIGURE 2 Three general types of deformation. (a) Tensile, (b) simple shear, and (c) bulk or hydrostatic compression.

force generated along the deformation axis that reflects the resistance to further deformation. If the amount or cross-sectional area of the rubber band is increased, the force will also increase for the same elongation. This suggests the need to normalize the size of the test specimen so that the results from specimens of different sizes can be compared. This is done by one of two approaches. The first and most common is to divide the measured force by the initial cross-sectional area of the test specimen. Referring to Fig. 2a, which shows deformation along the Z axis, this would be represented by dividing F by the product of $l_{0x}l_{0y}$. This product is the initial cross-sectional area, which we will denote by A_0 and which is *not* a function of deformation. This ratio of F/A_0 provides what is commonly known as the engineering stress σ_0 . Utilizing σ_0 rather than the values of force will, in principle, lead to the same result for the stress–elongation behavior of two identical materials irrelevant of their cross-sectional area.

A second means of defining stress is to use the true stress, denoted by σ_t . This parameter is defined as the force divided by the actual cross-sectional area A that exists at the time the force is determined. Generally A is a function of the degree of deformation, and this implies that it is necessary to determine the cross-sectional area over the entire deformation range if true stress is to be expressed. As indicated in Fig. 3, for any material that undergoes considerable deformation, such as a rubber band, there is an ever increasing difference between the true stress and the actual stress as deformation proceeds, because A is becoming smaller with respect to A_0 as elongation increases. The result is that, if one were to express the tensile strength (stress at break σ_B), there would be a considerable difference between these two values depending on which choice of stress were utilized; clearly the accurate value would be that based on the true stress. However, for the sake

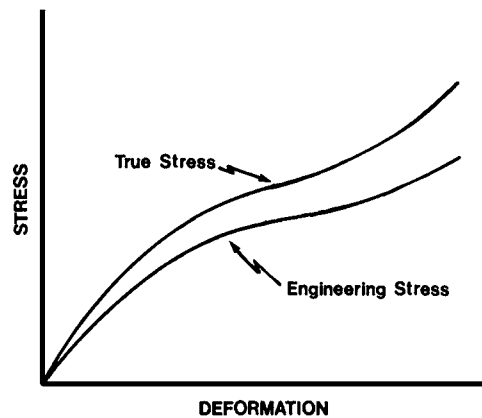


FIGURE 3 General plot of stress versus deformation showing the difference between true and engineering stress in a uniformly deforming system.

of convenience, it is common for results to be reported utilizing the engineering stress in contrast to true stress, thereby underestimating the actual stress at the time of failure for materials that show significant deformation. For specimens that undergo low deformation before fracture (e.g., glassy polystyrene), the difference between these two stress parameters is not great and of course becomes zero in the limit of no deformation. An important point here is related to the presentation of results; it would be misleading to report stress arbitrarily without specifying whether it is engineering stress or true stress. As will be discussed later, one may often be able to relate σ_t to σ_0 for homogeneous constant volume deformations. In the case of shear deformation, if simple shear is imposed, there is no change in the cross-sectional area and hence only a single stress value must be reported. This is conventionally denoted by τ (a shear stress) in contrast to σ (a tensile stress).

As an aside, the state of stress for any volume element of a system under load that is under stress can be described in terms of a tensorial representation, as indicated in Fig. 4, where the τ_{ij} terms are a simple means of representing the three “normal” stresses as well as the six shear stresses on this element, as indicated by the small double-subscripted components within the tensor. Although we will not need to utilize this tensorial representation in our basic discussions, it is important to recognize that the diagonal components of this tensor represent the stresses that act normal and along the principal axes of this volume element, whereas the six off-diagonal components are representative of the shear stress that act on a given face (first subscript) of which the shear direction is along the axis denoted by the second subscript. It can be shown that, through the coordinate rotation of the principle axes, symmetry can be maintained with the off-diagonal components, that is, $\tau_{ij} = \tau_{ji}$.

To express the magnitude of the deformation, we shall introduce four parameters. The first is denoted by ε and is called the engineering strain (it is also called the Cauchy strain by material scientists). Again, utilizing the tensile mode of deformation, the strain along a principal axis is given as

$$\varepsilon_i = (l_i - l_{0i})/l_{0i}, \quad (1)$$

where l_i represents the new length along the i th axis and l_{0i} represents its initial dimension before deformation. Similar values for the strain along the other two principal axes can also be specified. Generally, the strain value of interest is that along the principal deformation axis. Clearly, in the uniaxial deformation of a rubber band, this value of strain would increase from zero, whereas the two orthogonal strain values along the thickness and width direction would decrease to negative values as deformation occurs.

$$\text{STRESS} = \begin{vmatrix} \sigma_{11} & \tau_{12} & \tau_{13} \\ \tau_{21} & \sigma_{22} & \tau_{23} \\ \tau_{31} & \tau_{32} & \sigma_{33} \end{vmatrix}$$

(a)

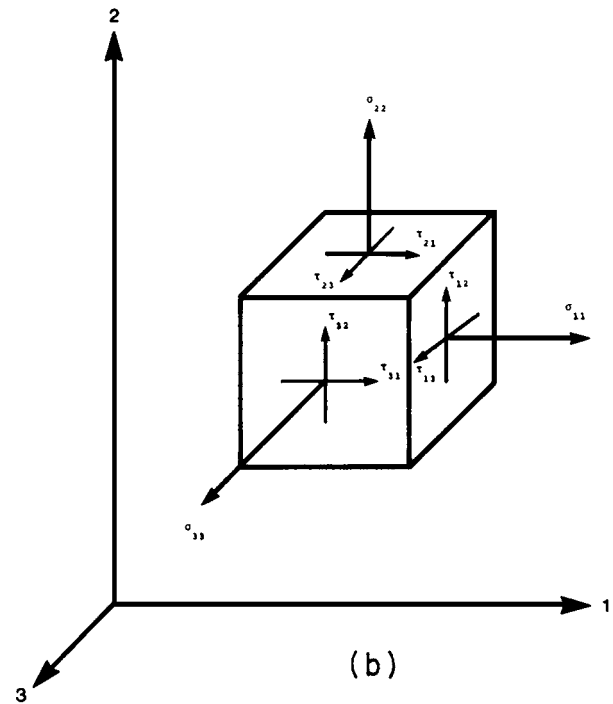


FIGURE 4 (a) Tensorial form of the representation of stress on a volume element of a material; σ_{11} , σ_{22} , σ_{33} , represent tensile or normal stress values, while the τ_{ij} values refer to shear stresses. (b) Three-dimensional representation of stress on a volume element.

In the case of simple shear (see Fig. 2b) the shear strain is expressed for small deformations as x/y , which again is a dimensionless number, as are the values of ε . In the case of shear strain, however, the common symbol is γ rather than ε . Note also from Fig. 2b that there would be no finite strains induced in the other two directions. For shear deformation, it is noted that for the same degree of movement in the shear direction (i.e., the x direction in Fig. 2b), the “thickness” of the element undergoing deformation influences the level of shear strain in a reciprocal manner. To illustrate this point further, if one considers adhering (gluing) two broken substrates together with a thin bond line, if the two substrate pieces are slid together with the polymeric adhesive between, although it may appear that little deformation has occurred for the adhesive material,

due to the thin bond line, considerable shear strain may well have been imposed.

Returning to tensile deformation, the principal strain or deformation direction is correlated to another common parameter that is often used to express the level of deformation, that is, the percent elongation:

$$\% \text{ elongation} = \varepsilon \times 100. \quad (2)$$

A third means of expressing deformation is to use the extension ratios or draw ratios, which we shall denote by λ_i . Three such values exist, one correlated to each of the principal axes. These are defined as

$$\begin{aligned} \lambda_x &= l_x/l_{0x}, \\ \lambda_y &= l_y/l_{0y}, \\ \lambda_z &= l_z/l_{0z}. \end{aligned} \quad (3)$$

In the limit of zero deformation, each λ_i takes on the value of unity, in contrast to 0 for the respective values of ε_i . Hence, there is a numerical factor of unity that relates λ_i to ε_i , that is,

$$\lambda_i = \varepsilon_i + 1. \quad (4)$$

There are certain relationships between the λ terms that are useful with regard to noting how the dimensions of a specimen change in a given deformation. In particular, for materials that undergo a constant-volume deformation, the product $\lambda_x\lambda_y\lambda_z$ is unity. In fact, good elastomers nearly follow this behavior, and since they deform uniformly (homogeneously), it can be shown that for uniaxial deformation along z

$$\lambda_x = \lambda_y = \lambda_z^{-1/2}. \quad (5)$$

The same approximation can often be used to define the deformation of many other materials, although some error is introduced, as pointed out in Section III.

Although the derivation will not be carried out here, it can be shown that if a constant volume homogeneous tensile deformation occurs be it uniaxial, biaxial, etc., then utilizing the fact that the product of the three extension ratios is unity, it follows that the true stress in a given principal deformation direction is equal to the engineering stress in that same direction multiplied by the respective extension ratio along that same axis. This can be a useful relationship to interconvert between true and engineering stress when the assumption of constant volume deformation is well approximated.

A final parameter describing the degree of deformation is the true strain ε_t . We establish this parameter by utilizing a differential form of our earlier definition of strain above, that is,

$$d\varepsilon_i = dl_i/l_i. \quad (6)$$

Integration of Eq. (6) leads to

$$\varepsilon_t = \ln(l/l_0). \quad (7)$$

One immediately notes that ε_t (also known as the Henky strain) is also given by the natural logarithm of the respective extension ratio for the corresponding axis. In the deformation behavior of polymeric systems, the true strain variable is not often utilized and it is more common for one of the other three parameters to be quoted. However, some data do exist in the literature in the form of true strain; this variable is quite different from the others due to its logarithmic nature.

III. IMPORTANT STRESS-STRAIN DEFORMATION PARAMETERS

The mode of tensile deformation will be used to elucidate some of the important parameters describing the mechanical properties of a material. Figure 5 is a general sketch of a common stress-strain response exhibited by many polymeric materials—particularly ductile semicrystalline materials like polyethylene or polypropylene. What can one extract from these data that might help convey the mechanical response of the system and that may be useful in deciding on the applicability of a given material? Often, the values of σ_b and ε_b (see Fig. 5) will be of importance since these are related to the stress at break and to the strain at break, the latter of which can now easily be converted to percent elongation, the extension ratio, or true strain at break. The values σ_y and ε_y are particularly important and should be distinctly noted if this “peak” occurs in the stress-strain response. The respective stress and strain correlated with this peak

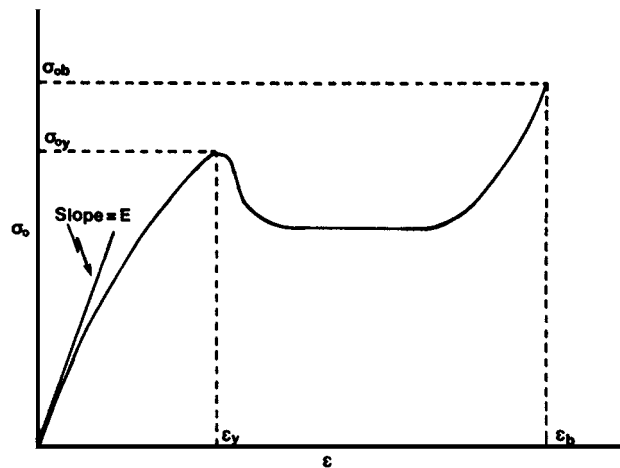


FIGURE 5 Generalized stress-strain curve that shows distinct yield.

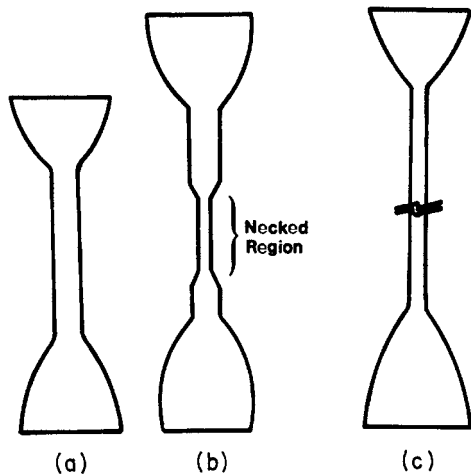


FIGURE 6 Schematic of a sample that undergoes necking and drawing. (a) Undeformed, (b) necking has occurred with some draw, and (c) neck is transformed throughout the material, generating a uniform cross-sectional area in the drawn region.

are known as the yield stress and yield strain. These values are crucial, for they indicate the stress and strain beyond which a material will no longer return to its initial dimensions; that is, plastic deformation or permanent set will generally be induced in the material. The tensile deformation of polyethylene utilized in the packaging of a “sick-pack” often leads to the formation of a “neck” and the necked material will not recover its original dimensions (Fig. 6). Indeed, if a material displays a distinct yield point or maximum in the stress–strain response as shown in Fig. 5, this almost certainly implies that a neck has been induced. It is apparent why engineering stress is a convenient indicator of the stress level since after inducement of a neck, two distinct cross-sectional areas may reside within the material until the neck is transformed through the specimen. At the onset of neck inducement, if the force is now divided by the new cross-sectional area of the thinned-down region or necked region, the distinct peak shown in Fig. 5 is often nearly removed, and hence the downturn in σ_0 is often principally a result of our representation of the stress utilizing the initial cross-sectional area. Again referring to Fig. 5, the region following the yield point might imply that “strain softening” is occurring, but this is often principally a result of the decrease in cross-sectional area and hence is not an entirely appropriate term to use for such behavior. Following this downturn, however, the long, rather uniform stress value obtained over considerable deformation is the result of ductile or cold drawing of the material and represents the transformation of the neck throughout the length of the sample (Fig. 6c). At the end of this transformation, an upturn is seen, which finally leads to the point of failure, σ_b . This upturn can definitely be referred to as strain hardening since it is the entire neck that

undergoes further elongation, and in the case of polymeric systems, this tends to promote further chain alignment or molecular orientation until failure occurs at σ_b and ϵ_b .

A final parameter, which is very significant in Fig. 5, is the initial slope of the stress–strain curve. This slope is called Young’s modulus, the tensile modulus, or modulus of elasticity and is given the symbol E . By definition this can be written

$$E = \lim_{\epsilon \rightarrow 0} (d\sigma_0/d\epsilon). \quad (8)$$

This parameter is an index of the stiffness of the material since it represents the stress generated in the limit of small deformation. This stiffness parameter is particularly significant in this article. It might be pointed out that if the stress–strain curve displays an initial “toe” in its behavior prior to it displaying a linear region, this is often due to a poorly mounted sample. As a result, the modulus would then be determined from the linear region that is generated following the “toe” as the sample “tightens up” in its initial stages of deformation. At this point it is also suitable to introduce the shear modulus and bulk modulus (refer to Fig. 2 for these modes of deformation). It follows from Figs. 2b and c that the shear modulus G and the bulk modulus B are given, respectively, by

$$G \equiv \lim_{\gamma \rightarrow 0} (d\tau/d\gamma), \quad (9)$$

$$B \equiv \lim_{\Delta P \rightarrow 0} [\Delta P / (\Delta V / V_0)], \quad (10)$$

where

$$\Delta V = V_0 - V. \quad (11)$$

In the case of Eq. (10), the bulk modulus approaches infinity as the material becomes incompressible, that is, $\Delta V = 0$. Furthermore, the reciprocal of the bulk modulus is correlated with the thermodynamic isothermal compressibility of the material. Hence, the bulk modulus is a very fundamental parameter.

Another common parameter, one used particularly in the industrial sector, is the secant modulus. By example, we shall define what is meant by the term 10% secant modulus. In Fig. 7, a secant has been drawn from the origin to the stress at 10% elongation. The slope of this line represents the 10% secant modulus, and in this case it will be less than Young’s modulus. Similarly, other secant moduli could be defined by the slopes of similar lines taken to any point on the stress–strain curve, but it is obvious that the degree of elongation must be correlated to these calculated slopes respectively. The use of secant modulus values helps convey information about the general stress–strain behavior when the whole curve is not to be presented.

Returning to Fig. 5, another parameter to be defined is the energy for failure or rupture energy. The energy or work of failure can be written

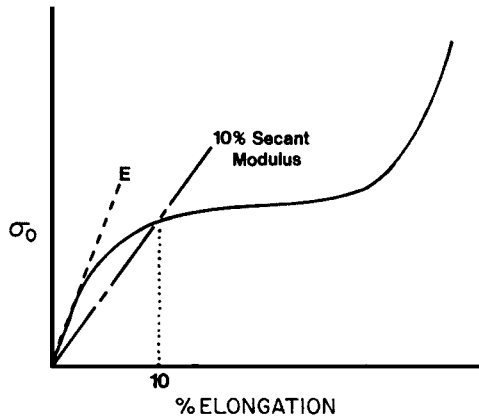


FIGURE 7 Generalized stress–elongation plot illustrating how a secant modulus is calculated.

$$W = \int_{l_0}^{l_{\text{break}}} f \, dl. \quad (12)$$

Note that this integral is similar to the integration of a stress–strain curve in that σ_0 ($\sigma_0 = F/A_0$) carries the variable of force and strain represents length in an indirect manner. To bring these two relationships together, first we divide both sides of Eq. (12) by A_0 , which will bring σ_0 into our relation. Realizing that

$$d\varepsilon = dl/l_0, \quad (13)$$

we now make the appropriate substitution for dl in Eq. (12) but must also recognize that l_0 is specifically related to the tensile direction and is not either of the dimensions involved with describing A_0 . Since this new length is a constant it can be moved outside the integral and divided into the left-hand side accordingly to give

$$\frac{W}{V_0} = \frac{W}{A_0 l_0} = \int_0^{\varepsilon_b} \sigma_0 \, d\varepsilon. \quad (14)$$

Hence, the integral of a stress–strain curve based on engineering stress and engineering strain provides the energy of rupture normalized per unit volume V_0 of the initial sample—a convenient result. Many modern instruments often provide direct integration of a stress–strain curve, thereby giving the rupture energy as a commonly reported parameter.

Figure 8 illustrates another common form of stress–strain behavior observed in many deformable polymers; note that no yield stress is observed. This behavior would be common to many elastomeric systems. Although only one curve is provided for the loading cycle, three curves, A, B and C, are possible candidates for the unloading cycle. Which of these unloading cycles might occur, say, for a rubber band? This is an easy question to answer on the basis of our discussion of the energy to break. Specifically,

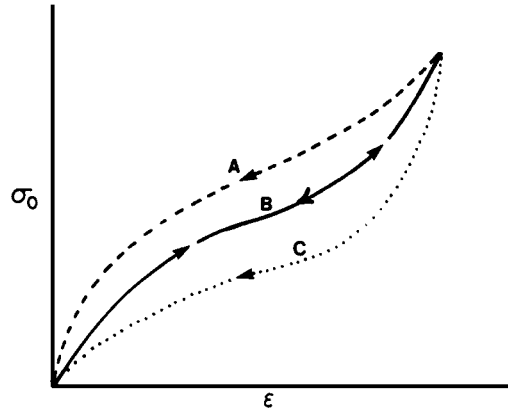


FIGURE 8 Generalized stress–strain behavior for cyclic deformation. Curve B represents the loading path; curves A, B, and C are discussed in the text with respect to unloading pathways.

the area under the loading curve is the energy expended into deforming this system, and hence if curve A were the associated unloading cycle, a higher energy under that curve would be returned than what was placed into the deformation of the sample. That is, energy would be created, which is in opposition to the first law of thermodynamics. Curve B as an unloading cycle is also not expected since it would imply perfect reversibility and, in this case, due to the nonlinear behavior the material would be described as a nonlinear elastic material. This is not common in the cyclic deformation of real materials due to the molecular slippage and segmental friction that dissipates some of the mechanical energy in the form of heat. Hence, curve C is the only expected path and this indicates that the energy regained following deformation is less than that expended for the deformation. Because some of the energy was stored and recovered while the remaining fraction was dissipated, this material would be described as a nonlinear viscoelastic system, which is very common for the behavior generally observed for polymeric materials.

This introduces the concept of mechanical hysteresis (MH). The percentage of mechanical hysteresis can be expressed as

$$\%MH = \left(\frac{\int_{\text{(loading)}} \sigma_0 \, d\varepsilon - \int_{\text{(unloading)}} \sigma_0 \, d\varepsilon}{\int_{\text{(loading)}} \sigma_0 \, d\varepsilon} \right) \times 100. \quad (15)$$

This parameter is a direct measure of energy dissipated per cycle (viscous behavior). Since the energy is dissipated in the form of heat, we realize the practical significance of measuring mechanical hysteresis in that it represents energy that can no longer be recovered. It may also serve as a significant source of internal heating of a material undergoing cyclic deformation. A prime example of mechanical heating is the cyclic deformation of tires at high

speeds. Due to the poor thermal conductivity of the polymeric tire, the rise in temperature of the internal part of the tire can be considerable, and in fact severe degradation would rapidly develop were it not for the appropriate chemical stabilizer package added during rubber compounding. Although hysteresis may be viewed somewhat as a disadvantage in some cases (i.e., generation of heat), it may also serve a useful role in helping to “dampen out” the transfer of energy in systems undergoing cyclic loading. For example, such damping materials might be utilized as vibrational mounts. Indeed, recognition of the hysteresis properties of materials is very important in many applications.

It should be pointed out that hysteresis implies that the unloading cycle returns the system to its original dimensions. However, there is a somewhat looser use of this term in defining similar behavior for materials whereby the initial dimensions are not totally recovered in the unloading cycle. That is, permanent set or irrecoverable flow (unrecovered strain) may be introduced in the initial cycle (Fig. 9). However, the mechanical hysteresis as defined by Eq. (15) is still a useful index.

We now ask if there is any relationship between the three fundamental moduli defined so far. For isotropic materials, there is a distinct relationship, but a new parameter, Poisson’s ratio, μ , must first be introduced. This can be defined at small tensile deformation as

$$\mu = -\text{transverse strain/longitudinal strain.} \quad (16)$$

The longitudinal strain represents the principal deformation axis, whereas either of the other two orthogonal directions could be utilized for the transverse strain. The purpose of the negative sign is to generally make Poisson’s ratio positive since the transverse strain will be negative based on our earlier definitions. In brief, this parameter

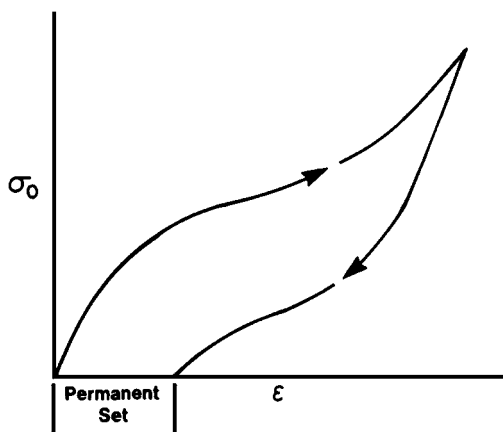


FIGURE 9 General stress–strain behavior illustrating the phenomenon of permanent set.

implies how the material will change in volume in tensile deformation. (The volume does not change in simple shear.) In brief, for an incompressible constant-volume deformation behavior, μ equals 0.5, whereas for all other isotropic systems, μ is less than 0.5 and usually ranges between 0.3 and 0.4 for glassy and semicrystalline polymeric materials. For elastomers, however, μ may indeed approach 0.5 and be as high as 0.496. An important point to recognize is that as μ becomes less than 0.5, tensile deformation of the material will cause an increase in volume. At small deformation, this change in volume can be written

$$\Delta V/V_0 = (1 - 2\mu)\epsilon. \quad (17)$$

From this relationship one notes that, when μ equals 0.5, there is no change in volume. Such behavior, along with uniform deformation, was the basis for the development of Eq. (5).

Regarding the dilation or volume increase, often in tensile testing a “whitening” of a material may be noted where it has undergone deformation. This whitening, though sometimes caused by strain-induced crystallization, is more often caused by the inducement of void formation, which leads to major fluctuations in refractive index relative to the bulk material and hence opaqueness due to the scattering of light. Not all materials show this whitening effect even though the value changes occur, because the dilation may be more uniform in terms of the volume fluctuations. In other materials the changes in volume may be considerable on a local scale, leading to the lack of transparency. As an example, an increased turbidity often occurs in the ambient deformation of a common material like semicrystalline high-density polyethylene or polypropylene, whereas during the tensile deformation of glassy polycarbonate, transparency is maintained even though the volume initially increases with deformation.

With μ defined, we now can write the well-known relationship among the three moduli defined above for an *isotropic* material:

$$E = 2G(1 + \mu) = 3B(1 - 2\mu). \quad (18)$$

(If the system is anisotropic, additional parameters are needed to interrelate the moduli, which are directionally dependent.) This relationship shows that for incompressible materials $E = 3G$ and that the bulk modulus must go to infinity. Since good elastomers have values of μ close to 0.5, this upper limit is often a very good approximation in that an elastomer is three times stiffer in tension than in shear. However, due to the fact that μ is typically between 0.3 and 0.4 for glassy or semicrystalline systems, it follows that Young’s modulus will still always be somewhat greater than a factor of 2 above the shear modulus. This result is a strong indicator that, when a material is

under a given loading profile, it will most likely undergo deformation by shear if allowed, since its resistance to that mode of deformation is less than that in tension. It should be noted that the bulk modulus is not infinity even for good elastomers; however, the volume of the bulk modulus, B , for such systems far exceeds the values of E or G .

IV. EFFECT OF TEMPERATURE ON STRESS–DEFORMATION BEHAVIOR

Let us now address how macromolecular systems may respond to external variables, one of the most important being temperature. Let us assume at the beginning that we are deforming a high molecular weight un-cross-linked amorphous system such as un-cross-linked high molecular weight polybutadiene (a rubbery system under ambient conditions). If we were to undertake the uniaxial deformation of samples of this material and carry out the loading of *each sample at the same rate of deformation*, the general stress–strain behavior that would be observed at different temperatures might be as shown in Fig. 10. We would find that at low temperatures (i.e., well below the glass transition temperature T_g of the system) the material displays a high modulus and relatively low strain to break (i.e., brittle behavior). (Not all amorphous polymers display brittle behavior below T_g ; some may display ductile behavior if the deformation conditions are suitable.) Above the glass transition temperature (approximately -90°C for amorphous *cis*-1,4-polybutadiene), a lower modulus is observed, and it continually decreases but not necessarily in a monotonic manner with temperature. The important point here is that temperature strongly influences the mechanical response of a macromolecular material, and it is therefore necessary to understand this thermomechanical response. One common way of illustrating this dependence on temperature is by a thermomechanical spectrum, which is the plot of a given mechanical property versus temperature. Although many such parameters could be selected, such as the energy to rupture, stress at break, and strain at break, these are ultimate properties and their values are often influenced by the presence of molecular orientation as well as defects in the material (voids, cracks, etc.). Thus, they are not always truly representative of the inherent macromolecular system before deformation. This is also often true of the yield stress and yield strain values. However, a principal means of illustrating the behavior dependence of the *initial structure* on the variable of temperature is to utilize the low-deformation parameter of modulus. If the test is in tension the value of E would be plotted, whereas if it were in shear (torsion) the value of G would be the appropriate variable. Generally, bulk deformations are not common,

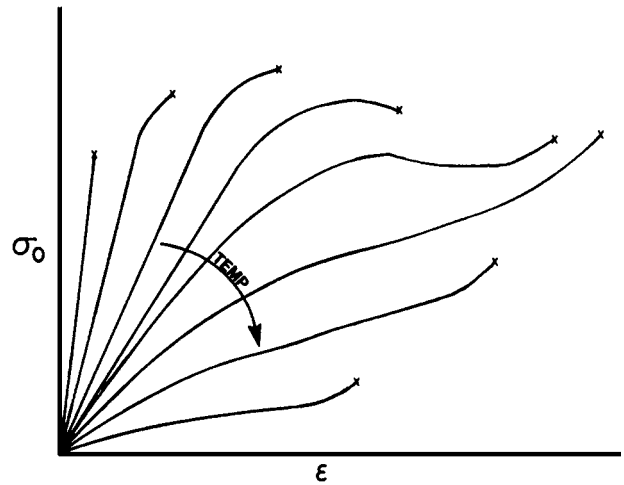


FIGURE 10 Generalized stress–strain curves showing the effect of temperature.

and hence we will not refer to the term B in the present discussion.

If modulus is plotted versus temperature based on the stress–strain experiment described above for the un-cross-linked high-molecular-weight amorphous material, the general behavior is as shown in Fig. 11. There are two rather distinct regions that are not strongly dependent on temperature, whereas there are two others that show a considerable dependence on temperature, particularly the lower temperature region. The lowest region, A, which is not strongly dependent on temperature would display a modulus nearly equivalent to that of organic glass (10^9 – 10^{10} Pa), and hence this region is known as the glassy state

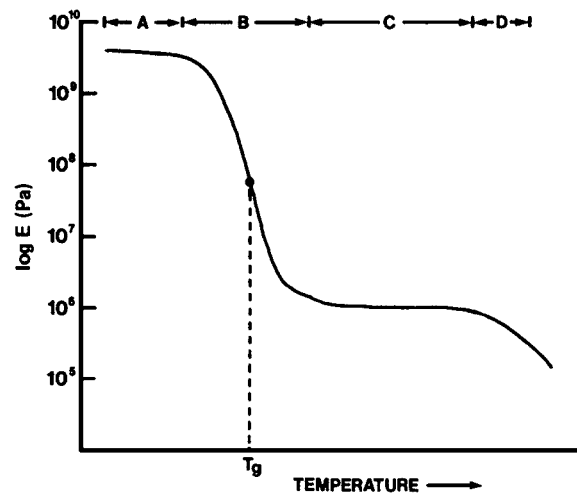


FIGURE 11 Typical plot of log Young's modulus E versus temperature for a high-molecular-weight un-cross-linked amorphous polymer.

or glassy region of the thermal mechanical spectrum. The other region that is not strongly dependent on temperature would display the properties and modulus behavior of a soft elastomer (10^5 – 10^6 Pa), and hence this region, C, is known as the rubbery state or rubbery region of the spectrum. The modulus decreases by a factor of between 1000 and 10,000 on going from a glass to a soft elastomer—an extremely large change. For this reason the temperature range over which this change occurs is crucial in characterizing the mechanical properties of polymers. This transition region is known as the glass transition region, and the inflection point in Fig. 11 is typically taken as one index of the glass transition temperature T_g —likely the most important thermal mechanical transition that occurs in an amorphous material. The range of temperature over which this transition occurs for homopolymers may be as small as 10 to 30°C, and hence an awareness of the location of this transition is imperative with respect to the mechanical applications of a specific polymer.

Above the rubbery region is another, more strongly temperature dependent region, which is the viscous flow region (see Fig. 11). In this thermal region, general polymer melt processing occurs for such amorphous materials (i.e., 100–200°C above the glass transition temperature).

It must now be explained why we have chosen to base this thermal mechanical spectrum on an amorphous, un-cross-linked high-molecular-weight polymer. Specifically, if cross-links were allowed such that an infinite network structure (gel) developed, the viscous flow region would be eliminated since an infinite network cannot undergo further softening or steady-state flow. Rather, such a material would display only an extension of the rubbery region until the onset of degradation. If the material remained un-cross-linked but was of low molecular weight, there would be no rubbery plateau region observed due to the fact that the molecular system did not have a critical length for the development of *molecular entanglements* between the chains (Fig. 12). These entanglements are important for inducing the rubbery region in un-cross-linked systems. Finally, if crystallinity had been present, a melting point T_m would enter the discussion, which of course would be located well above T_g . It should be pointed out that the melting of crystals within a polymeric material is typically not a sharp transition and in fact can occur over tens of degrees in some materials. Alterations in chain symmetry due to short-chain branches, the presence of added comonomer, and changes in stereoregularity are some of the causes that lead to a broad distribution in melting behavior but variation in cooling rate can also alter the perfection obtained within the crystalline state, thereby also leading to a lowering of the melting point and a broader distribution associated with that transition.

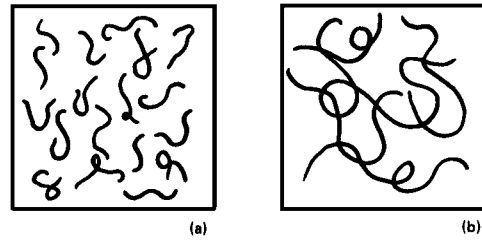


FIGURE 12 Schematic of molecular structures of an amorphous material having (a) molecular weight below the critical value for entanglements and (b) molecular weight above the critical value for entanglements.

Whereas crystallinity has a relatively small effect on the modulus below T_g of the amorphous phase, it has a strong influence above this thermal transition and in fact may cause the inflection point T_g in the modulus temperature curve to shift upward with increasing crystallinity. In addition, the level of crystallinity will strongly enhance the modulus in the rubbery region between T_g and T_m . Above the melting point, however, the viscous flow state would once again be reached as long as the semicrystalline system had not been cross-linked into an infinite network; if so, it would likely show the modulus taking a value typical of elastomers.

Recognition of the specific regions of the thermal mechanical spectrum given above is crucial to understanding many of the mechanical properties of polymeric systems. However, we first consider an additional variable and describe its influence on behavior. Let us return to Fig. 10 and question how we might be able to generate a similar series of stress–strain curves but at a constant temperature. The principal variable that makes this possible is deformation rate. A familiar example of such behavior involves the polymeric “silly putty” material that one can obtain from a hobby shop. On the application of a low rate of extension or shear deformation of this material at ambient conditions, it will display low modulus and nearly liquidlike behavior. This implies that it would represent one of the low-modulus curves in Fig. 10. However, if the same material is reformed into a test specimen and deformed at a high rate of deformation in either shear or extension, it will display a much higher modulus and brittle fracture, thereby more closely representing one of the upper curves in Fig. 10. Hence, if the modulus behavior is plotted against deformation rate, that is strain rate $\dot{\epsilon}(d\epsilon/dt)$ or shear rate $\dot{\gamma}(d\gamma/dt)$. Typically, because the range of deformation rates is considerable (several decades) it is more suitable to plot the modulus against the logarithm of the deformation rate constant temperature (Fig. 13). Granted, the specific temperature chosen for the measurements will influence which rates are necessary for this behavior to be

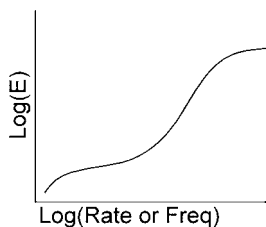


FIGURE 13 General plot of log modulus versus rate (or log rate) of deformation for many amorphous polymeric materials.

denoted. In Fig. 13 a mirror image of the behavior given in Fig. 11 is observed, where rate of deformation was assumed constant and the temperature was then varied. In fact, since rate can be viewed as frequency (i.e., reciprocal time), this clearly shows that time and temperature are strongly interrelated, and we will have to address this important fact. Before we do so, it is important to point out that the variable of pressure may be used to influence the stress-strain or modulus behavior at a constant temperature and deformation rate. As indicated in Fig. 14, for a process in which the temperature and rate are constant, an increase in the hydrostatic pressure will tend to promote higher modulus behavior in general. These remarks are meant to be general, for there are some specific effects of pressure that can be taken into account, such as its influence on the melting point (T_m), T_g , etc. Also, sometimes increased pressure can promote a higher strain to break. In brief, however, the effects of hydrostatic pressure on the general mechanical property behavior of polymers are not particularly important except in cases involving high hydrostatic pressure, for example, in deep oceanic applications.

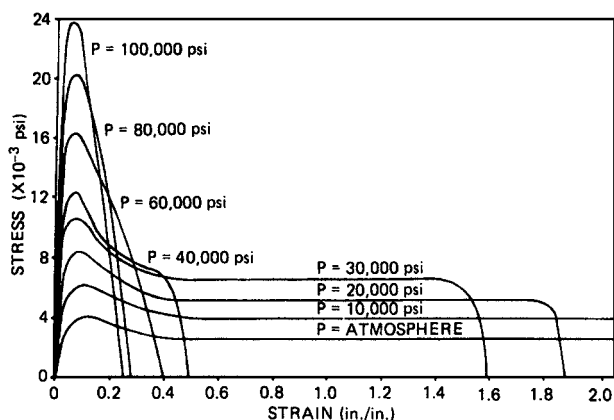


FIGURE 14 Plot of stress versus strain for polypropylene being measured at ambient temperature but at different hydrostatic pressures. [Reprinted with permission from Nielson, L. E. (1974). "Mechanical Properties of Polymers and Composites," Vol. 2, Dekker, New York. Copyright 1974 Marcel Dekker.]

V. TIME AND TEMPERATURE WITH RESPECT TO MOLECULAR CONSIDERATIONS

To interrelate the variables of temperature and time (rate of deformation), we must focus on the types of materials we are discussing, that is, systems composed of macromolecular chains. As mentioned earlier, the length-to-diameter ratio, or aspect ratio, of linear polymers is considerable and is much greater by far than the typical strands of spaghetti that are often used as an analogy for linear polymers. Besides this large mismatch in aspect ratio, there is another major discrepancy in the common comparison of macromolecules with spaghetti. This concerns the lack of mobility or motion of a spaghetti strand. A more suitable analogy, and one that is consistent with developments in the theories of reptation for the flow of polymer melts (viscous flow), compares linear polymers with long, stringy earthworms. Though somewhat crude and simplistic, this analogy has some merit in terms of the discussions that follow. In particular, long, stringy earthworms have many of the same response characteristics as polymer molecules. For example, placing them in liquid nitrogen would indeed produce a more "glasslike material" whereas placing them on a hot stove would tend to create a much higher degree of motion (at least for a short time!) within their backbones similar to the effect of thermal energy (kT) on macromolecules. In fact, let us be so simplistic as to consider stress-strain experiments carried out on entangled worms if indeed they could be mounted into a suitable mechanical testing device. There is little doubt that, at a constant deformation rate, the variable of temperature (in the framework indicated above) would lead to stress-strain curves that would have the general characteristics given by the same temperature function as indicated earlier in Fig. 10. The cause of the lower modulus and higher strain behavior, in general, simply arises from the fact that *within the time scale of the experiment* (constant loading rate) the worms would have sufficient time to respond to the imposed stress, thereby allowing some disentanglement and sliding of one backbone by another. The segmental friction would lead to a viscous dissipation, that is, loss of mechanical energy. However, as the temperature decreased and the backbone motion of the worms also decreased (an analogy with less thermal Brownian motion), there would be less chance for disentanglement *in the same time-scale*, and hence the general entanglement network character would provide a higher modulus behavior similar to that noted for macromolecular systems.

As can be imagined, varying the chemical structure of a polymer can alter its conformational freedom or backbone flexibility thereby influencing the average molecular

weight between entanglements with neighboring chains. To help clarify this issue, the reader will note that Table I provides a listing of the critical molecular weight between entanglements (often determined from melt rheological measurements) for many of the common polymers. As a comparison, one notices that the first three entries, polyethylene, polypropylene, and polystyrene, which all possess the same carbon-carbon backbone, are quite

TABLE I Critical Weight Average Molecular Weight between Entanglements (M_{wc})^a

Polymer	(M_{wc})
Polyethylene	3800
Polypropylene	7000
Polystyrene	35,000
Poly(vinyl chloride)	6250
Poly(vinyl acetate)	24,500
Poly(vinyl alcohol)	5300
Polyacrylamide	9100
Poly(a-methyl styrene)	40,800
Polyisobutylene	15,200
Poly(methyl acrylate)	24,100
Poly(ethyl acrylate)	31,300
Poly(methyl methacrylate)	31,000
Poly(<i>n</i> -butyl methacrylate)	60,400
Poly(<i>n</i> -hexyl methacrylate)	91,900
Poly(<i>n</i> -octyl methacrylate)	114,000
Poly(2-ethylbutyl methacrylate)	42,800
Poly(dimethyl siloxane)	24,500
Poly(ethylene oxide)	4400
Poly(propylene oxide)	7700
Poly(tetramethylene oxide)	2500
<i>Cis</i> -polyisoprene	7700
Hydrogenated polyisoprene	4000
<i>Cis, trans</i> , vinyl-polybutadiene	4500
<i>Cis</i> -polybutadiene	5900
1,2-Polybutadiene	12,700
Hydrogenated 1,2-polybutadiene	26,700
Poly(ϵ -caprolactam) nylon 6	5000
Poly(hexamethylene adipamide) nylon 66	4700
Poly(decamethylene succinate)	4600
Poly(decamethylene adipate)	4400
Poly(decamethylene sebacate)	4500
Poly(diethylene adipate)	4800
Poly(ethylene terephthalate)	3300
Poly(carbonate of bisphenol A)	4900
Poly(ester carbonate of 1-bisphenol A and 2-terephthalic acid)	4800
Poly(ester of bisphenol A and diphenyl sulfone)	7100

From Zhang, Y. H., and Carreau, P. J. (1991). *J. Appl. Polym. Sci.* **42**, 1965.

^a Generally determined from melt rheological measurements.

different in their values of M_{wc} . The first two are of relatively low M_{wc} , this is due to the fact these chains are very flexible and therefore can easily entangle with neighboring chains. However, in the case of polystyrene, it has large bulky phenyl groups on alternate backbone carbons and therefore makes the conformational freedom of that chain more restricted thereby leading, as the usual case, to a distinctly higher value of M_{wc} . The reader might look over the other entries in Table I to note the wide variability that occurs between different chemical structures for these linear polymers.

On the basis of the above remarks, an additional concept can be introduced. It is based on the definition of the Deborah number D_e , which is a ratio of two times and therefore is dimensionless. For our purposes this can be defined as

$$D_e = \frac{\text{molecular response or relaxation time}}{\text{experimental or observation time}}. \quad (19)$$

In Eq. (19) the numerator refers to a general characteristic time or relaxation time over which the molecular system in question can respond. For example, this would mean that molecular movement is possible in this time-scale, and therefore the material would appear somewhat liquid-like if the time-scale of the experiment were appropriate. The denominator concerns the time frame over which the observation occurs, that is, the experimental window or observation time. In brief, if the Deborah number is greater than unity, this means that the molecular response time is longer than the experimental time, and hence the material will behave or appear more as a rigid solid. When the Deborah number is less than unity, however, this means that the molecular response time is less than the experimental time frame, and hence relaxation or flow may be observed in this period. The exact value of the Deborah number is of relatively little concern here. In general terms, if it is large the material is more "solid-like," whereas as the number becomes less than unity the behavior of the material becomes more liquid-like. Temperature influences the Deborah number for a given experimental time frame by affecting the numerator. Specifically, as temperature increases, the molecular response time decreases and the Deborah number therefore decreases. Some exceptions to this can occur in polymeric materials. For example, a material raised to a higher temperature may first become somewhat liquid-like, but then due to the higher temperature, which may promote crystallization in selective systems, the presence of developing crystals may begin to increase the relaxation time due to the restrictions placed on molecular mobility. One can also change the Deborah number by changing the experimental time frame. The appropriate variable here is deformation rate, be it in shear or elongation. Although the rate of deformation carries

reciprocal time, increasing this variable essentially shortens the observation time scale and hence decreases the denominator in Eq. (19). Now whereas the denominator is controlled specifically by the observation time, which is inversely related to deformation rate, the numerator is controlled by many factors, many of which extend from internal variables such as molecular weight, cross-linking, molecular architecture, chain stiffness as related through chain chemistry, and crystallinity. As mentioned earlier, it is important to recognize the balance between three types of energy: intermolecular, intramolecular, and thermal energy. Indeed, the numerator in Eq. (19) is highly dependent on the balance of these energies. In summary, the Deborah number concept is important for rationalizing the mechanical behavior of a polymeric material when tested under different loading rates and environmental conditions.

Utilizing our earthworm concept of polymeric species, let us strengthen our understanding of the effect of deformation rate. Suppose we hold temperature constant, for example, at ambient temperature, and carry out a series of stress-strain experiments, but the changing variable is now deformation rate, be it in shear or extension. There is little doubt that again the response expected would mimic what is displayed in Fig. 10. At low rates of deformation, due to the backbone motion of the worms, they could move within the time frame of a slow deformation experiment, thereby leading to considerable strain and low-modulus behavior. On the other hand, at very high rates of deformation, there is little doubt as to what the result would be! Crude as the analogy seems, the response of the worms would now provide a higher modulus due to the inability to disentangle, thereby leading to chain scission and more brittle-like behavior similar to what we discussed earlier with reference to the “silly putty” polymeric material. Indeed, one can show that chain scission occurs in real macromolecular systems under suitable rates and temperatures by utilizing electron spin resonance studies to reveal the presence of free radicals generated by the breaking of covalent bonds.

With this somewhat simplistic but useful earthworm analogy we have a firm grasp of the general interplay between temperature and loading rate. Our desire now is to quantify the relative degree of storage of mechanical energy or (elastic behavior) caused by an entangled network-like behavior in contrast to the dissipation of mechanical energy (viscous dissipation) through chain slippage and general segmental frictional forces that are related to important mechanical properties, such as hysteresis, discussed earlier. A common way to quantify the relative degree of the viscous and the elastic components in these viscoelastic materials is by means of dynamic mechanical analysis (DMA) techniques. This approach allows a direct measurement of these two components generally by

using low-strain deformations that are carried out over a range of both temperature and frequency. The basics of the technique are best explained by first considering the response of a pure elastic body to an oscillatory dynamic strain such as is expressed by

$$\varepsilon(t) = \varepsilon_0 \sin(\omega t), \quad (20)$$

where $\omega = 2\pi$ frequency. A linear elastic body would be that of a Hookean spring whose relationship of strain to stress in tension is given by

$$\sigma_0(t) = E\varepsilon(t). \quad (21)$$

This relationship clearly shows that the stress on the system is a function only of the displacement and carries no other time-dependent characteristics. Hence, with Eq. (20) for the time-dependent strain, the time-dependent Hookean stress becomes

$$\sigma_0(t) = E\varepsilon_0 \sin(\omega t). \quad (22)$$

Hence, a general plot of these two functions together would appear as shown in Fig. 15a. Note that the amplitude of the stress function varies in proportion to its modulus but that both the stress and strain oscillate in phase; that is, a zero phase angle exists.

To represent a linear viscous body, Newton's law of viscosity suffices, which can be stated in tension as

$$\sigma_0(t) = \eta(d\varepsilon/dt), \quad (23)$$

where η represents a Newtonian viscosity; that is, it is independent of the deformation rate. Utilizing this equation in conjunction with Eq. (20) for the time-dependent strain shows that the time-dependent stress for a purely viscous material is

$$\sigma_0(t) = \eta\omega\varepsilon_0 \cos(\omega t), \quad (24)$$

which is strikingly different in its time-dependent behavior from the Hookean stress elastic response. In particular, the amplitude now varies linearly with the deformation rate (frequency), a factor that had no importance in the elastic or Hookean behavior. Particularly important is the fact that, for a purely viscous response, the stress and strain are out of phase by 90° (see Fig. 15b). (The stress will “lead” that of the strain, since the material will not undergo deformation without sensing stress.) It then should be obvious that, if a viscoelastic material is placed under an oscillatory deformation at small strains where its response should be linear, and if one can monitor the stress and strain response via suitable electronic techniques, this will allow a direct measurement of the phase angle between these two functions. This measurement will clearly provide a direct measure of the viscous response. As one might expect, a viscoelastic polymer undergoing cyclic

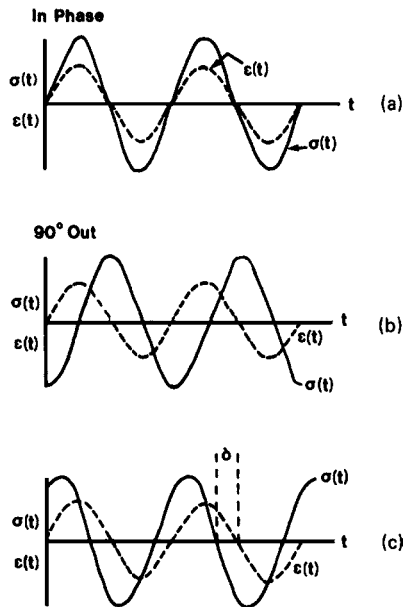


FIGURE 15 Generalized behavior of the phase relationship between stress and strain in a sinusoidal loading experiment. (a) Hookean or pure elastic behavior, (b) Newtonian or pure viscous behavior, and (c) viscoelastic behavior, which is typical of polymeric materials.

or dynamic loading as a function of temperature will display a finite phase angle whose magnitude is dependent on both the loading rate and temperature (Fig. 15c). (Think of how the worms would react.) Such dynamic loading patterns are characterized by the dynamic modulus (E^* and G^*) written below in terms of both tensile and shear deformation:

$$E^* = E' + iE'' \tag{25a}$$

$$G^* = G' + iG'' \tag{25b}$$

The conventional symbolism used here represents complex plane notation, where i denotes the square root of -1 and is of little importance in our discussion. Rather, it is most suitable for us to view E^* or G^* as a vector quantity made up of both the viscous and elastic components, as indicated in Fig. 16, where the respective elastic component (E' or G') and viscous component (E'' or G'') lie along the x and y axes, respectively. It therefore follows that the phase angle will be denoted by δ , and thus we reach the obvious and important result that

$$\tan \delta = E''/E' = G''/G' \tag{26}$$

Hence, measurement of the phase angle provides a direct ratio of the viscous (loss) to elastic (storage) components, and this is a useful parameter for describing the mechanical response of a material under a given loading rate and temperature. It should also be clear that, due to the interrelationship of $\tan \delta$ and the respective viscous and

elastic components, only two of the three quantities are independent, and thus all three are usually not reported. Generally, the elastic component and one of the other two parameters, either $\tan \delta$ or E'' (or G'') are given.

Some specific examples of such a response obtained in dynamic testing are shown in Figs. 17a–c. Some significant observations can be made. First, under dynamic conditions the elastic component E' displays the same characteristics as the modulus term discussed above in terms of the thermal mechanical spectrum, and in fact the two are essentially the same if the time frame of measurement is equal for both. Hence, the dynamic mechanical technique is very convenient and useful for generating the thermal mechanical spectrum. Second, $\tan \delta$ (see Fig. 17c) or E'' displays various maxima as a function of temperature, indicating distinct “loss peaks.” Note that some peaks occur below the glass transition temperature, whereas the major loss peak is typical at the glass transition. In fact, for un-cross-linked materials that are amorphous, $\tan \delta$ at T_g will be of the order of 1.0 or somewhat above, indicating that the viscous component is equal to or exceeds that of the elastic component [recall Eq. (26)]. Above the glass transition temperature, however, the general loss again decays as is indicated, even though the material shows higher mobility due to the enhancement of thermal energy (i.e., increased kT). If this is surprising, the reader may view it in the following framework. At a suitable rate and temperature, the dynamic loading resonates with the motion of the macromolecular system, whose rapidity of motion increases as temperature increases. At the glass transition temperature these local modes of motion within the macromolecular chain can be somewhat viewed as being in phase with the applied dynamic loading. Hence, “mechanical resonance” results, leading to a considerable absorption of energy and high values of $\tan \delta$. However, with enhanced thermal motion, there is a dephasing of the applied dynamic loading with that of the molecular motion, and a decrease in $\tan \delta$ occurs as E' (or G') decreases. It is clear that there is a further softening of the material by enhanced motion

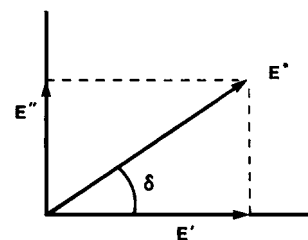


FIGURE 16 General plot showing the vectorial relationship between the loss and storage parts (E'' and E') with respect to the dynamic Young's modulus E^* . The phase angle between these two quantities is denoted by δ .

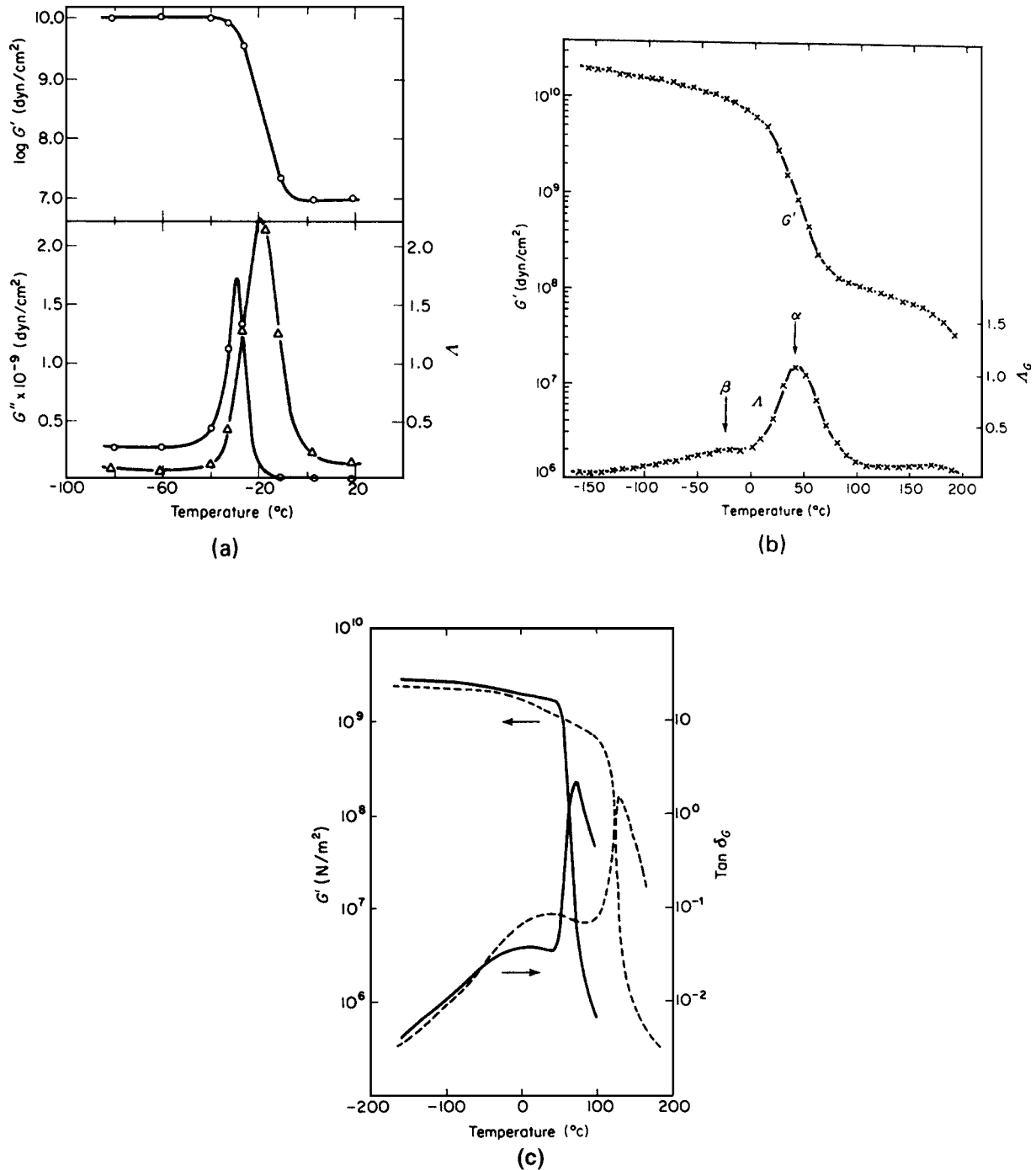


FIGURE 17 Dynamic mechanical behavior and respective parameters for (a) polyacetaldehyde, (b) polyvinylidene chloride, and (c) conventional or atactic polymethyl methacrylate (dashed curves) along with its high isotactic configuration (solid curve). [Reprinted with permission from McCrumb, N. G., Reed, B. G., and Williams, G. (1967). "Anelastic and Dielectric Effects in Polymeric Solids," Wiley, New York. Copyright 1967 John Wiley and Sons.]

due to the obvious decrease in modulus but that this drop varies in terms of its temperature dependence, as pointed out earlier in the discussion of the thermal mechanical spectrum.

Addressing the temperature dependence in Figs. 17a–c we realize that, below the glass transition temperature, modulus is only slightly dependent on the temperature because there is insufficient thermal energy for the overall

cooperative segmental motion of the backbone, that is, a “crank shaft” type of motion, which would lead to a much larger scale mobility and potential flow. However, there may be sufficient thermal energy to provide the onset of local-scale motions such as the rotation of side groups, oscillations of side groups, and oscillations and partial torsional rotations of backbone components. All of these motions lead to the dissipation of energy, and hence a distinct loss peak is noted in the thermal mechanical spectrum. These low-temperature loss peaks are considered to have great significance because their magnitude and number represent molecular means by which energy can be dissipated in the glassy state. We shall return to this discussion when we consider impact properties. It should be mentioned in passing that the two techniques of dielectric spectroscopy and solid-state NMR are also used considerably, since these methods can provide information on the local molecular motions discussed above.

If a material is amorphous, it is not likely that additional loss mechanisms will be observed above the glass transition temperature, although there has been some controversy relating to this point. If, however, crystallinity is present within the system, additional loss mechanisms may well be observed due to motions within the crystal phase or at the crystal interface. These motions are of importance in terms of the mechanical response of the crystalline phase under loading conditions and in fact may play a considerable role in determining the appropriate draw temperatures in the mechanical processing of fibers and films. The magnitude of these crystalline loss mechanisms can be influenced by the thermal processing history, as might be expected, since this will influence crystal perfection.

From our discussion of dynamic mechanical spectroscopy and its correlation with the time–temperature response of macromolecular systems, it now should be obvious how a dynamic mechanical spectrum will change as the frequency of loading is increased. This is illustrated in Fig. 18 and should come as no surprise in view of our discussion of the response of “earthworms.” The spectrum is shifted upscale on the temperature axis as the rate of deformation is increased. This, of course, follows from the fact that, for motion to occur and allow a lowering of modulus, a higher degree of thermal energy and faster molecular motion will be required for the experiment with the highest loading rate or shortest time frame (recall our discussion of the Deborah number). In fact, a general rule is that the glass transition temperature, as denoted by either the maximum in E'' or $\tan \delta$ (as well as the inflection point in E') will shift roughly 3–5°C per decade of loading rate increase. The same rule, however, does *not* directly apply to the sub- T_g or crystal loss peaks accordingly. It should be mentioned that the transition peak in $\tan \delta$ typically appears at a higher

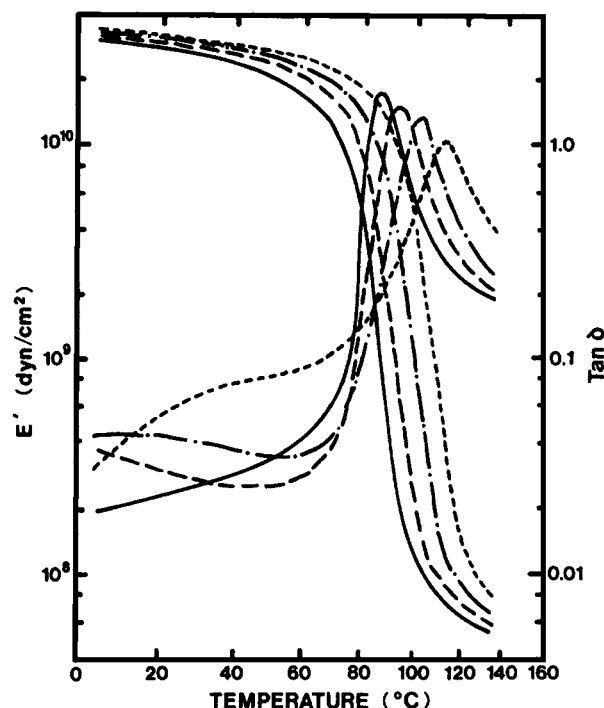


FIGURE 18 Plot of the real part of the dynamic Young's modulus versus temperature for atactic polyvinyl chloride as obtained at four different frequencies (—, 5 cps; — —, 50 cps; - · - ·, 500 cps; - - -, 5000 cps). [Reprinted with permission from Aklonis, J. J., and McKnight, W. J. (1983). "Introduction to Polymer Viscoelasticity," 2nd ed., Wiley-Interscience, New York. Copyright 1983 John Wiley and Sons.]

temperature than the corresponding peak in E'' . Thus, when reporting a transition temperature as determined by DMA, one must specify which parameter is utilized.

The sub- T_g loss peaks are generally more dependent on loading rate or frequency and, in fact, analysis shows that, as loading rate increases, the lower temperature loss mechanisms shift more rapidly upward toward the glass transition response peak. This response with deformation rate is denoted by a plot of the logarithm of the dynamic frequency versus the reciprocal temperature where the peak temperature in E'' or $\tan \delta$ is indicated. An example of this is illustrated in Figs. 19a and 19b, which show the spectra obtained for a cross-linked epoxy at different frequencies and the corresponding $1/T$ (Arrhenius) plot to indicate the frequency response. Typically, linear or near linear behavior is observed in Fig. 19b for this plot, the slope of which therefore provides an activation energy—an index of the frequency or temperature dependence. This works particularly well for sub- T_g loss peaks that follow Arrhenius behavior. However, due to the non-Arrhenius nature of the glass transition, this form of analysis is less reliable when applied to the glass transition region. The general shape of the modulus temperature curve in Fig. 19a is not altered

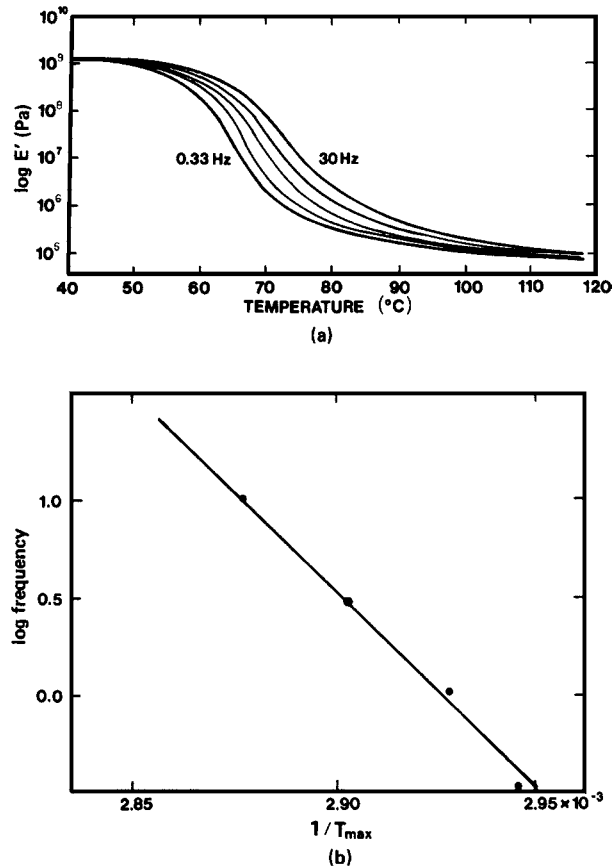


FIGURE 19 (a) Plot of the real part of dynamic Young's modulus E' versus temperature for a lightly cross-linked epoxy ($1^\circ\text{C}/\text{min}$). The three intermediate lines represent intermediate frequencies with respect to the two that are labeled. (b) Plot of log frequency versus $1/T_{\max}$ for the same epoxy material. The T_{\max} values were obtained from the $\tan \delta$ data not shown. [Reprinted with permission from Wetton, R. E., and Stone, M. R. (1983). *Proc. Trans. Relax. Polym. Mater.*, Melbourne, 1983.]

greatly with a change in frequency. However, this is not to indicate that there is no change, for in fact the breadth of the transition may often undergo alteration over a range of loading frequencies. This clearly must be correlated with a distribution in the relaxation times associated with the specific mechanism responsible for a given loss peak, be it a side group rotation, cooperative backbone motion, or otherwise.

A. Factors Influencing Dynamic Loss Behavior

As might be expected, variables that affect dynamic mechanical behavior are such important factors as level of cross-linking, the presence of plasticizer, and phase separation as may occur in block or segmented copolymers, polymer blends, and semicrystalline systems. Though we cannot explore all of these effects, we shall make a few

important points. Cross-linking tends to decrease the magnitude of the glass transition, loss behavior and sometimes causes it to broaden, as might be expected due to an influence on the spreading of the relaxation times for cooperative backbone motion. Addition of plasticizer tends to decrease the glass transition temperature and often broaden the loss response, although different plasticizers function in quite different ways in influencing the breadth of the respective loss behavior. This allows some control of the thermal range over which damping occurs. Antiplasticizers can, in fact, depress or eliminate one or more of the sub- T_g loss responses due to limiting the mobility of the corresponding molecular group responsible for that transition.

As a final example demonstrating the utility of dynamic mechanical spectra, let us consider the impact behavior of polymeric systems. It is well known that bisphenol A polycarbonate is a very high impact glassy polymer under ambient conditions, whereas atactic polystyrene is a brittle glass under similar high loading rate or impact conditions. The glass transition temperature of polycarbonate at low frequencies is $\sim 150^\circ\text{C}$, whereas that of polystyrene is taken to be $\sim 100^\circ\text{C}$; hence, polycarbonate can be viewed as 50° "deeper" in the glassy state than polystyrene at room temperature. The latter phrase should be taken lightly and is meant only to elucidate the difference between these two polymers in terms of impact properties. That is, the impact characteristics do not arise from the fact that polystyrene has a lower T_g ! Specifically, the dynamic mechanical spectrum of bisphenol A polycarbonate is shown in Fig. 20. Bisphenol A polycarbonate displays a particularly strong sub- T_g dissipation mechanism, which may well assist in dissipating energy when the glass is rapidly loaded. Polystyrene displays a low-temperature loss mechanism, but it is not of great magnitude; hence, this polymer exhibits less mobility in the glassy phase (data not shown). This indicates the potential use of dynamic mechanical spectroscopy in looking for differences in dissipative modes of energy below the glass transition temperature. Another important feature is apparent from Fig. 21, which illustrates the frequency dependence of the loss peaks of polycarbonate. In particular, due to the strong sensitivity of the sub- T_g peak to loading rate, the peak rapidly shifts upward under high loading rate conditions and may well be operative under ambient conditions as a prime source for dissipating mechanical energy placed into the material. The actual mechanism is more complex, but the point here is to illustrate the worth of dynamic mechanical spectroscopy in light of a very important mechanical property, namely, impact strength. Note that the loss peak associated with T_g shifts upscale with loading rate at only about 3 to $5^\circ\text{C}/\text{decade}$, as discussed earlier.

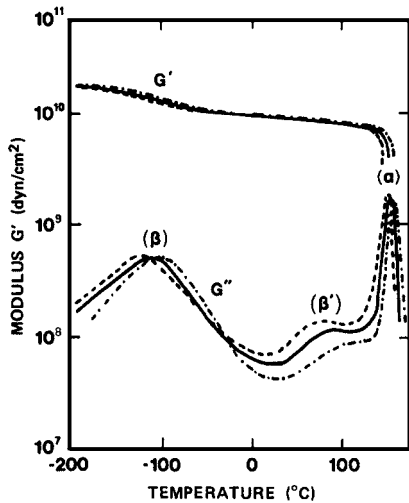


FIGURE 20 Plot of the real part of the dynamic shear modulus G' versus temperature for three frequencies (---, 0.1 Hz; —, 1 Hz; - - - -, 10 Hz) as obtained on conventional polycarbonate. [Reprinted with permission from Boden, H. E. (1984). *Adv. Polym. Technol.* 3(4), 383.]

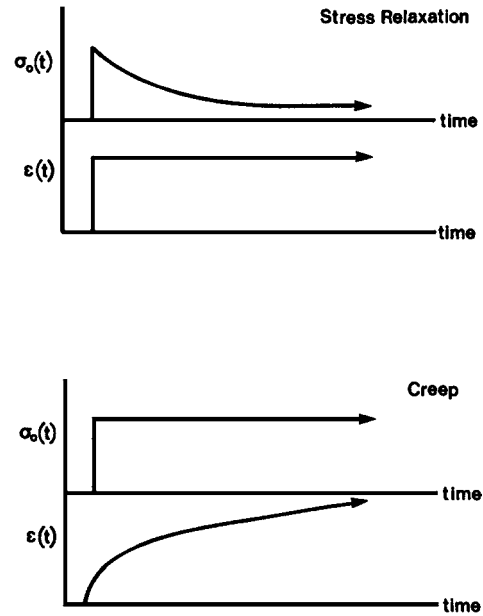


FIGURE 22 General time-dependent behavior of stress and strain for the conditions of stress relaxation and creep.

VI. STRESS RELAXATION AND CREEP BEHAVIOR

Two important mechanical tests that have not yet been mentioned are those of stress relaxation and creep. Both can be carried out in either tension or in shear, but for convenience we shall continue our discussion in terms of tensile deformation. The general characteristics of both the stress relaxation and creep tests are indicated in Fig. 22, where it can be seen that in stress relaxation

a fixed strain is imposed on a material and held while the stress is monitored as a function of time. The reverse situation occurs for creep; that is, dimensional changes occur with time under a fixed load or stress. The response obtained by these different tests can be viewed in terms of the earthworm analogy of macromolecules and the Deborah number concept. Picture a stress relaxation experiment under ambient conditions utilizing “silly putty.” We expect a finite stress to develop when

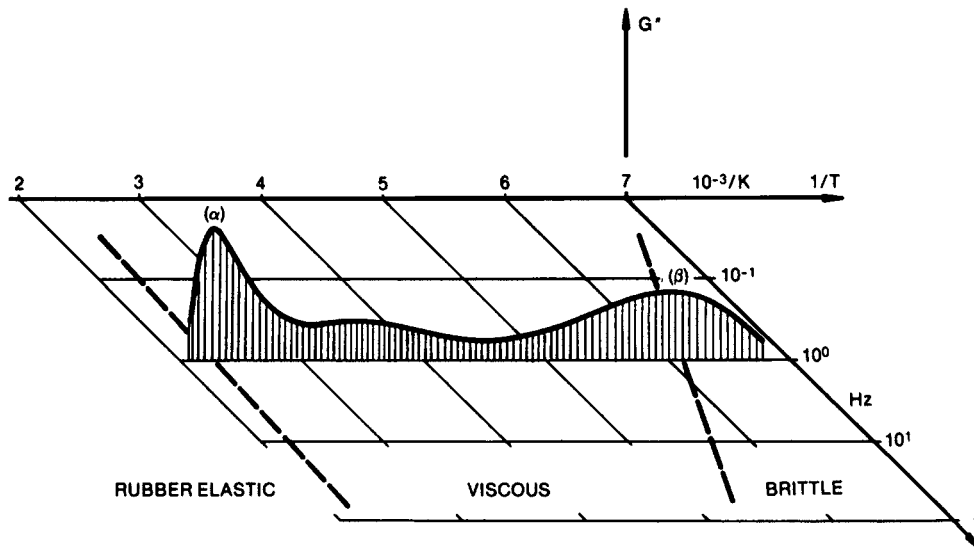


FIGURE 21 Three-dimensional plot displaying the variables of G'' , reciprocal temperature, and frequency for conventional polycarbonate. [Reprinted with permission from Boden, H. E. (1984). *Adv. Polym. Technol.* 3(4), 383.]

a rapid fixed strain is imposed on the material but realize that this stress would quickly decay due to the fairly rapid flow and sliding of the polymer macromolecules under ambient conditions (it displays a low Deborah number). This would lead to a zero stress in a short period of time. Similarly, if a fixed load were placed on the “silly putty” material, we would anticipate that the material would undergo deformation with time (creep) but not necessarily in a linear fashion. The initial response would likely be somewhat elastic, but due to the capacity of these macromolecules to flow at room conditions, the material dimensions would increase quite rapidly with time.

Let us contrast the behavior of the “silly putty” with that of a cross-linked rubber band. In stress relaxation one would anticipate that some rapid decay in stress would occur due to the slipping of chain entanglements as well as any loose chains or loops that make up the network. However, an equilibrium stress value would be obtained following the completion of the relaxation of these loose chain ends, loops, or un-cross-linked chains within the system. That is, the final “fish net” or gel macromolecular structure would reach an equilibrium stress value at some later time. With respect to the same material response in creep, one would expect a quick rise in strain due to the imposition of a load, but the strain would then rise much more slowly and reach a final equilibrium value at the point

where all chain entanglement effects had been relaxed out and again the “fish net” or gel structure served as the resistance for further deformation.

A final example is that of a cross-linked epoxy material or glassy network at room temperature. Here one would expect relatively little stress relaxation in short times, even if un-cross-linked chains existed in the system. That is since we are below the glass transition temperature, large-scale cooperative motion cannot occur rapidly within the same time frame as in the preceding experiment (a large Deborah number is displayed). With respect to the creep behavior of this cross-linked glass, one would also expect very little strain to result and little change with time for reasons that should be envious. It should then be evident that the tests of stress relaxation or creep, coupled with the variables of temperature and time, serve as convenient methods with which to monitor the viscoelastic response of polymeric systems.

These response times will be influenced accordingly by levels of cross-linking, crystallinity, molecular weight, molecular chain architecture (branched versus linear) plasticizer content, and so on, as is clear from the arguments based on wormlike motions. These same variables should be considered with respect to ultimate properties and yield behavior, as well as the low deformation (modulus) response. As an example, consider Fig. 23, which

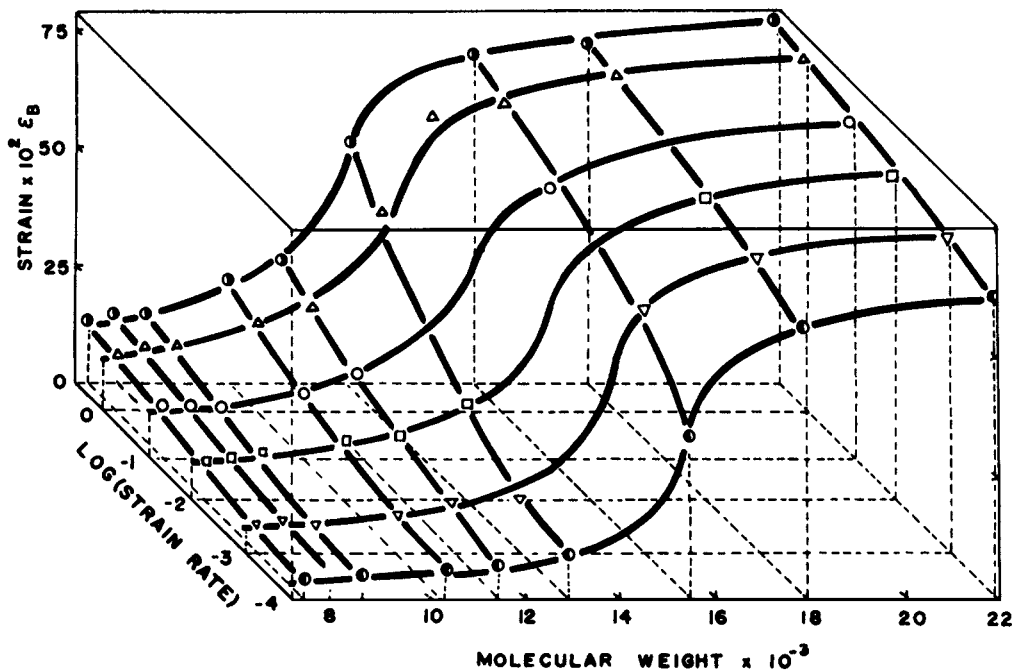


FIGURE 23 Three-dimensional plot illustrating the relationship between strain to break, log strain rate, and molecular weight for conventional polycarbonate as determined at ambient conditions. [Reprinted with permission from Morton, J. R., Johnson, J. F., and Cooper, A. R. (1972). *J. Macromol. Sci. Rev. Macromol. Chem.* **C8**(1), 57.]

shows the strain at break (ultimate property) as a function of molecular weight at a given temperature. There is a decrease in the strain at break for this polycarbonate system as rate is increased in this range of $\dot{\epsilon}$ as expected. A particularly important point is that, at a fixed $\dot{\epsilon}$, there is a major change in behavior above a critical molecular weight, which is of the order of 10,000 g/mol for this material. This critical molecular weight occurs where the length of these macromolecules is sufficient to promote molecular entanglements, which in turn lead to a pseudo network—a more useful material for structural applications. This critical molecular weight varies for different macromolecular chain chemistry depending on the relative chain stiffness and the mass of the repeat unit.

VII. EFFECT OF CRYSTALLINITY ON PROPERTIES

Because many of today's polymers are semicrystalline, we shall discuss briefly how crystallinity influences mechanical properties, as well as other important properties such as optical transparency. Let us first consider the effect of crystallinity on stiffness or modulus behavior. If the system is unoriented (oriented systems will be discussed in Section X) and if one is below the glass transition temperature of the amorphous phase, increasing the crystallinity of a material has relatively little effect on modulus; that is, modulus will be of the order of 10^9 to 10^{10} Pa, regardless of the level of crystallinity. On the other hand, if one is above the glass transition temperature of the remaining amorphous component, the presence of crystallinity will strongly influence modulus and cause it to increase accordingly, as long as one is below the melting point of the crystals. A general sketch of this behavior is illustrated in Fig. 24, where the general thermal mechanical behavior is shown with respect to level of crystallinity.

If stress-strain measurements were being made above the glass transition temperature of the amorphous phase, the modulus would be enhanced in these measurements as well, but so would other properties such as strain to break and stress at break. In the presence of crystallinity, a distinct yield point is often displayed (see Fig. 5). Generally, the presence of crystallinity may also strongly influence the nature of cold drawing or ductile flow, although the crystallinity does not have to exist for this phenomenon to occur. It certainly must, however, if a yield or ductile character is to be observed above the glass transition for a nonfilled homopolymeric material. Crystallites also serve basically as "physical cross-links" and therefore strongly dominate the mechanical properties above T_g . It is not our

goal to discuss the morphological textures of semicrystalline polymers, but it is important to point out that by varying the methods of crystallization (quench rates, etc.) one can change the morphological textures in a given polymer, thereby affecting the mechanical behavior even though the level of crystallinity may not greatly vary. It is therefore important to be aware of the crystallization procedures in conjunction with the level of crystallinity if one hopes to predict the mechanical behavior of a semicrystalline system.

VIII. EFFECT OF COVALENT CROSS-LINKING

Placing covalent cross-links into a system influences the mechanical properties in a fairly predictable manner. Below the glass transition temperature, cross-links increase the modulus, but the effect is somewhat like that of crystallinity in that the increase is not a large one. As the level of cross-linking increases and places restrictions on the thermal Brownian motion of a chain segment, the glass transition temperature is generally shifted upward. Often this transition is broadened and produces behavior similar to that of crystallinity (Fig. 24). It is clear, however, that (as pointed out earlier) when sufficient cross-linking exists to promote an infinite network (i.e., the gel point is reached), the viscous flow region is no longer available to the thermal mechanical spectrum. As expected, the degree of cross-linking is directly correlated with the modulus behavior in the *rubbery region*. In fact, if the level of cross-linking becomes considerable, rubbery behavior (modulus of 10^5 to 10^6 Pa) is not likely to be found, but rather the material will be stiffer and have the properties of a leather-like system. In fact, with excessive cross-linking, the glass transition temperature may never be observed before thermal degradation! Of course, cross-linking can be placed into polymeric materials by different means, such as sulfur vulcanization, peroxide cross-linking, or radiation, but the details of these methods will not be discussed.

IX. EFFECT OF FILLERS ON MECHANICAL BEHAVIOR

Often polymers are modified by the placement of soft particulates within them (e.g., rubber particles within a hard glassy matrix). The reverse approach is also undertaken. An example of the latter is the placement of hard particles in a softer matrix such as calcium carbonate or glass particles placed in a rubbery matrix. Also in the growing field of composites, polymeric components serve typically as the

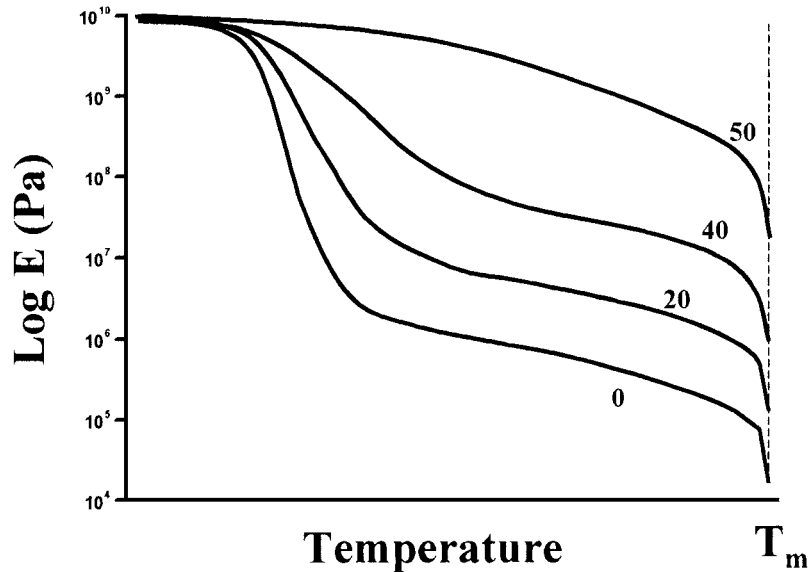


FIGURE 24 Generalized plot of the log of Young's modulus versus temperature contrasting the effect of levels of crystallinity ranging from 0 to 50%.

matrix material, whereas glass, carbon, or graphite fibers or other materials serve as fiber components that are generally stiff (high modulus) relative to the polymeric matrix. This is a highly complex area in terms of how these fillers or fibers influence mechanical properties, but a few important points can be made. In addition, there is a considerable literature available.

As stated above, there are two categories of particulate-filled systems that we will address here. The first is a soft filler in a hard matrix component, an example being a rubber particle or a void in a glassy polymer. In this case, if a stress is applied along some specific axis, such as in tension, the filler particle serves as a stress concentrator; that is, the stress field is altered in the general locality of the matrix near the filler particle (Fig. 25). Mechanics show that the soft filler will concentrate the stress to a maximum point at the equatorial region of the particle–matrix interface (Fig. 25). This forces the matrix material to undergo shear yielding or crazing—two important mechanisms by which energy dissipation occurs and which can promote a higher degree of toughening of the initial matrix system. An example of the crazing mechanism is shown in Fig. 26, where rubber particles in a glassy polystyrene matrix have promoted localized crazing in the equatorial regions. Without the presence of these rubber particles, polystyrene would show low strain to break and relatively low toughness, in contrast to the rubber-modified version. There are other ways in which rubber-toughening morphologies can be induced such as in high-impact polystyrene, but they are outside the scope of this article.

The phenomenon of crazing may not always be induced; rather, yielding by shear can be promoted, (Recall that yielding indicates plastic deformation and energy dissipation, which add to the toughness of a given material.) Softer phase particulates are often placed in the matrix for purposes of promoting toughness by one or both of the mechanisms indicated above. The price that is paid for placing a soft component into a hard matrix is that the modulus and yield stress will be sacrificed to some degree by the presence of the softer species.

The second system is a hard phase located in a soft matrix, such as a glass sphere placed within an elastomeric

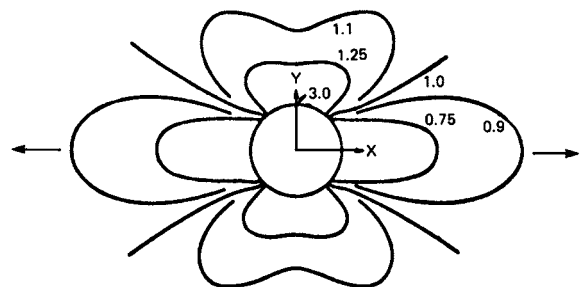


FIGURE 25 Schematic showing the relative stress levels around a hole that has been placed in a tensile sample loaded with the stress σ_0 along the x axis. The relative numbers on the contours imply the stress intensity factor above that of σ_0 . Note that the highest value is located at the equators and is a factor of 3. In the case of a spherical inclusion, the stress levels change in a similar way except that the maximum value is a factor of 2 at the equator. [Reprinted with permission from Nielsen, L. E. (1974). "Mechanical Properties of Polymers and Composites," Vol. 2, Dekker, New York. Copyright 1974 Marcel Dekker.]

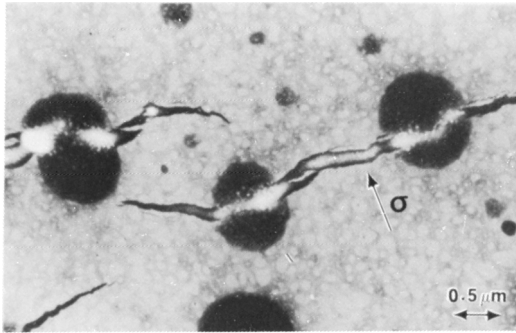


FIGURE 26 Transmission electron micrograph showing crazes induced in the equatorial regions of rubber particles that are embedded in the glassy polystyrene matrix. The arrow labeled with a σ represents the direction of tensile strain. [Reprinted with permission from Agarwal, B. D., and Broutman, L. J. (1980). "Analysis and Performance of Fiber Composites," Wiley, New York. Copyright 1980 John Wiley and Sons.]

slab. If attention is now placed on the rubber slab component, there is a desire for this softer material to elongate and to "thin down" around the hard inclusion, thereby placing a hoop stress on the equatorial region of the particle, which is very different from the system discussed above. In addition, the matrix tends to elongate and pull away from the "north" and "south" poles of the particulate, leading to a possible dewetting or cavitation phenomenon around

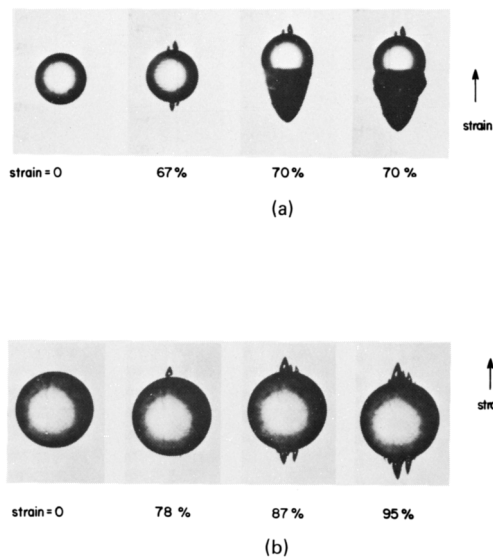


FIGURE 27 (a) Photomicrographs showing a glass bead embedded in a silicone elastomer that is undergoing elongation as indicated by the percentages. The blackish regions at the "poles" indicate where dewetting or cavitation is occurring, causing a scattering of light and a black region to be observed. (b) Surface of the particle has been treated such that it bonds well with the silicone elastomer matrix. Less dewetting or cavitation is observed, indicating a stronger interface. [Reprinted with permission from Gert, A. N., and Park, B. (1984). *J. Mat. Sci.* **19**, 1950 and 1951.]

the particles. An example of this is illustrated in Fig. 27a, where poor wetting of the particle existed between the elastomer and the glass sphere. In Fig. 27b, a coupling agent was used to bond the particle with the matrix to help minimize the cavitation process when elongation was undertaken. The particle that was bonded showed much less cavitation at equivalent or higher elongations than did the system without the bonding component.

To summarize the two types of particulates discussed above, it is clear that whether the matrix is hard relative to the particle, or vice versa, the effect of the dispersed phase is to modify the stress in the area of that inclusion. The exact behavior, however, is influenced by the difference in modulus characteristics of the dispersed phase relative to that of the matrix.

The effect of fibers versus particulates will not be discussed here. We shall simply point out that because a fiber has a much higher aspect ratio than more spherical-like particles, there is an effect on the stress transfer along the fibrous component. This will allow a greater stiffness to be gained and explains why high-strength composites often contain fibrous fillers in contrast to particulates. A final point regarding geometrically anisotropic filler particles is that their state of physical orientation will influence the local mechanics of the stress field and hence this feature must be considered in any analysis of such filler-containing materials.

X. MOLECULAR ORIENTATION AND ANISOTROPIC SYSTEMS

The use of polymers for many mechanical applications depends on the fact that previous molecular orientation of molecules has occurred for purposes of influencing the properties along specific directions. The simplest example is that of a drawn fiber in which the strength properties are important along the fiber axis but generally of little importance perpendicular to the same axis. Hence, by orientation of the molecules along the stretch direction or draw axis, the modulus is typically enhanced, as is tensile strength. Furthermore, the yield point can be eliminated since the system will have already gone through an orientation step. Generally, maximum or perfect orientation is not obtained through the drawing operations of bulk systems due to entanglement effects. This can lead to points of stress concentration and failure long before perfect alignment of all chains is attained.

There is much interest today in trying to achieve maximum orientation of polymer chains for purposes of obtaining ultrahigh-modulus/high-strength systems. Linear polyethylene has the characteristics to provide an extremely high modulus material of the order of 300 GPa, in

TABLE II Comparison of Moduli for Several Different Types of Materials^a

Material	Poisson's ratio, μ	Young's modulus, G	Shear modulus, G (GPa)	Bulk modulus, B (Gpa)	Density, ρ (g cm ³)	Specific properties	
						10 ⁶ E/ ρ (m ² /sec ²)	10 ⁶ G/ ρ (m ² /sec ²)
<i>Metals</i>							
Cast iron	0.27	90	35	66	7.5	12.0	4.7
Steel (mild)	0.28	220	86	166	7.8	28.0	11.0
Aluminum	0.33	70	26	70	2.7	26.0	9.6
Copper	0.35	120	45	134	8.9	13.5	4.5
Lead	0.43	15	5.3	36	11.0	13.6	4.8
<i>Inorganics</i>							
Quartz	0.07	100	47	39	2.65	38.0	17.8
Vitreous silica	0.14	70	31	33	2.20	32.0	14.0
Glass	0.23	60	25	37	2.5	24.0	9.8
<i>Polymers</i>							
Polystyrene	0.33	3.2	1.2	3.0	1.05	3.05	1.15
Poly(methyl methacrylate)	0.33	4.15	1.55	4.1	1.17	3.55	1.33
Nylon-6,6	0.33	2.35	0.85	3.3	1.08	2.21	0.79
Polyethylene (low density)	0.45	1.0	0.35	3.33	0.91	1.1	0.385
Ebonite	0.39	2.7	0.97	4.1	1.15	2.35	0.86
Rubber	0.49	0.002	0.0007	0.033	0.91	0.002	0.00075

^aAlso included are Poisson's ratio and density. The last two columns show the specific Young's and shear moduli.

contrast to 1 to 3 GPa for compression-molded polyethylene of the same species (i.e., unoriented). The value of the modulus just quoted is actually greater than what is presently achieved with high-strength/high-modulus liquid crystalline polymeric fibers such as poly-*p*-aromatic amide systems. Again it is apparent that molecular orientation can strongly influence mechanical parameters. In addition, an awareness of any previous orientation inducement in a system before its measurement may be very important in deciding how to test the final material. In multiphase or multicomponent systems, the level of orientation is not necessarily equal in each phase (i.e., crystalline versus amorphous), and hence if orientation is being taken account of, component or phase orientation should be considered rather than necessarily a system average. Indeed, in oriented semicrystalline systems, typically the crystal phase is much more easily oriented than that of the remaining amorphous phase. In fact, for fully amorphous systems, the orientation levels obtained are not particularly high by conventional processes. However, the induced mechanical anisotropy in these systems is still very considerable and therefore of great practical importance.

Due to the fact that orientation has such an impact on mechanical properties, it is one of the principal reasons why promoting orientation of the molecular chains is of high importance in achieving high stiffness and other properties (along the stretch direction). Of related interest is

that any property that is determined, when normalized on the basis of the density of the material, provides what is known as a *specific* property such as specific modulus. This normalization procedure therefore allows comparisons between all types of structural materials and an example of this is illustrated in Table II, which provides comparisons of polymers with inorganics as well as metallic systems. As is noted from Table II, which contains the parameters of Poisson's ratio, Young's modulus, shear modulus, bulk modulus, density, and the specific Young's modulus and specific shear modulus, the effects of the normalization procedure bring many of these materials in line with one another relative to their non-normalized moduli values. When orientation in addition is taken into account for polymeric systems, which can drastically alter the modulus as referred to earlier in this section, the specific moduli can distinctly exceed that of many metallics or inorganics as is illustrated in Fig. 28. Here one notes that the material designated as Spectra[®], which is a very highly oriented and highly crystalline linear polyethylene fiber material, has a much higher specific tensile strength as well as modulus relative to steel or glass fibers.

XI. MISCELLANEOUS CONSIDERATIONS AND FINAL REMARKS

Many important parameters have not been discussed in this article. For example, the wear characteristics of polymer

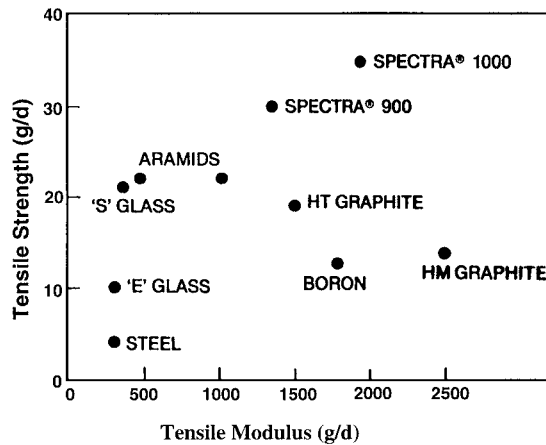


FIGURE 28 Plot of specific modulus versus specific tensile strength for several materials including steel, glass-oriented polyethylene (Spectra[®]), liquid crystalline aromatic polyamides (Kevlar[®]), etc.

surfaces are highly important, but it is not always easy to measure them by a simple test and apply the results to a specific application. Other important parameters are the tear characteristics and fatigue and cyclic loading behavior of materials. Picture, for example, an application of a polymeric hinge where folding back and forth occurs over its life-time. How many cycles of folding can occur at a given rate and temperature before failure is induced? Another important area is environmental stress crack resistance where certain agents, such as detergents or oil components, may promote the cracking of polymeric systems if they are under stress.

As the reader is aware, there are several materials that are used structurally but which are of a cellular nature, i.e., open-cell and closed-cell foams along with other materials such as even wood itself. Often the closed-cell foams are for insulation purposes or to help lighten the weight of a system. Polymeric structural foams are often utilized in a diversity of applications, including as automobile bumpers. In contrast, the open-cell foams allow air to pass through when the system is loaded as is common in the cushioning applications of polyurethane foams. Of importance is to recognize that the nature of the cellular structure does influence the mechanical properties of the materials and as a result can play an important role, when analyzing such materials. Although not discussed in this paper, the interested reader should consult the reference by Gibson and Ashby (1988) for more information on cellular materials and their mechanical behavior.

On a different note, if a polymeric system is below its glass transition temperature, one tends to often think that the system is stable mechanically since there is limited backbone motion. However, this can be very far from the truth. Typically, when glassy materials are prepared, they

are quenched from either the melt or from above T_g into the glassy state. The viscosity rises greatly as the glass transition temperature is approached during the cooling process causing the material not to be able to maintain its true equilibrium structure as it passes into the glassy state, thereby placing it into a nonequilibrium state. Specifically, the material will possess a greater amount of “free volume” due to the fact that equilibrium thermal contraction could not occur. As a result, this excess free volume, small as it may be, slightly lowers the density of the quenched glassy material and, as a result of possessing this excess free volume, its mechanical properties are also altered relative to what its true equilibrium state would provide. Generally, the result is that during aging below T_g , commonly called physical aging, the system undergoes slow densification of the material if *local-scale* molecular motion can occur as we have discussed is common for polymers in the glassy state. The degree and rate of physical aging is dependent on a number of factors such as how far below the glass transition temperature one stores the material and how rapid the cooling process was. (How far from equilibrium was the structure when placed into the glassy state?) Of much importance is that this slow densification or physical aging process has drastic effects on a number of parameters, one of these being yield stress. In particular, as shown in Fig. 29, amorphous polyethylene terephthalate (PET) shows that the yield stress distinctly grows with time upon aging a quenched sample at room temperature, which is approximately 40°C below its glass transition temperature (1 Hz). A number of other mechanical parameters are also altered with time but the author will not focus on additional detail in this basic paper. However, those working with materials that are polymeric glasses or contain glassy phases should become more acquainted with

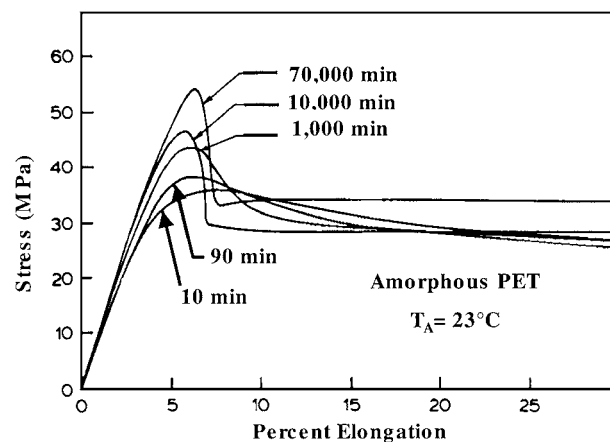


FIGURE 29 Engineering stress–engineering strain plots for quenched glassy poly(ethylene terephthalate) determined at different times following physical aging at 23°C. [From Tant, M. R., and Wilkes, G. L. (1981). *J. Appl. Polym. Sci.* **26**, 2813.]

the process of physical aging because it can have drastic effects on the time-dependent characteristics of those materials. In this respect, the reader may wish to consult the reference by Struick (1978).

An attempt has been made to acquaint the reader with the philosophy that the author uses in understanding the structure–property behavior of polymeric systems. Specifically, the earthworm analogy and the Deborah number concept are believed to be highly useful, and the reader should attempt to apply this thinking when encountering the behavior of polymeric materials.

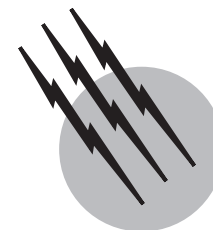
SEE ALSO THE FOLLOWING ARTICLES

COMPOSITE MATERIALS • ELASTICITY, RUBBERLIKE • FRACTURE AND FATIGUE • GLASS • HYDROGEN BOND • MACROMOLECULES, STRUCTURE • PLASTICIZERS • POLYMER PROCESSING • RUBBER, NATURAL

BIBLIOGRAPHY

Agarwal, B. D., and Broutman, L. J. (1980). "Analysis and Performance of Fiber Composites," Wiley, New York.

- Aklonis, J. J., and McKnight, W. J. (1983). "Introduction to Polymer Viscoelasticity," 2nd ed., Wiley-Interscience, New York.
- Boden, H. E. (1984). *Adv. Polym. Technol.* **3**(4), 383.
- Boyer, R. F. (1981). *Eur. Polym. J.* **17**, 661.
- Dealy, J. M. (1982). "Rheometers for Molten Plastics," Van Nostrand Reinhold, New York.
- Gent, A. N., and Park, B. (1984). *J. Mater. Sci.* **19**, 1947.
- Gibson, L. J., and Ashby, M. E. (1988). "Cellular Solids: Structure and Properties," Pergamon Press, New York.
- Kausch, H. H., and DeVries, K. L. (1975). *Int. J. Fract.* **11**, 727.
- McCrum, N. G., Read, B. E., and Williams, G. (1967). "Anelastic and Dielectric Effects in Polymeric Solids," Wiley, New York.
- Morton, J. R., Johnson, J. F., and Cooper, A. R. (1972). *J. Macromol. Sci. Rev. Macromol. Chem.* **C8**(1), 57.
- Nielsen, L. E. (1974). "Mechanical Properties of Polymers and Composites," Vol. 2, Dekker, New York.
- Nielsen, L. E. (1977). "Polymer Rheology," Dekker, New York.
- Randall, R. C., ed. (1984). "NMR and Macromolecules," Sequence, Dynamic, and Domain Structure, ACS Symposium Series, Vol. 247.
- Samuels, R. J. (1974). "Structured Polymer Properties," Wiley, New York.
- Struick, L. C. E. (1978). "Physical Aging in Amorphous Polymers and Other Materials," Elsevier Scientific Publishing Co., New York.
- Tant, M. R., and Wilkes, G. L. (1981). *J. Appl. Polym. Sci.* **26**, 2813.
- Ward, M., ed. (1975). "Structure and Properties of Oriented Polymers," Applied Sciences, London.
- Wetton, R. E., and Stone, M. R. (1983). *Proc. Trans. Relax. Polym. Mater.*, Melbourne, 1983.
- Zhang, Y. H., and Carreau, P. J. (1991). *J. Appl. Polym. Sci.* **42**, 1965.



Polymers, Photoresponsive (in Electronic Applications)

Elsa Reichmanis
Omkaram Nalamasu
Francis Houlihan

Bell Laboratories, Lucent Technologies

- I. Introduction
- II. Polymer Materials Requirements
- III. Historical Perspective
- IV. Chemically Amplified Resists
- V. Polymers for Sub-150-nm Imaging Applications
- VI. 157-nm Resist Design
- VII. Conclusion

GLOSSARY

Chemically amplified resists Resists where the initial exposure to either light or radiation generates a catalyst which then acts on the surrounding material to initiate a series of reactions that lead to solubility changes in the matrix.

Contrast The maximum rate change of normalized resist thickness per input energy (on a logarithmic scale) achieved upon development of a resist.

Conventional photoresist A photoresist material that is largely comprised of a substituted novolac resin and a diazonaphthoquinone dissolution inhibitor. Such materials represent the largest fraction of photoresists used in the production of semiconductor devices today.

Developer A solvent- or aqueous-based liquid medium that will selectively remove either the irradiated portions of a resist film in the case of positive resists or unexposed areas in the case of negative acting resists.

Dissolution-inhibition resists Resists that are composed of an inherently aqueous-base-soluble matrix resin and a second component that is insoluble in aqueous media that renders the matrix insoluble in aqueous solution as well. Irradiation effects a structural change in dissolution inhibitor such that dissolution rate of exposed areas is more than that of the matrix resin, thus causing a dissolution promotion.

Etching resistance A measure of how effectively a resist will withstand the etchants used to transfer images that have been defined in the resist into the device substrate.

Extreme ultraviolet (EUV) Refers to “soft” X-ray radiation in the wavelength range of 13 to 25 nm.

Lithographic process (lithography) The process for manufacturing semiconductor devices that involves transferring a circuit pattern into a thin polymer film and then transferring that pattern into the underlying substrate.

Photoacid generator A molecule that generates acid molecules upon irradiation. One class of such materials is the onium salts.

Post-exposure bake The baking step required for most chemically amplified resists whereby the photo- or radiation-generated acid catalytically reacts with pendant groups on relevant resist components to effect a change in solubility of the resist.

Resist (photoresist) A radiation- and/or photosensitive polymer material that replicates the circuit pattern on a photomask. The circuit patterns are subsequently transferred into the desired substrate materials. Resists can be classified as either negative or positive acting. Negative resists become less soluble in a given developer upon irradiation, while positive resists become more soluble in a developing medium.

Resolution The resolution capability of a resist is typically the minimum resolvable feature size.

Sensitivity The incident input energy per unit area required to achieve the desired chemical response in a resist.

Very large-scale integration (VLSI) Used as an adjective to refer to an integrated circuit having a very large degree of complexity.

THE INVENTION OF the point contact transistor in 1947 heralded the dawn of the microelectronics era,¹ which has had impact on every aspect of our lives. Materials chemistry in general, and organic and polymer chemistry in particular have enabled the unprecedented advancements in microelectronics technology. The business is driven by the need to build devices that contain an increasing number of individual circuit elements on a semiconductor material. Over time, device complexity and functionality have increased while minimum feature size has dramatically decreased.² This trend is perhaps best illustrated by Fig. 1, which compares a state-of-the-art, fully processed silicon substrate containing hundreds of complex devices with millions of transistors each to the first macroscopic, single silicon-based transistor fabricated in 1947. The ability to shrink the feature size is critically dependent upon the technologies involved in the delineation of the circuit pattern. Thus, high-resolution imaging materials could be considered to be the cornerstone of today’s device industry.

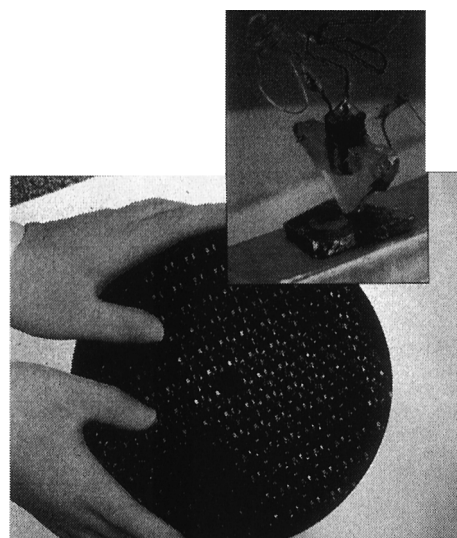


FIGURE 1 Photographic comparison of a state-of-the-art silicon device substrate and the first macroscopic silicon-based transistor fabricated in 1947.

I. INTRODUCTION

A modern integrated circuit is a complex three-dimensional structure of alternating, patterned layers of conductors, dielectrics, and semiconductor films. This structure is fabricated on an ultrahigh-purity wafer substrate of a semiconducting material such as silicon. The performance of the device is, to a large degree, governed by the size of the individual elements. As a general rule, the smaller the elements, the higher the device performance will be. The structure is produced by a series of steps used to precisely pattern each layer. The patterns are formed by lithographic processes that consist of two steps: (1) delineation of the patterns in a radiation sensitive thin-polymer film called the resist, and (2) transfer of that pattern using an appropriate etching technique. A schematic representation of the lithographic process is shown in Fig. 2.² Materials that undergo reactions that increase their solubility in a given solvent (developer) are called *positive-tone resists*, while those that decrease their solubility are known as *negative-acting materials*. The focus of this review concerns the design and selection of polymer materials that are useful as radiation-sensitive resist films. Such polymers must be carefully designed to meet the specific requirements of each lithographic technology and device process.

An overwhelming preponderance of devices continues to be fabricated via “conventional photolithography” employing 350 to 450 nm light. Incremental improvements in tool design and performance with concomitant refinements in the novolac/diazonaphthoquinone resist

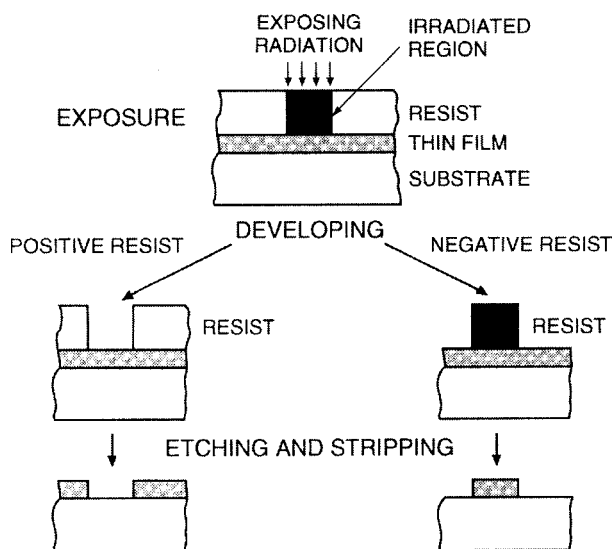


FIGURE 2 Schematic representation of the lithographic process.

materials chemistry and processing have allowed the continued use of this technology to produce ever-smaller features (Table I). The cost of introducing a new technology, which includes the costs associated with the development and implementation of new hardware and resist materials, is a strong driving force pushing photolithography to its absolute resolution limit and extending its commercial viability.³

The technological alternatives to conventional photolithography are largely the same as they were a decade ago: short-wavelength (>250 nm) photolithography, scanning or projection electron-beam, X-ray or EUV, or ion-beam lithography.^{2,4} Unfortunately, conventional photoresists are not appropriate for use with these new, alternative lithographic technologies. The most notable deficiencies of these materials are their inherent low sensitivity and absorption characteristics that are too high for shorter wavelength exposure to allow uniform imaging through practical resist film thicknesses (about 0.5 to 1 μm). Thus, no matter which technology becomes dominant after photolithography has reached its resolution limit, new resists and processes will be required.⁵ The introduction of new resist materials and processes will also require considerable lead time to bring them to the performance level currently realized by conventional positive photoresists.

There are significant trade-offs between optimum process performance and the chemical design of new resists. The ultimate goal of any lithographic technology is to be able to produce the smallest possible features with the lowest cost per level and with wide process latitude. The best solution will invariably require compromises, and an understanding of materials and process issues is essential to select the correct compromise.

II. POLYMER MATERIALS REQUIREMENTS

Resist chemistry must be carefully designed to meet the specific requirements of a given lithographic technology. Although these requirements vary according to the radiation source, device process requirements, and exposure tool design, the following are ubiquitous: sensitivity, contrast, resolution, etching resistance, purity, and manufacturability.⁶ As noted in Table II, each of these properties is affected by specific molecular characteristics of the resin and can be tailored by careful manipulation of polymer structure, molecular properties, and synthetic methods.⁷

The polymer resins must:

- Exhibit solubility in solvents that allow the coating of uniform, defect-free, thin films.
- Be sufficiently thermally stable to withstand the temperatures and conditions used with standard device processes.
- Exhibit no flow during pattern transfer of the resist image into the device substrate.
- Possess a reactive functionality that will facilitate pattern differentiation after irradiation.
- For photoexposure, have absorption characteristics that will permit uniform imaging through the thickness of a resist film.

In general, thermally stable (>150°C), high glass-transition-temperature ($T_g > 90^\circ\text{C}$) materials with low absorption at the wavelength of interest are desired. If other additives are to be employed to effect the desired reaction, similar criteria apply. Specifically, they must be non-volatile, be stable up to at least 175°C, possess a reactive functionality that will allow a change in solubility after irradiation, and have low absorbance. The sections that follow outline many of the chemistries that have been applied to the design of resist materials for microlithography. The reader is referred to additional major overviews of the field for additional information.^{2,7-10}

III. HISTORICAL PERSPECTIVE

A summary of the evolution of lithographic technologies and the associated materials and devices is presented in Table I.² The first devices were fabricated on 1-inch silicon substrates, were comprised of 256 transistors, and had minimum features in the range of 15 to 20 μm . The radiation-induced chemical processes used to effect patterning in this era were crosslinking reactions that led to negative acting resists. As time progressed, alternative higher resolution, positive-acting material choices became

TABLE I Evolution of Lithographic and Semiconductor Device Technologies

Year	Lithographic imaging technology	Resist imaging chemistry	Device parameters
1967	Contact printing	Cyclized rubber (-)	15–20 μm features; 256 DRAM; 0.2 cm^2 device size; 1" Si substrate
1971	Near contact	Cyclized rubber (-) Novolac/diazoquinone (+)	8–12 μm ; 1K DRAM; 0.3 cm^2 ; 2" Si substrate
1974	Near contact	Novolac/diazoquinone (+)	6 μm ; 4K DRAM; 0.4 cm^2 ; 2.5" Si substrate
1977	1:1 projection; 360–420 nm	Novolac/diazoquinone (+)	4 μm ; 16K DRAM; 0.6 cm^2 ; 3" Si substrate
1980	Step and repeat; 5–10 \times reduction optics; 420–436 nm	Novolac/diazoquinone (+)	<3 μm ; 64K DRAM; 0.8 cm^2 ; 4" Si substrate
1984	Step and repeat; 5 \times reduction optics; 436-nm (g-line)	Novolac/diazoquinone (+)	1.5 μm ; 256K DRAM; 1 cm^2 ; 6" Si substrate
1988	Step and repeat; 5 \times reduction optics; 436-nm (g-line)	Novolac/diazoquinone (+)	0.9 μm ; 1.8 cm^2
1990	Step and repeat; 5 \times reduction optics; 365-nm (i-line)	Novolac/diazoquinone (+)	0.7 μm ; 4M DRAM; 1.3 cm^2
1993	Step and repeat 5 \times reduction optics; 365-nm (i-line)	Novolac/diazoquinone (+)	0.5 μm ; 16M DRAM; 1.6 cm^2 ; 8" Si substrate introduced
1995	Step and repeat; 4–5 \times (i-line); deep-UV (248 nm)	Novolac/diazoquinone (+)	0.35 μm ; 64MB DRAM; 2 cm^2
1998	Step and repeat; deep-UV (248 nm)	Chemically amplified	0.25 μm ; 256M DRAM; 3 cm^2
2001	Step and repeat; deep-UV (248, 193 nm)	Chemically amplified	0.18 μm ; 1G DRAM; 5 cm^2 ; 8–12" Si wafers
2007	Deep-UV (193, 157 nm); EUV (13 nm); projection e-Beam; X-ray	Chemically amplified	<0.1 μm ; 16G DRAM; 8 cm^2 ; 12" Si wafers

available. The following sections outline the “traditional” materials chemistry options.

A. Two-Component Crosslinking Resists

During the early stages of the semiconductor industry (1957 to 1970), the minimum size of circuit features exceeded 5 μm , and the primary resist used dur-

ing this time consisted of cyclized poly(*cis*-1,4 isoprene) and an aromatic azide crosslinking compound.⁹ The *bis*-aryldiazide, 2,6-*bis*(4-azidobenzal)-4-methyl cyclohexanone, effectively initiates crosslinking of the matrix resin upon exposure to near-ultraviolet (UV) light (Fig. 3). The resolution of this highly sensitive, two-component resist was limited due to solvent-induced swelling followed by stress relaxation of the developed resist images. Enhanced

TABLE II Selected Resist Requirements as They Relate to Device Issues and Materials Molecular Characteristics

Lithographic parameter	Device issue	Molecular characteristic
Absorption	Resolution	No olefinic or aromatic moiety
Etching stability	Process flexibility	High levels of structural carbon, low oxygen content
Aqueous base solubility	Process flexibility, environmentally friendly	Base solubilizing groups such as OH, COOH, NH, etc.
Substrate adhesion	Yield	Presence of polar moieties
Sensitivity (photospeed)	Throughput	Catalytic chain length for acidolysis, quantum yield for acid generation, acid strength, protective group chemistry
Post-exposure delay and substrate sensitivity	Resolution, process flexibility, yield	Catalytic chain length for acidolysis, protective group chemistry, acid strength
Outgassing	Throughput	Protective group and photoacid generator chemistry
Aspect ratio of images	Resolution, yield	Surface tension effects and mechanical strength of materials
Low metal ion content	Yield	Synthesis and scale-up methodology
Manufacturability and cost	Manufacturing feasibility	Synthesis and materials scale-up methodology and lithographic process requirements

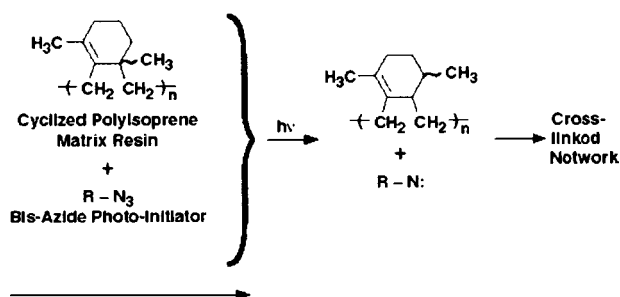


FIGURE 3 Structural representation of the polyisoprene negative-acting resists.

resolution was achieved by Iwayanagi *et al.*^{11,12} Employing an aryazide in conjunction with an aqueous-base-soluble poly(hydroxystyrene) matrix, submicron patterns were defined upon 250-nm exposure. However, the high optical density of the material at 250 nm afforded undercut resist profiles. Appropriate choice of the crosslinking agent allows extension of the chemistry of this system into the mid-UV range.¹³

B. Single-Component Crosslinking Resists

Concurrent with the rapid development of electron-beam lithographic tools for both optical mask making and direct write applications was the commercialization of single-component negative resists. The electron-beam exposure requirements of these materials were compatible with the dose outputs ($\sim 1 \mu\text{C}/\text{cm}^2$ at 10 kV) of raster scan machines developed by Bell Laboratories.¹⁴ These resists typically contained epoxy, vinyl, and halogen functionalities.^{15,16}

Exposure of polymers containing epoxy,^{17–19} vinyl, and allyl²⁰ affords a radical or cationic species that can react with the same (intramolecular crosslink) or neighboring (intermolecular crosslink) polymer chain. This process continues via a chain reaction leading to the formation of an insoluble polymer network. Though this reaction sequence affords high resist sensitivity, the propagation of radiation-generated reactive species continues in the vacuum environment of an electron-beam exposure tool. The consequence is that those features that were exposed first will have dimensions that are different from those exposed last.²¹ In certain cases, the feature-size difference can exceed the maximum allowable variation specified for a particular device level, thus these chemistries have limited usage today.

On the other hand, the halogenated styrene negative resists crosslink by a radiation-induced reaction that involves radicals that recombine and do not propagate.²² Since the reaction sequence does not involve a post-exposure curing reaction and, additionally, the incor-

poration of styrene into the resist improves the dry etching characteristics of the polymers, these materials are often favored over aliphatic-based resists. Specific examples of halogenated styrene-based resists are chlorinated²³ or chloromethylated²⁴ polystyrene and poly(chloromethylstyrene).^{25,26} In addition to being sensitive electron-beam resists, the latter also have sensitivity to deep-UV²⁷ and X-ray²⁸ exposure. In one case, the halogenated material chlorostyrene was copolymerized with glycidyl methacrylate (Fig. 4a) to afford a very sensitive e-beam resist that exhibits little of the curing phenomena typically observed with epoxy crosslinking reactions.^{29–31}

While the aromatic styrene ring affords improved dry-etching resistance, further improvement in this parameter can be achieved through incorporation of silicon. For instance, Hatzakis *et al.*³² showed that polysiloxane polymers such as poly(vinylmethyl siloxane) readily provide e-beam sensitivity in the 1- to $2\text{-}\mu\text{C}/\text{cm}^2$ range. These materials have a high silicon content ($>30 \text{ wt } \%$), and as such have found use in bilevel lithographic processes (see References 2 and 9 for a definition of bilevel). Other resists which exhibit acceptable thermal properties and etching resistance for bilevel applications are copolymers of trimethylsilyl-^{33,34} and trimethylstannylstyrene³³ with chlorostyrene (Fig. 4b). Additionally, copolymerization of trimethylsilylmethyl methacrylate with chloromethylstyrene yields a viable electron-beam and deep-UV negative resist even through the homopolymer of the silicon-containing methacrylate is a positive-acting material.³⁵ In this case, at the exposure dose employed, crosslinking of the chloromethylstyrene unites predominates.

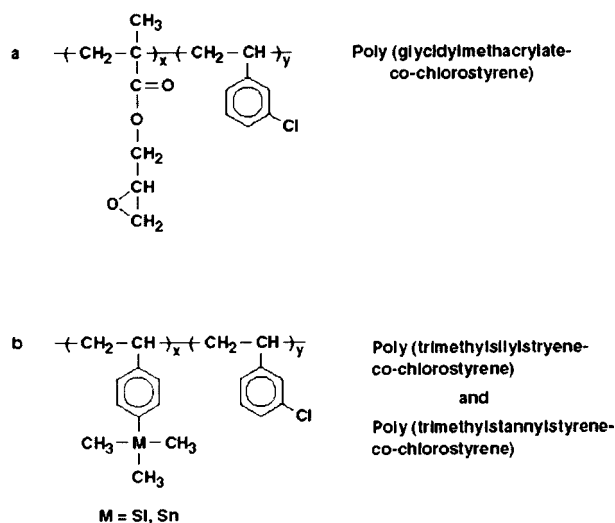


FIGURE 4 (a) Structural representation of the negative resist, poly(glycidyl methacrylate-co-chlorostyrene), and (b) the copolymers of chlorostyrene and trimethylsilyl- or trimethylstannylstyrene.

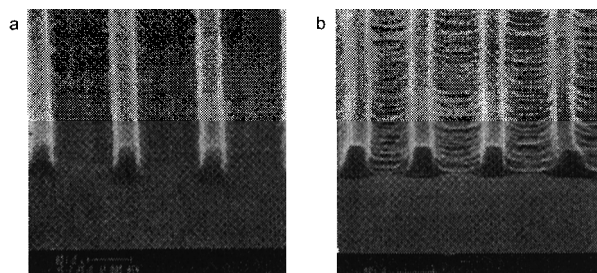


FIGURE 5 SEM micrographs depicting the effect of developer selection on a solvent-developed, negative-acting resist.

For the resists discussed in this section, lithographic performance is hindered by the extent to which the materials swell in organic developing solvents. This phenomenon is shown in Fig. 5, which depicts how developer selection can affect image quality in a styrene-based negative resist. The type of pattern distortion shown in this figure ultimately limits the resolution capability of these resists. Novembre and co-workers³¹ found that the extent of swelling could be minimized by proper choice of developer using a method based upon the Hansen three-dimensional solubility parameter model. They determined that developers found to be thermodynamically poor, but kinetically good, solvents afford resist materials such as poly(glycidyl methacrylate-co-3-chlorostyrene) (GMC) with enhanced resolution capability (Fig. 5a). This methodology facilitates selection of an optimal developer without the tedious trial-and-error approach commonly used.

C. Main-Chain Scission Positive Resist Chemistry

Positive resists exhibit enhanced solubility after exposure to radiation. The principles leading to this increased solubility are chain scission and/or polarity change. Positive photoresists that operate on the polarity change principle have been widely used for the fabrication of VLSI devices because of their high resolution and excellent dry-etching resistance. The chain scission mechanism typically operates at photon energies below 300 nm where the energy is sufficient to break main-chain bonds and will be reviewed first.

Substituted methacrylates are probably the most extensively investigated polymers that fall into this category. Poly(methyl methacrylate) (PMMA) undergoes chain scission when exposed to radiation.³⁶ Coupled with this scission process is dissolution behavior that leads to minimal swelling resulting in extremely high-resolution imaging capability. The ability to delineate submicron images in PMMA is, however, offset by its low sensitivity and relatively poor dry-etching resistance. Electron-beam and deep-UV exposure doses in excess of $50 \mu\text{C}/\text{cm}^2$ at

10 kV ³⁷ and $1 \text{ J}/\text{cm}^2$,^{38,39} respectively, have been required for patterning purposes.

Efforts to improve the sensitivity of PMMA have spawned many research efforts, including:

- Introduction of electronegative substituents⁴⁰
- Incorporation of bulky substituents⁴¹
- Incorporation of fluorine into the ester group⁴²
- Generation of inter- and intramolecular anhydride linkages⁴³
- Copolymerizing methyl methacrylate (MMA) with other methacrylate-based monomers to effect improved absorption characteristics⁴⁴ or etching resistance⁴⁵

Materials based upon poly(methyl isopropenyl ketone) (PMIPK) are also known to undergo radiation-induced chain scission.⁴⁶

Copolymers of an alkene or vinylaryl compound with sulfur dioxide are another major class of chain scission resists and are widely used for the fabrication of chromium photomasks.⁴⁷ Interest in the poly(olefin sulfone)s as resists arose from results of Bowmer and O'Donnell,⁴⁸ who reported a $G(s)$ value of ~ 10 for poly(1-butene sulfone). Upon irradiation, the relatively weak main-chain carbon-sulfur bond⁴⁹ cleaves, inducing depolymerization to yield the starting monomers as the major products. The copolymer containing 1-butene (PBS) (Fig. 6) is a highly sensitive ($< 1 \mu\text{C}/\text{cm}^2$ at 10 kV) electron-beam resist.⁵⁰ An O_2 -reactive, ion-etching-resistant material can be obtained using silylated monomers such as *p*-trimethylsilylstyrene and *p*-pentamethyldisilylstyrene.⁵¹

Linear silicon backbone polymers (i.e., polysilanes) have also been reported to function as positive-acting deep-UV resists.⁵² Exposure results in cleavage of the main-chain Si—Si bond, resulting in a decrease in molecular weight. These materials exhibit high quantum yields for scission, nonlinear photobleaching, and submicron resolution. One interesting variant of this approach involves plasma-induced deposition of networked polysilane-like films from methylsilane. Irradiation of this material in the presence of oxygen affords a silicon-oxide-like material (Fig. 7). Either the irradiated, oxidized regions or the parent silane can then be removed through plasma processing with the requisite reagent.⁵³ The reader is referred to recent reviews of lithographic applications of silicon-containing polymers for additional information.⁵⁴

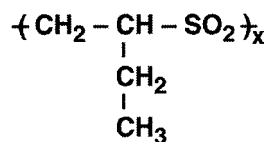


FIGURE 6 Structural representation of poly(1-butene-sulfone).

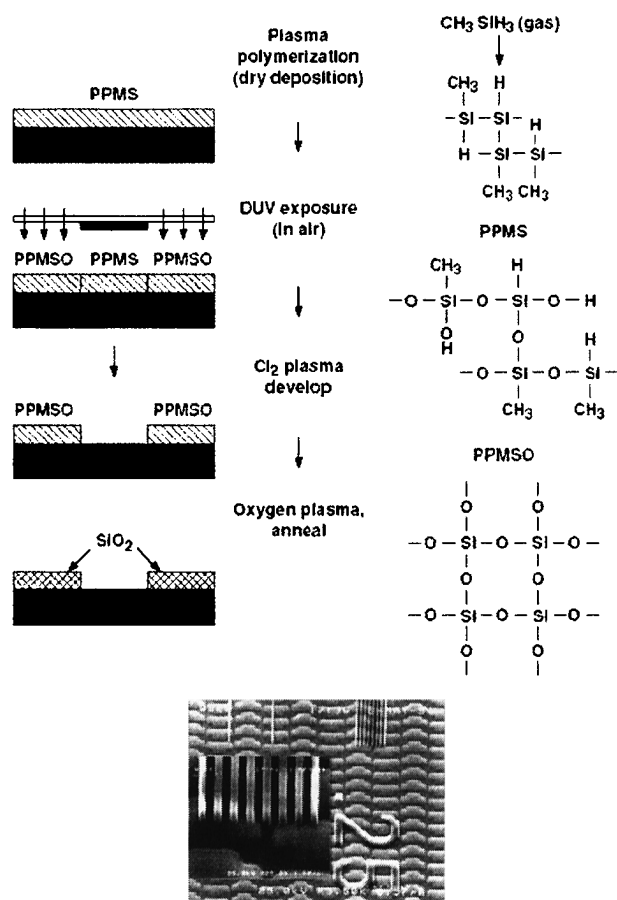


FIGURE 7 Structural representation of the chemistry and processes associated with plasma-polymerized methylsilane photoresists with an SEM image depicting 0.25- μm images obtained in this resist.

D. Dissolution-Inhibition Resists

Photolithography represents the workhorse technology for device manufacture and has traditionally used a Hg or Hg–Xe discharge lamp as the radiation source. Resist systems that have been developed to respond favorably to this energy spectrum (250–450 nm) are often called “conventional photoresists” (Fig. 8) and are typically comprised of two components: an aqueous alkali-soluble resin and a photosensitive dissolution inhibitor.^{2,55} The alkali-soluble resin, a novolac, is prepared via condensation polymerization of a substituted phenol and formaldehyde. These resins, and modifications thereof, are formulated to exhibit low absorbance in the near- and mid-UV region, are glassy amorphous materials at room temperature, and can be dissolved in a variety of organic solvents useful for spin-coating applications. In addition to alkyl substituents, silicon-bearing moieties have been examined for enhancement of oxygen-reactive ion-etching resistance.⁵⁶ The second component of conventional photoresists is

a hydrophobic, substituted diazonaphthoquinone (DNQ) dissolution inhibitor (DI). Addition of this component to the novolac renders the polymer matrix insoluble in aqueous-base developers. Upon irradiation, the DNQ undergoes a Wolff rearrangement followed by hydrolysis, yielding indene carboxylic acid. The photogenerated acid is hydrophilic and allows the exposed regions of the film to be dissolved in aqueous alkaline solution. The remaining, nonexposed regions are unaffected and do not swell in the developer. The dissolution mechanism has long attracted the attention of many workers. Most recently, Reiser⁵⁷ has postulated a mechanism based on percolation theory. In this model, the diffusion of base is regulated by the density of hydrophilic percolation sites in the solvent penetration zone. This density can be changed by the introduction of additives (i.e., the inhibitor) which block some of the hydrophilic sites, and it can be changed by irradiation (i.e., conversion of inhibitor to indene carboxylic acid). The novolac–DNQ chemistry affords high resolution and, as a consequence of the aromatic nature of the resin, good dry-etching resistance for pattern-transfer processes.

The performance of conventional resists depends on the precise structure of the photosensitive DI and the novolac resin.^{58,59} Most photoresists designed for 365- to 436-nm exposure utilize a 1,2-diazonaphthoquinone-5-sulfonate ester that exhibits absorbance maxima at ~ 340 , 400, and 430 nm. Changes in the position of the aryl substituent can lead to variations in sensitivity and light absorption. For example, the 4-aryl sulfonate analogs exhibit absorption characteristics that are more appropriate for shorter wavelength exposure (i.e., 313 and 365 nm).⁵⁸ This substitution pattern leads to the appearance of a bleachable absorbance at ~ 315 and 385 nm, extending the sensitivity of conventional resists to shorter wavelengths. Optimization of resist sensitivity for a particular exposure tool requires an understanding of the effect of substituents on the absorption characteristics of the materials. This approach was used effectively by Miller and coworkers,⁵² who coupled such studies with semi-empirical calculations to facilitate the design of diazonaphthoquinone dissolution inhibitors for mid-UV applications.

The high absorbance of conventional photoresists prevents their application to shorter wavelength (<280 nm) lithographies. As a result, alternative resins and dissolution inhibitors have been proposed. Examples include dissolution inhibitors based on 5-diazo-Meldrum's Acid chemistry for novolac resins⁶⁰ and 2-nitrobenzyl carboxylates⁶¹ (Fig. 9). In the case of the nitrobenzyl carboxylates, optimum results were obtained for ester derivatives of large-molecule organic acids such as cholic acid. These esters are nonvolatile and allow conversion of a relatively large volume fraction of resist from an alkali-insoluble to an alkali-soluble state. While these resists

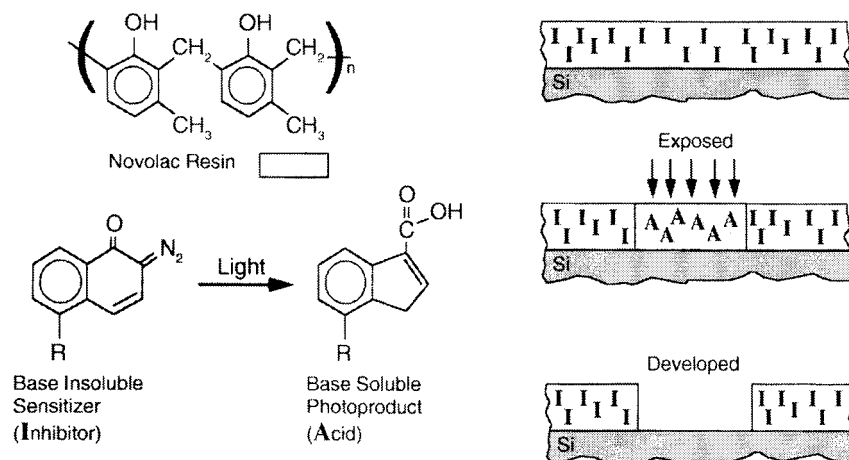


FIGURE 8 Schematic representation of conventional, diazonaphthoquinone–novolac, positive-resist chemistry.

exhibit high sensitivity and contrast and are capable of submicron resolution, their aliphatic nature provides only marginal dry-etching resistance.⁶² Improvements in the transparency at sub-250-nm wavelengths of the matrix resin used in dissolution inhibition resists while maintaining the good dry-etching characteristics can be obtained by replacing the novolac with poly(4-hydroxystyrene) (PHS) and its substituted analogs.⁶³ Alternatively, alicyclic methacrylates have been used to develop etching-resistant 193-nm resist materials.⁶⁴

Conventional positive photoresists based on novolac–DNQ chemistry have application not only to photolithography, but also to electron-beam and X-ray lithography.⁶⁵ One drawback to their use however, is poor sensitivity. The use of polymeric dissolution inhibitors in novolac

resins has been shown to overcome this issue and produce electron-beam sensitive-positive resist materials. Bowden *et al.*⁶⁶ have shown that a two-component system consisting of a novolac and a poly(olefin sulfone) as the dissolution inhibitor can generate a resist having electron-beam sensitivities in the 3- to 5- $\mu\text{C}/\text{cm}^2$ range at 20 kV. The specific sulfone is poly(2-methyl-1-pentene sulfone) (PMPS) which, when formulated with a novolac resin, renders the novolac insoluble in alkaline media. Exposure to electrons results in spontaneous depolymerization of PMPS to its volatile monomers. The dissolution inhibitor is thus effectively “vaporized,” thereby allowing dissolution of the remaining aqueous base-soluble novolac resin (Fig. 10).⁶⁷ Similar materials have been reported by other workers.⁶⁸

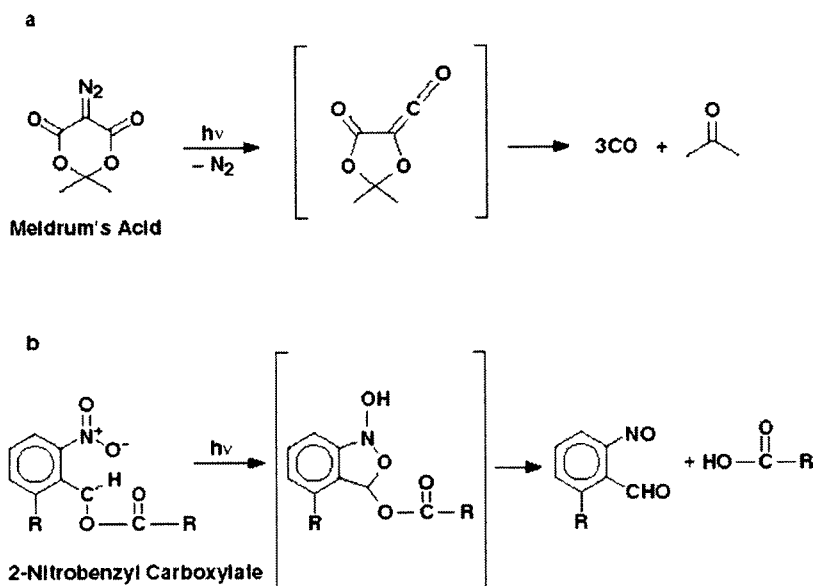


FIGURE 9 Structural representation of (a) Meldrum's Acid and (b) *o*-nitrobenzyl ester dissolution inhibitor chemistry.

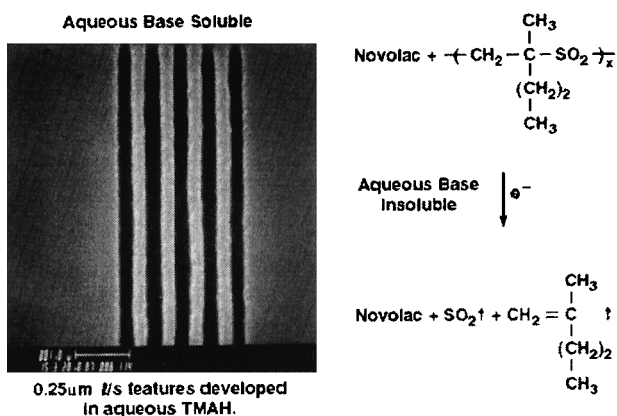


FIGURE 10 The chemistry and imaging characteristics of a novolac–poly(methyl-2-pentene sulfone) electron-beam resist; the SEM image depicts nominal 0.25- μm line/space patterns developed in aqueous tetramethyl ammonium hydroxide.

E. Image Reversal Chemistry

Knowledge that carboxylic acids undergo base-catalyzed decarboxylation led a number of groups to explore the possibility of creating negative tone images in conventional positive photoresist.⁶⁹ For instance, addition of small amounts of base additives such as monazoline, imidazole, or triethanolamine to diazoquinone novolac resists, followed by exposure, post-exposure baking, and finally development in aqueous base generates high-quality negative-tone images. The chemistry and processes associated with this system are shown in Fig. 11. Effectively, thermally induced, base-catalyzed decarboxylation of the indene carboxylic acid destroys the aqueous-base solubility of the exposed resist. Subsequent flood exposure renders the previously masked regions soluble in aqueous base, allowing generation of negative tone pat-

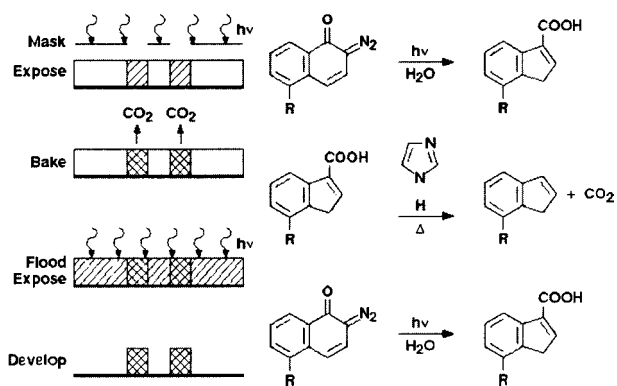


FIGURE 11 The chemistry and process sequence for a conventional diazonaphthoquinone–novolac photoresist used in an “image reversal” mode.

terns. Depending on the precise process conditions that are employed, the final flood exposure step may be unnecessary. Also, it is not always necessary to add base to the resist prior to exposure. Alternate image reversal processes have been developed involving treatment of exposed photoresist with a gaseous amine in a vacuum environment.⁷⁰

IV. CHEMICALLY AMPLIFIED RESISTS

As device feature sizes approached 0.25 μm and the industry moved towards using 248 as the exposing wavelength for advanced lithographic applications, the materials community saw the first truly revolutionary change in resist materials chemistry to be adopted (Table I). Conventional resists are fundamentally too absorbant to allow uniform imaging through the thickness of the film. Additionally, the available light at the exposure plane of commercial, 248-nm exposure tools is insufficient to provide for manufacturable processes when the quantum efficiency of a resist is less than 1.⁷¹ This knowledge laid the foundation for the breakthrough that ultimately led to the adoption of 248-nm lithography as the technology of choice for advanced device fabrication: the announcement of what has been termed the “chemically amplified” resist mechanism.^{72,73}

A. Deprotection Chemistry

The pioneering work relating to the development of chemically amplified resists based on deprotection mechanisms was carried out by Ito *et al.*⁷² These initial studies dealt with the catalytic deprotection of poly(4-*tert*-butoxycarbonyloxystyrene) (PTBS) in which the thermally stable, acid-labile *tert*-butoxycarbonyl group is used to mask the hydroxyl functionality of poly(vinylphenol). As shown in Fig. 12, irradiation of PTBS films containing small amounts of an onium salt such as diphenyliodonium hexafluoroantimonate with UV light liberates an acid species that, upon subsequent baking, catalyzes cleavage of the protecting group to generate poly(*p*-hydroxystyrene). Loss of the *tert*-butoxycarbonyl group results in a large polarity change in the exposed areas of the film. While the substituted phenol polymer is a nonpolar material soluble in nonpolar lipophilic solvents, poly(vinylphenol) is soluble in polar organic solvents and aqueous base. These resists have been used successfully in the manufacture of integrated circuit devices.⁷⁴

Alternative resins have been investigated for chemically amplified resist applications. The parent polymer is typically an aqueous-base-soluble, high T_g resin. Examples include poly(hydroxystyrene),⁷⁴ poly(vinyl benzoate),⁷⁵ poly(methacrylic acid),⁷⁶ *N*-blocked maleimide-styrene resins,⁷⁷ poly(hydroxyphenyl methacrylate),⁷⁸ and

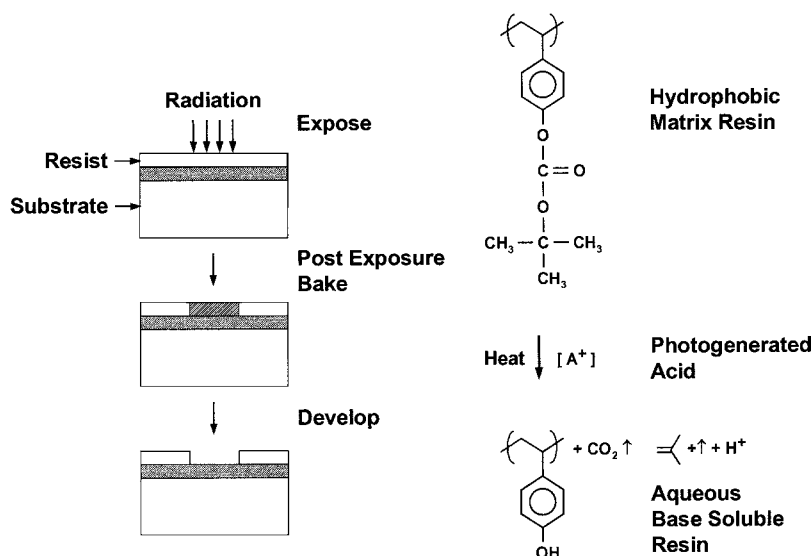


FIGURE 12 Structural representation of the chemistry and process associated with the first positive-acting, chemically amplified resist based on poly(*t*-butoxy-carbonyloxystyrene) matrix resin chemistry.

poly(4-*t*-butoxycarbonyloxystyrene-sulfone).⁷⁹ An interesting feature of the styrene sulfone copolymer is its propensity to undergo radiation-induced C–S bond scission to generate either sulfinic or sulfonic acid end groups that subsequently induce the deprotection reaction.⁸⁰ Thus, additional acid-generating components are unnecessary in this case.

A wide range of protective group chemistries have been demonstrated to be applicable as well. Examples of thermally stable yet acid labile substituents that have been employed include *tert*-butyl,⁸¹ tetrahydropyranyl, dihydropyranyl,⁸² and α - α -dimethylbenzyl.⁸³ Hydrolyzable groups such as trimethylsilyl⁸⁴ and various acetals and ketals⁸⁵ have also been employed. Issues related to acetal chemistry include a decrease in the linewidth of unirradiated patterns with increasing delay intervals.⁸⁶ This phenomenon arises from acid migration at room temperature and may be alleviated through the use of bulky acids and/or organic base additives.

The concept of acid-catalyzed deprotection may also be applied to resist formulations utilizing a small molecule acting as a dissolution inhibitor for an aqueous alkali-soluble resin. This approach possesses a key advantage, namely reduced shrinkage. By using a small molecule dissolution inhibitor, the content of the volatile, acid-cleavable group can be minimized, thus increasing the thermal stability of developed images. Materials that may effectively be used in dissolution inhibitor processes include carbonates or ethers of phenols,^{82,87} esters of carboxylic acids,⁸⁸ acetals,⁸⁹ or orthocarboxylic acid esters.⁸⁹ In one example, the *t*-butyl ester of cholic acid is used

as a dissolution inhibitor for a phenol-formaldehyde matrix resin.⁸⁸ Alternatively, a 193-nm resist has been developed using a substituted methacrylate resin in connection with a cholate-based inhibitor.⁶³ When formulated with an acid generator, irradiation affords a strong acid, which upon mild heating liberates cholic acid. The irradiated regions may then be removed by dissolution in aqueous base. Workers at Fuji Film have applied their knowledge of traditional novolac–DNQ dissolution inhibitor chemistry to the design of improved inhibitors for deep-UV applications.⁹⁰ Notably, hydrophobicity, molecular size, and dispersity of the acid-cleavable groups were influential in defining performance. The dissolution inhibitor may also be combined with the acid generator functions into a single chemically amplified resist additive.⁹¹

B. Depolymerization Chemistry

Chemically amplified resists that act through a polymer depolymerization mechanism can be broadly divided into two classes: those that act through a thermodynamically induced depolymerization mechanism, and those requiring catalytic cleavage of a polymer backbone. The former process depends upon the use of low-ceiling-temperature polymers that have been stabilized by suitable end capping. Introduction of a photocleavable moiety either at the end-cap or along the polymer backbone may then allow depolymerization to take place after irradiation and mild heating. A variant of this approach utilizes an end-cap or polymer chain that may be cleaved by photogenerated acid.^{75,92} An example is presented in Fig. 13.

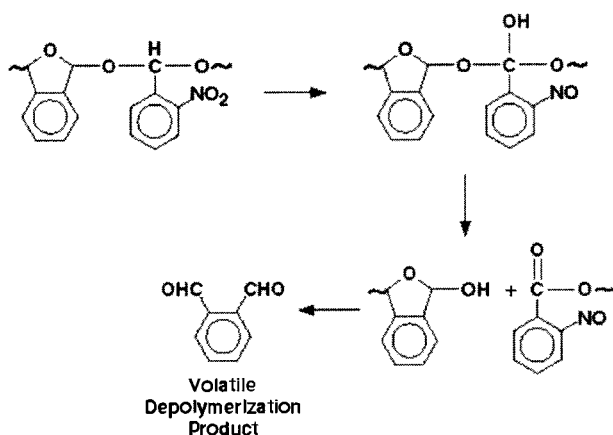


FIGURE 13 Structural representation of the polyphthalaldehyde acid-induced depolymerization mechanism.

C. Crosslinking Mechanisms

Chemical amplification through acid catalyzed crosslinking for negative-working resist applications has been achieved through various mechanisms. These include cationic polymerization, condensation polymerization, electrophilic aromatic substitution, and acid catalyzed rearrangement. The acid species may be generated from a variety of materials.⁹³

1. Cationic Polymerization Mechanisms

The first chemically amplified resist systems to be developed were those based on the cationic polymerization of epoxy materials.^{73,94} In general, the resolution of sub-0.5- μm features in resists based on this mechanism is difficult due to distortion resulting from solvent-induced swelling of the irradiated regions. Utilizing aqueous base soluble materials such as poly(hydroxystyrene-dicyclopentylloxy methacrylate), Allen⁹⁵ was able to circumvent the issue of swelling to develop a highly sensitive, aqueous-base-soluble i-line and e-beam resist.

2. Condensation Polymerization Mechanisms

Condensation polymerization mechanisms are probably the most prevalent in the design of chemically amplified negative resists. These systems utilize a polymer resin with reactive site(s) (also called a binder) for crosslinking reactions (e.g., a polymer containing a hydroxy functionality), a radiation-sensitive acid generator, and an acid-activated crosslinking agent.⁹⁶ Figure 14 depicts some of the alternative structures for the above components. The photogenerated acid catalyzes the reaction between the resin and crosslinking agent to afford a highly crosslinked

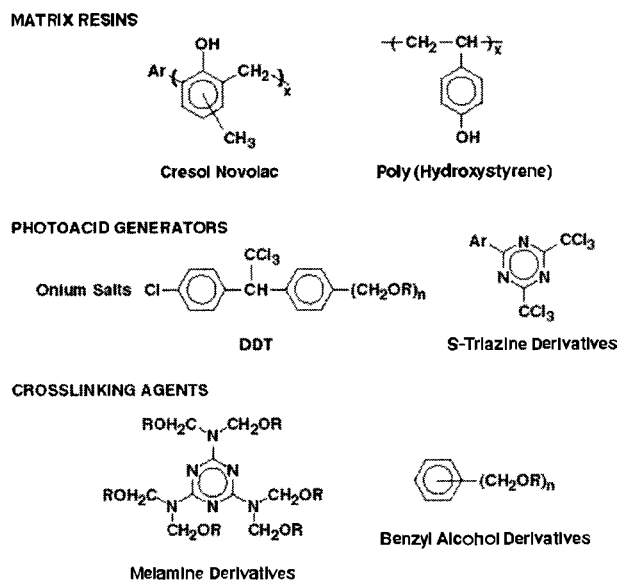


FIGURE 14 Structural representation of representative components that may be employed in negative-acting, chemically amplified resists that undergo acid-catalyzed condensation polymerization.

polymer network that is significantly less soluble than the unreacted polymer resin. A post-exposure bake step prior to development is required to complete the condensation reaction as well as to amplify the crosslinking yield to enhance sensitivity and improve image contrast. Sub-0.5- μm features could be resolved with deep-UV⁹⁷ and electron-beam⁹⁸ radiation with wide process latitude and high sensitivity using this chemistry. Figure 15 depicts 0.5- μm images obtained in such a material upon 248-nm UV exposure. Very sensitive X-ray and e-beam resist formulations based on similar chemistry using

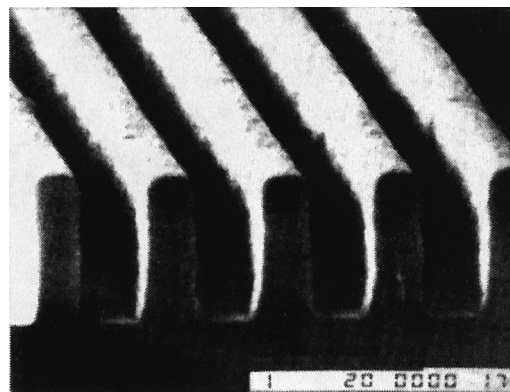


FIGURE 15 SEM images depicting 0.5- μm line/space images obtained in a negative-acting, chemically amplified resist based upon selected components shown in Fig. 15. [Courtesy of The Shipley Co.]

melamine and benzyl alcohol derivatives as crosslinking agents, formulated with onium salt photoacid generators in novolac or poly(hydroxystyrene) binders, have shown 0.2- μm line space resolution.⁹⁶ Other additives that undergo acid-induced condensation include compounds such as diphenylsilanediol,⁹⁹ polysiloxanes,¹⁰⁰ and diphenylcarbinol.¹⁰¹

3. Electrophilic Aromatic Substitution Mechanisms

Photo-induced crosslinking can be achieved in styrene polymers that are susceptible to electrophilic aromatic substitution by addition of latent electrophile (i.e., a carbocation precursor) and a photoacid generator.¹⁰² The photogenerated acid reacts with the latent electrophile during a post-exposure bake step to generate a reactive carbocation that then reacts with an aromatic moiety in the matrix affording a crosslinked network. The latent electrophile may be either an additive or a monomer that is copolymerized into the polymer binder. Examples of latent electrophiles include dibenzylacetate and copolymers of acetyloxymethylstyrene¹⁰² and 1,3-dioxlane-blocked benzaldehyde.¹⁰³

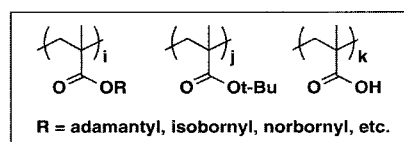
V. POLYMERS FOR SUB-150-NM IMAGING APPLICATIONS

The initial focus for designing 193-nm resists centered on derivatized acrylate and methacrylate copolymers. By and large, these polymers are effectively transparent at 193 nm and exhibit excellent resolution, but lack plasma-etching resistance and other requisite materials properties for lithographic performance. For instance, the first example of a high-speed, 193-nm acrylate resist was demonstrated in a collaboration between MIT and IBM. This material consisted of a methacrylate terpolymer containing acidolytically labile *t*-butylmethacrylate repeat units formulated with a diphenyliodonium triflate onium salt PAG.¹⁰⁴ Thus, the fundamental design challenge that has emerged appears to be the necessary trade-off between plasma-etching resistance and requisite materials properties for lithographic performance. On the whole, high-carbon-content copolymers functionalized with pendant alicyclic moieties possess adequate etching resistance but tend to be brittle, display poor adhesion, and have sub-optimal imaging characteristics due to poor aqueous base solubility. Decreased alicyclic carbon content results in improved lithographic performance at the cost of etching resistance. Examples of substituents that have been employed include menthyl,¹⁰⁵ adamantyl,¹⁰⁶ isobornyl,¹⁰⁷ and tricyclodecyl.¹⁰⁸

Recent approaches for addressing this fundamental design challenge include: (1) careful tailoring of polymer properties to maximize lithographic performance with minimal sacrifice in etching performance, and (2) development of three-component systems in which high-carbon-content alicyclic additives not only serve as dissolution inhibitors but also enhance the resistance of the matrix as a whole to plasma environments.

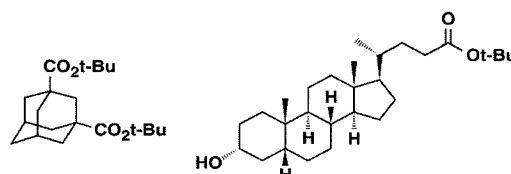
A. Alicyclic Polymers for 193-nm Imaging

As noted above, the first materials platforms that were examined for the purpose of providing transparent, 193-nm, imagable matrices were based on methacrylate resin chemistry (Fig. 16). While methacrylate-based resist platforms are attractive from an economic perspective, they suffer from the fundamental drawback of possessing a linear, oxygen-rich scaffold whose poor plasma-etching stability can be offset only partially by functionalization with more stable pendant groups. In a more ideal resist platform, greater intrinsic plasma stability might be imparted through incorporation of alicyclic, etching-resistant moieties directly into the polymer backbone. In addition, minimizing oxygen content by designing oxygenated functionalities to play only necessary imaging, adhesion, and solubilizing roles would be beneficial. Alternative routes to achieve the goal of an “all alicyclic backbone” are shown in Fig. 17 for the alicyclic alkene, norbornene. These routes are ring-opening metathesis polymerization (ROMP),¹⁰⁹ metal-catalyzed vinyl polymerization,¹¹⁰ and radical-promoted vinyl polymerization.¹¹¹ Over the years, several groups have taken such all-alicyclic approaches towards 193-nm resins.¹¹²



Methacrylate-based matrices

• IBM/Lincoln Labs, NEC, Fujitsu, Matsushita, others ...



Aliphatic dissolution inhibitors

FIGURE 16 Examples of alicyclic esters of acrylate resins and selected dissolution inhibitors that have been examined in 193-nm lithographic applications.

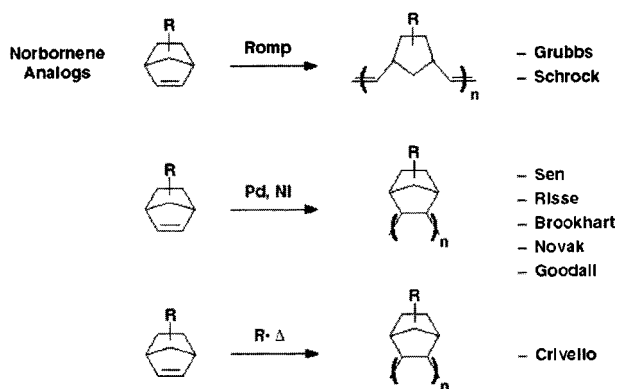


FIGURE 17 Schematic representation of alternative synthetic routes to preparing alicyclic polymers.

Cyclo-olefin-maleic anhydride alternating copolymers may provide an attractive alternative to methacrylate-based matrix resins.¹¹³ Compelling features of these copolymers include: (1) facile synthesis via standard radical polymerization, (2) a large pool of cycloolefin feed stocks, and (3) a generic structural motif that incorporates alicyclic structures directly into the polymer backbone and provides a latent water-solubilizing group that may also be useful for further structural elaboration. A large number of cycloolefins are known to copolymerize with maleic anhydride.

Norbornene-maleic anhydride copolymerizations¹¹⁴ were first described in a patent that provided two key insights: (1) copolymerization provides a material with a 1:1 composition regardless of monomer feed ratio, and (2) incorporation of small percentages of other vinyl monomers without disruption of the essentially alternating nature is tolerated. The alicyclic monomer readily undergoes free-radical-induced copolymerization with maleic anhydride to afford an alternating, high T_g polymer. Recent work by Ito *et al.*¹¹⁵ has shown that, although some polymerization systems are reasonably well behaved, most notably that of MA with NB and acrylates, other systems involving methacrylates or larger substituted alicyclics may be more problematic.

Aqueous-base solubility can be induced in the norbornene/maleic anhydride alternating copolymer via incorporation of acrylic acid. Free-radical polymerization of the cycloolefin and maleic anhydride in the presence of acrylic acid and/or its derivatives provides a controllable method for synthesizing aqueous-base-soluble resins (Fig. 18).¹¹³ Such materials were readily soluble in standard organic solvents used to spin-coat resist films and additionally were soluble in aqueous base media such as 0.262-N tetramethyl ammonium hydroxide (TMAH), the developer of choice for the electronics industry. Notably, thin films of these polymers cast onto

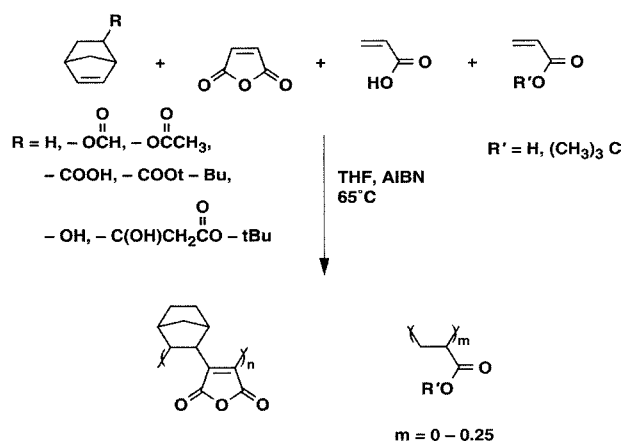


FIGURE 18 Schematic representation of the free-radical-induced synthesis of substituted norbornene-maleic anhydride alternating copolymer systems incorporating acrylic acid dopants.

quartz substrates display excellent transparency at both 248 and 193 nm, with the absorbance per micrometer of typical poly(norbornene-co-maleic anhydride-co-acrylic acid) materials being approximately 0.2 AU/ μm .

The norbornene-based matrix resins can be used in a variety of resist approaches (Fig. 19). The strategies that have been examined include the use of a protected polymer in conjunction with a photoacid generator (PAG) in a two-component, chemically amplified resist process; a three-component system using the parent acidic terpolymer, a dissolution inhibitor (DI), and a PAG; and a hybrid approach that uses both a DI and a partially protected matrix.¹¹³ Figure 20 depicts a schematic representation of the chemistry associated with the hybrid approach.

The inherent simplicity of the norbornene-maleic anhydride approach has led to the investigation of other similar resins based upon copolymerization with MA. The acronym COMA has been coined to signify copolymer resins of maleic anhydride with a single large alicyclic monomer. Representative examples of systems that have been investigated are shown in Fig. 21.¹¹⁶ Of particular interest is that COMA-based resists systems better withstand pattern collapse during processing¹¹⁷ and CD slimming occurring during SEM inspection than methacrylate or acrylate resin based upon pendant alicyclic groups.¹¹⁸

To summarize, there are three classes of 193-nm resist resins: resins with acrylate or methacrylate backbones containing pendant alicyclic groups, the COMA-based resins, and the all-alicyclic approach. Of these three, the first two are currently the only ones available as commercial resists. The third system, although promising from the plasma etch-resistance perspective, is late coming into the marketplace. Furthermore, despite great strides which have been made in reducing metal content in these materials, there is still concern over this issue.

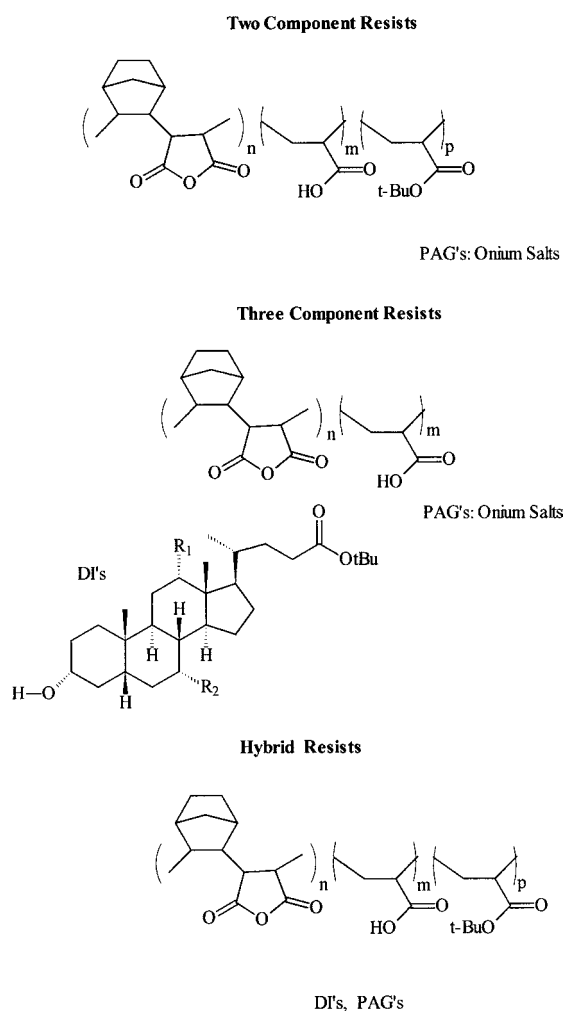


FIGURE 19 Examples of resist approaches that can be used to effect imaging when norbornene-maleic anhydride resins are used as matrices for 193-nm resist applications.

B. Dissolution Inhibitor Design

There has been much interest in acid-cleaveable cholate derivatives in which the cholates undergo acidolysis and the free cholic acids then act as dissolution promoters. The prototype for this design, albeit nonchemically amplified, was some early work at Bell Laboratories on 2-nitrobenzyl cholates for use as dissolution inhibitors in aqueous-base-soluble resist systems.⁶¹ Later work by others applying this concept to chemically amplified resists relied upon the derivatization of the cholate moiety with acidolytically labile groups such as *tert*-butyl esters.^{88,119} Bell Laboratories has also described the use of monomeric cholate materials, such as *tert*-butyl cholate in 193-nm poly(norborne/maleic anhydride)-based resins, and the use of a new class of dimeric and oligomeric cholates in which multiple acid cleaveable groups are present on the same molecule, giv-

ing rise to high contrast.¹²⁰ The oligomeric dissolution inhibitors are very soluble in norbornene-maleic anhydride-acrylate (NB/MA/AA) polymers and exhibit no tendency towards phase separation at loadings even as high as 40 wt%. Recent work has shown that the blendability of cholate DIs in general improves with increasing carboxylic content of the resin.¹²¹ Generally, the oligomeric inhibitors improved not only the contrast and solubility of the exposed areas in 0.262-*N* TMAH, but also reduced the unexposed film loss. The optimum adhesion and contrast were obtained by using a mixture of oligomeric DI with a polar "monomeric" material such as *t*-butyl cholate. Recently, a detailed study of the dissolution inhibition and promotion capability of a wide range of *tert*-butyl carboxylates derivatives in a p(NB/MA/AA) resin was carried out.¹²¹ It has been found that increasing hydrophobicity increased dissolution inhibition ability. The highest dissolution inhibition was found to occur for hydrophobic steroidal carboxylates having largest van der Waals surfaces for interaction with the polymer matrix. Dissolution promotion tracked with the number of carboxylic acid moieties and the hydrophobicity of carboxylic acid moieties released upon acidolytic cleavage of the *tert*-butyl carboxylate. Knowing the relative dissolution inhibition for *tert*-butyl carboxylates and promotion for carboxylic acids measured for a p(NB/MA/AA) matrix it was possible to predict trends in both contrast and maximum rate of dissolution measured in a p(NB/MA/TBA/AA) (TBA, *tert*-butyl acrylate) based resin.

C. Photoacid Generator Design Issues

While aromatic PAGs are highly absorptive at 193 nm, they are only needed in small quantities (typically <5%) in resist formulations. Consequently, 193-nm resists could be designed using the same PAGs as those that are in use with 248-nm resists. In addition to absorption, the considerations in designing a PAG are solubility, volatility of both the PAG and its photoproducts, acid strength, cost, and toxicity.⁹³ For *t*-butyl-substituted materials, high acid strength (often super-acids are required) coupled with high post-exposure bake (PEB) temperatures are required for complete removal of the ester appendage. Examples of applicable chemistries include photogenerators of perfluoroalkylsulfonic acids or aryl sulfonic acids highly activated with electron withdrawing groups.^{120,122} Although photoacid generators are not intended as dissolution inhibiting components in practice, some of these can act as very powerful dissolution inhibitors in COMA-based resists. Interestingly, iodonium or sulfonium salts of large perfluorinated anions (e.g., perfluorooctanesulfonate) tend to be poor dissolution inhibitors, while those of small anions (e.g., triflate, tresylate) tend to be good

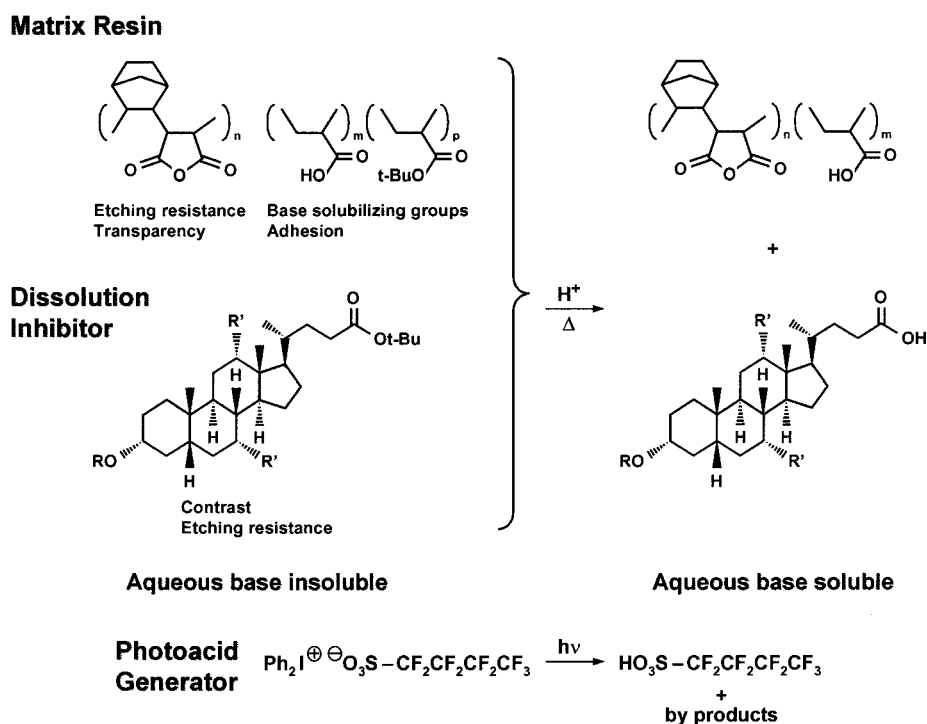


FIGURE 20 Structural representation of the chemistry associated with a 193-nm photoresist based upon norbornene–maleic anhydride matrix resin chemistry, a cholic acid dissolution inhibitor, and an onium salt photoacid generator.

dissolution inhibitors. Steric perturbation of PAG resin interactions by large perfluorinated anions may play a role in this behavior.¹²¹ Another consideration is the question of volatile outgassing. Outgassing during exposure, par-

ticularly of aromatic moieties, can lead to deposits on exposure tool lens elements.¹²³ A study has been done of the effect of PAG chemical structure on this phenomenon. It has been found that the best results are obtained with certain 2-nitrobenzyl sulfonates which, because of their photolysis mechanism, give no detectable outgassing.¹²⁴

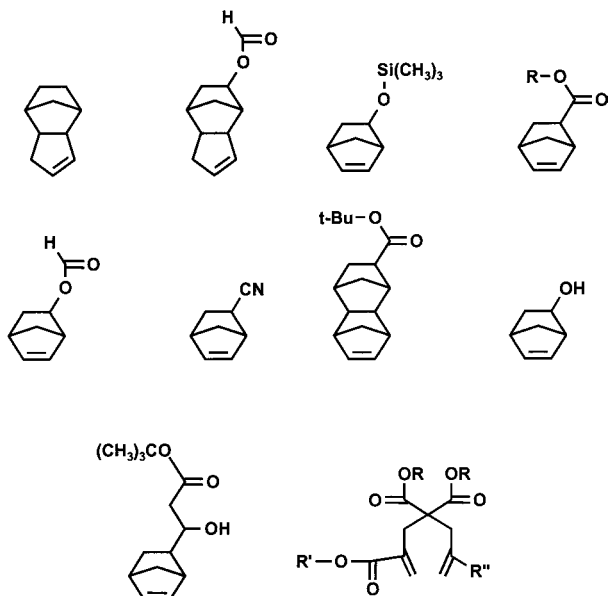


FIGURE 21 Structural representation of substituted alicyclic monomers that have been copolymerized with maleic anhydride for 193-nm lithographic applications.

D. Base Additives

While the acid-catalyzed deprotection reaction affords many advantages to designing sensitive lithographic materials, it induces several potential phenomena that unaddressed would preclude application of such mechanisms in “real-world” manufacturing. Some typical problems associated with chemically amplified technologies include diffusion of the photogenerated acid and depletion of acid at the resist–air interface. Depletion of acid can arise from either volatilization of the acidic species or more significantly from neutralization of the minute amounts of acid present at the resist–air interface by adventitious airborne amines present in most environments.¹²⁵ Acid diffusion is manifested as erosion or rather “slimming” of resolved lines with delays in post-exposure baking to effect deprotection, while either volatilization or neutralization of the catalyst results in what is termed “T-topping” of lines, a phenomenon that

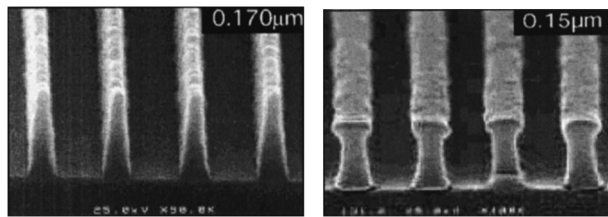


FIGURE 22 SEM images depicting the manifestation of line-width slimming and T-topping associated with chemically amplified resists.

also is aggravated upon delays in baking. **Figure 22** depicts examples of each of these issues. Base additives are known to reduce linewidth slimming, possibly by reducing the diffusion of acid¹²⁶ or, more probably, by scavenging small amounts of acid formed in nominally unexposed areas.¹²⁷ In the case of T-topping, base additives have been shown to alleviate this issue through either reduced volatilization of acid via decreased diffusion or, alternatively, creation of a low, uniform concentration of amine in the resist film which acts to overwhelm airborne basic contaminants depositing at the surface of the resist.¹²⁶

The possibility of utilizing photodecomposable aminosulfonate moieties capable of affording free aminosulfonic acids has been investigated.¹²⁸ In ester form, these materials are inherently basic, yet upon exposure to light they generate an acid, so they have been called photodefinable bases (PDB). It has been shown that the use of such materials leads to enhanced resist sensitivity because the aminosulfonate moiety is partially removed in the exposed resist film but remains unchanged in the unexposed areas where its basic properties act to limit diffusion. For instance, **Fig. 23** shows the structure of two different cyclamate materials employed as additives in a 193-nm single-layer resist based on a norbornene–maleic anhydride resist platform: The photodecomposable moiety gave a resolution dose of 22 mJ/cm², while the

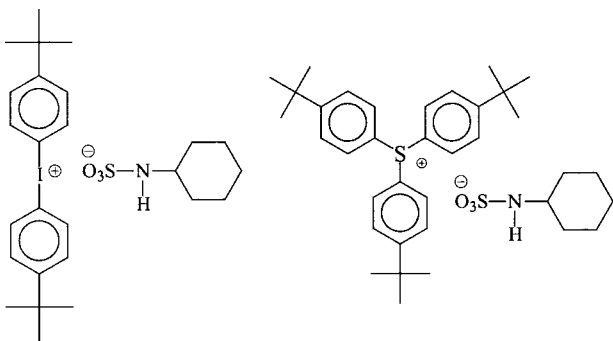


FIGURE 23 Structural representation of two cyclamates that could be employed as base additives in chemically amplified resists.

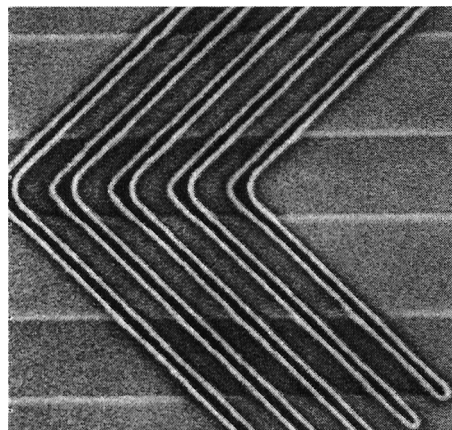


FIGURE 24 SEM images depicting nominal equal 60-nm line/space features printed in a norbornene–maleic anhydride based photoresist similar to that described in **Fig. 21**.

inert compound was far less sensitive (50 mJ/cm²).¹²⁸ Other groups have also applied the concept of photodecomposable base to 193-nm resins by using the more transparent trialkylammonium hydroxyde.¹²⁹

Figure 24 depicts representative images that can be achieved in alicyclic 193-nm lithographic materials. In this particular case, the polymer was a multicomponent material comprised of norbornene, maleic anhydride, *t*-butyl acrylate, and acrylic acid. A *t*-butyl cholate-based dissolution inhibitor was used in conjunction with an onium salt photoacid generator.

VI. 157-NM RESIST DESIGN

As device design rules continue to shrink, research directions transition towards future lithographic alternatives. The next logical extension of optical lithography involves the continued progression to still shorter wavelengths. As optical lithography has evolved over the past few decades, first from tools based on the 248-nm excimer laser (KrF), followed by 193-nm (ArF) systems, the next frontier utilizes fluorine, 157-nm UV sources.¹³⁰ Where optical transparency and etching resistance were the key concerns for the development of 193-nm lithographic materials, the overriding issue for 157-nm advanced optical lithography is resist materials transparency. Traditional resist materials platforms are too opaque to allow imaging in sufficiently thick films to address defect density concerns. For an optical density of 0.4, which is considered optimum for most resist applications, acrylic, phenolic, and cycloolefin polymer platforms would require resist thicknesses less than 100 nm (**Table III**).¹³¹ This value needs to be compared to the anticipated required film thickness for 50- to 100-nm

TABLE III Resist Thickness Required to Achieve an Optical Density of 0.4 for Three Classes of Resist Matrix Polymers²³

Materials platform	Thickness to achieve OD = 0.40
Acrylic	46–87 nm
Phenolic	48 nm
Cycloolefin	77 nm

imaging of 200 to ~400 nm, respectively.¹³¹ Thus, avenues leading to decreased absorbance need to be identified and explored for this application. This said, commercially available phenolic-, acrylate-, and cycloolefin-based resins have been evaluated as “tool testing” resists where “thinness” is not an obstacle. However, even in this application there is a need to suppress unwanted photochemical processes such as crosslinking or outgassing. The former leads to undesirable negative-tone behavior in a positive resist, while the latter can lead to outgassing which can deposit on the objective element of the exposure tool and lead to tool downtime. Such design considerations are crucial for all 157-nm systems. Of particular concern is outgassing of silicon-containing volatiles which can lead to irreversible damage and cannot be cleaned by irradiation in the presence of oxygen as is the case for carbon-based lens deposits.¹³²

A list of representative polymeric alternatives along with their 157-nm absorbance characteristics was reported by Kunz *et al.*¹³⁰ and is presented in Table IV. While hydro-

TABLE IV Survey of 157-nm Absorbance Characteristics of Selected Polymeric Platforms

Polymer	Absorbance (μm^{-1})	Film thickness (in nm for an OD = 0.4)
Si-O Backbone		
Poly(hydrosilsequioxane)	0.06	6667
Poly(dimethylsiloxane)	1.61	248
Poly(phenylsiloxane)	2.68	149
Carbon Backbone		
Fluorocarbon, 100% fluorinated	0.70	571
Hydrofluorocarbon, 30% fluorinated	1.34	298
Partially esterified hydrofluorocarbon, 28% fluorinated	2.60	154
Poly(vinyl alcohol)	4.16	96
Ethyl cellulose	5.03	80
Poly(methyl methacrylate)	5.69	70
Poly(norbornene)	6.10	66

carbon platforms do not provide sufficient transparency, fluorinated analogs do show potential, as do siloxane-based materials. Etching resistance and adhesion of the fluorinated materials to silicon substrates are concerns that will need to be addressed. Interestingly, the Kunz study demonstrated that the absorbance of many of the standard photoacid generator materials that have been used for both 248- and 193-nm chemically amplified resists have either similar or even lower absorbance at 157 nm than at the longer wavelengths,¹³⁰ thus alleviating concerns regarding the PAG component. An aspect of materials design that will be increasingly important at 157 nm is that of resist outgassing, or rather, the level of volatile species evolving from the resist film during exposure. These may include residual solvent, volatile resist components, or by-products generated upon irradiation of the resist film. Clearly, the evolution of volatile species must be kept to a minimum at 157 nm so that these products do not deposit onto critical lens surfaces, deleteriously affecting the lens transmission characteristics.

Several groups are beginning to explore materials alternatives for 157 nm applications. Willson¹³³ has utilized a “modular approach” in which chemical approaches to instilling necessary functionality into the 157-nm material is first tested in a model system. In this manner, he and his colleagues have identified the hexafluoroisopropyl group as an effective aqueous-base-solubilizing moiety and have shown that it can be protected with acid-labile alkyl acetal protecting groups while maintaining 157-nm transparency. Building from the 193-nm materials research that demonstrated the effectiveness of alicyclic backbone polymers for providing etching resistance, Willson¹³³ also showed that substitution of norbornene with an electron-withdrawing group such as fluorine or even a carbonyl group may afford resins with sufficient 157-nm transparency. For instance, the partially fluorinated poly(norbornene) shown in Fig. 25a has an absorbance of only 1.7 AU/micron. Although this absorbance is still too high for practical applications, it demonstrates substantial improvement over nonfluorinated analogs which can have absorbances as high as 7 AU/micron, and it represents a promising starting point for the design of new materials. Ober *et al.*¹³⁴ have reported two design approaches to achieving 157-nm transparency. One system is based upon a poly(trifluoromethylvinyl alcohol-co-vinyl alcohol) resin protected with acid-labile THP protecting groups, while in another approach they investigated the introduction of hexafluoropropyl groups onto cyclized polyisoprene (Fig. 25b). The material described to date does not have good transparency at 157 nm, but it does exhibit a high T_g (120–170°C) and good etching resistance. It is anticipated that hydrogenation of the olefinic moiety will address the

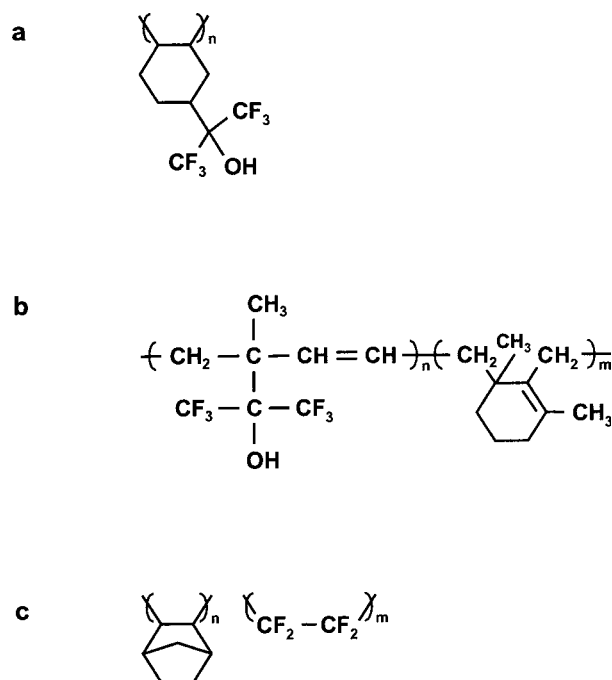


FIGURE 25 Examples of fluorinated matrix resin candidate chemistries under investigation for 157-nm lithographic applications.

absorbance issue. The DuPont¹³⁴ research team has shown some impressive initial results on at least one material that can be developed in aqueous base, has good transparency at 157 nm (2.9 AU/micron) and good thermal characteristics (T_g , 171°C), and may have good etching resistance. Preliminary investigations of imaging performance also show promise: 0.35- μm features have been obtained upon 157-nm exposure. Unfortunately, few structural details are known beyond the general poly(norbornene-co-tetrafluoroethylene) motif (Fig. 25c). One important advance recently has been the use of theoretical calculations of photoabsorption of molecules at 157 nm¹³⁶. Willson *et al.* have used this knowledge to aid them in the design of perfluorinated carbonyl-containing compounds and polymers having exceptionally low absorbance (i.e., 3 to 4 AU/ μm)¹³⁷. Although such materials are as yet not sufficiently transparent, they represent an important advance.

VII. CONCLUSION

Fundamental understanding of resist design concepts and structure–activity relationships between resist components and process performance has enabled the full integration of chemically amplified resists into device manufacture. It took about 20 years from the inception of the chemical amplification concept to full-scale acceptance

and use of such resists in full-scale semiconductor manufacturing, in spite of superior process latitude, mainly because of the dependence of resist performance on a set of new process variables such as the time elapsed between exposure to post-exposure bake, basic contaminants in the clean room, and substrate and the amount of protecting groups on the polymer.

Basic mechanistic understanding of the molecular structure and interactions of resist components (polymer, photoacid generator, base additive, protecting groups) as they relate to process performance have led to robust resist design. It is no exaggeration to say that such robust yet very high-resolution resist materials are responsible to a large extent for the extension of optical lithography capabilities to fabricate devices of design rules that are roughly half of the imaging wavelength. Figure 26 perhaps best depicts this. It is through understanding of the fundamental chemical issues that one can rationally design new manufacturable chemistries that overcome process issues such as severe T-typing presented on the right, and enable sub-100-nm imaging (left).

The lessons learned in implementing a revolutionary materials technology led to a parallel mode of development where new 193-nm resist concepts and materials were explored concomitant with their exercise in device fabrication. Such an approach has reduced the implementation time from 20 years with 248-nm resist technology to 5 to 7 years for 193-nm technology.

The challenge to design and manufacture 193-nm resists based on nonaromatic polymers turned out to be a very interesting research problem to a resist chemist and led to inventions of significance. Resist systems based on cycloolefin homo- or co-polymers and acrylates have been shown to meet much of manufacturability, cost, and process performance criteria and are in use for prototype manufacturing with 193-nm exposure tools.

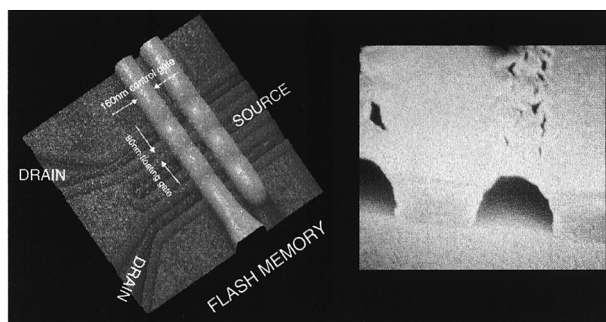


FIGURE 26 Images illustrating the issues associated with chemically amplified resists (left) and imaging capability (right) when materials chemistry and processes are optimized for the given technology.

The intense industry interest in 157-nm lithography has catalyzed activity in designing ultrathin resists that would most probably be based on fluoropolymers and/or siloxane chemistries. Such lithography also poses yet another challenge to the resist community and is the topic of intense research.

SEE ALSO THE FOLLOWING ARTICLES

INTEGRATED CIRCUIT MANUFACTURE • PHOTOCHEMISTRY, MOLECULAR • POLYMERS, MECHANICAL BEHAVIOR • THIN FILM TRANSISTORS

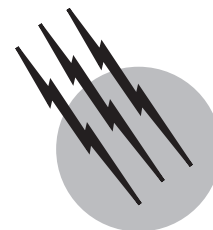
BIBLIOGRAPHY

1. Bardeen, J., and Brattain, W. H. (1948). *Phys. Rev.* **74**(2), 230.
2. Thompson, L. F., Willson, C. G., and Bowden, M. J. (1994). "Introduction to Microlithography," ACS Professional Reference Book, Washington, D.C.
3. McCoy, J. H., Lee, W., and Varnell, G. L. (1989). *Solid State Technol.* **32**(3), 87.
4. Takigawa, T. (1992). *Photopolymer Sci. Technol.* **5**(1), 1; DeJule, R. (1998). *Semiconductor Int.* **21**(2), 54; DeJule, R. (1999). **22**(3), 48; McClay, J. A., and McIntyre, S. L. (1999). *Solid State Technol.* **42**(6), 57.
5. Reichmanis, E., and Thompson, L. F. (1989). In "Polymers in Microlithography: Materials and Processes," ACS Symposium Series 412 (E. Reichmanis, S. A. MacDonald, and T. Iwayanagi, eds.), pp. 1–24, ACS, Washington, D.C.
6. Thompson, L. F. (1994). In "Introduction to Microlithography," pp. 269–375, ACS Professional Reference Book, Washington, D.C.
7. Reichmanis, E., and Thompson, L. F. (1989). *Chem. Rev.* **89**, 1273.
8. Moreau, W. M. (1988). "Semiconductor Lithography; Principles, Practices, and Materials," Plenum, New York.
9. Reiser, A. (1989). "Photoreactive Polymers: The Science and Technology of Resists," John Wiley & Sons, New York, pp. 22–65.
10. Reichmanis, E., and Neenan, T. X. (1998). In "Chemistry of Advanced Materials: An Overview" (L. V. Interrante, and M. J. Hampden-Smith, eds.), pp. 99–141, Wiley-VCH, New York.
11. Iwayanagi, T., Kohashi, T., Nonogaki, S., Matsuzawa, T., Douta, K., and Yanazawa, H. (1981). *IEEE Trans. Elec. Dev. Ed.* **28**(11), 1305–1310.
12. Nonogaki, S., Hashimoto, H., Iwayanagi, T., and Shiraishi, H. (1985). *Proc. SPIE* **529**, 189.
13. Hoshimoto, H., Iwayanagi, T., Shiraishi, H., and Nonogaki, S. (1985). "Proc. Regional Technical Conference on Photopolymers," Mid-Hudson Section SPE, Ellenville, NY, p. 11.
14. Herriott, D. R., Collier, R. J., Alles, D. S., and Stafford, J. W. (1975). *IEEE Trans. Electron. Devices* **ED-22**, 385.
15. Thompson, L. F., and Kerwin, R. E. (1976). *Ann. Rev. Materials Sci.* (R. A. Huggins, R. H. Bube, and R. W. Roberts, eds.), **6**, 267–301.
16. Tagawa, S. (1987). In "Polymers for High Technology: Electronics and Photonics," ACS Symposium Series 346 (L. F. Thompson, C. G. Willson, and J. M. Frechet, eds.), pp. 37–45, ACS, Washington, D.C.
17. Hirai, T., Hatano, Y., and Nonogaki, S. (1971). *J. Electrochem. Soc.* **118**(4), 669.
18. Feit, E. D., Thompson, L. F., and Heidenreich, R. D. (1973). *ACS Div. Org. Coat. Plast. Chem. Preprint*, 383.
19. Taniguchi, Y., Hatano, Y., Shiraishi, H., Horigome, S., Nonogaki, S., and Naraoka, K. (1979). *Jpn. J. Appl. Phys.* **28**, 1143.
20. Tan, Z. C., Petropoulos, C. C., and Rauner, F. J. (1981). *J. Vac. Sci. Technol.* **19**(4), 1348.
21. Novembre, A. E., and Bowden, M. J. (1983). *Polym. Eng. Sci.* **23**, 977.
22. Tabata, Y., Tagawa, S., and Washio, M. (1984). In "Materials for Microlithography" (L. F. Thompson, C. G. Willson, and J. M. J. Frechet, eds.), p. 161, ACS Symposium Series 266, ACS, Washington, D.C.
23. Hartney, M. A., Tarascon, R. G., and Novembre, A. E. (1985). *J. Vac. Sci. Technol.* **B3**, 360.
24. Imamura, S. (1979). *J. Electrochem. Soc.* **126**(9), 1268.
25. Choong, H. S., and Kahn, F. J. (1981). *J. Vac. Sci. Technol.* **19**(4), 1121.
26. Feit, E. D., Thompson, L. F., Wilkins, C. W., Jr., Wurtz, M. E., Doerries, E. M., and Stillwagon, L. E. (1979). *J. Vac. Sci. Technol.* **16**(6), 1287.
27. Imamura, S., and Sugawara, S. (1982). *J. Appl. Phys.* **21**, 776.
28. Yoshioka, N., Suzuki, Y., and Yamazaki, T. (1985). *Proc. SPIE* **537**, 51.
29. Thompson, L. F., and Doerries, E. M. (1979). *J. Electrochem. Soc.* **126**(10), 1699.
30. Thompson, L. F., Yau, L., and Doerries, E. M. (1979). *J. Electrochem. Soc.* **126**(10), 1703.
31. Novembre, A. E., Masakowski, L. M., and Hartney, M. A. (1986). *Poly. Eng. Sci.* **26**(6), 1158.
32. Hatzakis, M., Paraszcak, J., and Shaw, J. M. (1981). In "Micro-circuit Eng. 81" (A. Oosenburg, ed.), pp. 386–396, Swiss Fed. Inst. Technol., Lausanne.
33. MacDonald, S. A., Steinman, F., Ito, H., Lee, W.-Y., and Willson, C. G. (1983). Preprints. *ACS Div. Polymeric Materials: Sci. Eng.* **50**, 104.
34. Suzuki, M., Saigo, K., Gokan, H., and Ohnishi, Y. (1983). *J. Electrochem. Soc.* **130**, 1962.
35. Novembre, A. E., Jurek, M. J., Kornblit, A., and Reichmanis, E. (1989). *Polym. Eng. Sci.* **23**, 920.
36. Ranby, B., and Rabek, J. F. (1975). "Photodegradation, Photooxidation and Photostabilization of Polymers," John Wiley & Sons, New York, pp. 15–159.
37. Hatzakis, M. (1969). *J. Electrochem. Soc.* **116**, 1033.
38. Mimura, Y., Ohkubo, T., Takanichi, T., and Sekikawa, K. (1978). *Jpn. Appl. Phys.* **17**, 541.
39. Lin, B. (1975). *J. Vac. Sci. Technol.* **12**, 1317.
40. Helbert, J. N., Chen, C. Y., Pittman, C. U., Jr., and Hagnauer, G. L. (1978). *Macromolecules* **11**, 1104; Lai, J. H., Helbert, J. N., Cook, C. F., Jr., and Pittman, C. U., Jr. (1979). *J. Vac. Sci. Technol.* **16**(6), 1992; Helbert, J. N., Wagner, B. E., Caplan, J. P., and Poindexter, E. H. (1975). *J. Appl. Poly. Sci.* **19**, 1201; Chen, C. Y., Pittman, C. U., Jr., and Helbert, J. N. (1980). *J. Poly. Sci. Poly Chem. Ed.* **18**, 169.
41. Moreau, W. M. (1982). *Proc. SPIE* **333**, 2.
42. Kakuchi, M., Sugawara, S., Murase, K., and Matsuyama, K. (1977). *J. Electrochem. Soc.* **224**, 1648; Tada, T. (1979). *J. Electrochem. Soc.* **126**, 1829; Tada, T. (1983). *J. Electrochem. Soc.* **130**, 912.
43. Roberts, E. D. (1977). *ACS Div. Org. Coat. Plastics Chem. Preprints* **37**(2), 36; Moreau, W., Merritt, D., Moyer, W., Hatzakis, M., Johnson, D., and Pederson, L. (1979). *J. Vac. Sci. Technol.* **16**(6), 1989; Namaste, Y. M. N., Obendorf, S. K., Anderson, C. C., Krasicky, P. D., Rodriguez, F., and Tiberio, R. (1983). *J. Vac. Sci. Technol. B* **1**(4), 1160.

44. Reichmanis, E., and Wilkins, C. W., Jr. (1982). In "Polymer Materials for Electronics Applications," ACS Symposium Series 184 (E. D. Feit, and C. W. Wilkins, Jr., eds.), pp. 29–43, ACS, Washington, D.C.; Hartless, R. L., and Chandross, E. A. (1981). *J. Vac. Sci. Technol.* **19**, 1333.
45. Reichmanis, E., Smolinsky, G., and Wilkins, C. W., Jr. (1984). *Solid State Technol.* **28**(8), 130; Reichmanis, E., and Smolinsky, G. (1984). *Proc. SPIE* **469**, 38; Reichmanis, E., and Smolinsky, G. (1985). *J. Electrochem. Soc.* **132**, 1178.
46. Tsuda, M., Oikawa, S., Nakamura, Y., Nagata, H., Yokota, A., Nakane, H., Tsumori, T., and Nakane, Y. (1979). *Photogr. Sci. Eng.* **23**, 1290; MacDonald, S. A., Ito, H., Willson, C. G., Moore, J. W., Charapetian, H. M., and Guillet, J. E. (1984). In "Materials for Microlithography" (L. F. Thompson, C. G. Willson, and J. M. J. Frechet, eds.), pp. 179, ACS Symposium Series 266, ACS, Washington, D.C.
47. Brown, J. R., and O'Donnell, J. H. (1970). *Macromolecules* **3**, 265; Brown, J. R., and O'Donnell, J. H. (1972). *Macromolecules* **5**, 109.
48. Bowmer, T. N., and O'Donnell, J. H. (1981). *Radiation Phys. Chem.* **17**, 177.
49. Bowden, M. J., Thompson, L. F., and Ballantyne, J. P. (1975). *J. Vac. Sci. Technol.* **126**(6), 1294.
50. Bowden, M. J., and Thompson, L. F. (1979). *Solid State Technol.* **22**, 72.
51. Gozdz, A. (1987). *Solid State Technol.* **30**(6), 75; Gozdz, A., Ono, H., Ito, S., and Shelbourne, III, J. A. (1991). *Proc. SPIE* **1446**, 200.
52. Hofer, D. C., Miller, R. D., McKean, D. R., Willson, C. G., West, R., and Trefonas, R. T. (1984). In "Materials for Microlithography" (L. F. Thompson, C. G. Willson, J. M. J. Frechet, eds.), p. 283, ACS Symposium Series 266, ACS, Washington, D.C.; Miller, R. D., Hofer, D. C., and Willson, C. G. (1984). *Proc. SPIE* **469**, 16; Zeigler, J. M., Harrah, L. A., and Johnson, A. W. (1985). *Proc. SPIE* **539**, 166; Kunz, R. R., and Horn, M. W. (1991). "Proceedings, Regional Tech. Conf. Photopolymers," Mid-Hudson Section, SPE, Ellenville, NY, October 28–30, p. 291.
53. Weidman, T. W., and Joshi, A. J. (1992). *Appl. Phys. Lett.* **62**, 372; Dabbagh, G., Hutton, R. S., Cirelli, R. A., Reichmanis, E., Novembre, A. E., and Nalamasu, O. (1998). *Proc. SPIE* **3333**, 334.
54. Reichmanis, E., Novembre, A. E., Nalamasu, O., and Dabbagh, G. (2000). In "Silicon Containing Polymers" (R. G. Jones, W. Ando, and J. Chajnowski, eds.), pp. 743–762, Kluwer Academic, Netherlands.
55. Dammel, R. (1993). In "Diazonaphthoquinone-Based Resists" (D. Shea, ed.), p. 70, SPIE, Optical Engineering Press, Bellingham, WA.
56. Tarascon, R. G., Shugard, A., and Reichmanis, E. (1986). *Proc. SPIE* **631**, 40; Soatome, Y., Gokan, H., Saigo, K., Suzuki, M., and Ohnishi, Y. (1985). *J. Electrochem. Soc.* **132**, 909.
57. Yeh, T. F., Reiser, A., Dammel, R. R., Pawlowski, G., and Roeschert, H. (1993). *Macromolecules* **26**, 3862; Shih, Y.-H., Yeh, T. F., Reiser, A., Dammel, R. R., Merrem, H. J., and Pawlowski, G. (1994). *Proc. SPIE* **2195**, 514.
58. Miller, R. D., Willson, C. G., McKean, D. R., Tomkins, T., Clecak, N., Michl, J., and Downing, J. (1982). "Proc. Reg. Tech. Conf. On Photopolymers," Mid-Hudson Section SPE, Ellenville, NY, November 8–10, p. 111.
59. Hanabata, M., Furuta, A., and Uemura, Y. (1986). *Proc. SPIE* **631**, 76; Hanabata, M., Furuta, A., and Uemura, Y. (1987). *Proc. SPIE* **771**, 85; Hanabata, M., Oi, F., and Furuta, A. (1991). *Proc. SPIE* **1446**, 132; Templeton, M. K., Szmanda, C. R., and Zampini, A. (1987). *Proc. SPIE* **777**, 136; Trefonas, P., III, Daniels, B. K., and Fischer, R. K. (1987). *Solid State Technol.* **30**, 131.
60. Willson, C. G., Miller, R. D., and McKean, D. R. (1987). *Proc. SPIE* **771**, 2.
61. Reichmanis, E., Wilkins, C. W., Jr., and Chandross, E. A. (1981). *J. Vac. Sci. Technol.* **19**(4), 1338.
62. Pederson, L. A. (1982). *J. Electrochem. Soc.* **129**, 205; Gokan, H., Esho, S., and Ohnishi, Y. (1983). *J. Electrochem. Soc.* **130**, 154.
63. Pawlowski, G., Sauer, T., Dammel, R., Gordon, D. J., Hinsberg, W., McKean, D., Lindley, C. R., Merrem, H. J., Vicari, R., and Willson, C. G. (1990). *Proc. SPIE* **1262**, 391; Przybilla, K., Roeschert, H., Spiess, W., Eckes, C., Chatterjee, S., Khanna, D., Pawlowski, G., and Dammel, R. (1991). *Proc. SPIE* **1466**, 174.
64. Kaimoto, Y., Nozaki, K., Takechi, S., and Abe, N. (1992). *Proc. SPIE* **1262**, 66; Kuna, R. R., Allen, R. D., Hinsberg, W. D., and Wallraff, G. M. (1993). *Proc. SPIE* **1925**, 167; Abe, N., Takechi, S., Kaimoto, Y., Takahashi, M., and Nozaki, K. (1995). *J. Photopolymer Sci. Technol.* **8**(4), 637; Allen, R. D., Wan, I. Y., Wallraff, G. M., DiPietro, R. A., and Hofer, D. C. (1995). *J. Photopolymer Sci. Technol.* **8**(4), 623.
65. Shaw, J. M., and Hatzakis, M. (1979). *J. Electrochem. Soc.* **126**, 2026; Huber, H. L., Betz, H., Heuberger, A., and Pongrate, S. (1984). *Microelectronic Eng.* **84**, 325; Peters, D. W. (1988). *Proc. SPIE* **923**, 36.
66. Bowden, M. J., Thompson, L. F., Fahrenholtz, S. R., and Doerries, E. M. (1981). *J. Electrochem. Soc.* **128**, 1304.
67. Tarascon, R. G., Frackowiak, J., Reichmanis, E., and Thompson, L. F. (1987). *Proc. SPIE* **771**, 54; Frackowiak, J., Tarascon, R. G., Vaidya, S., and Reichmanis, E. (1987). **771**, 120.
68. Shiraishi, H., Isobe, A., Murai, F., and Nonogaki, S. (1984). In "Polymers in Electronics" (T. Davidson, Ed.), p. 167, ACS Symposium Series 242, ACS, Washington, D.C.; Chang, Y. Y., Grant, B. D., Pederson, L. A., and Willson, C. G. (1983). U.S. Patent. 4,398,001.
69. Moritz, H. (1995). *IEEE Trans. Electron Devices* **ED-32**, 672; Takahashi, Y., Shinozaki, F., and Ikeda, T. (1980). *Jpn. Kokai Tokyo Koho* **88**, 8032; MacDonald, S. A., Ito, H., and Willson, C. G. (1983). *Microelectronic Eng.* **1**, 269.
70. Alling, E., and Stauffer, C. (1985). *Proc. SPIE* **529**, 194.
71. Willson, C. G., and Bowden, M. J. (1988). In "Electronic and Photonic Applications of Polymers" (M. J. Bowden, and S. R. Turner, eds.), pp. 75–108, ACS Advances in Chemistry Series 218, ACS, Washington, D.C.; Iwayanagi, T., Ueno, T., Nonogaki, S., Ito, H., and Willson, C. G. (1988). In "Electronic and Photonic Applications of Polymers" (M. J. Bowden and S. R. Turner, eds.), pp. 109–224, ACS Advances in Chemistry Series 218, ACS, Washington, D.C.; Reichmanis, E., Houlihan, F. M., Nalamasu, O., and Neenan, T. X. (1991). *Chem. Mater.* **3**, 397.
72. Ito, H., and Willson, C. G. (1984). In "Polymers in Electronics" (T. Davidson, ed.), pp. 11–23, ACS Symposium Series 242, ACS, Washington, D. C.; Frechet, J. M. J., Eichler, E., Ito, H., and Willson, C. G. (1990). *Polymer* **24**, 995; Ito, H., Willson, C. G. (1983). *Polym. Eng. Sci.* **23**, 1012; Ito, H., Willson, C. G., Frechet, J. M. J., Farrall, M. J., and Eichler, E. (1983). *Macromolecules* **16**, 1510.
73. Crivello, J. V. (1984). In "Polymers in Electronics" (T. Davidson, ed.), pp. 3–10, ACS Symposium Series 242, ACS, Washington, D.C.
74. Maltabes, J. G. et al. (1990). *Proc. SPIE* **1262**, 2.
75. Ito, H., and Willson, C. G. (1987). *Proc. SPIE* **771**, 24.
76. Ito, H., Ueda, M., and Ebina, M. (1989). In "Polymers in Microlithography" (E. Reichmanis, S. A. MacDonald, and T. Iwayanagi, eds.), p. 57, ACS Symposium Series 412, ACS Washington, D.C.

77. Osuch, C. E., Brahim, K., Hopf, F. R., McFarland, M. J., Mooring A., and Wu, C. J. (1986). *Proc. SPIE* **631**, 68; Turner, S. R., Ahn, K. D., and Willson, C. G. (1987). In "Polymers for High Technology" (M. J. Bowden and S. R. Turner, eds.), pp. 200–210, ACS Symposium Series 346, ACS, Washington, D.C.
78. Przybilla, K. J., Dammel, R., Pawlowski, G., Roschert, J., and Spiess, W. (1991). "Proc. Regional Technical Conf. on Photopolymers," Mid-Hudson Section SPE, Ellenville, NY, October 28–30, p. 131.
79. Kanga, R. S., Kometani, J. M., Reichmanis, E., Hanson, J. E., Nalamasu, O., Thompson, L. F., Heffner, S. A., and Tai, W. W. (1991). *Chem. Mater.* **3**, 660; Houlihan, F. M., Reichmanis, E., Thompson, L. F., and Tarascon, R. G. (1989). In "Polymers in Microlithography" (E. Reichmanis, S. A. MacDonald, and T. Iwayanagi, eds.), pp. 39–56, ACS Symposium Series 412, ACS, Washington, D.C.
80. Novembre, A. E., Tai, W. W., Kometani, J. M., Hanson, J. E., Nalamasu, O., Taylor, G. N., Reichmanis, E., and Thompson, L. F. (1992). *Chem. Mater.* **4**, 278.
81. Crivello, J. V. (1989). *J. Electrochem. Soc.* **136**, 1453.
82. Hayashi, N., Hesp, S. M. A., Ueno, T., Toriumi, M., Iwayanagi, T., and Nonogaki, S. (1989). *Proc. Polym. Mat. Sci. Eng.* **61**, 417; Frechet, J. M. J., Kallman, N., Kryczka, B., Eichler, E., Houlihan, F. M., and Willson, C. G. (1988). *Polymer Bull.* **20**, 427; Frechet, J. M. J., Eichler, W., Gauthier, S., Kryczka, B., and Willson, C. G. (1989). In "The Effects of Radiation on High-Technology Polymers" (E. Reichmanis, and J. H. O'Donnell, eds.), pp. 155–171, ACS Symposium Series 381, ACS, Washington, D.C.; Hesp, S. A. M., Hayashi, N., and Ueno, T. (1991). *J. Appl. Polym. Sci.* **42**, 877; Schlegel, L., Ueno, T., Shiraishi, H., Hayashi, N., and Iwayanagi, T. (1991). *Microelectronic Eng.* **14**, 227; Talyor, G. N., Stillwagon, L. E., Houlihan, F. M., Wolf, T. M., Sogah, D. Y., and Hartler, W. R. (1991). *J. Vac. Sci. Technol.* **B9**, 3348.
83. Ito, H., and Ueda, M. (1988). *Macromolecules* **21**, 1475.
84. Yamaoka, T., Nishiki, M., Koseki, K., and Koshiha, M. (1988). "Proc. Reg. Tech. Conf. on Photopolymers," Mid-Hudson Section, SPE, Ellenville, NY, Oct. 30–Nov. 2, p. 27; Murata, M., Kobayashi, E., Yamachika, M., Kobayashi, Y., Yamota, Y., and Miura, T. (1992). *J. Photopolymer Sci. Technol.* **5**(1), 79; Uhrich, K. E., Reichmanis, E., Heffner, S. A., Kometani, J. M., and Nalamasu, O. (1994). *Chem. Mater.* **6**, 287; Schue, F., and Giral, L. (1989). *Makromol. Chem. Makromol. Symp.* **24**, 21.
85. Padmanabhan, M., Kinoshita, Y., Kudo, T., Lynch, T., Masuda, S., Nozaki, Y., Okazaki, H., Powloski, G., Przybilla, K. T., Roeschert, H., Spiess, W., Suehiro, N., and Wengenroth, H. (1994). *Proc. SPIE* **2195**, 61; Schwalm, R., Binder, H., Fischer, T., Funhoff, D., Goethals, M., Grassmann, A., Moritz, H., Reuhman-Huisken, M., Vinet, F., Dijkstra, H., and Krause, A. (1994). *Proc. SPIE* **2195**, 2.
86. Hattori, T., Schlegel, L., Imai, A., Hayashi, N., and Ueno, T. (1993). *J. Photopolymer Sci. Technol.* **6**, 497.
87. Schlegel, L., Ueno, T., Shiraishi, H., Hayashi, N., and Iwayanagi, T. (1990). *Chem. Mater.* **2**, 299; McKean, D. R., MacDonald, S. A., Clecak, N. J., and Willson, C. G. (1988). *Proc. SPIE* **920**, 60; Schlegel, L., Ueno, T., Shiraishi, H., Hayashi, N., and Iwayanagi, T. (1990). *J. Photopolymer Sci. Technol.* **3**, 281.
88. O'Brien, M. J. (1989). *Polym. Eng. Sci.* **29**, 846; O'Brien, M. J., and Crivello, J. V. (1988). *Proc. SPIE* **920**, 42.
89. Lingnau, J., Dammel, R., and Theiss, J. (1988). "Proc. Reg. Tech. Conf. on Photopolymers," Mid-Hudson Section, SPE, Ellenville, NY, Oct. 20–Nov. 2, pp. 87–97.
90. Aoai, T., Yamanaka, T., and Kokubo, T. (1994). *Proc. SPIE* **2195**, 111.
91. Schwalm, R. (1989). *Proc. Polymer. Mater. Sci. Eng.* **61**, 278; Houlihan, F. M., Chin, E., Nalamasu, O., and Kometani, J. M. (1992). *Proc. ACS Div. Polym. Mater. Sci. Eng.* **66**, 38.
92. Ito, H., Ueda, M., and Schwalm, R. (1988). *J. Vac. Sci. Technol.* **B6**, 2259.
93. Reichmanis, E., Houlihan, F. M., Nalamasu, O., and Neenan, T. X. (1991). *Chem. Mater.* **3**, 394.
94. Stewart, K. J., Hatzakis, M., Shaw, J. M., Seeger, D. E., and Neumann, E. (1989). *J. Vac. Sci. Technol.* **B7**, 1734.
95. Allen, R. D., Conley, W. E., and Gelorme, J. D. (1992). *Proc. SPIE* **1672**, 513.
96. Lingnau, J., Dammel, R., and Theiss, J. (1989). *Solid State Technol.* **32**(9), 105; *Ibid.* (1989). **32**(10), 107; Feely, W. E. (1980). *Eur. Patent Appl.* **232**, 972; Buhr, G. (1980). U.S. Patent, 4,189,323; Berry, A. K., Graziano, K. A., Bogen, L. E., Jr., and Thackeray, J. W. (1989). In "Polymers in Microlithography" (E. Reichmanis, S. A. MacDonald, and T. Iwayanagi, eds.), pp. 87–89, ACS Symposium Series 412, ACS, Washington, D.C.
97. Thackeray, J. W., Orsula, G. W., Pavelch, E. K., and Canistro, D. (1989). *Proc. SPIE Adv. Resist Technol. Processing VI* **1086**.
98. Liu, H.-Y., deGrandpre, M. P., and Freely, W. E. (1988). *J. Vac. Sci. Technol.* **B6**, 379.
99. Toriumi, M., Shiraishi, H., Ueno, T., Hayashi, N., and Nonogaki, S. (1987). *J. Electrochem. Soc.* **134**, 334; Shiraishi, H., Fukuma, E., Hayashi, N., Tadano, K., and Ueno, T. (1991). *Chem. Mater.* **3**, 621.
100. Sakata, M., Ito, T., and Yamashita, Y. (1991). *Jpn. J. Appl. Phys.* **30**(11B), 3116.
101. Uchino, S., Katoh, M., Sakamizu, T., and Hashimoto, M. (1992). *Microelectronic Eng.* **17**, 261.
102. Reck, B., Allen, R. E., Twieg, R. J., Willson, C. G., Matsuzczak, S., Stover, H. D. H., Li, N. H., and Frechet, J. M. J. (1989). *Polymer Eng. Sci.* **29**, 960; Frechet, J. M. J., Matsuzczak, S., Stover, H. D. H., Willson, C. G., and Reck, B. (1989). In "Polymers in Microlithography" (E. Reichmanis, S. A., MacDonald, and T. Iwayanagi, eds.), pp. 74–85, ACS symposium series 412, ACS, Washington, D.C.
103. Schaedeli, U., Holzwarth, H., Muenzel, N., and Schulz, R. (1992). "Proc. Reg. Tech. Conf. on Photopolymers," Mid-Hudson Section, SPE, Ellenville, NY, Oct. 28–30, p. 145.
104. Kunz, R. R., Allen, R. D., Hinsberg, W. D., and Wallraff, G. M. (1993). *Proc. SPIE* **1925**, 167.
105. Shida, N., Ushirogouchi, T., Asakawa, K., and Nakase, M. (1996). *J. Photopolymer Sci. Technol.* **9**, 457.
106. Takahasi, M., and Takechi, S. (1995). *Proc. SPIE* **2438**, 422; Takechi, S., Takahashi, M., Kotachi, K., Nozaki, K., Yano, E., and Hanyu, I. (1996). *J. Photopolymer Sci. Technol.* **9**, 475.
107. Allen, R. D., Wallraff, G. M., DiPietro, R. A., Hofer, D. C., and Kunz, R. R. (1995). *Proc. SPIE* **2438**, 474.
108. Nakano, K., Maeda, S., Iwasa, S., Ohfugi, T., and Hasegawa, E. (1995). *Proc. SPIE* **2438**, 433.
109. Mathew, J. P., Reinmuth, A., Melia, J., Swords, N., and Risse, W. (1996). *Macromolecules* **29**, 2744; Safir, A. L., and Novak, B. M. (1995). *Macromolecules* **28**, 5396.
110. Goodall, B. L., Benedikt, G. M., McIntosh, L. H., III, and Barnes, D. A. (1995). U.S. Patent 5,468,819 (to B. F. Goodrich, Inc.); Cherdron, H., Brekner, M.-J., and Osan, F. (1994). *Angew. Makromol. Chem.* **223**, 121; Kaminsky, W. (1994). *Angew. Makromol. Chem.* **223**, 101.
111. Crivello, J. C., and Shim, S. Y. (1996). *Chem. Mater.* **8**, 376.
112. Allen, R. D., Wallow, T. I., Optiz, J., Larson, C., DiPietro, R. A., Sooriyakumaran, R., Brock, P., Brega, G., Hofer, D. C., Jayaraman, S., Vicari, R., Hüllihen, K., and Rhodes, L. (1998). *J. Photopolymer Sci. Technol.* **11**, 475; Okoroanyanwu, U., Byers, J., Shimokawa, T., and Willson, C. G. (1998). *Chem.*

- Mater.* **10**, 3328; Allen, R. D., Sooriyakumaran, R., Opitz, J., Wallraff, G., DiPietro, R., Breyta, G., Hofer, D., Kunz, R. R., Jayaraman, S., Shick, R., Goodall, B., Okoroanyanwu, U., and Willson, C. G. (1996). *Proc. SPIE* **2724**, 334; Varanasi, P. R., Maniscalco, J., Mewherter, A. M., Lawson, M. C., Jordhamo, G., Allen, R., Opitz, J., Ito, H., Wallow, T. I., Hofer, D., Langsdorf, L., Jayaraman, S., and Vicari, R. (1999). *Proc. SPIE* **3678**(5), 1-63; Wallow, T. I., Brock, P., DiPietro, R., Allen, R., Opitz, J., Sooriyakumaran, R., Hofer, D., Meute, J., Byers, J., Rich, G., McCallum, M., Schuetze, S., Jayaraman, S., Hullahen, K., Vicari, R., Rhodes, L., Goodall, B., and Shick, R. (1998). *Proc. SPIE* **3333**, 92.
113. Houlihan, F. M., Wallow, T. I., Nalamasu, O., and Reichmanis, E. (1997). *Macromolecules* **30**, 6517; Wallow, T. I., Houlihan, F. M., Nalamasu, O., Chandross, E. A., Neenan, T. X., and Reichmanis, E. (1996). *Proc. SPIE* **2724**, 355.
 114. Potter, G. H., and Zutty, N. L. (1966). U.S. Patent 3,280,080.
 115. Ito, H., Allen, R. D., Opitz, J., Tom, I., Wallow, T. I., Truong, H. D., Hofer, D. C., Varanasi, P. R., Jordhamo, G. M., Jayaraman, S., and Vicari, R. (2000). *Proc. SPIE* **3999**, 2.
 116. Patterson, K., Okoroanyanwu, U., Shimokawa, T., Cho, S., Byers, J., and Willson, C. G. (1998). *Proc. SPIE* **3333**, 425; Rushkin, I. L., Houlihan, F. M., Kometani, J. M., Hutton, R. S., Timko, A. G., Reichmanis, E., Nalamasu, O., Gabor, A. H., Medina, A. N., Slater, S. G., and Neisser, M. (1999). *Proc. SPIE* **3678**, 44; Allen, R. D., Opitz, J., Ito, H., Wallow, T. I., Casmier, C. E., Larson, R., Sooriyakumaran, R., Hofer, D. C., and Varanasi, P. R. (1999). *J. Photopolymer Sci. Technol.* **12**(3), 501; Jung, J.-C., Bok, C.-K., and Baik, K.-H. (1998). *Proc. SPIE* **3333**, 11; Klopp, J. M., Pasini, D., Frechet, J. M. J., and Byers, J. D. (2000). *Proc. SPIE* **3999**, 23; Park, J.-H., Kim, J.-Y., Seo, D.-C., Park, S.-Y., Lee, H., Kim, S.-J., Jung, J.-C., and Baik, K.-H. (2000). *Proc. SPIE* **3999**, 1163.
 117. Domke, W. D., Graffenberg, V. L., Patel, S., Rich, G. K., Cao, H. B., and Nealey, P. F. (2000). *Proc. SPIE* **3999**, 313.
 118. Neisser, M., Kocab, T., Beauchimin, B., Sarubbi, T., Wong, S., and Ng, W. (2000). "Proc. Interface 2000," Arch. Microlithographic Symposium, Nov. 5-7, p. 43.
 119. Allen, R. D., Wan, I. Y., Wallraff, G. M., DiPietro, R. A., Hofer, D., and Kunz, R. R. (1995). *J. Photopolymer Sci. Technol.* **8**, 623.
 120. Houlihan, F. M., Wallow, T., Timko, A., Neria, E., Hutton, R. S., Cirelli, R. A., Nalamasu, O., and Reichmanis, E. (1997). *Proc. SPIE* **3049**, 84; Houlihan, F. M., Wallow, T. I., Timko, A. G., Neria, E., Hutton, R. S., Cirelli, R. A., Kometani, J. M., Nalamasu, O., and Reichmanis, E. (1997). *J. Photopolymer Sci. Technol.* **10**, 511.
 121. Yan, Z., Houlihan, F. M., Reichmanis, E., Nalamasu, O., Reiser, A., Dabbagh, G., Hutton, R. S., Osei, D., Sousa, J., and Bolan, K. (2000). *Proc. SPIE* **3999**, 127; Dabbagh, G., Houlihan, F. M., Rushkin, I., Hutton, R. S., Nalamasu, O., Reichmanis, E., Yan, Z., and Reiser, A. (2000). *Proc. SPIE*, **3999**, 120; Houlihan, F. M., Dabbagh, G., Rushkin, I. L., Hutton, R. S., Osei, D., Sousa, J., Bolan, K., Nalamasu, O., Reichmanis, E., Yan, Z., and Reiser, A. (2000). *J. Photopolymer Sci. Technol.* **13**, 569; Houlihan, F. M., Dabbagh, G., Rushkin, I. L., Hutton, R. S., Osei, D., Sousa, J., Bolan, K., Nalamasu, O., and Reichmanis, E. (2000). *Chem. Mater.* **12**(11), 3516.
 122. Allen, R. D., Opitz, J., Larson, C. E., Wallow, T. I., DiPietro, R. A., Breyta, G., Sooriyakumaran, R., and Hofer, D. C. (1997). *J. Photopolym. Sci. Technol.* **10**(4), 503.
 123. Kunz, R. R., and Downs, D. K. (1999). *J. Vac. Sci. Technol.* **17**(6).
 124. Houlihan, F. M., Rushkin, I. L., Hutton, R. S., Timko, A. G., Reichmanis, E., Nalamasu, O., Gabor, A. H., Medina, A. N., Malik, S., Neisser, M., Kunz, R. R., and Downs, D. K. (1999). *J. Photopolymer Sci. Technol.* **12**, 525; Houlihan, F. M., Rushkin, I. L., Hutton, R. S., Timko, A. G., Reichmanis, E., Nalamasu, O., Gabor, A. H., Medina, A. N., Malik, S., Neisser, M., Kunz, R. R., and Downs, D. K. (1999). *Proc. SPIE* **3678**, 264; Houlihan, F. M., Rushkin, I. L., Hutton, R. S., Timko, A. G., Reichmanis, E., Nalamasu, O., Gabor, A. H., Medina, A. N., Malik, S., Neisser, M., Kunz, R. R., and Downs, D. K. (1999). "Proc. Interface 1999," Arch. Microlithographic Symposium, Nov. 14-16, p. 133.
 125. MacDonald, S. A., Clecak, N. J., Wendt, H. R., Willson, C. G., Snyder, C. D., Knors, C. J., Deyoe, N. B., Maltabes, J. G., Morrow, J. R., McGuire, A. E., and Holmes, S. J. (1991). *Proc. SPIE* **1466**, 2; Nalamasu, O., Reichmanis, E., Cheng, M., Pol, V., Kometani, J. M., Houlihan, F. M., Neenan, T. X., Bohrer, M. P., Mixon, D. A., Thompson, L. F. (1991). *Proc. SPIE* **1466**, 13; MacDonald, S. A., Hinsberg, W. D., Wendt, R. H., Clecak, N. J., Willson, C. G., and Snyder, C. D. (1993). *Chem. Mater.* **5**, 348; Hinsberg, W. D., MacDonald, S. A., Clecak, N. J., and Snyder, C. D. (1994). *Chem. Mater.* **6**, 481.
 126. Asakawa, K., Ushiroguchi, T., and Nakase, N. (1995). *Proc. SPIE* **2438**, 563.
 127. Hinsberg, W., Houle, F., Sanchez, M., Morrison, M., Wallraff, G., Larson, C., Hoffnagle, J., Brock, P., and Breyta, G. (2000). *Proc. SPIE* **3999**, 148.
 128. Houlihan, F. M., Kometani, J. M., Timko, A. G., Hutton, R. S., Cirelli, R. A., Reichmanis, E., Nalamasu, O., Gabor, A. H., Medina, A. N., Biafore, J. J., and Slater, S. G. (1998). *Proc. SPIE* **3333**, 73; Houlihan, F. M., Kometani, J. M., Timko, A. G., Hutton, R. S., Cirelli, R. A., Reichmanis, E., Nalamasu, O., Gabor, A. H., Medina, A. N., Biafore, J. J., and Slater, S. G. (1998). *J. Photopolymer Sci. Technol.* **11**(3), 419.
 129. Padmanaban, M., Bae, J.-B., Cook, M., Kim, W.-K., Klauck-Jacobs, A., Kudo, T., Rahman, M. D., and Dammel, R. R. (2000). *Proc. SPIE* **3999**, 1136.
 130. Burggraaf, P. (2000). *Solid State Technol.* **43**(1), 31; Rothschild, M., Bloomstein, T. M., Fedynshyn, T. H., Kunz, R. R., Liberman, V., and Switkes, M. (2000). *J. Photopolymer Sci. Technol.* **13**(3), 369.
 131. Kunz, R. R., Bloomstein, T. M., Hardy, D. E., Goodman, R. B., Downs, D. K., and Curtin, J. E. (1999). *Proc. SPIE* **3678**, 13; Fedynshyn, T. H., Kunz, R. R., Doran, S. P., Goodman, R. B., Lind, M. L., and Curtin, J. E. (2000). *Proc. SPIE* **3999**, 335.
 132. Kunz, R. R., Downs, D. K., Fedynshyn, T. H., Sinta, R., and Sworin, M. (2000). "Proc. of the First Int. Symp. on 157-nm Lithography," Dana Point, CA, May 8-11, p. 635.
 133. Patterson, K., Yamachika, M., Hung, R., Brodsky, C., Yamada, S., Somervell, M., Osborn, B., Hall, D., Dukovic, G., Byers, J., Conley, W., and Willson, C. G. (2000). *Proc. SPIE* **3999**, 365; Chiba, T., Hung, R. J., Yamada, S., Trinke, B., Yamachika, M., Brodsky, C., Patterson, K., Heyden, A. V., Jamison, A., Lin, S.-H., Somervell, M., Byers, J., Conley, W., and Willson, C. G. (2000). *J. Photopolymer Sci. Technol.* **13**(3), 657.
 134. Schmaljohann, D., Bae, Y. C., Dai, J., Weibel, G. L., Hamad, A. H., and Ober, C. K. (2000). *J. Photopolymer Sci. Technol.* **13**(3), 451; Bae, Y. C., Schalmjohann, D., Hamad, A. H., Dai, J., Weibel, G. L., Yu, T., and Ober, C. K. (2000). "Proc. of the First Int. Symp. on 157-nm Lithography, Dana Point, CA, May 8-11, p. 727.
 135. Crawford, M. K., Feiring, A. E., Feldman, J., French, R. H., Periyasamy, M., Schadt F. L., III, Smalley, R. J., Zumsteg, F. C., Kunz, R. R., Rao, V., and Holl, S. M. (2000). *Proc. SPIE* **3999**, 357.
 136. Matsuzawa, N. N., Mori, S., Yano, E., Okazaki, S., Ishitani, A., and Dixon, D. A. (2000). *Proc. SPIE* **3999**, 375.
 137. Willson, C. G. (2000). "Proc. Interface 2000," Arch. Microlithographic Symposium, Nov. 5-7, p. 135.



Polymers, Recycling

Richard S. Stein

University of Massachusetts

- I. Nonrenewable Resources
- II. Means for Dealing with Plastic Waste
- III. Recycling
- IV. Overview

GLOSSARY

Alcoholysis Degradation accomplished by reaction with alcohol.

Degradation The chemical conversion of a material to lower molecular weight products.

Entropy A measure of the degree of thermodynamic disorder of a system.

Hydrolysis Degradation accomplished by reaction with water.

Incineration The burning of material.

Primary recycling Recycling involving physical changes without modification of the chemistry of the material.

Pyrolysis Degradation accomplished through heat.

Recycling The conversion of a waste product into a useful new one.

Secondary recycling Recycling in which chemical changes are carried out, such as by degradation, pyrolysis, or hydrolysis.

Trash-to-energy Incineration accomplished with energy recovery.

THE RAPID GROWTH in the use of polymers has resulted in concern about (1) their influence on the consump-

tion of nonrenewable resources and (2) the environmental burden arising from their manufacture and disposal. The volume of polymers used exceeds that of metals and is rapidly growing, particularly as the “third world” industrializes. The driving forces for this trend are (1) the economics of their use as compared with alternate materials, (2) their superior properties for many applications, and (3) their positive environmental impact resulting from weight savings, superior insulation, and decreased pressure on agricultural resources. The trend for increased use appears inevitable, so consideration of how best to modify practices to accommodate this is essential.

I. NONRENEWABLE RESOURCES

The concern about the effect of polymer use on consumption of nonrenewable resources may be excessive. The principal feed stock for polymer production is petroleum. About 90% of petroleum is currently used as fuel, about 4–5% goes for petrochemical production, and only 2–3% goes to polymer manufacture. The amount of petroleum saved through the use of polymers for weight reduction in automobiles and aircraft and for reduced heating oil consumption due to better insulation is probably greater than that needed to produce the polymers. Such would occur as

a result of a 5% improvement in car gasoline needs, which could readily be achieved by weight reduction.

As petroleum becomes more scarce and expensive, as is bound to happen, industry will turn to more value-added use. Thus, there will be diversion toward the more profitable petrochemical applications, and more of the burden will result from increased fuel costs. Thus, a wiser investment of research resources would be into energy-saving schemes and alternate energy production approaches, many of which are aided by the use of polymers for applications such as fuel cell membranes, solar panels, and wind turbine blades.

Alternate feed stock such as natural gas, coal, or biomaterials for polymer production is feasible, but, at present, not economical. It may be that as petroleum becomes scarcer, such approaches will become more favorable, but this does not appear to be so in the immediate future.

Recycling certainly has a role in reducing the need to produce new polymers (as well as other materials), but without governmental intervention, such as subsidies or tax rebates, society is unlikely to adopt uneconomical measures. Of course, the total cost of polymer use, including that of disposal of waste polymers, needs to be considered. Measures such as subsidizing recycling based upon savings of disposal might be reasonable. While improved means for recycling should be strongly encouraged, it should be realized that there are limits on the fraction of plastic waste that can be economically recycled. Such limits depend upon petroleum costs, recycling technology, and the associated infrastructure costs involved in collecting and sorting. At present, this fraction may be in the range of 30–40% of the polymer waste, but this number is bound to increase as petroleum becomes scarcer, technology improves, and infrastructure develops.

II. MEANS FOR DEALING WITH PLASTIC WASTE

A. Use Reduction

For some purposes, particularly in the “first world,” there is probably excessive polymer use. Consumer products often have too much packaging, and polymer can be saved by distributing liquid products as more concentrated solutions. (There is no point in packaging water.) Improved technology can result in less need for polymers. With improved polymer technology resulting in better mechanical properties, plastic bags and bottles can be made thinner.

The choice of substitute materials should be made with care. The consumer at the supermarket is often offered the choice of “plastic or paper” in choosing a shopping bag. Of course, the best choice is to say “neither” and bring an old bag for reuse. However, the choice of the alternative

of paper is not necessarily the wisest choice since the production of paper can be a polluting and water- and energy-consuming process. Also, the lighter plastic bags lead to lower shipping costs and a consequent reduction in fuel needs. Some of the properties of plastic bags such as moisture resistance and better “wet strength” are superior to those of paper. An advantage over paper is the ability they offer to carry a greater number of plastic bags because of their handles. Thus, the decision is dependent upon the environmental efficiency of production (and disposal) of the alternative products.

These considerations point to two important factors: (1) reuse is often superior to recycling and (2) energy saving as well as materials saving should be considered. By adopting the common European practice of not supplying new shopping bags, but expecting consumers to supply their own, a “good” plastic shopping bag could be reused perhaps 50 times, while if its plastic content were recycled, only two or three cycles might be possible before deterioration of properties occurred.

For energy considerations, the production, use, and disposal of any product require energy. The production of such energy often requires use of petroleum or other feed stocks common to the production of new polymers. Therefore, both energy and materials need to be considered together in the choice. For example, some environmentalists contend that natural fibers such as wool and cotton are a better choice than synthetic ones such as nylon and polyester. In making this decision, one needs to compare the energy and materials necessary to produce the synthetic fiber with that needed for fertilizer, tractor fuel, harvesting, and processing the natural one, along with a consideration of the greater maintenance requirements (laundering, ironing, dry cleaning) necessary for the product produced from the natural fibers. The choice is not always clear-cut and depends on societal factors and the efficiency of utilizing these alternatives. For much of the “third world,” food is scarce, and the production of the natural product competes with the agricultural requirements for food production.

B. Recycling

Recycling, next to reduced use and use of substitutes, is often the best environmental approach. This is the main focus of this article and will be considered in detail in later sections.

C. Degradation

Polymers can be intentionally made so as to degrade by photolysis or bacterial action during a predetermined time period. Until recently, the efforts of polymer scientists

and engineers have been devoted to making polymers last longer, but the problems associated with accumulated waste have shifted the focus. It should be realized that degradation results in a loss of polymeric material, which, while decreasing the burden of waste accumulation, has some negative environmental limitations. Polymers represent a state of matter of low entropy (low disorder), and degradation, where the polymers revert to lower molecular weight materials, represents an increase in their entropy. The second law of thermodynamics tells us that for isolated systems, entropy spontaneously increases (they become disordered), and that an investment of energy is required to reverse this trend. Thus, the entropy increase associated with degradation is equivalent to an energy expenditure necessary to produce the reverse, with its consequential environmental impact. A combination of entropy and energy considerations (thermodynamically expressed as “free energy”) is necessary in considering alternatives.

On the positive side, degradation of waste polymers reduces litter and decreases the need for means for otherwise dealing with the waste polymers, which are often energy demanding and environmentally damaging. The importance of such “cosmetic” measures depends on the nature of the society, and is probably more important in “first world” environments where neatness and absence of litter are highly valued.

Some successes of the employment of degradation should be cited. The “rings” used to bind beverage cans together are often made from long-lasting polyethylene. When these are discarded, they can lead to strangling of birds and marine life. Such polyethylene can be rendered photodegradable by introducing ultraviolet light-absorbing carbonyl groups through the use of carbon monoxide as well as ethylene in its synthesis. The absorption of light by such groups induces photochemical reactions leading to scission of the polymer chains and their reduction to a sufficiently low molecular weight so that further degradation by bacterial action becomes possible. The time for such degradation may be controlled by varying the concentration of such groups. This practice proves economical and is sometimes required by law.

Polyethylene sheets are sometimes used as “mulch” in farming to cover fields and prevent the growth of weeds. A problem can be the disposal of such sheets at the end of the growing season. By making these photodegradable with an appropriate lifetime, the sheets can degrade at the end of the growing season, eliminating the need and cost for their removal.

The above uses involve photodegradation. While most polymers resist bacterial degradation, it is possible to introduce structures that are susceptible to attack by bacteria or enzymes. There is an appreciable industrial effort economically to produce such polymers which still maintain

good mechanical properties. While such materials have their application, it seems unlikely that such practices will have a major impact on problems associated with the use of commodity or engineering plastics.

A problem with centrally disposing of degradable polymers is that degradation does not readily occur in dry landfills, and those with water present lead to leachants, which may contaminate ground water if they are not properly contained. The best way of dealing with them is through a composting facility in which liberated gases like methane can be captured and used as fuel, and the resulting compost can be utilized to benefit agriculture. Unfortunately, such facilities are rare, so their lack has limited the success of this approach. For example, disposable diapers can constitute 1–2% of landfill volume, so efforts have been made to fabricate them from degradable components. However, this effort has not gained favor, largely because of the lack of the required infrastructure.

While the impact of degradable polymers in affecting the plastic waste problem may be limited, they can be of great importance in medical applications such as for fabricating biodegradable sutures which degrade as wounds heal and for controlled release of drugs which may be dissolved or dispersed in a biodegradable polymer matrix.

D. Incineration

Incineration involves the burning of polymers. To do this in an environmentally desirable way, the liberated energy should be captured and used, usually to generate electricity in a “trash-to-energy” facility. Polymers are an excellent fuel, with heating value comparable to oil, and better than coal and most components of trash. The principal products of complete burning of most polymers are water and carbon dioxide, which are relatively environmentally benign (other than effects of CO₂ as a “greenhouse gas”). The procedure has not been favored by most environmentalists and the public since the vision is conditioned by old incinerators which are not state of the art and are polluting, producing toxic fumes and ash.

From a thermodynamic point of view, trash-to-energy procedures are superior in that the energy content of the plastic is recovered, so beyond reuse and recycling, it is a viable approach, provided the polluting aspects can be eliminated. This is possible, and it has been shown that modern incinerators do not produce toxic fumes, regardless of the polymer content of their feed stock. The toxic fumes usually result from incomplete combustion, which can be avoided by operating the incinerator at a proper temperature with adequate oxygen supply. Furthermore, any toxic substances in the effluent that might result could be detected through proper monitoring of the effluent and eliminated by “scrubbing” the fumes.

Toxic materials in the ash are almost always not of polymer origin, but arise from other materials, usually containing heavy metals, that are mixed with the polymer feed stock. A desirable approach is to have a crude sorting of the feed stock so as to prevent their mixing with the polymer content. Their inclusion could be reduced through parallel societal efforts such as making available ready means for recycling items like batteries and possibly encouraging the use of such recycling facilities through offering reverse deposits. Also, the ash can be converted to a low-solubility slag through addition of materials like lime to the feed stock. In any case, incineration considerably reduces the volume of the waste so as to make its proper disposal more feasible.

A consideration is what might happen to this possible content of toxic material had incineration not been done. It would then probably enter into the landfill, probably in a more soluble form, and eventually leach out and enter the environment in an uncontrolled manner. Is it to concentrate it in the form of an insoluble slag of reduced volume which can be disposed of in a more satisfactory manner.

A societal problem in providing state-of-the-art incinerators is their cost. In the short run, the approach is often more expensive than alternative disposal means, but in the long run, it becomes cost-effective and environmentally desirable. It is a problem, however, to persuade the public and politicians to adopt the long-range view, particularly for the latter, where reelection is often influenced by the short-range consequences of their term of office.

There is sometimes public resistance to the locating of incinerators and the adoption of the "not in my backyard" syndrome. However, this problem has been conquered, for example, by the Japanese, who combine the facilities with heated swimming pools and greenhouses, which win public acceptance. With proper design, these can be better neighbors than composting facilities or landfills.

III. RECYCLING

The practice of recycling has won strong favor among environmentalists. They have favored legislation requiring specified levels for recycling. Unfortunately, such legislation sometimes ignores thermodynamic and economic limitations, leading to their opposition by polymer producers and fabricators. It seems sensible to convert waste products into articles having a second or more use. Entropy concepts can be applied in that the use of plastic articles leads to their wear and eventual discarding, representing an increase in disorder and entropy. The second law tells us that to convert these waste products back to useful products, energy must be expended. The viability

of such recycling depends on whether the economic value of the resulting products exceeds the cost of the energy necessary to bring about the recycling. Such energy considerations should include that expended in collecting and sorting the waste feed stock, in addition to that utilized in its processing.

A. Primary Recycling

Primary recycling involves the conversion of waste plastic into a new product by a physical process, such as melting and remolding, without chemical modification of the polymer chemistry. It is the cheapest way to recycle, but is limited in application. It may be applied to mixed or "commingled" polymers or to those which are separated into separate types.

Most collected waste plastics consist of mixtures of different composition and color, and the product formed by their primary recycling usually will be inferior in properties to the original components. Most plastics of different chemical structure are immiscible. That is, when melted, they will be phase separated and consist of domains of their components having a size dependent upon the processing conditions. The boundaries between such polymer phases of different composition are often weak and lead to mechanical failure when the article is subject to strain. For this reason, articles fabricated from such commingled polymers often have inferior mechanical properties leading to limited application and diminished value. They may be used for applications such as park bench and pier construction and parking barriers, where the mechanical demands are not great. For such applications, they can be superior to the usual alternative, wood, in that they resist rot and do not require the application of preservatives, which are often polluting. However, the number of such applications is not great enough to accommodate the amount of material available for recycling.

Boundaries between immiscible polymers can be strengthened by use of "compatibilizers" that are often copolymers having affinities for both components, which serve to bind them together. A peripheral advantage in using such agents is that they usually result in the domains being smaller, resulting in improved mechanical and optical properties. A disadvantage is that the use of such agents adds to the cost. In some cases, the components are sufficiently reactive toward each other that chemical binding can occur when the mixture is heated with possible addition of a catalyst.

Where appearance is important, the use of mixtures of polymers of different color can be a problem. The mixture assumes an intermediate color, so uses are often selected where color is not important or where a dark color is acceptable.

For some sophisticated processing applications, molecular properties such as molecular weight and its distribution, branching, and tacticity can be important. Thus, even though the polymers that are mixed are of the same chemical composition, there may be difficulties if they differ in these molecular properties.

The recycle value of separated polymers is superior, but the difficulty of acquiring separated feed stock is greater. One approach is to select readily identifiable objects that a consumer will have no difficulty in separating from others. A prime success story is that of beverage bottles, usually made from polyethylene terephthalate (PET or polyester), which has the added advantage that it is a high value-added polymer. Consumers can be encouraged to return such bottles to recycle centers, either through social pressure or monetary encouragement, such as receiving a deposit when the empty bottle is returned for recycling. The use of "reverse deposit machines" in supermarkets which automatically identify the returned bottle, return the deposit to the consumer, and grind the plastic for compact shipment greatly facilitates the process.

The beverage bottle case serves to indicate an important aspect. Originally, such PET bottles were made with polyethylene bases. While these functioned well, they had to be removed for effective recycling, which added to the cost. Since the design and introduction of an all-PET bottle was slightly more expensive, manufacturers were reluctant to do so until forced to by legislation. The lesson is that recycling can proceed more effectively if one designs products with recycling in mind. This must sometimes be encouraged by means such as legislation.

A task is to identify other products where a single species of polymer can be readily identified and economically collected for recycling. The cost of collecting and separating mixed polymers from diverse sources is great, so increasing the efficiency of this process is a challenge. One such source is from used automobiles which are turned in upon purchase of a new car. Reuse is best through their sale as used cars, but ultimately the state of the car becomes sufficiently poor that it is scrapped. Increasingly, plastic parts are employed in cars and the large-scale scrapper is sufficiently knowledgeable to identify parts and classify them according to plastic type. The process can again be facilitated by "design for recycling" in which the number of different kinds of plastic which are used is reduced, and fasteners are such as to permit the easy separation of plastic parts from other components. A desirable measure is the establishment of databases for car parts so that the recycler may readily identify them and sort and return them to the proper place.

Another area of growth for recycling is for carpet, with the principal polymer components being nylon-6 and

nylon-66. New carpets are usually installed by professionals, who remove and carry away the old carpets. This constitutes a potential source of recycle feed stock, which is dealt with by relatively experienced personnel. A problem is that the nylon components are usually bound to a backing, often jute, which must be separated to permit effective recycling. Efforts are underway to develop means to do so. Most currently effective techniques involve secondary recycling, as discussed later.

Recycling means are often affected by public pressure, sometimes based on emotional rather than rational thinking. Styrofoam fast food utilities had been effectively recycled, with collection at establishments being rather efficient. Styrofoam was effectively converted into articles like plastic trays. However, in response to misguided public pressure, most such establishments have converted to the use of substitute materials with questionable environmental consequences.

Regulations often limit the use of the products of primary recycling. There is concern by FDA about bacterial content of recycled articles that may be used in contact with food, although fabrication temperatures are probably sufficiently high in most cases to sterilize the articles.

There remains a large quantity of waste plastics arising from sources not leading to ready separation. The economy of using such mixed plastic depends on the means available for separation and collection. Consumer separation can be facilitated by the requirement that identifying symbols be placed on plastic articles. However, the effectiveness is limited by the conscientiousness and the ability of the consumer to carry out the recommended procedures. Also, the sorting is time dependent, so the real economics is dependent upon the value of alternate use of the time of the consumer.

Once sorting is done by the consumer, it is necessary that these sorted polymers be kept separate during collection and delivery to the recycling facility. This requires the use of vehicles having bins to keep the various polymer types separate. This adds to the cost of the operation.

As an alternative to sorting by the consumer, one can employ "postconsumer sorting," in which the process is carried out in a central facility. This may be done manually or by using automatic sorting equipment. The effectiveness of manual sorting depends on the availability of adequately trained personnel willing to perform this rather monotonous procedure. There have been impressive developments in devising automatic devices for sorting based upon spectroscopic and other signals. This is a difficult task considering the variety of kinds, sizes, and shapes of articles encountered. The equipment is relatively expensive and the economics is dependent on the ability to develop equipment capable of adequate sorting at reasonable cost.

One approach that can be economical is through use of devices that depend upon the density differences of components. Sometimes components of a pulverized polymer may be separated in air streams, while in other cases, the use of liquid baths might be employed. In the latter case, separation may sometimes be aided through use of detergents or surface-active agents that selectively interact with one of the components and aid its floating or sinking.

The effectiveness of any sorting procedure is dependent upon its accuracy. The properties of a separated polymer can be appreciably affected by the presence of small amounts of a different one. The cost of the sorting process increases, as does the need for its accuracy, so it is necessary to seek a compromise between purity and cost.

Separation of polymers prior to processing is usually essential since polymer melts are usually very viscous and separation procedures for the melt are virtually impossible. This suggests the need for procedures involving depolymerization to reduce molecular weight and render the mixture more susceptible to conventional procedures.

B. Secondary and Tertiary Recycling

These approaches involve chemical modification so as to reduce the molecular weight of the polymeric species, often reducing them back to monomers. Such low-molecular-weight materials may then be separated by conventional means such as distillation, after which they may serve as the feed stock for repolymerization or other chemical operations. The means for molecular weight reduction may involve pyrolysis, hydrolysis, or alcoholysis, the choice being dependent upon the kind of bonding occurring in the polymers involved.

A disadvantage of these procedures is that they are usually demanding of energy necessary for breaking the chemical bonds holding the monomer units together in the polymer. They are in opposition to the desire for preventing entropy increase in that one is converting a low-entropy polymer species into higher entropy monomers.

An advantage is that cleaner separations are possible, and the reduced molecular weight material may be separated from other components such as fillers and reinforcing fiber by processes such as filtration. Application is possible to materials like carpets, disposable cameras, and laminated bottles, where separation by primary recycling means is difficult or impossible. Also, the materials pro-

duced by these means are free of concerns about bacterial contamination.

IV. OVERVIEW

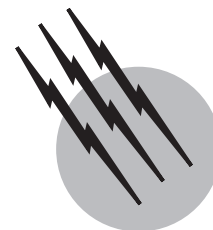
It is evident that there is no single solution for polymer recycling. The choice of an approach is often governed by economics, and at present it is unlikely that the majority of plastic waste can be economically recycled. This fraction will increase with employment of more "design for recycling," improvement of means for sorting, and development of infrastructure. Societal and legislative considerations can be as important as technical aspects in affecting such changes. However, there will always be a portion of the waste stream for which recycling is not the best choice, so alternatives such as generation of energy are viable considerations.

SEE ALSO THE FOLLOWING ARTICLES

BIOPOLYMERS • ENERGY FLOWS IN ECOLOGY AND IN THE ECONOMY • HAZARDOUS WASTE INCINERATION • RENEWABLE ENERGY FROM BIOMASS • WASTE-TO-ENERGY SYSTEMS

BIBLIOGRAPHY

- Andrews, G. D., and Subramanian, P. M. (eds.). (1992). "Emerging Technologies in Plastic Recycling," American Chemical Society, Washington, DC.
- ARC. (1999). "ARC'99. 6th Annual Recycling Conference Proceedings," SPE Recycling Division.
- Brandrup, J., Bittner, M., Michaeli, W, and Menges, G. (eds.). (1996). "Recycling and Recovery of Plastics," Hanser, Munich.
- Ehrig, R. J. (ed.). (1992). "Plastics Recycling, Products and Processes," Hanser, Munich.
- Le Mantia, F. P. (ed.). (1993). "Recycling of Plastic Materials," Chem Tec Toronto.
- Mishra, M. K. (ed.). (1999). "Special issue on polymer and fiber recycling," *Polymer Plastics Technol. Eng.* **38**.
- Rader, C. P., Baldwin, S. D., Cornell, D. D., Sadler, G. D., and Stockel, R. F. (eds.). (1995). "Plastics, Rubber, and Paper Recycling, A Pragmatic Approach," American Chemical Society, Washington, DC.
- Stein, R. S. (1992). "Polymer recycling: Opportunities and limitations," *Proc. Natl. Acad. Sci. USA* **89**, 635-838.



Polymers, Synthesis

Timothy E. Long
James E. McGrath

Virginia Polytechnic Institute and State University

S. Richard Turner

Eastman Chemical Co., Kingsport, TN

- I. Review of Fundamental Definitions
- II. Basic Considerations
- III. Linear Step-Growth Polymerizations
- IV. Linear Chain-Growth Polymerizations

GLOSSARY

Chain-grown (addition) polymerization Transformation of a reactive small molecule (often containing an alkene group) via radical or ionic intermediates into a macromolecule by a series of addition reactions which may involve several distinct kinetic chain-growth steps such as initiation, propagation, and possibly termination.

Chain isomerism Geometric (*cis*, *trans*, etc.), stereochemical (isotactic, syndiotactic, heterotactic), or regio (head-to-tail, head-to-chain configurations) isomerisms.

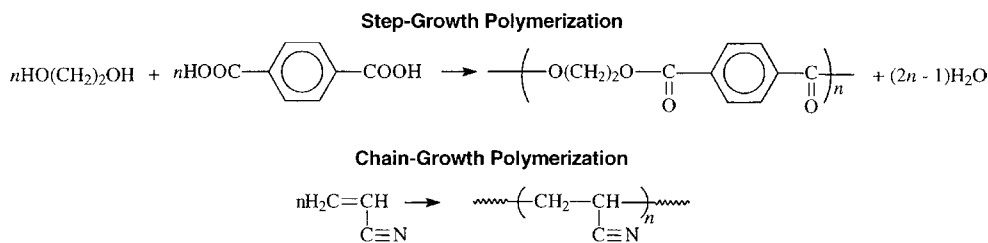
Composition Characteristic of a material defining whether it will have, for example, weak intermolecular forces, as illustrated by a hydrocarbon elastomer (e.g., polybutadiene), or be strongly hydrogen bonded, as in the case of a fiber-forming polyamide. The term is also related to the question of whether one is dealing with a

single repeating unit, which is called a homopolymer, or more than one chemical repeating unit in the chain structure.

Degree of polymerization (molecular weight) Number of repeating units in the macromolecule or polymeric chain structure. The molecular weight of the chain is then a simple product of the degree of polymerization multiplied by the molecular weight of the structure within the repeating unit.

Living and controlled polymerization Polymerization reaction wherein the terminal unit of the growing chain species has an indefinitely long lifetime and will essentially react only with the monomer.

Step-growth (polycondensation) polymerization Process by which a macromolecule is built up via a series of reactions between functional groups, for example, the hydroxyl-carboxyl reaction, to produce a macromolecule at very high conversions (>99.9%).



SCHEME 1 Synthesis of polymers.

I. REVIEW OF FUNDAMENTAL DEFINITIONS

The major routes to polymerization are summarized in [Scheme 1](#) (see below). *Step-growth polymerization* is illustrated by the reaction of ethylene glycol and terephthalic acid to produce poly(ethylene terephthalate) (PET) plus water as a by-product. This reaction is also referred to as a *condensation polymerization*. The pioneers in the field called these types of reaction *condensation processes* since a small molecule (i.e., water) was eliminated in the process. The alternative approach to producing high-molecular weight linear chains is illustrated by the transformation of acrylonitrile to polyacrylonitrile. *Chain-growth polymerizations* are also referred to as *addition* or *vinyl polymerizations*. The terms *condensation* and *addition* thus have their basis in composition and structure, whereas the more modern terms *step-* and *chain-growth polymerization* are related to the kinetics and the mechanisms of the processes. In fact, step-growth polymerization terminology is considered more universal and includes polymerization reactions between functional groups in the absence of condensate formation, e.g., polyurethane formation from diisocyanates and diols.

A. Chain Isomerism

This refers to the possibility of geometric (*cis*, *trans*, etc.), stereochemical (isotactic, syndiotactic, heterotactic), or regio (head-to-tail, head-to-chain configurations) iso-

merisms. The nature of the chain isomerism plays a major role in defining the chain symmetry and hence the physical behavior of macromolecules, even when the structures are nominally very similar.

B. Composition

The chemical composition defines whether a material will have, for example, weak intermolecular forces, as illustrated by a hydrocarbon elastomer (e.g., polybutadiene), or be strongly hydrogen bonded, as in the case of a fiber-forming polyamide. The term is also related to the question of whether one is dealing with a single repeating unit, which is called a homopolymer, or more than one chemical repeating unit in the chain structure. The presence of two dissimilar units defines a copolymer, three a terpolymer, and so on. The arrangement of the monomer units may be statistical, alternating, or blocklike. Sequential arrangements that are particularly long are referred to as segmented or blocklike structures. Fundamentally, this is related to the sequence distribution of the two species in a copolymer chain. If long, chemically distinct sequences are pendant to the main chain, they are referred to as graft copolymers. These features are illustrated in [Table I](#).

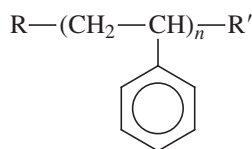
C. Degree of Polymerization (Molecular Weight)

The number of repeating units in the macromolecule or polymeric chain structure is referred to as the degree of polymerization. The molecular weight of the chain is then a simple product of the degree of polymerization

TABLE I Chemical Compositions of Polymers

Polymer type	Composition
Homopolymer	~~~~~AAAAAAAAAAAAAAAAAAAAAAAAAAAAAAAA~~~~~
Statistical or random copolymer	~~~~~AABABBBBABBBABBBABABAABBBBB~~~~~
Block or segmented copolymer	~~~~~AAAAAAAA~AAAAABBBBBB~BBBBBBBBB~~~~~
Graft copolymer	~~~~~AAAAAAAAAAAAAAAAAAAAAAAAAAAAAAAA~~~~~ <div style="display: flex; justify-content: space-around; width: 100%;"> <div style="text-align: center;"> B B B B </div> <div style="text-align: center;"> B B B B </div> </div>

multiplied by the molecular weight of the structure within the repeating unit. The molecular weights of synthetic macromolecules usually exhibit a distribution in size. The distributions are often Gaussian, but may also approach the Poisson distributions in living and more controlled polymerization processes. An example is provided below for polystyrene. Thus, M_n is the number-average molecular weight, which is a product of N , the degree of polymerization, times 104 g/mole. The end groups R and R' are negligible at high M_n :



D. Living and Controlled Polymerization

Polymerization reactions wherein the terminal unit of the growing chain species has an indefinitely long lifetime and will essentially react only with the monomer are called living or controlled polymerizations. Such behavior permits molecular weight to increase linearly with conversion and provides terminally active species, which may initiate distinctly different monomer structures, thus producing blocklike copolymers. This is particularly important for carbanion polymerizations, as illustrated by the organolithium polymerizations of hydrocarbon monomers. Research has shown that other types of reactive intermediates, including coordination species with particular attention to metallocene and single-site catalysts, appropriate cationic or oxonium ion species and reversibly stabilize free radical processes. Recent efforts in controlled radical polymerization processes have focused on stable free radical polymerization (SFRP) using nitroxide mediation, atom transfer radical polymerization (ATRP), and radical addition fragmentation transfer (RAFT). The use of “living” or “controlled” terminology depends on the mechanism of polymerization, and the “living” classification is often reserved for processes where the rates of transfer or termination equal zero during propagation.

E. Step-Growth (Polycondensation) Polymerization

In these processes a macromolecule is built up via a series of reactions between functional groups, for example, the hydroxyl–carboxyl reaction, to produce a macromolecule at very high conversions (>99.9%).

F. Chain-Grown (Addition) Polymerization

In this process a reactive small molecule (often containing an alkene group) is transformed via radical or ionic intermediates into a macromolecule by a series of addi-

tion reactions. The latter may involve several distinct kinetic chain-growth steps such as initiation, propagation, and possibly termination. The reaction is most important for the preparation of poly(ethylenes), poly(acrylates), poly(styrenes), poly(dienes), and related mono- or disubstituted analogs.

II. BASIC CONSIDERATIONS

A number of important requirements must be met if small molecules (on the left side of the arrows in [Scheme 1](#)) are to be efficiently transformed into macromolecular structures. One critical concept is the idea of functionality. In a step-growth polymerization, in order to achieve high molecular weight, it is essential that the reactions be perfectly difunctional. For example, if we reacted only one of the hydroxyl or carboxyl groups, we would make simply a small molecule. Indeed, the idea of a step-growth reaction is that the reaction can proceed from both ends of the molecule. It must proceed until high values of n , the degree of polymerization, are achieved. Typical number-average molecular weights for step-growth polymers, such as poly(ethylene terephthalate), are 20,000–30,000 g/mole (Da).

By contrast, typical chain-growth reactions are required to proceed to significantly higher molecular weights, perhaps 100,000–200,000 g/mole or higher in the case of polyacrylonitrile and related so-called vinyl polymers. The term *vinyl polymer* refers to the fact that the chain molecule is derived from a “vinyl-containing” starting material, even though the addition produces a saturated chain. The chain-growth reaction occurs in several distinct steps. Initiation, propagation, and terminated processes are involved as the kinetic chain begins to react, propagates, and finally terminates. Thus, there are a number of differences between these two fundamental routes of polymerization. In the step-growth case, only one reaction is responsible for polymer formation. In the example, this is esterification. By contrast, in the chain-growth case, initiation, propagation, and termination reactions proceed at different rates and possibly different mechanisms. During the polymer-growth step, any two molecular species present can react during a step process, and one typically observes a slow, random growth taking place. Again, by contrast, the growth step in the chain reaction usually occurs by the rapid addition of one unit at a time to the active end of the polymer chain. As we shall demonstrate later, the active ends will be the typical intermediates of organic chemistry, such as radicals, anions, cations, and coordination complexes. The point of the discussion here is that the molecular weights vary quite differently as a function of conversion for the two systems. This is illustrated in [Fig. 1](#). In the case of the step-growth reactions, molecular weight increases only slowly until one reaches very high conversions. In fact, the overall process is governed by

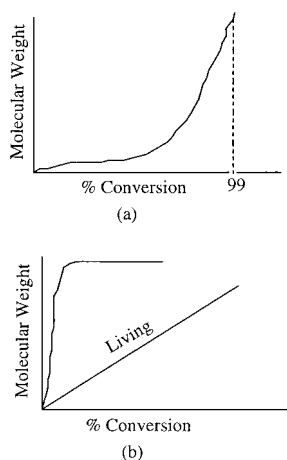


FIGURE 1 Molecular weight versus percent conversion for (a) step-growth polymerization and (b) chain growth polymerization and living polymerization processes.

the fractional extent of conversion, usually designated P . For example, if one started a reaction with 1 mole of carboxylic acid, it would be necessary to consume $\sim 99\%$ of that mole; in other words, reduce the concentration to 0.01 mole, before one could anticipate reaching high molecular weight. The degree of polymerization is proportional to $1/(1 - P)$, where P is the fractional extent of reaction.

This means that there are a number of requirements for obtaining high molecular weight. First, one must work with very pure monomers. Typical purities of commercial-grade monomers are 99.99%. If they were less than 99% pure, it would be impossible to make more than 100 units in a chain, which would generally be insufficient to obtain adequate mechanical properties. Second, if coreactants are utilized, a perfect stoichiometric balance of the two difunctional monomers must be introduced. Third, there must be no side reactions. Finally, conditions must exist that will allow the reaction to be pushed to very high conversions. This implies the absence of any side reactions. In essence, step-growth polymerization can be viewed as a form of quantitative organic chemistry. Most organic reactions are not suitable for obtaining such high yields. Surprisingly, however, a large number of systems have been produced in the laboratory, not only from simple polyesters and polyamides, but also from high-temperature materials, such as polyimides and liquid crystalline polymers. The only necessity is that the four requirements discussed above be met for any of the step-growth polymerization systems.

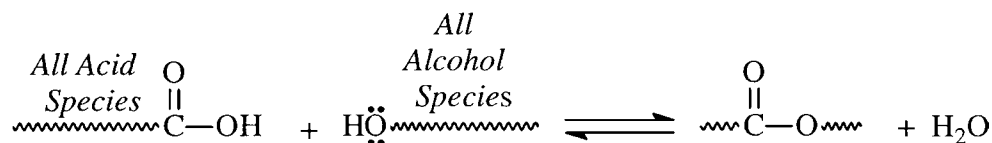
Chain-growth reactions, by contrast, often show molecular weight versus conversion curves, as illustrated in the lower portion of Fig. 1. Free-radical reactions that involve initiation, propagation, and termination often yield high-molecular weight chains at very low conversions.

Thus, one can imagine only a small percentage of the monomer being activated per unit time, and perhaps only about 10^{-8} mole/liter of growing chains may be active at any one time. In this case, the monomer concentration will decrease steadily throughout the reaction. Living polymerizations continue to receive intense academic and industrial attention. In a living polymerization, in which the chain-end activity is maintained throughout the overall polymerization (the rate of any transfer or termination steps is essentially zero), one may observe molecular weight increasing linearly with conversion. Such polymerizations are of great interest since they allow predictable molecular weights and narrow molecular weight distributions to be obtained, as well as the possible generation of block copolymers by the use of the active chain end of one species to initiate a new monomer.

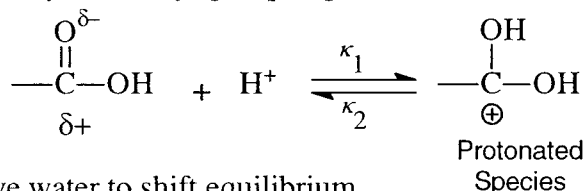
III. LINEAR STEP-GROWTH POLYMERIZATIONS

In Scheme 2, a direct esterification process illustrates linear step-growth polymerization. The implication is that all of the oligomeric species are capable of reacting with suitably terminated species. Therefore, as the molecular weight slowly builds through the early portion of the reaction, a variety of oligomeric sizes exist that must react with one another to ultimately generate high molecular weight. These reactions are often protic or Lewis acid-catalyzed, as illustrated, to allow the protonated species to be more readily attacked by the nucleophile. This is consistent with the usual mechanics in small-molecule esterification.

Since the esterification is an equilibrium process, water typically has to be removed in order to drive the reaction to the right, that is, toward higher molecular weight. The polymerization rate in such a case is proportional to the group collision frequency and not dependent on the diffusion rate of the entire chain. The statistical segment is more mobile than the whole molecule. Many workers have demonstrated that the second functional group on a growing chain is not influenced by the first if several carbon atoms separate it. Essentially, this leads to the principle of equal reactivity. This implies essentially that the reactivity of the growing molecules will not change significantly during most of the polymerization process. There are some exceptions to this, based on highly sterically restricted groups, and, of course, heterogeneous processes would also not fall into this category. Nevertheless, the principle of equal reactivity has made it possible to treat these reactions statistically. The fact that the molecular weights and molecular distributions can be predicted this way is an indication that the principle is typically correct. Another way of looking at this process is summarized in Scheme 3. Any two species in the reaction mixture must



1. Catalyzed by acid prototation of carboxyl, carbonyl group, e.g.,

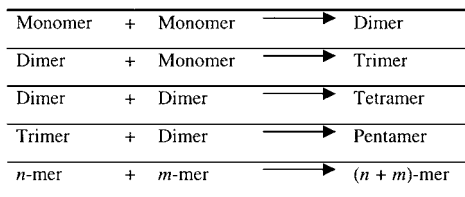


2. Remove water to shift equilibrium to right (e.g., toward higher MW)
3. Can follow reaction by titrating for unreacted -COOH, e.g., $R_p = -d(\text{COOH})/dt$

SCHEME 2 Linear step-growth processes: polyesterifications.

react with one another, whether they are dimers reacting with monomers, trimers, or higher species. In the general case, one considers an n -mer reacting with an m -mer to produce the next higher oligomer. This whole process must continue until P begins to approach 0.99 or higher.

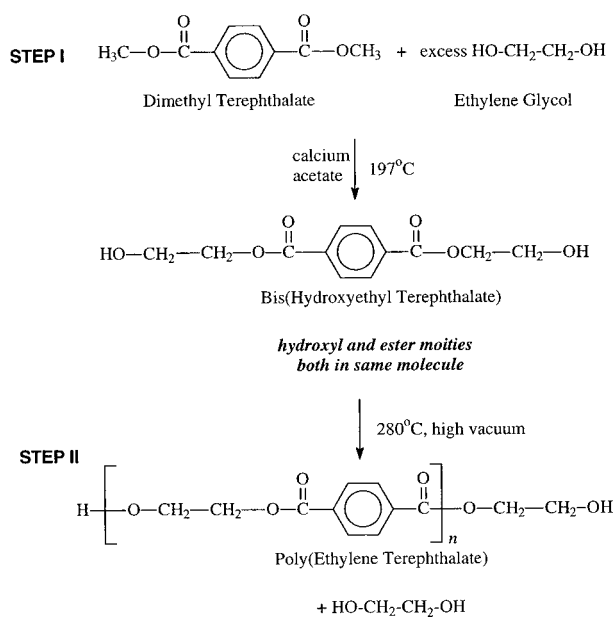
A second illustration of a linear step-growth polymerization is the synthesis of polyesters via ester interchange processes (Scheme 4). Here, one utilizes the dimethyl ester of terephthalic acid with, initially, an excess of ethylene glycol. Historically, the choice of the dimethyl ester was based on considerations of monomer purity. Thus, in early industrial practice, it was not feasible to produce nearly 100% pure terephthalic acid. Since terephthalic acid cannot be distilled, early investigators took recourse to producing the dimethyl ester, which could be vacuum-distilled and also crystallized, thus allowing one to meet the criterion of extremely high monomer purity. The dimethyl ester then will react with a diol, such as ethylene glycol, in the manner indicated.



SCHEME 3 Examples of step-growth polymerization. Any two species in the reaction mixture can react with one another.

Ester interchange processes will proceed and produce methanol, which is removed. Ideally, the structure is bis(hydroxyethyl) terephthalate. Actually, some higher oligomers may also be formed at this stage, but the point is that the new structure has both hydroxyl and ester functionality in the same molecule.

Sometimes it is common to term such a new monomer an AB system. This is contrasted with a so-called AA +



SCHEME 4 Synthesis of polyesters via ester interchange.

BB system, which requires two distinct molecules to be reacted together in the step-growth or polycondensation process. In the second stage of the ester interchange route to polyesters, application of heat and a gradually increasing vacuum down to a fraction of a torr eliminates any excess ethylene glycol that may be present. Then (usually in the presence of a catalyst), ester interchange processes begin where a hydroxyl end group can attach an in-chain ester carbonyl. On removal of additional ethylene glycol, the molecular weight and degree of polymerization begin to decrease.

Finally, when the n value in [Scheme 4](#) approaches a few hundred, which corresponds to molecular weights of $>20,000$ g/mole, one may stop the process. Clearly, for different applications somewhat different molecular weights may be required, but typically 20,000–30,000 would be a representative value. As the interchange process takes place, the reaction proceeds to higher and higher molecular weight. Typically, this is done 25°C above the crystalline melting point in order to achieve adequate reactivity. Although one could intuitively propose the use of longer polymerization times to achieve higher molecular weight products, the importance of relatively slow side reactions during the polymerization process becomes more important when using either longer polymerization times or higher polymerization temperatures. For example, the manufacture of PET is accompanied by the formation of diethylene glycol (DEG), vinyl esters, and acetaldehyde during the polymerization process. DEG is incorporated into the chain during the polymerization and its presence in the backbone has been shown to negatively affect the chemical resistance, crystallization rate, thermal stability, and ability for strain-induced crystallization in many PET product applications. In addition, acetaldehyde has been observed to affect the packaging of beverage and other food products. Typically, the process is completed at slightly below the crystalline melting point in what is often termed a solid-phase finishing step. In addition to reducing the propensity of undesirable side reactions, the lower temperature solid-phase or solid-state process serves to efficiently remove any small molecular impurities that were generated in the previous higher temperature melt-phase process.

As discussed earlier, a salient feature of step-growth polymerization processes is the gradual increase in molecular weight throughout the polymerization process. This observation is a direct result of the stepwise addition of reactive species (monomers, dimers, trimers, tetramers, etc.) to give high molecular weight. In contrast, high-molecular weight products are obtained very quickly in chain polymerization processes and are typically accompanied by highly exothermic reactions. Consequently, the gradual increase in melt viscosity and the absence of highly exother-

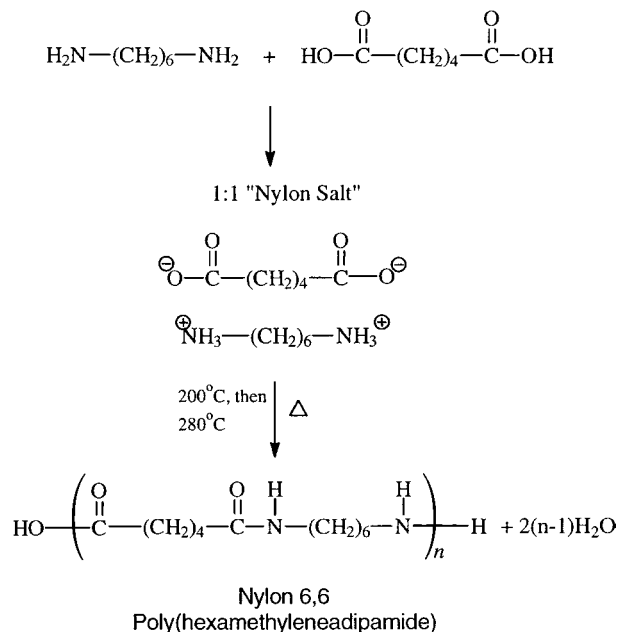
mic reactions facilitates the use of bulk polymerization processes in step-growth polymerization. For example, polyesters and polyamides are manufactured commercially in the absence of solvents and the final products are directly usable without further isolation and purification. Although molecular weights gradually increase throughout most of a step-growth polymerization process, the final stages of the polymerization process involve the rapid increase in molecular weight. It is well known that the melt viscosity for thermoplastics increase with the 3.4 power of the weight-average molecular weight. It is not surprising, therefore, that significant attention has been devoted in recent years to the development of novel agitation and reactor designs to facilitate the transport of the viscous melt and the transport of polymerization by-products in the latter stages of step-growth polymerization processes.

Although high molecular weight is often required for the maximization of thermal and mechanical properties, the synthesis of difunctional oligomers (less than 10,000 g/mole) is accomplished in step-growth polymerization using monofunctional reagents or a stoichiometric excess of a difunctional monomer. The difunctional oligomers are suitable starting materials for the preparation of crosslinked coatings, adhesives, or segmented block copolymers. Due to the reactive nature of many polymers prepared using step-growth polymerization processes, reactive end groups and internal reactive functionalities offer the potential for subsequent derivatization, chain extension, or depolymerization. For example, the depolymerization of polyesters is easily accomplished with the addition of a suitable difunctional acid or glycol. In addition, polyester and polycarbonate blends are easily compatibilized in a twin-screw extruder to prepare optically clear coatings.

Polyesters derived in part from unique rigid aromatic monomers including hydroquinone and biphenyl derivatives offer the potential for new families of high-temperature, high-performance polyester resins. Although liquid crystalline polyesters (LCPs) were discovered in the late 1960s, this family of engineering thermoplastics continues to receive intense academic and industrial attention. In addition to inherent flammability resistance, LCPs offer exceptional moldability due to the shear-induced alignment of the rigid polyester backbones. Therefore LCPs have become very important in the manufacture of small parts for the electronics and other industries. Ticona (formerly Hoechst-Celanese) has pioneered the commercialization of all-aromatic liquid crystalline polyesters based on 2-hydroxy-6-naphthoic acid (HNA) and *p*-hydroxybenzoic acid (PHB). Ester formation based on the reaction between an aromatic carboxylic acid and an aromatic phenol is not suitable for polyester manufacture, and all-aromatic polyesters

require the *in situ* acetylation of the aromatic phenols. Condensation of the acetate and aromatic carboxylic acid readily occurs at 250°C with the liberation of acetic acid, and the polymerization mechanism is often referred to as acidolysis. Although the polymerization mechanism appears straightforward, Hall and coworkers have recently elucidated the very complex nature of this polymerization process. Industrial attention has focused on the development of suitable manufacturing processes that can handle the corrosive reaction environment and the high polymerization temperatures required in the viscous melt phase. Significant attention has also been devoted to the preparation of liquid crystalline polyesters derived from aliphatic glycols and biphenyl dicarboxylic acids.

Many excellent reviews are available on the synthesis of nylons. Melt-phase polycondensation processes synthesize most aliphatic and partially aromatic nylons commercially. In cases where crystalline polyamides are prepared and melt-phase viscosities limit desired molecular weight formation, solid-state polymerization processes have been employed. For nylons, the formation of the “nylon salt” is very useful in purifying the monomers and obtaining the exact stoichiometry to be able to get a high degree of polymerization. Unlike polyesters, the equilibrium in a polyamide condensation lies for to the right and thus the polymerizations can be charged stoichiometrically and initially run under pressure to react all the diamine and maintain the stoichiometry. The step-growth process for polyamides is illustrated in Scheme 5. The reaction product of hexamethylenediamine and adipic acid produces



SCHEME 5 Synthesis of polyamides.

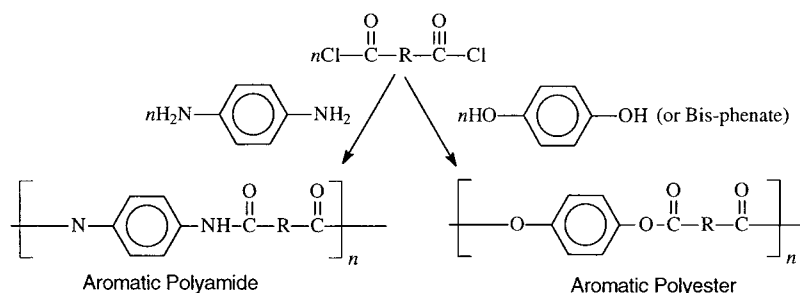
the largest volume polyamide, or nylon, in the world. This is called poly(hexamethylene adipamide), but in addition, the common nylon terminology is frequently used. Nylon nomenclature is based simply on the number of carbons in the reactants. Thus, there are six methylenes in hexamethylenediamine and six carbons in adipic acid, hence, the term Nylon 6,6.

In order to achieve perfect stoichiometry in the AABB system, one relies on the capacity of these species to form a one-to-one “nylon salt,” which essentially is an ammonium carboxylate, as indicated. On carefully heating the ammonium carboxylate to ~200°C initially, then as high as 280°C in order to exceed the crystalline melting point of the polymer, one can transform the ionic carboxylate into amide bonds with the release of water. The terminal amine groups of the oligomeric polyamides react with terminal carboxylic acid groups until appropriate high-molecular weight materials are obtained. The molecular weight is typically 20,000–30,000 for many fiber-forming polymers.

Many variations on polyesters and polyamides are possible, and in the case of wholly aromatic systems it is common to use either solution or interfacial processes, as depicted in Scheme 6. Due to the lower reactivity of aromatic amines and aromatic bisphenols, it is often necessary in these cases to utilize the more reactive acid chloride derivative of carboxylic acids. Thus, many aromatic polyamides and polyesters are known and are important in both fiber and thermoplastic materials technology. In these systems, either terephthaloyl or isophthaloyl chlorides or mixtures of the two are used frequently to disrupt the chain symmetry and produce amorphous materials. Utilization of a single component may allow crystalline textures to be produced that are important, for example, in fiber technology.

A much different solution process involves the use of diaryl halides and diamines to prepare aramids via the Heck carbonylation reaction. This route to aramids was first disclosed using dibromo aromatics. Relatively low molecular weight polymers were formed. Diiodo aromatics were found to react at a much higher rate and to give polymers of much higher ultimate molecular weight, presumably due to fewer side reactions. This process eliminates the use of corrosive and moisture-sensitive acid chlorides, but requires the use of expensive palladium catalysts.

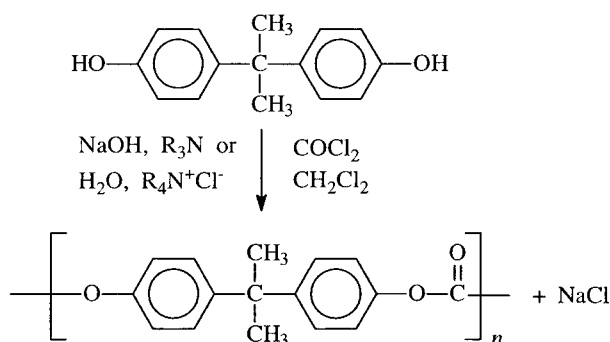
Other important polymers are synthesized via step-growth polymerization, although we shall provide only four additional examples that have received significant attention. Since the early 1960s polycarbonates have become an extremely important and fast-growing, clear, amorphous thermoplastic for injection molding and extruded sheet products. The workhorse polycarbonate resin is based on bisphenol A (BPA PC) and has a unique



SCHEME 6 Examples of acid chloride reactants. Such reactants are more reactive than carboxyl, should be used with less reactive “glycols” (bisphenols) or aromatic diamines, and should also be used in solution or interfacially.

set of properties, which include a very high glass transition temperature of 150°C and excellent toughness. These properties along with the low color and excellent clarity of products from BPA PC have propelled consumption to approximately 2.6 billion lb in 1996 with a growth rate of 8–10% a year.

Scheme 7 illustrates polycarbonate synthesis via an interfacial or phase-transfer-catalyzed process. In this case, one converts the starting bisphenol to its water-soluble sodium salt by the reaction of sodium hydroxide with the bisphenol. The simple diacid chloride is added in methylene chloride and, in principle, the phenate will react rapidly with phosgene to produce first chloroformates and then the important polycarbonates. In order to facilitate the process, one uses what has come to be known as a phase transfer catalyst. Typically this is a tertiary amine or a quarternary halide. The quarternary halide can exchange partially with the alkali metal cation to produce a quarternary cation, which makes the phenate much more organically soluble. The resulting phenate then quickly reacts with the acid chloride to produce the polycarbonate structure. The by-product of the process, then, is either sodium chloride or the quarternary chloride, which migrates back to

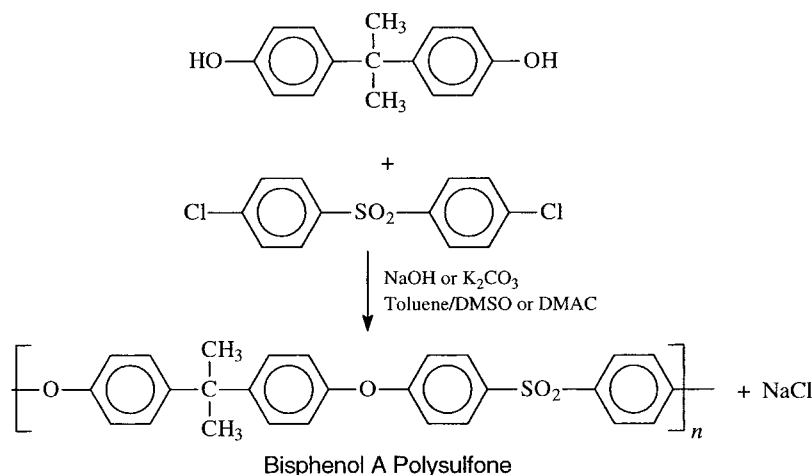


SCHEME 7 Polycarbonate aqueous caustic (interfacial, phase-transfer-catalyzed) process. The $\text{R}_4\text{N}^+\text{Cl}^-$ is thought to facilitate the transfer of phenate from the aqueous to the organic layer, where it reacts with COCl_2 .

the aqueous phase, thus completing the phase transfer cycle. There are several excellent reviews describing laboratory and industrial synthetic process for polycarbonates. Polycarbonates are prepared in solution or interfacially using bisphenol and phosgene in the presence of a base to react with the hydrochloric acid that is liberated. Due to the toxicity of phosgene and methylene chloride and the problems with disposal of the large amounts of sodium chloride that are generated during production of polycarbonate, there has been a very large interest in developing melt-phase processes. Catalyzed transesterification based on the reaction of bisphenol A with diphenyl carbonate is accomplished at temperatures as high as 320°C under vacuum in order to obtain the high molecular weights needed for good mechanical properties. Various lithium salts and other additives are used as catalysts. Considerable research continues in this area to minimize the degradation reactions, color formation, etc., that accompany these high-temperature melt-phase processes.

Another example of a step-growth polymer synthesis is a nucleophilic aromatic substitution reaction, which produces poly(arylene ether sulfones), as illustrated in **Scheme 8**. Poly(arylene ether sulfones) are very resistant to hydrolysis by water and thus can be used in situations that are not appropriate for polyesters, polycarbonates, or polyamides, which are eventually hydrolyzed in water. In **Scheme 8**, one first produces the bisphenate and utilizes a coreactant that is a class of activated aromatic halides. The sulfone group activates the carbon attached to the chlorine and facilitates the attack of the phenate nucleophile to generate the ether bond in the polymerization step. The by-product sodium chloride must be eliminated, but since it is water soluble, this is not difficult. In order for these processes to proceed efficiently, one normally requires an aprotic dipolar solvent such as dimethyl sulfoxide or dimethyl acetamide which can stabilize the intermediate structures and facilitate the formation of the ether bond in the polymerization step.

All of the same requirements discussed earlier are necessary in these systems as well. It is, for example,



SCHEME 8 Synthesis of poly(arylene ether sulfones) via step-growth polymerization.

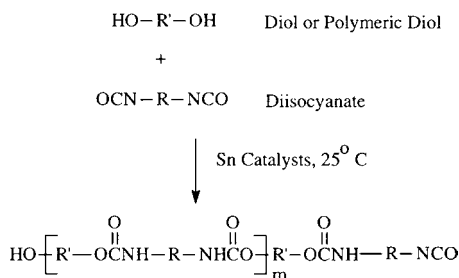
important to conduct these reactions under fairly dry conditions so that the activated halide is not prematurely hydrolyzed. Otherwise, this will upset the stoichiometry and limit the molecular weight to an undesirably low value. One approach that facilitates this process is to utilize the weak base potassium carbonate. This will react with the bisphenol only at elevated temperatures, where it is easier to obtain an anhydrous system.

An example of a step-growth polymerization process that does not involve the liberation of a low-molar-mass condensate is polyurethane synthesis. In 1998, approximately 9 billion lb of polyurethanes (PURs) was produced for three major classes of applications in rigid and flexible foams, elastomers, and coatings. Urethane formation can be produced in solution, in bulk, or interfacially. The reactions are very fast and can proceed far below room temperature at high rates. Catalysts have been developed to allow the reaction rates to be varied from seconds to hours. The inclusion of these catalysts is very important in many applications that involve the reactive processing of the monomers. Another way the reactivity of these systems is controlled is by blocking the isocyanate group with a group that comes off on heating to regenerate the reactive isocyanate group. This chemistry has found considerable application in coating technologies.

The great flexibility in choosing the starting polyisocyanate and the polyol leads to the capability to design polyurethanes with a wide-range of properties. Most flexible foam is based on toluene diisocyanate (TDI) with various polyols. These foams are used primarily for cushioning applications, for example, car seats, furniture cushions, and bedding. The technology for blowing these foams, flame retarding, stabilizing, etc., is very involved and key to the enormous commercial success. Rigid PUR foams generally are based on polymeric methylenediphenyl iso-

cyanates (PMDI) and are used as insulation in transportation vehicles and appliances, among others. These foams are characterized by their dimensional stability, structural strength, and insulation performance. The polyols most widely used are generally based on polyether or polyester backbones. Polyurethane elastomers are based on hard-soft segment type polymeric structures and can exist as cast elastomers or as thermoplastic elastomers. These elastomers generally possess good chemical and abrasion resistance and maintain their properties over wide temperature ranges. The hard segments that phase separate in the elastomer are primarily based on methylenediphenyl isocyanate (MDI).

A final example of a linear step-growth polymerization involves the synthesis of polyimides. Polyimides are classically prepared via the addition of an aromatic dianhydride to a diamine solution in the presence of a polar aprotic solvent such as NMP, DMAc, and DMF at 15–75°C to form a poly(amic acid). The poly(amic acid) is either chemically or thermally converted to the corresponding polyimide via cyclodehydration. The general chemistry for this two-stage, step-growth polymerization process for the preparation of Kapton polyimide is depicted in [Scheme 9](#). It is important to note that the formation of the poly(amic acid) is an equilibrium reaction and attention must be given to ensure that the forward reaction is favored in order to obtain high-molecular weight poly(amic acids). If the final polyimide is insoluble and infusible, the polymer is generally processed in the form of the poly(amic acid). Caution must be exercised when working with classical poly(amic acid) solutions due to their hydrolytic instability, and shelf-life is limited unless properly stored at low temperatures. This is due to the presence of an equilibrium concentration of anhydride and their susceptibility to hydrolytic degradation in solution.



SCHEME 9 General polyurethane synthesis.

On the other hand, poly(amic diesters) can be stored for indefinite periods of time without degradation due to the inability to form an intermediate carboxylate anion and have been utilized reproducibly in microelectronics applications. Earlier studies have shown that the formation of tri- and tetramethylesters of dianhydrides increased the likelihood of N-alkylation side reactions and a corresponding decrease in the molecular weight and mechanical properties of the final product. A similar side reaction has been observed in attempts to prepare polyamide esters using dimethyl esters of terephthalic acid.

Melt-processible thermoplastic polyimides are prepared by the addition of flexible units, bulky side groups, or, as mentioned earlier, flexible difunctional oligomers. Examples of these modifications include GE's Ultem (ether units), Amoco's Torlon (amide units), Hoechst-Celanese's P150 (sulfone units), and GE's Siltem (siloxane segments). Ultem polyimide is manufactured by General Electric and is an injection-moldable thermoplastic poly(ether imide). This commercial product exhibits high mechanical properties including modulus and strength, excellent ductility, and high thermal stability. Although polyimides have been prepared using a myriad of other synthetic methodologies including aryl coupling with palladium catalysts, poly(amic silylesters), silylethers with activated halides, and transimidization, this section has focused on only two of the commercial polyimides in the marketplace today. Many specialty polyimides for composite applications have also evolved including LARC-TPI and CPI (Mitsui Toatsu) and Hoechst-Celanese's fluorinated polyimides. Due to the tremendous scope of polyimide research and applications, several excellent comprehensive texts have been devoted to this family of high-temperature polymers.

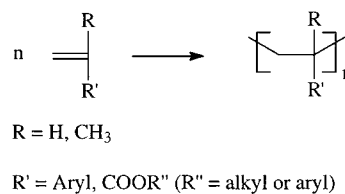
It is easy to understand, based on the above discussions, the serious restrictions that severely limit the number of suitable organic reactions that have been used for the successful preparation of high-molecular weight products via step-growth polymerization. Although many synthetic organic reactions appear to be suitable for the preparation of macromolecules via a step-growth polymerization process, most organic reactions do not meet all the necessary

requirements and have not been utilized in commercial products. *A challenge remains to broaden the scope of suitable polymerization chemistries and processes leading to new families of high-performance polymeric products.*

IV. LINEAR CHAIN-GROWTH POLYMERIZATIONS



The transformation of a vinyl or alkene monomer into a long-chain macromolecule via a chain reaction process is depicted in [Scheme 10](#). This process basically involves the addition of a monomer to an activated or initiated form of the monomer. The reaction as indicated involves a change in the bonding from an sp^2 bond to an sp^3 bond. This process of chain polymerization is usually not spontaneous, but rather must be catalyzed or initiated. For most monomer systems of this type, there are at least three basic individual steps in the overall process of polymerization: the initiation step, the propagating or growth step, and the termination step. The details of these three individual events will be highly dependent on the exact mechanism of polymerization. The active intermediates may be categorized as radicals, anions, cations, or coordinated species. For some of these mechanistic processes, notably anionic and controlled radical polymerization, it is often possible to avoid or significantly reduce the termination step. There are many monomers that can be transformed into long-chain linear macromolecules via an addition or chain reaction process. A number of these are illustrated in [Table II](#). The common feature is that one is converting the unsaturated carbon-carbon bond into a saturated moiety. All samples here have a functionality of 2; divinylbenzene, in contrast, would have a functionality of 4 and would form networks.

The nature of the pendent group will help discern which reaction mechanism must be followed in order to effect this transformation. We have indicated that, in all cases, we are converting a carbon-carbon double bond to a long-chain macromolecule. However, it should be pointed out that chain reaction polymerization is not limited simply to carbon-carbon bond polymerization but includes many other reactions. Nevertheless, it is most useful to illustrate chain reaction polymerization via a discussion of



SCHEME 10 Polymerization of an alkene monomer into polymer.

TABLE II Addition Polymers

Monomer		Polymer	Name of polymer
$n\text{CH}_2=\text{CH}_2$	→	$-(\text{CH}_2-\text{CH}_2)_n-$	Poly(ethylene)
$n\text{CH}_2=\text{CH}$ CH_3	→	$-(\text{CH}_2-\text{CH})_n-$ CH_3	Poly(propylene)
$n\text{CH}_2=\text{CH}$ Cl	→	$-(\text{CH}_2-\text{CH})_n-$ Cl	Poly(vinyl chloride)
$n\text{CH}_2=\text{CH}$ 	→	$-(\text{CH}_2-\text{CH})_n-$ 	Poly(styrene)
$n\text{CH}_2=\text{C}$ CH_3 $\text{C}=\text{O}$ OCH_3	→	$-(\text{CH}_2-\text{C})_n-$ CH_3 $\text{C}=\text{O}$ OCH_3	Poly(methyl methacrylate)
$n\text{CF}_2=\text{CF}_2$	→	$-(\text{CF}_2-\text{CF}_2)_n-$	Poly(tetrafluoroethylene)

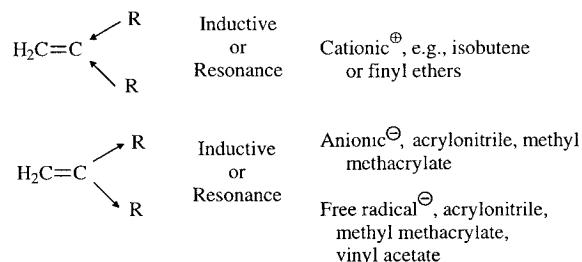
carbon-carbon bond reactions. The types of initiators or catalysts for addition or chain reaction polymerization are briefly outlined in Table III. Ordinarily, radical, cationic, anionic, or coordination-type catalysts are the most effective for initiating polymerizations. The radical initiators include peroxides, azo compounds, redox combinations, UV light, and, in general, any process that will efficiently produce an active radical species that is capable of interacting with a monomer. High-energy radiation, for example, from ^{60}Co , is also a suitable radical initiation agent. The mechanism in the case of radiation can be quite complex. Ordinarily, such high-energy radiation processes are radical-type polymerizations. Under certain anhydrous conditions, however, it has been demonstrated that either cationic or anionic polymerization can be initiated with high-energy radiation. More traditional cationic species include Lewis acids such as BF_3 and alu-

minum trichloride and various oxonium ions. Anionic processes have been studied in great detail through the use of organoalkali compounds such as the alkylolithiums. Electron transfer reagents, such as sodium naphthalene complexes, are also used. One of the most important types of polymerization, especially in terms of volume of materials produced, is coordination or Ziegler-Natta catalysis, which involves a variety of transition metal complexes. For example, these are usually based on titanium, vanadium, or chromium compounds, as we shall discuss later.

Since we have indicated that various polymerization processes may occur via different mechanisms, one might ask how one defines which type of mechanism may be operative for a particular monomer. From a fairly simplistic point of view, we can get some idea of the nature of the required catalyst from the structure of the monomer. For example, Scheme 11 indicates that a monomer that

TABLE III Examples of Initiators for Chain Reaction Addition Polymerizations

Radical	Cationic	Anionic	Coordination
Peroxides	Proton or Lewis	Organo alkalis	Transition metal complexes
Azo compounds	Carbocations	Lewis bases	
Redox systems	Oxonium ions	High-energy radiation (anhydrous)	
Light	High-energy radiation (anhydrous)		
High-energy radiation			



SCHEME 11 Vinyl chain polymerization. Electron density at the double bond may determine whether a particular monomer polymerizes via an anionic, cationic, or free-radical mechanism. Some monomers (e.g., styrene) can polymerize via two or all three routes.

contains electron-donating groups either via resonance or inductive interactions will polymerize via a carbocation mechanism. Examples are isobutene and the vinyl alkyl ether systems. Monomers of this type are very responsive to cationic type of initiators, such as Lewis acids. Thus, the electron density at the double bond can determine whether a monomer polymerizes via a cationic or an anionic process. A second example is a monomer in which electron-withdrawing groups such as ester groups or nitrile groups are attached to the reactive site. Such a monomer is quite stable to cationic species but can very often be rapidly polymerized by anionic initiators. On the other hand, there are a number of monomers of somewhat intermediate electron densities, for example, vinyl acetate. These monomers are primarily polymerized by only free-radical type of initiators. Such monomers may contain groups that would interfere with cations or anions (e.g., vinyl halides) and therefore must be polymerized only by free-radical processes.

A. Free-Radical Chain Polymerizations

If one were to use a peroxide-type initiator, it would be of great interest to understand how the groups attached to the oxygen bond influence the polymerization. Table IV lists several peroxide initiators and some suitable temperature ranges where they could be used. The common feature here is the relatively weak oxygen–oxygen bond, which is susceptible to homolytic cleavage. However, the groups attached to the peroxy bond particularly influence the stability of the radicals that are formed, and this in turn defines more or less the temperature range within which a partic-

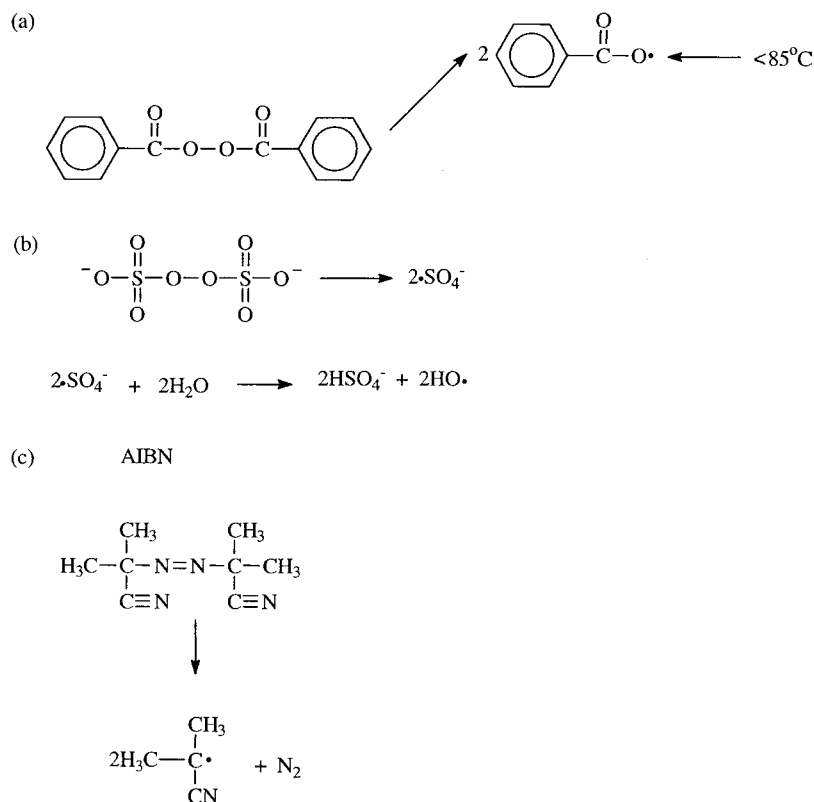
ular peroxide molecule could be used to effect polymerization. For example, a tertiary butyl group on a peroxide will produce a tertiary butoxy radical, which is relatively stable. Therefore, initiators containing these groups are useful at relatively high temperatures. The other principal effect of structure is related to the solubility of a peroxide initiator. A high percentage of organic groups will promote organic solubility, which is important in certain types of polymerizations, such as “suspension” reactions. On the other hand, if one wishes to have a water-soluble initiator, the initiator of choice may be potassium persulfate since the potassium salt form is quite soluble in aqueous media. A wide range of initiator structures has been prepared, and many of these are commercially available. Nevertheless, there are some occasions when one wishes to generate a free-radical species at room temperature or slightly above.

Some additional free-radical decompositions are depicted in Scheme 12. In particular, one should comment on the important class of azo initiators. The most important of these is azobisisobutyronitrile (AIBN), which decomposes to generate a molecule of nitrogen plus a nitrile-stabilized alkyl radical. The half-life of the polymerization initiators can often be quite readily predicted, at least for model systems. The reaction rate follows first-order kinetics. There is a wide variety of vinyl monomers that will undergo free-radical polymerizations. In general the pendant group is usually capable of producing resonance stabilization to the growing radical species. Scheme 13 shows several of the most important types of monomers that readily undergo free-radical polymerization; these include styrene, vinyl acetate, the acrylic and methacrylate monomers, the vinyl halides, acrylonitrile, and the dienes. Various free-radical resonance forms can be written in the case of styrene. The initiator molecule first decomposes into radical species, which add to the carbon–carbon double bond. One should note that there is a marked preference for so-called head-to-tail addition in most vinyl radical polymerizations. The head-to-tail addition is favored both for the resonance reasons indicated and also because of steric effects. Head-to-head placement in the case of styrene would produce two phenyl units adjacent to one another, which would be a very unlikely situation. For these reasons, head-to-tail addition is the predominant mode of chain configuration for vinyl polymerizations. The exceptions to this generality usually involve monomers that have very small pendant groups, which cannot contribute much resonance stabilization to the growing radical. The most important class of such monomers probably comprises the fluorine-containing monomers, since fluorine is small and does not have much tendency to resonance-stabilize a growing chain end. There are a number of systems of this type

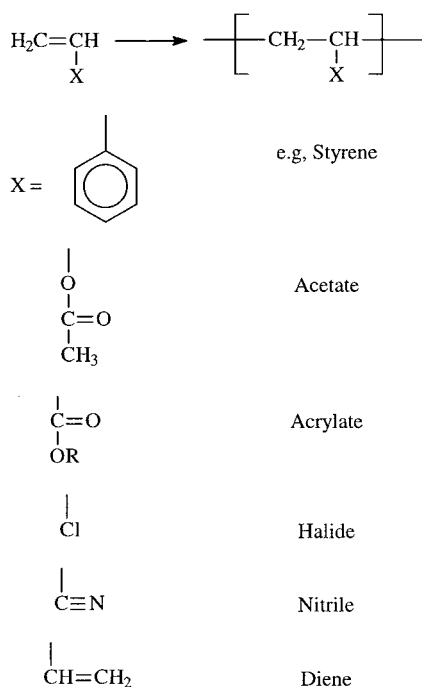
TABLE IV Peroxide Initiators^a

Structure	Polymerization temperature range (°C)
$\text{KO}-\overset{\text{O}}{\parallel}{\text{S}}-\text{O}-\text{O}-\overset{\text{O}}{\parallel}{\text{S}}-\text{OK}$	30–80
$\text{H}_5\text{C}_6-\overset{\text{O}}{\parallel}{\text{C}}-\text{O}-\text{O}-\overset{\text{O}}{\parallel}{\text{C}}-\text{C}_6\text{H}_5$	40–100
$\begin{array}{c} \text{CH}_3 \\ \\ \text{H}_5\text{C}_6-\text{C}-\text{O}-\text{O}-\text{H} \\ \\ \text{CH}_3 \end{array}$	50–120
$\begin{array}{c} \text{CH}_3 \quad \text{CH}_3 \\ \quad \\ \text{H}_3\text{C}-\text{C}-\text{O}-\text{O}-\text{C}-\text{CH}_3 \\ \quad \\ \text{CH}_3 \quad \text{CH}_3 \end{array}$	80–150

^a Groups bonded to the peroxide structure primarily affect thermal stability and/or solubility.



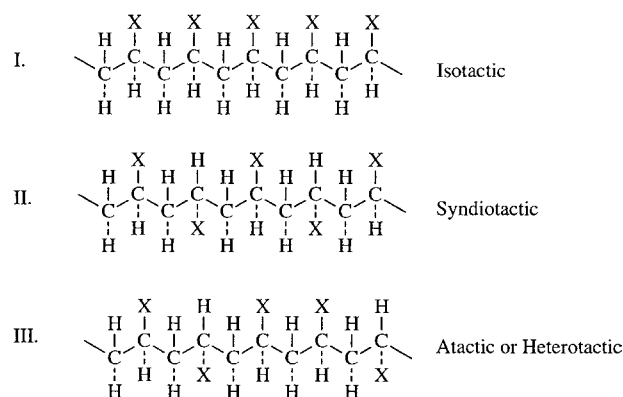
SCHEME 12 Generation of some typical free radicals.



SCHEME 13 Free radical polymerization; X provides resonance stabilization to the growing radical.

that do have small but significant quantities of head-to-head and tail-to-tail addition steps. This has most often been demonstrated through the use of ^{19}F NMR spectroscopy. Even in this case, the abnormal addition is relative minor and is of the order of $\sim 10\%$ of the overall chain structure.

The tacticity or stereochemistry of vinyl chains is a very important parameter. Following the definitions of Natta (Scheme 14) it is common to depict chains as isotactic, syndiotactic, or atactic. The isotactic chains are capable of undergoing crystallization and, indeed, isotactic polypropylene made via coordination polymerization is a polymer of major commercial importance. Further comments on this process will be made later. Syndiotactic polymers have placements of the R group on opposite sides of an extended chain. It is also quite popular to characterize the stereostructure by NMR in terms of meso or racemic types of placements, diads, triads, pentads, and so on. In general, one should not that free-radical polymerization tends to produce mostly atactic or heterotactic placements. There is some tendency to produce moderately high syndiotactic structures in certain polar monomers, such as vinyl chloride or acrylonitrile. Moreover, the syndiotactic structure is favored as one reduces the polymerization temperature.



SCHEME 14 Tacticity. Free-radical polymerization is most commonly atactic. Low temperature favors syndiotactic placement. Coordination polymerization produces stereoregular chains.

1. Thermodynamics of Polymerization

The possibility of polymerizing monomers such as α -olefins and their derivatives and various other vinyl monomers depends on whether the free energy of such a process will be favorable. The free energy in turn is dependent on the values of the enthalpy or heat of polymerization. Table V lists values for the ΔH of polymerization for a number of vinyl monomers. In general the transformation of an alkene to a polymeric species is quite exothermic. The exact value is dependent on the detailed structure of the monomer. One important correlation between monomer structure and heat of polymerization is related to whether the tertiary carbon contains a hydrogen or a methyl group. For example, the value for α -methylstyrene is approximately one-half that of styrene. This structural correlation can be seen more clearly in Table VI. As already mentioned, the

heat of polymerization will help determine whether the polymerization process can proceed. Another useful term in connection with polymerization thermodynamics is the so-called ceiling temperature. The ceiling temperature can be defined either by the equation in Table VI or by the idea that at the ceiling temperature the propagation rate will be essentially equivalent to the depropagation rate. The ceiling temperature phenomenon is not of particular significance for monomers like ethylene, propylene, or even styrene where the ceiling temperature is far removed from normal polymerization temperatures; however, it becomes quite significant for monomers such as methyl methacrylate and extremely important for systems such as α -methylstyrene or acetaldehyde. Methyl methacrylate

TABLE V Heats of Polymerization^a

Monomer	$-\Delta H_p$ (kcal/mole)
Ethylene	22.7
Propylene	20.5
Isobutene	12.3
1,3-Butadiene	17.4
Isoprene	17.8
Styrene	16.7
α -Methylstyrene	8.4
Vinyl chloride	22.9
Vinylidene chloride	18.0
Tetrafluoroethylene	37.2
Methyl acrylate	18.8
Methyl methacrylate	13.5
Vinyl acetate	21.0

^a ΔH_p refers to the conversion of liquid monomer to amorphous or slightly crystalline polymer.

TABLE VI Heats of Polymerization and Ceiling Temperatures^a

Monomer	Heat of polymerization ΔH (kcal/mole)	Ceiling temperature T_c (bulk) ($^{\circ}\text{C}$)
Styrene	16	235
α -Methylstyrene	7	61
Methyl acrylate	20	—
Methyl methacrylate	13	164
Formaldehyde	13	-26
Acetaldehyde	0	-11
Acetone	6	—
Vinyl chloride	22	—
Vinylidene chloride	14	—
Ethylene	26	407
Propylene	21	300
Isobutene	17	50

$T_c = \Delta H / (\Delta S + R \ln[M_e])$

$\text{---} R_{n*} + M \xrightleftharpoons[k_D]{k_p} (R_n + 1)$

At T_c , propagation and depropagation are equally probable.

can be easily polymerized to 100% conversion. However, the ceiling temperature concept also has ramifications for polymer degradation. For example, if polymethyl methacrylate (PMMA) is exposed to free radicals at high temperatures, one can basically unzip the polymer chain and regenerate nearly quantitatively the monomeric species. The monomer α -methylstyrene has been widely studied, and it is well known that it is very difficult to polymerize this structure to high molecular weight unless one uses rather low temperatures. It is possible to use an anionic mechanism at -78°C and completely polymerize α -methylstyrene.

2. Kinetics of Free-Radical Polymerization

The propagation or the growth step involves the rapid addition of additional monomer to the initiated species. If this grows with a rate constant k_p , where R now represents a long chain, one can define the propagation reaction by the equation shown. An important assumption here is that all the chains have the same reactivity. Another reasonable assumption is that the initiation step involves the reaction of only one monomer molecule and the propagation involves the addition of many monomer molecules. The rate of the polymerization can be designated R_p and may be shown to be basically equivalent to the rate of propagation. The rate of propagation or polymerization, then, will be given by the product of the rate constant k_p , the monomer concentration, and the concentration of the growing species. Free radicals involve unpaired electrons, and hence their lifetime is rather short (e.g., a fraction of a second). Therefore, the growth step is basically at some stage quickly terminated, usually by one of the two schemes shown in Scheme 16. Some typical rate constants are summarized in Table VII. Moreover, it is easy to see that the termination rate constant is much faster than that of either of the other two steps. This allows one to make a steady-state assumption in which one can set the rate of initiation equal to the rate of termination. An advantage of doing this is that it becomes possible to solve the equation

TABLE VII Typical Rate Constants

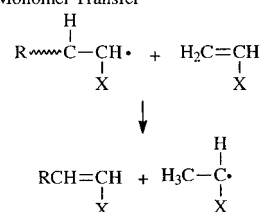
k_1	Low rate constant
k_p	$\cong 10^2$ – 10^3 liters/mole sec
k_T	$\cong 10^7$ – 10^9 liters/mole sec
Hence, a steady state of free radicals, e.g.,	
$R_i = R_T$	
$2k_d[I] = 2k_t[M\bullet]^2$	
$[M] = \left(\frac{k_d}{k_T}[I]\right)^{1/2}$	(difficult to measure)
$R_p = k_p \left(\frac{k_d}{k_T}[I]\right)^{1/2} [M]$	

shown in Table VII in terms of the radical concentration. On substituting this value into the rate expression, one obtains a final rate expression that is quite useful. Basically, it states that the rate of polymerization will depend on several constants, but that it will also be proportional to the first power of the monomer concentration and to the square root of the initiator concentration. Thus, as one doubles the initiator concentration, the expected rate should increase only by a factor of ~ 1.4 . If one plots the rate of polymerization versus the log of the initiator concentration for a variety of monomers and initiators such as methyl methacrylate and AIBN or styrene and benzyl peroxide, for example, one observes slopes equal to $1/2$. An additional term in the rate of expression is f , the fraction efficiency of initiation: For 100% efficiency, f has a value of 1.0. This is never achieved, although in some cases, particularly with some azo initiators, many people have reported values as high as 0.9. More recent work has tended to indicate that this value may be rather high.

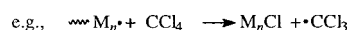
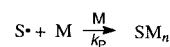
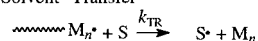
A fourth process in polymerization kinetics is called the chain transfer reaction. This reaction is very important in a variety of cases, as outlined in Scheme 15. Here, we depict a growing chain interacting with a small molecule XY in such a way that a portion of the small molecule can terminate the active radical chain and at the same time produce a new radical Y. Basically, this step regulates the molecular weight. It does not necessarily decrease the rate of polymerization if one assumes that the new radical Y will again reinitiate more monomer and



(a) Monomer Transfer



(b) "Solvent" Transfer



(lowers molecular weight)

(c) Initiator Transfer

(d) Transfer to Polymer

(e) Transfer to Modifier

SCHEME 15 Chain transfer.

the rate of polymerization can proceed basically as before.

There are many types of chain transfer steps, such as transfer to monomer, to a solvent, to an initiator, to a polymer, or even to a modifier. In all cases, the molecular weight will be decreased. The quantitative decrease will be dependent on the reactivity of the growing macroradical with the small-molecule species. The extent to which this happens is very dependent on the structure of the agent in question and can be roughly related to its reactivity with a small-molecule radical species. Some typical data are shown in Table VIII. An aromatic molecule, such as benzene, would not be expected to interact particularly effectively with radicals and, indeed, the chain transfer constant here is rather small. On the other hand, molecules such as carbon tetrachloride or certainly mercaptans have enormous activity with macroradicals and are very efficient chain transfer agents. One can assess the effectiveness of a chain transfer agent by conducting polymerizations at various ratios of the chain transfer agent to the monomer and plotting the reciprocal of the number-average molecu-

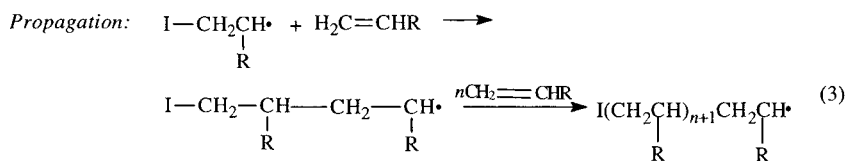
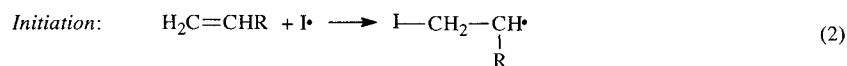
TABLE VIII Chain Transfer Constants of Various Agents to Styrene at 333 K

Agent	$10^4 C_S$
Benzene	0.023
<i>n</i> -Heptane	0.42
<i>sec</i> -Butylbenzene	6.22
<i>m</i> -Cresol	11.0
CCl ₄	90
CBr ₄	22,000
<i>n</i> -Butylmercaptan	210,000

lar weight or the number-average degree of polymerization versus this ratio.

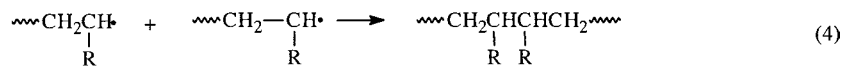
An overview of the kinetics of free-radical polymerizations that takes into account chain transfer is provided in Scheme 16. Chain transfer to the polymer chain produces a particular type of structure, namely, a branched macromolecule.

To this point, we have not discussed any detailed aspect of the polymerization process itself. There are essentially

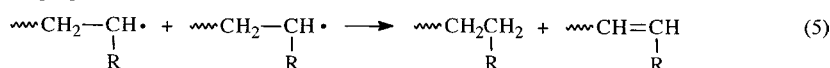


Termination (by radical coupling, disproportionation, or chain transfer)

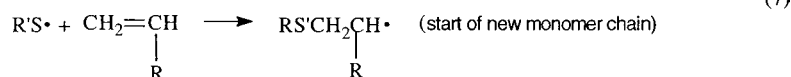
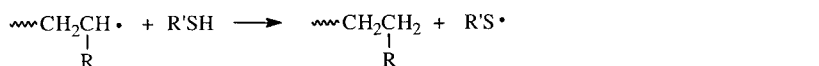
Radical Coupling:



Disproportionation of Two Radicals:



Chain Transfer:



SCHEME 16 Overview of free-radical kinetics.

TABLE IX Comparison of Homogeneous Polymerization Processes

Type	Advantages	Disadvantages
Bulk (batch type)	Low impurity level Casting possible	Thermal control difficult
Bulk (continuous)	Improved thermal control	Isolation difficult Requires devolatilization
Solution	Improved thermal control	Difficult to remove solvent Solvent recovery costly Chain Transfer may limit molecular weight

four important processes. First, one can have a bulk reaction in which basically only the monomer and possibly the initiator are used. Alternatively, a solution reaction process may be used which has a monomer, initiator, and a solvent present. Bulk and solution reactions are sometimes referred to as homogeneous processes. The other two processes are often termed heterogeneous processes, and they are known as suspension and emulsion reactions. Several advantages and disadvantages of the various polymerization processes are given in [Tables IX](#) and [X](#).

The bulk process has the advantage of allowing for a relatively low impurity level. Furthermore, it is possible under some conditions to perform the polymerizations discussed earlier. For example, some gasoline station signs are produced from cast polymethylmethacrylate (PMMA). One can imagine, however, that it would be very difficult, if not impossible, to control the temperature of such a reaction, recalling the heat of polymerization discussed earlier. Moreover, the viscosity becomes enormous rather quickly, and one has to find a way to dissipate the heat of polymerization. The advantage of continuous processes is that in a series of reactions, for example, it may be possible to achieve greater control of the temperature

than in one bulk batch-type process. However, one probably would still have to isolate the polymer by a relatively high vacuum devolatilization step. This could be done and is done commercially, but nevertheless it might be considered a disadvantage. In addition, a series of reactors requires one to design the engineering so as to be able to recycle monomer back to the first reaction for additional polymerization.

Conducting a solution process with an inert solvent can solve several of these problems. This enables one to improve the thermal control and decrease the viscosity, but it is still difficult to remove quantitatively the solvent at the end of this process. Moreover, the solvent may serve as a chain transfer agent, which will limit the molecular weight to lower values than may be desired. In the suspension processes, an agent such as polyvinyl alcohol or perhaps an inorganic oxide, such as zinc oxide, stabilizes the growing polymer particles and prevents them from coalescing together. The generation of particles then essentially produces a relatively low viscosity particle system, which is desirable. If one converts all the monomer to polymer, then isolation becomes a fairly simple process of filtering off the finished polymer particles from the aqueous media. Many important “glassy” polymers are made via suspension processes; polystyrene and polyvinyl chloride are made in this manner. On the negative side, it is necessary to agitate very carefully, especially early in the reaction. Otherwise, the growing polymer particles might aggregate rather than stay in discrete small particles. At the end of the reaction, one has to accept the fact that the polymer will contain a small residual amount of the suspending agent.

In emulsion reactions, as in the suspension case, water is the heat transfer medium and hence it is easy to obtain good thermal control. Very small particle sizes of the order of a few hundred to a few thousand angstroms can be obtained. In emulsion polymerization, surfactants,

TABLE X Comparison of Heterogeneous Polymerization Processes

Type	Advantages	Disadvantages
Suspension	Low viscosity	Highly sensitive to agitation rate
	Simple polymer isolation	Particle size difficult to control
	Easy thermal control	Possible contamination by suspending agent
	May be of direct usable particle size	Washing, drying, and compaction necessary
Emulsion	Low viscosity	Emulsifier, surfactants, and coagulants must be removed
	Good thermal control	High residual impurity level may degrade certain polymer properties
	Latex may be directly usable	High cost
	100% conversion may be achieved	Washing, drying, and compacting may be necessary
	High MW possible at high rates	
	Small particle size product can be obtained	
	Operable with soft or tacky polymers	

TABLE XI Emulsion Polymerization Compared with Other Radical Techniques

Advantages	Disadvantages
Faster rates	Recovery of solid polymer more difficult
High molecular weights	Difficult to free completely from emulsifier
Good heat transfer	
May be directly usable (latex)	
500–5000 Å	

which are anionic or nonionic (or both), are used at the level of several percent. If they are not removed from the final product, they will contribute to the degradation of at least certain polymer properties. In particular, optical properties and electrical properties can be influenced negatively by residual of a surfactant. From Table XI we see that, compared with other processes, emulsion polymerizations have the distinct advantage of providing a fast rate at the same time as allowing for high molecular weight. Good heat transfer is achieved because of the use of water as the heat transfer medium. They may also be directly useful. For example, one can imagine deriving a paint by taking an emulsion polymer and simply adding pigments such as TiO₂. The kinetics of emulsion polymerization is quite different from that of the other types of polymerization already described. Bulk, solution and suspension reactions are often referred to as following homogeneous free-radical chain kinetics. It may be surprising that suspension processes are considered to follow homogeneous reactions, but in a sense they are like a microbulk reaction. Emulsion processes are quite complex, and we shall now discuss some of the essential features of these systems.

In an emulsion polymerization, there are typically several components: the monomer, water, the emulsifier or the surface-active agent, a water-soluble initiator, and, optionally, a chain transfer agent. The rate will suddenly begin to increase at a fairly rapid rate at some critical micelle concentration (CMC). It is considered that at this CMC, about 50–100 soap molecules will aggregate into tiny micelles. The small soap micelles have a very large surface area. An important result of this is that they will capture nearly all of the radicals generated in the aqueous phase. It has been calculated that there are $\sim 10^{18}$ micelles per cubic centimeter versus only $\sim 10^{11}$ monomer droplets per cubic centimeter. Therefore, most of the radicals and some of the monomer become part of the micelles. It is believed that the polymerization begins in the soap micelles. As the monomer polymerizes, new monomer may diffuse in from the aqueous phase. Essentially, the macromonomer droplets can saturate the aqueous phase,

and one may observe pseudo-zeroth-order kinetics for such polymerizations. The radical micelle then initiates the polymerization, which essentially continues until all of the local monomer in the micelle is consumed or until a second radical diffuses in to terminate the growing chain. The termination rate is low since a second radical would also have to pass through the interfacial boundary. On the average, then, the micelle is believed to contain only one growing chain for most of its lifetime. The rate of polymerization is often approximated by the expression

$$R_p = k_p[M]N/2,$$

where N is the number of colloiddally dispersed particles. The rate, then, is proportional to the number of colloiddally dispersed particles, which means that, if one increases the surfactant concentration or the soap concentration, it is possible to increase the number of particles and hence also increase the polymerization rate. This is a very fundamental way in which one can *decouple* the effects of initiator concentration on molecular weight and polymerization rate. Thus, the rate can be increased more or less independently of the concentration of the initiator. Emulsion processes are the only free-radical chain polymerizations that present this opportunity. Therefore, they are somewhat unique in producing very high molecular weight polymers at very fast rates. It is not difficult, for example, to make one million-molecular weight polystyrene or polybutadiene.

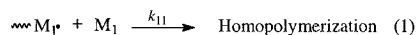
As the polymerization proceeds, the locus of the reaction is believed to change from the micelles to a monomer-swollen polymer particle at about 10–20% conversion. The swollen polymer particle is stabilized at its interface by residual surfactant. Therefore, when all of the monomer is consumed, the polymer dispersion, or latex, as it is frequently termed, can be quite stable, at least for a small range of temperatures and pH. Quantitative studies of the emulsion kinetics are available in the literature and are discussed in greater depth in the references listed in the Bibliography.

B. Copolymers

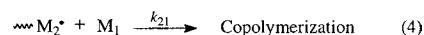
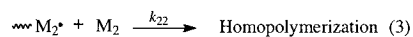
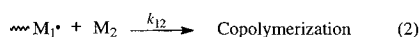
In addition to the synthesis of homopolymers, in which there is only one chemical structure in the repeating unit, it is possible to prepare copolymers or even terpolymers by chain reaction processes. There are various types of copolymers, as indicated earlier in Table I. Among the most common are the statistical copolymers, in which two monomers are randomly distributed throughout the chain molecule. A second type is a perfectly alternating copolymer. Two additional types are block and graft copolymers. We will not discuss block and graft

Critical Assumption: Steady State

e.g., $R_I = R_t$



e.g., Terminal radical on chain derived from monomer M_1



SCHEME 17 "Random free-radical chain polymerization.

copolymers in this article, but they are discussed in some detail in the references. Very briefly, these copolymers contain very long sequences joined either from the end or from the sides of the chain. We shall limit our discussion here mostly to random copolymers and only very briefly touch on alternating copolymers. The simplest reaction sequence for random free-radical chain copolymerization is given in Scheme 17. Here, four possible reactions may lead to either a copolymer unit or a homopolymer unit being formed.

In each case cross-initiation of the other monomer by a different macroradical chain end will produce elements of a copolymer. Copolymers of this type are usually of interest because they can display a number of desirable averaged properties. One usually attempts to relate the rate of depletion of the two monomers with their rate of entry into the copolymer chain. It is possible to derive a copolymer composition that yields the molar ratio of the two units that are formed in the copolymer to the reaction copolymerization kinetics. By assuming a steady state and by making further manipulations it is possible to derive a so-called copolymer equation that relates the mole ratio of the two units that are found in the copolymer to the respective monomer molar charge ratios through the use of reactivity ratios or coefficients.

The reactivity ratios are basically the ratio of the homopropagation rate constants to the copolymerization rate constants for each of the monomer species under investigation. The values of the reactivity ratios (r_1 and r_2) have considerable significance. As indicated in Table XII, r values of between 0 and 1 imply that two monomers will probably be copolymerized in a fairly random fashion. If

TABLE XII Reactivity Ratios

r values of $0 \leq 1$	Imply monomers will copolymerize
$r_1 > 1$	Prefers to homopropagate
$r_1 \cong 0$	Prefers to alternate
$r_1 \cong r_2 \cong 1$	Perfectly random
$(r_1)(r_2) \cong 1$	Termed "ideal" system, by analogy
$r_1 = 1/r_2$	With vapor-liquid equilibria

either of the values is greater than 1, that means that the growing chain end will homopropagate rather than cross-initiate the other monomer. On the other hand, if the reactivity ratio is very small, for example, if it approaches 0, this implies that the growing chain end will cross-initiate the other monomer rather than add to its own chain end. In the best situation the reactivity ratios are approximately equal and their product is nearly 1. Such a system is termed a perfectly random copolymer.

The copolymerization equation can be transformed into mole fractions, which are frequently more useful. If one does this, it is possible to derive an expression that generates r values by a graphical procedure. Thus, to determine whether two monomers will copolymerize, it is necessary to perform a series of experiments in which one varies the monomer feed ratios and, at low conversions, assesses the concentration of the two species in the formed copolymer; there are basically three possibilities (Table XIII). If one has similar reactivity ratios or if one limits the polymerization to a low conversion, it is possible to make a rather uniform random copolymer.

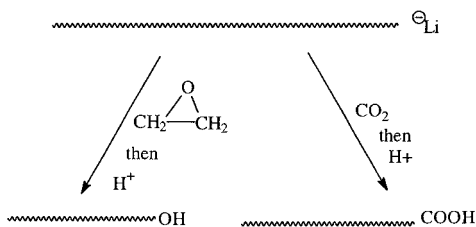
By this we mean that the distribution of the monomer units may be considered to be relatively random. Nonuniform copolymers of this type are usually undesirable since one may exceed the lifetime of the growing radical and thus generate homopolymers. This occurs if one has widely different reactivity ratios and if the reaction is carried to high conversion. Clearly, as the faster reacting monomer becomes consumed, it becomes apparent that the composition of the chain will be heterogeneous. Indeed, in later stages of such a reaction, homopolymer is derived from the slower reacting monomer in the system. This is to be avoided because the homopolymer will tend to be incompatible with the copolymer and the resulting material characteristics will usually be rather poor. If the reactivity ratios do not differ by too great a margin, it may be possible slowly to add the faster reacting monomer to the system and hence to maintain a more or less constant comonomer composition. By this method, it is possible to produce a relatively uniform copolymer, even though the reactivity ratios may be somewhat different.

TABLE XIII Three Possibilities of Formed Copolymers

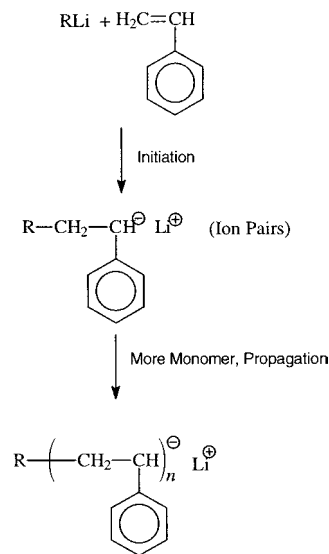
1. Uniform copolymer	Same reactivity ratios, or Low conversion, or Constant comonomer composition
2. Nonuniform copolymer	Different reactivity ratios carried to high conversion
3. Alternating copolymer	Reactive radical accepting comonomer that will not homopolymerize Charge transfer complex

C. Ionic Polymerization

In this section, we shall outline some of the characteristics of anionic polymerization. One important feature is that, under certain conditions, there may be no termination step. This is possible with organolithium initiators, hydrocarbon monomers like styrene or butadiene, and hydrocarbon solvents like cyclohexane or benzene. The reason for this is no doubt related to the enhanced stability of the carbanion relative to that of other chain intermediates such as radicals or even carbonium ions. The anionic chain end can be considered to have sp^3 -type bonding as opposed to the sp^2 -type bonding associated with radicals or carbonium ions. This lack of a termination step (in the strict absence of water, oxygen, etc.) then means that one is dealing simply with initiation and propagation steps. In turn, this enables one to predict molecular weight on the basis of the ratio of the monomer concentration to the initiator concentration. Thus, each initiator may start one chain. Another feature is that one can synthesize polymers that have a very narrow molecular weight distribution and that tend to follow a Poisson distribution, as opposed to the much broader Gaussian-type distributions. In addition, it is possible to produce a relatively high 1,4 structure in polybutadiene and polyisoprene. Not only can one have *cis*- and *trans*-1,4 structure, but one can also have isotactic or syndiotactic placement in the 1,2 geometric isomer. The lithium systems were discovered in about 1955 by workers at Firestone to produce a very high 1,4 structure in both polybutadiene and polyisoprene. Moreover, the polyisoprene could actually be produced in a relatively high *cis*-1,4 configuration, as high as 93% in some cases. At about the same time, M. Szwarc and coworkers found that, under certain conditions, polymerizations utilizing electron transfer initiation could also be termination-free. This was quickly developed commercially by the production of polybutadiene and certain polybutadiene–styrene copolymers by the Phillips Petroleum Company. An additional feature of anionic polymerization is the ability to produce functional end groups. For example, reacting a macromolecular carbanion with ethylene oxide can produce a hydroxyl group, and by treating the same carbanion with carbon dioxide, it is possible to generate a carboxylate or, after neutralization, a carboxyl group (Scheme 18). The



SCHEME 18 Functional termination.

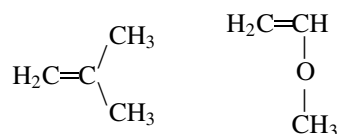


SCHEME 19 Initiation via alkyl lithium compounds. The alkyl lithium initiator and the growing polymer chain are homogeneous and hydrocarbon soluble. The reaction proceeds via nucleophilic addition to the unsaturated double bond.

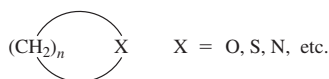
two major types of anionic polymerization mechanisms that have been studied are achieved by electron transfer reagents and by organolithium compounds (Scheme 19).

The nature of the chain end anion, as we have already seen, is greatly affected by the nature of the solvent and the counterion. Therefore, one can speak of tight ion pairs, loose ion pairs, and even free ions, which may contribute to the copolymerization. Therefore, caution should be used when applying the classical copolymerization criteria to ionic polymerization. However, some useful copolymerization data have been generated by the use of the methods described in Section III.A. However, in many cases one particular anion may be incapable of initiating a second unit. For example, methyl methacrylate enolate anion is incapable of reinitiating a hydrocarbon monomer like styrene. Therefore, the anionic statistical copolymerization of monomers like styrene and methyl methacrylate becomes a rather moot point. The last important feature of anionic polymerization to be mentioned is that it offers a very clean synthesis for block copolymers.

Vinyl or 1-alkene monomers bearing suitable electron-releasing groups, such as the alkyl groups or ether bond in isobutene or vinyl methyl ether, respectively, will polymerize via a carbocationic mechanism:



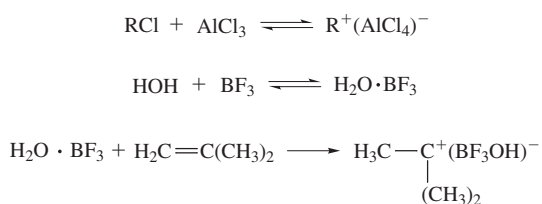
The electron enrichment may occur by either inductive or resonance routes. Moreover, numerous heteroatom-containing cyclic monomers, such as



can also be polymerized via positively charged species (e.g., oxonium ions).

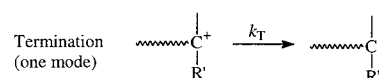
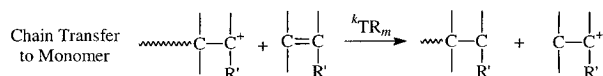
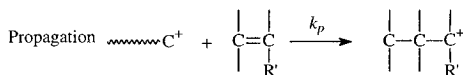
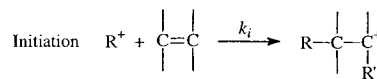
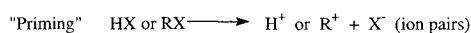
The reactive growing chain end will have much sp^2 -type character in the case of carbocationic polymerizations. Thus, it should not be surprising that these chain reactions have much shorter lifetimes than the previously discussed anionic systems. The carbocationic chain end has traditionally been referred to as a carbonium ion. However, many workers in the polymerization field now prefer the term *carbenium ion* as a better choice for a trigonal, trivalent sp^2 -hybridized species.

Carbocationic polymerizations of 1-alkenes can be initiated by a variety of homogeneous or heterogeneous Lewis acids,



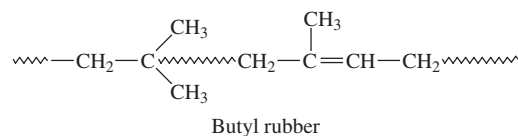
such as BF_3 , TiCl_4 , AlCl_3 , and $\text{Al}(\text{C}_2\text{H}_5)_2\text{Cl}$. The process is somewhat analogous to reactions such as alkylations that are very familiar to organic chemists. The reactions may require that either a proton donor (e.g., water) or cation donor (e.g., a tertiary halide) be present. Thus, isobutene is inert in the presence of BF_3 if the system is rigorously dry. Reaction will begin immediately if catalytic quantities of, say *tert*-butyl halide or water are added. The initiation mechanism may be quite complex. However, J. P. Kennedy and colleagues demonstrated that the chain end (“HEAD” group) formed in the presence of cation donors is, in fact, derived from the cation. Thus, they consider the proton or cation source to be the initiator and the Lewis acid to serve as the coinitiator.

An overview of the carbocationic polymerization is given in Scheme 20. One major difficulty with many cationic polymerizations is that many other chain transfer or chain-breaking reactions can effectively compete with the chain growth step. Carbonium (carbenium) ions can undergo many reactions such as alkylation, isomerization, and so on. In a carbocationic polymerization these reactions have the net result of lowering the molecular weight, often to lower than desired values. Fortunately, one may “freeze out” many of these events by lowering the polymerization temperature. Thus, poly(isobutene) or



SCHEME 20 Mechanism of carbenium ion polymerization. Often low temperature is required to achieve high molecular weights. Controlled end groups can be provided.

butyl rubber (a copolymer with a small amount of isoprene) is probably produced commercially at -40°C or lower:



Carbocationic polymerizations may also be used to polymerize other alkenes such as propylene or styrene to moderately high molecular weight. However, these polymerizations are not stereoregular and the commercial utility has been quite limited.

The advent of Ziegler–Natta catalysis in the mid-1950s amplified and greatly expanded the idea that ionic polymerizations can be stereochemically controlled via coordination of the growing chain end with its monomer and counterion. The industrial importance of these reactions is apparent from the fact that coordination polymerization is used to produce linear (high-density) polyethylene (HDPE), linear low-density polyethylene (LLDPE), isotactic polypropylene, isotactic poly(1-butene), various ethylene–propylene co- and terpolymers, *cis*-1,4-polybutadiene, and *cis*-1,4-polyisoprene. The volume of these important rubbers and plastics probably exceeds that of polymeric materials produced by all other chain (or step-growth) processes. K. Ziegler and G. Natta received the Nobel Prize in 1963 for their contributions.

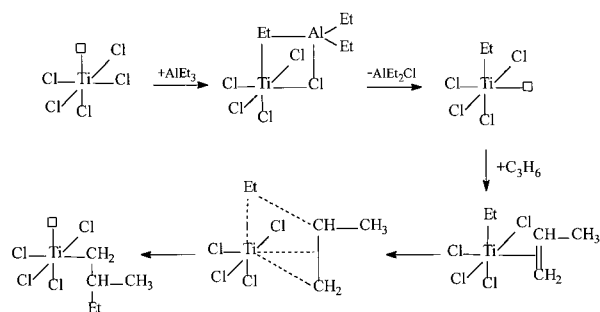
The components of a Ziegler–Natta catalyst are listed in Table XIV. The utilization of these usually heterogeneous catalysis is well developed. However, because of the enormous complexities, mechanistic understanding has been relatively slow to evolve. One should also note that the catalysts may themselves also be deposited on supports such

TABLE XIV Typical Ziegler–Natta Catalyst Components

Transition metal halide [Me(I)]
TiX ₄ , TiX ₃ , VX ₄ , VX ₃ , VOX ₃
Co, Ni complexes
Organometallic compound [Me(II)]
AlR ₃ , AlR ₂ X, ZnR ₂ , LiR, etc.
Generally agreed
Mi(II) alkylates, reduces Me(I)
Alkylated Me(I) responsible for chain growth
AlEt ₃ + TiCl ₄ → TiCl ₃ Et + AlEt ₂ Cl
TiCl ₃ Et → TiCl ₃ + Et
AlEt ₃ + TiCl ₃ → TiCl ₂ R + AlEt ₂ Cl
Cl ₂ TiR + x(monomer) → Cl ₂ Ti(monomer) _x R

as silica or alumina. The most generally accepted mechanism is shown in [Scheme 21](#). Although free radicals can be produced, they are not involved in these types of polymerizations. The olefin is believed to coordinate first via π bonding with vacant *d* orbitals in the transition metal complex. The availability and stability of these coordination sites can be influenced significantly by the metal alkyl. Nevertheless, it is usually now considered to be a monometallic mechanism. The coordination species must undergo a *cis* rearrangement both to yield the stereoregular placement and to produce a new vacancy in the transition metal structure, which may coordinate with the next monomer unit (the propagation step).

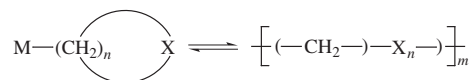
Most of the industrial interest has centered on 1-alkenes, dienes, or ethylene polymerizations. Many other monomers, such as methyl methacrylate and vinyl alkyl ethers, have also been studied. Heteroatom-containing monomers have further sites for coordination and hence can yield stereospecific polymerizations under even



SCHEME 21 Evolution of ideas on the mechanism of olefin coordination polymerization. The essential steps are as follows. An octahedral titanium complex has a chlorine vacancy. Alkylation occurs, giving an alkylated titanium species that still has a chlorine vacancy. Monomer is adsorbed on the vacancy and is π -bonded to the titanium atom. A “cis migration” occurs, leading to a new titanium-carbon bond.

“homogeneous” conditions. This enormously important mechanism remains an active area of research.

The process of transforming a heteroatom-containing ring to a linear chain is often described as a ring-opening polymerization:



This process almost always involves anionic, cationic, or coordination initiation (catalysis). Only in very special situations have free-radical initiators been successful.

Some major types of cyclic monomers that undergo ring-opening reactions are shown in [Table XV](#). The thermodynamic feasibility of such a process for cyclic ethers as a function of ring size is shown in [Table XVI](#). For small rings such as ethylene oxide, the reaction is highly exothermic, and polymerization proceeds with either anionic or cationic initiators. Dioxane has not been polymerized. Larger cyclic ethers such as tetrahydrofuran are initiated only by oxonium salts such as (C₂H₅)₃O⁺(BF₄)⁻. Presumably, the oxonium salt initiates by coordination with the electron pair of the cyclic ether. Propagation then

TABLE XV Some Important Examples of Ring-Opening Polymerization

Cyclic monomer	Ring-opening reaction
Ethers	
Acetals	
Esters (lactones)	
Amides (lactams)	
Siloxanes	
Phosphazines	

TABLE XVI Heats and Entropies of Polymerization for Cyclic Ethers

Monomer	Ring size	$-\Delta H$ (kcal/mole)	$-\Delta S$ (cal/k mole)
Ethylene oxide	3	22.6	—
Oxacyclobutane	4	16.1	—
3,3-Bis(chloromethyl)-oxacyclobutane	4	20.2	19.9
1,3-Dioxolane	5	6.2	—
Tetrahydrofuran	5	5.3	11.5
Tetrahydropyran	6	0.4	—
<i>m</i> -Dioxane	6	0.0	—
1,3-Dioxepane	7	3.6	—

proceeds by nucleophilic attachment of monomer at the carbon next to the oxonium ion. Other counterions, such as $(PF_6)^-$ and $(SbCl_6)^-$, are also utilized. In some systems, there are essentially “living” or nonterminated oxonium ions, which are somewhat analogous to the “living” carbanionic polymerizations discussed earlier. Many ring-opening polymerizations display ring-chain equilibrium, and hence one may have to separate cyclic monomer from high-molecular weight linear chains at the end of the polymerization.

D. Controlled and Living Radical Polymerization

Controlled polymerization routes permit the synthesis of well-defined macromolecules with controlled chemical composition, predictable molecular weight, and narrow molecular weight distribution. The ability to control polymer architecture is essential in advanced technological applications where well-defined macromolecular architectures are required. Control of chain-growth polymer architecture has been traditionally achieved using living anionic, cationic, or group-transfer polymerization procedures. Synthetic methodologies for controlled polymerization have been expanded with recent developments in stable free-radical polymerization (SFRP), atom transfer radical polymerization (ATRP), and the radical addition and fragmentation technique (RAFT).

The basic feature of controlled polymerization is the absence of transfer and termination processes in chain growth reactions as discussed earlier. Szwarc first defined such systems as “living polymerizations” in 1956 based upon his work on anionic polymerizations. Several decades later, the idea of living polymerizations was extended to free-radical systems. The use of initiator-transfer-agent-terminators, or iniferters, to reduce irreversible chain termination in free-radical polymerization processes is a viable approach. The reversible radical

termination steps help to control irreversible chain termination and result in polymerization behavior with linear molecular weight increase with time similar to living anionic polymerizations. Based on the earlier work of Rizzardo *et al.* in nitroxide-mediated stable free-radical polymerization of methyl acrylate, Georges *et al.* first reported the preparation of polystyrene with low polydispersity using bulk free-radical polymerization of styrene initiated by a conventional free-radical initiator, benzoyl peroxide (BPO), in the presence of the stable nitroxide free radical, 2,2,6,6-tetramethyl-1-piperidinyloxy (TEMPO) at 125°C. The SFRP process involves a desirable reversible equilibrium between nitroxide-capped polymer chains and uncapped polymer radicals. The uncapped polymer radicals are then able to chain extend via styrene monomer addition. The success of this method arises from the unique feature that the nitroxide radicals will react with carbon radicals at near-diffusion-controlled rates, but will not react with other oxygen-centered radicals or initiate additional polymer chains.

One drawback of the initial SFRP technique is that the polymerization requires long reaction times to achieve high conversion. The addition of camphorsulfonic acid dramatically increases the rate of styrene polymerization and high yields could be achieved with reaction times less than 6 hr. Addition of acylating agents such as acetic anhydride to styrene SFRP dramatically reduces reaction time. The development of unimolecular initiators for SFRP is a viable method to control molecular weight. The classic initiating system is bimolecular and consists of benzoyl peroxide as the initiating radical together with TEMPO as the mediating radical. Disadvantages of the bimolecular initiating system include lack of control over structural features such as molecular weight, chain ends, and architecture. A unimolecular initiator can be synthesized from benzoyl peroxide, TEMPO, and styrene. Using this unimolecular initiator as well as derivatives, the synthesis of narrow-polydispersity materials with controlled molecular weights, chain ends, and chain architectures is feasible.

A very successful approach to the controlled nitroxide-mediated polymerization of acrylates uses β -phosphonate-substituted nitroxide with 2,2'-azobisisobutyronitrile (AIBN) as the initiating radical source. Two major structural features of the β -phosphonate-substituted nitroxide distinguish it from previously studied nitroxides. First, it is acyclic; second, it contains a α -hydrogen to the nitroxide functionality. Both of these features are expected to decrease the stability of nitroxide and increase decomposition. It is anticipated that the limitation of polymerization of acrylates and other monomer families is the control of excess free nitroxide that accumulates during polymerization. Therefore, the decreased stability

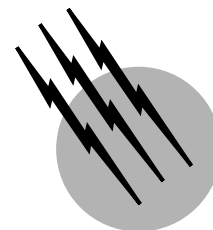
of the acyclic β -phosphonate-substituted nitroxide bearing a α -hydrogen leads to decreased accumulation of excess nitroxide during reaction and results in improved control over the polymerization of acrylates. Several acyclic α -hydrogen-bearing alkoxyamines were found to be successful for the controlled polymerization of both styrene and acrylates. Two structures in particular have been found to be very robust and successfully polymerized styrene: they are acrylate-, acrylamide-, and acrylonitrile-based monomers with controlled molecular weights from 1000 to 200,000 g/mole and polydispersities of 1.05 to 1.15. Hawker also reported the synthesis of narrow-polydispersity block and random copolymers based on combinations of the above monomers.

SEE ALSO THE FOLLOWING ARTICLES

CATALYSIS, INDUSTRIAL • MACROMOLECULES, STRUCTURE • ORGANIC CHEMISTRY, SYNTHESIS • POLYMERS, RECYCLING • POLYMERS, THERMALLY STABLE

BIBLIOGRAPHY

- Bhanu, V. A., and Kishore, K. (1991). *Chem Rev.* **91**(2), 99–118.
- Colombani, D. (1997). "Chain growth control in free radical polymerizations," *Prog. Polym. Sci.* **22**(8), 1649–1720.
- Culbertson, B. M., and McGrath, J. E. (eds.). (1985). "Advances in Polymer Synthesis," Vol. 31, Plenum Press, New York.
- Ferguson, J. (1984). "Step growth polymerization. Part 1. Polyesters, polycarbonates, polyamides, and polyimides," *Macromol. Chem.* **3**, 76–92.
- Heitz, W. (1995). "Metal-catalyzed polycondensation reactions," *Pure Appl. Chem.* **67**(12), 1951–1964.
- Hogen-Esch, T., and Smid, J. (eds.). (1987). "Recent Advances in Anionic Polymerization," Elsevier, New York.
- Kendall, J. L., Canelas, D. A., Young, J. L., and DeSimone, J. M. (1999). "Polymerizations in supercritical carbon dioxide," *Chem. Rev.* **99**(2), 543–563.
- Labadie, J. W., Hedrick, J. L., and Ueda, M. (1996). "A survey of some recent advances in step-growth polymerizations," *ACS Symp. Ser.* **624**, 294–305.
- Long, T. E., and Turner, S. R. (2000). "Step growth polymerization," In "Applied Polymer Science 21st century (2000)" (C. D. Craver and C. E. Carraher, eds.), pp. 979–998, Elsevier, New York.
- Nuyken, O., and Pask, S. (1989). "Telechelic polymers," In "Encyclopedia of Polymer Science and Engineering" (J. J. Kroschwitz, ed.), Vol. 16, pp. 494–532, Wiley, New York.
- Odian, G. (1985). "Chain-reaction polymerization. In "Encyclopedia of Polymer Science and Engineering" (J. J. Kroschwitz, ed.), Vol. 3, pp. 247–288, Wiley, New York.
- Sparrow, D. J., and Walton, I. G. (1984). "Step growth polymerizations, Part II. Developments in polyurethanes," *Macromol. Chem.* **3**, 93–97.
- Tirrell, D. A. (1985). "Copolymerization," In "Encyclopedia of Polymer Science and Engineering" (J. J. Kroschwitz, ed.), Vol. 4, pp. 192–233, Wiley, New York.
- Turner, S. R. (1999). "Historical development and progress in step growth polymerization," *Polym. Mater. Sci. Eng.* **80**, 285.
- Wagener, K. B., and Davidson, T. A. (1996). "Non-conjugated and conjugated dienes in acrylic diene metathesis (ADMET) chemistry," In "New Macromolecular Architecture and Functions. Proceedings OUMS '95" (M. Kamachi and A. Nakamura, eds.), Springer, Berlin.



Polymers, Thermally Stable

J. P. Critchley

Royal Aerospace Establishment

- I. Thermally Stable Polymers
- II. Carbocyclic Aromatic Systems
- III. Heterocyclic Aromatic (Heteroaromatic) Systems

GLOSSARY

Ablative coating Polymeric material providing thermal protection whereby high levels of heat flux are absorbed in the course of the pyrolytic thermal decomposition of the exposed surface layer.

Creep (cold flow) Reversible change in shape sustained by thermoplastic materials under sustained loading.

Cross-linking Formation of three-dimensional or network polymer systems by polymerization of monomers with functionality greater than two or by covalent bonding between preformed linear molecules.

Cyclopolycondensation Process in which a stable heterocyclic ring is formed as part of the polymer chain backbone with elimination of condensation volatiles. The process can occur via chain extension or postpolymerization of a preformed precursor polymer.

Interlaminar shear strength (ILSS) Design critical feature of fiber-reinforced composites relating to the absolute stress level required to separate individual layers of reinforcement. For optimum levels of fiber strength and loading a valuable analytic tool for predicting compressive and flexural strengths of individual composites formulated from different resin matrices.

Interpenetrating network system (IPN) An intimate mixture of two or more polymeric networks held together predominantly by permanent entanglements.

These entanglements restrict the segmental motion such that the creep and flow phenomena of the participating polymers can be radically reduced.

Ladder (double-strand) systems Relates to linear as opposed to network polymers in which two molecular strands are linked often via complex ring systems. "Perfect" ladder polymers require the rupture of at least two bonds within the same ring before major reduction in molecular weight can occur.

Liquid crystallinity Is exhibited in melt (thermotropism) or solution (lyotropism) by polymers having rigid rod-like structures; such polymers showing spontaneous anisotropy and readily induced orientation in the liquid crystalline state. Processing (i.e., fiber spinning) from this state can lead to materials with great strength in the direction of orientation.

Molecular composites Utilize the extended chain structure of a rigid-rod segment as reinforcement, copolymerized or blended at molecular level with the flexible matrix component which may be, typically, a thermoplastic polymer. To achieve optimum properties for the composite, there should be little or no phase separation between rigid-rod and matrix components.

Polymer degradation Involves the chemical modification of main-chain backbone and/or side groups of the macromolecule. The process requires rupture of primary valence bonds and results in reduced molecular

weight, cross-linking, or cyclization. As a general criterion, degradation adversely affects those polymer properties critical for commercially viable plastics, fibers, or rubbers.

Reinforced plastics Composite nonmetallic materials for which the basic resin system is combined in varying proportion with a fibrous additive in order to improve the mechanical strength and modulus of the matrix.

Rigid-rod polymers Formed from benzenoid and heterocyclic moieties, the molecules are colinearly arranged and have rotational flexibility within the polymer backbone only at the junction of phenyl and heterocyclic rings.

Thermal analysis Measurement and evaluation of polymer thermal stability by monitoring a specific polymer property with respect to temperature. Analytic data includes polymer weight loss measured by dynamic or isothermal thermogravimetric analysis (TGA); glass transition temperature (T_g) measured calorimetrically by differential scanning calorimetry (DSC)/differential thermal analysis (DTA) or mechanically by torsional braid analysis (TBA)/thermomechanical analysis (TMA); monitoring volatile by-products by effluent gas analysis (EGA).

Thermoplastic polymer Relates to a plastic material that can be repeatedly softened when heated and hardened when cooled.

Thermosetting resin Polymer capable of being modified into a predominantly and permanently infusible and insoluble material due to the effects of heat or chemical processes.

THE KEY Requirement for a successful “working” thermally stable (heat-resistant) polymer is that functioning within clearly defined parameters of temperature, time, and environment it should retain a high proportion of those practically useful properties in material form (e.g., film, fiber, resin matrix, or metal-to-metal adhesive) that were demonstrated under ambient conditions. The temperature–time limitations most frequently imposed include 230–260°C for several thousand hours, 360–370°C for hundreds of hours, 550–560°C for 1 hr, and 750–800°C (ablative conditions) for minutes only. The environment within which the polymer must function will include the prevailing atmosphere surrounding the polymer (inert gas, air/oxygen, or vacuum), possible exposure to chemical attack and/or radiation, and the individual or combined mechanical stress factors (tensile, compressive, shear) encountered under static or dynamic loading conditions.

The 1990s saw significant changes in the direction taken by developments in the field of thermally stable materials,

away from an emphasis on predominantly military applications into aspects of multidisciplinary studies. Thus, while research into high-temperature polymers has continued to be directed toward aerospace requirements, there has also been a move toward environmental objectives, which has led, for example, to studies into dielectrics for electronic applications, polymer sensors, resist materials, and polymeric membranes. Associated basic studies, while continuing to examine the design and synthesis of thermally stable systems, have concentrated efforts into those areas of polymer chemistry linked to chain architecture and the control of end-group structure. The previous overriding emphasis on stability, both thermal and thermo-oxidative, which frequently led to brittle “brick dusts,” has shifted noticeably toward efforts to provide an optimum thermal/thermo-oxidative stability allied with a capacity to produce processible materials that can provide manufactured products (see Section 1.C) by melt, solution, or dispersion processing.

I. THERMALLY STABLE POLYMERS

A. Essentials of Polymer Stability

Two basic mechanisms control property deterioration of polymers at elevated temperature. One, linked predominantly to thermoplastics, involves a reversible wholly temperature-dependent softening phenomenon; the other an irreversible degradative process time, temperature, and environment dependent relates to thermosets.

To increase the polymer softening point, or more critically the glass transition temperature (T_g), it is necessary to maximize contributions from both interchain attractive forces and chain regularity:

Interchain forces	Chain regularity
Polar side groups	Crystallinity
Hydrogen bonding	<i>para</i> -Linked cyclics
Cross-linking	Extensive orientation

Observations from the purely thermal degradation of several polymers with closely related structures have emphasized the following features as important for high thermal stability:

1. Maximum bond strength via resonance stabilization
2. Minimum of low-energy paths allowing rearrangement processes
3. Maximum influence of the polybonding effect

Bond dissociation energies (kJ/mol)											
C—S	273	C—N	307	C—H	416	P—O	528	C=C	609	B—O	777
B—H	294	Si—H	319	C—F	428	P—C	580	C=N	617		
		Si—C	328	Si—N	437			Ti—O	672		
		C—Cl	340	Si—O	445						
		C—C	349								
		C—O	361								
		C—B	374								
		B—N	386								

The choice of the highest bond strength combinations (see below), though important, is certainly not the final arbiter of thermal stability since ultimately all polymer systems degrade by lowest energy routes.

The exploitation of inorganic high-temperature polymers has been, for example, severely restricted due to the intervention of preferred low-energy processes leading to hydrolytic or oxidative breakdown. With the semiorganic polysiloxanes, although notably successful as elastomers, low-energy paths have resulted in a relatively more facile cleavage of the Si—O bond with concomitant formation of low-molecular-weight cyclics than would have been expected from an apparently high (445 kJ/mol) bond strength. In fully organic systems energetically favored eliminations (e.g., hydrogen fluoride from hydrofluoro polymers) and unzipping (stepwise) breakdown of aliphatic polymer chains are characteristic causes of instability. Contrary to the situation described above, however, bond strengths of aromatic and hetero-aromatic nuclei are significantly strengthened through resonance stabilization and polymers that incorporate these systems exhibit an enhanced thermo-oxidative stability. Ideally, fused ring/ladder polymers should be more stable than the ring-chain analogs since, with multiple bonding, chain disruption should not occur on cleavage of a single bond. In practice, however, the stability of ladder systems seldom reaches the optimum.

B. Structure and Thermal Stability and Tractability

Assumptions regarding potentially thermally stable polymer systems based on a study of model compounds have been of only limited value since polymer stability depends critically on the structure, reactivity, and mutual interaction of the macromolecules. Variations in thermal stability have, for example, been observed in ordered as opposed to limited order or random copolymers. The extent of cross-linking or chain branching is an important feature as are those physical characteristics such as molecular weight and degree of crystallinity. Frequently the presence of unstable end groups, weaklinks, and trace impurities leads

to a discrepancy in the theoretically predicted and experimentally observed stability of the polymer. Factors influencing the choice of aromatic/heteroaromatic ring structures in thermal/thermo-oxidatively stable polymers have been highlighted above. However, polymer systems incorporating long sequences of directly linked rings are invariably insoluble and infusible and structural modifications required to allow processing and fabrication of practically useful materials often result in a reduced stability.

For aromatic/heteroaromatic ring-containing polymers the following main conclusions regarding structure-property relationships have, therefore, been established:

1. The highest thermal/thermo-oxidative stabilities are reserved for ladder (double-strand) polymers although synthetic difficulties—incomplete ladder formation—frequently reduce the observed stability to that of “conventional” aromatic systems.
2. For polymers containing phenylene groups, *para*-linked rings produce the highest thermal stability but also the highest softening points and lowest solubilities. The use of *meta*- or *meta/para*-linked rings provides a compromise in processability versus stability.
3. Substitution of hydrogen in phenylene groups leads to a reduced thermal stability. This is not always reflected in other ring systems (e.g., chlorine substitution in polyxylylene or phenyl substitution in polyquinoxalines) where stability is increased.
4. Interposition of flexible groups midchain leads to a reduction in thermal stability in all cases but that reduction is minimized by using the following: —CO—, —COO—, —CONH—, —S—, —SO₂—, —O—, (CF₂)_n. The relative stability (ITGA) in air of phenylene polymers containing these linkages is shown in Fig. 1.

C. Material Developments and Applications

High costs associated with the provision of novel raw materials and difficult processing and fabrication requirements for thermally stable/heat-resistant polymers have limited their marketability to the relatively narrow, specialized field of aerospace and in particular that of

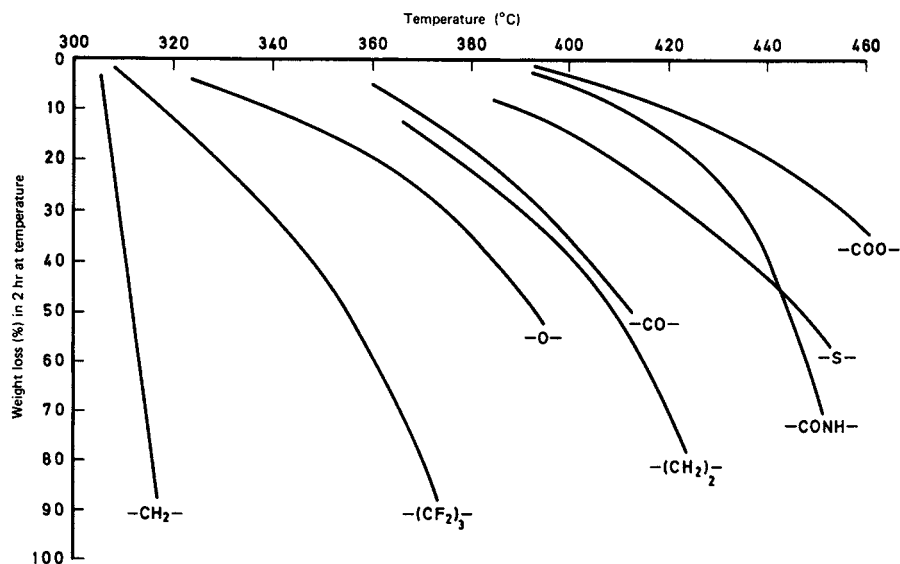


FIGURE 1 Comparison of stability of phenylene polymers with different linking groups in oxidizing atmosphere. [Reprinted with permission from Wright, W. W. (1975). Comparison of stability of phenylene polymers with different linking groups in oxidizing atmosphere. In "Degradation and Stabilization of Polymers" (G. Gueskens, ed.), pp. 43–45, Elsevier, New York.]

advanced military aircraft, space craft, and missiles. Principal areas of materials development and real or potential application in these advanced technology areas are listed here:

1. *Films/varnishes/membranes*: Wire and cable insulation, heat-sealable or pressure-sensitive tapes, electrically conductive film, electric motor slot liners, flexible printed circuits, magnetic wire coatings, reverse osmosis membranes.

2. *Adhesives*: Film and B-staged (on fiber substrate), cryogenic and high-temperature application. Bonding metal-to-metal (stainless steel, titanium, or beryllium alloy adherends), metal-to-composite, and composite-to-composite use in honeycomb structures.

3. *Fibers*: Heat/flare resistant and high strength/high modulus. Protective clothing, armor, and shields. Reinforcement for composites, fire hoses, V-belts. Hot gas filtration systems, deceleration parachutes, solid rocket motors, nozzles, exist cones.

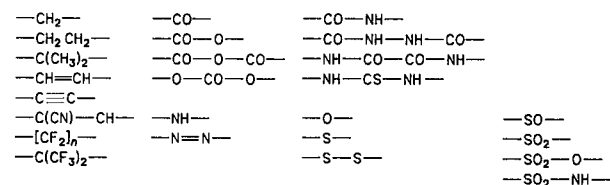
4. *Molding materials*: Binders (brake pads, abrasive wheels, etc.), self-lubricating bearings, friction-resistant flap track surfaces; abradable seals; rotors/vanes for pumps; activators, piston rings, electrical connectors.

5. *Composites*: Matrix and reinforcement materials for laminating and filament winding applications. Radomes, engine nacelles, fan and compressor blades, fan frames.

6. *Foams*: Blown and syntactic. In-fill materials, aircraft fire barriers, space shuttle insulation.

II. CARBOCYCLIC AROMATIC SYSTEMS

Linear poly-*p*-phenylene is not a commercially available material; indeed it is rather typical of those intractable systems generally referred to as "brick dusts." However, as perhaps the simplest example of a wholly aromatic-linked polymer it is the standard against which the thermal/thermo-oxidative stability of more complex aromatic and heteroaromatic polymers has been measured. Considerable improvements in tractability and processibility have followed the introduction of the midchain flexible units shown below.

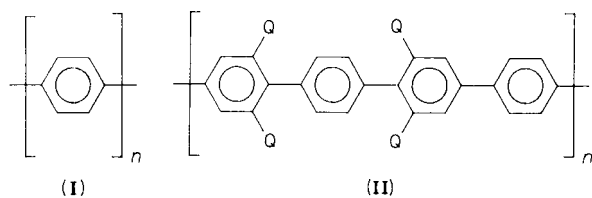


Discussion will be restricted to those systems that have combined a high level of thermal stability with some practical utility.

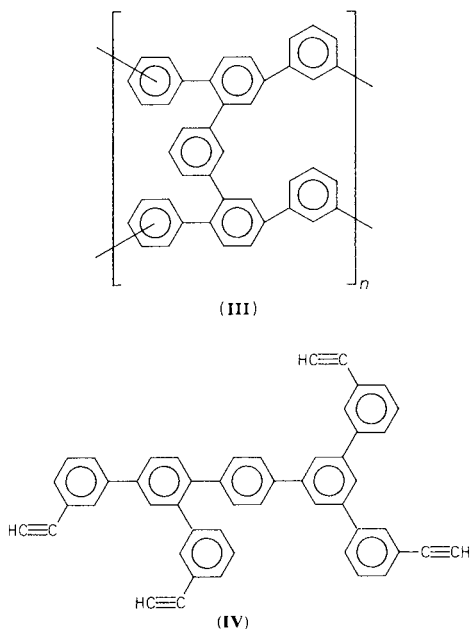
A. Polyphenylenes and Polyxylylenes

Poly-*p*-phenylene (**I**) has been synthesized by several conventional reactions—direct coupling of benzene/*p*,*p*'-derivatives, via a (soluble) poly-1,3-cyclohexadiene intermediate, or by Diels–Alder addition of diethynylbenzene

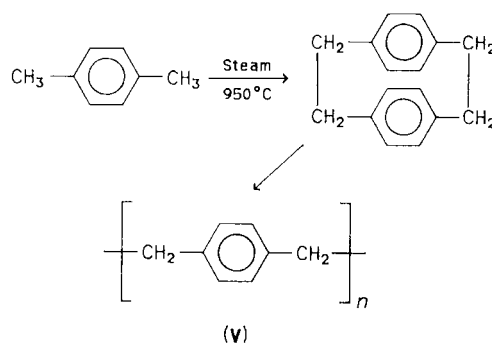
and an unsubstituted bispyrene—using the relevant catalyst. The product from these reactions is a crystalline intractable material that is extremely difficult to process. The introduction of phenyl substituents (Q) into the polymer (II) has resulted in soluble, noncrystalline materials with relatively high molecular weight ($3-6 \times 10^4$).



Highly branched polyphenylenes have been produced involving, however, different reaction schemes than those used for linear systems. Polymer (III) is obtained via cure (274°C) of a soluble, processible intermediate while oligomer (IV) cures (cross-links) at temperatures above melt flow ($>150^\circ\text{C}$). Both materials have been used in high-temperature resin applications, the former specially as the matrix in carbon fiber-reinforced composites.



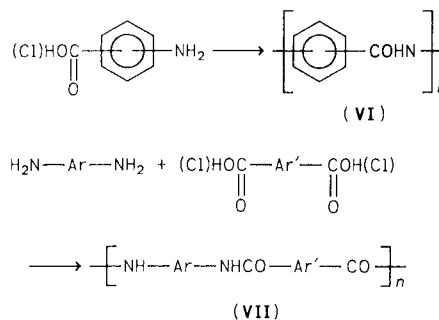
Poly-*p*-xylylene (V) has been most successfully prepared by the controlled (steam/ 950°C) pyrolysis of *p*-xylylene/chlorinated *p*-xylylene via a cyclic dimer that rearanges (*in vacuo*) to yield the crystalline high-molecular-weight ($\sim 500,000$) polymer as a hard, impervious coating.



Poly-*p*-xylylene coatings (Parylenes) involving both unsubstituted and chloro-substituted products have been successfully marketed in electrical/electronic coatings applications used in air and inert atmospheres at around 150 and 220°C , respectively. A comparison of properties, particularly electrical, of typical Parylene, silicone, and epoxy coatings formulations is shown in Table I. The deleterious effect, however, of the alkylene ($-\text{CH}_2-\text{CH}_2-$) linking unit, particularly on thermooxidative stability, is clearly apparent from the isothermal TGA curves (Fig. 2).

B. Polyamides

The extensive development of aromatic polyamides (aramids) as high-temperature polymers, particularly as thermally stable fibers, followed naturally from the commercial successes of the wholly aliphatic systems (nylon; nylon 6,6 etc.). Aramids (VI and VII) are produced from amino acids (A-B condensations) and from diacid/diamine combinations (AA-BB condensations), respectively, by low-temperature interfacial or high-temperature solution polymerization techniques.



The use of highly polar solvents such as dimethylformamide (DMF), hexa-methylphosphoramide (HMP), and *N*-methyl-pyrrolidone (NMP), among several others, has been critical to the success of many high-temperature polymerization reactions used to produce both aromatic and heteroaromatic polymers.

A large number of aramids have been obtained from widely varied A-B and AA-BB precursors. Generally,

TABLE I Comparison of Properties of Xylylene Polymers with Epoxy and Silicone Materials^a

Property	Poly- <i>p</i> -xylylene (Parylene N)	Polymonochloro- <i>p</i> -xylylene (Parylene C)	Polydichloro- <i>p</i> -xylylene (Parylene D)	Epoxy	Silicon
Density	1.11	1.289	1.418	1.11–1.40	1.05–1.23
Tensile strength (MPa)	45	69	76	28–90	6–7
Elongation at break (%)	30	200	10	3–6	100
24-hr water absorption (%)	0.06	0.01	—	0.08–0.15	0.12 (7 days)
Melting or heat distortion temperature (°C)	405	280	>350	Up to 220	Up to 300
Linear coefficient of expansion (10 ⁻⁵ /°C)	3.5	6.9	—	4.5–6.5	25–30
Dielectric strength (V/mil)	7000	5600	5500	2300	2000
Volume resistivity 23°C 50% RH (Ω-cm)	1 × 10 ¹⁷	6 × 10 ¹⁶	2 × 10 ¹⁶	1 × 10 ¹⁴	1 × 10 ¹⁵
Surface resistivity 23°C 50% RH (Ω-cm)	10 ¹³	10 ¹⁴	5 × 10 ¹⁶	5 × 10 ³	3 × 10 ¹³
Dielectric constant					
60 Hz	2.65	3.15	2.84	4.2	2.6
10 ³ Hz	2.65	3.10	2.82	3.9	2.6
10 ⁶ Hz	2.65	2.95	2.80	3.4	2.6
Dissipation factor					
60 Hz	0.0002	0.020	0.004	0.03	0.0005
10 ³ Hz	0.0002	0.019	0.003	0.03	0.0004
10 ⁶ Hz	0.0006	1h0.013	0.002	0.04	0.0008

^a Reprinted with permission from Critchley, J. P., Knight, G. J., and Wright, W. W. (1983). "Heat Resistant Polymers—Technologically Useful Materials," Plenum, New York. Copyright 1983 Plenum Press.

the polymers are characterized by a combined low solubility and high melt temperature, most prominent in wholly *para*- and least in wholly *meta*-oriented systems. Various approaches have been applied toward "tailoring" the

aramid system in order to obtain the maximum thermal stability benefits from high polymer melt temperatures while increasing the most important feature in the spinning of high-quality fiber, that is solubility. Typically, the

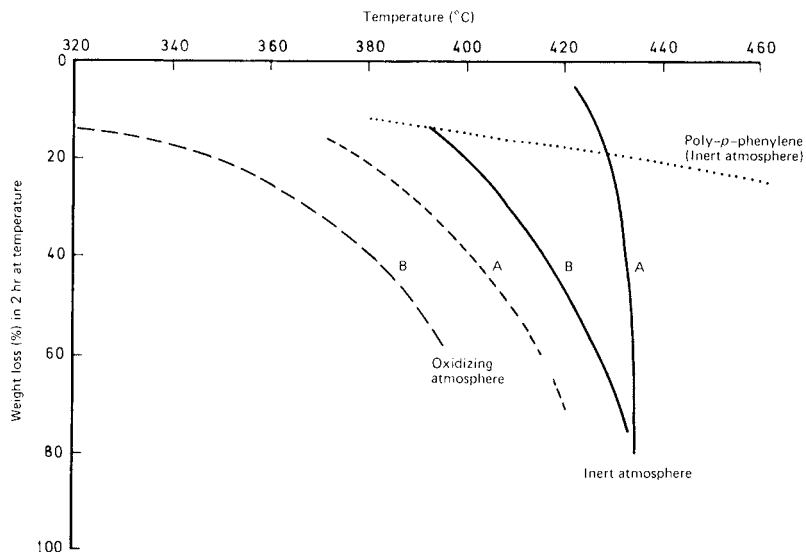


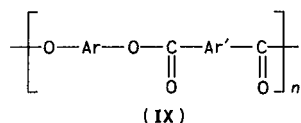
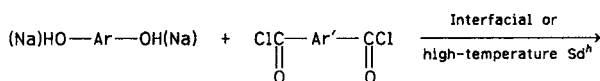
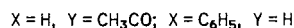
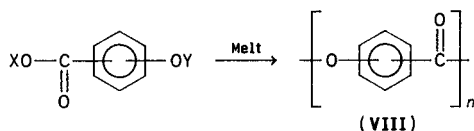
FIGURE 2 Thermal stability envelopes for poly-*p*-xylylenes in inert and oxidizing atmospheres. (A) From Wurtz reaction and (B) from pyrolysis of *p*-xylylene. [Reprinted with permission from Critchley, J. P., Knight, G. J., and Wright, W. W. (1983). "Heat Resistant Polymers—Technologically Useful Materials," Plenum, New York. Copyright 1983 Plenum Press.]

introduction of additional flexible links mid-chain [e.g., —O—, —S—, —SO₂—, and —(CH₂)—] as well as substitution in the aromatic rings increased solubility but reduced polymer melt temperature. More successfully, the development and application of alternating ordered copolyamides containing a high proportion of *para*-substituted phenylene, and heteroaromatic rings yielded soluble, high melt systems in which a high level of crystallinity could be induced, most significantly after the spinning process. The thermal/thermooxidative stability and retention of fiber tenacity at temperature (300°C) for extended periods increases in the alternating co-aramids as the content of *para*-substitution increases.

In spite of the considerable activity referred to above only two aramid systems have been recognized commercially. The first poly-*m*-phenyleneisophthalamide (**VII**, Ar = Ar' = *m*-C₆H₄), marketed as Nomex for its principal use in flame-resistant fabrics, the second originated as poly(*p*-benzamide) (**VI**, *p*-C₆H₄), marketed as Fiber B/PRD-49, but a later ultrahigh modulus material development (Kevlar 49) was based on poly(1,4-phenyleneterephthalamide) (**VII**, Ar = Ar' = *p*-C₆H₄). These *para*-linked aramids form lyotropic liquid crystalline solutions which can be spun to high-strength/high-stiffness fibers. A comparison of the thermal stability (TGA) underlines the superiority in both inert and oxidizing atmospheres of the *para/para*-linked aramid (rapid degradation begins above 500°C) as opposed to the *meta/meta* isomer (rapid degradation begins above 400°C).

C. Polyesters

Like the aramids, an impetus for the assessment of aromatic polyesters in a thermally stable role was the commercial success generated in the aliphatic series, in this case poly(ethyleneterephthalate), a fiber- and film-forming material. Research effort was directed to a wide area of aromatic polymers, (**VIII**) and (**IX**), produced by A–B or AA–BB condensation processes.

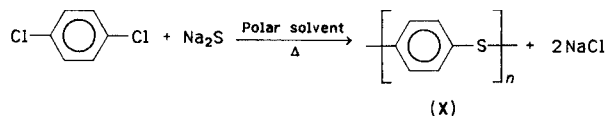


The latter process has produced a wide range of polyesters from which it was possible to assess property–structure relationships. The replacement of wholly *para*-linked unsubstituted rings in a homopolymer system by *meta*-links, incorporation of midchain flexible groups [e.g., —C(CF₃)₂—, —C(CH₃)₂—, —CH₂—, —O—] or interposition of ordered alternating copolymer structures resulted in an increased solubility/processibility paralleled, however, by a reduced thermal stability [as much as 150°C (TGA) in air or nitrogen].

The commercial development of useful high-temperature aromatic polyesters has been based on A–B type melt condensations of *p*-hydroxybenzoic acid derivatives and is limited to a homopolymer [Ekonol; **VIII** (*p*-linked)] and two related copolymer compositions, Ekkcel C-100 and Ekkcel I-2000. A comparison of the thermal stability (isothermal weight loss in air) of the three polymer systems is demonstrated in Fig. 3. Ekonol, because of its very high crystallinity/melting, is processed under exceptional conditions of compressive sintering (370°C/70 MPa) or plasma spray while Ekkcell C-100 and I-200 are compression and injection molded, respectively. Comparative property data for Ekonol versus selected high-temperature alternatives are detailed in Table II.

D. Poly(Phenylene Sulfide)

Although other synthetic approaches have been reported, the most successful and also commercial route to linear poly(phenylene sulfide) (**X**) is illustrated in the following reaction sequence:



As prepared, the polymer is moderately crystalline (~65%) exhibiting both a *T_g* (85°C) and *T_m* (285°C) and elevated temperature cure involving cross-linking and chain extension processes results in an insoluble but ductile network polymer. The stabilizing effect of oxidative cross-linking processes is well illustrated in a comparison of isothermal weight loss in air and nitrogen (Fig. 4). Poly(phenylene sulfide) (**X**) in its commercial form (Ryton) can be used in molding and laminating resin and surface coating applications. As a “base” material for bearings it exhibits considerable high-temperature benefits over conventional epoxy resins (Fig. 5); carbon fiber laminates incorporating poly(phenylene sulfide) as a matrix resin maintain a high level of tensile and flexural hot and hot/wet property retention (Table III).

Further research activity has now produced a series of related aromatic polysulfides. However,

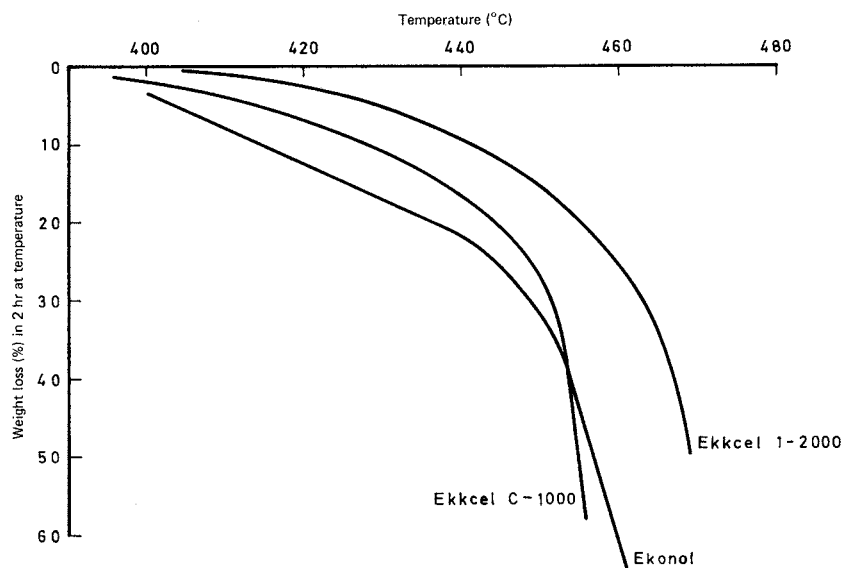


FIGURE 3 Comparison of the thermo-oxidative stability of *p*-hydroxybenzoic acid-based polymers. [Reprinted with permission from Critchley, J. P., Knight, G. J., and Wright, W. W. (1983). "Heat Resistant Polymers—Technologically Useful Materials," Plenum, New York. Copyright 1983 Plenum Press.]

poly(*p*-phenylene sulfide) (PPS) remains the only major commercial development for this class of thermoplastic aromatic polymer. Although alternative PPS products are beginning to be marketed by others (General Electric, Bayer AG, Mobay, and Hoechst-Celanese), the Phillips' Ryton material still controls around 95% of the market. A widening range of high-temperature applications has emerged for both reinforced and unreinforced PPS, including, ball valves, chip- and fiber-carriers, encapsulants,

and camshafts. In tailoring the properties of PPS to suit the specific application, both amorphous and crystalline versions of the resin have been investigated, and in this regard the potential of PPS fibers has been investigated. The application of zone-drawing and zone-annealing techniques has recently been used to improve the mechanical properties of PPS fibers.

PPS is characterized as a thermosetting thermoplastic. "Curing" occurs on heating in oxygen or in the pres-

TABLE II Comparison of Properties of a Polyester (Ekonol) with Other High-Temperature Resistant Polymers^a

Property	Polyester (Ekonol)	Polysulfone (Astrel 360)	Polyimide (Vespel)	Polytetrafluoroethylene
Density (g/ml)	1.44	1.36	1.40	2.13
Flexural strength (MPa)	74	119	81–97	—
Flexural modulus (GPa)	7.1	2.7	3.2	0.6
Compressive strength (MPa)	226	124	166	7
Dielectric strength (V/mil)	660	300	430	620
Dielectric constant	3.8	3.9	3.6	2.1
Dissipation factor ($\times 10^4$)	2	30	34	3
Volume resistivity (Ω -cm)	10^{15}	10^{13}	10^{16} – 10^{17}	10^{18}
Water absorption, 24 hr at RT (%)	0.02	0.22	0.30	0.01
Coefficient of static friction	0.10–0.16	—	0.25–1.2	0.05–0.08
Thermal conductivity 10^{-4} cal/(sec)(cm) ² (°C/cm)	18.0	6.0		6.0

^a Reprinted with permission from Mark, H. F., Gaylord, N. G., and Bikales, N. M., eds. (1971). "Encyclopedia of Polymer Science and Technology," Vol. 15, p. 292, Wiley (Interscience), New York. Copyright 1971 John Wiley & Sons, Inc.

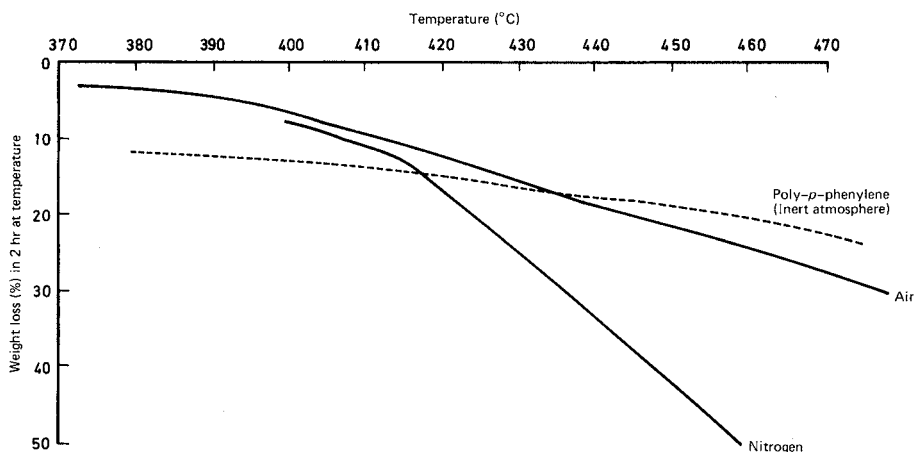


FIGURE 4 Thermal stability of poly(phenylene sulfide) in air and nitrogen. [Reprinted with permission from Critchley, J. P., Knight, G. J., and Wright, W. W. (1983). "Heat Resistant Polymers—Technologically Useful Materials," Plenum, New York. Copyright 1983 Plenum Press.]

ence of sulfur (argon atmosphere at 290°C) with an increase in molecular weight, toughness, ductility, and insolubility. An increase in sulfur from 0 to 0.94% by weight raised the impact strength from 52,800 to 85,600 J/m², although thermal stability is reduced when significantly larger amounts of sulfur cross-links are incorporated in the polymer. A comparison of the crystallinity of PPS with polyetheretherketone (PEEK) and polyetherketone (PEK) (see Section II.E) has shown all three to have an orthorhombic crystal structure. Solution-grown

crystals have multilayered, sheaflike lamellae which are chain-folded with the fold plane parallel to the growth direction of the crystal. The degree of crystallinity developed by PPS during drawing is related to the drawing temperature. PPS is an insulating material, but UV irradiation at room temperature increases the conductivity of film material by three orders of magnitude. Addition of inorganic (AsF₅, SbF₅) or organic [tetracyanoethylene (TCNE), dichlorodicyanobenzoquinone (DDQ)] additives renders PPS electrically conductive. An

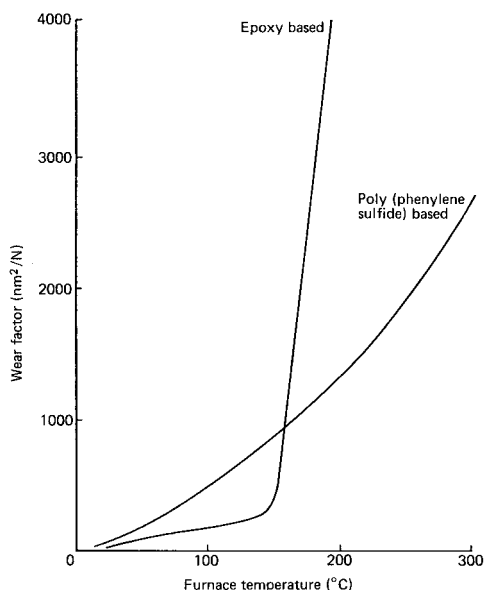


FIGURE 5 Wear-rate of poly(phenylene sulfide) and epoxy resin-based bearings as a function of temperature. [Reprinted with permission from West, G. H., and Senior, J. M. (1973). *Tribology* 6, 269. Copyright 1973 IPC Science and Technology Press Ltd.]

TABLE III Mechanical Properties of a Poly(Phenylene Sulfide)/Carbon Fiber (Ryton/T-300) Laminate^a

Property	Condition	Room temperature	121°C	177°C
Flexural strength (0°) (MPa)	Dry	1162	687	449
	Wet	755	517	339
Flexural strength (90°) (MPa)	Dry	195	126	103
	Wet	212	174	143
Flexural modulus (0°) (GPa)	Dry	84	86	73
	Wet	86	75	66
Flexural modulus (90°) (GPa)	Dry	11	9.0	8.4
	Wet	14	8.6	5.2
Tensile strength (0°) (MPa)	Dry	818	642	564
Transverse tensile strength (MPa)	Dry	103	78	67
Tensile modulus (0°) (GPa)	Dry	108	84	90
Transverse tensile modulus (GPa)	Dry	14	17	3.6

^a Reprinted with permission from Hartness, J. T. (1980). *Nat. SAMPE Symp. Exhib.* 25, 376.

area of increasing importance for PPS is as a thermoplastic matrix for advanced structural composites using carbon- or glass-fiber reinforcement. Blends of PPS with other systems such as Bisphenol-A/Polysulfone, nylon-6,6 and high-density polyethylene (HDPE), using glass fiber reinforcement, have been recorded.

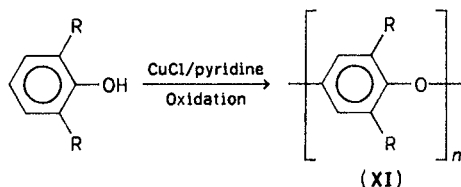
Individually, PPS with carbon fiber reinforcement is under investigation in advanced (aerospace) structures. Complex shapes such as I-beams and C-channels have been manufactured from laminates incorporating unidirectional, offaxis (90° , $\pm 45^\circ$) and fabric reinforcement. The lower interlaminar fracture toughness (G_{IC}) of epoxy (0.1 kJ/m^2) and polysulfone (0.63 kJ/m^2) compared with that of PPS (1.3 kJ/m^2) and PEEK ($1.4\text{--}2.4 \text{ kJ/m}^2$) has been ascribed to the bonding efficiency of PPS and PEEK to the carbon fiber reinforcement due, it is suggested, to the development of transcrystalline regions at the fiber surface in the latter two systems.

A very recent development has been the use of rigid-rod LCs to reinforce thermoplastics such as PPS (and PEEK). Using a novel mixing process, a blend of 10–20% LCP with PPS is extruded or blow-molded into film or tape. It is claimed that the dynamic torsional properties of LCP/PPS films are higher than for carbon fiber reinforced PPS.

E. Poly(Phenylene Ether), Poly(Phenylene Ether Sulfones), Poly(Phenylene Ether Ketone)

The ether-link is frequently used to promote an added flexibility to inherently rigid polymer chains without incurring too radical a reduction in thermal/thermo-oxidative stability. This approach, particularly effective in the heteroaromatic series of polymers to be discussed later, has also characteristically enhanced the low-temperature flexibility of the aliphatic fluoroalkylene chain in, for example, PTFE [poly(tetrafluoroethylene)] to produce fluoroether elastomers with specialized application.

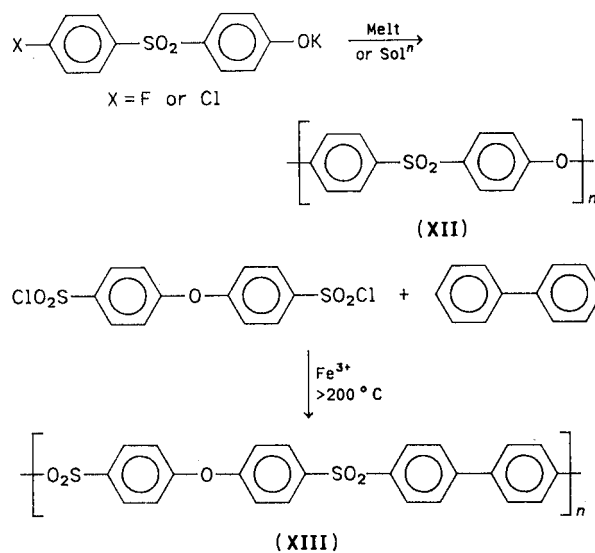
Carbocyclic poly[phenylene ethers (oxides)] (**XI**) are produced from substituted phenols by oxidative, free-radical, or replacement reactions.



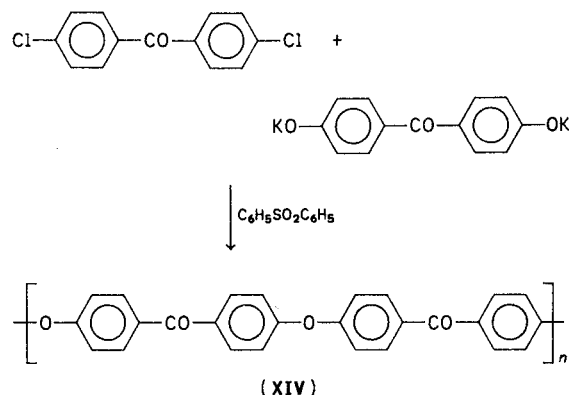
Thermal and thermo-oxidative stability decrease both with type and extent of substitution in the nucleus ($\text{H} > \text{C}_6\text{H}_5 > \text{CH}_3 > \text{CH}_3\text{O} > \text{OH} > \text{SO}_3\text{H} > \text{SO}_2\text{Cl}$); poly(1,4-phenylene ether) (**XI**, $\text{R} = \text{H}$) with a decomposition temperature (TGA/ITGA; air and nitrogen) of 570°C

exhibiting the highest stability. Nevertheless, only two materials (**XI**, $\text{R} = \text{CH}_3$ and $\text{R} = \text{C}_6\text{H}_5$) have demonstrated useful commercial application as thermoplastic molding products of intermediate heat resistance.

The utility of the ether-link in thermally stable carbocyclic polymers has proved most effective, applicationally, when combined with other flexibilizing units. Poly(phenylene ether sulfones) (**XII** and **XIII**) have typically been produced by polyetherification or polysulfonation processes:



Weight loss (Fig. 6) and property retention data at elevated temperature (Fig. 7) indicate continuous-use temperature for thermoplasts (**XII**, Polymer 200P and **XIII**, Astrel 360) of 175 and 200°C , respectively. Table IV indicates tensile strength retention versus temperature for carbon fiber reinforced poly(ethersulfone), while Table V compares tensile strength retention at various temperatures of typical glass fiber reinforced thermoplastics. Poly(phenylene ether ether ketone) (**XIV**, PEEK) is commercially produced via a polyetherification reaction:



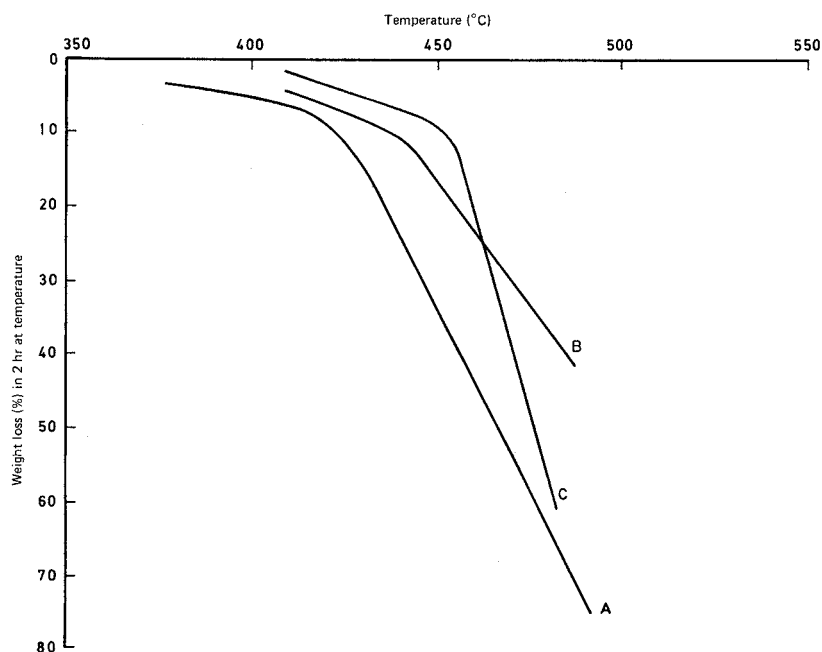
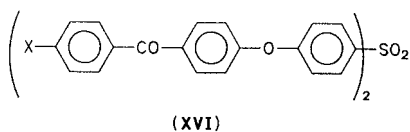
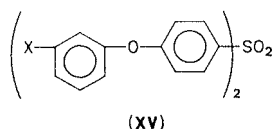


FIGURE 6 Thermal stability of poly(phenylene ether sulfones) in air. A is Udel P1700, B is Astrel 360, and C is Polyether sulfone 200P. [Reprinted with permission from Critchley, J. P., Knight, G. J., and Wright, W. W. (1983). "Heat Resistant Polymers—Technologically Useful Materials," Plenum, New York. Copyright 1983 Plenum Press.]

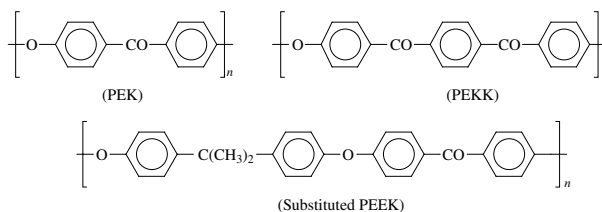
PEEK has been developed for wire coating (50,000 hr/200°C), injection molding, and reinforced composite applications. Like PPS materials, the mechanical properties of PEEK have been improved by zone-drawing/zone-annealing processes. Carbon fiber-reinforced PEEK has exhibited significantly improved properties after impact compared with carbon fiber/epoxy laminates. The stability (weight loss in air and nitrogen) is among the highest of aromatic polymers (Fig. 8). Oligomeric ether sulfones (XV) and keto-ether sulfones (XVI) have been polymerized/cured via intramolecular cyclization or trimerization reaction of terminal acetylene or nitrile groups yielding insoluble thermosets. Laminates from oligomer (XV)/carbon fiber composites demonstrated excellent property retention under dry and wet conditions at 175°C.



PEEK has continued to demonstrate a high level of property retention under extreme environmental conditions and

maintains a key position as a thermoplastic matrix resin for advanced composites.

Alternative polyaryletherketones (PAEKs) to the basic PEEK formulation have been reported; these include polyetherketone (PEK) and polyetherketoneketone (PEKK), as well as substituted versions of PEEK.



Limited characterization has been made of basic PEK and PEKK. PEK demonstrates a morphology similar to PEEK and PPS (see Section II.D); it exhibits, however, a higher T_g (160°C as opposed to 143°C) and a T_m of 365°C as opposed to 343°C, but it has a lower toughness (notched impact resistance) than PEEK. PEKK has a T_g approximately 12°C higher than PEEK, and it has an unusually high tensile modulus and a fracture toughness of 1.0 kJ/m² versus 0.1 kJ/m² for an untoughened aerospace epoxy. PEKK has a lower crystallinity than PEEK as well as lower density, heat of fusion, and melt viscosity. The introduction of fluorine (F or CF₃) into the polymer chain has been shown to increase solubility, reduce crystallinity, and improve the thermal stability of the polyetherketones.

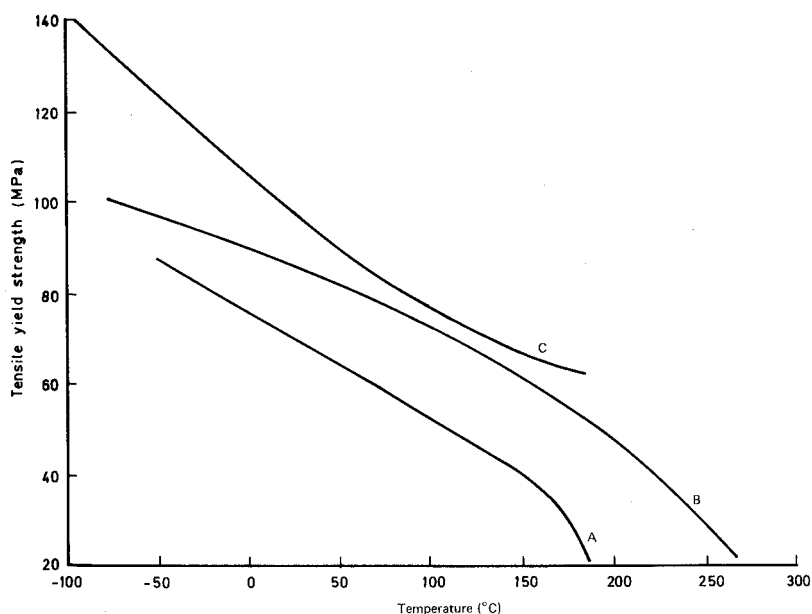


FIGURE 7 Tensile strength of polyethersulfones as a function of temperature. A is Udel P1700, B is Astrel 360, and C is Polyethersulfone 200P. [Reprinted with permission from Critchley, J. P., Knight, G. J., and Wright, W. W. (1983). "Heat Resistant Polymers—Technologically Useful Materials," Plenum, New York. Copyright 1983 Plenum Press.]

For PEEK itself, a large proportion of reporting has concentrated on polymer morphology relating, for example, the time and temperature of heating with the crystallinity of the microstructure. A study of PEEK/carbon fiber composites revealed that PEEK in combination with carbon fiber has a higher nucleation density than neat PEEK resin. Strong bonding at the resin–fiber interface is suggested to be caused by crystallization on the fiber surface. Morphology and consequential physical properties of the resin are greatly influenced by the processing conditions applied

TABLE IV Retention of Room Temperature Mechanical Properties of an Aromatic Poly(Ethersulfone) Carbon Fiber Composite (200P/AS) at Elevated Temperature^a

Property	Temperature (°C)	Retention of initial room temperature value (%)
Tensile strength	175	90
Tensile modulus	175	100
Compressive strength	175	73
Compressive modulus	175	100
Flexural strength	160	58
Flexural strength	145	73
Flexural modulus	160	100
Interlaminar shear strength	160	51
Interlaminar shear strength	145	61

^a Data from Hoggatt, J. T. (1975). *Nat. SAMPE Symp. Exhib.* **20**, 606.

during the fabrication of PEEK composites. To minimize deleterious thermal effects, it has been shown that PEEK composites are best fabricated under nonoxidative conditions at temperatures less than 400°C. Reheating the composite (e.g., in repair or readjustment of lay-up) results in significant morphological changes unless these processing conditions are retained.

Binary blends of PEEK and sulfonated PEEK (SPEEK) are miscible over the entire composition range with Torlon 4000 T (amide-imide) and Ultem 1000 (ether-imide). It has been suggested that electron donor-accepter complexes involving the phenylene rings of PEEK/SPEEK and *N*-phenylene units of the polyimides are responsible for this miscibility. A single, sharp T_g for each composition has been observed. The increase of T_g over that of PEEK for some of these compositions has suggested that blending may be a technique for improving the mechanical properties and increasing the heat distortion point for these thermoplastic materials. A further method for improving the thermal and mechanical properties of the PEEKs has involved polymer chain interaction/cross-linking via pendant or terminal maleimide, styryl, ethynyl, or nitrile groups.

Unreinforced PEEK is used in a number of applications, including high-temperature bearings and seals, wire and cable coatings, and in electronics. But the main growth area has been in advanced structural composites based on a carbon fiber reinforced PEEK(APC-2) developed by Imperial Chemical Industries (ICI) as one of their

TABLE V Comparison of Tensile Strength at Elevated Temperatures of Various Glass-Reinforced Thermoplastics^a

Polymer type	Glass content (wt%)	Tensile strength (MPa) at (°C)					
		23	95	150	175	205	230
Polysulfone (P1700)	40	119	103	16	8	—	—
Polyethersulfone (200P)	40	157	134	90	34	21	—
Polyarylsulfone (Astrel 360)	0	90	72	60	51	39	22
Poly(phenylene sulfide)	40	160	77	56	33	8	—
Poly- <i>p</i> -oxybenzoate	0	96	77	64	54	44	—
Polyimide	30	90	43	33	21	16	12
Polyamideimide	0	189	137	112	79	57	48
TFE/HFP copolymer	20	35	29	16	8	—	—
TFE/E copolymer	20	78	47	43	14	—	—

^a Courtesy of J. Theberge, LNP Corporation.

“Victrex” range. PEEK (Litrex K) has also been developed as a commercial material by Petrochemie Danubia GmbH.

APC-2 is a thermoplastic prepreg consisting of a 60% by volume unidirectional web of high-strength fiber impregnated with PEEK resin. Although it has demonstrated processing advantages over more conventional thermoset prepreps—shorter processing time, indefinite shelf-life—the APC-2 prepreg is stiff and inflexible (boardy). Two approaches have been made to improve the so-called drapability of the prepreg. In the first a filament-to-filament “co-mingled” blend of carbon and PEEK fibers is processed

by weaving, braiding, or knitting to give a drapable fabric. Heat and pressure has resulted in a consolidated composite with good carbon fiber dispersion. The other approach has involved the dispersion of fine PEEK powder (average particle size 7 μm) onto the carbon fiber reinforcement. The improved wettability of the fine particles has proved to be a significant advantage in the material handling characteristics. By comparison with conventional thermosets, thermoplastic composites such as PEEK and PPS exhibit improved mechanical properties at temperature, chemical/solvent resistance, and, critically, tolerance to accidental damage and environmental (particularly hot/wet)

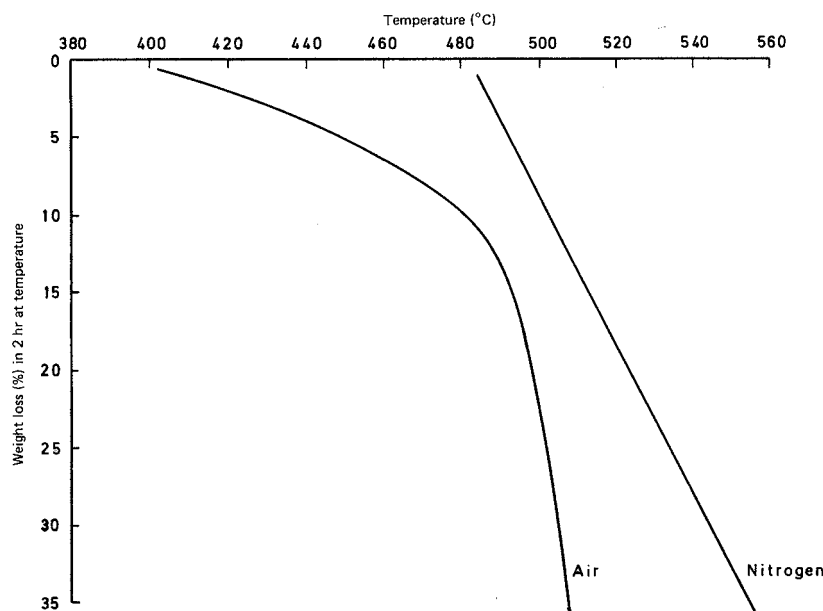


FIGURE 8 Thermal and thermo-oxidative stability of PEEK. [Reprinted with permission from Critchley, J. P., Knight, G. J., and Wright, W. W. (1983). “Heat Resistant Polymers—Technologically Useful Materials,” Plenum, New York. Copyright 1983 Plenum Press.]

resistance. PEEK in particular offers toughness under high levels of impact loading. A recent comparative study of PEEK(APC-2) and PPS studied the effect of drop-weight impact and compression after impact. Although PPS exhibited a high resistance to perforation, PEEK showed an ability to confine the damage and hence had a markedly improved damage tolerance.

Most current applications for PEEK composites are in aerospace. In both fixed- and rotary-wing aircraft, relatively small components such as access doors and leading edge structures are in service. A number of larger, more complex demonstrator structures involving main fuselage and tailplane are under development.

F. Liquid Crystal Polymers (LCPs)

Initial (pre-1985) commercial developments of LCPs included Aramid fiber (Kevlar), based on poly(1,4-phenylene terephthalamide), which is a lyotropic (solvent-processed) material, and the thermotropic Ekkcell I-200 (Xydar) based on *p*-hydroxybenzoic acid. Since 1985 thermotropic LCPs have been developed by duPont and Hoechst-Celanese based on aromatic and condensed aromatic (naphthalene-based) copolyesters which combine a high level of processability with durability and stiffness. Both amorphous and crystalline LCPs—the amorphous-crystalline terminology refers to secondary thermal transitions detected by TGA—have been processed by injection/blow-molding, extrusion (into film and sheet), and thermoforming techniques. The largest outlets for the LCPs are currently in the field of electronic and electrical components in which unreinforced and reinforced (glass- and mineral-filled) have been used. Surface-mount applications of these components require high dimensional and thermal stability provided by the LCPs during vapor phase or infrared soldering.

III. HETEROCYCLIC AROMATIC (HETEROAROMATIC) SYSTEMS

Heteroaromatic systems have been influential in the development of thermally stable organic polymers. Some 40 to 50 polymers have been produced in which phenylene rings alternate or are condensed with predominantly nitrogen containing 5- or 6-membered heterocyclic rings. Significantly, it has been possible to develop exceptionally high levels of stability in often insoluble and intractable polymers that have themselves been obtained from high-molecular-weight soluble and processable precursor polymers via “postpolymerization cyclization” reactions. Even so in some instances, for example, with certain polyquinoxalines and polybenzimidazoles, structural “tailoring” of the final macromolecule made it

possible to achieve an acceptable solubility and processability without intervention of a prepolymer. Synthetic activity was greatest during the 1960s and early 1970s; since then the effort has concentrated on applicational developments and, as a result, it has been necessary to compromise between thermal/thermooxidative stability and processability.

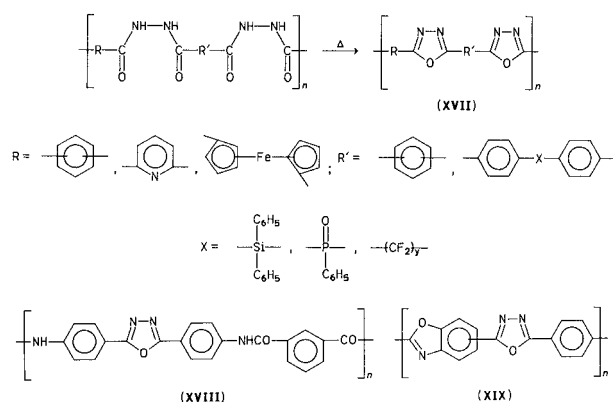
With the notable exception of the polyimides and aryl cyanate ester resins, as well as to a lesser extent the ordered (rigid-rod) polybenzazoles (see below), during the past decade there has been a marked decrease in published references to the heteroaromatic polymer systems, some of which are mentioned below. The continued presence of such systems in this account is, however, intended to reflect the intense activity directed into the development of these thermally stable polymers during the 1960s and 1970s.

A. Ring-Chain

1. Poly(1,3,4-Oxadiazoles)

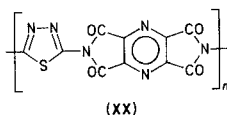
Several routes exist to aromatic poly(1,3,4-oxadiazoles) (XVII), however, cyclization of preformed polyhydrazides has proved most productive of useful (fibers, films) materials.

Aromatic polyhydrazides are soluble in polar solvents and can be solution-cast or spun into films and fibers, which on cyclodehydration yield insoluble intractable poly(1,3,4-oxadiazoles) in the same material form. The wholly aromatic system (XVII; R = *m*-C₆H₄, R¹ = *p*-C₆H₄) in the form of fiber or film exhibits a 60% strength retention in air after 24 hr at 400°C, 50% after 700 hr at 300°C. Introduction of flexible groups midchain leads to an increase in tractability but a decline in thermal/thermooxidative stability. Aliphatic-linked poly(1,3,4-oxadiazoles), for example, are readily soluble in polar solvents with melt temperatures around 150–200°C (aromatics > 400°C) and major (TGA) weight loss in both inert and oxidizing atmospheres between 300 and 350°C (aromatics 400–480°C).



The success of wholly aromatic poly(1,3,4-oxadiazoles) as fiber-forming materials generated interest in the inclusion of the 1,3,4-oxadiazole moiety into ordered heterocycle–amide copolymers (XVIII) and wholly ordered heterocycle copolymers (XIX). Although “tailored-in” improvements to mechanical properties, tractability, and even thermal/thermo-oxidative stability have been observed, a relatively poor light stability for these materials has limited useful development.

Analogous homo- and copoly(1,3,4-thiadiazoles, S replacing O in the heterocycle ring, are similarly film- and fiber-forming materials exhibiting somewhat higher thermooxidative stability than the 1,3,4-oxadiazoles. A hydrogen-free alternating imide–thiadiazole copolymer (XX) film showed outstanding thermal/thermooxidative stability (weight loss in air and nitrogen and retention of strength) up to 600°C.



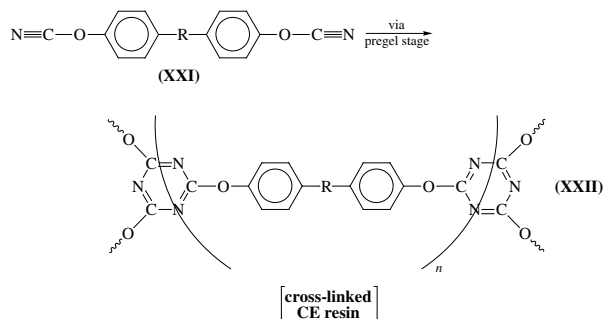
2. Aryl Cyanate Esters

The first successful route to the aryl cyanate esters (CEs), compounds containing the O—C≡N moiety, originated in the late 1960s via reaction of phenols with cyanogen chloride using a technology pioneered by Bayer AG. Further research and development of this process by Mitsubishi, Gas Chemical Corporation, Rhone Poulenc, Ciba Geigy, and Dow Chemical, among others, has provided a variety of commercially available, but relatively high priced, monomers and prepolymers. Of special significance has been the introduction of dicyanate esters (XXI) in which the bridging heteroatoms or groups (—R—) have provided a range of structure–property variations.

CEs (XXI) polymerize via a cyclotrimerization step-growth reaction, progressing from low-molecular-weight monomer, through a prepolymer (pregel) stage to the final cured polycyanurate resin (XXII). This conversion, frequently occurring with >98% efficiency, is promoted thermally, aided by transition metal salts or chelates in the presence of an active hydrogen cocatalyst. While the final resins are correctly referred to as polycyanurates, the term cyanate ester is most often used to describe both prepolymers and thermoset resins.

The excellent thermal stability of the CE resins is associated with the aromatic character of the *sym*-triazine ring system generated during the cyclotrimerization reaction and, as thermally stable systems, they occupy a position between epoxies and bismaleimides (BMIs). However, compared to these two systems, CE resins exhibit a rel-

atively low cross-link density (increased toughness), low moisture absorption, and a low dielectric constant. Significantly it is the relatively high T_g values of CE polymers linked to their hydrophobicity that has been instrumental in generating the major interest in potentially advanced applications.



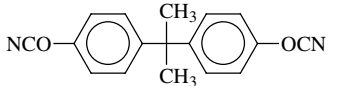
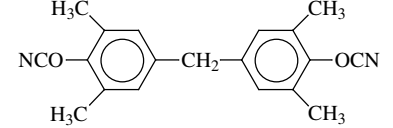
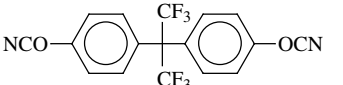
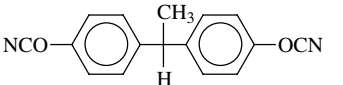
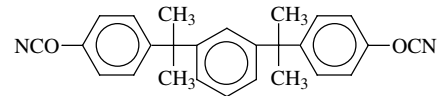
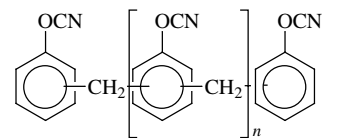
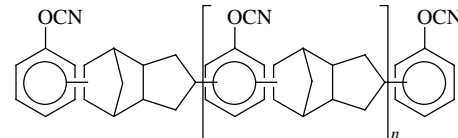
The low viscosity of monomers and prepolymers facilitates processing of CE resins using a variety of traditional techniques. This ease of processing, allied with their environmental stability has, during the 1990s, led to a number of “high-tech” applications for CE resins both as unreinforced and as carbon fiber composite materials. They have proved to be strong candidates in the choice of materials for a variety of general microelectronics applications as well as materials of choice in aerospace applications including their selection as structural composites in primary and secondary structures in both military and civilian aircraft.

Typical resin systems that have demonstrated limited commercial success are shown in Table VI, the limitation being the relatively high price of the resins. Despite the significant improvements in “use” properties shown by CE resins over comparable systems, for example, they exhibit twice the fracture toughness (G_{IC}) of typical epoxies, a broadening of their commercial potential has been achieved by the inclusion of toughening additives or the formation of blends.

The use of conventional rubber additives, for example, those based on butadiene acrylonitrile elastomers, improved the level of toughness but has resulted in some reduction in T_g and thermo-oxidative stability.

Oligosiloxane elastomers have been reported to toughen CEs without a commensurate limitation in such properties. Alternatively, thermoplastics (TPs) such as poly(arylene ether ketone) and poly(ether sulphone) have proved to be effective toughening agents for the resins. Up to fourfold increases in G_{IC} have been reported with little or no reduction in T_g . Thermoplastics have been incorporated either into the bulk of the CE resin or, alternatively, they have seen limited use in the interply/interlaminar (ILT) toughening of CE prepregs. It has been reported that cured ILT

TABLE VI Chemical Structure of Commercial or Developmental Cyanate Esters Available in Monomer and/or Prepolymer Form

Polycyanate monomer structure/precursor	Tradename/supplier	1994 cost (£/kg)	Melting point/viscosity at 25°C	Homopolymer property			
				T_g (°C)	% H ₂ O	D_k at 1 MHz	G_{IC} (Jm ⁻²)
 Bisphenol A	AroCy B/ Ciba-Geigy BT-2000/ Mitsubishi GC	29	Crystal 79°C	289	2.5	2.91	140
 Tetramethylbisphenol F	AroCy M/ Ciba-Geigy	44	Crystal 106°C	252	1.4	2.75	175
 Hexafluorobisphenol A	AroCy F/ Ciba-Geigy	99	Crystal 87°C	270	1.8	2.66	140
 Bisphenol E	AroCy L/ Ciba-Geigy	66	Liquid 90–120 cP Semisolid 29°C ^a	258	2.4	2.98	190
 Bisphenol M	RTX-366/ Ciba-Geigy	68	Liquid 8000 cP Semisolid 68°C ^a	192	0.7	2.64	210
 Novolac resin	Primaset PT/Allied Signal REX-371/ Ciba-Geigy	68	Semisolid 250,000 cP ^b	270– >350	3.8	3.08	60
 Dicyclopentadienyl bisphenol	XU-71787 Dow Chemical	—	Semisolid 1000 cP ^c	244	1.4	2.80	125

Cured state properties: T_g , glass transition temperature (DMA); % H₂O, water absorption at saturation (100°C); D_k , dielectric constant; G_{IC} , fracture energy (double torsion method).

^a Melting point of supercooled liquid; ^b PT30; ^c XU71787.02 (at 82°C).

composites show exceptional impact resistance allied to a dramatic reduction in delamination on impact.

An alternative approach to improving the properties of the base CE resin has involved a thermoset–thermoset

blending processes. Combining different CE monomers frequently improves not only their initial individual rheological behavior but it can also result in improved properties for the cured resin. By using the correct

blends, significant improvements have been observed for thermal/thermo-oxidative stability and hot-wet mechanical strength.

Epoxy resins are miscible with, and coreact with, CE resins resulting in hybrid products with improved properties, e.g., increased T_g and better electrical resistance compared with the parent epoxy.

A number of epoxy/CE systems have been used in applications where the relative cheapness of the epoxy resin makes a significant difference to the commercial viability of the product. Blending CEs with BMIs has enhanced the toughness characteristics of the latter resin systems and a range of blended materials (Skyflex^R BT resins) has been produced by Mitsubishi Gas Chemical Corporation. Originally it was believed that the CE/BMI resin systems coreacted on blending. However, it is now considered that an interpenetrating network (IPN) is established, indicated by the fact that two distinct T_g values are observed originating from the independent CE and BMI networks. The lower valued of these T_g values governs the “use” temperature of the blend.

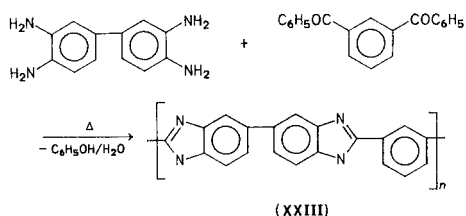
The introduction of reactive allyl groups into the CE monomer has been reported to facilitate copolymerization with the BMI component, producing a linked interpenetrating network (LPN) with a single high T_g and a G_{IC} higher than for either homopolymer.

B. Bi- and Tricyclic Polymers

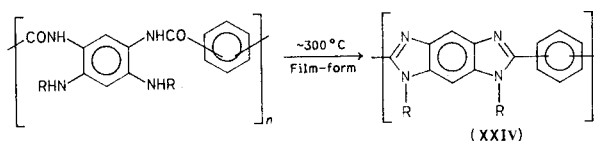
1. Polybenzazoles—Polybenzimidazoles

The extension of conventional polycondensation processes from simple aliphatic systems to high-temperature heteroaromatic polymers was first observed for the polybenzimidazoles (PBIs). Practical, semicommercial applications—adhesives, fibers, composites—were soon evaluated, but this initial progress was not sustained and the aromatic polyimides soon took, and retained, “center-stage” as the most important applicational heteroaromatic polymer system. However, techniques of synthesis, and structure versus property data evaluated for PBIs have been of considerable value in the development of other polyheteroaromatics.

The main synthetic route to PBIs involves the reaction of aromatic tetraamine with dicarboxylic acid esters under melt conditions, typified below for the formation of poly(2,2'-*m*-phenylene-5,5'-bibenzimidazole) (XXIII)

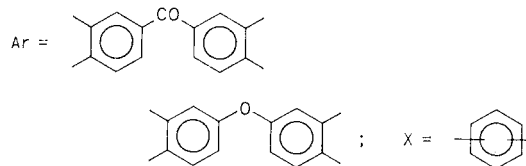
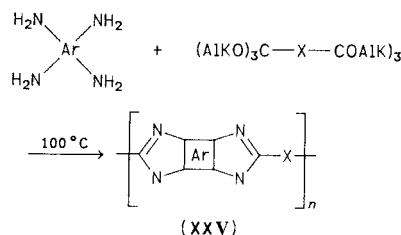
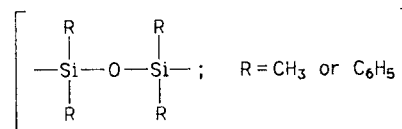


A staged heating (220–280°C) under nitrogen produces an oligomeric prepolymer with evolution of phenol and water; above 350°C (*in vacuo*) complete conversion to the high-molecular-weight, intractable PBI occurs via a solid-state process. Most PBI variants have been produced by this melt–polycondensation route; however, a limited number are prepared in solution using high boiling polar solvents. Examples are the formation of the substituted PBIs (XXIV) via the “open-chain” poly(aminoamide) intermediates:



and interaction of aromatic tetraamines with bisorthoesters to produce high-molecular-weight film- and fiber-forming PBIs (XXV).

Structural modifications to the wholly aromatic PBI system have involved incorporation of both relatively simple midchain flexible groups [$(-\text{CH}_2)_n$], $-\text{SO}_2-$, $-\text{O}-$] and more complex units such as siloxanes



In general, improvements that these groups make to the solubility/processibility of the polymers are linked with reductions in thermal/thermooxidative stability. However, the substitution of the imidazole N—H by *N*-phenyl (XXIV) provides an improvement to both processibility and long-term thermooxidative stability (Fig. 9). A comparison of weight loss data for typical wholly aromatic heterocyclic polymers, first under inert conditions (TGA) then in air (ITGA), highlights the basic oxidative instability of the PBI system:

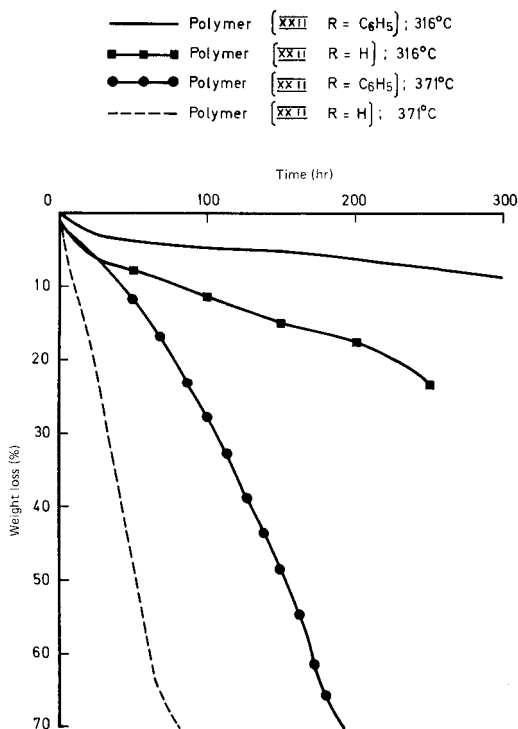


FIGURE 9 Isothermal weight loss in air for PBI and *N*-phenyl PBI. [Courtesy of Spain, R. G., and Ray, J. D. (1967). In "Conference on Stability of Plastics," pp. E1–E4, Society of Plastic Engineering, Washington, DC.]

1. Helium (TGA)

Polybenzothiazoles \geq polybenzimidazoles
 > polyimides > polybenzoxazoles
 > polyquinoxalines

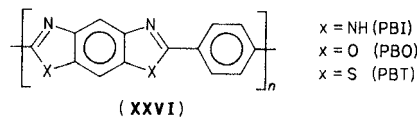
2. Air (ITGA)

Polyimides > polybenzoxazoles
 > polyquinoxalines > polybenzothiazoles
 > poly-*N*-phenylbenzimidazoles
 \gg polybenzimidazoles

Materials applications such as glass-reinforced composites and filament-wound structures, metal-to-metal adhesives, films, fibers, and foams have involved only the wholly aromatic PBI (**XXIII**). Processing is conducted at the prepolymer stage and, for the adhesives and laminates, a major drawback is that they must be stored under refrigerated conditions. The only application to have made some headway against strong competition from the polyimides is the PBI fiber. Postspinning techniques of orientation/crystallization of the predominantly amorphous fiber allow the attainment of optimum properties. PBI fibers exhibit outstanding nonflammability/low smoke generation in air under extreme conditions; fabrics have been chosen for the hazardous environments associated with aircraft and spacecraft.

2. Polybenzazoles—Ordered Polymers

Highly ordered (rodlike) polymers derived from wholly *para*-linked polybenzazoles (**XXVI**) have been developed primarily as high-temperature fibers and self-reinforcing resins.



Typically, PBO (**XXVI**, X = O) was originally developed as a fiber by the Stanford Research Institute. It is now marketed as Zylon^R by Dow Chemical, Co. who, in conjunction with the Toyobo Research Center (Japan), have devised a unique spinning technology to produce fiber with a tenacity >5.8 GPa.

Polybenzothiazoles (PBT) and polybenzoxazoles (PBO) have merited particular attention since, like the ordered aromatic polyamides, they form liquid crystalline solutions. They are prepared in polyphosphoric acid (PPA) solution with very high intrinsic viscosities \sim 30 dL/g. The spinning of the liquid crystalline solutions provides fibers of exceptional stiffness and strength. Typical of the heteroaromatic polymers, thermooxidative stability is high (superior to the ordered polyamides); for PBT, weight losses of 2% at 316°C and 50% at 371°C after 200 hr have been reported. A comparison of strength and modulus properties of PBT and conventional reinforcing fibers is shown in Table VII. In a further development both PBO and PBT are under investigation as high-strength/high-modulus resins. In this material form, the elimination of

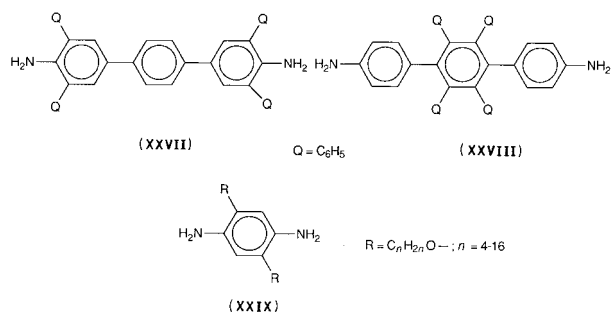
TABLE VII Tensile Properties of Ordered PBT Fibers Compared with Alternative Reinforcements^a

Fiber material	Tensile strength (MPa)	Tensile modulus (GPa)	Specific gravity
Boron	3174	414	2.60
Alumina	1380–3450	380	3.60
Silicon carbide	3450	290–331	3.20
Carbon	2346–5500	207–345	1.78
Polybenzamide	2760	131	1.45
Polyethylene	3001	90	0.95–0.98
Polybenzothiazole	1518	186	1.40
E Glass	1725	69	2.54
Polyterephthalamide (Kevlar 49)	3720	124	1.44

^a Reprinted with permission from Critchley, J. P., Knight, G. J., and Wright, W. W. (1983). "Heat Resistant Polymers—Technologically Useful Materials," Plenum, New York. Copyright 1983 Plenum Press.

difficulties associated with the processing and fabrication of conventional laminates together with those of fiber-resin property mismatch (e.g., difference in expansion coefficients) is of considerable importance.

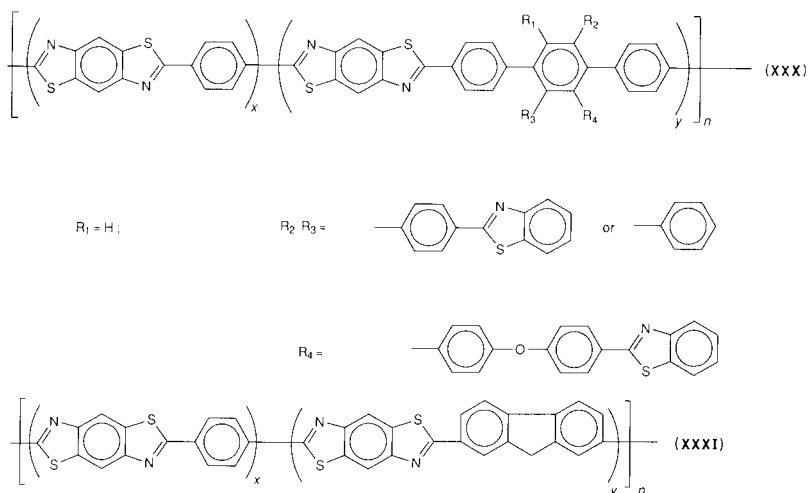
The heteroaromatic rigid-rod molecular composites continue to excite considerable research interest. Molecular composites are composed of binary blends of reinforcement having a high aspect, high strength, rigid structure dispersed in a flexible coil polymer matrix. Research has continued into PBT, PBO, PBI, and BBL (see Section II.C.2) as the rigid-rod polymers. Ordered polypyromellitimides produced from highly phenylated diamines (**XXVII** and **XXVIII**) or alkoxy-substituted diamines (**XXIX**) have been described.



PBT, however, remains the most frequently investigated of the rigid-rod polymer systems—heat-treated samples have demonstrated a tensile modulus of 330 GPa and a tensile strength of 3 GPa—acting in combination with a variety of flexible coil polymers such as nylon-6, 6-, poly-2,5(6)-benzimidazole, PEEK, and BBB (see Section II.C.2). One major barrier which has prevented the extensive characterization of structure and solid-state properties, as well as application of the rigid-rod/flexible coil matrix system, has been the problem of insolubility in

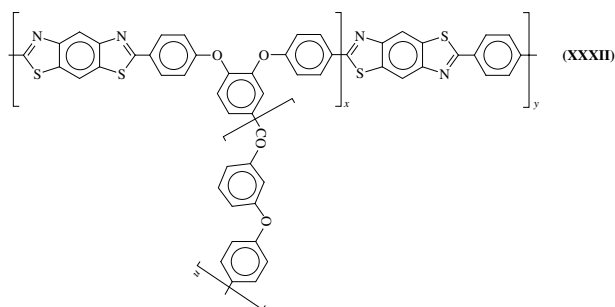
conventional organic solvents from which such materials could readily be processed into films, coatings, or fibers. While soluble in strong acids, e.g., methanesulfonic acid (MSA), such a corrosive medium presents extremely difficult processing problems, and attempts to resolve the dilemma have been made. PBT, is, for example, soluble (up to 10 wt%) in nitroalkanes or nitrobenzene which contain Lewis acids (e.g., FeCl₃, AlCl₃). Solvent casting onto glass, sapphire, or silicon wafers has given films of PBT/MX_n complexes which after immersion in non-solvent produce clear coatings of pure PBT. An alternative approach to the solubility dilemma has been to introduce hydroxy, alkoxy, alkyl, and sulfonic acid side groups into the basic PBT system. Highly ordered rigid-rod polyimide structures have been introduced into flexible coil matrices via a DMAC-soluble polyisoimide intermediate. The isoimide and flexible coil matrix (polysulfone or acetylene-terminated polyimide thermosets) were blended in solution. Heat treatment after coagulation and film-casting converts the isoimide to the rigid-rod polyimide structure. Characterization of these systems is under way.

Despite the ability of rigid-rod PBT to be spun into fibers having a nearly perfect uniaxial orientation with state-of-the-art tensile strength and modulus, it suffers from a relatively low axial compression strength (~450 MPa). The highly oriented polymer chain buckles under compressive loading, and attempts have been made to “tailor-in” resistance to this compressive weakness. Such techniques have included the introduction of bulky main-chain pendant groups e.g., (**XXX**) in order to disrupt the nematic packing order. In another approach, cross-linking via reactive fluorene units in-chain (**XXXI**) has been investigated. In neither of these approaches have improvements yet been observed to the compressive behavior of the basic PBT system.



Other potential cross-link sites have been introduced into the rigid-rod (PBT/PBO) molecules. These include methyl, halogen, ethynyl, phenylene sulfide, and cyclobutene (BCB) moieties. The cyclobutene derivatives are reported to cross-link via quinone methide intermediates, which then undergo cycloaddition or dimerization reactions. In the case of the PBT/BCB system, phase separation occurred between rigid-rod and matrix components and the desired synergistic effects were not realized. However, with the PBO/BCB system, there was no phase separation after heat treatment and this resulted in excellent tensile properties and improved resistance to delamination.

In a novel approach, bulk rigid-rod molecular composites (XXXII) have been obtained by powder consolidation of a copolymer with a PBT derivative as the backbone reinforcement and polyetherketone (PEK) thermoplastic side chains as the flexible matrix. Compared to PEK homopolymer, copolymers with a low rod content exhibited significant increases in T_g and tensile properties. However, higher rod content resulted in a significant phase separation and consequent decreases in T_g and reinforcement efficiency of the molecular composite.



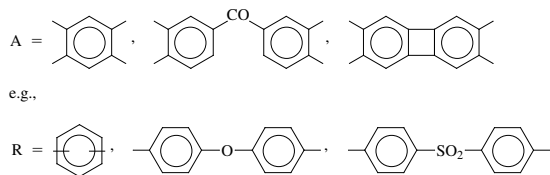
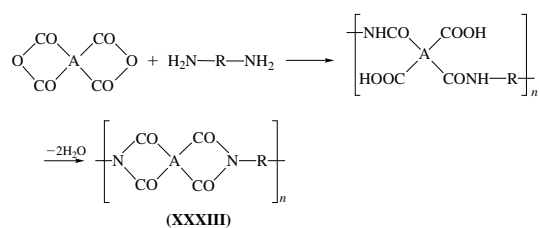
3. Polyimides

The emergence of polyimides as technologically and commercially viable materials remains the cornerstone of activity for thermally stable heteroaromatic polymers. This results both from the ability to adapt available synthetic routes to the increasing requirement for processable products as well as the high level of thermal/thermo-oxidative stability compared for example with other heteroaromatic systems (Fig. 10).

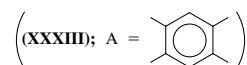
Research and development into the aromatic polyimides remains the most prolific and productive area of the heteroaromatic polymers. Activity has covered condensation and addition-type systems, the former produced predominantly via postpolymerization cyclization of precursor poly(amic-acids). Although condensation polymers were the first to be commercially exploited (e.g., H-film), the addition systems subsequently provided the major commer-

cial advances, particularly in the field of advanced composites. However, in the 1990s there was renewed interest in the synthesis, structure, and commercial potential of the condensation-type polymers.

a. Condensation polyimides. Wholly aromatic polyimides (XXXIII) are almost invariably insoluble and infusible; as a result while strictly not cross-linked, at least as prepared, they are referred to as “thermoset types.” Synthesis involves the low-temperature polycondensation (in dipolar aprotic solvents) of a dianhydride and diamine to produce a soluble/fusible intermediate poly(amic acid) followed by a chemically or, preferentially, thermally induced postpolymerization cyclization.



A vast array of aromatic polyimides—particularly polyarylethers—has been produced.



The approach via the soluble intermediate is especially suitable for the formation of films, coatings, and fibers but to achieve optimum properties (high molecular weight) the control of precursor purity and stoichiometry/mixing order is critical as is also the storage of the hydrolytically unstable poly(amic acid) under rigorously dry refrigerated conditions. For laminating/adhesive formulations the attainment of a high molecular weight is less important than are those processing problems associated with a limited shelf-lived intermediate, void-forming volatiles (water, high boiling solvent) liberated during cyclization, and the proximity of softening/flow temperature to that of cyclodehydration. These processing difficulties have been reduced using variously modified poly(amic acids) and, for example, the diacetylated intermediate (XXXIV) prepared in low-boiling solvents is hydrolytically stable with a

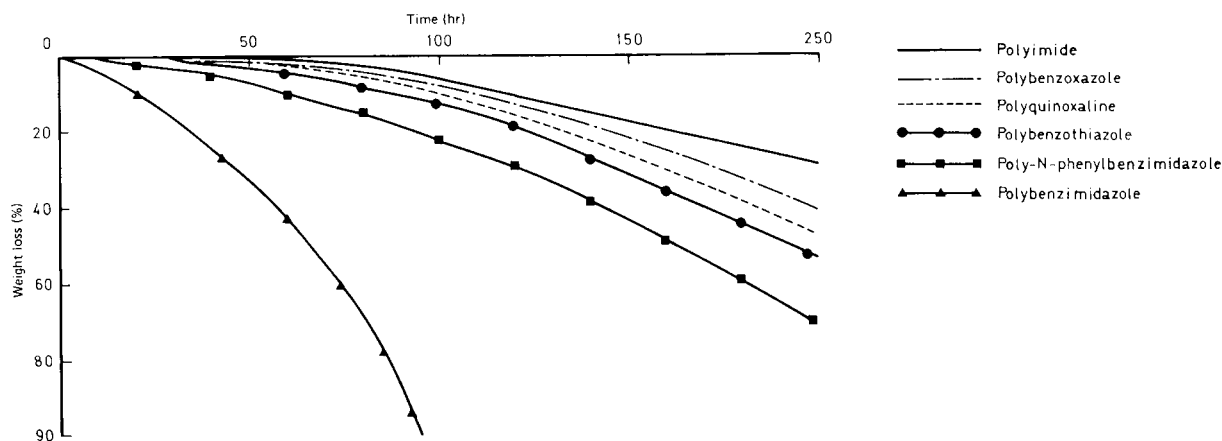
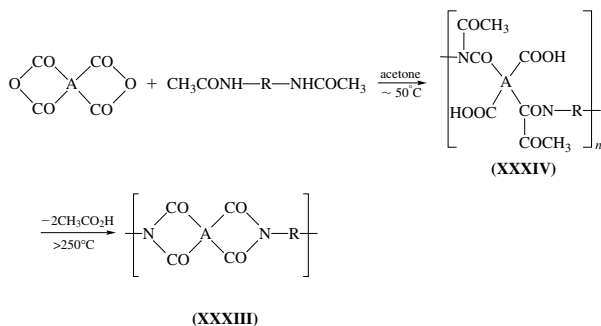


FIGURE 10 Isothermal weight loss in air (371°C) for various heteroaromatic polymers. [Reprinted with permission from Hergenrother, P. M. (1971). High temperature organic adhesives, *SAMPE Q*, 3, 1. Copyright 1971 SAMPE.]

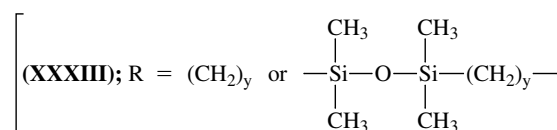
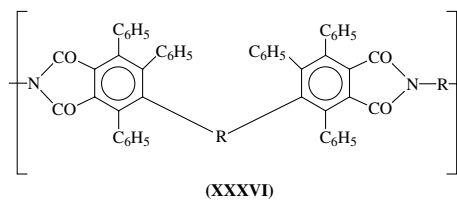
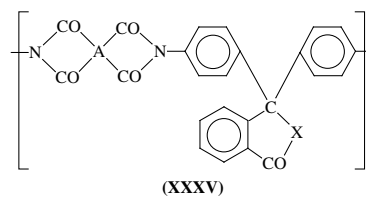
temperature of cyclization significantly above that of resin flow.



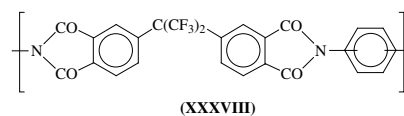
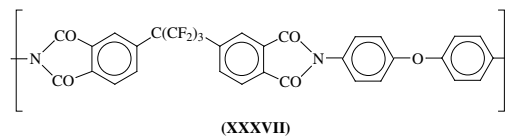
Commercial exploitation of thermoset polyimides based principally on pyromellitic dianhydride (PMDA) or benzofenone dianhydride (BTDA) includes Kapton H and HF (films), Pyre-ML (coating), Vespel (SP molding grades), Pyralin (glass prepreg), Skybond (solutions for films, coatings, varnishes), FM-34 (adhesive) and QX-13 (glass/carbon-reinforced prepreg).

“Thermoplastic” aromatic polyimides are designed to overcome the processing problems of the thermoset systems. Modifications to the basic polymer structure have conferred sufficient solubility and/or fusibility to allow, in some cases, fabrication by conventional thermoplastic techniques at the fully imidized stage. Bulky groups present in polymers. (XXXV) and (XXXVI), reduce crystallinity and close packing effects enhancing solubility (in polar solvents), but not fusibility (T_g values $>400^\circ\text{C}$), without affecting the characteristically excellent aromatic-imide thermal/thermooxidative stability.

Tractability and hence processability are significantly increased by introducing extended flexible “hinge” groups into the chain, but in polymers

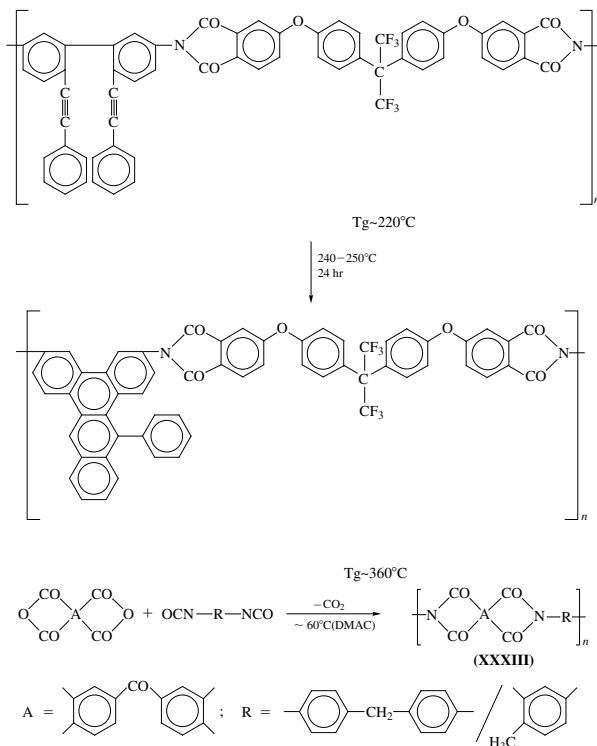


for example, the aliphatic content induces a much lower ($\sim 100^\circ\text{C}$ drop) thermo-oxidative stability. Alternatives have been investigated; in polymers (XXXVII) and (XXXVIII) adequate processability does not, however, preclude a high thermal or thermo-oxidative stability.



The application of these thermoplastic fluoro-polyimides as structural adhesives or laminating resins

at elevated temperatures ($>300^{\circ}\text{C}$) requires long-term strength retention above the initial T_g and processing temperatures. Postcyclization intermolecular crosslinking (above 340°C) leading to a thermoset system (with significantly increased T_g) has been one practical approach. Alternatively (see following discussion), intramolecular cycloaddition (IMC) of suitably active pendant groups increases chain-stiffening and ceiling-use temperature (final T_g) by increasing the proportion of in-chain fused rings.

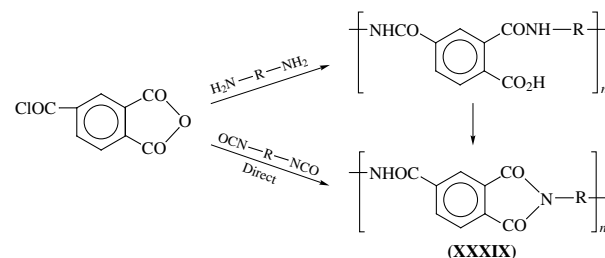


The advantages of “IMC cure”—absence of volatiles and an essentially linear (tough) rather than potentially brittle final structure—have been introduced into other heteroaromatic polymers, most notably the polyquinoxalines.

An increased processibility in fully cyclized aromatic polyimides is also introduced by the deliberate “tailoring” of a random sequence into the polymer chain, the resultant dissymmetry accentuating the amorphous as opposed to the usually extensive crystalline character of such materials. A polymer (XXXIII) produced, without formation of an open-chain intermediate, from dianhydride and mixed diisocyanates, is marketed (PI2080) as a molding resin and fiber/film-forming solution.

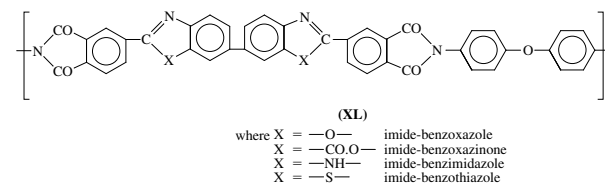
Copolyimides incorporating amide, ester, or ether groups are commercially widely applied thermoplastics whose relative ease of processing has been achieved with some sacrifice to thermal stability. Typically, poly(amide-imides) (XXXIX) are most frequently prepared by

reaction of diamines or diisocyanates and trimellitic anhydride:

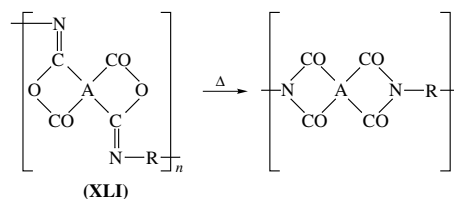


Used in laminating/molding resins or coating applications these amide-imides can withstand, depending on the nature of the R group, temperatures up to 290°C for 2000 hr.

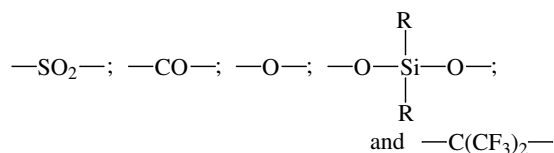
Heterocyclic-imide copolymers (XL) with ordered structures have high T_g values, crystallinity, and thermal/thermo-oxidative stability but commensurately reduced tractability. A limited solubility in polar solvents has allowed fabrication of high-modulus fibers. Processability more closely matched to that of amide-imide copolymers is practicable, however, when similar heteroaromatic groups are distributed in limited-or random-order through the polymer chain.



Commercially available condensation (thermoplastics) include polyimides: Avimid fluoropolyimides (solution and carbon fiber reinforced preregs), PI 2080 (molding resins and solution); amide-imides: Torlon (molding resin and carbon, glass and PTFE preregs), AI (solution), Kerimid 500 (solution); ester-imides: Terebec (solution), Isomid (solution); ether-imide: (molding- and matrix-resins); and benzheterocyclic-imide: PIQ (Film). The poly(amic-acids) (PAAs) continue to be used as intermediates in the formation of polyimides (PIs) in, for example, the production of fibers, films, and coatings. Improvements remain to be resolved in stability and processing properties of the PAAs, and the preparation of PIs from PAAs via the hydrolytically stable isoimides (XLI) in a dicyclohexyl carbodiimide medium is an attractive alternative.



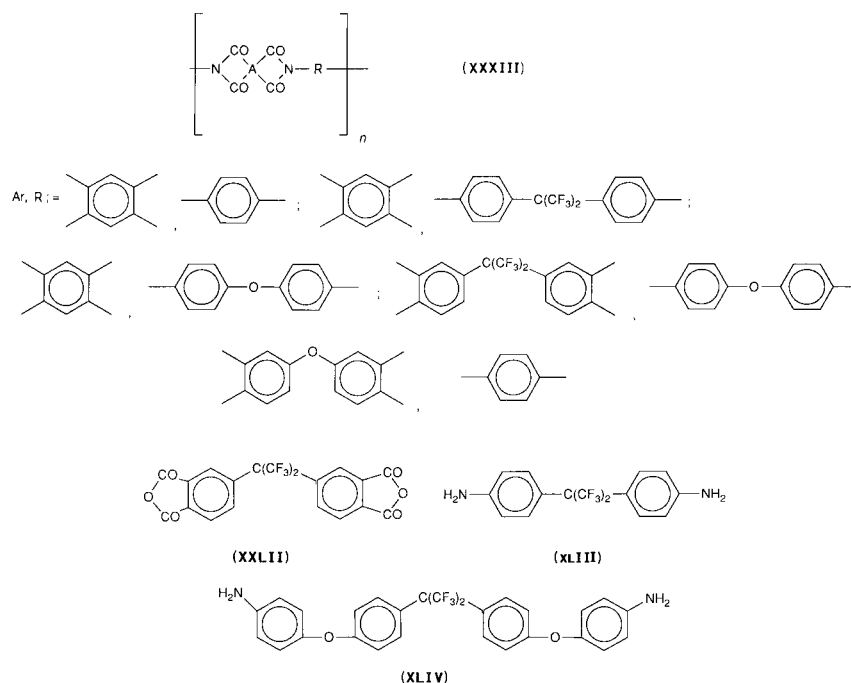
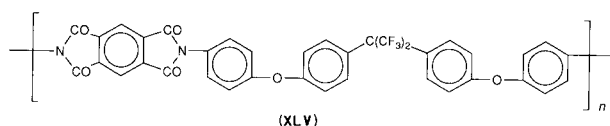
The search for thermoplastic replacements for the conventional thermosets remains a key factor in the advancement of condensation PIs. Studies of structure–property relationships on processing and fabrication have included an examination of the effects of wholly *para*- versus *meta*-*meta*- and *meta*-*para*-links between aromatic rings, as well as a continuing assessment of the most effective in-chain flexible “hinge-groups.” Based on frequency of appearance these are:



“Tailoring” of PI properties to meet specific product requirements can also be achieved via use of copolymers or polymer blends. Polymer blending is particularly attractive and frequently used due to the ease of property modification by this means. Binary blends of PIs with, for example, PBIs or PEEK have provided products miscible over the entire composition range. Blending of various PIs (XXXIII; see below)—best achieved at the intermediate soluble PAA stage—has also produced discrete products miscible over the whole composition range.

mers, random copolymers, and polymer blends of these PI systems. There is continuing R and D evidence to the value of the $\text{—C(CF}_3)_2\text{—}$ “hinge unit” in PI structures, introduced via the dianhydride (XLII) (6F) or diamines (XLIII) and (XLIV) (4-BDAF).

The first commercial fluorinated PI was based on dianhydride 6F. Known as Avimid-N (originally NR-150B), it exhibits quite outstandingly good stability and property retention, both as reinforced and unreinforced material. In particular, it exhibits considerable resistance to microcracking following thermal cycling. Certain fabrication difficulties caused its withdrawal from production in the mid-1980s, but it seems likely to be reintroduced in modified form in the near future. Diamine 4-BDAF is used in a number of PI research formulations. To date the partially fluorinated polyimide (XLV) has shown considerable promise as a thermoplastic matrix in carbon fiber reinforced molding resins. As a prototype jet engine accessory, after 100 hr at 357°C (in air), weight loss of the component was only 8%.



Comparisons have been made of the crystallinity, thermal stability, and mechanical properties of homopoly-

Condensation PIs are used extensively in the field of microelectronics as thin film dielectric interlayers in

semiconductor devices. By “tailoring” properties in the ways already described, the major in-built advantages of the PIs—high thermal stability, excellent mechanical properties, and low dielectric constant—can be reinforced by improved processibility (including highly planar coatings), increased adhesion, and low thermal expansion coefficient. Recently reported are polypyrrole-PI composite films which combine high electrical conductivity with high thermal stability. Two types of film are available: Type 1, a polypyrrole-coated PI with maximum conductivity of 10 Scm^{-1} and Type 2, a PI film loaded with finely divided polypyrrole particles, producing a maximum conductivity of $5 \times 10^{-4} \text{ Scm}^{-1}$. Both types having a thermal stability up to 350°C . Applications of the condensation PIs as matrix materials for structural composites are more limited than for addition-type PIs. A thermoplastic PI (LARC-TPI) has been developed as an adhesive or coating product from the (XXXIII) system above. It has also been commercialized (Duramid) as a tough and strong (tensile strength 153 MPa, tensile modulus 4.3 GPa) molding resin.

Perhaps the most novel reported application is that of film produced from a blend of PBI and a poly(siloxane-imide) copolymer. Conventional Kapton (PI film), used as a thermal blanket and protective coating on the space shuttle, is rapidly eroded by the action of atomic oxygen. In the blended film, however, the siloxane component continuously migrates to the film surface, where reaction with atomic oxygen converts it to a protective silica coating.

During the past decade continued efforts have been made further to capitalize on the stability and applicational development of condensation-type polyimides.

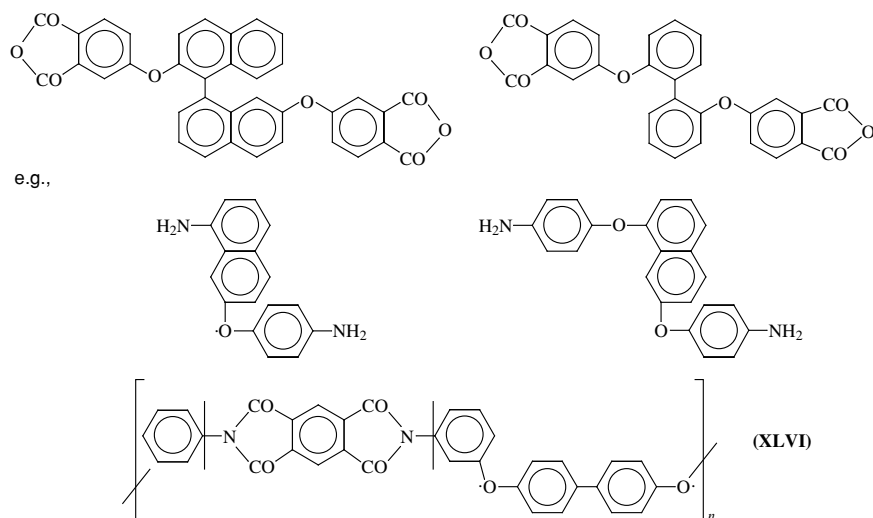
The link between polyimides (PIs) and silica referred to above has been extended to carbon fiber composites based

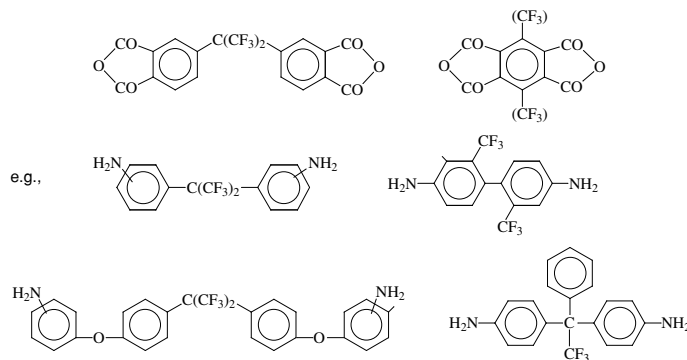
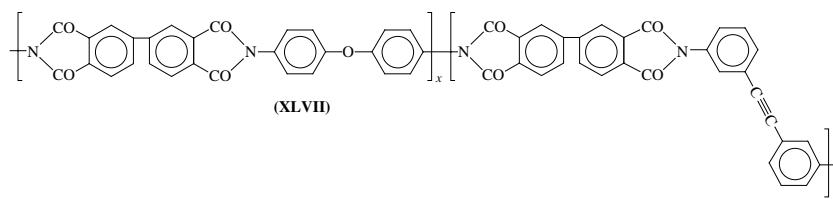
on PI/silica ceramers (polymer-ceramic hybrids). These ceramers contain nanoscale silica domains trapped in the PI matrix, the composites exhibiting lower thermal expansion and higher thermal stability compared with carbon fiber/PI-only composites.

Maintaining the thermal/thermo-oxidative stability of PIs, while simultaneously increasing their solubility and processibility, is an ongoing aspect of R&D. The introduction of large bulky units (e.g., the adamantane group) pendant to or in-chain continue to feature in breaking up the regular symmetric structure of aromatic PIs.

Significant advances in processibility have also been achieved in those thermoplastic PIs formed from the complex ether-linked dianhydride and diamine precursors examples of which are featured below. The “cranked/twisted” nature of these precursors confers a noncoplanar structure, which again inhibits chain packing in the polymer structure. The thermoplastic polyimide New TPI (XLVI) exhibits crystallization and melting behavior similar to high-performance poly(aryl ether ketones). However, both bulk crystallization and linear crystallization rates are significantly slower and the T_g higher in New TPI probably due to a decreased chain mobility. Blends of New TPI with other high-performance polymers have been reported.

Polyimides have featured prominently in the development of rigid-rod molecules and related molecular composites. Typically, a molecular composite has comprised a rigid-rod component (XXXIII), $A = \text{C}_6\text{H}_4\text{CO-C}_6\text{H}_4\text{-CH}_2\text{-C}_6\text{H}_4$ and a flexible matrix (XLVII). A high-modulus composite film has been obtained in which cross-linking of ethynyl groups afforded enhanced performance at higher temperatures.





Two aspects of polyimide development that have recently received strong research attention are, first, the use of polymer thin films as gas separation membranes (permeability and permselectivity) and, secondly, their use as low dielectric constant material for microelectronic devices. In both of these applications, the most recent advances have featured the introduction of fluoro groups as links between phenylene rings and/or as phenyl-ring substituents in the polymer chain. Examples of polyimide dianhydride and diamine precursors are shown below.

In both applications, the high thermal stability and excellent mechanical properties observed in polyimides are important. In the former case, simultaneous improvements to permeabilities and permselectivities have been achieved by the reducing packing and local motion of polymer chains in the fluoro-polyimides.

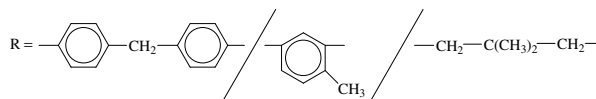
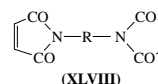
It has been suggested that the presence of, for example, $-\text{C}(\text{CF}_3)_2$ groups in the polyimide chain lowers the dielectric constant by decreasing interchain electronic interactions. Certainly, the key to the successful production of microelectronic components is the lowest attainable dielectric constant insulating material. The fluorinated polyimides referred to above have emerged as a favored class of such materials.

Applications that require this high level of performance include thin-film wiring in high-density electronic packaging such as large-scale and very-large-scale (LSI and VLSI) integrated circuits; fibers used in low dielectric constant laminates for high-speed multilayer printed wiring boards (PWBs); and foamed films (“nanofoams”), incorporating nanometer-length scale voids, which have been

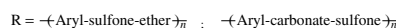
considered for use as very low dielectric constant insulating materials.

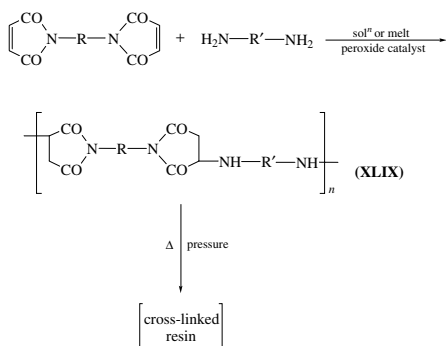
b. Addition polyimides. Addition polyimides are based on short pre-imidized units end-capped with reactive (unsaturated) aliphatic or cycloaliphatic groups. Polymerization occurs at relatively low temperature and pressure by chain extension/cross-linking processes. Good flow/wetting characteristics of the low-molecular-weight prepolymers have played a key role in the successful development of such systems as matrix resins in advanced carbon fiber reinforced composites.

Currently, bismaleimides (XLVIII) are considered to be the most successful of the addition polyimides based on their performance-to-cost characteristics. Alone, they are most effectively thermally polymerized, in the presence of free-radical catalysts, to produce the cured resin directly. Alternatively, using nonstoichiometric mixtures of BMI and aromatic diamine, under carefully controlled conditions, cured resins are produced via the initial formation of the polyaspartimide (XLIX).



or

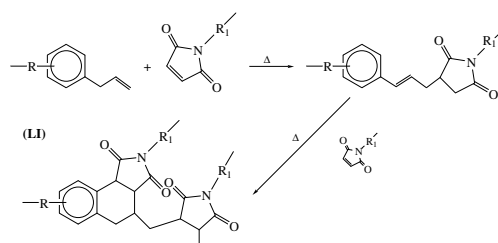
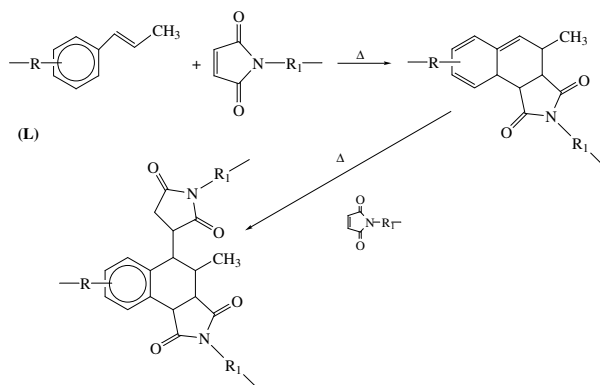




BMIs have attractive processing characteristics, similar to the epoxy resins but with the bonus of higher temperature performance. Prepregs are produced by impregnating fiber matrix from the melt or from a solution of the monomers. BMI resins are available in a wide range of commercial resin systems. Although single monomers can be used, they invariably produce rather brittle products and more frequently eutectic mixtures of monomers are supplied in order to lower the viscosity of the melt and improve the wetting/flow behavior on the fiber matrix.

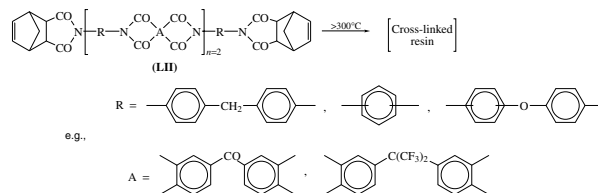
Other techniques have been used to improve the toughness characteristics of the BMIs. The introduction of flexible groups, e.g., urethane or epoxy segments in the polymer chain, while improving toughness, limits the thermal stability of the BMI resin. Addition of liquid rubber during cure has produced a two-phase system that contributes to a much tougher resin. Unfortunately, the presence of the rubber modifier also increases susceptibility to hot/wet degradation.

Improvements to the processing and mechanical properties of BMI resins have also been achieved by melt blending base monomers, including close-to-eutectic mixtures, with propenyl (**L**) or allyl (**LI**) substituted comonomers. Proposed reaction schemes that postulate Diels–Alder cycloaddition mechanisms are shown below.



The resulting modified materials have exhibited enhanced mechanical and environmental (hot/wet) properties over the base BMI resin system. For example, compared with a fracture toughness ($G_{IC} = 50 \text{ J/m}^2$) for base resin, the optimized cured BMI/allylphenyl comonomer blend exhibited significantly enhanced toughness ($G_{IC} = 500\text{--}600 \text{ J/m}^2$). Properties of the carbon fiber-reinforced laminates have reflected the improved properties of the unreinforced resins. As discussed earlier (Section 2), the blending of BMIs with cyanate ester (CE) resins has enhanced the toughness characteristics of the BMIs, resulting in a range of (Skyflex^R) BT resins.

The reactivity of the norbornylene (endomethylene tetrahydrobenzene) group to “pyrolytic polymerization” above 300°C forms the basis of the volatileless thermal cure of bisarylnadimides (**LII**) to yield cross-linked resins.



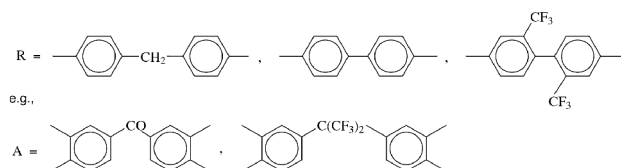
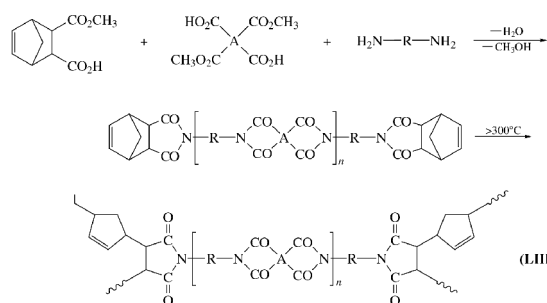
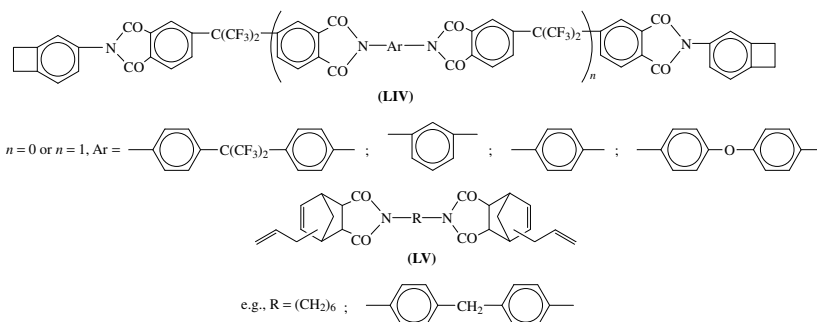
In the thermal polymerization, the rate-determining steps involve reverse Diels–Alder reactions to produce *N*-arylmaleimide moieties, which then provide the key monomers for the final polymerization to the cross-linked resin. Overall fabrication problems associated with this process led to the development of the PMR polyimides. These are formed by the *in situ* polymerization of monomeric reactants on the fiber matrix according to the scheme shown below.

Processing of fiber composites (prepregs) involves conversion of the initially formed low-molecular-weight prepolymer into the required component by compression or autoclave moulding.

PMR-15 (**LIII**, $\text{R} = \text{---C}_6\text{H}_4\text{---CH}_2\text{---C}_6\text{H}_4\text{---}$, $\text{A} = \text{---C}_6\text{H}_4\text{---CO---C}_6\text{H}_4\text{---}$), a key matrix resin for high temperature applications, is the most widely commercially accepted of the norbornene-terminated range of addition PIs. Compared with other high-temperature materials, it is relatively easy to process, and carbon fiber reinforced composites can be fabricated by a variety of techniques. Uses of these materials have been

directed mainly toward the aerospace industry. Recently, critical drawbacks to the use of PMR-15 have emerged which may limit its widespread commercial impact, including:

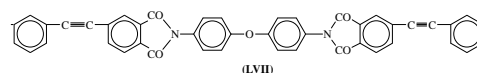
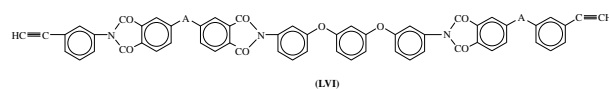
Aliphatic, cycloaliphatic, and aromatic-substituted allyl nadic imides (**LV**) have been reported to produce thermoset resins by thermal homopolymerization as well as being effective in bismaleimide comonomer blending.



- Problems associated with prepreg quality control and batch-to-batch variability.
- Microcracking of the resin matrix on thermal cycling of carbon fiber laminates due to mismatch of fiber-resin thermal expansion coefficients.
- Toxicity of the key methylene-dianiline (MDA) component. The fluorinated diamine (4-BDAF) (**XLIV**) has been used as a replacement both to reduce the level of toxicity and to enhance the basic toughness of the resin. Improved processing characteristics and higher operating temperatures than for PMR-15 have been claimed for resins incorporating fluorine-containing groups in either R and/or A segments of the PMR system (**LIII**).

Benzocyclobutene terminated imides (**LIV**) can be homopolymerized in the melt to yield temperature-resistant resins having a maximum of 24% weight loss after 200 hr at 371°C. These benzocyclobutenes have also produced modified resins by copolymerization with bismaleimides.

Carbon fiber matrix resins have been produced from acetylene (ethynyl)-terminated prepolymers. Typically, Thermid HR 600, imide oligomer (**LVI**, A = CO) cures *in situ* at 350°C to form a thermoset resin ($T_g > 350^\circ\text{C}$). Alternatives have been developed that improve the poor processibility (low solubility and limited gel time of 3 min/250°C). For example, in Thermid FA 700 [**LVI**, A = C(CF₃)₂], solubility has been improved and gel time increased on introduction of the hexafluoroisopropylidene unit into the polymer chain.



Aromatic polyimides prepared from phenylethyne-terminated imide monomers or oligomers (e.g., **LVII**) demonstrate many advantages over the ethynyl counterparts in their favorable processing and improved thermal/thermo-oxidative stability. In all of these systems, however, cyclotrimerization yields a complex of cross-linked structures rather than the predicted aromatic rings. Indeed, the cure reaction mechanism is still little understood.

Commercial addition polyimides include the bismaleimides: Kinel 500 (molding resin), Kerimids, e.g., Compimid, Matrimid and Desbimid (filament winding/laminating resins); arylnadimides: e.g., P10, P13N, P105A (solutions/molding resins); PMRs: e.g., PMR-15, PMR-11-50, LARC-160 and AFR 700B (solutions/carbon fiber prepreg); and acetylene-terminated imides. Thermid HR-600 (molding resin, carbon fiber prepreg).

TABLE VIII Comparison of Interlaminar Shear Strength versus Temperature and Time for Various Polyimide Matrix/Carbon Fiber Composites^a

Polyimide type	Interlaminar shear strength (MPa)	Temperature (°C)	Time (hr)
Condensation	83	260	1000
Addition—PMR	83	260	1000
Addition—bismaleimide	83	230	1000
Condensation	55	350	10
Condensation	55	320	1000
Thermoplastic	55	320	1000
Addition—PMR	55	320	500
Addition—PMR	55	290	1000
Thermoplastic	55	260	50000
Addition—PMR	55	260	10000
Addition—bismaleimide	55	260	1000
Thermoplastic	28	350	10
Addition—PMR	28	350	10
Addition—PMR	28	320	1000
Condensation	28	290	10000
Thermoplastic	28	290	10000
Addition—PMR	28	290	10000
Thermoplastic	28	230	50000
Addition—PMR	28	230	50000
Addition—bismaleimide	28	230	10000

^a Reprinted with permission from Critchley, J. P., and Wright, W. W. (1979). Polyimides as matrix resins for composites, *Rev. High-Temp. Mater.* **4**, 107. Copyright 1979 Freund Publishing House Ltd.

Interlaminar shear strength is used (Table VIII) to highlight levels of performance of key polyimide/carbon fiber composites as a function of time and temperature. Comparison (Fig. 11) of the thermo-oxidative stability of different polyimide types highlights the superior stability of the wholly aromatic condensation systems. The presence of polyene units in the polymers derived from acetylene-terminated oligomers is reflected in a lower-than-expected stability.

4. Quinoxaline Polymers

Without reproducing the considerable achievements in materials application of the polyimides, quinoxaline polymers have shown high levels of thermal and environmental stability together with the potential for commercial application in the fields of high-temperature adhesives and laminating resins.

Polymers (LVIII) are prepared from the condensation of aromatic tetraamines and aromatic tetra-carbonyl compounds (LIX) under melt or solution (polar solvent) conditions and without the intervention of an isolable "open-chain" intermediate.

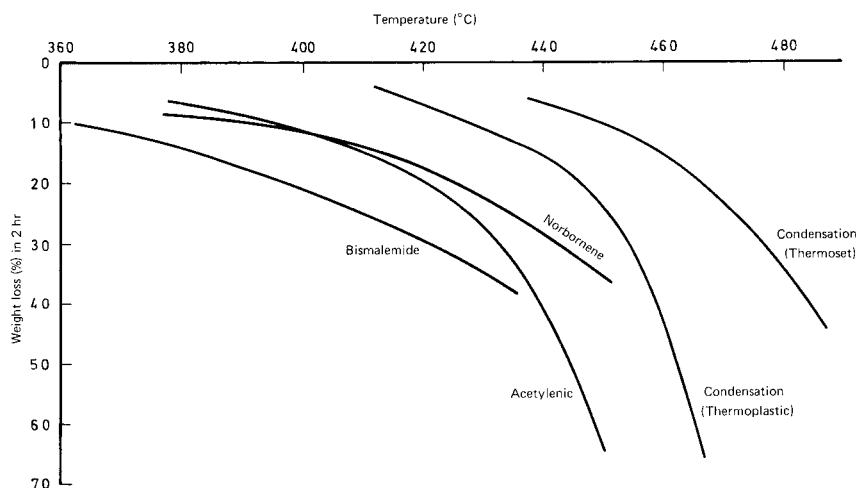
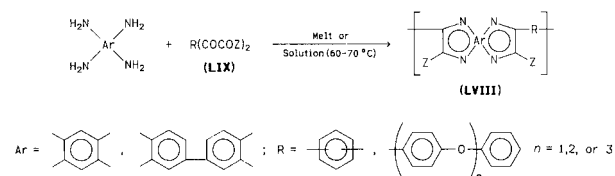


FIGURE 11 Comparison of thermo-oxidative stability of typical condensation and addition-type polyimides. [Reprinted with permission from Wright W. W. (1981). Application of thermal methods to the study of the degradation of polyimides. In "Developments in Polymer Degradation" (N. Grassie, ed.), Chap. 1. Elsevier, Barking, England. Copyright 1981 Elsevier Applied Science Publishers Ltd.]

Polyquinoxalines (**LVIII**, $Z = H$) (PQs) are formed from a bisglyoxal dihydrate (**LIX**, $Z = H$). Wholly aromatic systems with limited solubility and fusibility, however, have been successfully evaluated as metal-to-metal (steel and titanium adherends) adhesives and as high-temperature matrix resins in advanced carbon and boron fiber reinforced composites (Table IX). The high processing temperatures ($>400^\circ\text{C}$) for these resins (T_g values $> 300^\circ\text{C}$) have been reduced by the incorporation of flexible midchain units, for example, either linkages (T_g values $< 200^\circ\text{C}$) associated with, however, a concomitant reduction in thermo-oxidative stability (ITGA/ 400°C). Polyphenylquinoxalines (**LVIII**, $Z = \text{C}_6\text{H}_5$) (PPQs) with improved thermooxidative stability (Fig. 12) and processibility compared to the PQs have been obtained on replacement of bisglyoxals by more stable dibenzils (**LIX**, $Z = \text{C}_6\text{H}_5$) in the reaction sequence shown above. Advanced PPQ-based unidirectional carbon fiber reinforced composites and metal-to-metal (stainless-steel and titanium adherends) adhesive formulations exhibit superior retention of strength properties over the PQs at temperatures $> 300^\circ\text{C}$. However despite T_g values $> 300^\circ\text{C}$ for the wholly aromatic PPQs, long-term use above 250°C requires a postprocessing increase in the initial level of T_g in order to minimize the reduced property levels associated with thermoplasticity/creep deterioration. Several volatileless cross-linked systems have been investigated including cyano- or cyanato-chain-pendant groups (T_g increase on cure $\sim 100^\circ\text{C}$), but the most effective cycloaddition/cure processes have involved use of acetylenic-end groups.

Intramolecular cross-link cure (see polyimides) of vicinal pendant groups increases T_g ($\sim 120^\circ\text{C}$) solely by chain-stiffening effects induced by an increase in the content of fused rings.

Acetylene-terminated phenyl quinoxalines (**LX**, ATQs) chain extend/cross-link by intermolecular cycloaddition. Carbon fiber-reinforced ATQ laminates retain approximately 90% of their room temperature flexural strength and modulus at 260°C and, unlike carbon/epoxy laminates, these properties are maintained under hot wet conditions (Fig. 12).

C. Ladder/Highly Fused Ring Polymers

Ladder systems have extended the concept of heteroaromatic polymers into those “double-strand” structures incorporating essentially linear rather than cross-linked chains of fused rings. Despite wide predictions that such systems would exhibit improved thermal/thermo-oxidative stability allied to superior high-temperature properties, in practice they show little or no improvement over the best of the “conventional heteroaromatic” polymers. Numerous ladder polymers based on individual heterocyclic units have been synthesized; typically a wholly ladder polyquinoxaline (**LXI**) exhibited a TGA weight loss of 10% at 440 and 585°C in air and nitrogen, respectively, with a 38% loss in nitrogen at 800°C .

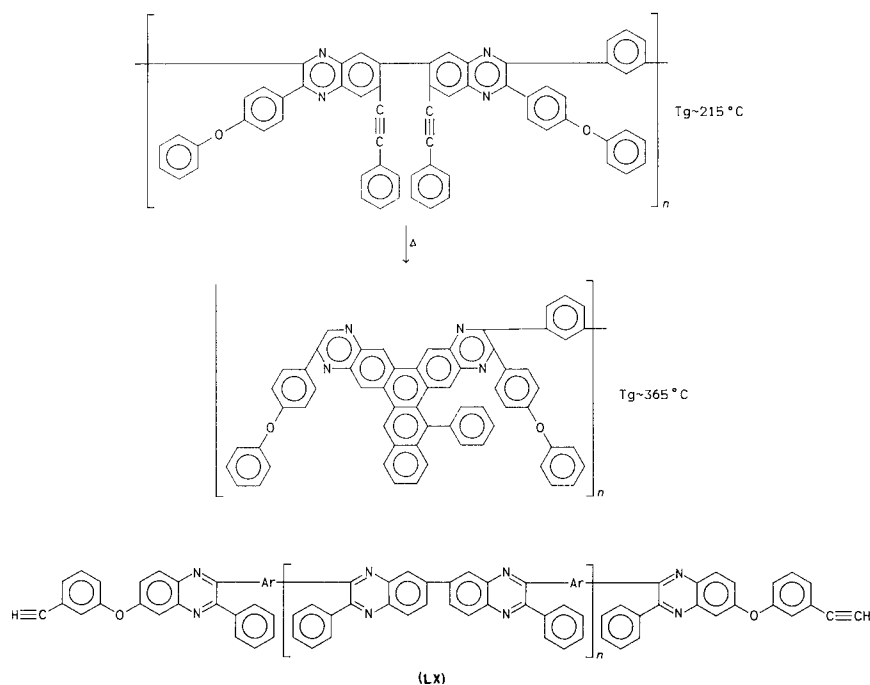
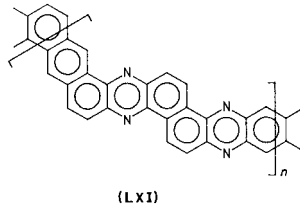


TABLE IX Properties of Polyquinoxaline/Boron and Carbon Composites

Test temperature (°C)/test condition	C-Fiber			B-Fiber	
	Flexural strength (MPa)	Modulus (GPa)	ILSS ^a MPa	Flexural strength (MPa)	Modulus (GPa)
RT	842	107	88	1746	292
133				1359	250
177				1384	259
212				1242	255
316				1524	167
316 after 1 hr/316	816	105	59		
316 after 100 hr/316	802	104	58		
316 after 200 hr/316	651	101	48		
361				1666	83
371 after 1 hr/371	748	104	61		
371 after 10 hr/371	713	100	61		

^a Interlaminar shear strength.



The majority of ladder systems are intractable “brick dusts” but two chemically related systems in particular, produced from the interaction of an aromatic

tetracarboxylic dianhydride and aromatic tetramine, have provided a range of structural materials that, though not currently commercially developed, has demonstrated definite potential in high-temperature applications.

1. Poly(benzimidazopyrrolones)—Pyrrones

Pyrrone polymers have been produced in full ladder (LXII) or semiladder via soluble (LXIII) form via soluble “open-chain” intermediates (cf. polyimides) or directly in polyphosphoric acid solution.

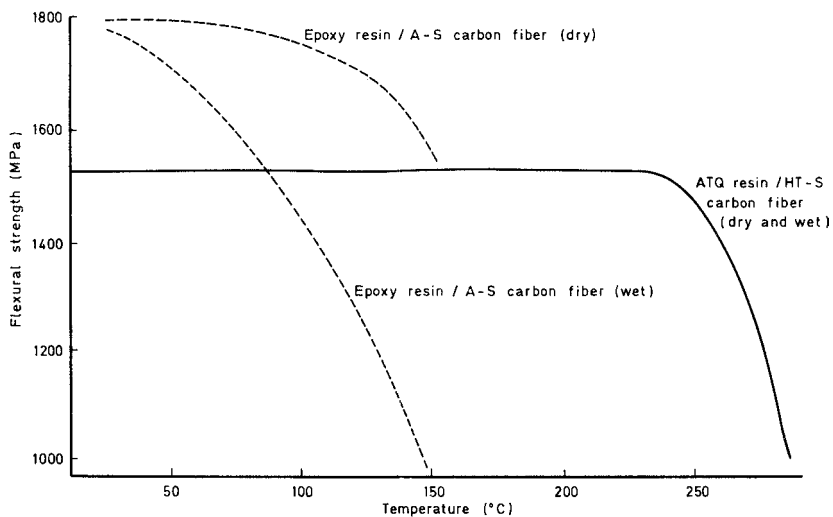
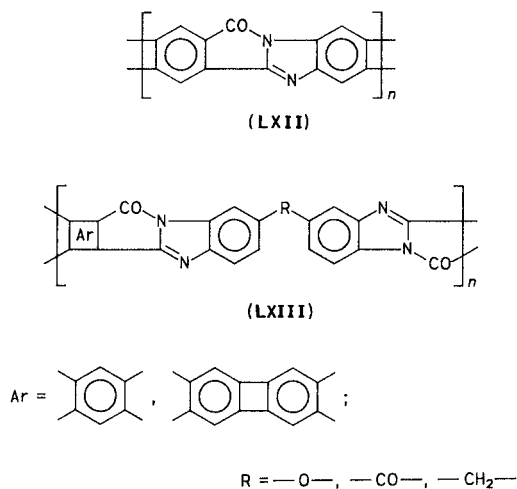


FIGURE 12 Flexural strength at elevated temperatures of dry and wet ATQ resin and epoxy resin carbon fiber composites. [Reprinted with permission from Critchley, J. P., Knight, G. J., and Wright, W. W. (1983). “Heat Resistant Polymers—Technologically Useful Materials,” Plenum, New York. Copyright 1983 Plenum Press.]



Applications such as films and fibers are formed at the “open-chain” stage with subsequent cyclization (250–325°C) to the pyrrone. For both material forms optimum performance is obtained from semiladder systems, for example, fibers from polymer **LXIII** Ar , R = single bond) retain room temperature tensile properties after exposure (12 hr) to 10% NaOH at 90°C or air at 400°C. Solid grades of ladder or semiladder homo- or heterocyclic (imide, benzimidazole, oxadiazole) copolymers have been produced by high-temperature/high pressure molding processes. The effect of isothermal heating in air (Fig. 13) highlights the unexpectedly low thermo-oxidative stability of the pyrrones.

2. Poly(bisbenzimidazo-benzophenanthrolines)

Ladder **LXIV** and semiladder (**LXV**) polymers are produced from the reaction of 1,4,5,8-naphthalenetetracarboxylic acid dianhydride and the appropriate tetraamine. Although a “staged” reaction via an open-chain intermediate is possible, most frequently the fully cyclized polymer is formed direct in PPA (150°C) or in the melt (300°C).

For the semiladder system the introduction of flexible groups [e.g., —O— and —C(CF₃)₂—] midchain has resulted in an increased solubility and tractability. However, for most practical applications, ladder system (**LXIV**) and semiladder polymer (**LXV**; R = single bond), so called BBL and BBB polymers, respectively, have been widely evaluated. For BBB in particular, fiber spun from concentrated sulfuric acid exhibits excellent tensile properties under ambient conditions and in air approximately 60% of initial tensile strength is retained after 30 hr at 360°C or 1 min at 600°C. Comparative strength retention at elevated temperature for BBB, PBI, and Nomex is shown in Fig. 14. However, the long-term strength of BBB at 360°C is inferior to a nonladder benzoxazole-imide copolymer fiber. Strong, high-modulus films of BBB and BBL polymers have been formed by precipitation (from methane sulfonic acid solution) and vacuum filtration. It is suggested that a high degree of interchain packing is responsible for this effect. Differences are observed for BBB and BBL polymer systems in dilute solution; the former exhibits flexible coil behavior while the latter demonstrates a rigid rod-like configuration.

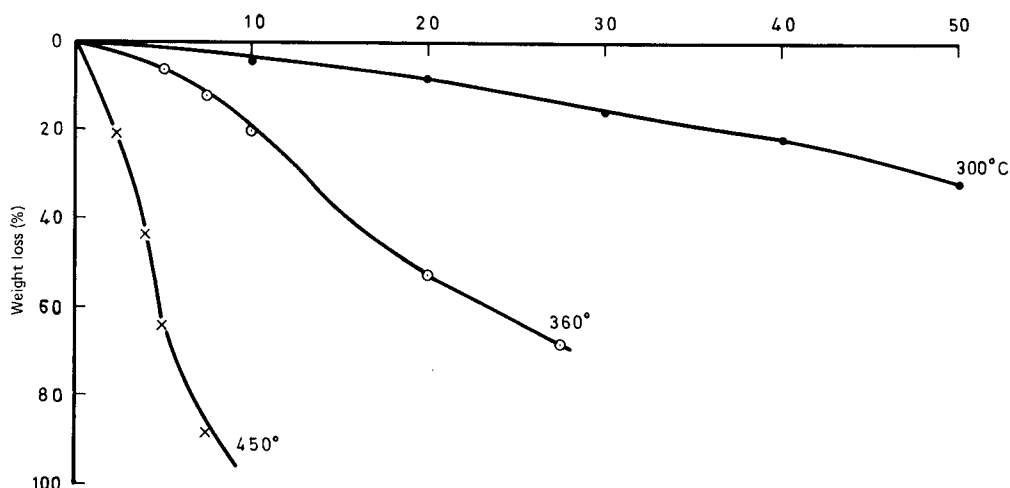


FIGURE 13 Isothermal weight loss of a partial ladder polypyrrone at three temperatures in air. [Reprinted with permission from Pezdirtz, G. F., and Johnston, N. J. (1971). Thermally stable macromolecules. In “Chemistry in Space Research” (R. Landal and A. Rembaum, eds.), pp. 155–252, Elsevier, New York.]

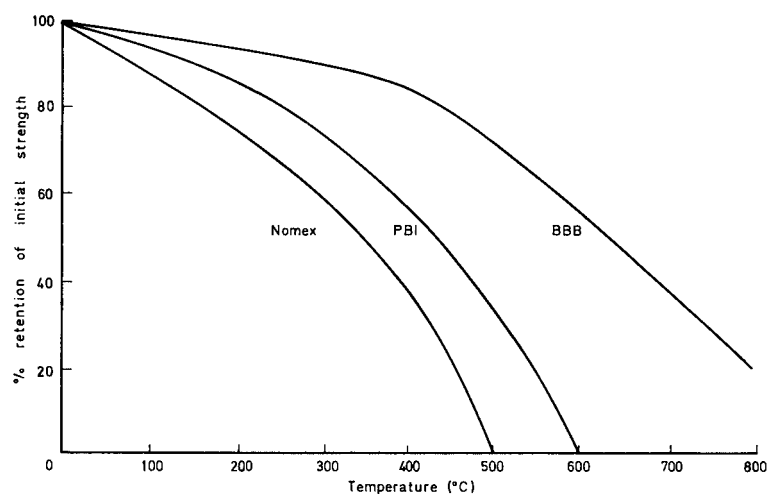
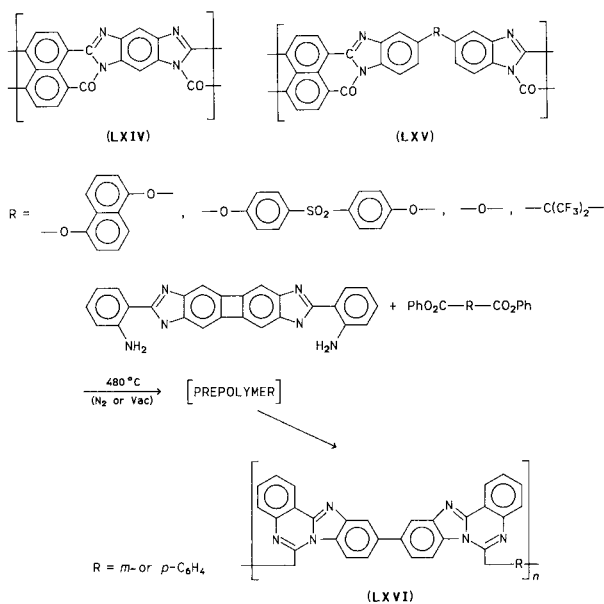


FIGURE 14 Strength retention of Nomex, PBI, and BBB fibers in air at various temperatures. [Reprinted with permission from Preston, J., Black, W., and De-Winter, W. (1969). *Appl. Polym. Symp.* 9, 145. Copyright 1969 John Wiley & Sons, Inc.]



3. Polyimidoquinazolines (PIQs)

Fused-ring PIQs (LXVI) are the only heteroaromatic ladder-type competitors to pyrrone—and BBB/BBL—systems as applicational high-temperature materials. Several synthetic routes based on aromatic tetraamines have been used; the most practically useful is reminiscent of PBI manufacture, involving the melt-polycondensation of 2, 2'-bis(*O*-aminophenyl)bibenzimidazole with aromatic dicarboxylic acids.

Like the PBIs, evolution of volatiles is a problem in processing but carbon fiber laminates with excellent retention

TABLE X Flexural Properties of a Polyimidoquinazoline/Carbon Fiber Laminate at Elevated Temperature^a

Heat aging conditions	Flexural strength (MPa)	Flexural modulus (GPa)	Retention of RT strength (%)
RT	1540	119	—
200 hr at 316°C	1249	115	81
500 hr at 316°C	1252	126	81
1000 hr at 316°C	598	81	39
RT	1939	119	—
1 hr at 371°C	1181	126	61
50 hr at 371°C	1187	117	61
100 hr at 371°C	992	100	51
RT	1617	116	—
1 hr at 426°C	1497	113	93
5 hr at 426°C	987	102	61
10 hr at 426°C	331	98	20
1 hr at 481°C	1181	110	73
1 hr at 536°C	629	63	39

^a Reprinted with permission from Gosnell, R. B., Fitzgerald, W. P., and Milligan, R. J. (1973). *Appl. Polym. Symp.* 22, 21. Copyright 1973 John Wiley & Sons, Inc.

of flexural properties at elevated temperature (>500°C) have been observed for the PIQ resins (Table X).

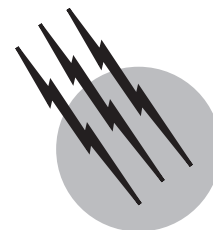
SEE ALSO THE FOLLOWING ARTICLES

COMPOSITE MATERIALS • HETEROCYCLIC CHEMISTRY
• MATERIALS CHEMISTRY • POLYMER PROCESSING •

POLYMERS, INORGANIC AND ORGANOMETALLIC • POLYMERS, MECHANICAL BEHAVIOR

BIBLIOGRAPHY

- Akita, H., *et al.* (1999). *J. Polym. Sci. Polym. Phys.* **37**, 199–207, 209–218.
- Auman, B. C., Myers, T. L., and Higley, D. P. (1997). *J. Polym. Sci. Polym. Chem.* **35**(12), 2441.
- Beehag, A., and Ye, L. (1996). *Composites* **27A**, 175.
- Ching, T.-S., and Kafchinski, E. R. (1996). *Polymer* **37**(9), 1635.
- Coleman, M. R., and Koros, W. J. (1994). The transport properties of polyimide isomers containing hexafluoroisopropylidene in the diamine residue. *J. Polym. Sci. Polym. Phys.* **32**(11), 1915.
- Critchley, J. P., Knight, G. J., and Wright, W. W. (1983). "Heat Resistant Polymers—Technologically Useful Materials," Plenum, New York.
- Eashoo, M., Buckley, L. J., and St. Clair, A. K. (1997). *J. Polym. Sci. Polym. Phys.* **35**(1), 173.
- Ghosh, M., and Mittal, K. L., eds. (1996). "Polyimides: Fundamentals and Applications," Marcel Dekker, New York.
- Goodwin, A. A. (1999). Thermal properties of a thermoplastic polyimide blend. *J. Appl. Polym. Sci.* **72**, 543.
- Grenier-Loustalot, M. F., Billon, L., Louartani, A., *et al.* (1997). *Polym. Int.* **44**(4), 435.
- Hamerton, I., ed. (1994). "Chemistry and Technology of Cyanate Ester Resins," Blackie Academic and Professional, Glasgow, UK.
- Han, J. L., and Li, K. Y. (1998). *J. Appl. Polym. Sci.* **70**(13), 2635.
- Hedrick, J. L., Di Pietro, R., and Plummer, C. J. G., *et al.* (1996). *Polymer* **37**, 5229.
- Ivanov, D. A., and Jones, A. M. (1998). *J. Polym. Sci. Polym. Phys.* **36**(5), 39.
- Kitagawa, T., Murase, H., and Yabuki, K. (1998). *J. Polym. Sci. Polym. Phys.* **36**(1), 39.
- Lovinger, A. J., Padden, F. J., and Davis, D. D. (1998). Crystal structure, morphology, thermal stability and crystallization kinetics of PPS. *Polymer* **29**, 229.
- Mascia, L., Zhang, Z., and Shaw, S. J. (1996). *Composites* **27A**, 1211.
- McGee, R. L., *et al.* (1997). *J. Polym. Sci. Polym. Chem.* **35**(11), 2157.
- Pater, R. H. (1994). *SAMPE J.* **30**, 29.
- So, Y.-H., *et al.* (1995). *J. Polym. Sci. Polym. Chem.* **33**(15), 2893.
- Song, H.-H. (1999). *J. Polym. Sci. Polym. Phys.* **37**(7), 661.
- Susuki, A., Kohno, T., and Kunugi, T. (1998). *J. Polym. Sci. Polym. Phys.* **36**(10), 1731.
- Toi, K., Tsuzumi, H., and Ito, T. (1999). *Polym. Polym. Compo.* **7**(1), 45.
- Zoia, G., *et al.* (1994). *J. Polym. Sci. Polym. Phys.* **32**(1), 53.



Rheology of Polymeric Liquids

Chang Dae Han

University of Akron

- I. Classification of Polymeric Liquids
- II. Unusual Characteristics of Polymeric Liquid Flow
- III. Definitions of Material Functions for Polymeric Liquids
- IV. Methods for Determining Rheological Properties of Polymeric Liquids
- V. Constitutive Equations for Predicting the Rheological Properties of Polymeric Liquids
- VI. Concluding Remarks

GLOSSARY

Dynamic viscosity Real component of complex viscosity in oscillatory shear flow.

Extrudate swell Swelling of extrudate upon exiting from a die.

Loss modulus Imaginary component of the complex modulus.

Normal stress difference Difference in the two primary normal stresses.

Normal stress effect Effect exhibiting the elasticity of polymeric liquid.

Shear thinning behavior Decreasing trend of viscosity with increasing shear rate.

Shear viscosity Viscosity in steady-state shear flow.

Storage modulus Real component of the complex modulus.

RHEOLOGY is the science of the deformation and flow of matter. Therefore, depending on the type of matter

one deals with, different branches of rheology may be considered. For instance, polymer rheology deals with polymeric materials and biorheology deals with biological fluids (e.g., blood, mucus, and synovial fluids). Polymeric materials cover a wide range of man-made materials, such as plastics, synthetic rubber, synthetic fiber, and many others. These materials have very large molecules consisting of many repeat units of small molecules. Because of the large size of the molecules, they exhibit unusual flow behavior under deformation. The study of the flow behavior of polymeric liquids is not only an intellectual challenge to scientists, but also is of fundamental importance to an advancement of polymer technology.

I. CLASSIFICATION OF POLYMERIC LIQUIDS

In a general sense, there are two types of polymeric liquids: thermoplastics and thermosets. Thermoplastic polymeric liquids are thermally reversible in that, when solidified,

they can be melted by heating to recover the original liquid state. Thermoset resins, in contrast, are thermally irreversible in that, once solidified, they cannot be melted. Thermoplastic polymer molecules are large, with molecular weights on the order of tens to hundreds of thousands. Furthermore, many of the repeat units are linked in a one-dimensional direction. The size of thermoplastic polymer molecules does not change during the fabrication of products. Thermoplastic polymers (e.g., polyethylene, polystyrene, poly(vinyl chloride), nylon, and polycarbonate) are used for manufacturing films, fibers, furniture, etc. Thermoset resins, however, have smaller molecules, with molecular weights on the order of a few thousand. They usually form three-dimensional networks in the presence of a catalyst (often referred to as curing agent), giving rise to strong structures. Therefore, parts made from thermoset resins are much stronger than those made from thermoplastic polymers and are widely used for structural purposes. Thermoset resins (e.g., unsaturated polyester, epoxy, and urethane) are used for manufacturing boat hulls, parts for automobiles and airplanes, bath tubs, buttons, etc.

Thus, in dealing with the flow properties of thermoplastic polymeric liquids, one need not be concerned with a change of molecular size, and in this sense, the measurement of the flow properties of thermoplastic polymeric liquids is much simpler than that of thermoset resins. In dealing with the flow properties of thermoset resins, however, one must understand that the molecules grow during fabrication. Consequently, measurement of the flow properties of thermoset resins is very difficult. An understanding of the flow behavior of thermoset resins during fabrication requires an understanding of the nature of the chemical reactions occurring during fabrication. Because of the complexity of the problems involved in dealing with the rheological behavior of thermoset resins, we shall be

concerned here primarily with the rheological behavior of thermoplastic polymeric liquids.

Thermoplastic polymeric materials may be classified in the following way, on the basis of chemical constituents: (1) bulk polymers (or polymer solutions), which are considered to be homogeneous liquids; (2) polymer liquid crystals; (3) polymer blends consisting of two or more similar or dissimilar polymers, the latter of which generally form heterogeneous phases in which one component is suspended in the other; (4) filled polymers in which particulates are suspended in the polymeric liquid; and (5) polymeric foams, in which gas bubbles are suspended in the polymeric liquid.

II. UNUSUAL CHARACTERISTICS OF POLYMERIC LIQUID FLOW

Before we quantitatively discuss the rheological behavior of polymeric liquids, let us observe some of their unusual flow characteristics. [Figure 1](#) demonstrates a dramatic difference between two types of liquid—a low-molecular-weight polybutene and an aqueous solution of polyacrylamide—when a rotating rod is dipped into them. The polyacrylamide solution climbs up the rotating rod, while the low-molecular-weight polybutene does not. Note that low-molecular-weight polybutene has a molecular weight of hundreds or thousands, whereas the polyacrylamide dissolved in water is believed to have a molecular weight of tens of thousands.

The direction in which the polyacrylamide solution climbs in [Fig. 1](#) is perpendicular to the rotating direction of the solution, and therefore one can conjecture that there ought to be a force generated by the liquid that overcomes the effect of centrifugal force and points in a direction perpendicular to the direction of rotation. The liquid

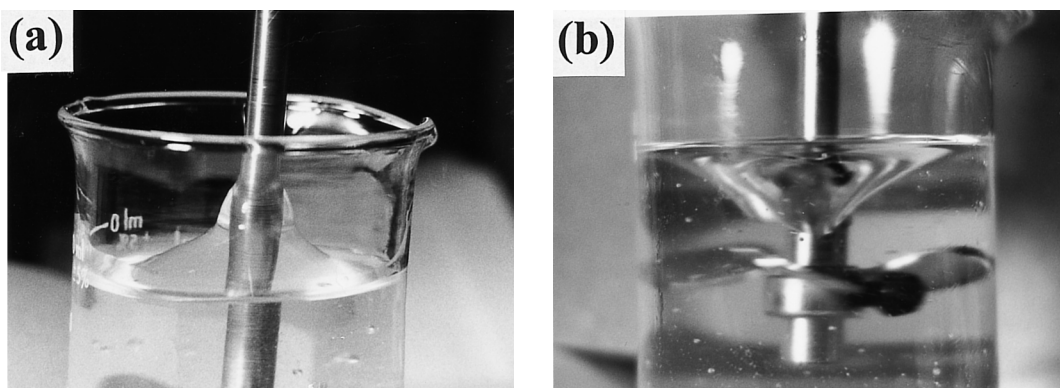


FIGURE 1 Photograph describing the liquid climb-up effect: (1) low-molecular-weight polybutene; (b) 2 wt% aqueous solution of polyacrylamide.

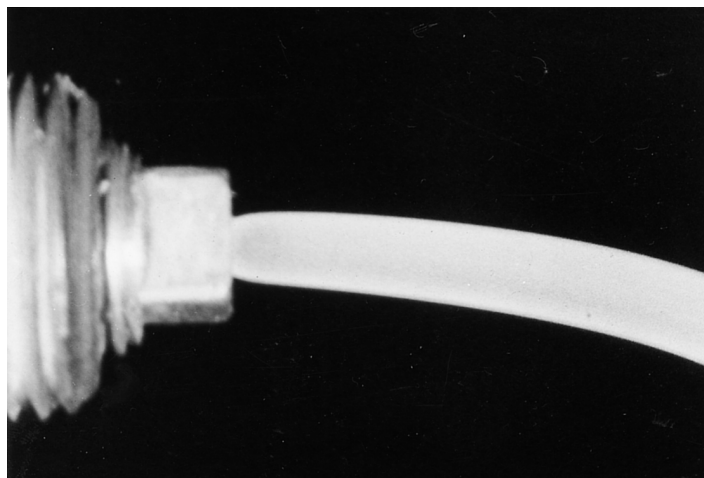


FIGURE 2 Photograph describing the swelling of a molten high-density polyethylene melt at 180°C exiting from a cylindrical tube.

climb-up effect shows that polymeric liquids exhibit a “normal stress” effect.

Figure 2 shows the swelling of a molten high-density polyethylene extrudate exiting from a cylindrical tube, which is believed to occur as a result of the recovery of the elastic deformation (or the relaxation of normal stresses) imposed on the polymeric liquid in the capillary.

III. DEFINITIONS OF MATERIAL FUNCTIONS FOR POLYMERIC LIQUIDS

Consider the flow fields in which a polymeric liquid can undergo shear deformation, which is encountered when the liquid flows through a confined geometry, such as through a pipe or channel. Under such circumstances, some practical questions come to mind. (1) How much pressure drop (or mechanical or electrical power) are required to maintain liquid flow through a pipe at a desired flow rate? (2) What would be the most cost-effective design for a pipe to transport a specific polymeric liquid at a desired flow rate? These questions can be answered intelligently only when we know the relationships between the rheological properties of the liquid and the rate of deformation and between the rheological properties of the liquid and its molecular parameters, such as the chemical structure, molecular weight, and molecular weight distribution.

Consider a flow of liquid flowing through two infinitely long parallel planes, where the upper plane moves in the z direction at a constant velocity \bar{V} (i.e., $v_z = \bar{V}$) at $y = h$ while the lower plane remains stationary (i.e., $v_z = 0$). Referring to Fig. 3, the gap opening h is very small compared to the width w of the plane (i.e., $h \ll w$). Under such a situation, the velocity field of the flow at steady state between the two planes is given by

$$v_z = f(y), \quad v_x = v_y = 0. \quad (1)$$

We then have a constant velocity gradient dv_z/dy ,

$$\dot{\gamma} = dv_z/dy = \text{constant}, \quad (2)$$

where $\dot{\gamma}$ is called steady-state shear rate. The flow field satisfying Eq. (1) is called “uniform shear” flow field or “simple shear” flow field.

When a liquid flowing through a long cylindrical tube, the velocity profile of the liquid may look like that shown in Fig. 4. The exact shape of the parabolic velocity profile may vary depending on the type of liquid dealt with; in other words, whether the liquid has small molecules or large molecules. The shape of the velocity profile can be predicted only when we have information on the flow properties of the liquid. It is clear from Fig. 4 that the axial velocity v_z is a function only of distance in the radial (r) direction in cylindrical coordinates, that is,

$$v_z = f(r), \quad (3)$$

and therefore the velocity gradient dv_z/dr varies with r ,

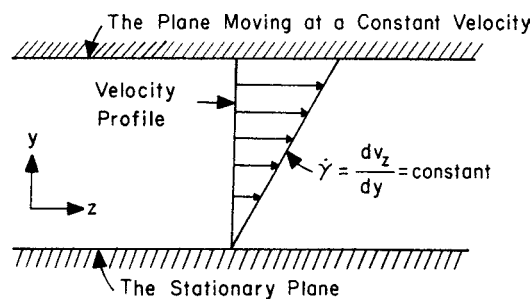


FIGURE 3 Schematic describing the velocity profile of a liquid flowing through two parallel planes.

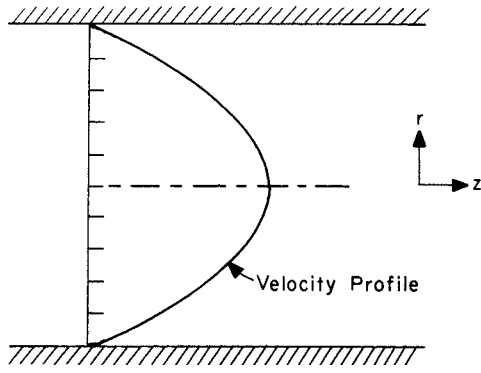


FIGURE 4 Schematic describing the velocity profile of a liquid flowing through a cylindrical tube.

$$dv_z/dr = g(r). \quad (4)$$

The flow field given by Eq. (4) is called “nonuniform shear” flow field. We can show that the velocity profile of a polymeric liquid may be given by

$$v_z(r) = \bar{V} \left(\frac{3n+1}{n+1} \right) \left[1 - \left(\frac{r}{R} \right)^{(n+1)/n} \right], \quad (5)$$

where \bar{V} is the average velocity, R is the radius of the tube, and n is a constant characteristic of the liquid. It can be shown easily that for $n = 1$, Eq. (5) reduces to

$$v_z(r) = 2\bar{V} \left[1 - \left(\frac{r}{R} \right)^2 \right]. \quad (6)$$

It is well-established that the majority of polymeric liquids have values of n less than unity. We describe later how one can determine experimentally the values of n for polymeric liquids.

Let us consider the three forces acting on the three faces (one force on each face) of a small cube element of fluid, schematically shown in Fig. 5. For instance, a force acting on face ABCD with an arbitrary direction may be resolved into three-component directions: the force acting in the x_1 direction is $S_{11}dx_1dx_3$, the force acting in the x_2 direction is $S_{12}dx_2dx_3$, and the force acting in the x_3 direction is $S_{13}dx_2dx_3$. Similarly, the forces acting on face BCFE are $S_{21}dx_1dx_3$ in the x_1 direction, $S_{22}dx_1dx_3$ in the x_2 direction, and $S_{23}dx_1dx_3$ in the x_3 direction. Likewise, the forces acting on face DCFG are $S_{31}dx_1dx_2$ in the x_1 direction, $S_{32}dx_1dx_2$ in the x_2 direction, and $S_{33}dx_1dx_2$ in the x_3 direction. Therefore, we may represent the components of the stress tensor S_{ij} in matrix form as

$$\mathbf{S} = \begin{vmatrix} S_{11} & S_{12} & S_{13} \\ S_{21} & S_{22} & S_{23} \\ S_{31} & S_{32} & S_{33} \end{vmatrix}, \quad (7)$$

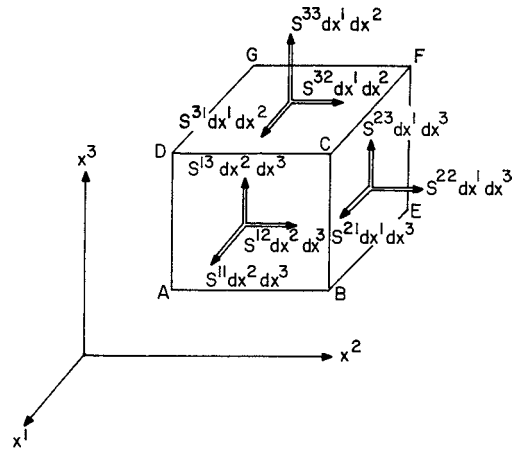


FIGURE 5 Stress components on a cube.

where the component S_{ij} of the stress tensor \mathbf{S} is the force acting in the x_j direction on the unit area of a surface normal to the x_i direction. The components S_{11} , S_{22} , and S_{33} are called normal stresses since they act normally (or perpendicular) to surfaces, and the mixed components S_{12} , S_{13} , etc., are called shear stresses.

If a liquid has been at rest for a sufficiently long time, there are no tangential components of stress on any plane of a cube and the normal components of stress are the same for all three planes, each perpendicular to the others. In such a situation, the normal component of stress is nothing but hydrostatic pressure. However, when a liquid is under deformation or in flow, additional stresses are generated. The components of the stresses may be divided into two parts and, in Cartesian coordinates, we have

$$S_{ij} = -p\delta_{ij} + \sigma_{ij}. \quad (8)$$

In Eq. (8), p is the hydrostatic pressure, and it has a negative sign since it acts in a direction opposite to a normal stress (S_{11} , S_{22} , S_{33}) which, for convenience, is chosen as pointing out of the cube (Fig. 5). The σ_{ij} term is the ij th component of the extra stress that arises due to the deformation of the liquid, and the subscripts i and j , respectively, range from 1 to 3.

If we now consider the state of stress in an isotropic material subjected to simple shear flow defined by Eq. (2), we have

$$S_{13} = S_{31} = S_{23} = S_{32} = 0, \quad S_{12} = S_{21} \neq 0. \quad (9)$$

Since the measurement of hydrostatic pressure is not possible when a liquid is under deformation or in flow, we now define hydrostatic pressure as

$$-p = (S_{11} + S_{22} + S_{33})/3 \quad (10)$$

Using Eqs. (9) and (10) in Eq. (8), we obtain three independent stress quantities of rheological significance—namely,

two differences of normal stress components and one shear component,

$$N_1 = \sigma_{11} - \sigma_{22}, N_2 = \sigma_{22} - \sigma_{33}, \text{ and } \sigma_{12}, \quad (11)$$

in which N_1 is called the first normal stress difference, N_2 is called the second normal stress difference, and σ_{12} is called the shear stress. Following the nomenclatures agreed up by the rheology community, hereafter σ instead of σ_{12} will be used to denote the shear stress. Note that $\sigma_{11} - \sigma_{33}$ becomes redundant since we have

$$\sigma_{11} + \sigma_{22} + \sigma_{33} = 0, \quad (12)$$

which follows from Eqs. (8) and (10).

Let us now define the following three material functions of rheological significance in steady-state shear flow:

$$\sigma = \eta(\dot{\gamma})\dot{\gamma}, \quad (13)$$

$$N_1 = \Phi_1(\dot{\gamma})\dot{\gamma}^2, \quad (14)$$

$$N_2 = \Phi_2(\dot{\gamma})\dot{\gamma}^2, \quad (15)$$

where $\eta(\dot{\gamma})$ denotes the shear viscosity function, which is considered to be a measure of the resistance to flow, Φ_1 is the first normal stress difference coefficient, and Φ_2 is the second normal stress difference coefficient, with subscript 1 denoting the direction of flow, subscript 2 the direction perpendicular to the flow, and subscript 3 the remaining (i.e., neutral) direction. We will show below how the quantities, σ , N_1 , and N_2 can experimentally be determined, and how such information can be used to characterize the rheological properties of polymeric liquids.

IV. METHODS FOR DETERMINING RHEOLOGICAL PROPERTIES OF POLYMERIC LIQUIDS

There are two basic types of apparatus for determining the rheological properties of polymeric liquids in shear flow: the rotational instrument and the capillary instrument. The rotational instrument may have one of three flow geometries: cone-and-plate, two parallel plates, or two coaxial cylinders.

Let us consider the flow of a polymeric liquid placed in the cone-and-plate fixture, in which a cone with a wide vertical angle is placed on a horizontal flat plate, as schematically shown in Fig. 6. The wedge-like space between the cone and plate is filled with the liquid under test. One of the surfaces is fixed and the other rotates around the axis of the cone. In using such an instrument, we wish to relate the torque \mathfrak{S} and the net thrust F (in excess of that due to ambient pressure) acting on the cone (or plate) to the angular velocity Ω . For an instrument having a small angle θ_c (e.g., less than 5°) between the cone and plate (Fig. 6)

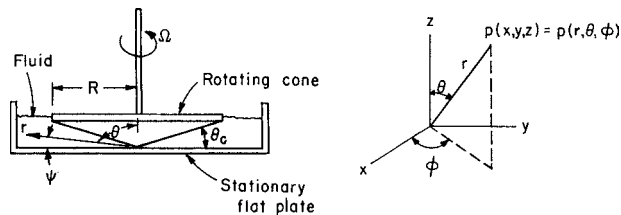


FIGURE 6 Schematic describing the cone-and-plate geometry.

and a small gap (say $50 \mu\text{m}$) between the cone and plate, one can derive the following expressions for steady-state shear flow:

$$\dot{\gamma} = -\Omega/\theta_c, \quad (16)$$

$$\sigma = 3\mathfrak{S}/2\pi R^3, \quad (17)$$

$$N_1 = 2F/\pi R^2, \quad (18)$$

where $\dot{\gamma}$ is the shear rate and R is the radius of the cone. Since we expect that the measured torque \mathfrak{S} and normal force F will vary with the angular velocity Ω of the cone (or plate), we should be able to obtain an experimental correlation between σ and $\dot{\gamma}$, and between N_1 and $\dot{\gamma}$.

Figure 7 gives logarithmic plots of η versus $\dot{\gamma}$ and logarithmic plots of N_1 versus $\dot{\gamma}$ for molten polystyrene and poly(methyl methacrylate), respectively, at 200°C , in which the data for $\dot{\gamma} < 20 \text{ sec}^{-1}$ were obtained using a cone-and-plate rheometer and the data for $\dot{\gamma} < 70 \text{ sec}^{-1}$ were obtained with a slit rheometer that will be discussed below. Note in Fig. 7 that the values of η and N_1 were determined using Eqs. (16) through (18) with the definition of η defined by Eq. (13). Many polymer solutions and polymer melts exhibit similar rheological behavior in steady-state shear flow as that shown in Fig. 7.

It can be seen in Fig. 7 that η stays constant at low $\dot{\gamma}$ and then starts to decrease as $\dot{\gamma}$ is increased further. This behavior of η can be described by the following expression:

$$\eta = \begin{cases} \eta_0, & \text{for } \dot{\gamma} < \dot{\gamma}_c, \\ K\dot{\gamma}^{n-1}, & \text{for } \dot{\gamma} \geq \dot{\gamma}_c, \end{cases} \quad (19)$$

where η_0 is called the zero-shear viscosity, $\dot{\gamma}_c$ is the critical shear rate at which η starts to decrease as $\dot{\gamma}$ is increased beyond that value, K is the power-law constant, and n is the power-law index. One can determine values of K and n from $\log \sigma$ versus $\log \dot{\gamma}$ plots in the shear-thinning region (i.e., at $\dot{\gamma} > \dot{\gamma}_c$). Behavior that exhibits a decreasing trend of η as $\dot{\gamma}$ is increased is referred to as shear thinning. Notice further in Fig. 7 that N_1 does not appear in the range of $\dot{\gamma}$ over which the η is constant and that N_1 begins to appear at the $\dot{\gamma}$ at which η begins to decrease as $\dot{\gamma}$ is increased. Note that at low $\dot{\gamma}$, N_1 increases as $\dot{\gamma}$ is increased with a slope of 2 in the $\log N_1$ versus $\log \dot{\gamma}$ plot, but at

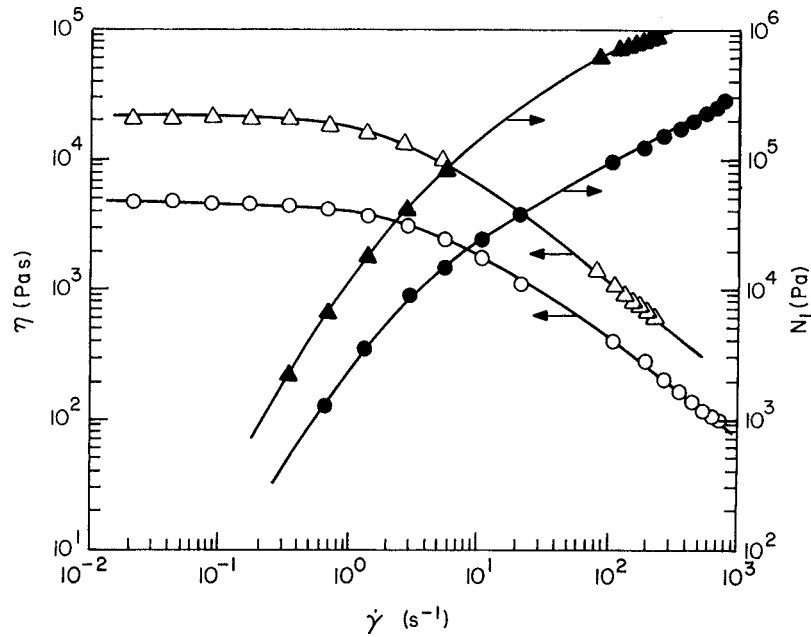


FIGURE 7 Plots of $\log \eta$ versus $\log \dot{\gamma}$ and $\log N_1$ versus $\log \dot{\gamma}$ for polystyrene (\circ, \bullet) and poly(methyl methacrylate) (Δ, \blacktriangle) at 200°C .

high shear rates, the slope of the $\log N_1$ versus $\log \dot{\gamma}$ plot becomes less than 2. Liquids exhibiting shear-thinning behavior are called non-Newtonian fluids and liquids exhibiting measurable N_1 are called viscoelastic fluids. It should be mentioned that polymeric liquids exhibiting the rod climb-up effect (Fig. 1) and extrudate swell (Fig. 2) also exhibit normal forces in a cone-and-plate instrument, and thus possess nonzero values of N_1 . Such liquids are said to exhibit normal stress effect or fluid elasticity.

When subjected to a cone-and-plate instrument, low-molecular-weight polybutene, for instance, has a constant value of viscosity and does not exhibit the normal force and hence has a zero value of N_1 . It should be remembered that when a rotating rod is dipped into a low-molecular-weight polybutene, it did not climb up the rotating rod (Fig. 1). The diameter of such a liquid, upon ejection from a capillary tube, would not swell. Such liquids are called Newtonian fluids.

In the use of the rotational instrument, another method widely used for determining the rheological properties of polymeric liquids is to subject the test fluid to sinusoidal strain as an input and to record the stress resulting from the deformed liquid as an output, as schematically shown in Fig. 8. Such an experimental technique is often referred to as oscillatory shear flow measurement or dynamic measurement. Since the sinusoidal motion can be represented in the complex domain, the following complex quantities may be defined as

$$\gamma^*(i\omega) = \gamma_0 e^{i\omega t} = \gamma'(\omega) + i\gamma''(\omega), \quad (20)$$

$$\sigma^*(i\omega) = \sigma_0 e^{i(\omega t + \varphi)} = \sigma'(\omega) + i\sigma''(\omega), \quad (21)$$

where γ_0 and σ_0 are the amplitude of the complex strain γ^* and the complex stress σ^* , respectively, and φ is the phase angle between them, the quantities with primes (γ' and σ') and double primes (γ'' and σ'') representing the real and imaginary parts of the respective complex quantities. In Eqs. (20) and (21), the response variable $\sigma^*(i\omega)$ is assumed to have the same frequency ω as the input variable $\gamma^*(i\omega)$. This is only true when the system (i.e., the liquid in oscillatory motion) is a linear body.

A perfectly elastic (i.e., Hookean) material can be described by

$$\sigma(t) = G\gamma(t), \quad (22)$$

and a purely viscous liquid can be described by

$$\sigma(t) = \eta\dot{\gamma}(t), \quad (23)$$

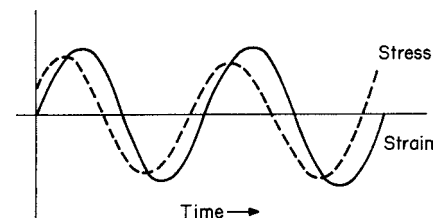


FIGURE 8 Schematic describing the sinusoidally varying stress and strain.

where $\sigma(t)$ is the stress, $\gamma(t)$ is the strain, and G is the elastic modulus.

Under an oscillatory shear flow, using the definitions given by Eqs. (20) and (21), one can derive from Eqs. (22) and (23) material properties of rheological significance. These are the complex modulus $G^*(i\omega)$ and the complex viscosity $\eta^*(i\omega)$, which can be defined as

$$G^*(i\omega) = \sigma^*(i\omega)/\gamma^*(i\omega) = G'(\omega) + iG''(\omega), \quad (24)$$

$$\eta^*(i\omega) = \sigma^*(i\omega)/\dot{\gamma}^*(i\omega) = \eta'(\omega) - i\eta''(\omega), \quad (25)$$

The term η^* in Eq. (25) can be expressed in terms of $G^*(i\omega)$ as

$$\eta^*(i\omega) = G^*(i\omega)/i\omega = (G''(\omega)/\omega) - i(G'(\omega)/\omega). \quad (26)$$

From Eqs. (25) and (26) we have

$$\eta'(\omega) = G''(\omega)/\omega, \quad \eta''(\omega) = G'(\omega)/\omega. \quad (27)$$

Here $G'(\omega)$ is an in-phase elastic modulus associated with energy storage and release in the periodic deformation and is called the storage modulus. The term $G''(\omega)$ is an out-of-phase elastic modulus associated with the dissipation of energy as heat and is called the loss modulus. The real (i.e., in-phase) component of the complex viscosity $\eta'(\omega)$ is called the dynamic viscosity. The relationships given in Eq. (27) serve a very useful role in correlating experimental data obtained from steady-state shear flow and oscillatory shear flow measurements.

Figure 9 gives plots of $\log \eta'$ versus $\log \omega$ and $\log G'$ versus $\log \omega$ for molten polystyrene at 200°C. For comparison, also given in Fig. 9 are plots of $\log \eta$ versus $\log \dot{\gamma}$ and $\log N_1$ versus $\log \dot{\gamma}$. It is seen that the shape of the $\log \eta'$ versus $\log \omega$ plot is very similar to that of the $\log \eta$ versus $\log \dot{\gamma}$ plot, and the shape of $\log G'$ versus $\log \omega$

plot is very similar to that of the $\log N_1$ versus $\log \dot{\gamma}$ plot. It should be mentioned that the use of the rotational instrument for polymeric liquids, especially very viscous molten polymers, is limited to low shear rates. The range lies below approximately 10 sec^{-1} for most commercially available molten thermoplastics, although the exact upper limit of operable shear rates may vary from material to material. It is well established that above a certain value of shear rate, say above 10 sec^{-1} , polymeric melts exhibit flow instability in cone-and-plate instruments. This phenomenon is commonly referred to as secondary flow or radial flow.

Another type of rheological instrument is the capillary rheometer, and it is not limited to low $\dot{\gamma}$. For this reason, the polymer industry has long used a plunger-type capillary instrument. In using such an instrument, one measures the pressure in the reservoir section of a capillary as a function of extrusion rate and then calculates the wall shear stress $\dot{\gamma}$ and consequently η . However, such a conventional instrument is limited to obtaining information on shear viscosity but not fluid elasticity. To overcome this limitation, it has been suggested that wall normal stresses be measured along the axis of a cylindrical or slit die with the aid of pressure transducers, as schematically shown in Fig. 10. According to this method, wall normal stresses must be measured far away from the entrance of the die and the axial profile of wall normal stress must be linear.

Figure 11 shows plots of wall normal stress profiles (often referred to as axial pressure profiles) along a cylindrical die for a low-density polyethylene melt at 180°C, and Fig. 12 shows similar plots for a low-molecular-weight polybutene at 35°C. It can be seen in Fig. 11 that the wall normal stress distribution is linear and the wall normal stresses extrapolated to the die exit plane (often referred

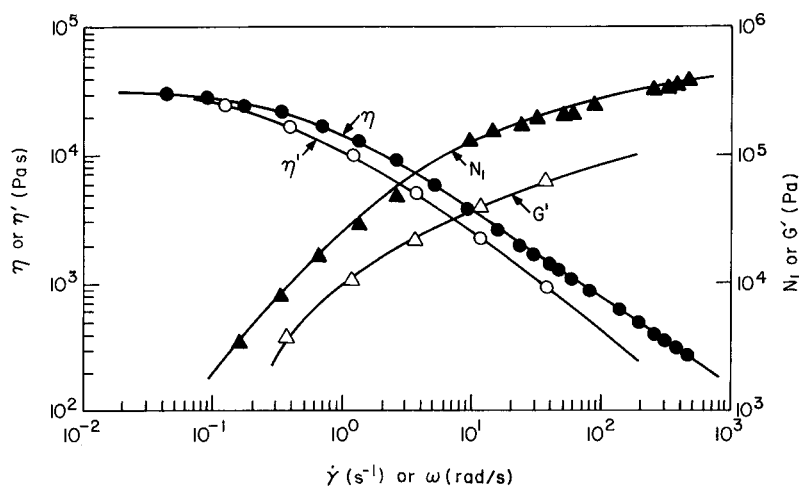


FIGURE 9 Plots of $\log \eta'$ versus $\log \omega$ (\circ), $\log G'$ versus $\log \omega$ (Δ), $\log \eta$ versus $\log \dot{\gamma}$ (\bullet), and $\log N_1$ versus $\log \dot{\gamma}$ (\blacktriangle) for a commercial polystyrene at 200°C.

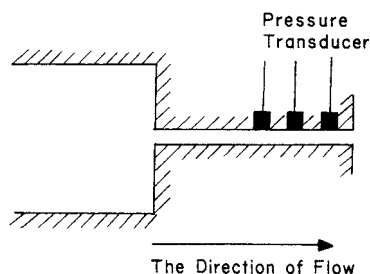


FIGURE 10 Schematic describing the measurement of wall normal stresses, with the aid of pressure transducers, along the axis of a cylindrical or slit die.

to as “exit pressure”) give rise to *nonzero* value, which increases with $\dot{\gamma}$. In contrast, in Fig. 12 the extrapolated wall normal stress to the die exit plane for polybutene gives rise to virtually *zero* value. It should be remembered that the same polybutene did not exhibit “rod climb-up” effect (see Fig. 1).

The slope of the pressure profile in Fig. 11 or Fig. 12 permits us to determine the wall shear stress with the following expression:

$$\sigma_w = (-\partial p/\partial z)(R/2), \quad (28)$$

here σ_w is the shear stress σ evaluated at the die wall, $-\partial p/\partial z$ is the pressure gradient, and R is the radius of the

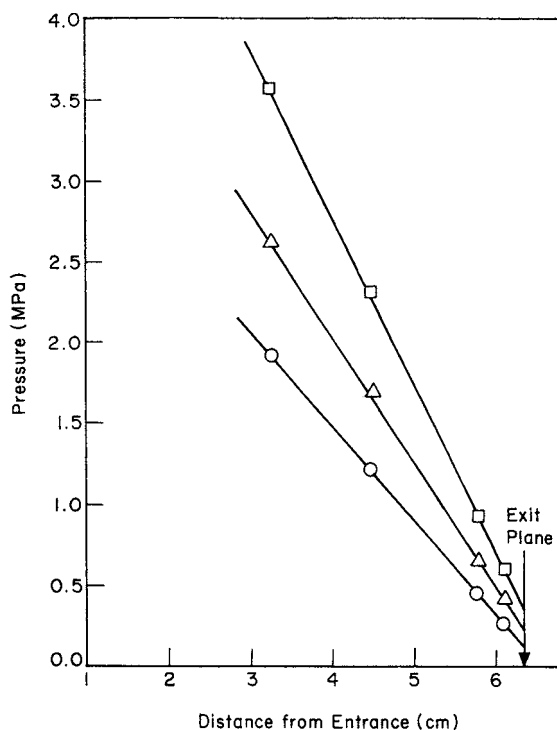


FIGURE 11 Profiles of wall normal stress along a capillary die axis for low-density polyethylene at 180°C for different shear rates: (○) 82.6 sec⁻¹, (△) 185.7 sec⁻¹, and (□) 432.5 sec⁻¹.

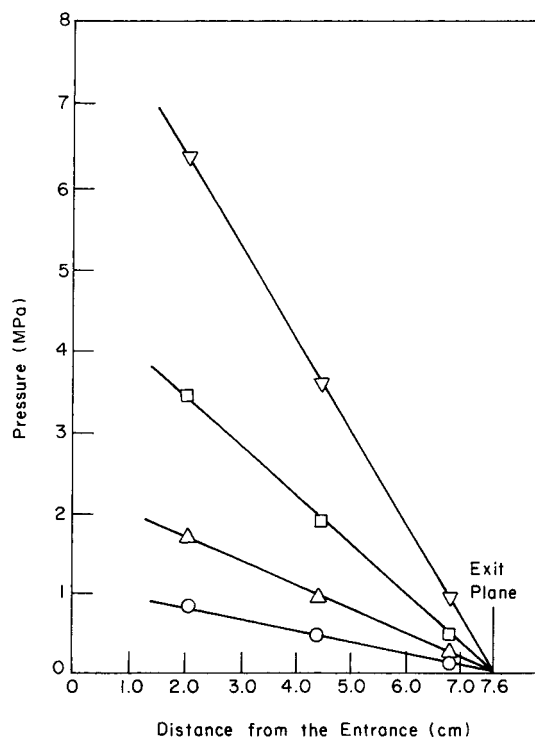


FIGURE 12 Profiles of wall normal stress along a capillary die axis for a low-molecular-weight polybutene at 35°C for different shear rates: (○) 20.5 sec⁻¹, (△) 38.6 sec⁻¹, (□) 77.7 sec⁻¹, and (▽) 157.3 sec⁻¹.

capillary. It can be seen in Figs. 11 and 12 that $-\partial p/\partial z$ increases with $\dot{\gamma}$, which is defined by

$$\dot{\gamma} = (4Q/\pi R^3)[(3n + 1)/4n], \quad (29)$$

where Q is the volumetric flow rate and n is the flow index introduced in Eq. (19). It should be remembered that Newtonian liquids (e.g., low-molecular-weight polybutene) have $n = 1$. Note that η can be determined by dividing σ_w by $\dot{\gamma}$.

If one uses a slit geometry, instead of a circular geometry, the following expressions must be used, instead of Eqs. (28) and (29), for σ_w

$$\sigma_w = (-\partial p/\partial z)(h/2), \quad (30)$$

and for $\dot{\gamma}$

$$\dot{\gamma} = (6Q/wh^2)[(2n + 1)/3n], \quad (31)$$

where h and w are the height and width of the slit die, respectively. It has been found that when the value of w is greater than 10 times the value of h (i.e., $w/h > 10$), the slit geometry yields the same values of σ_w and $\dot{\gamma}$ that the circular geometry does.

The nonzero value of “exit pressure” that can be seen in Fig. 11 is a manifestation of the fact that the molten

polyethylene has residual stress that is yet to be relaxed upon exiting from the die (Fig. 2). If there is no residual stress present in the liquid (e.g., low-molecular-weight polybutene) as it exits from the die, there will be no extrudate swell. Therefore, we can conclude that swelling of an extrudate originates from the existence of residual stress in the liquid at the exit plane of the die, that is, from the exit pressure. A theory has been advanced to relate the exit pressure to N_1 by

$$N_1 = P_{\text{exit}} \left[1 + \frac{d \ln P_{\text{exit}}}{d \ln \sigma_w} \right], \quad (32)$$

in which P_{exit} denotes the exit pressure. It should be remembered that N_1 represents fluid elasticity. It is then clear from Eq. (32) and Fig. 12 that the low-molecular-weight polybutene has *no* fluid elasticity owing to $N_1 = 0$. It should be mentioned that $\log \eta$ versus $\log \dot{\gamma}$ plots and $\log N_1$ versus $\log \dot{\gamma}$ plots given in Fig. 7 at high $\dot{\gamma}$ were obtained from wall normal stress measurements in a capillary die, i.e., η was determined by Eqs. (28) and (29) and N_1 by Eq. (32).

V. CONSTITUTIVE EQUATIONS FOR PREDICTING THE RHEOLOGICAL PROPERTIES OF POLYMERIC LIQUIDS

There are two primary reasons for seeking a precise mathematical description of the rheological equations of state (also often referred to as the constitutive equations or rheological models), which relate the state of stress to the state of deformation. The first reason is that such expressions can be used to identify the significant rheological parameters characteristic of the material, and to suggest the experimental procedure(s) for measuring them. One would then like to be able to correlate rheological properties with molecular parameters (e.g., molecular weight, molecular weight distribution, the degree of side chain branching, etc.). The second reason is that such an expression can be used, together with the equations of continuity, to solve the equations of motion (sometimes, also the equations of energy), in order to relate the rheological properties to flow conditions and flow geometry. There are two approaches to construct constitutive equations that enable one to predict the rheological properties of polymeric liquids: continuum (phenomenological) approach and molecular approach. Below we describe very briefly each of these two approaches, in order to convey the basic ideas behind the two approaches.

Continuum Approach to Constitutive Equations

In the continuum approach, emphasis is placed on formulating the relationships between the components of

stress and the components of deformation (or the rate of deformation), which should then properly describe the response of the material to a specific deformation imposed. The constants involved in a specific rheological equation of state presumably represent the characteristics of the material. It should be mentioned that the parameters appearing in a continuum theory often have to be determined by curve-fitting to experimental results. In this regard, constitutive equations based on a continuum approach are of little help, for instance, to the design of polymers with specific molecular characteristics. For such purposes, constitutive equations based on a molecular approach are needed, and this will be presented later.

In the development of rheological equations of state from a continuum point of view, basically there are two types of rheological equations of state, namely the differential type and the integral type. The differential type has the form that contains a derivative (or derivatives) of either the stress tensor or the rate-of-deformation tensor or both, and the integral type has the form in which the stress is represented by an integral over the deformation (or strain) history. Below we will present the basic ideas behind the development of continuum constitutive equations for both differential and integral types.

Let us consider the simplest instance in which one spring is attached to one dashpot, as schematically shown in Fig. 13. When a force F is acting on the spring downward at $t = 0$ (i.e., in one-dimensional flow), the deformation of the spring (i.e., Hookean material) may be described by

$$\sigma = G\gamma, \quad (33)$$

where σ is the stress (the force divided by the cross-sectional area), γ is the strain defined by $(L_0 - L)/L_0$, in which L_0 is the initial length of the spring (i.e., at $t = 0$) and L is its length at time t , and G is the proportionality constant, called the elastic modulus. On the other hand, the deformation of the dashpot (i.e., purely viscous fluid) may be described by

$$\sigma = \eta_0 \dot{\gamma}; \quad (34)$$

$\dot{\gamma} = d\gamma/dt$ is the rate-of-strain and η_0 is the proportionality constant, called viscosity. In other words, the spring

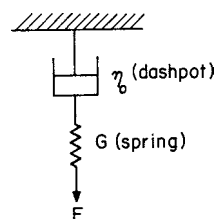


FIGURE 13 A spring-dashpot mechanical model of a viscoelastic fluid.

exhibits purely an elastic effect (i.e., as a Hookean solid) and the dashpot exhibits purely a viscous effect (i.e., as a Newtonian fluid).

Therefore, the total strain of the “spring and dashpot” at any time t is the sum of that due to the spring (reversible) and that due to the dashpot (irreversible). Combining Eqs. (33) and (34), we obtain

$$\sigma + \lambda_1 \frac{d\sigma}{dt} = \eta_0 \dot{\gamma} \quad (35)$$

which is known as the one-dimensional Maxwell mechanical model. Note that $\lambda_1 = \eta_0/G$ in Eq. (35) is a time constant, often referred to as the relaxation time. Equation (35) is capable of qualitatively explaining many well-known viscoelastic phenomena, such as stress relaxation following a sudden change in deformation and elastic recovery following a sudden release of imposed stress.

If the partial derivative $\partial/\partial t$, appearing in Eq. (35), is replaced with the convected derivative $\partial/\partial t$, we obtain

$$\sigma + \lambda_1 \frac{\partial \sigma}{\partial t} = \eta_0 \mathbf{d}. \quad (36)$$

This model predicts $\eta = \eta_0$ and $N_1 = 2\lambda_1 \dot{\gamma}^2$ for steady-state shear flow. There are many different types of non-linear rheological models suggested in the literature. One of the simplest modifications that can be introduced into Eq. (36), in order to empirically correct the inherent defects that the linear Maxwell model has in predicting the rheological properties of viscoelastic fluids, would be to make the material constants become shear dependent. There have been several attempts made to accomplish this, and one such generalization can be made as

$$\sigma + \lambda(\Pi) \frac{\partial \sigma}{\partial t} = 2\eta(\Pi) \mathbf{d}, \quad (37)$$

where Π represents the second invariant of the rate-of-deformation tensor \mathbf{d} . For steady-state shear flow, the two parameters $\lambda(\Pi)$ and $\eta(\Pi)$ may be expressed by

$$\eta(\dot{\gamma}) = \frac{\eta_0}{[1 + (\eta_1 \dot{\gamma}^2)^{(1-n)/2}]}, \quad (38)$$

$$\lambda(\dot{\gamma}) = \frac{\lambda_0}{[1 + (\lambda_1 \dot{\gamma}^2)^{(1-m)/2}]}. \quad (39)$$

There are many other differential-type constitutive equations that can be found in the literature.

For infinitesimally small deformations, the integration of Eq. (35) gives

$$\sigma(t) = 2 \int_{-\infty}^t \frac{\eta_0}{\lambda_1} e^{-(t-t')/\lambda_1} \mathbf{d}(t') dt'. \quad (40)$$

Since polymeric materials consist of many segments of different submolecules, the properties of a polymeric material may be thought of being given in terms of a spectrum

of these variables (e.g., λ_i and η_i for the i th submolecule). If one assumes that the components of a stress are linearly related to the components of the rate of deformation, then the overall response of the N submolecules may be expressed by

$$\sigma(t) = 2 \int_{-\infty}^t \sum_{i=1}^N \frac{\eta_0}{\lambda_i} e^{-(t-t')/\lambda_i} \mathbf{d}(t') dt'. \quad (41)$$

If one considers the rate of deformation as the cause and the stress as the resulting effect, then the observed “resulting effect” at the present time is due to the sequence of causes up to the present time t from the remote past.

For large deformations, one can still write differential-type rheological equations of state with integral representation, using appropriate transformations of the coordinate systems involved, as

$$\sigma(t) = 2 \int_{-\infty}^t m(t-t') \Gamma(t, t') dt', \quad (42)$$

where $m(t-t')$ is referred to as the memory function and $\Gamma(t, t')$ is the rate-of-deformation tensor in a coordinate system rotating with a fluid element. The memory function $m(t-t')$ for Eq. (40) is given by

$$m(t-t') = \frac{\eta_0}{\lambda_1} e^{-(t-t')/\lambda_1}. \quad (43)$$

One can derive expressions for three material functions, σ , N_1 , and N_2 , from Eq. (37), Eq. (40), or Eq. (42). Such expressions are well documented in the literature.

Molecular Approach to Constitutive Equations

The molecular approach is to relate the rheological behavior of polymeric liquids to their molecular parameters, such as molecular weight, molecular weight distribution, and the extent of side chain branching. It is not difficult to surmise that the rheological properties of polymers are greatly influenced by the molecular parameters. The predictions of the rheological properties of polymers on the basis of phenomenological theory is of little help either to control the quality of polymers produced or to improve the performance of polymers, unless the parameters appearing in various continuum constitutive equations are related to molecular parameters.

It is well established that the zero-shear viscosity (η_0) of polymer is proportional to the molecular weight (M) below a critical value M_c , whereas above M_c it increases rapidly and becomes proportional to $M^{3.4}$, i.e.,

$$\eta_0 = \begin{cases} KM, & \text{for } M \leq M_c, \\ KM^{3.4}, & \text{for } M > M_c. \end{cases} \quad (44)$$

The critical molecular weight M_c is believed to correspond to a value beyond which molecular entanglements (i.e.,

temporary couplings between neighboring chains) begin to dominate the resistance to flow. For concentrated solutions and molten polymers, the chain contours are extensively intermingled, so each chain is surrounded all along its length by a mesh of neighboring chain contours. Rearrangement of macromolecular chains on larger scales is restricted because the chain cannot cross through its neighbors. The molecular weight between entanglement couplings M_e is about one half of M_c , i.e., $M_c \approx 2M_e$. In the case of polymer solutions, both K and M_c in Eq. (44) change if a solvent is added to the polymer.

One can interpret the critical molecular weight M_c as a material constant signifying the lower limit of molecular weight for which non-Newtonian flow can be observed. It would then be expected that the onset of non-Newtonian behavior is strongly dependent on the molecular weight and the molecular weight distribution. Above M_c , the onset of non-Newtonian behavior occurs at lower shear rates as the molecular weight increases and as the molecular weight distribution broadens. A molecular interpretation of the viscoelastic behavior of polymeric liquids requires different concepts for the two regimes: (a) unentangled regime and (b) entangled regime.

Rouse introduced a “bead-spring” model, in which it is assumed that the long polymer molecule can be divided into submolecules and that fluctuations of the end-to-end length of a polymer molecule follow a Gaussian probability function. Then a polymer molecule is considered to be replaced by a chain of N identical segments joining $N + 1$ identical beads with completely flexible spring at each bead, as schematically shown in Fig. 14. The seminal study of Rouse dealt with dilute polymer solutions, which was later extended to polymeric melts by Zimm. The Rouse theory being valid in the linear regime (i.e., in the Newtonian regime), later Zimm extended the Rouse theory to predict shear-thinning (non-Newtonian) viscosity of a polymer, as well as the effect of polydispersity on shear viscosity.

We will now discuss predictions of the linear viscoelastic properties of unentangled polymer melts based on the Rouse theory. Consider the situation where a sudden strain

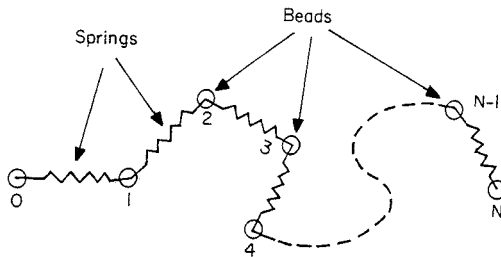


FIGURE 14 The bead-spring model for a linear polymer molecule.

is imposed on a polymer. The stress remaining in the specimen at time t can be determined from a material property referred to as the stress relaxation modulus $G(t)$, which for the Rouse model is given by

$$G(t) = \frac{\rho RT}{M} \sum_{p=1}^{\infty} \exp(-t/\tau_p), \quad (45)$$

where ρ is the density, R is the universal gas constant, T is the absolute temperature, M is the molecular weight, and τ_p is given by

$$\tau_p = \frac{\zeta b^2 N^2}{6\pi^2 p^2 k_B T}, \quad (46)$$

in which ζ is the segmental friction coefficient, b is the Kuhn statistical length, N is the number of identical segments, and k_B is the Boltzmann constant. Note that the largest or terminal relaxation time τ_1 for the Rouse chain, i.e., for $p = 1$ in Eq. (46), is given by

$$\tau_r = \tau_1 = \frac{(N\zeta)(Nb^2)}{6\pi^2 k_B T}, \quad (47)$$

where the quantities $N\zeta$ and Nb^2 describe the chains as a whole and are each proportional to the number of links in the chain backbone. Hereafter τ_r will be referred to as the Rouse relaxation time.

When $G(t)$ is known, one can obtain expressions for zero-shear viscosity η_0 , steady-state compliance J_e^0 , dynamic storage modulus $G'(\omega)$, and dynamic loss modulus $G''(\omega)$ from

$$\eta_0 = \int_0^{\infty} G(t) dt, \quad (48)$$

$$J_e^0 = \frac{1}{\eta_0^2} \int_0^{\infty} t G(t) dt, \quad (49)$$

$$G'(\omega) = \omega \int_0^{\infty} G(t) \sin \omega t dt, \quad (50)$$

$$G''(\omega) = \omega \int_0^{\infty} G(t) \cos \omega t dt, \quad (51)$$

in which ω is angular frequency applied in oscillatory shear flow. Substitution of Eq. (45) into Eqs. (48)–(51) gives

$$\eta_0 = (\pi^2 K \rho RT / 36) M, \quad (52)$$

$$J_e^0 = 2M / 5 \rho RT, \quad (53)$$

$$G'(\omega) = \frac{\rho RT}{M} \sum_{p=1}^{\infty} \frac{\omega^2 \tau_p^2}{1 + \omega^2 \tau_p^2}, \quad (54)$$

$$G''(\omega) = \frac{\rho RT}{M} \sum_{p=1}^{\infty} \frac{\omega \tau_p}{1 + \omega^2 \tau_p^2}. \quad (55)$$

Note that K in Eq. (52) is defined by

$$K = \frac{\zeta b^2 N^2}{\pi^2 k_B T M^2}. \quad (56)$$

The Rouse model allows us to determine that stress σ contributed by the polymer chains by

$$\sigma = \sum_{p=2}^{\infty} \sigma_p, \quad (57)$$

where σ_p denotes the stress contributed by the polymer chain at the p th mode ($p = 1, 2, \dots, \infty$), which can be evaluated from

$$\left(1 + \tau_p \frac{\partial}{\partial t}\right) \sigma_p = G_0 \delta, \quad (58)$$

where $\partial/\partial t$ is the upper convected derivative, τ_p is the relaxation times defined by Eq. (46), $G_0 = \rho RT/M$, and δ is the Kronecker delta function.

In steady-state shear flow the Rouse model predicts

$$\sigma = \frac{\rho RT}{M} \sum_{p=1}^{\infty} \tau_p \dot{\gamma}, \quad (59)$$

$$N_1 = \frac{2\rho RT}{M} \sum_{p=1}^{\infty} \tau_p^2 \dot{\gamma}^2, \quad (60)$$

$$N_2 = 0. \quad (61)$$

Use of Eq. (46) in Eq. (59) gives the zero-shear viscosity,

$$\eta_0 = \frac{\rho b^2 \zeta N_A N^2}{36M}, \quad (62)$$

where N_A is Avogadro's number. Since $N \propto M$, it can be concluded from Eq. (62) that $\eta_0 \propto M$ and it is independent of shear rate $\dot{\gamma}$, i.e., the Rouse model cannot predict shear-dependent viscosity. Equation (62) can be rewritten as

$$\eta_0 = \left(\frac{\rho b_0^2 \zeta_0 N_A}{36M_0^2}\right) M, \quad (63)$$

where b_0 is the length of monomer, ζ_0 is the monomeric friction coefficient, and M_0 is the molecular weight of monomer. The ζ_0 is one of the most important properties of macromolecules, which can be calculated from Eq. (63) by measurement of η_0 . With the aid of Eq. (63), Eq. (46) can be rewritten as

$$\tau_p = \frac{6\eta_0 M}{\pi^2 p^2 \rho RT}, \quad (64)$$

and thus the terminal (Rouse) relaxation time becomes

$$\tau_r = \tau_1 = \frac{6\eta_0 M}{\pi^2 \rho RT}. \quad (65)$$

The Rouse model is useful to predict the linear viscoelastic properties (Eqs. (52)–(55)) of polymer melts

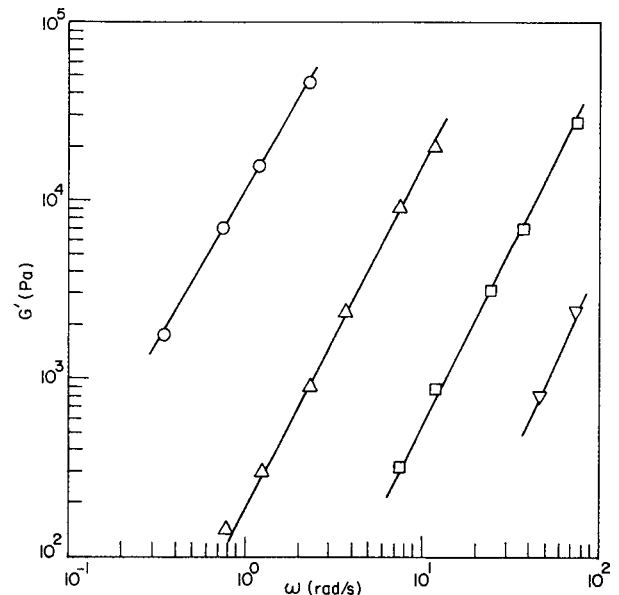


FIGURE 15 Plots of $\log G'$ versus $\log \omega$ for a nearly monodisperse polystyrene with molecular weight of 9×10^3 at various temperatures: (○) 120°C, (△) 130°C, (□) 140°C, and (▽) 150°C.

with molecular weight M less than M_c . Figure 15 gives plots of $\log G'$ versus $\log \omega$, and Fig. 16 gives plots of $\log G''$ versus $\log \omega$, measured at four different temperatures for a monodisperse polystyrene with $M = 9000$, which is much lower than the $M_c = 36,000$ of polystyrene. It can be seen in these figures that (a) at a constant value

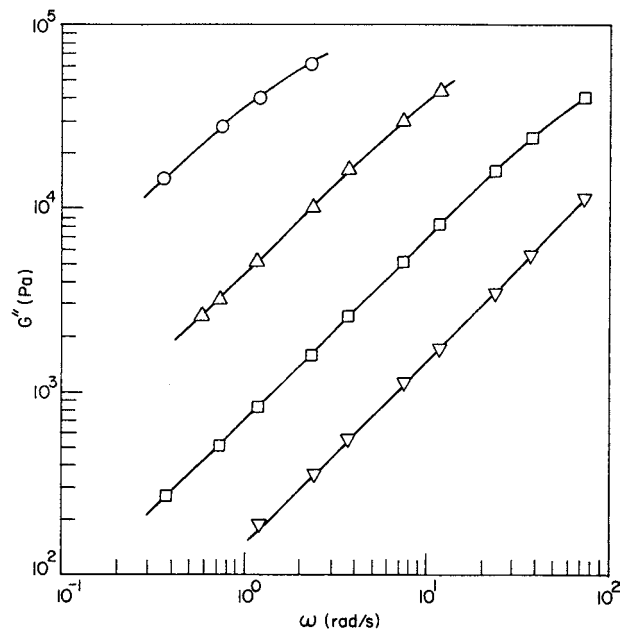


FIGURE 16 Plots of $\log G''$ versus $\log \omega$ for a nearly monodisperse polystyrene with molecular weight of 9×10^3 at various temperatures: (○) 120°C, (△) 130°C, (□) 140°C, and (▽) 150°C.

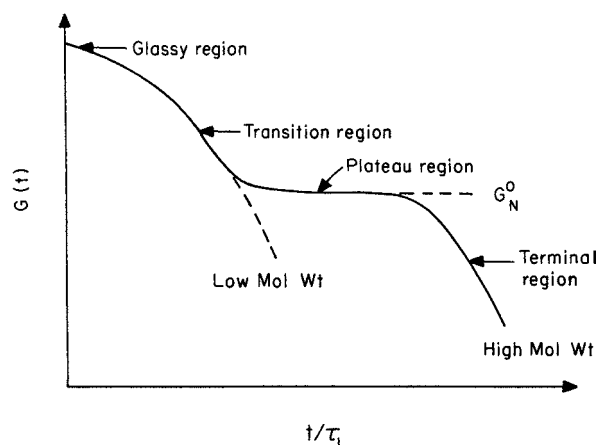


FIGURE 17 Schematic describing the relaxation of modulus of a polymer upon cessation of flow in terms of dimensionless time t/τ_1 with τ_1 being the terminal relaxation time of the polymer.

of ω , values of G' and G'' decrease with increasing temperature, (b) at a given temperature, values of G' and G'' increase with increasing ω , and (c) the terminal behavior is observed in both G' and G'' over the entire range of frequency investigated.

Experiment has shown that the stress relaxation modulus $G(t)$ of an entangled polymer with $M \gg M_c$ is quite different from that of an unentangled polymer with $M < M_c$, as shown schematically in Fig. 17. It can be seen in Fig. 17 that for entangled polymer melts there are two main dispersions: (1) relaxation at short times in the transition region is independent of chain length and appears to reflect only local rearrangements of chain conformation, and (2) relaxation at long times in the terminal region reflects the rearrangement of large-scale conformation. Its location and shape depends strongly on molecular parameters: chain length and chain-length distribution. Between the terminal region and transition region there appears a plateau region where $G(t)$ changes only slowly with time. It has been observed that the separation in time of these two dispersions increases rapidly with chain length, but the modulus in the plateau region G_N^0 , commonly referred to as plateau modulus, is insensitive to molecular parameter and depends only on polymer species and concentration. Notice in Fig. 15 that there is no plateau modulus for unentangled polymers. It should be mentioned that the plateau modulus is one of the most important viscoelastic properties that distinguish entangled polymers from unentangled polymers.

Figure 18 gives experimental data of reduced dynamic storage and loss moduli, $G'_r(\omega)$ and $G''_r(\omega)$, plotted against angular frequency $a_T\omega$ for a nearly monodisperse polystyrene with molecular weight M of 1.95×10^5 over a very wide range of temperatures, where a_T is a shift

factor that enables one to superpose experimental data obtained at different temperatures on a single master plot. Note in Fig. 18 that G'_r and G''_r are defined, respectively, by $G'_r = (\rho_0 T_0 / \rho T) G'(\omega)$ and $G''_r = (\rho_0 T_0 / \rho T) G''(\omega)$, where ρ_0 is the density at a reference temperature T_0 and ρ is the density at temperature T . The following observations are worth noting in Fig. 18: (a) in the terminal region the slope of $\log G''_r$ versus $\log a_T\omega$ plots is 2 and the slope of $\log G'_r$ versus $\log a_T\omega$ plots is 1; (b) there is a very long plateau region, from which the value of G_N^0 can be determined. A characteristic feature of the plateau region is that the magnitude of G'' is smaller than that of G' , as illustrated in Fig. 18.

Today it is a well-accepted procedure that once the value of G_N^0 is available, one can determine the molecular weight between entanglement couplings M_e from the relationship

$$G_N^0 = \rho RT / M_e. \quad (66)$$

It is a prevailing view today that the entanglement effects arise essentially from topological restrictions on the chain motions.

A molecular theory for concentrated polymer solutions and melts was developed by Doi and Edwards. Their theory is based on the premise that a polymer chain is confined within a fictitious tube, through which the polymer chain moves along the tube axis in reptative mode, as schematically shown in Fig. 19. The Doi-Edwards theory is often referred to as the "tube model," in which the principal molecular motion considered is that of reptation confined within a tube. If the characteristic length scale of motion is smaller than the tube diameter a , the entanglement effect is not important, and the dynamics are well described by the Rouse model (or the Zimm model if the hydrodynamic interaction is dominant). On the other hand, if the length scale of the motion becomes larger than the value of a , the dynamics of the chain is governed by reptation. There is experimental evidence indicating that reptation is the dominant motion of highly entangled polymer molecules. The reptation model has been successful in explaining many features of the viscoelastic behavior of concentrated polymer solutions and polymer melt, and also predicting some of the rheological behavior in a nonlinear regime.

In the tube model, the chains can stretch and contract along the tube or slide along the tube as a whole. The former motion equilibrates the fluctuation in the density of the chain segment along the tube, and the latter motion is related to the diffusion of the chain as a whole. The characteristic times of these processes can be derived easily from the Rouse model consisting of N segments. In other words, the Rouse chain remains the basic model, but now subject to spatial constraints in the form of a tube to represent the mesh.

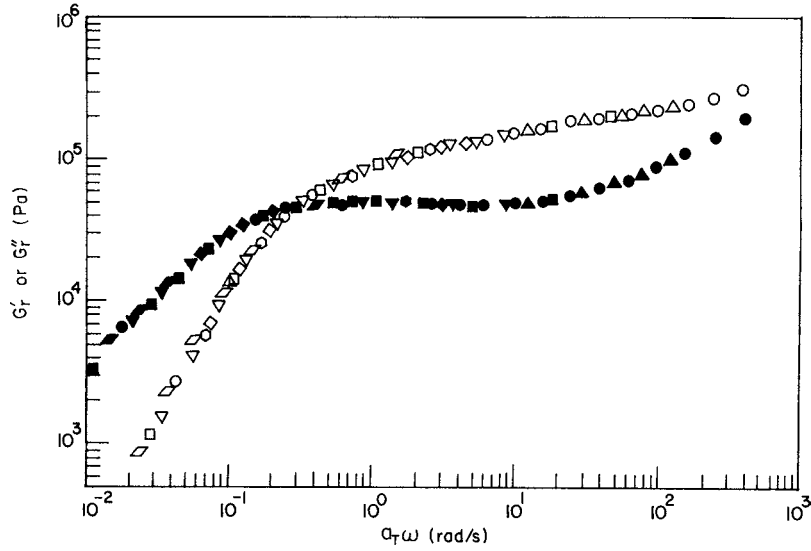


FIGURE 18 Plots of $\log G'_r$ versus $\log a\tau\omega$ (open symbols) and plots of $\log G''_r$ versus $\log a\tau\omega$ (filled symbols) for a nearly monodisperse polystyrene with molecular weight of 1.95×10^5 at various temperatures (\circ, \bullet) 160°C, ($\triangle, \blacktriangle$) 170°C, (\square, \blacksquare) 180°C, ($\nabla, \blacktriangledown$) 200°C, (\diamond, \blacklozenge) 210°C, (\circ, \bullet) 220°C, and (\oslash, \blacklozenge) 230°C.

The tube model yields the following expressions for the linear viscoelastic properties of concentrated polymer solutions or polymer melts:

$$\eta_0 = (\pi^2/12)G_N^0\tau_d, \quad (67)$$

$$J_e^0 = 6/5G_N^0, \quad (68)$$

$$G'(\omega) = \frac{8G_N^0}{\pi^2} \sum_{\text{odd } p} \frac{1}{p^2} \frac{(\omega\tau_d/p^2)^2}{1 + (\omega\tau_d/p^2)^2}, \quad (69)$$

$$G''(\omega) = \frac{8G_N^0}{\pi^2} \sum_{\text{odd } p} \frac{1}{p^2} \frac{\omega\tau_d}{1 + (\omega\tau_d/p^2)^2}, \quad (70)$$

where τ_d is the disengagement time defined by

$$\tau_d = \frac{\zeta N^3 b^4}{\pi^2 a^2 k_B T} = \left(\frac{K}{M_e}\right) M^3, \quad (71)$$

in which K is given by Eq. (56). Thus η_0 given by Eq. (67) can be rewritten as

$$\eta_0 = \left(\frac{0.10416 \rho b_0^2 \zeta_0 N_A}{M_e^2 M_0^2}\right) M^3. \quad (72)$$

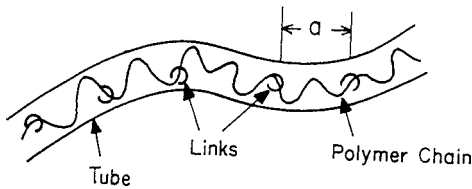


FIGURE 19 Schematic describing the tube model.

We therefore have the following relationships:

$$\tau_d \propto M^3; \quad \eta_0 \propto M^3; \quad J_e^0 \propto M^0. \quad (73)$$

On the other hand, it is well established experimentally that $\eta_0 \propto M^{3.4}$ for entangled polymer melts (see Eq. (44)). Thus the prediction of the tube model deviates from the well-established relationship between η_0 and M for entangled polymer melts.

While the Rouse model considers only intramolecular motions, the tube model deals with intermolecular interactions due to entanglement couplings and neglects intramolecular motions. The neglecting of intramolecular motions that may occur on the time scale shorter than the time scale of reptation motions was thought to be responsible for the 3.0 power dependence of η_0 on M , given in Eq. (72). Doi incorporated fluctuations of contour length into the tube model and obtained the following expression for η_0 :

$$\eta_0 = \left(\frac{\pi^2 K \rho R T}{15}\right) \left(\frac{M^3}{M_e^2}\right) [1 - 1.47(M_e/M)^{0.5}]^3. \quad (74)$$

It can be shown that values of η_0 predicted from Eq. (74) are numerically close to the 3.4 power of molecular weight M for $20M_e < M < 200M_e$.

By combining the molecular network theory and the tube model, the following expression for η_0 predicting a gradual transition from 3.5 power to 3.0 power dependence of η_0 on M as M/M_e ratio increases is reported:

$$\eta_0 = \left(\frac{0.001496 \rho N_A \zeta_0 b^2}{M_e^{2.5} M_0^2}\right) M^{3.5}. \quad (75)$$

It should be pointed out that Eq. (75) was derived without invoking fluctuations of contour length (i.e., without considering the Rouse motion in a reptating chain). The main idea behind the derivation of Eq. (75) is that since experimental data for η_0 is usually obtained from shear measurement, stress effect must be included into the reptation model; i.e., when a polymer is subjected to shear flow, a relaxation of polymer chains to reptate around the entangled junctions must be taken into consideration, in addition to the reptation of the overall center-of-mass motion. For very high-molecular-weight polymers, the approach used to derive Eq. (75) yields

$$\eta_0 = \left(\frac{0.02916 \rho \zeta_0 b_0^2 N_A}{M_e^2 M_0^2} \right) M^3. \quad (76)$$

It has been shown that the combination of Eqs. (75) and (76) predicts a gradual transition from a 3.4 power law to a 3.0 power law for $200M_e < M < 2000M_e$, which compares very favorably with experiment.

The tube model predicts, for steady-state shear flow, three material functions, η , N_1 , and N_2 , and they are expressed by

$$\eta = (G_0/\dot{\gamma}) \int_0^\infty m(s) F_1(\dot{\gamma}s) ds, \quad (77)$$

$$N_1 = G_0 \dot{\gamma} \int_0^\infty sm(s) F_1(\dot{\gamma}s) ds, \quad (78)$$

$$N_2 = -G_0 \int_0^\infty m(s) F_2(\dot{\gamma}s) ds, \quad (79)$$

where $\dot{\gamma}$ denotes shear rate, $m(s)$ is a memory function, and $F_1(\dot{\gamma}s)$ and $F_2(\dot{\gamma}s)$ are complicated expressions not shown here.

VI. CONCLUDING REMARKS

In studying the rheology of a specific type of material, one needs to perform the following three basic steps: (1) define the flow field in terms of the velocity components and the coordinates that are most appropriate; (2) choose a rheological equation of state for the description of the material under deformation, and (3) decide which of the experimental techniques available are most suitable for determining the rheological properties of the material under consideration.

There are two reasons for seeking a precise mathematical description of the rheological models, which relate the state of stress to the state of deformation. The first is that such an expression can be used to identify the significant rheological parameters characteristic of the materials and to suggest the experimental procedure for measuring them. One would then like to correlate the rheological

parameters with the molecular weight, molecular weight distribution, and molecular structure. The second reason is that such an expression can be used, together with the equation of continuity, to solve the equations of motion that relate the rheological parameters to flow conditions and die geometry.

In the past, much effort has been put into developing rheological models for predicting the rheological properties of polymeric liquids. There are two approaches to describing the rheological behavior of viscoelastic polymeric liquids. One approach is to view the material as a continuum, and then to describe the response of this continuum to stress or strain by a system of mathematical statements having their origin in the theories of continuum mechanics. Another approach is to describe the rheological behavior of the material from molecular considerations. In either approach, one basically has to establish a relationship (or relationships) on the basis of either a rigorous mathematical physical theory or empiricism, or both, which describes the deformation of a fluid in terms of the components of the deformation history or the rate of deformation and the components of the stress.

As an important application of rheology, one can cite processing of polymeric materials. The polymer processing industry constantly strives to improve its existing processing techniques and to develop new ones with the purpose of finding optimum processing conditions for each new material that comes on the market. Therefore, the development of a method or methods for evaluating the processibility of a new polymeric material and for improving existing processing conditions is an essential step in improving the mechanical or other properties of the final product. On the basis of the information presented here, it can be concluded that processibility is very closely related to the rheological properties of the polymeric materials in the molten state and that a good understanding of any polymer processing operation requires knowledge of several branches of science and engineering, such as polymer chemistry, polymer physics, polymer rheology, and mass and energy transports.

SEE ALSO THE FOLLOWING ARTICLES

FLUID DYNAMICS (CHEMICAL ENGINEERING) • LIQUID CRYSTALS • LIQUIDS, STRUCTURE AND DYNAMICS • PLASTICS ENGINEERING • POLYMER PROCESSING • POLYMERS, MECHANICAL BEHAVIOR • RUBBER, SYNTHETIC • STEREOCHEMISTRY

BIBLIOGRAPHY

Bird, R. B., Armstrong, R. C., and Hassager, O. (1987). "Dynamics of Polymeric Liquid," 2nd edition, Vol. 1, Wiley, New York.

- Collyer, A. A., and Clegg, D. W., eds. (1998). "Rheological Measurement," 2nd edition, Chapman & Hall, London.
- Doi, M., and Edwards, S. F. (1986). "The Theory of Polymer Dynamics," Clarendon Press, Oxford.
- Ferry, J. D. (1980). "Viscoelastic Properties of Polymers," 3rd edition Wiley, New York.
- Han, C. D. (1976). "Rheology in Polymer Processing," Academic Press, New York.
- Han, C. D. (1981). "Multiphase Flow in Polymer Processing," Academic Press, New York.
- Han, C. D. (1998). *In* "Rheological Measurement," A. A. Collyer and D. W. Clegg, eds., 2nd edition, pp. 190–209, Chapman & Hall, London.
- Larson, R. D. (1988). "Constitutive Equations for Polymer Melts and Solutions," Butterworth, Stoneham, MA.
- Walters, K. (1975). "Rheometry," Chapman & Hall, London.



Rubber, Natural

Stephen T. Semegen

STS Technical Services

- I. Introduction
- II. Agriculture
- III. Preparation
- IV. Modified Rubber and Derivatives
- V. Properties
- VI. Product Usages
- VII. Economics
- VIII. Research

GLOSSARY

Crystallization, polymer Arrangement of previously disordered polymer segments of repeating patterns into geometric symmetry.

Latex, rubber Colloidal aqueous dispersion of rubber.

Monomer Low-molecular-weight substance consisting of molecules capable of reacting to form a polymer.

Polymer Three-dimensional substance of molecules characterized by repetition of one or more monomer units.

Rubber Material that is capable of recovering (retracting) quickly from large deformations.

Rubber product Item of commerce whose major portion consists of rubber.

Rubber, raw Vulcanizable macromolecular material, used to produce a rubber product.

Tack, rubber Property causing contacting surfaces of raw rubber to adhere to each other.

Transition, first order Reversible change in phase of a material, as in melting or crystalization of polymers.

Transition, glass Reversible change in a material from a viscous or rubbery state to a brittle glassy state.

Vulcanization Irreversible process changing the chemical structure of a rubber (cross-linking), becoming less plastic, more elastic, and extending the usable temperature range.

NATURAL RUBBER is a *cis*-1,4-polyisoprene obtained from a botanical source and is the oldest known rubber. It is also the most versatile one for fabrication into rubber products. Before World War II, natural rubber accounted for practically 100% of all rubber usage. Two-thirds of this total usage is for tires. However, natural rubber did not become an important industrial commodity until the discovery of sulfur vulcanization in 1839 and the invention of the pneumatic tire in 1888.

Even so, natural-rubber-containing trees originally grew wild in the jungles of South America. They had to be domesticated and raised as an agricultural crop on cultivated farms and plantations. Finally, a tapping

system had to be devised to remove the rubber latex from the tree without permanent damage to the tree. By 1900, the modern rubber industry had been born. Today, natural and synthetic rubbers enjoy a symbiotic relationship.

I. INTRODUCTION

Natural rubber is a high-molecular-weight polymer of isoprene, whose chemical structure is 2-methyl-1,3-butadiene. Natural rubber most commonly is obtained from the latex of the *Hevea brasiliensis* tree. The *Hevea* tree is indigenous to South America, especially in the Amazon valley. However, for the past hundred years, it has been cultivated in many tropical areas around the world. Principally, this species is grown in Southeast Asia, especially Malaysia and Indonesia. As a rule, regions that are 5–10° latitude north or south of the equator can grow rubber trees. Heavy rainfall over the full year, temperatures holding between 70 and 90°F, and elevations preferably no higher than a thousand feet above sea level are necessary for commercial growth.

More than 14 million acres, currently containing more than 2 billion rubber trees, had to be cleared out of dense jungles and rain forests in Southeast Asia. Conversely, the *Hevea brasiliensis* tree is practically no longer cultivated in its South American birthplace, because of its susceptibility to leaf blight disease. The latter is caused by a fungus, *Dothidella ulei*. Some progress has been made recently in controlling the disease, but not yet on a commercial scale. Two *Hevea* species are known that are resistant to the leaf blight—*Hevea benthaniama* and *Hevea pauciflora*. Efforts have been made to cross-breed *Hevea brasiliensis* in order to develop high-yielding progeny and high-quality rubber.

Natural rubber is present in varying degree in at least 200 different species of plants, including such common weeds as goldenrod and dandelion (Table I). All these species fall short of *Hevea* in yield, purity, frequency of

tapping, and longevity. All contain more resin, that is, acetone-soluble material. For example, the Russian dandelion *koksagys* contains only 10% rubber hydrocarbon, gathered from the roots. Goldenrod is reputed to have about 8% rubber in its stems. During World War II, several of these species were utilized when the Asian sources were cut off. Guayule has recently been reactivated in a joint program by Mexico and the United States. Its ideal aim is freedom from dependency on overseas sources. In practical reality, it is a program by the U.S. Department of Agriculture and the U.S. Bureau of Indian Affairs to provide employment in Mexico and the southwestern United States.

A. Historical Background

Natural rubber has been traced back to the eleventh century when the Mayan Indians made simple articles from it. First scientific observations were made by the French, Charles de la Condamine and C. F. Fresneau. They identified the rubber trees as the species *Hevea Brasiliensis*.

Economic growth of natural rubber was hampered by its thermoplastic behavior. In 1939, independent discovery of vulcanization with sulfur was independently made in the United States by Charles Goodyear and in England by Thomas Hancock.

In 1888, the Englishman, John Dunlop developed the pneumatic tire, for bicycles. With the advent of the automobile, the current rubber industry was born. However, natural rubber was native to only Central and South America, where it was highly susceptible to yellow leaf blight disease.

In 1876, Sir Henry Wickham gathered 70,000 *Hevea* rubber seeds in Brazil. These were ultimately planted as seedlings throughout Southeast Asia. From these plants, 75% of the total cultivated rubber in the world has sprung.

Plantation rubber became a reality in 1888. Henry N. Ridley, director of the Botanic Gardens in Singapore, discovered the current method of “tapping” a tree to obtain the latex. He is known as the father of the modern plantation industry.

Within a decade, Indonesia, Sri Lanka, and Malaya started rubber plantations. Ridley later showed that rubber trees could be planted in regular rows in clear areas, that trees could be tapped every few days, and that the trees would produce latex efficiently for at least 30 years. Rapid growth of rubber production followed (Table II).

II. AGRICULTURE

A. Botanical Studies

The *Hevea* tree is a tall tree, averaging 60 ft in height, and reaching as high as 120 ft. The bark is smooth and

TABLE I Some Common Rubber-Bearing Plant Species

Name	Habitat
<i>Funtumia elastica</i>	Africa
<i>Landolphia</i>	Africa
<i>Castilloa elastica</i>	Mexico
<i>Manihot glaziovii</i> (Ceara)	South America
<i>Ficus elastica</i>	India, Burma
<i>Taraxacum koksagys</i>	Russia
<i>Parthenium argentatum</i> (Guayule)	Mexico, United States (California)
<i>Cryptostegia grandiflora</i>	United States (Florida)

TABLE II Early Consumption of Natural Rubber

Year	Metric tons
1825	30
1840	380
1850	1,500
1860	2,700
1870	8,000
1880	13,000
1890	23,000
1900	50,000

of a variable color, mostly light brown, but mottled with gray-green coloration. The tree can live for more than 100 years. The base circumference of the tree can be as much as 15 ft. However, most trees have a girth of 3 to 4 ft. Although the tree sheds its leaves once a year, latex tapping can be continued. Normally, latex yields are lower during the weathering season, usually about February. The fruit of the tree is a pod consisting of three sections, each with a seed. This is a characteristic of the Euphorbiaceae.

B. Pathology (Diseases)

Disease is a major enemy of the rubber tree. Yellow leaf blight has been mentioned. Brown bast, which attacks the tree trunk, is a canker causing physiological disturbance. *Oidium heveae* is a fungus that attacks the leaves. *Corticium salmonicolor* is another fungus setting in the forks between branches. *Phytophthora palmivora* thrives on the tapping panel. *Fomes* is a fungus resulting in moldy rot of the roots. It is small wonder that pathology is a major function of rubber research and production. Fortunately, there are known fungicides that are effective in preventing the spread of such diseases.

C. Planting and Cultivation

The tree has a tap root that goes deeply into the ground, anchoring the tree against wind damage, providing food, and resisting water drought. The most suitable soils are loamy, sandy clays, naturally drained, shade covered, and rich in mineral nutrients and organic matter.

In the past, *Hevea* trees were ready for tapping 5–6 years after planting. Recent research, however, has reduced the period of immaturity to 3 or 4 years. Peak efficiency is reached when the tree is almost 15 years old.

Once the land has been cleared, young *Hevea* can be planted. The young plants are obtained by germinating seeds in a bed, then transplanting the young seedlings to a nursery. The early technique consisted of planting seeds

that had been selected from trees known to be high in latex yield.

Selected seeds come from several sources: (1) natural, random pollination of flowers of a high yielding tree, (2) natural cross-pollination between trees in the same clone, and (3) artificial cross-pollination of high yielding trees. The latter provides the best seedlings.

Bud grafting was the next advance. A bud from a high-yielding tree is inserted under the bark of the lower stem of a young tree. If successful, the rest of the tree above the graft can be removed. The new branch then takes over, and becomes the main trunk of the mature tree. All trees derived by vegetive reproduction from a single mother tree are said to constitute a clone.

The vast majority of plantation acreage has been replanted with such high-yielding clones since 1945. These clones are less than two dozen in number. Typical names are Avros 49, Tjirandji 1, Bodjong Datar 5, Prang Besar 86, RRIM 501, RRIM 600, RRIM 703, etc. (Table III). Currently, second and third generations of the RRIM 600 series have been yielding up to 6000 lb/year/acre in small, pilot-scale plantings.

Young plants are raised in a nursery for the first year. The trees are then planted in a permanent field in regular rows about 14 to 20 ft apart. These are finally thinned out until 100 to 150 trees are left per acre. Legumes, such as soy bean plants, provide ground cover among the trees, and also furnish fixed nitrogen for fertilizer. Phosphate fertilizers are also used extensively.

D. Tree Tapping and Collection

The bark is the most important part of the rubber tree. It is here that the latex vessels are found. These vessels are living cells, within whose walls the latex is found. Latex vessels are a network of capillary tubes that exist in all parts of the tree. In the trunk, these are vertical bundles inclined from right to left at about a 5° angle. These bundles, arranged in a series of concentric rings, are concentrated near the cambium layer and are only 2–3 mm thick. The latex vessels are living cells that convert plant food materials into rubber hydrocarbon.

TABLE III Yields by Decades

Decade	Clone	Yield (lb/acre per year)
1920	Unselected	500
1930	Pil 384	1000
1940	PB 86	1200
1950	RRIM 501	1500
1960	RRIM 600	2300
1970	RRIM 703	3300

Ridley originally developed the herringbone pattern for the tapping panel, shaving 1–2 mm of bark with each cut or tap. The cut is made at an optimum angle of 25° from the horizontal. At the lower end is a vertical channel terminating in a metal spout below which is attached a latex collecting cup.

Tapping is usually performed in the early morning hours, although rainfall will seriously curtail the flow of latex. After flowing for several hours, the latex vessels plug up with coagulum. If the cut is reopened the next day, latex flow begins again. This indicates the rapid regeneration of latex by the tree.

At each successive tapping, a shaving of bark about $\frac{1}{16}$ in. thick is made, along the lower edge. This tapping system is known as spiral tapping. Other tapping systems are the “half spiral alternate daily” and the “full spiral fourth daily.” Another unusual system is the double tap, on opposite sides of the tree, with one cut about 4 ft higher than the other cut.

Latex from the tree (fresh, whole field latex) is 30–40% total solids by weight. The tapper is paid according to the “drc” (dry rubber content), as measured by a hydrometer. The contents of each tapping cup are collected in 5 gallon containers, then taken to nearby collecting stations for pickup trucks to deliver to large storage tanks at bulking stations. This practice is similar to the way dairy farmers handle milk.

A drop of ammonia is usually placed inside each cup before tapping, to prevent premature coagulation in the cup. Collected latex is further stabilized by the addition of about 0.01% ammonia, 0.05% sodium sulfite, or 0.02% formaldehyde. Fresh latex has a normal pH of 7.

Residue in the latex-collecting cup coagulates naturally, and is called cup lump. This is salvaged by the tapper during his next tapping, when he also removes the coagulated latex skin over the tapping cup. This is called tree lace. Any latex that drops on the ground is collected every few months. Such rubber is named earth scrap (Table IV).

About 10% of tree latex is concentrated and shipped to consumer countries, for conversion into finished latex products, such as a host of dipped goods, foam for

bedding or carpet backing, and adhesives. The percentage is higher in such producing countries as Malaysia and Liberia.

Latex is concentrated from an original 30% to about 60%. Such processes include centrifugation, evaporation, or creaming. Centrifuged latex accounts for about 90% of the total. The residual serum contains about 5% rubber, which is recovered and known as skim rubber.

Evaporated latex is prepared by passage through film evaporators at elevated temperatures. The final concentrate is usually higher than 60% solids and also contains the smallest rubber particles.

Creamed latex is the smallest volume type. It is prepared by mixing the latex with a creaming agent, such as ammonium alginate. Creaming occurs as the Brownian movement of the rubber particles slows down. The process may take several weeks. Creamed latex is primarily used in the manufacture of latex thread.

1. Yield Stimulation

The selection of planting material was the first step in improving the yield of rubber foam trees. This was followed by the application of certain chemicals, called plant “hormones,” to the bark near the tapping panel. Most common were 2,4-dichlorophenoxyacetic acid (2,4-D), 2,4,5-tri-chlorophenoxyacetic acid (2,4,5-D), and even copper sulfate. Such increases in yield are temporary, and treatment must be repeated frequently. Yield increases of 25% are common, although some areas respond more or less, say 20–40%.

Such stimulants presumably operate by increasing the surface area of bark drained by the tapping cut. Of course, this implies a physiological change that is not known. At least, prolonged use of such stimulants does not appear to be harmful to the tree.

In recent years, a major breakthrough was accomplished in the field of yield stimulation. This stemmed from a study of the “plugging” process of latex vessels. It now appears that the difference between a high-yielding tree and a low-yielding tree is the length of time of latex flow before plugging, that is, coagulation at the cut end of the latex vessel.

Specific chemicals were found that inhibited the closing off of the vessels. Most effective was ethylene gas, among a host of others. Today, commercial compounds that slowly liberate ethylene are used. Among these is one called Ethrel, 2-chloroethyl phosphonic acid (Table V). The most common application is to prepare a 10% slurry of Ethrel in palm oil. Application by hand with a paint brush on the bark near the tapping panel is the next step. Within a very few days enough hydrolysis has occurred to permit ethylene absorption within the tree tissues. The

TABLE IV Distribution of Dry Rubber Types

Source	International type	Total (%)
Chem. coag. latex	Pale crepe/smoked sheets	80.0
Cup lump, tree lace	Estate brown crepes	15.5
Bark scrap	Thin brown crepes, ambers	2.0
Earth scrap	Flat bark crepe	2.0
Factory salvage	Flat bark crepe or higher	0.5
	Total	100.0

TABLE V Effect of Ethylene on Yield

Clone	Untreated	Treated (lb/year/acre)
Tjir 1	1280	2480
PB 86	1300	2920
PR 107	1890	2250
GT 1	2420	3030
RRIM 501	2170	2640
RRIM 605	1400	2650
RRIM 623	1760	2900
RRIM 600	2950	5490

dramatic yield increase is immediate. Renewed application is optimum at 2-month intervals.

Since the largest components of operating (and final) costs on a rubber estate are tapping and collecting of latex, the utilization of ethylene or newer generation stimulants has tremendous economic and social impact.

III. PREPARATION

Collected latex upon arrival at the producing factory is strained and blended in large tanks holding about 700 gallons or more. The latex is then diluted with water to about 15% solids (for sheets) and 20–25% (for pale crepe). It is then transferred into coagulating aluminum tanks of 200–400 gallons capacity. To 100 parts of diluted latex may be added 5 parts of either a 0.5% formic acid solution or a 1% acetic acid solution.

The tanks are about 16 in. deep with removable aluminum partitions. Coagulation is complete in several hours, but usually is done overnight. The soft, smooth, and gelatinous slabs are then processed into sheets or crepes.

A. Grades and Types

1. Pale Crepe

Only 5–10% of total field latex is made into pale crepe. This is a premium rubber, noted for lightness of color. As such, it goes into white sidewall tires, drug sundries, surgical goods, and certain domestic products.

Prior to coagulation, latex is treated with 0.5% sodium bisulfite to prevent darkening of the rubber by enzymes. A bleaching agent, such as 0.1% xylyl mercaptan, may also be utilized. Another method is fractional precipitation by first adding only 15% of the total coagulating solution, which coagulates about 10% of the latex. The latter is skimmed off and contains most of the natural occurring protein and β -carotene, the yellow coloring pigment in natural rubber. This produces sole crepe.

The coagulum is passed through a series of several grooved rolls on creping machines. After about eight passes through such creping rolls, operating at a differential speed, and sprayed continuously with water, the final sheet is thin, has a creped surface, and is slightly yellow–white in color. The sheets are then dried in well-ventilated sheds or hot-air tunnel driers at 40–45°C. This may take up to 6 days to dry. Pale crepe is carefully inspected and packed as 75–160 lb bales in multiwall paper bags or wooden boxes.

2. Smoked Sheets

Ribbed smoked sheets (RSS) are prepared much as is pale crepe. However, even speed rollers are used, with a final embossing roll to provide the characteristic ribbed surface. The rib pattern is intended to provide increased surface area for a faster rate of drying.

The ribbed sheets are placed on racks mounted on trolleys, then placed in a smoke-house, then a drying chamber. The total cycle takes 2–4 days, with entry temperature at 40°C and exit temperature at 60°C. Most estates convert 80–85% of their total crop into RSS.

Smoking is done with wood fires. The smoke provides the characteristic odor of RSS. Some people feel that the cresols, phenols, and other components of the smoke confer antioxidant properties to the rubbers. Most probably, some antiseptic effects are gained. Indeed, if the smoke is eliminated, air-dried sheets result. These are becoming more popular, with their amber or light brown color.

3. Brown Crepe

Such crepes constitute the largest single type of rubber made from raw material other than field latex. Since the raw material is so variable, that is, cup lump, tree lace, etc., it must be soaked overnight in a dilute solution of sodium bisulfite to lighten the color and to remove surface dirt. After maceration, the slabs are sheeted and treated as with pale crepe. Due to varying degrees of enzyme darkening, color may be quite variable and mottled. Such crepes can be baled bareback (as with RSS) in 250 lb cubical bales, bound with rust-proof bands, or wrapped in burlap.

4. Blanket Crepe (Ambers)

Such rubber type is made from RSS clippings and remilled cup lump.

5. Standard Grades

There are 35 grades of dry natural rubber sold on the market. The market operates as with any other agricultural

commodity on a trading exchange. These grades are segregated into eight types, depending on the preparation and the raw scrap used. Each type is subdivided into grades based on quality. In the past, quality has mainly been determined by visual examination. Of special concern are dirt, cleanliness (absence of foreign substances such as bark), color, freedom from blemishes, and general uniformity.

The above types and grades are officially endorsed by organizations from consuming and producing countries. In the United States, this means the Rubber Trade Association of New York and the Rubber Manufacturers' Association of Washington, D.C. An official manual, titled "International Standards of Quality and Packing for Natural Rubber Grades," describes these rubbers. The manual is commonly called "The Green Book." The most recent edition was approved at the *Fourth International Rubber Quality and Packing Conference (IRQPC)* held in Brussels, Belgium, in June 1968.

B. Specifications

Natural rubber is a rather uniform material leaving the tree. It is the subsequent handling and processing that introduce variability. Of the 35 official grades, there are really only about eight major types. These are summarized in a visual grading scheme.

Type	Source	Grades
Ribbed smoked sheet	Field latex	1×, 1, 2, 3, 4, 5
Pale crepe	Field latex	1×, 1, 2, 3 (thick and thin)
Estate brown crepe	High grade natural coagulum	1×, 2×, 3× (thick and thin)
Compo crepe	Coagulum, tree scrap	1, 2, 3
Thin brown crepe	Natural coagulum, unsmoked sheets	1, 2, 3, 4
Thick blanket crepe	Natural coagulum, unsmoked sheets	2, 3, 4
Flat bark crepe	Natural coagulum, earth scrap	Standard and hard
Pure smoked	Remilled RSS or cuttings	
Blanket crepe		

C. Packing and Shipping

Natural rubber was originally shipped in wooden cases, similar to tea. Unfortunately, wood splinters often became imbedded in the rubber. About 1930, burlap or jute bags were used, but again the fibers were troublesome. The standard practice finally became "bareback" baling. Rubber sheets are piled together and squeezed with a hydraulic press into a 5 ft³ bale, weighing 250 lb. The outer wrap of

rubber sheet is coated with a very light slurry of soapstone, talc, or whiting in water, preventing the bales from sticking in transit.

IV. MODIFIED RUBBER AND DERIVATIVES

A. Anticrystallizing Rubber

This form of natural rubber, isomerized by chemical treatment, is used in low-temperature applications.

B. Cyclized Rubber Masterbatch

This rubber is prepared by heating stabilized latex with strong sulfuric acid, mixing with untreated latex containing an equal quantity of rubber, and coagulating. The coagulum is washed, machined, and dried in the usual way. Cyclized rubber masterbatch is useful in the preparation of stiff vulcanizates.

C. Heveaplus MG Rubber

These rubbers are made by polymerizing methyl methacrylate monomer *in situ* in latex so that polymer chains are attached to the rubber molecule. The resultant latex is coagulated and the coagulum made into a crepe. Two products are available, MG 30 containing 30% methyl methacrylate, and MG 49 containing 49%. Their special value is in adhesives for bonding rubber to plastics.

D. Partially Purified Crepe (PP Crepe)

This rubber contains less than half the normal amount of protein and mineral matter present in pale crepe and is prepared from latex that has been centrifuged to remove some of the naturally occurring nonrubber substances.

E. Rubber Powder

There are several types of rubber powder that are made in different ways. They are usually in the form of granules about $\frac{1}{32}$ in. in diameter. They may be slightly vulcanized and contain appreciable quantities of dusting powder to prevent massing on storage.

F. Skim Rubber

When latex is concentrated by centrifuging, the by-product skim latex is coagulated and made into smoked sheet, thick crepe, or granulated rubber. It contains a higher proportion of nonrubbers than ordinary sheet or crepe and is rapid-curing.

G. Softened or Peptized Rubber

Softened or peptized rubber is prepared by adding a small quantity of a softening agent or peptizer to latex, which is then coagulated and made into sheet or crepe. It has the advantage that it can be easily broken down to a suitable plasticity as a first step in the manufacture of rubber articles.

H. Superior Processing Rubbers

Various types of superior processing rubbers are available, for example, SP smoked sheet, SP crepe, SP air-dried sheet, SP heveacrumb, SP brown crepe, PA 80, and PA 57. The first four mentioned are made by mixing 20% by weight of vulcanized latex with 80% by weight of unvulcanized latex. The mixtures are coagulated and the coagula processed and dried in the normal manner. SP brown crepe is made by first coagulating a mixture of 80% vulcanized and 20% unvulcanized latex; one part of the resultant wet crumb is mixed with three parts of wet scrap on power mills and processed as estate thin brown crepe.

PA 80, a concentrated form of SP rubber, is made by drying the coagulum of 80% vulcanized and 20% unvulcanized rubber. The dry crumb is finally pressed into a block. PA 57, another concentrated form of SP rubber, is made by drying the coagulum produced from a mixture of 70 parts of latex consisting of 80% vulcanized and 20% unvulcanized latex rubber together with 30 parts of a non-staining processing oil. The oil is added to give an easier processing concentrated SP rubber.

SP rubbers must conform to the technical specification of swell on compound extrusion and Mooney viscosity before they may be sold. Their special value lies in improved extrusion and calendaring properties.

I. Technically Classified Rubber

Technically classified rubber, TC rubber, is supplied in three classes marked with a blue, yellow, or red circle, respectively. The rate of vulcanization of samples of a consignment is measured in an ACS 1 test compound prior to dispatch. Slow-curing rubbers are marked red, rubbers with a medium rate of cure yellow, and fast-curing rubbers blue. In the ACS 1 test compound with additional stearic acid, and in carbon black compounds, these differences are diminished and natural rubber is then of high uniformity regarding rate of cure. TC rubber reduces the variability in rate of cure in gum-type compounds and eliminates the extremes of fast-curing and slow-curing rubbers. It can be made available in any grade but present output is mainly confined to No. 1 RSS.

J. New Rubber Processes

While the standard methods of preparing and packing natural rubber have worked well in the past, the synthetic rubber industry by 1955 had set high standards of presentation of synthetic rubber in small, plastic film-wrapped bales, prepared and sold to technical specifications.

Dr. L. Bateman began to alert the industry to the weaknesses and backwardness of the visual grading system. By 1965, Malaysian research groups were ready to unveil Standard Malaysian Rubber (SMR) (Table VI).

Other producing countries, such as Indonesia, Singapore, Thailand, and Sri Lanka have similar versions of standard technically specified rubbers. Latex concentrate has been made to technical specifications for many years.

SMR technical specifications were first developed in 1965. Current technical specifications were revised in 1970 (Table VII).

1. SMR-5L is the same as SMR-5, except the former is extra light in color.
2. SMR-EQ is also available as a special, extra-pure grade, above SMR-5L.
3. SMR-5CV is a constant viscosity type.

Normally, all natural storage hardens with time. This may be at least 10–20 Mooney units in a few months. Since such stiff rubber requires premastication prior to factory use, the viscosity stabilized form of SMR-5 was developed. By treatment of latex with as little as a few tenths of 1% of a monofunctional amine, such as hydroxylamine (hydrochloride salt), aldehyde sites along the rubber chain

TABLE VI Annual Tonnage Standard Malaysian Rubber

Year	Metric tons
1966	9,000
1967	24,000
1968	83,000
1969	140,000
1970	228,000
1971	319,000
1972	280,000
1973	364,000
1974	405,000
1975	433,000
1977	542,000
1979	576,000
1985	820,000
2000	1,100,000

TABLE VII SMR Technical Specifications

Maximum limits	5L ^a	5 ^a	10	20	50
Dirt content (%)	0.05	0.05	0.10	0.20	0.50
Ash content (%)	0.60	0.60	0.75	1.00	1.50
Nitrogen content (%)	0.65	0.65	0.65	0.65	0.65
Volatile matter (%)	1.00	1.00	1.00	1.00	1.00
PRI (min) ^b	60.	60.	50.	40.	30.
Wallace plasticity (min)	30.	30.	30.	30.	30.
Color (Lovibond)	6.	—	—	—	—

^a Restricted entirely to whole field latex origin.

^b Plasticity retention index, based on Wallace. Dirt is that retained on a 44- μ m aperture mesh.

are blocked, and prevented from cross-linking or hydrogen bonding.

1. Heveacrumb Process

The Rubber Research Institute of Malaysia (RRIM) invented a mechanochemical method for making crumb rubber. The process utilizes an incompatible oil such as castor oil, added to latex at amounts less than 0.5%. The acid-coagulated slab passes through the usual creping rolls. A fine, rice-particle-size crumb is produced, rather than a sheet. The washed crumb is readily dried in trays or continuously on a belt moving through hot-air dryers. The "Hevea-crumb" is then compressed into small bales, polythene-film wrapped, and shipped on a 1-ton wooden palletized crate or loose, in large containers.

High amounts of petroleum extending oils or carbon black or both can also be incorporated within the latex before crumbling. Other materials, such as zinc stearate or silicone oils, may be used. The excess of crumbling agents is removed during the washing process. Hence, no loss of natural tack or vulcanizate adhesion is encountered.

2. Comminution Process

Many producers and consumers prefer to use SMR made without a chemical crumbling agent. Such a strictly mechanical process reduces the coagulum to pea-sized particles with a rotary knife cutter or a granulator, such as the Cumberland. Additionally, a hammermill may be used, to ensure friability of any occasional large chunk. The larger chunks may not dry completely, and could result in what is known as "wet knuckles."

While the Heveacrumb process is primarily restricted to field latex origin, the mechanical process usually employs natural coagulum such as cup lump or tree lace. Otherwise, washing, drying, packing, and shipping steps are the same as for Heveacrumb.

3. Extruder–Dryer Process

Very large production capacity can be obtained by using extruder–dryers, as with synthetic rubber. Wet coagulum is shredded, washed, put through a dewatering press (which reduces water content below 15%), then finally goes through a second screw extruder. Heating during extrusion is regulated to remove residual water without excessive heat oxidation of the rubber. One to three tons of rubber can be processed each hour. Hence, only the largest producer can economically use the process.

The SMR and other TSR types are compressed into bales of 70–75 lb each. These may measure 28 × 14 × 6.5 or 22.5 × 15 × 7 in. Polythene-wrapped bales are stacked in a wooden pallet of 1100 mm (43.4 in.) × 1425 mm (58.1 in.) × 915 mm (36 in.) in height.

K. Speciality Rubbers

Several of the modified rubbers, such as AC, MG, SP, TC, PP, and skim, have been described earlier in the Green Book of Specifications. Others are also available, some commercially while others only experimentally. These include the following.

1. Depolymerized Rubber

Depolymerized rubber has been liquefied by exposure for several hours at 140°C. These can be vulcanized and are used for casting molds, potting compounds, and binders for abrasive wheels.

2. Cyclized Rubber

Cyclized rubber is prepared by treating sheeted rubber for 1–4 hr at 125–145°C in the presence of a catalyst. Catalysts such as sulfuric acid, *p*-toluenesulfonic acid, phosphoric acid, and trichloroacetic acid may be used.

Amphoteric halides, such as the chlorides of various heavy metals, including tin, antimony, aluminum, or titanium, may be utilized to produce cyclized rubber.

Excellent adhesives for rubber to metal may be made from cyclized rubber. Protective paints and coatings for metal have also been commercialized.

3. Chlorinated Rubber

Natural rubber can react by substitution or addition with chlorine. Passage of chlorine gas through a solution of rubber in an inert solvent (such as carbon tetrachloride) at 80°C is the usual manufacturing process. Removal of solvent by steam distillation leaves a fine, white powder. It is also possible to chlorinate latex directly, with suitable protection against coagulation.

Fully chlorinated rubber is 65% chlorine, with a specific gravity of about 1.65. It can be dissolved in aromatic hydrocarbons for use as chemically resistant paints and in bonding rubber to metal.

4. OENR

Natural rubber has a tremendous capacity for absorbing oil. If imbibed without mastication, remarkably little is lost in vulcanized physical properties of the rubber. Such rubber has been shown to be superior for traction on dry snow or ice, as a winter tire.

5. DPNR

Deproteinized natural rubber is a premium rubber, wherein enzymes have broken down the naturally occurring proteins. The resultant rubber has exceptional resistance to fatigue failure and to rate of stress relaxation of the vulcanizate. Its use is aimed at engineering applications, especially under dynamic working conditions.

6. Epoxyrene

Epoxyrene is a chemical modification of natural rubber resulting in vulcanizates of increased oil resistance, enhanced adhesive properties, high degree of damping, and reduced gas permeation. Functional group interaction results in compatible blends with a range of synthetic polymers.

7. Thermoplastic Rubber (TPR)

TPR is a blend of natural rubber and polypropylene plastic fluxed at high temperatures. It is flexible at room temperature, but can be reworked and remilled at elevated temperatures.

8. Novor

Natural rubber can be vulcanized with isocyanates, resulting in high temperature resistance. It is known as Novor.

9. Biological Synthesis

The ideal goal of forming new genes has progressed as far as developments of roots and plantlets, through the exploration of tissue culture.

V. PROPERTIES

A. Chemical Properties

The first recorded analysis of natural rubber was by M. Faraday. He reported rubber to be a hydrocarbon in

TABLE VIII Nonrubber Constituents in Latex^a

Constituent	Percentage by weight
Fatty acid soaps (e.g., ammonium oleate)	0.5
Sterols and sterol esters	0.5
Proteins	0.8
Quebrachitol (a sugar)	0.3
Choline	0.1
Glycerophosphate	0.1
Water-soluble carboxylic acid salts	0.3
Amino acids and polypeptides	0.2
Inorganic salts (carbonates, phosphates)	0.2
Total	3.0

^a Trace elements can include potassium, magnesium, copper, manganese, and iron. The proteins and fatty acids are highly useful as cure activators.

the ratio of C₅H₈. Williams discovered in 1860 that destructive distillation of rubber produced isoprene as the building unit. Tilden reported that the probable structure was 2-methyl-1,3-butadiene. Bouchardat recognized that isoprene could be polymerized into rubber in 1879.

Analysis of typical samples of natural rubber reveals a small, but important amount of non-rubber constituents (Table VIII).

While the nonrubber constituents of latex and dry rubber are important, the hydrocarbon portion is still the most significant aspect of the total composition (Table IX).

Much evidence for the chemical structure of rubber is based on the products formed when the double bond is cleaved with oxidizing agents or ozone. The structure is essentially 1,4-isoprenoid, with units joined "head-to-tail."

B. Physical Properties

The physical properties of rubber may vary slightly, because of the nonrubbers present, or the degree of crystallinity (Table X). Rubber is colloiddally dispersed in latex.

TABLE IX Composition of Typical Natural Rubber^a

Ingredients	Average (%)	Range (%)
Moisture	0.5	0.2–1.0
Acetone extract	2.5	1.5–3.5
Protein (calc. from nitrogen)	2.8	2.2–3.4
Ash	0.3	0.2–0.8
Rubber hydrocarbon	93.0	
Total	100.0	

^a The acetone extract contains the fatty acids, sterols, and esters. Certain of these are believed to be natural antioxidants for rubber.

TABLE X Some Physical Properties of Natural Rubber

Density	0.92
Refractive index (20°C)	1.52
Coefficient of cubical expansion	0.00062 °C ⁻¹
Cohesive energy density	63.7 cal cm ⁻³
Heat of combustion	10,700 cal g ⁻¹
Thermal conductivity	0.00032
Dielectric constant	2.37 cal s ⁻¹ cm ⁻² °C ⁻¹
Volume resistivity	10 ¹⁵ Ω cm ⁻³
Dielectric strength	1,000 V mil ⁻¹

The average diameter of the latex particles is about 0.5 μm. These particles are constantly in motion due to Brownian movement. Each particle carries a negative electric charge, hence repelling each other and imparting stability to the latex.

Natural rubber has both a sol and gel phase. Differences are illustrated by their behavior to solvation. Highly branched and lightly cross-linked gel resists solvation. Effective solvents for sol rubber are aliphatic and aromatic hydrocarbons, chlorinated hydrocarbons, ethers, and carbon disulfide. Nonsolvents include the lower alcohols, ketones, and certain esters.

The gel phase can be broken down into processible rubber by mechanical shearing (mills, mixers, plasticators), or oxidation (assisted by heat), or chemically (peptizers). Rubber with high gel content is undesirable for calendaring, extrusion, or other fabrication processes.

1. Molecular Weight

Since rubber is a high-molecular-weight substance, ranges of values exist. Viscosity measurements of the dry rubber in shear are commonly used for relative assessment of molecular weight. Solution viscosity of the sol rubber in organic solvents is also valuable.

Fractionation of rubber from solution reveals a range of polymers of varying molecular weight. Such fractions will range from 200,000 to 400,000 in *average* molecular weight. The electron microscope has permitted measurement of the size of the molecular particles. Size/frequency data can then be converted into a molecular weight distribution curve.

2. Crystallinity

There are two geometric configurations for natural rubber. These are the *cis* and *trans* isomeric forms. The normal standard rubber, such as sheets and crepes, has the *cis* form. Balata or gutta-percha has the *trans* form. The latter is hard and horny (crystalline) at room temperature.

When heated to about 80°C, it becomes soft and tacky, indistinguishable from RSS at that temperature.

X-Ray diffraction studies of rubber in the unstretched state show a pattern of two concentric amorphous bands. When stretched to elongations short of rupture, such as 700%, a fiber pattern is revealed. This consists of well-defined interference spots, called “crystallites.” The regular arrangement indicates a unit cell with a repeat distance along the chain structure of 8.1 Å.

Raw rubber also shows a property called “racking.” If rubber is stretched repeatedly and rapidly near its ultimate breaking elongation, followed each time by cooling (dry-ice bath), a highly fibrous structure develops. These fibers are very stiff and strong.

Other thermal effects are noted in rubber. When rubber is stretched rapidly, it heats up noticeably, contrary to the behavior of most materials. Also, if rubber is stretched under a load, while held at the other end, it will retract as the temperature is raised. These two thermal effects are jointly known as the Gough–Joule effect.

Finally, the prime importance of crystallization in natural rubber is its self-reinforcing effect. As elongation increases, so does crystallization, contributing to the ultimate tensile strength of natural rubber. It is this factor that makes natural rubber superior in strength or pure gum or non-black-filled vulcanizates.

C. Biosynthesis

Natural rubber is structurally a simple example of terpenes and terpenoids, one of the most important groups of natural products. Terpenes are related from the usually regular union of the isopentane carbon skeleton of isoprene. This is described in the Ruzicka “Biogenetic Isoprene Rule.” The important implication is that all terpenes and terpenoids have a common precursor. This was found to be isopent-3-enyl pyrophosphate (IPP), the addition product of pyrophosphoric acid to isoprene.

The search for such precursors only became possible through isotopic labeling techniques. The conversion of IPP into rubber is complex and detailed, best summarized to include the role of acetic acid as a precursor in all rubber plants, and that of IPP as the monomer.

VI. PRODUCT USAGES

Although much blending of raw material is performed with field latex and/or natural coagula, such as cup lump, efforts to attain uniformity are intensive. With standard rubber grades, such as sheets and crepes, the manufacturer still resorts to blending of various shipment lots. With technically specified rubbers, such blending is usually not necessary.

A. Test Recipes

The Crude Rubber Committee of the Rubber Division of the American Chemical Society has recommended test recipes. These are used by the consumer as standard reference compounds. The ACS-I test recipe is as follows:

Natural rubber (test sample)	100.
Zinc oxide (Amer. Proc.—low lead)	6.
Stearic acid (Comm.—double pressed)	0.5
Mercaptobenzothiazole (MBT, Captax)	0.5
Sulfur (rubber makers' grade)	3.5
Total	110.5
Cure: 20, 30, 40, 60, 80 min at 127°C (260°F)	
Tests: Modulus at 500, 600, and 700% elongation; Tensile strength, breaking elongation on all cures	

Some rubbers tend to be slower than normal in cure rate, usually because of insufficient naturally occurring activators. In such cases, the same Crude Rubber Committee recommended a test recipe with higher fatty acid content (ACS-II test recipe):

Natural rubber	100.
Zinc oxide	6.
Stearic acid	4.
Mercaptobenzothiazole	0.5
Sulfur	3.5
Total	114.
Cure: 5, 10, 15, 20, 30, 45, 65, 100, 150, 225 min at 141°C (286°F)	

Pure gum vulcanizates exhibit erratic test results. In addition, MBT is no longer the most common cure accelerator for natural rubber. Also, there is some merit in using carbon-black-loaded vulcanizates, to accommodate synthetic rubber comparisons. For these reasons, the Crude Rubber Subcommittee of D-11, ASTM has recommended the following test recipe (ASTM test recipe 1-I):

Natural rubber (or <i>cis</i> -polyisoprene)	100.
Zinc oxide	5.
Stearic acid	2.
<i>N-tert</i> -Butyl-2-benzothiazole sulfenamide	0.7
Oil furnace black	35.
Sulfur	2.25
Total	144.95

Depending upon the ultimate product usage, either or both the pure gum and black loaded recipe may be tested.

TABLE XI Product Usage of Natural Rubber^a

Product	Percentage
Tires and tire products	68.0
Mechanical goods	13.5
Latex products	10.0
Footwear	3.0
Adhesives	1.5
Miscellaneous	2.0
Total	100.0

^a It is interesting to note that synthetic rubber consumption is also distributed among products in much the same percentages.

B. Distribution by Product

The percentage distribution of natural rubber usage by product category has remained remarkably steady for the past 20 years (Table XI).

C. Latex Products

Natural rubber latex is often used in blends with various synthetic rubber latices. This is because of conferring properties of superior wet gel strength, tear resistance, strength, and wet tack. Product uses are in foam backing for carpets, foam for bedding and upholstery, dipped goods, surgical goods, gloves, drug sundries, adhesives, and thread. Compounding is done by the addition of aqueous dispersions of rubber chemicals.

Recently, latex allergy sensitivity has been claimed, especially with latex gloves. Latex containing high protein levels are particularly targeted. In addition, powdered gloves have been reported to provide an aerosol to carry the allergens. Extra safety has been provided by double-centrifuging the field latex and also by enzyme treatment to destroy 95% of the proteins.

D. Tire Products

As a general rule of thumb, the larger the tire, the higher the percentage content of natural rubber. In passenger tires, natural rubber is primarily used in the carcass, for hot strength properties, low heat build-up in service, superior building tack, and better ply adhesion. In radial tires, much higher amounts of natural rubber are used, especially for essential green stock strength during the forming and building operations.

It is the commercial vehicle in which the majority of natural rubber is consumed. This includes aircraft, truck, tractor, and any off-the-road application. These use natural rubber in the tread and sidewall, as well as the carcass. Resistance to blowout, tread groove cracking, and rib tearing are the outstanding features.

E. Industrial Products

Industrial products represent the largest class of products. Hence, each product specifies the properties required, and determines the kind of rubber required.

Conveyor belting, both carcass and cover, may be composed of natural rubber. A hot ore environment is a typical one best served by natural rubber.

Seals, especially for underground pipelines to handle sewage, gas, and water, are best served by natural rubber. These are to seal joints in the lines.

Mechanical goods include a host of tank linings, hose, rubber-covered rolls, domestic goods, coated fabrics, hard rubber, sporting goods, and many extrusions.

F. Engineering Applications

Natural rubber is outstanding in its dynamic usage, especially for fatigue resistance. As such, it is widely used in bridge bearings, vibration isolators, building pads, motor mounts, suspension systems, rail pads, and even in asphalt road surfacing.

G. Recycled Rubber

Vulcanized rubber scrap has increasingly become a problem. About 2700 million tires per year require disposal.

Reclaiming rubber is no longer viable, due to costs. During the past decade interest has increased in recycling the rubber scrap. Recycling methods involve ambient or cryogenic grinding down to about 10–20 mesh. Such regrind can be added incrementally to fresh compound, or added to asphalt to resurface roads, playgrounds, or athletic running tracks.

VII. ECONOMICS

A. Natural Rubber versus Synthetic Rubber

Before World War II, the total rubber consumption was almost exclusively natural rubber, although several forms of synthesized rubber were already known. However, the capture of rubber-producing areas in Southeast Asia by Japan in World War II forced the United States to develop its own source of rubber, resulting in the tremendous growth of the synthetic rubber industry.

After World War II, the consuming demand for rubber products was great enough to require all the rubber available, both natural and synthetic (Table XII).

Based on technological properties, there is no doubt that both natural and synthetic rubbers will continue to be used by the rubber industry. Each has its own merits, often exhibiting symbiotic advantages when blended together.

TABLE XII United States Total Rubber Consumption^a

Year	Total rubber consumption	NR usage	NR (%)	SR usage	SR (%)
1960	1580	487	30.7	1100	69.3
1965	2090	523	25.0	1560	75.0
1969	2660	608	22.8	2060	77.2
1973	3150	712	22.6	2440	77.4
1977	3280	804	24.5	2480	75.5
1990	2810	796	28.3	2014	71.7

^a 10³ metric tons; NR; natural rubber; SR, Synthetic rubber.

B. Petrochemical Influence

It is doubtful that the synthetic rubber industry would have flourished so rapidly had it not been for the vast, readily available, and low cost source of petroleum raw material. With an assist from the coal industry, the rubber chemical industry rose to its maturity. All synthetic rubbers are based on such hydrocarbon sources.

C. Future Market

The demand for natural rubber, and also synthetic rubber, is directly related to general economic growth, both in the United States and worldwide (Table XIII).

The advent of the synthetic rubber industry during World War II, and inability of the natural rubber industry to keep up with the demand of the consuming industry,

TABLE XIII Natural Rubber Consumption^a

Year	United States	Rest of world	Total
1900	20,000	30,000	50,000
1910	43,000	57,000	100,000
1920	206,000	92,000	298,000
1930	376,000	334,000	710,000
1940	648,000	462,000	1,110,000
1950	720,000	1,002,000	1,722,000
1960	480,000	1,585,000	2,065,000
1970	568,000	2,425,000	2,993,000
1975	634,000	2,724,000	3,358,000
1977	800,000	3,100,000	3,900,000
1990	760,000	4,544,000	5,340,000
1996	1,002,000	5,118,000	6,120,000
1999	1,110,000	5,808,000	6,908,000
2000	1,125,000	5,945,000	7,070,000

^a Metric tons.

TABLE XIV Natural Rubber Consumption by Country^a

Country	1996	1999
United States	796,000	1,100,000
United Kingdom	146,000	195,000
France	197,000	202,000
Germany	237,000	231,000
Other W. Europe	520,000	690,000
Eastern Europe	328,000	438,000
Japan	664,000	720,000
China	620,000	827,000
South Korea	262,000	280,000
Other Asia	1,010,000	1,310,000
Latin America	180,000	274,000
Africa	120,000	180,000
All others	260,000	480,000
Total	5,340,000	6,908,000

^a Metric tons.

restricted the total growth consumption of natural rubber. It is also interesting to note that since 1940 the “rest of the world” has shown a greater rate of increased usage of natural rubber than the United States. Of course, this illustrates the normal pattern of growth for industrially developing countries (Table XIV).

Until 1945, the United States consumed more natural rubber than the rest of the world combined. Since then, as economic development surged in Asia and Europe, the United States percentage consumption has steadily declined to about 20% by 1977.

There is no average price for natural rubber. It is traded on the open market just as any commodity. It is subject to the law of supply and demand, as well as inflationary forces common to all industrially developing countries. To a degree, it is also influenced by market prices for synthetic rubber. (See Table XV.)

TABLE XV Natural Rubber Production by Country^a

Country	1983	2000
Malaysia	1,562,000	2,200,000
Indonesia	997,000	2,350,000
Thailand	587,000	1,400,000
Sri Lanka	140,000	270,000
Africa	250,000	360,000
India	168,000	250,000
All Others	306,000	240,000
Total	4,010,000	7,070,000

^a Metric tons.

VIII. RESEARCH

The natural rubber industry was formed and nurtured by the fruits of labor of a mixed lot of individuals, during the eighteenth and nineteenth centuries. It would be difficult to classify these pioneers as scientists in the classical sense. They were a mixed lot of botanists, civil servants, adventurers, explorers, everyday laymen, and opportunists.

However, the twentieth century witnessed the emergence of organized rubber research, first with the Dutch in Holland at Delft in 1909. This was followed by rubber research institutes in the Dutch East Indies at Bogor (Java) and Medan (Sumatra).

The British formed rubber research institutes in Sri Lanka (Ceylon) and at Kuala Lumpur in Malaysia. The latter, now known as the Rubber Research Institute of Malaysia (RRIM), celebrated its Golden Anniversary in 1975. RRIM is now the largest agricultural research institute in the world devoted to a single crop.

British and Malaysian planters financed the British Rubber Producers' Research Association in England. It is now known as the Malaysian Rubber Producers' Research Association. This laboratory is famed for its scientific research on elasticity, viscoelastic behavior, isomerism, biochemistry of latex, abrasion, strength properties, ozone and oxidation mechanism, vulcanization, and physics of rubber.

In 1936, the International Rubber Research and Development Board was formed. Its members include RRIM, MRPRA, Institut Fran cais Du Caoutchouc, and institutes from South Africa, Cambodia, Vietnam, Sri Lanka, and Indonesia. Its aims are to improve natural rubber quality, to reduce costs, and to develop new markets through wider applications.

Closely allied, although more concerned with synthetic polymers, are the United States rubber manufacturers' research laboratories, the Polymer Institute of the University of Akron in Ohio, the large chemical companies, such as Bayer and Leverkusen, and various polymer research institutes in Russia.

SEE ALSO THE FOLLOWING ARTICLES

ELASTICITY, RUBBERLIKE • PLASTICIZERS • POLYMER PROCESSING • POLYMERS, SYNTHESIS • RUBBER, SYNTHETIC • SOL-GEL PROCESSING

BIBLIOGRAPHY

Allen, P. W. (1972). “Natural Rubber and the Synthetics.” Wiley, New York.

- Babbit, R. D. (ed.) (1978). "The Vanderbilt Rubber Handbook," R. T. Vanderbilt Company, Norwalk, Connecticut.
- Bateman, L. (ed.) (1963). "Chemistry and Physics of Rubber-Like Substances," Maclaren and Sons, London.
- Blow, C. M. (ed.) (1971). "Rubber Technology and Manufacture," Butterworths, London.
- Davis, C. C., and Blake, J. T. (1937). "Chemistry and Technology of Rubber," Reinhold, New York.
- LeBras, J. (1957). "Rubber, Fundamentals of Its Science and Technology," Chemical Publishing Co., New York.
- Morton, M. (ed.) (1973). "Rubber Technology," Van Nostrand-Reinhold, New York.
- Naunton, W. J. S. (ed.) (1961). "The Applied Science of Rubber," Edward Arnold, London.
- Noble, R. J. (1953). "Latex in Industry, 2nd ed.," Hildreth Press, Bristol, Connecticut.
- Stern, H. J. (1967). "Rubber: Natural and Synthetic, 2nd ed.," Maclaren and Sons, London.



Rubber, Synthetic

Stephen T. Semegen

STS Technical Services

- I. Introduction
- II. Types
- III. Production by Types
- IV. Economics and Future Outlook

GLOSSARY

Catalyst Chemical that promotes the reaction of monomers into long polymer chains.

Coagulation Irreversible agglomeration of particles originally dispersed in a rubber latex.

Comonomer One of the two or more monomer species that react to form a polymer.

Copolymer Polymer formed from two or more types of monomers.

Diene polymer Polymer formed from one or more monomer species, at least one of which is a diolefin.

Formula (recipe) List of materials and description of procedure used to prepare a polymer.

Gel, latex Semisolid system consisting of a network of aggregates in which a liquid is held.

Homopolymer Polymer formed from a single monomer species.

Polymer network Three-dimensional structure formed by chemical or physical linking of polymer chains.

Short stop Chemical that stops the polymerization process at the required chain length.

Viscoelasticity Combination of viscous and elastic properties in a material with the relative contribution of each dependent on time, temperature, stress, and strain rate.

SYNTHETIC RUBBER represents perhaps the greatest chemical engineering accomplishment of modern times. Although a laboratory curiosity 200 years ago, no type of synthetic rubber was used commercially until almost 1940. The loss of natural rubber sources during World War II led to a tremendous industry and government program to develop poly(styrene-butadiene) rubber as a substitute for natural rubber. By the end of the war in 1945, annual production exceeded 700,000 tons. Although a synthetic form of natural rubber exists that is chemically and physically almost identical to *cis*-1,4-polyisoprene natural rubber, there are at best 20 distinct chemical types of synthetic rubber available today. No one is better than all others in an absolute sense. The best choice depends on the properties required for end usage. Modern industry and technology could not exist as they are today without synthetic rubber.

I. INTRODUCTION

A. Historical Background

The basic chemistry for synthetic rubber had been worked out in the early 1800s. In 1826, Michael Faraday had shown natural rubber to consist of a hydrocarbon with five

atoms of carbon for eight atoms of hydrogen. In 1860, G. Williams pyrolyzed raw natural rubber by dry distillation and called the distillate isoprene.

By 1887, W. A. Tilden in England, G. Bouchardat in France, and O. Wallach in Germany had some success in converting isoprene back into a rubberlike substance. Tilden was also able to obtain isoprene from turpentine. In 1909, the first patent for synthetic rubber was granted to F. Hofman in Germany, who used isoprene obtained from mineral sources.

Kondakov, a Russian chemist, discovered that an elastic polymer could be more easily made from another hydrocarbon, dimethylbutadiene. In 1910, the English chemists F. E. Mathews and E. H. Strange and the German chemist G. C. Harries independently found that sodium was an effective catalyst to speed up the polymerization process.

In Germany, lack of access to natural rubber sources during World War I accelerated work on synthetic rubber. By 1916, Leverkusen was producing 150 tons of methyl rubber from dimethyl-butadiene each month. After World War I, Hermann Staudinger of Freiburg University in Germany discovered that rubber consists of molecules with very long chain lengths and high molecular weight.

After investigators switched to butadiene as the monomer and sodium as the catalyst, two new types were found by 1929. One was a copolymer of butadiene and styrene. The other was a copolymer of butadiene with acrylonitrile. Both were made in an aqueous emulsion, so that the rubber was obtained first as a latex and then could be coagulated to yield a dry rubber. By the start of World War II in Europe, Germany had a synthetic rubber production capacity of 175,000 tons per year in 1939. In Russia, synthetic rubber production reached 90,000 tons in 1939.

In the United States, the first commercial efforts were concentrated on oil-resistant types of rubber, which natural rubber and poly(butadiene-styrene) rubber are not. In 1927, J. C. Patrick produced a rubber by reacting ethylene dichloride with sodium tetrasulfide. This is now the polysulfide class of elastomers. In 1931, Du Pont introduced commercially the polymers of chloroprene (2-chloro-1,3-butadiene). Popular legend attributes early laboratory discovery to Father Nieuwland at Notre Dame University.

In 1937, W. J. Sparks and R. M. Thomas invented poly(isobutylene-isoprene), or butyl rubber, at the Standard Oil Company in New Jersey. By 1939, the B. F. Goodrich Company in Akron, Ohio, began production of poly(butadiene-acrylonitrile), or Ameripol rubber. After World War II arrived, the rest became history. By 1945, a turning point was reached that proved to be of major significance to the rubber industry, and indeed to all industry.

B. Chronological Discovery of Types

The early history of synthetic rubber development has been mentioned. Perhaps the synthesis of a polyisoprene in 1887 in the laboratory was the first step in a long journey. Certainly, the production of the Buna rubbers in 1929 was a major first leap. The United States' entry with polysulfide rubber in 1927 and chloroprene rubber in 1931 was a significant commercial advance. A quantum breakthrough was, of course, the establishment of the giant styrene-butadiene rubber plants in the United States during the 1940s. Since then, there have been a host of different synthetic rubber types developed, each with its own specific combination of properties and uses.

1. Silicone Rubber

First patent application for silicone elastomers was in 1944. Original suppliers were the General Electric Company and the Dow Corning Corporation. Their unique properties stem from a silicone backbone instead of an organic carbon-carbon backbone.

2. Polyacrylic Rubber

Homopolymers of esters of acrylic acid were developed during World War II by the B. F. Goodrich Company and regional laboratories of the U.S. Department of Agriculture. In 1948, B. F. Goodrich commercialized copolymers of the ester types with reactive halogen-containing types. The latter are useful for vulcanizing sites.

3. Fluorocarbon Elastomers

The fluorocarbon elastomers are based primarily on vinylidene fluoride and hexafluoropropylene. These were developed originally by the Kellogg Company in the 1950s. Current producers are the 3M Company and Du Pont in the United States, Japan, Italy, and Russia are also producers.

4. Polybutadiene

Polybutadiene (PB) made in an aqueous solution is not new. However, PB rubber made in an organic solvent solution system with stereospecific catalysts is much more scientifically and commercially important. These were the polymerization catalyst systems discovered by Karl Ziegler in Germany and by Giulio Natta in Italy.

Phillips Petroleum Company announced high *cis*-polybutadiene rubber in 1956.

5. Polyisoprene

Stereoregular polyisoprene was first commercialized by the Shell Chemical Company in 1960. This was quickly

followed by Goodyear and Goodrich-Gulf, although Sam Horne had successfully obtained high *cis*-1,4 polyisoprene in 1955. This was the first truly synthetic “natural rubber.”

6. Poly(ethylene-propylene) and Terpolymers

The copolymers of ethylene and propylene are normally crystalline plastics or resins. However, Karl Ziegler and Giulio Natta were able to choose catalysts that produced an amorphous structure with rubbery properties. By 1961, elastic poly(ethylene-propylene) (EPM) was available in small quantities. In 1962, a third monomer was added. This is usually a diene, which permits conventional sulfur vulcanization. Commercial production followed in 1963 in the United States.

II. TYPES

There is only one chemical type of natural rubber, *cis*-1,4-polyisoprene. In contrast, there are many different chemical types of synthetic rubber. Such types can comprise repeating chains of one, two, or even three monomers of different chemical and physical properties. In recent years, the use of blends of different synthetic rubbers has greatly increased. Often, a symbiotic improvement in physical properties and end product performance has resulted.

A. Poly(styrene-butadiene) and Polybutadiene

The copolymer of styrene and butadiene is called poly(styrene-butadiene) (SBR). It consists approximately of 25% of styrene units distributed among 75% of butadiene units in the polymer chain. It is the most widely used type of synthetic rubber in the world; it also surpasses the total usage of natural rubber. (See Table I.) It is interesting to note that by the mid-1960s, total volume usage of synthetic rubber finally exceeded that of natural rubber worldwide.

TABLE I Consumption of Synthetic Rubber (SR) and Natural Rubber (NR) Worldwide

Year	SR	NR	Total (metric tons)
1900	—	50,000	50,000
1920	—	300,000	300,000
1940	100,000	1,100,000	1,200,000
1950	700,000	1,600,000	2,300,000
1960	1,700,000	2,100,000	3,800,000
1970	4,600,000	2,300,000	6,900,000
1980	8,600,000	3,200,000	11,800,000
1996	9,560,000	6,120,000	15,680,000
2000	10,976,000	7,070,000	18,046,000

Actually, in North America that crossover had occurred by 1955.

Polybutadiene comes in a variety of types. These may have low to high *cis* contents. They may be made in organic solvent solution or in aqueous emulsions. They possess the highest resilience of any rubber, even including natural rubber. However, its most important use is to blend with SBR or natural rubber because of its superiority for abrasion resistance and low temperature resistance. As such, its use is highly desirable in tire treads. It is also capable of absorbing very high amounts of petroleum oils without undergoing a serious drop in the level of its beneficial physical properties. This is most helpful as a cost-reducing factor.

B. Polychloroprene

Polychloroprene (CR) is similar to isoprene in its chemical structure. The main difference is a chlorine atom in place of a methyl group as a side chain. This confers greater resistance to oil and solvents than does SBR or natural rubber. It is also more resistant to aging and weathering. However, it is less resistant to stiffening at low temperatures. It also has a degree of flame resistance.

C. Poly(acrylonitrile-butadiene)

Nitrile rubber (NBR) is a copolymer of acrylonitrile and butadiene in which the acrylonitrile content may vary from 18 to 40%. The higher the acrylonitrile content, the better the oil resistance, which is still better than that for chloroprene. Its heat aging resistance is also better, but not its resistance to weathering. Low temperature resistance also becomes poorer with increasing acrylonitrile content.

D. Poly(isobutylene-isoprene)

Poly(isobutylene-isoprene) (IIR) is a solution polymer, often called butyl rubber. The isoprene content ranges only from 1 to 4%. The latter is present to permit vulcanization with sulfur. Its outstanding property is its very low permeability to air and other gases. Its resistance to aging and weathering is very good, but it has a low degree of resilience and poor low-temperature properties.

In addition, butyl rubber is incompatible with other rubbers and will not covulcanize. This problem can be overcome to a degree by a small degree of reaction with chlorine or bromine to form halogenated butyl rubber.

E. Poly(ethylene-propylene) and Terpolymers

Copolymers of ethylene and propylene can be randomly formed from 40:60 to 70:30 ratios. These are called

poly(ethylene-propylene) (EPM) rubbers and can only be vulcanized with peroxides. Terpolymers may be made by adding a small amount of a diene. This can be 1,4-hexadiene, dicyclo-pentadiene, or ethylidene norbornene. Such rubbers are called EPDM rubbers and can then be vulcanized with sulfur. Both EPM and EPDM rubbers are excellent for heat aging and weathering. Their resistance to low temperatures is also quite good. In addition, they lend themselves to very high extension with hydrocarbon oils without a high degree of loss in physical properties. In addition, a moderate amount of these rubbers can be blended with other rubbers satisfactorily.

F. Specialty Polymers

There are several synthetic rubbers whose volume usage is not very large but that fill very important roles.

1. Fluorocarbon Elastomers

The most common of the fluorocarbon elastomers (CFM) are based on vinylidene fluoride, hexafluoropropylene, and tetrafluoromethylene. These are expensive rubbers, ranging upward from about \$15 per pound. In addition, their specific gravity is almost double that of other synthetic rubbers. Their main virtue lies in their heat resistance above 200°C and their extremely good resistance to corrosive chemicals. Most of these types do not have good resistance to low temperatures.

2. Silicone Rubbers

Silicone (SI) rubbers are not considered to be carbon organic compounds. Based on alternate atoms of silicon and oxygen, they are most useful for their wide operating temperature range, from below -100°C to above +200°C. In addition, they have excellent electrical insulating properties, excellent resistance to many chemicals, and a property of being very unsticky.

3. Polysulfide Rubber

Polysulfide (T) rubbers are the reaction products of an organic dihalide and sodium polysulfide. The FA type is a copolymer of ethylene dichloride and dichloroethyl formal. The ST type is a polymer of dichloroethyl formal with 2% of trichloropropane. Further treatment produces thiol groups. Zinc oxide is most commonly used as the vulcanizing agent. Paraquinone dioxime may also be used with zinc oxide. The rubbers are very resistant to most classes of organic solvents. Resistance to aging and weathering is also excellent, as is its impermeability to gases. It also has a strong, characteristic sulfurous odor.

TABLE II U.S. Consumption of Synthetic Rubber (1985)

Type	Metric tons	% Total
SBR	1,960,000	59
Polybutadiene	560,000	17
Polychloroprene	175,000	5
Nitrile	95,000	3
Butyl	190,000	6
EPDM	190,000	6
Polyisoprene	90,000	3
Others	40,000	1
Total	3,300,000	100

4. Polyacrylates

The polyacrylates (ACM) are highly heat- and oil-resistant polymers. They were developed specifically for use in seals for the automotive industry. Most commonly used rubbers employ ethyl acrylate with 1 to 5% of a chlorine containing cure site, such as 2-chloroethyl vinyl ether. Strong bases, such as polyamines, are the vulcanizing agents. Alkali metal stearates with sulfur have been used predominantly. Resistance to heat, aging, and weathering is also excellent. Due to a sluggish state of cure, post-tempering in a hot-air oven is often used to increase resilience.

5. Others

In recent years, a host of other synthetic rubbers have been developed. These include the fluorosilicones, polyepichlorhydrin types, chlorosulfonated polyethylene (CSM), millable polyurethanes (Ue), vinyl acetate ethylene rubber (EVAC), and a large class of thermoplastic elastomers (TPE). The last is expected to have a bright future, due to the ease with which it is processed and fabricated into products. Since the materials do not require vulcanization, residual scrap can be recycled. Styrene block copolymers with dienes were the earliest commercial types. These are polystyrene hard segments connected by a rubbery linear segment of polybutadiene, polyisoprene, or polyisobutylene. (See [Table II](#).)

III. PRODUCTION BY TYPES

Reference has been made to polymerization processes for synthetic rubbers. Economic production requires a low-cost, plentiful raw material supply; a fast and controllable polymerization process; the ability to stop the reaction at the desired molecular weight or chain length; recovery of

unreacted monomers; and coagulation and drying of the rubber.

A. Polymerization Systems

1. Poly(styrene-butadiene) and Polybutadiene

The source of butadiene is petroleum. It is obtained by “cracking” or dehydrogenation of ethylene, by dehydrogenation of butylene in refineries, or by dehydrogenation of butanes from natural gas. Butadiene gas is liquefied with high pressure and low temperature prior to storage and use.

Styrene, or vinyl benzene, is a liquid. Its source is dehydrogenation of ethyl benzene from alkylation of benzene.

Most SBR is made by the water emulsion polymerization process. The monomers are mixed together with water and soap to form an emulsion. The polymerization catalyst and activator are then added, and the reaction proceeds in a closed vessel for several hours at a designated temperature. A shortstop is then added to stop the reaction at the desired chain length. Unreacted monomers are recovered by stripping. The resultant latex is coagulated with dilute acid or salt into crumbs. The crumbs are water washed, filtered, and dried. The dried crumbs are pressed into bales of 35 kg, wrapped in polyethylene bags, and stored.

Emulsion polymerization recipes can be as follows:

Hot process (50° C)	
Butadiene	75
Styrene	25
Water	180
Soap	5
Potassium persulfate	0.3
Dodecyl mercaptan	0.5

Cold process (5° C)	
Butadiene	75
Styrene	25
Water	200
Soap	4.5
Alkyl peroxide	0.1
Ferrous sulfate	0.03
Trisodium phosphate	0.5
EDTA	0.04
Dodecyl mercaptan	0.2

Solution recipes would replace water with cyclohexane. The catalyst would be the metal alkyl types of Ziegler–Natta or anionic types. Such types require recovery of the

solvent and care in drying. The rubbers are more linear with less branching than the emulsion types.

2. Polychloroprene

Neoprene is made from the monomer 2-chloro-1,3-butadiene. The monomer was originally made from acetylene gas and hydrogen chloride with a cuprous chloride catalyst. Currently, it is made from butadiene and chlorine, followed by sodium hydroxide treatment.

Chloroprene is emulsified with water and soap and then catalyst and modifier are added, polymerization proceeds at the designated time and temperature, and the reaction is terminated with a shortstop. The rubber is obtained by freeze drying a coagulated film on a cold roll. The film is then washed and dried and formed into ropes or chips. It is usually stored in sealed fiber drums.

3. Poly(acrylonitrile-butadiene)

Poly(acrylonitrile-butadiene) is prepared very similarly to the SBR process. It can also be made by the hot or cold process.

Hot process (50° C)	
Butadiene	70
Acrylonitrile	30
Soft water	180
Soap	4
Potassium persulfate	0.3
Dodecyl mercaptan	0.5

A stabilizer is also added prior to coagulation. This is usually an antioxidant to prevent oxidation and cross-linking during drying and subsequent storage. The rubber is finished as with SBR.

4. Poly(isobutylene-isoprene)

Butyl rubber is prepared by copolymerizing isobutylene with 1.5 to 4.5% of isoprene. Both monomers are obtained by petroleum refinery cracking. Isobutylene must have very high purity, at least 99%. Isoprene is much more difficult to obtain by extractive distillation with acetone and must be at least 92% pure.

The polymerization process is continuous rather than batch operated. It must also proceed at very low temperatures, such as -96°C .

The monomers are blended with an inert diluent, methyl chloride. The catalyst is aluminum trichloride; the reaction is known as a Friedel–Crafts reaction. The polymerization is instantaneous. The suspension of rubber particles and

liquid medium is dumped into hot water. Methyl chloride and unreacted monomers are recovered and stored. The wet crumbs are dried by passage through extruder mill driers, weighed, and baled.

5. Poly(ethylene-propylene) and Terpolymers

Both EPM and EPDM polymers are also prepared in a solvent solution, usually in hexane. The catalysts are a combination of metal alkyls and transition metal halides. Complete dryness is necessary, since moisture destroys the catalysts. In fact, the polymerization reaction is terminated by the addition of water or alcohol. Oil is added at this point, if the rubber is to be an oil-extended type. The rubber solution is then coagulated into crumbs by agitation in boiling water. The hexane solvent is recovered by distillation, while the rubber is dried by passage through extruder driers. It is then compressed into 75-lb bales measuring $7 \times 14 \times 28$ in. The bales are wrapped in polyethylene film and packed in large unit cartons.

6. Fluorocarbon Elastomers

Fluorocarbon elastomers are produced by high-pressure polymerization in an emulsion system using water as the medium. The emulsifier is a fluorocarbon soap. Persulfates are used to initiate the reaction and polymerization regulators are used to control the molecular weight of the polymer. The production process is very similar to that for SBR.

7. Silicon Rubbers

Silicon polymers are prepared by a complex series of chemical reactions. Starting materials are sand and alkyl or aryl halides. Sand, preferably quartz, is first reduced to elemental silicon by heating with carbon in an electric furnace. Eugene Rochow of the General Electric Company developed the "direct process" of converting silicon into silicone. This consists of heating silicon and copper powder in a tube with methyl chloride gas to produce a mixture of methyl trichlorosilane, dimethyl dichlorosilane, and trimethyl chlorosilane. Dimethyl dichlorosilane is the basic ingredient for dimethyl silicone gums. It is separated by fractional distillation. The silane is then hydrolyzed to form a siloxane.

This siloxane is then converted to the silicone gum. This is done by a condensation polymerization reaction. Another process utilizes cyclic dimethyl siloxanes, which can be catalyzed with a base to open the ring and form a high-molecular-weight gum. Other types can be formed by adding phenyl or vinyl groups to the intermediates.

8. Polysulfides

The polymers are prepared by the addition of an organic dihalide to a heated and stirred aqueous solution of sodium polysulfide. Soaps or detergents are used to produce small rubber crumbs upon coagulation with acid. The FA type is a linear copolymer of ethylene dichloride and dichloroethyl formal. The ST type is principally dichloroethyl formal with 2% of trichloropropane.

Ethylene dichloride is made by reacting ethylene and chlorine. Dichloroethyl formal is made by reacting ethylene oxide with hydrochloric acid to form ethylene chlorohydrin. The latter is then reacted with formaldehyde to form the formal. Sodium polysulfide is made by reacting sulfur with sodium hydroxide.

9. Polyacrylates

Polyacrylate elastomers can be prepared by any of several methods. These include the water emulsion system, suspension system, solvent solution method, or even the mass (bulk homogenous) polymerization process. Most are made by the water emulsion (latex) or the suspension method. Peroxides or persulfate initiated free radical systems are most commonly used in the presence of heat. Polymerization is usually taken to completion. Coagulation is best with salts, followed by water washing and drying with hot air, vacuum, or extrusion.

B. Chemical and Physical Properties

The properties of the raw, unvulcanized rubbers are not generally important, except for their specific gravity and molecular weight. The latter is usually expressed in a relative fashion, such as Mooney viscosity units. In addition, most synthetic rubbers are lacking in strength properties unless compounded with reinforcing fillers, such as carbon blacks or fine-particle-size silicas.

1. Poly(styrene-butadiene)

Poly(styrene-butadiene) is most useful when sulfur vulcanized and reinforced with fillers. (See [Table III](#).)

2. Polybutadiene

Polybutadiene is almost always used in blends with SBR or natural rubbers. This is primarily because of poor processing properties. However, it is the most resilient of all rubbers. (See [Table IV](#).)

3. Polychloroprene

Polychloroprene rubber has a wide range of useful properties. However, none of them is supreme among

TABLE III Properties of SBR Rubbers^a

Property	Average rating
Tensile strength (gum)	Poor
Tensile strength (filler)	Very good
Elongation at break	Very good
Abrasion resistance	Very good
Tear resistance	Fair
Low temperature resistance	Good
Compression set at room temperature	Good
Compression set at 100°F	Poor
Heat resistance	Poor
Oxidation resistance	Poor
Weather and ozone resistance	Fair
Oil resistance	Poor
Gasoline resistance	Poor
Acid and base resistance	Fair
Flame resistance	Very poor
Electrical resistance	Good
Gas permeability resistance	Fair

^a Noteworthy properties are strength and wear resistance.

synthetic rubbers. It is a good general-purpose rubber. (See [Table V](#).)

4. Polyisoprene

Polyisoprene rubber is chemically and physically almost identical to natural rubber. It can replace natural rubber

TABLE IV Properties of PB Rubbers^a

Property	Average rating
Tensile strength (gum)	Very poor
Tensile strength (filler)	Fair
Elongation at break	Fair
Abrasion resistance	Excellent
Tear resistance	Poor
Low temperature resistance	Excellent
Compression set at room temperature	Good
Compression set at 100°F	Poor
Heat resistance	Fair
Oxidation resistance	Fair
Weather and ozone resistance	Fair
Oil resistance	Poor
Gasoline resistance	Poor
Acid and base resistance	Fair
Flame resistance	Very poor
Electrical resistance	Good
Gas permeability resistance	Poor

^a Outstanding properties are wear resistance and low-temperature performance.

TABLE V Properties of CR Rubbers^a

Property	Average rating
Tensile strength (gum)	Good
Tensile strength (filler)	Very good
Elongation at break	Very good
Abrasion resistance	Good
Tear resistance	Good
Low temperature resistance	Fair
Compression set at room temperature	Good
Compression set at 100°F	Fair
Heat resistance	Good
Oxidation resistance	Good
Weather and ozone resistance	Good
Oil resistance	Good
Gasoline resistance	Good
Acid and base resistance	Good
Flame resistance	Good
Electrical resistance	Good
Gas permeability resistance	Good

^a The outstanding feature of CR rubber is its versatility; a specific gravity of 1.25 is high among general purpose rubbers.

almost 100% in most applications. Hence, it is a militarily and economically strategic material. (See [Table VI](#).)

5. Poly(acrylonitrile-butadiene)

Poly(acrylonitrile-butadiene) is most widely used because of its high resistance to oil and gasoline. Low temperature resistance becomes a problem. (See [Table VII](#).)

6. Poly(isobutylene-isoprene)

The IIR rubbers are noteworthy for their resistance to air and gas permeability. They are also excellent for resistance to heat aging and weathering. Their inability to resist low temperatures and poor compatibility with other polymers have restricted their wider acceptance. (See [Table VIII](#).)

7. Poly(ethylene-propylene) and Terpolymers

The EPM and EPDM rubbers have been allied with the poly(isobutylene-isoprene) rubbers. In many respects, they have similar properties, but are more compatible with other rubbers. (See [Table IX](#).)

8. Fluorocarbon Elastomers

Fluorocarbon elastomers (CFM rubbers) are expensive, and hence have very specialized uses. They do not blend well with other polymers. (See [Table X](#).)

TABLE VI Properties of IR Rubbers^a

Property	Average rating
Tensile strength (gum)	Good
Tensile strength (filler)	Very good
Elongation at break	Excellent
Abrasion resistance	Fair
Tear resistance	Good
Low temperature resistance	Very good
Compression set at room temperature	Very good
Compression set at 100°F	Poor
Heat resistance	Poor
Oxidation resistance	Poor
Weather and ozone resistance	Poor
Oil resistance	Poor
Gasoline resistance	Poor
Acid and base resistance	Good
Flame resistance	Very poor
Electrical resistance	Very good
Gas permeability resistance	Fair

^a Outstanding feature is its ability to replace or extend natural rubber.

9. Silicon Rubbers

Silicon rubbers are usable over a much higher range of temperatures than are carbon-based rubbers. Their electrical and chemical resistances also find wide application in aerospace and medical applications. (See [Table XI](#).)

TABLE VII Properties of NBR Rubbers^a

Property	Average rating
Tensile strength (gum)	Poor
Tensile strength (filler)	Good
Elongation at break	Good
Abrasion resistance	Very good
Tear resistance	Good
Low temperature resistance	Fair-poor
Compression set at room temperature	Fair
Compression set at 100°F	Fair
Heat resistance	Good
Oxidation resistance	Fair-good
Weather and ozone resistance	Fair
Oil resistance	Excellent
Gasoline resistance	Excellent
Acid and base resistance	Fair-good
Flame resistance	Poor
Electrical resistance	Poor
Gas permeability resistance	Good

^a Because of its solvent resistance, NBR is very useful in seals, linings, printing rolls, and bearings.

TABLE VIII Properties of IIR Rubbers^a

Property	Average rating
Tensile strength (gum)	Fair-poor
Tensile strength (filler)	Fair
Elongation at break	Good
Abrasion resistance	Fair
Tear resistance	Fair
Low temperature resistance	Very poor
Compression set at room temperature	Fair-poor
Compression set at 100°F	Good
Heat resistance	Very good
Oxidation resistance	Excellent
Weather and ozone resistance	Excellent
Oil resistance	Poor
Gasoline resistance	Poor
Acid and base resistance	Good
Flame resistance	Poor
Electrical resistance	Very good
Gas permeability resistance	Excellent

^a Low permeability to air makes IIR highly useful in tire inner tubes and as an inner liner in tubeless tires.

10. Polysulfide Rubbers

The T rubbers are very inert to oils and many solvents. These are highly useful in building and civil engineering uses. (See [Table XII](#).)

TABLE IX Properties of EPDM Rubbers^a

Property	Average rating
Tensile strength (gum)	Poor
Tensile strength (filler)	Fair
Elongation at break	Fair
Abrasion resistance	Fair
Tear resistance	Fair
Low temperature resistance	Good
Compression set at room temperature	Good
Compression set at 100°F	Very good
Heat resistance	Very good
Oxidation resistance	Excellent
Weather and ozone resistance	Excellent
Oil resistance	Poor
Gasoline resistance	Poor
Acid and base resistance	Excellent
Flame resistance	Very poor
Electrical resistance	Good
Gas permeability resistance	Good

^a Its resistance to weathering makes it a desirable blending material for sidewalls in tires.

TABLE X Properties of CFM Rubbers^a

Property	Average rating
Tensile strength (gum)	Very poor
Tensile strength (filler)	Fair
Elongation at break	Fair
Abrasion resistance	Fair
Tear resistance	Fair
Low temperature resistance	Very poor
Compression set at room temperature	Fair
Compression set at 100°F	Poor
Heat resistance	Excellent
Oxidation resistance	Excellent
Weather and ozone resistance	Excellent
Oil resistance	Excellent
Gasoline resistance	Excellent
Acid and base resistance	Excellent
Flame resistance	Good
Electrical resistance	Good
Gas permeability resistance	Good

^a Its outstanding heat resistance up to 250°C and its resistance to weathering, hydrocarbons, and corrosive chemicals make it very useful in aerospace and automotive applications.

11. Polyacrylates

The ACM rubbers were early leaders for use against oils and lubricants in the automotive industry. (See [Table XIII](#).)

12. Epichlorhydrin Rubbers

Epichlorhydrin (ECO) rubbers are specialty types with excellent fuel and ozone resistances. Combined with low gas permeability, they have a better balance of overall physical properties than do other oil-resistant rubbers. They find outlets in the aircraft and automotive industries. (See [Table XIV](#).)

C. Product Usages

Owing to the wide range of synthetic rubbers, there is seldom a product application unique to only one elastomer. The final choice is often based on cost, availability, processing, and fabrication requirements, or most often, on a blend of two or more rubbers. (See [Table XV](#).) Conversely, it is useful to tabulate the synthetic rubber types, to determine their principal application outlets. (See [Table XVI](#).) As with natural rubber, the largest single outlet for synthetic rubbers is in tires and tire products. Of course, this accounts for the overwhelming volume consumption of the polybutadiene-styrene and polybutadiene types. (See [Table XVII](#).)

TABLE XI Properties of SI Rubbers^a

Property	Average rating
Tensile strength (gum)	Very poor
Tensile strength (filler)	Fair
Elongation at break	Fair
Abrasion resistance	Poor
Tear resistance	Fair-poor
Low temperature resistance	Excellent
Compression set at room temperature	Good
Compression set at 100°F	Excellent
Heat resistance	Excellent
Oxidation resistance	Excellent
Weather and ozone resistance	Excellent
Oil resistance	Good
Gasoline resistance	Poor
Acid and base resistance	Poor
Flame resistance	Poor
Electrical resistance	Excellent
Gas permeability resistance	Very poor

^a SI polymers do not blend well with other rubbers. They have unique nonstick properties.

IV. ECONOMICS AND FUTURE OUTLOOK

As with natural rubber, the early research on synthetic rubber was mainly conducted by individual scientists working independently. This approach would no

TABLE XII Properties of T Rubbers^a

Property	Average rating
Tensile strength (gum)	Very poor
Tensile strength (filler)	Poor
Elongation at break	Good
Abrasion resistance	Poor
Tear resistance	Poor
Low temperature resistance	Fair-good
Compression set at room temperature	Fair
Compression set at 100°F	Fair
Heat resistance	Excellent
Oxidation resistance	Excellent
Weather and ozone resistance	Excellent
Oil resistance	Excellent
Gasoline resistance	Excellent
Acid and base resistance	Fair
Flame resistance	Poor
Electrical resistance	Fair
Gas permeability resistance	Excellent

^a The T rubbers are not used in blends with other rubbers, often due to the sulfurous odor they emit.

TABLE XIII Properties of ACM Rubbers^a

Property	Average rating
Tensile strength (gum)	Poor
Tensile strength (filler)	Fair
Elongation at break	Fair
Abrasion resistance	Fair
Tear resistance	Fair
Low temperature resistance	Poor
Compression set at room temperature	Fair
Compression set at 100°F	Poor
Heat resistance	Very good
Oxidation resistance	Very good
Weather and ozone resistance	Very good
Oil resistance	Excellent
Gasoline resistance	Excellent
Acid and base resistance	Poor
Flame resistance	Very poor
Electrical resistance	Poor
Gas permeability resistance	Good

^a There are increasing applications for ACM latex to treat paper, textile, and leather products.

longer apply. Efficiency and integration dictate the “group approach.”

In fact, it required the military needs of World War II to accelerate the vast government program on polybutadiene-styrene rubber. Over 50 government plants were constructed and operated in the United States and Canada. Today, there are about 150 plants worldwide. Total investment probably exceeds \$4 billion.

TABLE XIV Properties of ECO Rubbers

Property	Average rating
Tensile strength (gum)	Poor
Tensile strength (filler)	Fair
Elongation at break	Fair
Abrasion resistance	Fair
Tear resistance	Fair
Low temperature resistance	Good
Compression set at room temperature	Good
Compression set at 100°F	Poor
Heat resistance	Good
Oxidation resistance	Good
Weather and ozone resistance	Good
Oil resistance	Excellent
Gasoline resistance	Excellent
Acid and base resistance	Good
Flame resistance	Very poor
Electrical resistance	Poor
Gas permeability resistance	Excellent

TABLE XV Product Usages of SR Types

Product	Primary SR used
Tires and tire products	SBR, PB, IR, CR, IIR, EPDM
Hoses and belting	SBR, CR, CRM, T
Engines and seals	CR, NBR, EPDM, CFM, SI, T, ACM
Footwear	SBR, CR, NBR
Adhesives	CR, NBR
Sporting goods	SBR, IR, CR, NBR
Pharmaceuticals	IR, NBR, IIR, SI
Food equipment	SBR, NBR, SI, IR
Textiles	SBR, CR, NBR, ACM
Cellular products	CR, EPDM, SBR
Electrical equipment	SBR, CR, IIR, EPDM, SI
Building and construction materials	SBR, IR, CR, NBR, EPDM, T

The selling price of synthetic rubbers can vary with the economic health of the world, the cost of the raw materials provided by oil supplies, and, to some degree, the price of natural rubber. As a traded commodity, natural rubber has ranged from as low as 4¢/kg to as high as \$4/kg. In recent years, the more steady prices of general-purpose rubbers, such as SBR, have greatly stabilized the price of all rubbers.

Since 1945, production of synthetic rubbers has approximately doubled every 10 years. This may continue as long as financial capital is available and as new uses for rubber are developed. Originally, the auto industry accounted for the rapid increase in the use of rubber. Today, this has

TABLE XVI SR Types and Their Main Applications

SR type	Main application
SBR	Tires, hoses and belting, footwear, sporting goods, food equipment, textiles, electrical equipment, construction materials, cellular products
BR	Tires
IR	Tires, sporting goods, pharmaceuticals, food equipment, construction materials
CR	Tires, hoses and belting, footwear, adhesives, sporting goods, textiles, cellular products, electrical equipment, construction materials
NBR	Seals, footwear, adhesives, food equipment, textiles, construction materials
IIR	Tires, pharmaceuticals, electrical equipment
EPDM	Tires, seals, electrical equipment, construction materials
CFM	Hoses and belting, seals
SI	Seals, pharmaceuticals, food equipment, electrical equipment
T	Hoses and belting, seals, construction materials
ACM	Seals, textiles

TABLE XVII Product Usage of Synthetic Rubber

Product	Percent
Tires and tire products	67
Mechanical goods	15
Footwear	5
Latex products	4
Drug sundries	4
Adhesives	2
Construction materials	2
Miscellaneous products	1
Total	100

extended to the space program, the construction industry, civil engineering uses, road constructions, agriculture, mining, and medicine. Already, the per capita consumption of rubber in the United States exceeds 20 kg per year. The role of synthetic rubber as a primary raw material and as a finished commodity in modern society appears to be assured and unchallenged. (See [Table XVIII](#).)

Leaders in the research and production of synthetic rubber continue to be the major tire manufacturers, chemical companies, and petroleum corporations worldwide. Most

TABLE XVIII Synthetic Rubber Consumption by Country^a

Country	1996	2000
U.S.	2,187,000	2,565,000
Japan	1,124,000	1,179,000
Germany	478,000	535,000
France	436,000	455,000
S. Korea	440,000	425,000
Brazil	300,000	329,000
Italy	291,000	309,000
Taiwan	274,000	285,000
Canada	242,000	285,000
U.K.	230,000	226,000
Spain	201,000	230,000
Rest of World	3,357,000	3,720,000
Total	9,560,000	10,543,000

^a Metric tons.

of these are loosely allied for promoting and providing information about synthetic rubber within the International Institute of Synthetic Rubber Producers, Inc., headquartered in Houston, Texas.

Despite the development of polyisoprene, the quest for a synthetic replacement of natural rubber continues to be advocated. Both economic and technical reasons have hindered such research. On the average, natural rubber continually sells for 40% less than synthetic polyisoprene.

SEE ALSO THE FOLLOWING ARTICLES

ELASTICITY • ELASTICITY, RUBBERLIKE • MACROMOLECULES, STRUCTURE • PLASTICIZERS • POLYMER PROCESSING • POLYMERS, MECHANICAL BEHAVIOR • POLYMERS, RECYCLING • POLYMERS, SYNTHESIS • RUBBER, NATURAL • THERMODYNAMICS

BIBLIOGRAPHY

- Babbit, R. D. (ed.) (1978). "The Vanderbilt Rubber Handbook," R. T. Vanderbilt, Norwalk, Connecticut.
- Bateman, L. (ed.) (1963). "Chemistry and Physics of Rubber-like Substances," Maclaren and Sons, London.
- Billmeyer, F. W., Jr., (1984). "Textbook of Polymer Science, 3rd ed.," Wiley, New York.
- Blackley, D. C. (1983). "Synthetic Rubbers: Their Chemistry and Technology," Applied Science Publishers, London.
- Bueche, F. (1962). "Physical Properties of Polymers," Interscience, New York.
- Flory, P. J. (1953). "Principles of Polymer Chemistry," Cornell University Press, Ithaca, New York.
- Kennedy, J. P., and Tornqvist, E. (eds.) (1968–1969). "Polymer Chemistry of Synthetic Elastomers," Vols. 1 and 2. Interscience, New York.
- Morton, M. (1987). "Rubber Technology, 3rd ed.," Van Nostrand-Reinhold, New York.
- "Office of Rubber Reserve Reports," Library of Congress, Washington, D. C. (1946–1950).
- Penn, W. S. (1960). "Synthetic Rubber Technology," Maclaren and Sons, London.
- Stern, H. J. (1967). "Rubber: Natural and Synthetic, 2nd ed.," Maclaren and Sons, London.
- Whitby, G. S., Davis, C. G., and Dunbrook, R. F. (eds.) (1954). "Synthetic Rubber," Wiley, New York.